UNIVERSIDAD DE EXTREMADURA

**TESIS DOCTORAL**

# TERAPIAS AVANZADAS BASADAS EN CÉLULAS MADRE Y VESÍCULAS EXTRACELULARES: CARACTERIZACIÓN Y APLICACIONES EN MODELOS ANIMALES

**FEDERICA MARINARO**

**PROGRAMA DE DOCTORADO EN BIOLOGÍA MOLECULAR Y CELULAR, BIOMEDICINA Y BIOTECNOLOGÍA**

**2021**

UNIVERSIDAD DE EXTREMADURA

**TESIS DOCTORAL**

# TERAPIAS AVANZADAS BASADAS EN CÉLULAS MADRE Y VESÍCULAS EXTRACELULARES: CARACTERIZACIÓN Y APLICACIONES EN MODELOS ANIMALES

**FEDERICA MARINARO**

**PROGRAMA DE DOCTORADO EN BIOLOGÍA MOLECULAR Y CELULAR, BIOMEDICINA Y BIOTECNOLOGÍA**

Conformidad de los directores

Fdo. Dr. D. Javier García Casado

Fdo. Dra Esther López Nieto

**2021**

# FUNDING SOURCES

This thesis was supported by a MAFRESA S.L. grant (part of Grupo Jorge, promoted by Jesús Usón Gargallo) to Federica Marinaro; "Sara Borrell" grant (CD19/00048) from the National Institute of Health Carlos III (ISCIII) to Esther López Nieto; Miguel Servet I" grant "MS17/00021" [co-funded by ERDF/European Social Fund (ESF) "A way to make Europe"/"Investing in your future"] and projects "CP17/00021" and "PI18/0911" (co-funded by ERDF/ESF) from ISCIII and "IB16168" grant (co-funded by ERDF/ESF) by Junta de Extremadura to Javier García Casado; grant "CB16/11/00494" from CIBER-CV and Ayuda Grupos de Investigación de Extremadura (GR18199) from Consejería de Economía, Ciencia y Agenda Digital (cofunded by European Regional Development Fund – ERDF) to Francisco Miguel Sánchez Margallo and by Jesús Usón Minimally Invasive Surgery Centre (CCMIJU). This thesis has been developed at the ICTS Nanbiosis (Unit 14 — Stem Cell Therapy, Unit 21 — Experimental Operating Rooms, Unit 22 — Animal Housing, Unit 23 — Assisted Reproduction, Unit 24 — Medical Imaging) in collaboration with CNIC (Centro Nacional de Investigaciones Cardiovasculares, Spain), INIA (Instituto Nacional de Investigación y Tecnología Agraria y Alimentaria), University of Extremadura (Spain), University of Marburg (Germany), University of Porto (Portugal), and Federal University of Santa Maria (Brazil).

The funders had no role in study designs, data collection and analysis, decision to publish, or preparation of the manuscripts collected in this thesis.

MAFRESA
EL IBERICO DE CONFIANZA S.L.

Unión Europea
Fondo Europeo de Desarrollo Regional "Una manera de hacer Europa"
MINISTERIO DE CIENCIA E INNOVACIÓN
Instituto de Salud Carlos III
JUNTA DE EXTREMADURA
Consejería de Economía, Ciencia y Agenda Digital

Centro de Cirugía de Mínima Invasión
Minimally Invasive Surgery Centre
Jesús Usón

nanbiosis
Infrastructure for the Production and Characterization of Nanomaterials, Biomaterials and Systems in Biomedicine

# TABLE OF CONTENTS

**ABBREVIATIONS** ..... **6**

**RESUMEN** ..... **7**

**ABSTRACT** ..... **9**

**GRAPHICAL ABSTRACT** ..... **10**

**INTRODUCTION** ..... **11**

STEM CELLS ..... 11

*General characteristics of stem cells* ..... *11*

*Stem cell classification according to their origin* ..... *14*

*Mesenchymal Stem/Stromal Cells* ..... *15*

EXTRACELLULAR VESICLES ..... 28

*General characteristics of extracellular vesicles* ..... *28*

*Isolation and characterisation of EVs* ..... *29*

*Clinical applications* ..... *30*

CHARACTERISATION OF ADULT STEM CELL- AND EXTRACELLULAR VESICLE-BASED THERAPY AND APPLICATION IN ANIMAL MODELS ..... 33

*SECTION I: Application of MSC- and EV-based therapy on hernia* ..... *34*

*SECTION II: Application of MSC- and EV-based therapy on myocardial infarction* ..... *36*

*SECTION III: Application of MSC- and EV-based therapy on assisted reproduction technologies* ..... *38*

**AIM OF THE THESIS** ..... **40**

RATIONALE OF THE THESIS ..... 42

**RESULTS AND DISCUSSION** ..... **43**

SECTION I: APPLICATION OF MSC- AND EV-BASED THERAPY ON HERNIA ..... 43

SECTION II: APPLICATION OF MSC- AND EV-BASED THERAPY ON MYOCARDIAL INFARCTION ..... 47

SECTION III: APPLICATION OF MSC- AND EV-BASED THERAPY ON ASSISTED REPRODUCTION TECHNOLOGIES ..... 52

General contribution to knowledge and limitations of this thesis ..... 57

**CONCLUSIONS ..... 60**

**CONCLUSIONES ..... 61**

**BIBLIOGRAPHY ..... 63**

**APPENDIX 1: PUBLICATIONS FORMING PART OF THIS THESIS ..... 93**

Publications ..... 93

Informe de los directores – Grado de contribución ..... 241

Copyright ..... 246

**APPENDIX 2: CO-AUTHORED PUBLICATIONS NOT FORMING PART OF THIS THESIS ..... 250**

Indexed publications not included in this thesis ..... 250

Non-indexed publications ..... 250

Presentations and proceedings ..... 250

Book chapters ..... 253

Awards ..... 254

**APPENDIX 3: INTERNATIONAL PHD MENTION ..... 255**

# ABBREVIATIONS

AMI: Acute Myocardial Infarction

ART: Assisted Reproductive Technology

BM-MSCs: Bone Marrow Mesenchymal Stem/Stromal Cells

CCL: Chemokine (C-C Motif) Ligand

CDCs: Cardiosphere-Derived Cells

COVID-19: Coronavirus Disease 19

CSF1: Colony Stimulating Factor 1

CXCR: C-X-C Chemokine Receptor

EMA: European Medical Agency

endMSC: Endometrial Mesenchymal Stem/Stromal Cells

ESCs: Embryonic Stem Cells

EVs: Extracellular Vesicles

EV-CDCs: Extracellular Vesicles from Cardiosphere-Derived Cells

EV-endMSCs: Extracellular Vesicles from Endometrial Mesenchymal Stem/Stromal Cells

FDA: American Food and Drug Administration

GM-CSF: Granulocyte Macrophage-Colony Stimulating Factor

GO: Gene Ontology

HGF: Hepatocyte Growth Factor

HLA: Human Leukocyte Antigen

IDO: Indoleamine 2,3-dioxygenase

IFNγ: Interferon γ

IFNγ/EV-CDCs: Extracellular Vesicles from IFNγ-primed Cardiosphere-Derived cells

IFNγ/EV-endMSCs: Extracellular Vesicles from IFNγ-primed Endometrial Mesenchymal Stem/Stromal Cells

Ig: Immunoglobulin

IL: Interleukin

IL6R: Interleukin 6 Receptor

iPSCs: Induced Pluripotent Stem Cells

ISCT: International Society for Cellular Therapy

IVF: *In vitro* Fertilisation

M-CSF: Macrophage Colony-Stimulating Factor

MHC: Major Histocompatibility Complex

miRNAs: microRNAs

MISEV: Minimal Information for Studies of Extracellular Vesicles

MSCs: Mesenchymal Stem/Stromal Cells

NK: Natural Killer

PD-L1: Programmed Death Ligand 1

PDGF: Platelet-Derived Growth Factor

PGE2: Prostaglandin E2

qPCR: Real-time Quantitative Polymerase Chain Reaction

ROS: Reactive Oxygen Species

TGFβ: Transforming Growth Factor β

Th1: T Helper cell

TNFα: Tumour Necrosis Factor α

Tregs: Regulatory T cells

VEGF: Vascular Endothelial Growth Factor

# RESUMEN

En los últimos veinte años, las terapias basadas en el uso de células madre se han convertido en una prometedora herramienta terapéutica en el campo de la biomedicina. En este escenario, las células más estudiadas y que más se han usado en medicina regenerativa son las células madre mesenquimales (MSCs), gracias a su capacidad de diferenciación, sus efectos paracrinos y su multipotencialidad. A pesar de ello, este tipo de terapias tiene sus limitaciones, principalmente relacionadas con la seguridad, y en ciertos tipos de células, implicaciones éticas. Es por este motivo por el que la investigación se ha centrado en el uso de terapias alternativas no celulares que presentan todas las ventajas de la administración de células madre, disminuyendo los posibles riesgos. Una de estas terapias no celulares consiste en la administración de vesículas extracelulares, las cuales son secretadas por las MSCs para ejercer su efecto paracrino.

En la actualidad, se están llevando a cabo numerosos estudios clínicos y preclínicos basados en la administración de células madre, algunos de los cuales ya han sido aprobados por la Agencia Europea del Medicamento y por la American Food and Drug administration. Por el contrario, existen muy pocos ensayos clínicos basados en la administración de vesículas extracelulares. Es importante indicar que, a día de hoy este tipo de terapias presentan muchas desventajas y su aplicación clínica sigue siendo un tema controvertido.

Por esta razón, el objetivo de esta tesis ha sido caracterizar y evaluar el efecto de las terapias celulares basadas en la administración de MSCs y de sus vesículas extracelulares sobre modelos animales. Para la evaluación de ambas terapias se utilizaron tres condiciones patológicas/fisiológicas, cuya aplicación clínica aún no se ha desarrollado

Así, los modelos animales de hernia abdominal, infarto de miocardio y estudios de fecundación *in vitro* nos han permitido dilucidar si estas opciones terapéuticas avanzadas pueden ser útiles para prevenir y tratar enfermedades humanas, mejorando y prolongando la calidad de vida.

# ABSTRACT

Stem cell therapies have represented one of the brightest promises in the biomedical science in the last twenty years. Mesenchymal stem cells (MSCs) have been broadly studied and their extensive use in and regenerative medicine can be attributed to their differentiation ability, multipotentiality, and paracrine potential. Despite this, stem cell therapies have some limitations, safety concerns and, depending on cell type, even some ethical issues. Because of that, researchers have focused their attention on cell-free therapies that present all the advantages related to stem cells, but avoid most of the hypothetical risks. One of these cell-free therapies involves extracellular vesicles (EVs) secreted by MSCs which are responsible of most of their paracrine activity.

Currently, cell-based therapies are undergoing numerous preclinical and clinical trials, having, some of them, already been approved as advanced therapies by the European Medical Agency and by the American Food and Drug administration. In contrast, very little ongoing clinical trials are testing the clinical use of cell-free therapies based on extracellular vesicles. Both therapies still present some disadvantages and their clinical application is still a controversial issue.

For this reason, the aim of this thesis was the characterization and evaluation of cell- and cell-free therapies, based on MSCs and EVs, respectively, in animal models. Three pathological/physiological conditions, whose resolutive clinical approach has not been defined yet, will be used for the evaluation of these cell- and cell-free therapies.

Hence, animal models of abdominal hernia, myocardial infarction and *in vitro* fecundation studies allowed us to elucidate if these advanced therapeutic options may be useful to prevent and treat human diseases, improving and prolonging quality of life.

# GRAPHICAL ABSTRACT

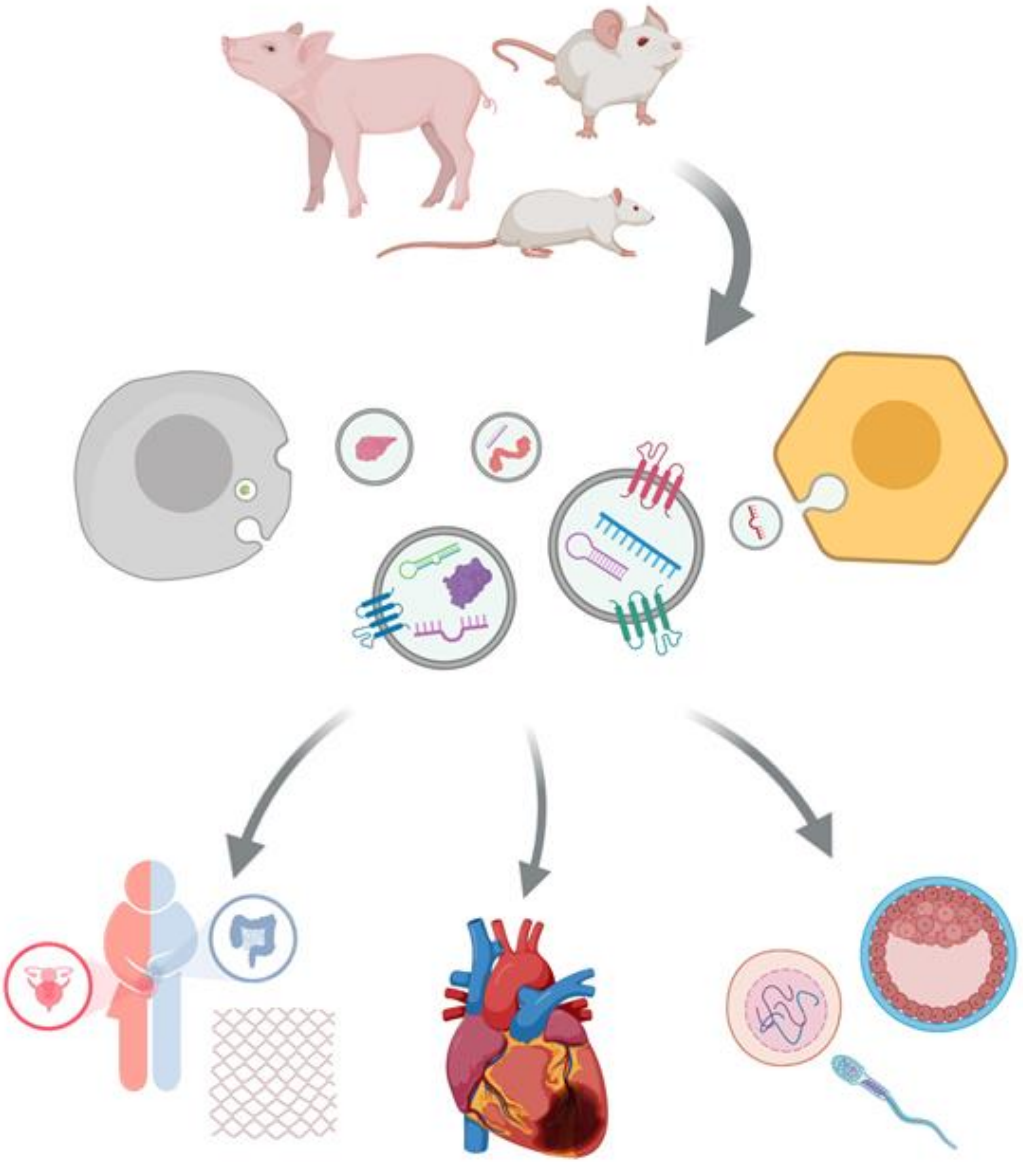

# INTRODUCTION

## STEM CELLS

Stem cells are unspecialised cells found in any multicellular organism in the animal and plant kingdoms (1). In 1868, the German biologists Ernst Haeckel hypothesised the existence of an ancestor unicellular organism that gave rise to all multicellular organisms according to Darwin's theory of evolution. This ideal ancestor was called “stem cell”. Afterwards, in 1877, Ernst Haeckel used the term “stem cell” to describe also the fertilised egg giving rise to all the cells of the living creatures. At the end of 19$^{th}$ century, in the light of the theories of August Weismann, Theodor Boveri and Valentin Häcker, the term “stem cell” started to be used to refer to what are nowadays called “primordial germ cells” (2). After that, more theories and more investigation led to the first evidence of the existence of a common hematopoietic stem cell by James Till and Ernest McCulloch in 1961. The first isolation of embryonic stem cells from murine embryos by Martin Evans and Matthew Kaufman in 1981 (3) and from human embryos by James Thomson in 1998 (4), started the stem cell era, where mammalian stem cells have been, and are being, thoroughly studied.

### GENERAL CHARACTERISTICS OF STEM CELLS

#### SELF-MAINTENANCE AND SELF-RENEWAL, DIFFERENTIATION, AND QUIESCENCE

Stem cells are represented by fixed and representative characteristics. **Self-maintenance** is the ability of stem cells to maintain their own number. **Self-renewal**, on the other hand, is the ability of maintaining multipotency and tissue regeneration potential during multiple proliferation cycles. Stem cells have a long term self-renew ability that is preserved throughout the lifetime of the animal. Frequency and timing of self-renewal divisions of stem cells are strictly regulated by different mechanisms. This fine regulation controls the proliferative potential of stem cells, preventing tissue atrophy, premature ageing, abnormal tissue development, and cancer (5,6). Stem cell proliferation can occur through symmetric or asymmetric cell divisions. Symmetric divisions can be self-renewing or differentiative. Self-renewing divisions are aimed to expand the stem pool, while symmetric differentiating divisions generate two differentiated progenies. In contrast, asymmetric cell divisions

generate one self-renewing and one differentiated progeny in a single division (7,8). Stem cell fate toward a symmetric or an asymmetric division can be induced by signalling molecules from stem cell niche or distant tissues, or from intrinsic determinants, as cytoskeleton polarization (9).

**Differentiation** is the ability of stem cells to switch to more specialised cells, losing some of their developmental potential (5). Cell differentiation can be induced by soluble factors (i.e., growth factors and cytokines) present in stem cell microenvironment, by cell-cell and cell-extracellular matrix contacts, and physical forces. Stem cells do not differentiate towards a random specialised cell type: their fate is strictly dependent on tissue-specific ligand and receptor expression and on a variety of autocrine and paracrine signals that may reach the stem cell niche as long as they develop and adapt (10). Thanks to their proliferation and differentiation capacity, stem cells are directly involved in tissue regeneration in case of injury. Firstly, they proliferate to replenish the tissue, then they differentiate into progenitor cells. Subsequently, progenitor cells differentiate into lineage-specific and functionally mature cell types, restoring the damaged tissue (11). The capacity of stem cells to differentiate to restore the injured tissue of course depends on their lineage commitment, which, in turn, depends on their developmental potency (12).

**Quiescence** is a reversible stop of cell cycle leading to the absence of cell proliferation. Within uninjured tissues, stem cells that remain in a quiescent and undifferentiated state until they receive activation stimuli from the stem cell niche. Subsequently, they re-enter the cell cycle and resume proliferation (5,11).

### DEVELOPMENTAL POTENCY OF STEM CELLS

In the process of fertilization, after sperm entrance in the oocyte, the very first embryonic diploid cell, the zygote, is formed. The mouse zygote cleaves into blastomeres of equal developmental potency for no more than three cell divisions, reaching the 8-16-cell embryo stage. The zygote and these early blastomeres are **totipotent stem cells**, that can give rise to any embryonic or extraembryonic tissue (13). When early blastomeres start to fuse forming a morula (E2.5), they enter the first differentiation event, where the blastomeres residing in the external surface of the morula commit to the trophectoderm lineage, while the blastomeres residing in the centre of the morula commit to the inner cellular mass lineage. When four days have passed since oocyte fertilization, the embryo is at the blastocyst stage and rolls into the uterine cavity. The inner cell mass and the trophectoderm cells start to be physically divided by a fluid-filled cavity called blastocoel (14,15). Before hatching from the zona pellucida, hence before implantation, a second differentiation event occurs: the inner

cellular mass (expressing *Nanog and Gata*6 mRNA) differentiates into epiblast (expressing *Nanog*) and primitive endoderm (expressing *Gata6*). Initially (E3.25), epiblast and primitive endoderm have a random spatial distribution into the inner cell mass. In the late blastocyst (E4.5) *Nanog* positive cells remain in the internal core of the inner cell mass, while *Gata6* positive cells move to the borders, separating the epiblast from the blastocoel (16). At this stage, trophectoderm and primitive endoderm cells commit to form extraembryonic tissues, being this process essential for implantation. On the other side, the epiblast cells remain undifferentiated and are **pluripotent stem cells** (17)**,** with an unlimited differentiation capacity towards all the embryonic tissues of the organism. From E6.5 to E8.5, the primitive streak, the site of migration of the pluripotent cells, is formed in the middle of the epiblast. In this process, called gastrulation, the pluripotent epiblast cells undergo another differentiation process towards the ectodermal, mesodermal, and endodermal cell layers (18). Cells from the three germ layers are **multipotent stem cells**, with the potential of differentiating into specific cell lineages depending on the layer of origin. Organogenesis is led by these multipotent stem cells (Figure 1). After birth, adult stem cells can be found in almost all parts of the body. Their function is to allow healing, growth, and replacement of senescent or damaged cells. Among the big adult stem cell population, multipotent, **oligopotent**, and **unipotent stem cells** can be found, with an increasingly lower range of differentiation options (15). Even though pluripotent stem cell presence within adult tissues has been reported, it is likely that they are isolation or culture artefacts (19).

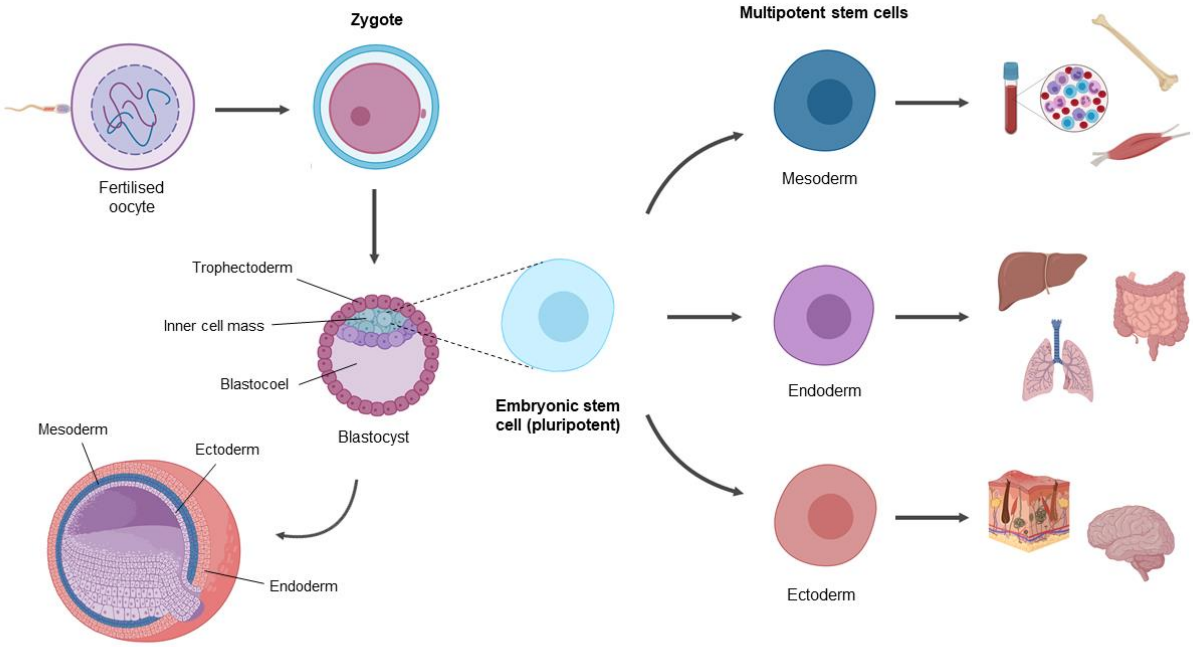


**Figure 1. Multipotent stem cell formation from the fertilised oocyte.** The pluripotent embryonic stem cells from the inner cell mass differentiate towards multipotent mesodermal, ectodermal, or endodermal stem cells during gastrulation. These multipotent cells further differentiate and create specialised organs. Figure created with Biorender (https://biorender.com/).

## STEM CELL CLASSIFICATION ACCORDING TO THEIR ORIGIN

### PLURIPOTENT STEM CELLS

Pluripotent stem cells are characterised by unlimited self-renewal and differentiation capacity. To be defined "pluripotent", stem cells have to: I) rise from a pluripotent cell population; II) be immortal; III) propagate indefinitely in the undifferentiated state; VI) be clonally derived, but capable of differentiating into the three germ layers; V) form teratomas *in vivo*; VI) maintain of a normal karyotype *in vitro* (20,21).

**Embryonic stem cells** (ESCs) derive and can be isolated from the inner cell mass of pre-implantation blastocysts. They can be expanded rapidly *in vitro* and cultured as immortal cell lines. Additionally, they show a high differentiation capacity, being able to differentiate into all embryonic cell types.

Their properties are regulated by various transcription factors, as Kruppel-Like Factor 4 (*KLF4*), Myc Proto-Oncogene (*MYC*), Nanog Homeobox (*NANOG*), Octamer binding transcription factor (OCT) 3/4, and SRY (Sex Determining Region Y)-Box 2 (*SOX2*). ESCs use for cell therapy is strongly discouraged since they also show a high oncogenic potential and trigger immune rejection. Additionally, they are not free of ethical concerns (20,22–24).

In 2006, the group of Yamanaka discovered that differentiated somatic cells, transfected with the transcription factors *Oct3/4*, *Sox2*, *Klf4* and *c-Myc*, could be reprogrammed to pluripotent cells, called i**nduced pluripotent stem cells** (iPSCs) (13,22,24). This reprogramming method has been further improved by downregulating genes promoting genome stability, as *p53*. iPSC technology avoids ethical implications and can generate patient-specific pluripotent stem cells. Nevertheless, the high risk of single mutations, insertions and changes in the epigenetic signatures in non-genetic and genetic regions, at the moment, limits their therapeutic use (15,20,25).

### Adult stem cells

After birth, tissue repair is guaranteed by a variety of adult stem cells (26). Compared to ESCs, they are more difficult to isolate and expand *in vitro*, and their recovery often involves invasive interventions. Additionally, depending on the site where adult stem cells are, their proliferation can be more or less efficient. Consequently, it is more likely to retrieve an abundant number of adult stem cells from bone marrow than from pancreas. Regarding their potency, unipotent (e.g. satellite and epidermal stem cells) (27); oligopotent (corneal and limbal stem cells) (28); and multipotent adult stem cells (neuronal, haematopoietic, and mesenchymal stem cells) (23,26) can be found in the adult body. Regardless of their differentiation potential, adult stem cells are a valuable source of self-renewing cells for regenerative medicine purposes and they can be used in autologous and allogenic therapies, without the risk of immune rejection (20,25).

## Mesenchymal Stem/Stromal Cells

Mesenchymal stem/stromal cells (MSCs) are a type of cell culture with immunomodulatory and regenerative properties (29). They are fibroblast-like cells (30) that can be isolated from perinatal tissues (umbilical cord, cord blood, placenta, and amniotic fluid) and adult tissues (bone marrow, adipose tissue, synovial fluid, and periosteum). MSCs can differentiate towards the osteogenic,

chondrogenic, and adipogenic lineages, but also towards connective tissue, smooth muscle, and haematopoietic stroma, being so defined as “multipotent”. Their multipotentiality is increased under certain culture conditions, that can induce MSC differentiation towards cardiac, lung, endothelial cells, and astrocytes, among other cell types (22,31,32). The acronym “MSC” has generated confusion over time, being sometimes indiscriminately associated to the terms “mesenchymal stem cells”, “multipotent stromal cells” (33), or “medicinal secretory cells” (34). Discrepancies and overlapping hallmarks between these three terms have been thoroughly described by Paolo Bianco in 2014 (33) and by Arnold Caplan in 2017 (34). To avoid misunderstandings, the International Society for Cellular Therapy (ISCT) in 2006 published the Minimal Criteria for defining multipotent mesenchymal stromal cells (35). This position statement defined that any cell culture deriving from bone marrow or other tissues could be labelled as “multipotent mesenchymal stromal cells” only accomplishing three criteria: I) adherence to plastic; II) expression of the specific surface antigens CD105, CD73 and CD90, and lack of expression of CD45, CD34, CD14 or CD11b, CD79a or CD19 and HLA-DR; III) multipotent differentiation potential towards osteoblasts, adipocytes and chondroblasts (35). Furthermore, without contradicting ISCT guidelines, authors have also described MSCs as fibroblastoid/cuboidal cells forming colonies, expressing additional surface markers, as CD44, CD49, CD51, CD62, CD117, CD166, CD271, and Stro-1, and not expressing glycophorin A, CD11a, and CD31. While adherence to plastic and colony formation can be easily assessed though inverted microscopy, the expression of surface antigens requires flow cytometry analysis. On the other hand, MSC differentiation potential needs to be demonstrate through the use of *in vitro* differentiation media and specific staining (Alcian blue for chondroblasts, Alizarin Red or von Kossa staining for osteoblasts; Oil Red O for adipocytes) (22,31,33,35).

### Therapeutic use of MSCs

In the last decades, the regenerative and immunomodulatory potential of MSCs has been demonstrated on numerous occasions over time. MSCs were so proposed as a promising therapeutic approach for the treatment of autoimmune diseases, transplantations, and any disease causing an exacerbated inflammatory reaction. Hence, to assess the beneficial effects of local or systemic administration of MSCs, a multitude of *in vitro* and preclinical studies have been focused on the most disparate conditions, as acute myocardial infarction (36); autoimmune disorders (37); burns (38); cardiac diseases (39); cartilage repair (40); chronic lung allograft dysfunction (41); Crohn's disease (42), fracture repair (43); graft-versus-host disease (44); hernia (45); kidney transplantation (46); liver transplantation (47); lung diseases (48); multiple sclerosis and

amyotrophic lateral sclerosis (49); osteoarthritis (50); osteonecrosis (51); Parkinson disease (52); rheumatoid arthritis (53), small bowel transplantation (54); spine fusion (55); spinal cord injury (56); stroke (57); synovitis (58); systemic lupus erythematosus (59), temporomandibular joint disorders (60); and vascular diseases (61).

Nowadays, MSC-based therapies are object of various clinical trials [1] (62), having a wide range of applications in many different diseases (63–65). In the last year, MSCs have also been proposed as potential therapy to counteract acute lung injury and to inhibit the cell-mediated inflammatory response in Coronavirus Disease 19 (COVID-19). To date (the 25th of April, 2021), seven registered clinical trials have been completed and involved MSCs of umbilical chord (ClinicalTrials.gov Identifiers: NCT04288102, NCT04573270, NCT04355728), adipose (NCT04522986), embryonic and induced pluripotent (NCT04535856), bone marrow (NCT04492501), and unspecified (NCT04713878) origin. Among the active or recruiting trials, the most proposed MSCs are autogenic (NCT04428801) or allogenic adipose (NCT04366323) and from umbilical cord (NCT04273646, NCT04457609), even though also dental pulp MSCs (NCT04302519), allogenic pooled olfactory mucosa-derived MSCs (NCT04382547), placenta-derived MSCs (NCT04461925), iPSC) and mesenchymoangioblast-derived MSCs have been proposed (NCT04537351). The administration route, when mentioned, is usually intravenous. Unfortunately, no results from the completed clinical trials have been reported yet, however the outcomes of some small trials have already been published (66–68). In general, the infusion of MSCs in COVID-19 patients resulted in less deaths than in placebo group, but the small sample sizes and various eligibility criteria make the interpretation of these results challenging.

Regarding the approved cell therapies, seven of them have currently been approved by the European Medical Agency (EMA)[2]. These advanced therapy medicinal products are aimed to treat cancer (B-cell lymphoma, acute lymphoblastic leukaemia, diffuse large B-cell lymphoma, high-risk blood cancer) and inflammatory or immune-related diseases (perianal fistulas in Crohn´s disease, cartilage

[1] https://stemcellsportal.com/stem-cells-translational-medicine-clinical-trials-portal

[2] https://www.ema.europa.eu/en/human-regulatory/marketing-authorisation/advanced-therapies/advanced-therapy-classification/summaries-scientific-recommendations-classification-advanced-therapy-medicinal-products

defects in the knee joint, adenosine deaminase severe combined immunodeficiency and severe limbal stem cell deficiency) (69). On the other side of the ocean, the American Food and Drug Administration (FDA) has approved fourteen advanced cell therapies [3], for the treatment of cancer (B-cell precursor acute lymphoblastic leukaemia, Incorporated B-cell lymphoma), inflammatory or immune-related diseases (full-thickness cartilage defects of the knee, wounds of the oral soft tissue defects, disorders affecting the hematopoietic system), and even for aesthetic purposes (severe nasolabial fold wrinkles in adults) (70). Cell therapies approved by EMA and FDA use autologous, allogeneic, or genetically engineered immune cells, adult somatic cells, or stem cells (haematopoietic cells or MSCs).

Regardless of the type, starting materials for cell therapy need to be characterized; manufacturing processes must be reproducible, consistent, and must include well-defined raw materials and methods under Good Manufacturing Practice (GMP). Additionally, appropriate characterization of cell products and quality control is necessary to guarantee safety or efficacy (71). Nevertheless, important risks may arise from the nature of the cells (tumorigenicity, immunogenicity), and others from the cell-implantation procedure (72). This makes the approval of cell-based advanced therapies tough and the number of currently approved cell-based advanced therapies incredibly smaller than the number of launched preclinical and clinical trials.

### Therapeutic properties of MSCs

In addition to differentiative and proliferative potential, aimed to support the tissues *in vivo*, MSCs can interact with a wide range of immune cells. In the past their efficacy as alternative therapy relied on their presumed trans-differentiation capacity. However, many *in vitro* and *in vivo* studies and, more recently, preclinical and clinical trials, have reported that the immunomodulatory and regenerative properties of MSCs, exerted in a paracrine fashion, are the key for the treatment of many diseases (31,33,73). This paracrine effect derives from the so-called “secretome”, that refers to all the soluble factors and extracellular vesicles that are secreted by MSCs (74). Nevertheless, the molecular and cellular mechanisms supporting the immunomodulatory potential of MSCs, as well as their effect on the immune system after their administration are still under investigation (75).

[3] https://www.fda.gov/vaccines-blood-biologics/cellular-gene-therapy-products/approved-cellular-and-gene-therapy-products

*In vivo*, MSCs immunoregulatory responses depend on the local conditions of the environment in which they reside (73,76). *In vitro*, MSCs harvested from different tissues and under different culture conditions show dissimilar phenotypes and have a unique cytokine secretion signature (75). Even though a plethora of inconsistent results can be found in the literature, a general profile of MSC potential can be portrayed.

### Effect of MSCs on the immune system

MSCs have been demonstrated to effectively modulate adaptive immune system (by acting on T lymphocytes and B lymphocytes) and innate immune system (by acting on natural killer cells, dendritic cells, monocytes, macrophages, and neutrophils) (73,77).

MSCs immunomodulatory effect on immune cells has been mostly attributed to soluble factors secretion, however new pieces of evidence are suggesting that also cell-cell interactions play an important role in MSC-mediated immunomodulation.

MSCs interact with immune cell types through the secretion of anti-inflammatory and pro-inflammatory factors. Among the factors secreted by MSCs, there are cytokines, chemokines and prostaglandins. To cite some examples, Transforming Growth Factor Beta (TGFB) and Interleukin 6 (IL6) are involved in the direct induction of regulatory T cells, regulatory macrophages, and regulatory B cells, enhancing their immunosuppressive effects. Interleukin 8 (IL8), Chemokine (C-C Motif) Ligand (CCL) 2 and CCL8 are chemokines secreted by MSCs to attract immune cells. In particular, IL8 is a neutrophil chemo-attractant chemokine, while CCL2 attracts monocytes. Chemokine secretion is aimed, in some cases, to attract reactive immune cells to enhance, for instance, their immunosuppressive actions. In other cases, MSCs use chemokines to attract immune activated cells and keeping them at a distance that is close enough to inhibit their function (73,76). Prostaglandin E2 (PGE2) is used by MSCs to reprogramme macrophages into anti-inflammatory cells and to shift T Helper cell (Th) responses from type 1/type 17 responses to type 2 responses (73,76).

Regarding cell-cell interaction between MSCs and immune cells, it occurs through surface proteins, as the co-stimulatory CD40; the co-inhibitory programmed death ligand 1 (PDL1) and Fas ligand (FasL); and some adhesion molecules, like Intercellular Adhesion Molecule 1 (ICAM1) and Vascular Cell Adhesion Molecule 1 (VCAM1), that are expressed by MSCs to interact with activated immune cells (73,76).

MSCs are also involved in the control of metabolic pathways. To cite some examples, the enzyme indoleamine 2,3-dioxygenase (IDO) is used by human MSCs to metabolise L-tryptophan to L-kynurenine. When L-tryptophan is depleted from the milieu and high levels of L-kynurenine can be detected, lymphocyte proliferation is suppressed. Moreover, MSCs constitutively express ecto-5′-nucleotidase (CD73) that acts with CD39 on regulatory T cells to catabolize ATP to adenosine. In this way, the immune-activating effect of ATP is replaced by the immune-inhibiting effect of adenosine (73,76).

### *Effect of mesenchymal stem cells on T Lymphocytes*

MSCs can modulate adaptive immune system by acting on T cell activation, proliferation, and differentiation. During immune responses, an antigen is presented on the surface of an antigen-presenting cell, in the context of a major histocompatibility complex (MHC) molecule. This complex is recognised by the T cell receptor and, at the same time, CD28 on the T cell interacts with CD80 or CD86 on the antigen-presenting cell. These co-stimulatory signals, summed together, adequately activate T lymphocytes and, subsequently, induce their proliferation (77).

In this framework, MSCs have been reported to suppress both naïve and memory T lymphocyte activation and proliferation. MSCs directly produce soluble factors or trigger other cells to release factors aimed to inhibit T lymphocyte activity. Among these factors, there are TGF-β, hepatocyte growth factor (HGF), PGE2, IDO, human leukocyte antigen G (HLA-G) protein, IL10, galectins, and PD-L1, among others (32).

MSCs effect on T cell activation has been demonstrated by the fact that, during their activation, T lymphocytes express and secrete molecules like CD38, CD25, CD69, IL-2, HLA-DR, Cytotoxic T-Lymphocyte Associated Protein 4 (CTLA4), IFNγ, and TNFα. By using T cells activators like phytohemagglutinin, anti-CD3/CD28 or antibodies in presence of MSCs, it was demonstrated that the expression of the early activation markers CD25, CD69, and CD38 and IFNγ were decreased in CD4+ and CD8+ T cell, populations (77).

Regarding T lymphocyte proliferation (CD4+ and CD8+ subsets), MSCs have been demonstrated a suppressive activity in a dose-dependent manner (77–80). The inhibitory activity of MSCs towards the proliferation of CD4+ and CD8+ T cells seems to be mediated by Galectin 1. Moreover, T lymphocyte apoptosis was reported to be induced by MSCs via the secretion of PD-L1 (75).

MSCs interfere also with T cells differentiation, regulating the balance of inflammatory T lymphocyte sub-populations and their production of cytokines. After T cells clonal expansion, helper T cells CD4+

(Th0) can differentiate into Th1, Th2, Th17, or regulatory T cell (Tregs) population. Then, depending on the T-cell microenvironment, each population secrete some cytokines to carry out their intrinsic function in the inflammation milieu (77). MSCs have been demonstrated to drive naïve T cells (CD45RA+) differentiation towards Th1 or Th2 lineage. Indeed, MSCs can inhibit IFNγ secretion by Th1 cells and stimulating Interleukin 4 (IL4) secretion by Th2 cells via IDO secretion. A shift from Th1 to Th2 cells, so from the pro-inflammatory to the anti-inflammatory phenotype, respectively, was shown to be induced by MSCs, altering the secreted cytokine secretion, as well (75,77). Also naïve CD4+ lymphocyte differentiation towards Th17 can be prevented by MSCs, that inhibit the production of the pro-inflammatory cytokines Interleukin 17 (IL17), Interleukin 22 (IL22), IFNγ, and TNFα (77).

Last but not least, MSCs have an active role in formation and maintenance of distinct Tregs populations, involved in autoimmunity prevention. It has been widely demonstrated that allogeneic MSCs promote an increase in CD4+CD25+CTLA-4+ Foxp3+ Tregs populations from CD4+ or CD8+ cells, CD3+, CD3+CD45RO+, or CD3+CD45RA+ T lymphocyte populations (33,77). The induction of CD4+CD25+FoxP3+ Tregs was shown to be a key process for tolerance induction in a kidney allograft transplantation model (75).

In addition, clinical studies demonstrated an increase of CD4+CD25+Foxp3+ and Treg1 populations and a decrease of Th17+ induced by MSCs in patients with Graft-Versus-Host Disease (GvHD) and systemic lupus erythematous (33,77).

#### *Effect of mesenchymal stem cells on B Lymphocytes*

B lymphocytes, belonging to the adaptive immune response, are responsible for humoral immunity. When stimulated by antigens, they produce and secrete antibodies and, in addition, they are involved in antigen presentation and cytokine production (77,81). Different studies have demonstrated that MSCs can trigger a suppression of B cell proliferation, the inhibition of plasma cell differentiation, as well as immunoglobulin (Ig) production and regulatory B cells proliferation. This inhibitory effect can be directly exerted by MSCs via soluble factors and cell–cell contact, or through the intermediation of other immune cells, such as T cells.
First, MSCs revealed a suppressive activity on B lymphocyte proliferation, which seemed to be more effective after IFNγ or TNFα pre-conditioning and mediated by T-cells and Galectin 9 (77,81). On one hand, the inhibition of B lymphocyte differentiation was reported and attributed to the secretion of IL1-RA by MSCs or IFNγ by T cells and, in T-cell absence, by IFNγ-preconditioned cells (75). On the other hand, MSCs have been demonstrated to enhance the differentiation of B cells towards IL10-producing regulatory B cells, involved in immunological tolerance. This stimulatory

effect seems to be dependent on cell-cell contact and to induce an indirect T cell-immunomodulation by converting effector CD4+ T cells into Foxp3+ Tregs (75).
MSCs were demonstrated to trigger alterations in the chemotactic properties of B cells by downregulating the chemokine receptors C-X-C Chemokine Receptor Type 4 (CXCR4), C-X-C Chemokine Receptor Type 5 (CXCR5), and C-C Chemokine Receptor Type 7 (CCR7) and immunoglobulins IgM, IgG, and IgA (77,81).
Despite most of the studies indicate an inhibitory effect of MSCs on B lymphocytes, contradictory results suggest that further clarifying studies are required (81).

### *Effect of mesenchymal stem cells on Monocytes*

Monocytes are precursors for macrophages and dendritic cells *in vitro* and can be divided into different subsets based on CD14 and CD16 expression. Bone Marrow Mesenchymal Stem/Stromal Cells (BM-MSCs), promote the recruitment of monocytes and macrophages into inflamed tissues to support wound repair through chemokine ligands CCL2, CCL3, and CCL12 secretion. Moreover, MSCs secrete HGF in order to act on peripheral blood derived CD14+ monocytes, thus modulating T cell function and to induce splenic CD14+ monocytes expansion before becoming adherent macrophages (82). HGF and IL6 production of MSCs induce the formation of IL10-secreting anti-inflammatory monocytes, with decreased TNFα, IL12p70, and IL17 expression. IL10-producting monocytes are characterized by high levels of CD11b, CD45R, and MHC II and can inhibit the activity of T lymphocytes and preventing monocyte differentiation into dendritic cells (75).

### *Effect of mesenchymal stem cells on Macrophages*

Macrophages are involved in phagocytise apoptotic cells and pathogens and interact with activated T and B lymphocytes in the development of acquired immunity. Likewise, they produce immune effector molecules, contributing to host protection and to the pathogenesis of inflammatory and degenerative diseases (83–85). Macrophage differentiation from monocytes can generate two different phenotypes. On one side, the pro-inflammatory classically activated M1 macrophages, with antimicrobial activity and secreting IFNγ and TNFα. On the other side, the anti-inflammatory alternatively-activated M2 macrophages, with important roles in tissue regeneration and secreting high levels of IL10 and TGFβ1 and low levels of IL1, IL6, IFNγ and TNFα (82–84,86).

In the presence of a pro-inflammatory environment, MSCs contribute to maintain tissue homeostasis and to reduce inflammation by inducing either the direct differentiation of monocytes towards M2 macrophages or triggering the switch between M1 and M2 macrophages (82,86,87). Monocyte differentiation towards M2 macrophages can be regulated by cell-cell contact or PGE2, IDO, IL6, or

IL10 release by MSCs (82,86,87). MSCs can also trigger macrophage polarisation from M1 to M2 phenotype through PGE2, IL6, IL1 receptor antagonist (IL1RA), and granulocyte macrophage-colony stimulating factor (GM-CSF) (88).

Macrophages co-cultured with MSCs showed a CD206+ immunophenotype, producing high levels of the anti-inflammatory IL10 and IL6, and a higher level of phagocytic activity. Low levels of the pro-inflammatory IL12 and TNFα were also reported (89,90). These MSC-induced macrophages also demonstrated an increased proliferation and migration ability (91), showing a potential significant role in tissue repair.

MSC action on macrophages can further be aided by activated T cells. The latter, secreting pro-inflammatory cytokines, as IFNγ and TNFα, triggers COX2 and IDO production by MSCs, hence inducing macrophage polarisation. M2 macrophage polarization by MSCs has been coupled with FoxP3+ Tregs induction from CD4+ T cells. In short, it has been demonstrated that Tregs induction was due to the constitutive secretion of TGFB1 by MSCs, along with CCL18 produced by M2 polarized macrophages (82,86).

#### *Effect of mesenchymal stem cells on Dendritic Cells*

Dendritic cells are antigen presenting cells also involved in self-tolerance (32,77,92). Dendritic cells differentiate from BM-CD34+ cells *in vivo* and from monocytes *in vitro*. It has been reported that MSCs can interfere with dendritic cell differentiation, maturation, and function (31). MSCs can inhibit monocyte differentiation into dendritic cells through the secretion of factors like PGE2. As a result, CD1a, CD40, CD80, CD86, and MHC expression in dendritic cells is reduced (32,77). Furthermore, monocytes exposed to maturation factors, such as TNFα or lipopolysaccharide, and in presence of MSCs, differentiate into immature dendritic cells with lower levels of CD83, CD80, and CD86 (93) and incapable of activating T cells (77). Instead, mature dendritic cells co-cultured with MSCs result to be pushed toward an immature state, with reduced expression of HLA-DR, CD1a, CD80, and CD86 and altered TNFα, IL10 and IL12 secretion (75,77,94).

#### *Effect of mesenchymal stem cells on Natural killer (NK) cells*

NK cells are effectors of innate immunity that act against cancer, infections and MHC class I negative cells. NK cytotoxic potential, can be either spontaneous or antibody-dependent (31). MSCs express low levels of MHC class I and present activator ligands for NKs on their surface, being so potentially susceptible to be killed by NK cells. If some authors have stated that MSCs are completely vulnerable to NK-mediated killing, other authors have evidenced MSC resistance (77). Various

theories have been proposed, but it seems that the balance between NK activating and inhibitory signals and protecting factors released by other immune cells may diminish NK cytotoxicity and protecting MSC from being killed by NKs (95). For instance, IFNγ-primed MSCs are protected by NK cytotoxicity via MHC I up-regulation (32).

Nonetheless, MSCs have been shown to change NK cell phenotype and to inhibit their proliferation, cytotoxic potential, and cytokine secretion through mediators like IDO, PGE2, IL6, TGF-β1, and nitric oxide (31,32,75,77).

#### *Effect of mesenchymal stem cells on Neutrophils, complement, and mast cells*

MSCs immunomodulatory effect is exerted also by recruiting neutrophils, promoting their survival, and enhancing their phagocytic and burst activity. This activity is mediated by the secretion by MSCs of cytokines and chemokines as IL6, IL8, GM-CSF, Macrophage Migration Inhibitory Factor (MIF), and IFNγ in response to inflammatory stimuli (82).

Regarding complement system, the components C3a and C5a were demonstrated to act as chemotactic agents to lead MSCs towards the site of inflammation and then to induce MSCs proliferation, while inhibiting apoptosis (82). MSCs, in turn, are thought to induce complement activation through all three complement pathways (classical, lectin or alternative), but an inhibiting role has also been investigated (82). On one side, MSCs partially protect themselves from complement activation through the surface inhibitory proteins CD46, CD55, and CD59 (82). On the other hand, MSCs, especially in presence of TNFα and IFNγ, inhibit complement activation by producing factor H (96).

Mast cells are part of innate immunity involved in allergic inflammation and autoimmunity. MSCs from bone marrow can interact with histamine, produced by mast cells, through specific receptors. As a result, MSCs produce IL6, that, in turn, prevents neutrophils apoptosis and increase superoxide production in phagocytic cells (82).

### Effect of MSCs on tissue repair

Besides their effect on immune system, MSCs are also involved in tissue regeneration. MSCs exert their effect on regenerative processes through paracrine signalling involving not only growth factors and cytokines, but also extracellular matrix components, extracellular vesicles, and organelles (97). It has been demonstrated that chemoattractant gradients attract MSCs towards injury sites. After migration, MSCs overexpress intercellular adhesion molecules and engraft in the damaged tissue,

modulating the activity of the cells residing in the microenvironment they encounter via paracrine communication (98). Among the tissue regeneration processes influenced by MSCs, cell migration, proliferation, differentiation, angiogenesis, and extracellular matrix formation have been proposed (99).

Tissue regeneration is induced by MSCs primarily through secretion of trophic factors that promote cell survival. Among these growth factors, HGF, epithelial growth factor (EGF), nerve growth factor (NGF), stromal derived factor-1 (SDF1), tissue angiogenesis vascular endothelial growth factor (VEGF), transforming growth factor-alpha (TGFα), and insulin-like growth factor (IGF1), can be mentioned (98).

Although cytokine secretion by MSCs is especially related to their immunomodulatory capacity, it has also been related to tissue regeneration. For instance, MSCs were associated to a reduction fibrotic injury through IL6 secretion leading to STAT3 inactivation in renal tubulointerstitial fibrosis and acute kidney injury model (98). MSCs were also considered to be accountable for inducing the restoration of the stem cell pool in damaged intestinal crypt by secreting IL11 (97). In contrast, secretion of immunosuppression mediators like PGE2, COX2, and IDO by MSCs counteract tissue impairment caused by exacerbate effect production of proinflammatory cytokines in the injured area (97).

MSCs were also shown to secrete microRNAs (miRNAs) with the capacity of regulating the platelet-derived growth factor (PDGF), WNT, and TGFβ signalling pathways, preventing the depletion of the stem cell pool in damaged tissues. Moreover, some miRNAs were demonstrated to reduce fibrosis and formation of myofibroblasts (97).

### Drawbacks of MSC-based therapies

MSCs have been, and still are, considered “off-the-shelf” products. They are low immunogenic and are considered “immune privileged”, expressing low levels of surface HLA-I, no HLA-II, and no costimulatory molecules CD40, CD80, and CD86, under standard culture conditions (100). The transcriptional and synthesis levels of these markers were demonstrated to be increased by inflammatory stimuli, such as IFNγ. Nonetheless, it was also reported that surface HLA-I undergoes a clathrin-independent dynamin-dependent endocytosis, so reducing the potential MSC immunogenicity (100). Moreover, MSC-based therapies showed, in most cases, no tumorigenic and teratogenic potential and no serious adverse effects in the short term (101). Notwithstanding, MSC-based therapies have shown in several instances lack of efficacy, immunogenicity, and side effects.

Allogenic MSCs were reported to induce immune cell responses and being targets of the immune system, triggering a mechanism of rejection. *In vitro* and *in vivo* assays showed allogenic MSCs lysis by CD8+ T cells, by activated Natural Killer (NK) cells, or the induction of antibody responses (33,73,76). Additionally, MSC-based therapies have often been considered responsible of various side effects, such as fibrosis of the interstitial renal tissue, atrophy of the renal tubules, thrombus formation, pulmonary embolism (101), bacterial, viral, and fungal infections, interstitial pneumonia, and arrhythmia (102). Additionally, animal models revealed that MSCs may promote tumour growth and metastasis. The factors affecting potential tumorigenesis may be related to the MSC donor (age), the host (immunosuppression) or the MSC themselves (culture conditions, dose, cell heterogeneity), but a clear comprehension is still missing (101).

It is worth mentioning that the findings on MSC regenerative potential thrilled researchers from the moment they were discovered. This enthusiasm resulted in thousands of registered clinical trials, but very few cell therapies have been approved by the relevant authorities. Unfortunately, scientists have exaggerated MSC real potential over time, and some physicians and mass media exploited it for their own economic interests. As a consequence, many unproven stem cell interventions have been performed on human patients without the appropriate validation and authorisation by the authorities (103). In other cases, the authors of unproven cell therapies were able to trick the authorities, as in the famous Italian case called “Stamina method” (104). Luckily, it seems that this “method”, based on bone marrow-derived MSCs, did not produce any adverse effect on the recruited patients, nearly all children with degenerative diseases, but no improvements were recorded (105). In worse cases, unvalidated cell therapies led to a variety of adverse effects, as infections, brain and spinal cord lesions, severe vision loss, pulmonary embolism, cardiac arrest, and death (103).

It is true that, from a technical perspective, obtaining safe and effective MSC-based therapies is still challenging. The first obstacle researchers must overcome is getting enough cells. However, long-term *in vitro* cultures of MSCs can cause a decrease in telomerase activity and induce morphological changes, genetic instability and chromosomal aberrations that may lead to malignant transformation (101). The second obstacle is finding the most appropriate administration route for MSCs. The systemic intravenous (IV) infusion is the most used and feasible cell administration in experimental and clinical trials. Nevertheless, most of the infused cells remain trapped in the lungs without reaching the area of injury (106) and show low engraftment and short viability (107). This happens with other systemic administration routes, as well, such as the intraperitoneal (108), and the intra-arterial (109). Hence, topical administration routes have been proposed, as the intraventricular (109), intracoronary, transendocardial, intramyocardial (110), intrapericardial (111),

intracranial, intracerebral, and subcutaneous (108). Unfortunately, more biodistribution and tracking studies are required to clarify which is the best delivery method depending on the condition that needs to be treated. For the above-mentioned issues and taking into consideration that MSCs therapeutic potential resides in the paracrine mediators they release, extracellular vesicle-based therapies are now in the cross hairs.

# EXTRACELLULAR VESICLES

It has been widely demonstrated that MSCs exert their therapeutic potential through the paracrine secretion of growth factors, chemokines, and cytokines, among other proteins, as well as mRNAs, and miRNAs (112). It is likely that these factors are almost exclusively carried by extracellular vesicles (EVs) released by MSCs as paracrine mediators. It has been shown by numerous studies that EVs from MSCs have a direct role in several events, such as immunomodulation processes, wound healing, apoptosis inhibition, and angiogenesis promotion, among others. These properties are exerted by the molecular cargo of EVs, that can strictly depend on the source cells (113).

## GENERAL CHARACTERISTICS OF EXTRACELLULAR VESICLES

Extracellular vesicles (EVs) are lipid bilayer-enclosed particles released by cells, in the extracellular space (114). According to their size, biogenesis, release, content, and function, EVs are grouped into three subtypes: exosomes, microvesicles and apoptotic bodies (115).

**Exosomes** (30–150 nm in diameter) form by multivesicular bodies arising, in turn, from early endosomes. As for microvesicles and apoptotic bodies, they are identified by the presence of the tetraspanin markers CD63, CD9 and CD81. Exosomes also present the specific markers Alix, TSG101, HSC70, and HSP90β (115).

**Microvesicles** (50-1000 nm) form by plasma membrane budding and cleavage. Besides having tetraspanins as common EV markers, microvesicles are also identified by the presence of annexin A1, annexin V, CD40, selectins, flotillin-2, and integrins (114).

**Apoptotic bodies** (50-5000 nm) are released by dying cells as blebs. Their markers are phosphatidylserine, histones, C3b, TSP, and annexin V (114). Apoptotic bodies are a mere result of cell disassembly, however, their role in paracrine signalling, is under investigation (116).

Under physiologic conditions or under stress, a variety of cells produce vesicles with an active cargo that depends on their cell source and on the microenvironment where they reside (117). It is known that EV cargo, so their function, substantially changes under different stimuli, as thermal and oxidative stress, hypoxia, serum starvation, acidic conditions, ultraviolet light, irradiation, inflammation, senescence, and cell death (113,114). Nucleic acids, sugars, lipids, lipid mediators,

and proteins, including cytokines, chemokines, lipid metabolism enzymes, and transmembrane proteins have been found to be enclosed in EVs. Packed EVs are then released in the extracellular space, where they act as short- and long-distance mediators of cell–cell communication. To exert their effect, they are recognised and bound by specific membrane receptors on the target cells, and EV cargo is directly delivered by internalization. Once the "message" has been delivered, a multitude of outcomes can be expected, ranging from the regulation of immune responses, to angiogenesis, lymphogenesis, cell maintenance, differentiation, migration, proliferation, and tumour progression (114,115).

## Isolation and characterisation of EVs

After their first discovery in 1981 (118), EVs have been successfully isolated from body fluids (115), cell culture-conditioned media, and dissociated tissues (114). For EV isolation, differential centrifugation, polymer-based precipitation, and techniques based on size exclusion, immunoaffinity capture, and microfluidics have been commonly used (113,115). Once isolated, particle size and concentration of EVs have been measured with different techniques, such as nanoparticle tracking analysis, electron microscopy, and dynamic light scattering. Finally, to characterise EV composition and content, various approaches, like flow cytometry, western blotting, and proteomics have been documented (115).

In order to standardise the big variability and complexity of future findings, the International Society for Extracellular Vesicles published a position statement on the "Minimal information for studies of extracellular vesicles" (MISEV) in 2014 (119), followed by an update in 2018 (120). According to the MISEV 2018, forthcoming studies involving EVs should be take into consideration that:

- "Extracellular vesicle" (EV) should be used to describe the lipid bilayer-enclosed particles without functional nucleus that are naturally released from cells. Information about their size, density, biochemical composition, and cell of origin should be specified;
- A complete description of cell culture and harvesting conditions, or of the biological fluid and its donor, plus information about the starting sample or the isolated EVs should be provided to allow reproducibility;
- EV separation (also called "purification" or "isolation") can be performed with all those techniques that guarantee a complete separation of all EVs from all the other components of the starting sample, or of one type of EVs from the other types; EV concentration

(sometimes called “enrichment”) can be performed with techniques that increase EV presence in a smaller volume of the starting sample, without requiring EV separation;

- Quantification of particle number, total protein, lipids, or RNA amount can be performed, but it is not representative of the total quantity of EVs in the sample;
- EV presence should be justified by identifying membrane proteins, as tetraspanins, MHC class I, and integrins, or cytosolic proteins with membrane-binding ability, as ALIX, or annexins;
- EV purity needs to be justified by quantifying lipoproteins and protein/nucleic acid aggregates in the sample;
- EV characterization should be performed with a combination of optical and biophysical/biochemical techniques;
- EV separation is required to perform functional tests, that should always be performed to demonstrate EV biological functions.

## CLINICAL APPLICATIONS

Research is particularly focused on the study of EVs as disease biomarkers, since their cargo is strongly influenced by the cells from which they are produced and released. Among the advantages of using EV cargo as biomarker, there is the fact that it is protected by a lipid bilayer and less prone to undergoing enzymatic and hydrolytic degradation. Additionally, EVs can be easily retrieved from body fluids, providing so a non-invasive diagnostic method in the clinical setting. Promising biomarkers have been found in EVs from various diseases, as acute kidney injury, glioblastoma, vascular damage, Parkinson’s disease, type II diabetes, ovarian, breast, pancreatic, and lung cancer (114,115).

Given that EVs carry a cargo that reflects their parent cells it has been evidenced several times that EVs released by MSCs may be used as a safer therapeutic alternative for MSC-based therapy. As a matter of facts, EVs-based therapies exclude most of the drawbacks related to MSCs, as immunological reactions, tumourigenicity, teratogenicity, and short half-life (114). For this reason, EVs from various cell types have been, and still are, under investigation to completely decipher their therapeutic potential. For instance, EVs from umbilical cord stem cells (114), neural stem cells, immune cells (121), amniotic epithelial cells (122,123), endothelial progenitor cells (124), MSCs (125), cardiomyocyte progenitor cells (125), and embryonic stem cells (126) produced numerous

effects, as tissue regeneration, reduction of apoptosis, fibrosis, inflammation, promotion of neovascularization, immunomodulation, suppression of hyperproliferative pathways, migration of endothelial cells, reduction of infarct size, recovery of cardiac functions, and maintenance of pluripotency (114,121–126). Hence, EVs have been proposed for the treatment of various diseases, such as myocardial infarction (114), ischemic stroke, atherosclerosis (121), liver and pulmonary fibrosis (122,123), ischemia-reperfusion injury (125), diabetes, tissue/organ damages, circulatory, kidney, and bone diseases (124), among others.

Moreover, different techniques as electroporation, co-incubation, sonication, permeabilization with saponin, freeze-thaw cycles, and extrusion are being used to create EV-based drug-delivery systems (113). EVs loaded with drugs, proteins, miRNAs, short hairpin RNA (shRNAs), and Short interfering RNA (siRNAs) are being explored as alternatives for liposomes and polymer-based synthetic nanoparticles for the treatment of inflammatory, genetic diseases, cancer (113), and COVID-19 (127). Other therapeutic strategies include the development of vaccines, including anticancer vaccines, with engineered or unmodified EVs, being known their involvement in antigen presentation (114,115).

Last but not least, strategies to block biogenesis, release, up-taking and target cell response are now being investigated where EVs may be responsible of diseases, as cancer (114).

At present, 222 clinical trials are listed in the official database of the U.S. National Library of Medicine[4] under the terms “extracellular vesicle” (83), “microvesicle” or “microparticle” (115), and “exosome” (83). Most of these clinical trials are focused on the use of EVs as biomarkers to detect or monitor certain diseases after a treatment; nevertheless, only few clinical trials are focused on EVs themselves as a treatment. In the last year, MSCs-derived EVs have been proposed as potential therapy for COVID-19. To date (the 25$^{th}$ of April, 2021), the aerosol inhalation of exosomes from MSCs has been tested in two completed registered clinical trials (NCT04276987, NCT04491240) with still unpublished results. Additionally, the aerosol inhalation of MSC-derived exosomes is object of a recruiting trial (NCT04602442), as well as their intravenous delivery (NCT04798716) and the intramuscular injection of secretomes from hypoxia-primed MSCs (NCT04753476).

[4] www.clinicaltrials.gov

Numerous *in vitro* and *in vivo* studies are now demonstrating efficacy and safety of EVs, compared to MSCs, as a therapeutic and regenerative strategy for a variety of conditions, such as nerve tissue disorders (128), cancer (129), renal (130), autoimmune (131), degenerative disc (132), central nervous system (133), joint (134), and musculoskeletal diseases (135), ischemia–reperfusion (136), acute lung injuries (137), myocardial infarction (138), and other cardiovascular diseases (139).

In light of the above, the use of EVs as therapeutic tools is promising, but further characterisation and *in vivo* and clinical studies should be performed. Moreover, EV-based therapies still need to be standardised to be approved by the regulatory agencies.

## CHARACTERISATION OF ADULT STEM CELL- AND EXTRACELLULAR VESICLE-BASED THERAPY AND APPLICATION IN ANIMAL MODELS

Looking at the scientific literature about MSC- and EV-based therapies, most of the original articles recognize their effectiveness and their clinical potential. In contrast, systematic reviews and meta-analyses strongly remark that there is a lack of standardization in *in vitro* studies, preclinical and clinical trials involving MSCs and EVs. These works have always revealed a great degree of variability in methodology (MSCs sources, MSC and EV isolation protocols, cell passage numbers, MSC and EV doses, administration), participants (small or large animal models with induced or spontaneous diseases), and assessment of the clinical outcome (timing and follow up). Under these circumstances, the application of MSC- and/or EV-based therapies to the clinical setting is still tough.

In the light of the above, we decided to study three conditions whose therapeutic approach have not been optimized yet, being still cause of low quality of life, pain, and also death for patients in human and veterinary medicine. These three conditions and their therapeutic approaches are described in the following sections.

## SECTION I: APPLICATION OF MSC- AND EV-BASED THERAPY ON HERNIA

Hernias are protrusions of internal organs through weakened muscles and connective tissue for iatrogenic causes, trauma, or congenital defects (140,141). Surgeons use to repair hernia through open suturing and/or surgical mesh implantation through open surgery procedures or laparoscopic approaches. Surgical meshes are sterile, chemically, and physically inert prosthetic materials that guarantee the reinforcement of abdominal wall more effectively than suturing (142). Nevertheless, the implantation of surgical meshes often leads to complications, such as infection, adhesions, foreign body reaction, formation of scar tissues, postoperative pain, and hernia recurrence (143). In order to reduce the risk of these complications, new surgical techniques have been proposed (144), as well as a variety of materials and manufacturing processes to produce surgical meshes with different mechanical properties (143). Additionally, mesh coatings with antibiotics (145), bioactive compounds (146), and hydrogels (147) have been developed to protect the prosthesis from degradation, decrease post-surgical inflammation, minimize foreign body reaction, reduce the risk of infections, and decrease adhesions (140,145,146). In the last years, cell-based therapy has also been applied to mesh-aided hernia repair to improve the healing outcome of damaged tissues.

When studying hernia repair and tissue reinforcement, biomechanically accurate abdominal wall models are still missing, so resorting to animal models is necessary (148). Models of incisional hernia have been described in mice, rats, rabbits, and pigs (149). The creation of an incisional hernia model just requires a laparotomy incision through the fascia of the midline linea alba and cutting the peritoneum sac below the fascial incision under anaesthesia (150). Incisional hernia models are easy to perform with reproducible results, however large animal models with congenital hernias resemble more closely the clinical human condition. The incidence of abdominal and inguinal hernias for genetic causes (151) ranges from 1.7% to 6.7% in different swine breeds (152). This makes pigs with congenital hernia good candidates for hernia repair studies.

Murine models offer some undoubtable advantages compared to larger animal models, especially concerning the availability of laboratory reagents and the lower costs (149). Nevertheless, pigs are clinically relevant animal models, being comparable to humans in terms of body mass, metabolism, organ sizes, omnivorous diets (153,154), gastrointestinal anatomy (155), and skin histology and anatomy (156–160).

The application of cell therapy on surgical meshes for abdominal hernia repair has become an attractive tool to improve mesh biocompatibility and reduce foreign-body reaction. Effectiveness

and safety of differentiated cells or MSCs on surgical meshes for hernia treatment have been assessed in a variety of *in vitro* and preclinical studies (161). Unfortunately, current studies are too heterogeneous and hard to compare to understand benefits and drawbacks of the combination of surgical meshes and cell therapy (Figure 2).

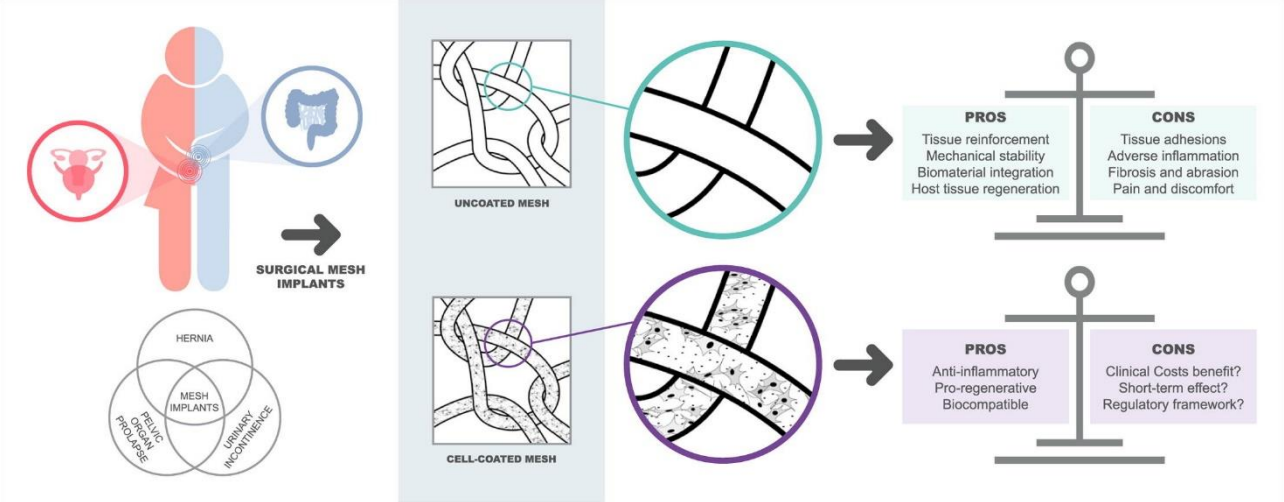


**Figure 2.** Benefits and drawbacks of the implantation of surgical meshes without any modification (uncoated mesh) or combined with stem cell therapy (cell-coated meshes). Figure from Marinaro et al., 2019 (161).

## SECTION II: APPLICATION OF MSC- AND EV-BASED THERAPY ON MYOCARDIAL INFARCTION

Acute myocardial infarction (AMI) is a major cause of death and disability worldwide (Figure 3). It results from the occlusion of a coronary artery and the subsequent myocardial ischemia. The generated ischemia leads to cell death, triggering a strong inflammatory process involving immune cells and soluble mediators that finally results in scar formation (162). The treatment of choice for reducing acute myocardial ischemic injury and limiting infarct size is an early and effective myocardial reperfusion. Myocardial reperfusion is performed using thrombolytic therapy or primary percutaneous coronary intervention, together with the administration of aspirin, antiplatelet and antithrombotic agents. Unfortunately, the process of reperfusion can trigger a myocardial reperfusion injury, where cardiomyocyte undergo cell death (163,164).

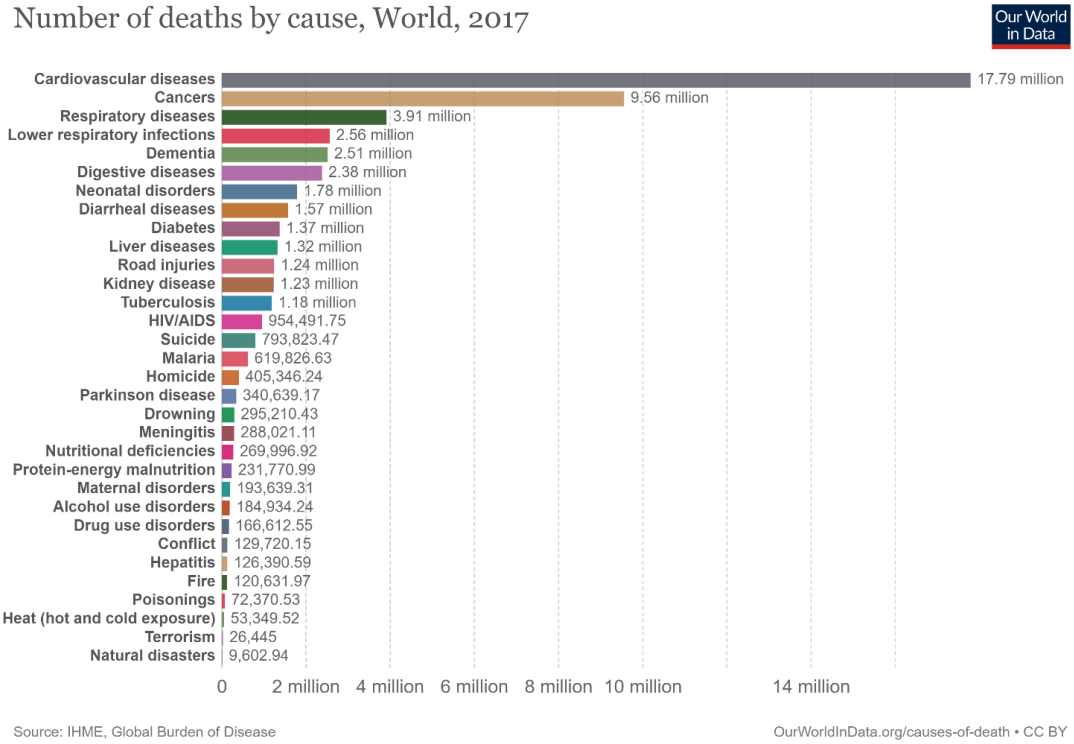


**Figure 3. Chart representing the number of deaths worldwide by cause in 2017.** As it can be seen, cardiovascular diseases represent the first cause of death, corresponding to 31.8% of the total number of deaths in 2017. Data from the Global Burden of Disease Study 2017 (165) and chart from Our World in Data (https://ourworldindata.org/causes-of-death#what-do-people-die-from).

No therapy exists for myocardial reperfusion injury yet, but it can be prevented or reduced by therapeutic targeting of oxidative stress, calcium overload, pH correction, and inflammation (163). Nowadays, a variety of anti-inflammatory therapies are under evaluation (166). Among them, autologous and allogenic progenitor cells administered post-infarction have been proposed to modulate an adverse and unbalanced inflammation (167,168) and to promote tissue regeneration (164). At present, their real effectiveness and biological mechanisms are still unclear (164).

The biological mechanisms involved in cardiovascular disorders and the evaluation of safety aspects and efficacy of novel therapies for AMI need to be tested in clinically relevant large animal models. The porcine model is similar to humans in terms of anatomy, physiology and biochemical parameters (169). Moreover, anatomy, cardiomyocyte metabolism, electrophysiological properties and response to an ischemic insult of the porcine heart are quite comparable to the human one (170).

The closed-chest model of myocardial infarction has been widely described as an approach to simulate human AMI in pigs (171). The best protocol, in terms of similarity with human AMI, involves the standardized endovascular model of 90 min balloon occlusion (172). For the follow-up of the porcine AMI model, electrocardiography, echocardiography, cardiac magnetic resonance, and the detection of cardiac enzymes (173) in plasma are usually performed. Histological staining, such as tetrazolium chloride, can be used for an anatomopathological analysis *post-mortem* (174).

Cell-based therapies delivered by intrapericardial administration (111) have been presented as a promising therapeutic option for myocardial regeneration for a long time (175). Notably, cardiosphere-derived cells have emerged as a promising cell type to promote cardiac immunomodulation and repair (39). However, the administration of MSCs has also shown many contradictory results in terms of beneficial effects on myocardial infarction (176). Given that MSC beneficial effect on target tissues is due to their paracrine communication, the intrapericardial injection of EVs from MSCs may be a valid alternative option to MSC administration.

To understand the mechanisms underlying EV effect on target cells, omic technologies, as transcriptomics and proteomics, coupled to system biology approaches, are particularly useful. These technologies help to make predictions faster than traditional *in vitro* assays, so they should be carefully used to avoid conceptual mistakes at the root of unsuccessful preclinical trials.

## SECTION III: APPLICATION OF MSC- AND EV-BASED THERAPY ON ASSISTED REPRODUCTION TECHNOLOGIES

Infertility affects almost 200 million people worldwide (177). It has been estimated that in 2017 the global age-standardized prevalence rate of female infertility increased by 14.96% since 1990, while the corresponding rate of male infertility increased by 8.22% (178) (Figure 4). Infertility can be due to disease, iatrogenic or unexplained causes (179), or advanced maternal age (180). Delayed motherhood is often linked to poor ovarian function, due to a decrease in the number of follicles, oocyte aneuploidy and a decrease in endometrial receptivity (181).

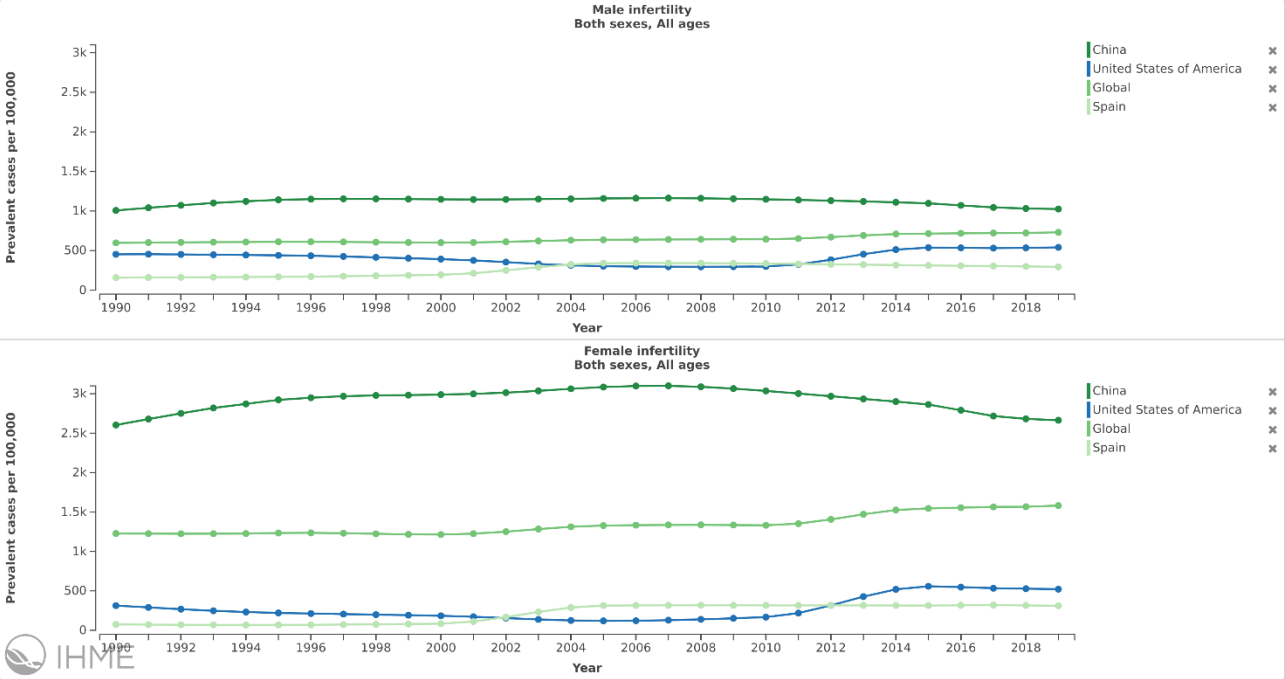


**Figure 4. Estimated prevalence of male and female infertility (per 100 000 population).** Data and plots from the Global Burden of Disease Compare application (Institute for Health Metrics and Evaluation, University of Washington, https://www.thelancet.com/lancet/visualisations/gbd-compare).

Assisted reproductive technologies (ARTs) have become routine treatments for infertile couples. However, ARTs are still characterized by low fertilization, implantation and pregnancy rates (182), due to chromosomal abnormalities in gametes and embryos, defective endometrium, immunological factors (183), or oxidative stress (184), among others. Special attention has been

focused on supplements of *in vitro* fertilization or embryo culture media to support the embryo-maternal cross-talk and to reduce the excess of reactive oxygen species (185,186).

MSCs and EVs may represent valid co-adjutants in *in vitro* fertilisation (IVF) and embryo culture media. MSCs from different sources have already been explored to induce the differentiation and expansion of male and female germ cells (187). Moreover, results in animal models suggest that MSCs play a role in the treatment of male and female infertility, restoring spermatogenesis, suppressing the antisperm antibody, reducing germ cell apoptosis, improving folliculogenesis, and enhancing ovarian function (187). MSCs were also related to improvements in oocyte yield and *in vitro* embryo production (188) and to contribute to the regeneration of damaged endometrium (189). Regarding the use of EVs from different sources to improve ART results, they were related to a better quality of cryopreserved sperms (187), to higher efficiency in oocyte *in vitro* maturation, enhanced blastocyst rates, decreased global DNA methylation and hydroxymethylation levels, better blastocyst quality and embryo hatching (190).

Menstrual blood is a particularly promising source of MSCs from the endometrium (endMSCs). endMSCs and their EVs are strictly involved in embryo-maternal interactions (191) and in endometrial receptivity (192), moreover they are both well-known for their regenerative potential and to play an important role in immunomodulatory processes (193). During embryo implantation in the uterus, the maternal immune system is completely altered to prevent the rejection of the blastocyst (194). Hence, it may be hypothesized that endMSCs and their EVs are particularly promising for ART improvement.

The definition of pros and cons of the use of endMSCs and their EVs in reproduction has not been defined yet and the use of animal models is necessary. Mice represent the most used animal model for research in reproduction. Even though their use for studying human pregnancy and placentation has been criticised in the last years (195), mice are optimal for genetic manipulations and are time- and cost-effective (196). Preclinical studies, coupled to omic technologies and system biology approaches may finally clarify if cell- and EV-based therapies may help to overcome the lasting trauma of infertility.

# AIM OF THE THESIS

Altogether, the main aim of this PhD project is the application of adult stem cell- and extracellular vesicle-based therapies on the three medical conditions described in Section I, II, and III. The methodological tools are based on *in vitro* and *in vivo* assays using omic technologies. Moreover, animal models of disease will help to elucidate benefits and burdens of advanced therapies. Three main aims have been established:

1. **Combination of mesenchymal stem cells and derived extracellular vesicles with surgical materials: safety and mechanisms of action using animal models.**
    a. Fibrin glue mesh fixation combined with mesenchymal stem cells or exosomes modulates the inflammatory reaction in a murine model of incisional hernia
    b. Laparoscopy for the treatment of congenital hernia: use of surgical meshes and mesenchymal stem cells in a clinically relevant animal model
    c. Meshes in a mess: mesenchymal stem cell-based therapies for soft tissue reinforcement
2. **Application of extracellular vesicles derived from mesenchymal stem cells in ischemic events: biomarkers in myocardial infarction and immunomodulatory effects of extracellular vesicles.**
    a. Altered hematological, biochemical and immunological parameters as predictive biomarkers of severity in experimental myocardial infarction
    b. Identification of very early inflammatory markers in a porcine myocardial infarction model
    c. The intrapericardial delivery of extracellular vesicles from cardiosphere-derived cells stimulates M2 polarization during the acute phase of porcine myocardial infarction
    d. The immunomodulatory signature of extracellular vesicles from cardiosphere-derived cells: a proteomic and miRNA profiling
3. **Application of extracellular vesicles derived from mesenchymal stem cells in assisted reproduction: applicability in embryo culture development.**
    a. Murine embryos exposed to human endometrial MSCs-derived extracellular vesicles exhibit higher VEGF/PDGF AA release, increased blastomere count and hatching rate
    b. Extracellular vesicles derived from endometrial human mesenchymal stem cells improve IVF outcome in an aged murine model

c. Extracellular vesicles derived from endometrial human mesenchymal stem cells enhance embryo yield and quality in an aged murine model
d. Unraveling the molecular signature of extracellular vesicles from endometrial-derived mesenchymal stem cells: potential modulatory effects and therapeutic applications

# RATIONALE OF THE THESIS

COHERENCIA E IMPORTANCIA UNITARIA DE LA TESIS

This PhD has been fully developed in the Stem Cell Therapy Unit, including a short stay in the 3B's laboratory at the University of Minho. According to supervisor´s recommendations, the objectives and results of the thesis are closely related with the scientific priorities of the host institution. In this sense, the host institution (Minimally Invasive Surgery Centre Jesús Usón) is a non-profit organization with multidisciplinary team members focused on: I) the preclinical validation of stem cell-based therapies, II) the development of advanced therapies for the treatment of inflammatory-based diseases, and III) optimization of surgical procedures and implantable devices.

Based on that, the main objectives of this thesis were closely related with the research interests of this institution. In this sense, the three main sections, which include several scientific publications in peer reviewed journals are based on the evaluation of innovative ideas for the successful application of stem cell-based therapies. The characterization of vesicles derived from MSCs, the application of these vesicles in assisted reproduction together with the use of MSCs for surgical implantations meshes have a common goal which is the application of advanced cell-based therapies and unravelling the biological mechanisms involved.

Considering that PhD is a learning and cross-disciplinary process, it is important to note that the different sections of this thesis are especially interconnected in terms of methodology. The first section (Application of MSC- and EV-based therapy on hernia) involves preclinical research using clinically relevant animal models, the second section (Application of MSC- and EV-based therapy on myocardial infarction), is basically focused on animal models and cell-based analyses. Finally, the third section (Application of MSC- and EV-based therapy on assisted reproduction technologies) is much more focused on molecular studies, and omic approaches.

Altogether, the objectives, methodologies and results sections developed in this thesis cover basic and applied research in the fields of stem cell biology, inflammatory-mediated diseases, and reproduction.

# RESULTS AND DISCUSSION

## SECTION I: APPLICATION OF MSC- AND EV-BASED THERAPY ON HERNIA

Surgical mesh implantation is the gold-standard procedure for tissue reinforcement in abdominal hernia-related complications (140). Due to the numerous adverse effects reported by patients after hernia repair (197–199), scientists and physicians are striving to improve meshes and surgical techniques. Unfortunately, safety and effectiveness concerns over the use of surgical meshes have been a matter of debate in the Food and Drug Administration and European Medicines Agency in the last years (200,201) and many devices were removed from urogynaecological use because of safety concerns (202). Cell therapy has been proposed as a tool to break the vicious circle where surgical meshes are implanted to repair hernia, but the adverse inflammatory response after implantation leads to mesh removal and hernia recurrence.

So, in the study entitled "*Fibrin glue mesh fixation combined with mesenchymal stem cells or exosomes modulates the inflammatory reaction in a murine model of incisional hernia*" (149), the biological effect of mesenchymal stromal cells (MSCs) from murine bone marrow and the derived extracellular vesicles (EVs) was evaluated in a murine model of incisional hernia. While bone marrow-derived MSCs (BM-MSCs) were already tested in previous studies using animal models of hernia (203–205), EVs from MSCs were never combined with surgical meshes before. The murine BM-MSCs and the derived EVs where firstly characterised. The cells were positive for stemness surface markers having differentiation capacity towards the adipogenic, osteogenic, and chondrogenic lineages. EVs, in turn, were characterised in terms of concentration and particle size and they were shown to express the tetraspanin CD9 (206). BM-MSCs and EVs where then mixed with fibrin sealant, a biological adhesive widely used in tissue engineering (207,208). In this case, fibrin sealant was used as vehicle to seed cells and EVs onto polypropylene surgical meshes. Afterwards, cell/EV-coated meshes were implanted in murine models of incisional hernia. Thanks to the adhesive property of the fibrin sealant, no additional fixation method was required. After one week, meshes were explanted and inflammatory and tissue response to the bioactive surgical meshes were explored. Histological analyses and flow cytometry demonstrated that the fibrin sealant triggered the infiltration of CD45+ leukocytes and this response was counteracted neither by BM-MSCs nor EVs. Fibrin glue was already shown to recruit leukocytes (209,210), with a putative

beneficial effect on tissue incorporation (211). In this study, both cells and EVs produced a decrease in the M1 inflammatory macrophages infiltrated in the surgical mesh, compared to hernia repair with conventional meshes. MSCs-coated meshes were already demonstrated to polarise macrophages towards the M2 anti-inflammatory phenotype (45) and MSC-derived vesicles were associated to a shift in the balance of macrophages towards a M2 phenotype (212). In this study, an increase in M2 macrophages was observed with both cells and EVs, but it was significant only in EVs-coated meshes. Additionally, the enhancement in M2 polarisation by BM-MSCs and EVs was confirmed by qPCR analysis of TH1/TH2 cytokines, where *IL4* expression was increased in cell-coated meshes, while *IL13* expression increased in both cell- and EV-coated meshes, compared to conventional meshes. It is difficult to state that EVs were more effective than MSCs to induce an M2 polarisation, since the anti-inflammatory effect of MSCs is known to be mediated through paracrine mechanisms (213). However, it may be hypothesised that EV-coated meshes contained more concentrated MSC-secretomes, or that EVs lasted longer than cells when encapsulated in the fibrin sealant. Of course, further studies should confirm this hypothesis. The last aim of this study was to evaluate the regenerative potential of MSC- or EV-coated meshes. Hernia patients usually present variations in connective tissue (214), with altered collagens (214–216) and matrix metalloproteinases (MMPs) (214). One week after mesh implantation, MSC- and EV-coated meshes triggered a decrease in *MMP2*, *COL1A1*, and *COL3A1* gene expression, compared to uncoated meshes. Additionally, BM-MSCs caused the increase of *MMP9* expression and in the ratios between MMPs and tissue inhibitors of metalloproteinases (TIMPs) *MMP9*/*TIMP1* and *MMP9*/*TIMP2*. A decrease in the ratios *MMP2*/*TIMP1* and *MMP2*/*TIMP2* was also triggered by cell-coated meshes, when compared with the uncoated ones. Given that collagen synthesis re-organization (23–25) and MMP release (26,27) were already shown to be induced by stem cells, these results may suggest that neovascularization (217), angiogenesis (218), and wound-healing (219) were induced. This study (149) proved that fibrin sealants can be used as cell/EV vehicle as well as fixation method for surgical meshes. Moreover, it suggests that these bioactive meshes may improve the short-term response of an incisional hernia patient to the surgery. Although promising, in this study MSC- and EV-based therapies were tested on a small animal model of ventral incision, that was already used in previous studies (220–223). Unfortunately, even though this model could be appropriate for incisional hernias following laparotomies, it is not suitable for more frequent hernias, such as umbilical or inguinal hernias.

Hence, in the second study included in this section, entitled "*Laparoscopy for the Treatment of Congenital Hernia: Use of Surgical Meshes and Mesenchymal Stem Cells in a Clinically Relevant Animal Model*" (224), the effects of MSC-based therapy were assessed in a pigs with congenital

umbilical hernia. These large animal models were chosen to resemble human patients with abdominal hernias. Similarly to the previous study (149), fibrin sealant was used as a vehicle for porcine BM-MSCs fulfilling the "Minimal criteria for defining multipotent mesenchymal stromal cells" defined by the International Society for Cellular Therapy (35). This compound was then spread on the top of polypropylene surgical meshes. The bioactive meshes were implanted in pigs after the approximation of hernia borders and fixed with helicoidal staples. In this study, fibrin sealant could not be used as a mesh fixation method due to the pathological situation of the pigs and to the longer follow-up (one week and one month). It should be remembered that these pigs were not models of ventral incision but presented a natural abdominal wall defect with related complications. All the surgical procedures were performed by laparoscopy to avoid the open-surgery related complications. Hernia size was measured through ultrasonography prior to surgical mesh implantation and one week and one month after mesh implantation. Even though a statistically significant reduction in terms of hernia mean size was observed with cell-coated meshes one week after implantation, this result was for sure due to different suture closures and heterogeneity of animals in terms of weight and hernia size. The response of the abdominal tissues to cell-coated meshes was evaluated by histology, flow cytometry, and gene expression analysis. Contrarily to the previous study (149), no significant change was found in the expression of M1/M2 markers and TH1/TH2 cytokines, except for *TNF* gene expression. The increase in *TNF* expression in the cell group one month after implantation could be related to the implantation of polypropylene meshes that causes inflammation *per se* (225). The analysis of T cell subsets infiltrating the surgical mesh did not reveal significant changes with cell-coated meshes, suggesting neither positive, nor detrimental effects of the bioactive meshes on the surrounding tissues. Additionally, in the histological evaluation of connective tissue and vascularization, cell-coated meshes caused just a slight reduction in *VEGF* expression one month after implantation, probably helping to minimise severe scarring of the wound (226,227). This was the first preclinical study where a clinically relevant swine model with congenital abdominal hernia was implanted with stem cell-coated meshes by laparoscopy. Unfortunately, if large animal models with congenital hernia could be advantageous in terms of similarity with the human patient, the poor homogeneity and the ethical issues arising for biopsies and follow up, made it difficult to understand the therapeutic effect of cell therapy in hernia repair. In order to combine cell therapy and surgical meshes more efficiently, preclinical trials should be strictly standardised to avoid inconclusive results and waste of money, time, and animal lives.

The lack of standardisation in preclinical studies was clear when a complete overview of the state-of-the-art of cell therapy-based hernia repair was presented in the review entitled "*Meshes in a mess:*

*mesenchymal stem cell-based therapies for soft tissue reinforcement*"(161). In this work it was shown that differentiated cells, as well as MSCs, have been repeatedly tested in *in vitro* and preclinical studies. First, combinations of various differentiated cells, from fibroblast to platelets, and different biologic and synthetic meshes showed beneficial effects especially in terms of neovascularization and foreign body reaction. Second, when MSCs from bone marrow, adipose, or endometrial origin were used, neovascularization, collagen deposition, inflammatory cell infiltration, and improvement of physical-mechanical mesh properties, among the most frequent findings, were triggered. However, in both cases, a comparison between cell types, mesh material, and methodological procedures for cell coating was challenging, due to the heterogeneity of the different studies (161).

So, the evaluation of stem cell-based therapies for the treatment of hernia is quite hard when the available preclinical trials have been performed on various animal models (mice, rats, rabbits, sheep), using stromal cells of different origin (placental, endometrial, adipose, etc.), different surgical materials (synthetic non-absorbable, synthetic absorbable, and biological meshes), several surgical procedures (open surgery, laparoscopy), and have been focused on different purposes (abdominal hernias or pelvic organ prolapse, among others) (161). As a consequence, to date, no registered clinical trials involving surgical meshes and stem cell therapy for hernia repair exist, even though a case report was published in 2017 (228) and an open label trial was performed recently (229). In the case report, autologous BM-MSCs and platelet-rich plasma were seeded on a biological mesh and implanted in a woman with an abdominal incisional hernia. According to the authors, hernia relapse and adhesion formation were prevented, and mesh biocompatibility was improved (228). In the open label trial, 128 patient with inguinal hernia were recruited and using the Lichtenstein repair (230), standard polypropylene meshes were compared with autologous bone marrow cell-coated meshes. The authors claimed that cell-coated meshes reduced hospital stay, post-operative pain and complications (229). Taking into consideration the questionable reliability of open-label trials (231) for the high risk of bias (232), only a standardisation of preclinical trials may avoid inconvenient outcomes in the clinical setting.

Hernia continues to be an unresolved issue, where patients learn to live with discomfort, chronic pain, and disability. Of course, the improvement in MSC-based therapies and the development of engineered cell-vehicles might improve patient outcomes.

# SECTION II: APPLICATION OF MSC- AND EV-BASED THERAPY ON MYOCARDIAL INFARCTION

Acute myocardial infarction (AMI) is a common cause of heart failure (233), which is the most common death cause worldwide (165). Heart failure can emerge right after AMI or later in time (233), and it is hard to predict (234). The risk of heart failure is usually monitored by imaging techniques, electrocardiography (ECG), chest X-ray, and laboratory test values, among others (235). The identification of biomarkers in peripheral blood may help to predict and monitor the evolution of the disease, but there is no evidence for their use in the clinical practice yet (235). To date (the 15th of April, 2021) a basic search in Clarivate Analytics Web of Science[5] with the words "*myocardial infarction*" leads to 306 853 results. This number seems incredibly small when it is compared with the 3 510 023 results corresponding to "*cancer*" and it just doubles the novel "*COVID-19*" (144 358 results). This means that although very common, AMI still needs to be thoroughly studied. It is widely accepted that the closed-chest model of AMI in swine is one of the most appropriate approaches for cardiovascular research (236,237), and it has been used to identify biomarkers to predict the severity of AMI (174,238).

In our first study from this section, entitled "*Altered haematological, biochemical and immunological parameters as predictive biomarkers of severity in experimental myocardial infarction*" (174) several biochemical, haematological, and immunological parameters were analysed at different time points: before AMI model creation, 24 hours and 7 days after AMI. Briefly, significant changes in transaminases, myeloid cells, erythrocytes, and platelets were found when the three time points were compared. Additionally, direct or indirect correlations between haematological/biochemical parameters with ejection fraction, infarction area and cardiac enzymes were found. No immunological parameters appeared to be significantly altered at different time points. Considering that ischemia during AMI activates the immune system, it was likely that some relevant immunological changes may have occurred at earlier time points. This study, whose results are supported by previous findings (239–247), suggests that the proposed biochemical and haematological parameters (gamma-glutamyl transferase, glutamic pyruvic transaminase, red

[5] https://www.webofknowledge.com

blood cell counts, haemoglobin concentration, haematocrit, platelet count, and plateletcrit) may be used as biomarkers to predict the severity of myocardial infarction in human patients (174).

With all this in mind, in our following study entitled "*Identification of very early inflammatory markers in a porcine myocardial infarction model*" (238), peripheral blood was collected 1 hour after myocardial infarction induction in the same experimental model. Lymphocytes were then isolated and then characterized to identify potential early biomarkers for myocardial infarction severity (238). Only one hour after balloon deflation, some variations in lymphocyte subsets distribution and in cytokine gene expression were found. In short, there were significant changes in the T cell ratio CD4+/CD8+ and in lymphocyte differentiation/activation status, as confirmed by previous studies (248–250). Regarding the expression of genes encoding cytokines secreted by lymphocytes, some significant differences were reported 1 hour after myocardial infarction, compared to the basal state. *IFNγ*, *IL4*, *CELA*, and *BPI* expression was reduced, suggesting a prompt rearrangement in Th1 and Th2 lymphocytes, and in neutrophils. Expression levels of *IFNγ* and *IL4* was already proposed as a diagnostic tool to evaluate the success of percutaneous coronary intervention after AMI (251) and also neutrophils were considered predictive cells in coronary heart diseases (252,253). Moreover, there was an increase in *ARG1* expression, suggesting that monocytes are immediately recruited to the site of infarction, as previously hypothesised (254). As in our previous work (174), correlations between the altered parameters and classic cardiac variables (cardiac enzymes, ejection fraction and infarction area) were found. These results suggest that patients that 1 hour after AMI onset present a high percentage of CD4+IFNγ+ lymphocytes, low *IL2, IFNγ,* and *CELA* expression, or high *NOS* and *IL5* expression, may have higher levels of Troponin I or CK-MB and lower left ventricular ejection fraction (LVEF) 1 week after AMI, indicating a worse prognosis (238). Additional studies with bigger sample sizes would elucidate if these parameters may be used as molecular biomarkers for the severity of AMI. This method would give the advantage to predict, in relatively short time, the prognosis of AMI in human patients as soon as they are admitted into hospital. Furthermore, knowing accurately the clinical context of the patient is necessary to test new treatments. In this scenario, the identification of immune biomarkers in the swine model of closed-chest AMI is particularly reliable, being the animals free of pre-existing immune disorders. These biomarkers can then be used to evaluate the efficacy of novel anti-inflammatory treatments.

The inflammatory process involving the cardiac tissues after AMI are well-known and MSC- and EV-based therapies are particularly of interest. Cardiosphere-derived cells (CDCs) were isolated for the first time in 2007 from human percutaneous endomyocardial biopsies (255). Primary cultures of these specimens are characterised by the formation of multicellular clusters called cardiospheres.

When CDCs migrate from these clusters, they are c-Kit+ and mesenchymal/fibroblasts (CD105+ CD90+) and endothelial (CD34+ CD31+) subpopulations can be found. Moreover, human and porcine CDCs demonstrated all characteristics of cardiogenic differentiation and to migrate and engraft to infarction zones in murine hearts (255). Following studies have demonstrated CDC therapeutic potential in myocardial infarction (256), especially for their anti-inflammatory properties (257–259). Different clinical trials involving CDCs (ClinicalTrials.gov Identifiers: NCT00893360, NCT02293603, NCT01458405, NCT03129568, NCT01273857, NCT01829750) have been performed. The completed trials (NCT00893360, NCT01273857, NCT01458405) demonstrated that the intracoronary administration of CDCs is feasible (260), safe (260–262), and effective (263), even at a long term (264). Unfortunately, the ALLSTAR clinical trial (NCT01458405) observed no reduction in scar size, although some cardiac improvements were induced by CDC-based therapy (262). The poor regenerative potential of cardiac tissue may be attributed to the fact that MSCs are effective when they can persist in the site of injury for a long time (265). Even though in all the cited trials, CDCs were delivered through the coronary artery, preclinical studies have demonstrated that the intrapericardial injection is as safe and effective as the intramyocardial, intracoronary, and intravenous administrations. However, the intrapericardial infusion guarantees longer retention of CDCs in the heart (39,111). This administration route was proposed for the administration of EVs from CDCs, that showed the same anti-inflammatory, anti-apoptotic, and pro-angiogenic effects of their source cells (266–268).

Hence, in the following study, entitled "*The intrapericardial delivery of extracellular vesicles from cardiosphere-derived cells stimulates M2 polarization during the acute phase of porcine myocardial infarction*" (269) porcine CDCs as well as EVs from porcine CDCs (EV-CDCs) were intrapericardially administered in infarcted hearts from swine. Neither CDCs nor EV-CDCs produced any effect on the cardiac function parameters (obtained by magnetic resonance imaging), on cardiac enzymes (troponin I), or in biochemical parameters (transaminases), showing a lack of effectiveness, but also of toxicity. Regarding the immunological parameters, EV-CDCs produced a significant increase of CD14+CD16+ cells, corresponding to M2 monocytes (270). This result is particularly interesting and it suggests that EV-CDCs may trigger the infiltration of these pro-angiogenic and immunomodulatory M2 monocytes in the infarcted heart, promoting tissue repair (271–273) and counteracting the exacerbated inflammatory response in AMI. This study confirmed the feasibility of the technique, but it did not elucidate the molecular mechanisms involved in the M2 polarisation.

In the last study from this section, entitled "*The Immunomodulatory Signature of Extracellular Vesicles From Cardiosphere-Derived Cells: A Proteomic and miRNA Profiling*", a detailed

characterisation of the proteome and the miRNome of EV-CDCs was performed (274). This kind of description is especially necessary in animal-derived EVs which are still poorly characterised to be successfully translated to the clinical setting. According to high-throughput proteomic analysis and following enrichment analysis, the top-abundant protein in EV-CDCs were found to be related with the processes *Immune system* (R-HAS-168256), *Hemostasis* (R-HSA-109582), and *Muscle Contraction* (R-HSA-397014), as defined in the database Reactome. Furthermore, several cardiac-related and immune-related miRNAs, as well as previously identified miRNAs in EVs from MSCs, were selected and their expression was quantified in EV-CDCs by qPCR. Five miRNAs (mir-23a-3p, mir-191-5p, mir-21-5p, mir-125b-5p, and let-7a-5p) appeared to be particularly abundant in EV-CDCs. Of note, *in silico* analyses revealed that these miRNAs target the gene *IL6R*. This receptor was considered an ideal target for coronary heart disease (275) and it is blocked by the monoclonal antibody Tocilizumab, which is now considered a good therapeutic strategy for coronary heart disease (276) and COVID-19 (277). These pieces of evidence suggest that EV-CDCs may have a therapeutic relevance for inflammatory-mediated diseases. Afterwards, MSC priming strategies were used to decipher any change in EV-CDC profile. Numerous priming strategies for different MSC types are currently under investigation, and our study aimed to optimise *in vitro* cell culture conditions (274). , providing stimuli as cytokines, chemical agents, hypoxia, or other molecules. Under these conditions, MSC properties are enhanced, being then "inherited" by the released EVs (de Pedro et al., manuscript in preparation). In this study (274), Briefly, CDCs were primed with IFNγ, and the molecular profile of the derived EVs (called IFNγ/EV-CDCs) was compared with EV-CDCs. First, IFNγ priming did not induced any difference in terms of size and concentration of EVs. Second, several proteins were up-regulated in IFNγ/EV-CDCs vs. EV-CDCs. Among these proteins, we identified IL6, whose function in the immune system pathway seems to be "contradictory". Indeed, it has been often considered as a pro-inflammatory cytokine (278), but also as an anti-inflammatory molecule (279), with a role in the alternative activation of macrophages (280). Third, mir-125b-5p was significantly up-regulated in IFNγ/EV-CDCs. This miRNA was found to be involved in cardiac regeneration after myocardial infarction (281) by acting on cardiomyocytes survival (282). Additional *in silico* analyses on the target network of mir-125b-5p identified a variety of genes targeted by this miRNA and involved in the processes *Metabolism* and *Immune System*, including IL6R. The immunomodulatory potential of EV-CDCs and IFNγ/EV-CDCs was then assayed on CD4+ and CD8+ T cell subsets. EV-CDCs reduced the *in vitro* differentiation of CD4+ and CD8+ T cells towards an effector-memory phenotype and the expression of activation markers, confirming previous findings on EVs from endometrial stem cells (283,284). In conclusion, even though the molecular mechanisms underlying the immunomodulatory potential of EV-CDCs still needs to be elucidated by functional

analyses, this study suggests a possible involvement of EV-CDCs and IFNγ/EV-CDCs in the IL6/IL6R axis. This insight may explain why in the previous study included in this section (269) EV-CDCs triggered the infiltration of M2 monocytes in the infarcted heart (285).

To conclude, the *in silico*, *in vitro*, and preclinical studies included in the four publications of this section, suggest that an accurate analysis of the immunological response during myocardial infarction would be very useful to predict the severity of the disease, and these immunological markers could be useful to evaluate the effectiveness of novel therapies. Finally, prior to a clinical application of CDCs and EV-CDCs further *in vivo* studies are required to evaluate the therapeutic efficacy in clinically relevant animal models.

# SECTION III: APPLICATION OF MSC- AND EV-BASED THERAPY ON ASSISTED REPRODUCTION TECHNOLOGIES

One of the most promising sources of Mesenchymal Stromal Cells (MSCs) is the human endometrium. Its functional and basal layers are the source of two types of MSCs: multipotent W5C5/SUSD2+ CD146+ perivascular cells (286,287), usually called "endometrial MSCs", and W5C5/SUSD2- CD146- "endometrial stromal fibroblasts" of mesenchymal origin (288). The W5C5/SUSD2+ CD146+ endometrial MSCs have self-renewal capacity and differentiate into myocytes, adipocytes, osteocytes, and chondrocytes. They are also progenitors of the endometrial stromal W5C5/SUSD2- CD146- cells (286,288), that are responsive to progesterone and differentiate to epithelial-like cells in the decidualization process (286). Both types of cells can be isolated from hysterectomy, biopsies of the endometrium, or by menstrual fluid collection. Menstrual fluid is a particularly advantageous and non-invasive source of cells of mesenchymal origin. Any pre-menopausal healthy women, without infections or immune disorders and who is not undergoing hormonal therapy, is a potential donor. The collection of menstrual blood can be performed using a menstrual cup and it is completely painless, quick, without any additional cost and ethical concern. Menstrual fluid is composed of endometrial tissue fragments comprising endometrial stroma, glands, and blood cells (193). Both W5C5/SUSD2+ CD146+ endometrial MSCs and endometrial stromal W5C5/SUSD2- CD146- cells (both hereinafter referred to as "endometrial-derived MSCs—endMSCs") can then be easily isolated by plastic adherence and *in vitro* expanded using standard culture conditions (289). In the last years, endMSCs have been deeply studied and have demonstrated a high proliferative rate and differentiation capacity, been particularly attractive from a therapeutic point of view (193,287). Moreover, they have also demonstrated immunosuppressive (290–292), anti-apoptotic, and pro-angiogenic capacities (293), which are mediated by paracrine factors. In this context, extracellular vesicles (EVs) are believed to be the principal mediators of MSC-related therapeutic potential. The molecular cargo of EVs has been found to be involved in adaptive/innate immune response, complement activation, antigen processing/presentation, signal transduction, cell proliferation, and apoptotic processes (294).

Hence, since EVs are known to mediate cell-to-cell communication, and the endometrium is known to establish a complex interplay with the embryo, an *in vitro* study, entitled "*Murine embryos exposed to human endometrial MSCs-derived extracellular vesicles exhibit higher VEGF/PDGF AA release, increased blastomere count and hatching rates*" (295) was performed. In this study, endMSCs and

their concentrated EVs (EV-endMSCs) were characterised. These cells showed to comply with the Minimal criteria for defining multipotent mesenchymal stromal cells proposed by the International Society for Cellular Therapy (35) and the EVs with the Minimal information for studies of extracellular vesicles by the International Society for Extracellular Vesicles (120). Then embryo development and hatching were *in vitro* evaluated by co-culturing EV-endMSCs with murine cell embryos for three days, showing a significant increase in total blastomere number and in hatching rates when EV-endMSCs were added to embryo cultures. These results suggest that EV-endMSCs may promote blastomere division during embryonic development and that this effect may be due to the protein content of these EVs. As a matter of facts, proteomic analyses of EV-endMSCs evidenced the presence of proteins as vinculin, fibronectin, metalloproteinase-2, -3, -9, and E-cadherine, that have already been positively linked to embryo development and implantation (295). On the other side, EV-endMSCs affected neither positively nor negatively, blastocyst rates of the 2-cell embryos, suggesting that EVs may intervene in the late phases of embryo development preceding implantation. Moreover, the absence of negative effects on blastocyst and hatching rates may indicate that EVs are not toxic when used as co-adjutants of embryo cultures. Regarding blastocyst response to EVs, PDGF-AA and VEGF were detected in embryo supernatants in an EV concentration-dependent manner. The mitogenic factor PDGF-AA was already associated to enhance embryo quality and developmental potential, while VEGF, usually known for being the conductor of the angiogenesis orchestra, was also linked with embryo development and implantation (295). Additionally, the quantified PDGF-AA and VEGF in embryo supernatants showed a significant correlation, suggesting that embryos may support angiogenesis, differentiation, and tissue remodelling of the endometrium during implantation (295). In conclusion, EV-endMSCs seemed to be an integrated part of a feedback loop where the endometrium supports embryo development and hatching, and the embryo supports endometrium remodelling during implantation.

The use of EV-endMSCs as co-adjutants for *in vitro* embryo culture seemed very promising and their beneficial effect was tested in embryos derived from aged female mice. In the study entitled "*Extracellular vesicles derived from endometrial human mesenchymal stem cells improve IVF outcome in an aged murine model*" (296), *in vitro* fertilization was performed with the gametes of old B6D2 female (24 weeks) and young male mice (8-12 weeks). Different concentrations of EV-endMSCs were co-cultured with presumptive zygotes and the impact on embryo developmental competence was explored. On one hand, the first mitotic divisions before the morula stage of mice embryos were not affected by the EVs, confirming the results from the study conducted with young female gametes (295). On the other hand, embryo division kinematics at the morula and blastocyst

stages were significantly increased by the presence of certain doses of EV-endMSCs, Furthermore, in accordance with the result from the previous study (295), blastocyst total cell number was significantly boosted with any of the tested concentration of EV-endMSCs (296,297). The implementation of embryo culture media with EVs from the female reproductive tract was already explored in mammals (190). Survival rate and number of cells of vitrified bovine embryos, improved when EVs from bovine oviductal epithelial cells were supplemented to embryo culture media (298). In another study, the same type of bovine EVs was reported to enhance blastocyst quality and embryo hatching rate (299). Recently, EVs from human umbilical cord MSCs were administered by intravenous injection in female mice with induced premature ovarian insufficiency. These EVs increased the number of oocytes retrieved, percentage of fertilized oocytes, cleaved embryos, and blastocyst rates in the infertile mice (300).

Thus, the enhancement of developmental competence in the morula and blastocyst stages of embryos from aged oocytes is crucial to improve blastocyst rates when assisted reproduction techniques are employed in the case of advanced maternal age. In the third study included in this section, entitled "*Extracellular vesicles derived from endometrial human mesenchymal stem cells enhance embryo yield and quality in an aged murine model*" (297), it was demonstrated that EV-endMSCs in supplemented embryo culture media were effectively internalised by embryo cells, allowing EV-cargo to directly interact with recipient cells. The proteomic analysis of the EV-endMSCs used throughout the study (297) revealed that the proteins in the EV cargo are involved in crucial Reactome pathways for fertilization and embryo implantation, as *Metabolism* (R-HSA-1430728), *Developmental biology* (R-HSA-1266738), and *Cellular response to oxidative stress* (R-HSA-2262752). The effect of EV-endMSCs on embryo quality was further confirmed by qPCR analyses in the murine blastocysts. The expression of genes involved in *Developmental biology* (vascular endothelial growth factor A-*Vegfa and* sex determining region Y-box 2 -*Sox2)* resulted to be significantly increased with some dosages of EV-endMSCs, as well as the gene glyceraldehyde-3-phosphate dehydrogenase – *Gapdh,* involved in *Metabolism*. It is worth mentioning that *Sox2* participates in trophectoderm/inner cell mass formation in the pre-implantation embryo, *Gapdh* is involved in the glycolytic pathway and *Vegfa* is strictly related with placentation. This means that EV-endMSCs may contribute to many events that sustain blastocyst development until implantation (297). On the other side, the expression of genes related to *Cellular response to oxidative stress* pathway *(*glutathione peroxidase 1 -*Gpx1*- and superoxide dismutase 1 -*Sod1*), encoding antioxidant enzymes, was significantly decreased with some dosages of EV-endMSCs, compared to controls (296,297). The impairment in reactive oxygen species metabolism is a detrimental factor for oocyte competence, especially if

aged, and for embryo development (296). A potential reactive oxygen species (ROS) scavenger activity of EV-endMSCs was already hypothesized in the setting of prostate tumours. Therefore, this reduction in antioxidant gene expression may indicate that EVs can lower ROS levels, contributing to increase embryo developmental competence (296,297).

The results from the previously described studies (295–297) suggested a possible role of endMSCs and EV-endMSCs in the early stages of embryo development until implantation. Since inflammation is necessary for embryo implantation (301), the aim of the subsequent study, entitled "*Unraveling the molecular signature of extracellular vesicles from endometrial-derived mesenchymal stem cells: potential modulatory effects and therapeutic applications*" (294), was to fully characterise the molecular signature of EV-endMSCs and its possible implication in immune-related events. EV-endMSC samples, were analysed by high-throughput quantitative proteomic techniques and revealed the presence of a total of 895 proteins, 617 being annotated in the Gene Ontology (GO) category *Extracellular exosome* (GO:0070062). In turn, Next Generation Sequencing (NGS) allowed us to identify 225 micro RNAs (miRNAs) with 937 target genes. The enrichment analysis of EV-endMSC proteins showed that they were predominantly localized in *Extracellular matrix* (GO:0031012), *Cytosol* (GO:0005829), and *Membrane* (GO:0016020) and involved in processes as *extracellular matrix organization* (GO:0030198) and *cell redox homeostasis* (GO:0045454). These results confirm previous studies were EV proteins were already hypothesized to be involved in biological processes such as cellular migration (302), invasion (303), tumour metastasis (304,305), and neutrophils recruitment during inflammation (306), among others. On the other side, miRNA-targeted genes were shown to be mainly localized in the nucleus (GO:0005634) and to be involved in *signaling transduction* (GO:0007165), *cell proliferation* (GO:0008283) and *apoptotic processes* (GO:0006915), among others. This result suggest that EV-endMSC cargo exert pleiotropic effects on the recipient cells, depending on the molecules that are delivered (294). Afterwards, endMSCs were primed with IFNγ, and the molecular profile of the derived EVs (called IFNγ/EV-endMSCs) was compared with EV-endMSCs. Under IFNɣ treatment, there was a significant change in 84 proteins, involved in *angiogenesis* (GO:0001525), *tumor necrosis factor signaling* (GO:0033209), and *innate immune response* (GO:0045087). Among the up-regulated proteins in IFNγ/EV-endMSCs, there was the cytokine Colony Stimulating Factor 1 (CSF1). CSF1 is a modulator of inflammatory responses which has been associated with M1/M2 polarization, and shifts towards homeostatic/reparative state (294). CSF1 levels were measured by ELISA and was found to be released and significantly increased in IFNγ/EV-endMSCs when compared to EV-endMSCs. This result suggests that EVs from IFNγ-primed MSCs may promote a M2 polarization. To further confirm the involvement of EV-

endMSCs and IFNγ/EV-endMSCs in macrophage polarisation, human monocyte differentiation towards M1-macrophages and M2-macrophages was firstly induced with GM-CSF and M-CSF (CSF1) respectively. Macrophage differentiation was compared with the effects of EV-endMSCs and IFNγ/EV-endMSCs co-cultured with monocytes. It was so shown that EVs could trigger monocyte differentiation towards M2 macrophages, regardless of their provenance from control or IFNγ-primed endMSCs (294). This finding remarks the role of MSC-derived EVs in promoting M2 differentiation (307), however it pinpoints the importance of finding the best priming strategy to amplify MSC immunomodulatory properties. Indeed, later studies demonstrated a clearly increased macrophage polarization capacity in EVs from IFNγ/TNFα-primed cells than in EVs themselves (308,309) suggesting that priming MSCs with IFNγ alone is not sufficient and should be modified or combined with different priming agents. Conversely, IFNγ priming significantly altered the expression of 18 miRNAs, whose targeted genes are involved in *IL-6/8/12 Signaling*, and in the *Role of Macrophages*, confirming that IFNγ/EV-endMSCs may have a potential role in macrophage polarization, but additional functional studies involving further priming strategies should be performed.

In conclusion, the bioinformatic, *in vitro*, and *in vivo* analyses collected in the four publications on which this section is focused, support the use of EV-endMSCs in the context of assisted reproduction technologies. Moreover, our results encourage their use as an innovative, cheap, and safe cell-free therapy for inflammatory-related conditions.

## GENERAL CONTRIBUTION TO KNOWLEDGE AND LIMITATIONS OF THIS THESIS

The use of animals for scientific purposes is still a matter of debate and many alternatives have been proposed over the last decade. Experimental *in vitro* techniques have incredibly improved and bioinformatics and computational biology are increasingly more accessible, nevertheless animal research is still essential to answer to a variety of scientific and medical questions. Advanced therapies based on stem cells and extracellular vesicles are appealing, but they are relatively new and need a strong validation in animal models of disease prior to the clinical translation. Currently, many clinical trials have not revealed the expected results, presumably due to an insufficient or inadequate *in vitro* and preclinical phase. In this regard, omic strategies and *in vitro* experiments should be carefully planned and combined prior preclinical trials. Preclinical trials, in turn, should be focused on clinically relevant animal models and standardised to evaluate the real effectiveness of MSC- and EV-based therapies. Nowadays, cell therapy is well-known even among non-healthcare professionals. It is especially useful in patients with inflammatory diseases, such as Crohn's disease, but its application to other medical conditions has not reached a consensus yet. On the other hand, the existence of extracellular vesicles was firstly deciphered in the eighties, but their characterization, classification and their exact clinical potential is still a matter of debate.

In this PhD thesis, bone marrow-derived MSCs and their EVs were combined with surgical meshes to reduce adverse inflammation reactions and induce tissue regeneration in a murine model with incisional hernia. This preliminary study was then followed by a clinically relevant study in a swine model of congenital hernia. The results obtained from these preclinical studies, as well as the considerations made in the related literature review, may be crucial to develop a standardised protocol to be evaluated in further clinical studies.

The intrapericardial administration of EVs from cardiosphere-derived MSCs was also assessed in a swine model of myocardial infarction. A detailed molecular characterisation of these EVs was provided and it demonstrated their potentiality to be a safe and effective approach to counteract adverse inflammatory events in acute myocardial infarction and triggering tissue regeneration.

Last but not least, a detailed characterization of EVs from menstrual blood-derived MSCs was provided, as well, and their use was investigated in a murine model of *in vitro* fecundation and embryo development. The use of EVs from MSCs as culture media supplements for assisted reproduction technologies may provide a relatively low-cost and safe strategy to raise the still low

success rates of assisted fecundation and to counteract implantation failure. Furthermore, EVs from endMSCs constitute promising end ethic concern-free tools for the treatment of immune system-related diseases.

In conclusion, adult stem cells and their EVs may be the off-the-shelf therapeutic alternative to reduce severity and costs associated to the recurrence of some diseases.

This thesis demonstrates that with the appropriate research and trials, MSC-and EV-based therapies will be a valuable therapeutic tool in clinical practice. Notwithstanding, it should be remarked that severe criticism about the concept of "extracellular vesicles" is arising in more recent times. To begin with, the term "extracellular vesicle" was used for the first time in 1971 in the *Journal of Ultrastructure Research*, while the term "exosome" was used to refer to EVs just in 1981 in *Biochimica et Biophysica Acta*. However, the term "exosome" became the most popular in the recent literature, until the participants to the "International Workshop on Exosomes" (then forming the International Society for Extracellular Vesicles) in 2011 agreed that the term "extracellular vesicle" should be the consensus generic term for lipid bilayer-enclosed particles secreted by cells (310). Nowadays, the nomenclature issue has been shelved, but the concept of EVs as cellular messengers is being jeopardised. Even though the theory of EVs as intercellular delivery tools may seem particularly attractive and there is plenty of publications in the literature about EVs/exosomes working miracles, numerous doubts have been shed on the "EV cargo transfer hypothesis" (311). After all, if the putative effects of EV cargo can be hypothesized and even demonstrated through system biology tools, or in *in vitro* experiments, but accurate *in vivo* validations still need to be performed. Additionally, rigorous EV isolation is challenging (311). The mere concentration of cell culture media does not discriminate between extracellular vesicles and other molecules in the cell secretome. So, many authors have mistakenly attributed the effects of cell-free based therapies to EVs, when cell secretomes are actually a conglomerate of growth factors, cytokines, chemokines, nucleic acids, lipids, and also extracellular vesicles (312). Last but not least, the determination of EV functionality has not been standardised yet and the interpretation of results can be as confusing as subjective (313). To summarise, it is becoming quite evident that the translation of EV-based therapies to the clinical setting still requires careful planning and that sometimes a step back is necessary to move forward.

It is also worth mentioning that some of the inconclusive results of the studies collected in this thesis, as well as many others that have been cited in the previous chapters, may be consequence the recent decadence where science is falling into. This "decadence of science" must not be

interpreted as a decrease in scientific production or as the lack of interest towards creating and spreading knowledge. Certainly, science is moving forward faster than ever, and the pandemic COVID-19 is the proof of the incredible effort that scientists make to let science progress quicker than ever. Nevertheless, we also live in a world where scientists "*publish or perish*" (314) and academic talent is measured as number of publications more than research and teaching ability. The exponential increase in scientific publications that has characterised the last decades has generated a significant amount of data that are often irrelevant, repeated, useless, unethical, or fraudulent. What authorities should learn from this pandemic, is that research is a primary good and that it is not industry, where production comes first. In research, health, respect, and ethics come first, or countless animal lives will be wasted, and innumerable patients will continue suffer and die in the name of scientific output.

# CONCLUSIONS

**Section I**

1. Fibrin sealants can be used as vehicle for MSCs and EVs, as well as for the fixation of bioactive surgical meshes in a murine model of incisional hernia. MSC- and EV-coated meshes have anti-inflammatory properties, inducing the recruitment of M2 macrophages and are involved in tissue remodelling.
2. Pigs with congenital hernia is an appropriate experimental model to explore new therapeutic strategies for abdominal hernia, and laparoscopy is a feasible approach to implant MSCs-coated meshes.

**Section II**

1. Haematological, biochemical, and immunological parameters can be used for an early prognosis of myocardial infarction and to predict the severity in a clinically relevant swine model.
2. The intrapericardial administration of CDCs or EV-CDCs in a porcine myocardial infarction is feasible, safe and counteract the inflammatory reaction increasing M2 monocytes.
3. The *in silico* analysis of proteins and miRNAs expressed in EVs from porcine CDCs and IFNγ-primed CDCs suggests a regulation of the IL6/IL6R axis.

**Section III**

1. EVs from human endMSCs increase the proliferation of murine blastocysts and the release of pro-angiogenic molecules.
2. EVs from human endMSCs increase blastocyst hatching in embryos derived from aged murine oocytes and induce alterations in oxidative stress-related genes.
3. EVs from human endMSCs can be internalised in murine embryos from aged oocytes and improve developmental competence as wells as total blastomere count.
4. The *in silico* analyses of the proteins and miRNAs of EVs from endMSCs allowed us to identify molecular interactions with adaptive/innate immune system, signal transduction, cell proliferation, and apoptosis.

# CONCLUSIONES

**Sección I**

1. Los selladores de fibrina pueden ser utilizados como vehículo para las MSCs y las EVs, así como para la fijación de mallas quirúrgicas bioactivas en un modelo murino de hernia incisional. Las mallas recubiertas de MSCs y EVs poseen propiedades antiinflamatorias, inducen el reclutamiento de macrófagos M2 y están involucradas en la remodelación tisular.

2. Los cerdos con hernia congénita son un modelo experimental apropiado para explorar nuevas estrategias terapéuticas, siendo la laparoscopia una técnica factible para implantar mallas recubiertas de MSCs.

**Sección II**

1. Los parámetros hematológicos, bioquímicos e inmunológicos obtenidos de un modelo porcino de infarto de miocardio pueden ser utilizados para emitir un pronóstico temprano y para predecir la gravedad de la enfermedad.

2. La administración intrapericárdica de CDCs o EV-CDCs en un modelo de infarto de miocardio porcino es factible, segura y contrarresta la reacción inflamatoria aumentando la población de monocitos M2.

3. El análisis *in silico* de proteínas y miRNAs expresados en EV-CDCs porcinos y CDCs precondicionados con IFNγ están relacionados con la regulación del eje IL6/IL6R.

**Sección III**

1. Las EV-endMSCs humanas aumentan la proliferación de blastocistos murinos y la liberación de moléculas proangiogénicas.

2. Las EV-endMSCs humanas aumentan la eclosión de blastocistos en embriones derivados de ovocitos murinos envejecidos e inducen alteraciones en genes relacionados con el estrés oxidativo.

3. Las EV-endMSCs humanas se internalizan en embriones murinos de ovocitos envejecidos y ayudan a mejorar su capacidad de desarrollo, así como el recuento total de blastómeros.

4. Los análisis *in silico* de las proteínas y miRNAs procedentes de EV-endMSCs permiten identificar interacciones moleculares con procesos del sistema inmune adaptativo/innato, transducción de señales, proliferación celular y apoptosis.

# BIBLIOGRAPHY


1. Chakraborty C, Agoramoorthy G. Stem cells in the light of evolution. *Indian J Med Res* (2012) **135**:813–819.

2. Ramalho-Santos M, Willenbring H. On the Origin of the Term “Stem Cell.” *Cell Stem Cell* (2007) **1**:35–38. doi:10.1016/j.stem.2007.05.013

3. Evans MJ, Kaufman MH. Establishment in culture of pluripotential cells from mouse embryos. *Nature* (1981) **292**:154–156. doi:10.1038/292154a0

4. Thomson JA, Itskovitz-Eldor J, Shapiro SS, Waknitz MA, Swiergiel JJ, Marshall VS, Jones JM. Embryonic stem cell lines derived from human blastocysts. *Science* (1998) **282**:1145–1147. doi:10.1126/science.282.5391.1145

5. Potten CS, Loeffler M. Stem cells: attributes, cycles, spirals, pitfalls and uncertainties. Lessons for and from the crypt. *Dev Camb Engl* (1990) **110**:1001–1020.

6. Fuchs E, Chen T. A matter of life and death: self-renewal in stem cells. *EMBO Rep* (2013) **14**:39–48. doi:10.1038/embor.2012.197

7. Daynac M, Petritsch CK. Regulation of Asymmetric Cell Division in Mammalian Neural Stem and Cancer Precursor Cells. *Results Probl Cell Differ* (2017) **61**:375–399. doi:10.1007/978-3-319-53150-2_17

8. Morrison SJ, Shah NM, Anderson DJ. Regulatory mechanisms in stem cell biology. *Cell* (1997) **88**:287–298. doi:10.1016/s0092-8674(00)81867-x

9. Venkei ZG, Yamashita YM. Emerging mechanisms of asymmetric stem cell division. *J Cell Biol* (2018) **217**:3785–3795. doi:10.1083/jcb.201807037

10. Clause KC, Liu LJ, Tobita K. Directed stem cell differentiation: the role of physical forces. *Cell Commun Adhes* (2010) **17**:48–54. doi:10.3109/15419061.2010.492535

11. Rumman M, Dhawan J, Kassem M. Concise Review: Quiescence in Adult Stem Cells: Biological Significance and Relevance to Tissue Regeneration. *Stem Cells Dayt Ohio* (2015) **33**:2903–2912. doi:10.1002/stem.2056

12. Rogers EH, Hunt JA, Pekovic-Vaughan V. Adult stem cell maintenance and tissue regeneration around the clock: do impaired stem cell clocks drive age-associated tissue degeneration? *Biogerontology* (2018) **19**:497–517. doi:10.1007/s10522-018-9772-6

13. Daley GQ. Stem cells and the evolving notion of cellular identity. *Philos Trans R Soc Lond B Biol Sci* (2015) **370**:20140376. doi:10.1098/rstb.2014.0376

14. Kaneko KJ. Metabolism of Preimplantation Embryo Development: A Bystander or an Active Participant? *Curr Top Dev Biol* (2016) **120**:259–310. doi:10.1016/bs.ctdb.2016.04.010

15. Zakrzewski W, Dobrzyński M, Szymonowicz M, Rybak Z. Stem cells: past, present, and future. *Stem Cell Res Ther* (2019) **10**:68. doi:10.1186/s13287-019-1165-5

16. Liebisch T, Drusko A, Mathew B, Stelzer EHK, Fischer SC, Matthäus F. Cell fate clusters in ICM organoids arise from cell fate heredity and division: a modelling approach. *Sci Rep* (2020) **10**: doi:10.1038/s41598-020-80141-3

17. Artus J, Chazaud C. A close look at the mammalian blastocyst: epiblast and primitive endoderm formation. *Cell Mol Life Sci CMLS* (2014) **71**:3327–3338. doi:10.1007/s00018-014-1630-3

18. Pijuan-Sala B, Griffiths JA, Guibentif C, Hiscock TW, Jawaid W, Calero-Nieto FJ, Mulas C, Ibarra-Soria X, Tyser RCV, Ho DLL, et al. A single-cell molecular map of mouse gastrulation and early organogenesis. *Nature* (2019) **566**:490–495. doi:10.1038/s41586-019-0933-9

19. Labusca L, Mashayekhi K. Human adult pluripotency: Facts and questions. *World J Stem Cells* (2019) **11**:1–12. doi:10.4252/wjsc.v11.i1.1

20. Parolini O, Soncini M, Evangelista M, Schmidt D. Amniotic membrane and amniotic fluid-derived cells: potential tools for regenerative medicine? *Regen Med* (2009) **4**:275–291. doi:10.2217/17460751.4.2.275

21. Pera MF, Reubinoff B, Trounson A. Human embryonic stem cells. *J Cell Sci* (2000) **113 ( Pt 1)**:5–10.

22. McKee C, Chaudhry GR. Advances and challenges in stem cell culture. *Colloids Surf B Biointerfaces* (2017) **159**:62–77. doi:10.1016/j.colsurfb.2017.07.051

23. Sobhani A, Khanlarkhani N, Baazm M, Mohammadzadeh F, Najafi A, Mehdinejadiani S, Sargolzaei Aval F. Multipotent Stem Cell and Current Application. *Acta Med Iran* (2017) **55**:6–23.

24. Takahashi K, Yamanaka S. Induction of pluripotent stem cells from mouse embryonic and adult fibroblast cultures by defined factors. *Cell* (2006) **126**:663–676. doi:10.1016/j.cell.2006.07.024

25. Mattioli M, Gloria A, Turriani M, Mauro A, Curini V, Russo V, Tetè S, Marchisio M, Pierdomenico L, Berardinelli P, et al. Stemness characteristics and osteogenic potential of sheep amniotic epithelial cells. *Cell Biol Int* (2012) **36**:7–19. doi:10.1042/CBI20100720

26. Dulak J, Szade K, Szade A, Nowak W, Józkowicz A. Adult stem cells: hopes and hypes of regenerative medicine. *Acta Biochim Pol* (2015) **62**:329–337. doi:10.18388/abp.2015_1023

27. Yin H, Price F, Rudnicki MA. Satellite cells and the muscle stem cell niche. *Physiol Rev* (2013) **93**:23–67. doi:10.1152/physrev.00043.2011

28. Majo F, Rochat A, Nicolas M, Jaoudé GA, Barrandon Y. Oligopotent stem cells are distributed throughout the mammalian ocular surface. *Nature* (2008) **456**:250–254. doi:10.1038/nature07406

29. Le Blanc K, Mougiakakos D. Multipotent mesenchymal stromal cells and the innate immune system. *Nat Rev Immunol* (2012) **12**:383–396. doi:10.1038/nri3209

30. Horwitz EM, Le Blanc K, Dominici M, Mueller I, Slaper-Cortenbach I, Marini FC, Deans RJ, Krause DS, Keating A, International Society for Cellular Therapy. Clarification of the nomenclature for MSC: The International Society for Cellular Therapy position statement. *Cytotherapy* (2005) **7**:393–395. doi:10.1080/14653240500319234

31. Clément F, Grockowiak E, Zylbersztejn F, Fossard G, Gobert S, Maguer-Satta V. Stem cell manipulation, gene therapy and the risk of cancer stem cell emergence. *Stem Cell Investig* (2017) **4**:67. doi:10.21037/sci.2017.07.03

32. Jacobs SA, Roobrouck VD, Verfaillie CM, Van Gool SW. Immunological characteristics of human mesenchymal stem cells and multipotent adult progenitor cells. *Immunol Cell Biol* (2013) **91**:32–39. doi:10.1038/icb.2012.64

33. Bianco P. “Mesenchymal” stem cells. *Annu Rev Cell Dev Biol* (2014) **30**:677–704. doi:10.1146/annurev-cellbio-100913-013132

34. Caplan AI. Mesenchymal Stem Cells: Time to Change the Name! *Stem Cells Transl Med* (2017) **6**:1445–1451. doi:10.1002/sctm.17-0051

35. Dominici M, Blanc KL, Mueller I, Slaper-Cortenbach I, Marini FC, Krause DS, Deans RJ, Keating A, Prockop DJ, Horwitz EM. Minimal criteria for defining multipotent mesenchymal stromal cells. The International Society for Cellular Therapy position statement. *Cytotherapy* (2006) **8**:315–317. doi:10.1080/14653240600855905

36. Crisostomo V, Casado JG, Baez-Diaz C, Blazquez R, Sanchez-Margallo FM. Allogeneic cardiac stem cell administration for acute myocardial infarction. *Expert Rev Cardiovasc Ther* (2015) **13**:285–299. doi:10.1586/14779072.2015.1011621

37. Prasad VK, Lucas KG, Kleiner GI, Talano JAM, Jacobsohn D, Broadwater G, Monroy R, Kurtzberg J. Efficacy and safety of ex vivo cultured adult human mesenchymal stem cells (Prochymal™) in pediatric patients with severe refractory acute graft-versus-host disease in a compassionate use study. *Biol Blood Marrow Transplant J Am Soc Blood Marrow Transplant* (2011) **17**:534–541. doi:10.1016/j.bbmt.2010.04.014

38. Bey E, Prat M, Duhamel P, Benderitter M, Brachet M, Trompier F, Battaglini P, Ernou I, Boutin L, Gourven M, et al. Emerging therapy for improving wound repair of severe radiation burns using local bone marrow-derived stem cell administrations. *Wound Repair Regen Off Publ Wound Heal Soc Eur Tissue Repair Soc* (2010) **18**:50–58. doi:10.1111/j.1524-475X.2009.00562.x

39. Blázquez R, Sánchez-Margallo FM, Crisóstomo V, Báez C, Maestre J, Álvarez V, Casado JG. Intrapericardial Delivery of Cardiosphere-Derived Cells: An Immunological Study in a Clinically Relevant Large Animal Model. *PloS One* (2016) **11**:e0149001. doi:10.1371/journal.pone.0149001

40. Buda R, Vannini F, Cavallo M, Baldassarri M, Luciani D, Mazzotti A, Pungetti C, Olivieri A, Giannini S. One-step arthroscopic technique for the treatment of osteochondral lesions of the knee with bone-marrow-derived cells: three years results. *Musculoskelet Surg* (2013) **97**:145–151. doi:10.1007/s12306-013-0242-7

41. Keller CA, Gonwa TA, Hodge DO, Hei DJ, Centanni JM, Zubair AC. Feasibility, Safety, and Tolerance of Mesenchymal Stem Cell Therapy for Obstructive Chronic Lung Allograft Dysfunction. *Stem Cells Transl Med* (2018) **7**:161–167. doi:10.1002/sctm.17-0198

42. Ciccocioppo R, Bernardo ME, Sgarella A, Maccario R, Avanzini MA, Ubezio C, Minelli A, Alvisi C, Vanoli A, Calliada F, et al. Autologous bone marrow-derived mesenchymal stromal cells in the treatment of fistulising Crohn's disease. *Gut* (2011) **60**:788–798. doi:10.1136/gut.2010.214841

43. Hernigou P, Poignard A, Beaujean F, Rouard H. Percutaneous autologous bone-marrow grafting for nonunions. Influence of the number and concentration of progenitor cells. *J Bone Joint Surg Am* (2005) **87**:1430–1437. doi:10.2106/JBJS.D.02215

44. Morata-Tarifa C, Macías-Sánchez MDM, Gutiérrez-Pizarraya A, Sanchez-Pernaute R. Mesenchymal stromal cells for the prophylaxis and treatment of graft-versus-host disease-a meta-analysis. *Stem Cell Res Ther* (2020) **11**:64. doi:10.1186/s13287-020-01592-z

45. Blázquez R, Sánchez-Margallo FM, Álvarez V, Usón A, Casado JG. Surgical meshes coated with mesenchymal stem cells provide an anti-inflammatory environment by a M2 macrophage polarization. *Acta Biomater* (2016) **31**:221–230. doi:10.1016/j.actbio.2015.11.057

46. Perico N, Casiraghi F, Remuzzi G. Clinical Translation of Mesenchymal Stromal Cell Therapies in Nephrology. *J Am Soc Nephrol JASN* (2018) **29**:362–375. doi:10.1681/ASN.2017070781

47. Detry O, Vandermeulen M, Delbouille M-H, Somja J, Bletard N, Briquet A, Lechanteur C, Giet O, Baudoux E, Hannon M, et al. Infusion of mesenchymal stromal cells after deceased liver transplantation: A phase I-II, open-label, clinical study. *J Hepatol* (2017) **67**:47–55. doi:10.1016/j.jhep.2017.03.001

48. Weiss DJ, Casaburi R, Flannery R, LeRoux-Williams M, Tashkin DP. A placebo-controlled, randomized trial of mesenchymal stem cells in COPD. *Chest* (2013) **143**:1590–1598. doi:10.1378/chest.12-2094

49. Karussis D, Karageorgiou C, Vaknin-Dembinsky A, Gowda-Kurkalli B, Gomori JM, Kassis I, Bulte JWM, Petrou P, Ben-Hur T, Abramsky O, et al. Safety and immunological effects of mesenchymal stem cell transplantation in patients with multiple sclerosis and amyotrophic lateral sclerosis. *Arch Neurol* (2010) **67**:1187–1194. doi:10.1001/archneurol.2010.248

50. Koh Y-G, Choi Y-J. Infrapatellar fat pad-derived mesenchymal stem cell therapy for knee osteoarthritis. *The Knee* (2012) **19**:902–907. doi:10.1016/j.knee.2012.04.001

51. Hernigou P, Daltro G, Filippini P, Mukasa MM, Manicom O. Percutaneous implantation of autologous bone marrow osteoprogenitor cells as treatment of bone avascular necrosis related to sickle cell disease. *Open Orthop J* (2008) **2**:62–65. doi:10.2174/1874325000802010062

52. Venkataramana NK, Kumar SKV, Balaraju S, Radhakrishnan RC, Bansal A, Dixit A, Rao DK, Das M, Jan M, Gupta PK, et al. Open-labeled study of unilateral autologous bone-marrow-derived mesenchymal stem cell transplantation in Parkinson's disease. *Transl Res J Lab Clin Med* (2010) **155**:62–70. doi:10.1016/j.trsl.2009.07.006

53. Li R, Zhang Y, Zheng X, Peng S, Yuan K, Zhang X, Min W. Synergistic suppression of autoimmune arthritis through concurrent treatment with tolerogenic DC and MSC. *Sci Rep* (2017) **7**:43188. doi:10.1038/srep43188

54. Ceresa CDL, Ramcharan RN, Friend PJ, Vaidya A. Mesenchymal stromal cells promote bowel regeneration after intestinal transplantation: myth to mucosa. *Transpl Int Off J Eur Soc Organ Transplant* (2013) **26**:e91-93. doi:10.1111/tri.12139

55. Gan Y, Dai K, Zhang P, Tang T, Zhu Z, Lu J. The clinical use of enriched bone marrow stem cells combined with porous beta-tricalcium phosphate in posterior spinal fusion. *Biomaterials* (2008) **29**:3973–3982. doi:10.1016/j.biomaterials.2008.06.026

56. Park JH, Kim DY, Sung IY, Choi GH, Jeon MH, Kim KK, Jeon SR. Long-term results of spinal cord injury therapy using mesenchymal stem cells derived from bone marrow in humans. *Neurosurgery* (2012) **70**:1238–1247; discussion 1247. doi:10.1227/NEU.0b013e31824387f9

57. Savitz SI, Misra V, Kasam M, Juneja H, Cox CS, Alderman S, Aisiku I, Kar S, Gee A, Grotta JC. Intravenous autologous bone marrow mononuclear cells for ischemic stroke. *Ann Neurol* (2011) **70**:59–69. doi:10.1002/ana.22458

58. Casado JG, Blázquez R, Vela FJ, Álvarez V, Tarazona R, Sánchez-Margallo FM. Mesenchymal Stem Cell-Derived Exosomes: Immunomodulatory Evaluation in an Antigen-Induced Synovitis Porcine Model. *Front Vet Sci* (2017) **4**:39. doi:10.3389/fvets.2017.00039

59. Wang D, Wang S, Huang S, Zhang Z, Yuan X, Feng X, Lu L, Sun L. Serum IFN-γ Predicts the Therapeutic Effect of Mesenchymal Stem Cells Transplantation in Systemic Lupus Erythematosus Patients. *Stem Cells Transl Med* (2017) **6**:1777–1785. doi:10.1002/sctm.17-0002

60. Serakinci N, Savtekin G. Modeling Mesenchymal Stem Cells in TMJ Rheumatoid Arthritis and Osteoarthritis Therapy. *Crit Rev Eukaryot Gene Expr* (2017) **27**:205–210. doi:10.1615/CritRevEukaryotGeneExpr.2017019380

61. Haack-Sørensen M, Friis T, Mathiasen AB, Jørgensen E, Hansen L, Dickmeiss E, Ekblond A, Kastrup J. Direct intramyocardial mesenchymal stromal cell injections in patients with severe refractory angina: one-year follow-up. *Cell Transplant* (2013) **22**:521–528. doi:10.3727/096368912X636830

62. Levy O, Kuai R, Siren EMJ, Bhere D, Milton Y, Nissar N, De Biasio M, Heinelt M, Reeve B, Abdi R, et al. Shattering barriers toward clinically meaningful MSC therapies. *Sci Adv* (2020) **6**:eaba6884. doi:10.1126/sciadv.aba6884

63. Sánchez A, Schimmang T, García-Sancho J. Cell and tissue therapy in regenerative medicine. *Adv Exp Med Biol* (2012) **741**:89–102. doi:10.1007/978-1-4614-2098-9_7

64. Reisman M, Adams KT. Stem cell therapy: a look at current research, regulations, and remaining hurdles. *P T Peer-Rev J Formul Manag* (2014) **39**:846–857.

65. Rajabzadeh N, Fathi E, Farahzadi R. Stem cell-based regenerative medicine. *Stem Cell Investig* (2019) **6**:19. doi:10.21037/sci.2019.06.04

66. Leng Z, Zhu R, Hou W, Feng Y, Yang Y, Han Q, Shan G, Meng F, Du D, Wang S, et al. Transplantation of ACE2- Mesenchymal Stem Cells Improves the Outcome of Patients with COVID-19 Pneumonia. *Aging Dis* (2020) **11**:216. doi:10.14336/AD.2020.0228

67. Shu L, Niu C, Li R, Huang T, Wang Y, Huang M, Ji N, Zheng Y, Chen X, Shi L, et al. Treatment of severe COVID-19 with human umbilical cord mesenchymal stem cells. *Stem Cell Res Ther* (2020) **11**:361. doi:10.1186/s13287-020-01875-5

68. Lanzoni G, Linetsky E, Correa D, Messinger Cayetano S, Alvarez RA, Kouroupis D, Alvarez Gil A, Poggioli R, Ruiz P, Marttos AC, et al. Umbilical cord mesenchymal stem cells for COVID-19 acute respiratory distress syndrome: A double-blind, phase 1/2a, randomized controlled trial. *Stem Cells Transl Med* (2021) **10**:660–673. doi:10.1002/sctm.20-0472

69. Eder C, Wild C. Technology forecast: advanced therapies in late clinical research, EMA approval or clinical application via hospital exemption. *J Mark Access Health Policy* (2019) **7**:1600939. doi:10.1080/20016689.2019.1600939

70. Golchin A, Farahany TZ. Biological Products: Cellular Therapy and FDA Approved Products. *Stem Cell Rev Rep* (2019) **15**:166–175. doi:10.1007/s12015-018-9866-1

71. Campbell A, Brieva T, Raviv L, Rowley J, Niss K, Brandwein H, Oh S, Karnieli O. Concise Review: Process Development Considerations for Cell Therapy. *STEM CELLS Transl Med* (2015) **4**:1155–1163. doi:10.5966/sctm.2014-0294

72. Mount NM, Ward SJ, Kefalas P, Hyllner J. Cell-based therapy technology classifications and translational challenges. *Philos Trans R Soc B Biol Sci* (2015) **370**: doi:10.1098/rstb.2015.0017

73. Hoogduijn MJ. Are mesenchymal stromal cells immune cells? *Arthritis Res Ther* (2015) **17**:88. doi:10.1186/s13075-015-0596-3

74. Xia J, Minamino S, Kuwabara K, Arai S. Stem cell secretome as a new booster for regenerative medicine. *Biosci Trends* (2019) **13**:299–307. doi:10.5582/bst.2019.01226

75. Weiss ARR, Dahlke MH. Immunomodulation by Mesenchymal Stem Cells (MSCs): Mechanisms of Action of Living, Apoptotic, and Dead MSCs. *Front Immunol* (2019) **10**: doi:10.3389/fimmu.2019.01191

76. de Witte SFH, Franquesa M, Baan CC, Hoogduijn MJ. Toward Development of iMesenchymal Stem Cells for Immunomodulatory Therapy. *Front Immunol* (2015) **6**:648. doi:10.3389/fimmu.2015.00648

77. Castro-Manrreza ME, Montesinos JJ. Immunoregulation by mesenchymal stem cells: biological aspects and clinical applications. *J Immunol Res* (2015) **2015**:394917. doi:10.1155/2015/394917

78. Aggarwal S, Pittenger MF. Human mesenchymal stem cells modulate allogeneic immune cell responses. *Blood* (2005) **105**:1815–1822. doi:10.1182/blood-2004-04-1559

79. Beyth S, Borovsky Z, Mevorach D, Liebergall M, Gazit Z, Aslan H, Galun E, Rachmilewitz J. Human mesenchymal stem cells alter antigen-presenting cell maturation and induce T-cell unresponsiveness. *Blood* (2005) **105**:2214–2219. doi:10.1182/blood-2004-07-2921

80. Rasmusson I, Ringdén O, Sundberg B, Le Blanc K. Mesenchymal stem cells inhibit lymphocyte proliferation by mitogens and alloantigens by different mechanisms. *Exp Cell Res* (2005) **305**:33–41. doi:10.1016/j.yexcr.2004.12.013

81. Fan L, Hu C, Chen J, Cen P, Wang J, Li L. Interaction between Mesenchymal Stem Cells and B-Cells. *Int J Mol Sci* (2016) **17**: doi:10.3390/ijms17050650

82. Le Blanc K, Davies LC. Mesenchymal stromal cells and the innate immune response. *Immunol Lett* (2015) **168**:140–146. doi:10.1016/j.imlet.2015.05.004

83. Martinez FO, Gordon S. The M1 and M2 paradigm of macrophage activation: time for reassessment. *F1000prime Rep* (2014) **6**:13. doi:10.12703/P6-13

84. Murray PJ, Wynn TA. Protective and pathogenic functions of macrophage subsets. *Nat Rev Immunol* (2011) **11**:723–737. doi:10.1038/nri3073

85. Shi C, Pamer EG. Monocyte recruitment during infection and inflammation. *Nat Rev Immunol* (2011) **11**:762–774. doi:10.1038/nri3070

86. Bernardo ME, Fibbe WE. Mesenchymal Stromal Cells: Sensors and Switchers of Inflammation. *Cell Stem Cell* (2013) **13**:392–402. doi:10.1016/j.stem.2013.09.006

87. Ter Horst EN, Naaijkens BA, Krijnen PA, Van Der Laan AM, Piek JJ, Niessen HW. Induction of a monocyte/macrophage phenotype switch by mesenchymal stem cells might contribute to improved infarct healing postacute myocardial infarction. *Minerva Cardioangiol* (2013) **61**:617–625.

88. Luz-Crawford P, Djouad F, Toupet K, Bony C, Franquesa M, Hoogduijn MJ, Jorgensen C, Noël D. Mesenchymal Stem Cell-Derived Interleukin 1 Receptor Antagonist Promotes Macrophage Polarization and Inhibits B Cell Differentiation. *STEM CELLS* (2016) **34**:483–492. doi:https://doi.org/10.1002/stem.2254

89. Kim J, Hematti P. Mesenchymal stem cell-educated macrophages: a novel type of alternatively activated macrophages. *Exp Hematol* (2009) **37**:1445–1453. doi:10.1016/j.exphem.2009.09.004

90. Eggenhofer E, Hoogduijn MJ. Mesenchymal stem cell-educated macrophages. *Transplant Res* (2012) **1**:12. doi:10.1186/2047-1440-1-12

91. Gao S, Mao F, Zhang B, Zhang L, Zhang X, Wang M, Yan Y, Yang T, Zhang J, Zhu W, et al. Mouse bone marrow-derived mesenchymal stem cells induce macrophage M2 polarization through the nuclear factor-κB and signal transducer and activator of transcription 3 pathways. *Exp Biol Med Maywood NJ* (2014) **239**:366–375. doi:10.1177/1535370213518169

92. Stockwin LH, McGonagle D, Martin IG, Blair GE. Dendritic cells: Immunological sentinels with a central role in health and disease. *Immunol Cell Biol* (2000) **78**:91–102. doi:10.1046/j.1440-1711.2000.00888.x

93. Jiang X-X, Zhang Y, Liu B, Zhang S-X, Wu Y, Yu X-D, Mao N. Human mesenchymal stem cells inhibit differentiation and function of monocyte-derived dendritic cells. *Blood* (2005) **105**:4120–4126. doi:10.1182/blood-2004-02-0586

94. Spaggiari GM, Abdelrazik H, Becchetti F, Moretta L. MSCs inhibit monocyte-derived DC maturation and function by selectively interfering with the generation of immature DCs: central role of MSC-derived prostaglandin E2. *Blood* (2009) **113**:6576–6583. doi:10.1182/blood-2009-02-203943

95. Moloudizargari M, Govahi A, Fallah M, Rezvanfar MA, Asghari MH, Abdollahi M. The mechanisms of cellular crosstalk between mesenchymal stem cells and natural killer cells: Therapeutic implications. *J Cell Physiol* (2020) doi:10.1002/jcp.30038

96. Tu Z, Li Q, Bu H, Lin F. Mesenchymal stem cells inhibit complement activation by secreting factor H. *Stem Cells Dev* (2010) **19**:1803–1809. doi:10.1089/scd.2009.0418

97. Sagaradze GD, Basalova NA, Efimenko AY, Tkachuk VA. Mesenchymal Stromal Cells as Critical Contributors to Tissue Regeneration. *Front Cell Dev Biol* (2020) **8**: doi:10.3389/fcell.2020.576176

98. Ayala-Cuellar AP, Kang J-H, Jeung E-B, Choi K-C. Roles of Mesenchymal Stem Cells in Tissue Regeneration and Immunomodulation. *Biomol Ther* (2019) **27**:25–33. doi:10.4062/biomolther.2017.260

99. Fu Y, Karbaat L, Wu L, Leijten J, Both SK, Karperien M. Trophic Effects of Mesenchymal Stem Cells in Tissue Regeneration. *Tissue Eng Part B Rev* (2017) **23**:515–528. doi:10.1089/ten.TEB.2016.0365

100. Wang Y, Huang J, Gong L, Yu D, An C, Bunpetch V, Dai J, Huang H, Zou X, Ouyang H, et al. The Plasticity of Mesenchymal Stem Cells in Regulating Surface HLA-I. *iScience* (2019) **15**:66–78. doi:10.1016/j.isci.2019.04.011

101. Musiał-Wysocka A, Kot M, Majka M. The Pros and Cons of Mesenchymal Stem Cell-Based Therapies. *Cell Transplant* (2019) **28**:801–812. doi:10.1177/0963689719837897

102. Lukomska B, Stanaszek L, Zuba-Surma E, Legosz P, Sarzynska S, Drela K. Challenges and Controversies in Human Mesenchymal Stem Cell Therapy. *Stem Cells Int* (2019) **2019**:e9628536. doi:https://doi.org/10.1155/2019/9628536

103. Bauer G, Elsallab M, Abou-El-Enein M. Concise Review: A Comprehensive Analysis of Reported Adverse Events in Patients Receiving Unproven Stem Cell-Based Interventions. *STEM CELLS Transl Med* (2018) **7**:676–685. doi:https://doi.org/10.1002/sctm.17-0282

104. Mautino B. *Stamina: una storia sbagliata*. Comitato Italiano per il Controllo delle Affermazioni sulle Pseudoscienze (CICAP) (2014).

105. Garattini S, Remuzzi G, Vago G, Zangrillo A. Stamina therapies: Time to call a halt. *Nature* (2014) **506**:434–434. doi:10.1038/506434b

106. Fischer UM, Harting MT, Jimenez F, Monzon-Posadas WO, Xue H, Savitz SI, Laine GA, Cox CS. Pulmonary Passage is a Major Obstacle for Intravenous Stem Cell Delivery: The Pulmonary First-Pass Effect. *Stem Cells Dev* (2009) **18**:683–691. doi:10.1089/scd.2008.0253

107. Eggenhofer E, Benseler V, Kroemer A, Popp F, Geissler E, Schlitt H, Baan C, Dahlke M, Hoogduijn MJ. Mesenchymal stem cells are short-lived and do not migrate beyond the lungs after intravenous infusion. *Front Immunol* (2012) **3**: doi:10.3389/fimmu.2012.00297

108. Zhang J, Huang X, Wang H, Liu X, Zhang T, Wang Y, Hu D. The challenges and promises of allogeneic mesenchymal stem cells for use as a cell-based therapy. *Stem Cell Res Ther* (2015) **6**:234. doi:10.1186/s13287-015-0240-9

109. Du G, Liu Y, Dang M, Zhu G, Su R, Fan Y, Tan Z, Wang LX, Fang J. Comparison of administration routes for adipose-derived stem cells in the treatment of middle cerebral artery occlusion in rats. *Acta Histochem* (2014) **116**:1075–1084. doi:10.1016/j.acthis.2014.05.002

110. Golpanian S, Schulman IH, Ebert RF, Heldman AW, DiFede DL, Yang PC, Wu JC, Bolli R, Perin EC, Moyé L, et al. Concise Review: Review and Perspective of Cell Dosage and Routes of Administration From Preclinical and Clinical Studies of Stem Cell Therapy for Heart Disease. *STEM CELLS Transl Med* (2016) **5**:186–191. doi:https://doi.org/10.5966/sctm.2015-0101

111. Blázquez R, Sánchez-Margallo FM, Crisóstomo V, Báez C, Maestre J, García-Lindo M, Usón A, Álvarez V, Casado JG. Intrapericardial administration of mesenchymal stem cells in a large animal model: a bio-distribution analysis. *PloS One* (2015) **10**:e0122377. doi:10.1371/journal.pone.0122377

112. Mendt M, Rezvani K, Shpall E. Mesenchymal stem cell-derived exosomes for clinical use. *Bone Marrow Transplant* (2019) **54**:789–792. doi:10.1038/s41409-019-0616-z

113. Wiklander OPB, Brennan MÁ, Lötvall J, Breakefield XO, Andaloussi SE. Advances in therapeutic applications of extracellular vesicles. *Sci Transl Med* (2019) **11**: doi:10.1126/scitranslmed.aav8521

114. Mallia A, Gianazza E, Zoanni B, Brioschi M, Barbieri SS, Banfi C. Proteomics of Extracellular Vesicles: Update on Their Composition, Biological Roles and Potential Use as Diagnostic Tools in Atherosclerotic Cardiovascular Diseases. *Diagn Basel Switz* (2020) **10**: doi:10.3390/diagnostics10100843

115. Doyle LM, Wang MZ. Overview of Extracellular Vesicles, Their Origin, Composition, Purpose, and Methods for Exosome Isolation and Analysis. *Cells* (2019) **8**: doi:10.3390/cells8070727

116. Li M, Liao L, Tian W. Extracellular Vesicles Derived From Apoptotic Cells: An Essential Link Between Death and Regeneration. *Front Cell Dev Biol* (2020) **8**: doi:10.3389/fcell.2020.573511

117. Abels ER, Breakefield XO. Introduction to Extracellular Vesicles: Biogenesis, RNA Cargo Selection, Content, Release, and Uptake. *Cell Mol Neurobiol* (2016) **36**:301–312. doi:10.1007/s10571-016-0366-z

118. Trams EG, Lauter CJ, Salem N, Heine U. Exfoliation of membrane ecto-enzymes in the form of micro-vesicles. *Biochim Biophys Acta* (1981) **645**:63–70. doi:10.1016/0005-2736(81)90512-5

119. Lötvall J, Hill AF, Hochberg F, Buzás EI, Di Vizio D, Gardiner C, Gho YS, Kurochkin IV, Mathivanan S, Quesenberry P, et al. Minimal experimental requirements for definition of extracellular vesicles and their functions: a position statement from the International Society for Extracellular Vesicles. *J Extracell Vesicles* (2014) **3**: doi:10.3402/jev.v3.26913

120. Théry C, Witwer KW, Aikawa E, Alcaraz MJ, Anderson JD, Andriantsitohaina R, Antoniou A, Arab T, Archer F, Atkin-Smith GK, et al. Minimal information for studies of extracellular vesicles 2018 (MISEV2018): a position statement of the International Society for Extracellular Vesicles and update of the MISEV2014 guidelines. *J Extracell Vesicles* (2018) **7**: doi:10.1080/20013078.2018.1535750

121. Klyachko NL, Arzt CJ, Li SM, Gololobova OA, Batrakova EV. Extracellular Vesicle-Based Therapeutics: Preclinical and Clinical Investigations. *Pharmaceutics* (2020) **12**: doi:10.3390/pharmaceutics12121171

122. Alhomrani M, Correia J, Zavou M, Leaw B, Kuk N, Xu R, Saad MI, Hodge A, Greening DW, Lim R, et al. The Human Amnion Epithelial Cell Secretome Decreases Hepatic Fibrosis in Mice with Chronic Liver Fibrosis. *Front Pharmacol* (2017) **8**: doi:10.3389/fphar.2017.00748

123. Tan JL, Lau SN, Leaw B, Nguyen HPT, Salamonsen LA, Saad MI, Chan ST, Zhu D, Krause M, Kim C, et al. Amnion Epithelial Cell-Derived Exosomes Restrict Lung Injury and Enhance Endogenous Lung Repair. *STEM CELLS Transl Med* (2018) **7**:180–196. doi:https://doi.org/10.1002/sctm.17-0185

124. Xing Z, Zhao C, Liu H, Fan Y. Endothelial Progenitor Cell-Derived Extracellular Vesicles: A Novel Candidate for Regenerative Medicine and Disease Treatment. *Adv Healthc Mater* (2020) **9**:2000255. doi:https://doi.org/10.1002/adhm.202000255

125. Nawaz M, Fatima F, Vallabhaneni KC, Penfornis P, Valadi H, Ekström K, Kholia S, Whitt JD, Fernandes JD, Pochampally R, et al. Extracellular Vesicles: Evolving Factors in Stem Cell Biology. *Stem Cells Int* (2015) **2016**:e1073140. doi:https://doi.org/10.1155/2016/1073140

126. Hur YH, Feng S, Wilson KF, Cerione RA, Antonyak MA. Embryonic Stem Cell-Derived Extracellular Vesicles Maintain ESC Stemness by Activating FAK. *Dev Cell* (2021) **56**:277-291.e6. doi:10.1016/j.devcel.2020.11.017

127. Popowski KD, Dinh P-UC, George A, Lutz H, Cheng K. Exosome therapeutics for COVID-19 and respiratory viruses. *View* **n/a**:20200186. doi:https://doi.org/10.1002/VIW.20200186

128. Galieva LR, James V, Mukhamedshina YO, Rizvanov AA. Therapeutic Potential of Extracellular Vesicles for the Treatment of Nerve Disorders. *Front Neurosci* (2019) **13**: doi:10.3389/fnins.2019.00163

129. Parfejevs V, Sagini K, Buss A, Sobolevska K, Llorente A, Riekstina U, Abols A. Adult Stem Cell-Derived Extracellular Vesicles in Cancer Treatment: Opportunities and Challenges. *Cells* (2020) **9**: doi:10.3390/cells9051171

130. Tang T-T, Lv L-L, Lan H-Y, Liu B-C. Extracellular Vesicles: Opportunities and Challenges for the Treatment of Renal Diseases. *Front Physiol* (2019) **10**: doi:10.3389/fphys.2019.00226

131. Tian J, Casella G, Zhang Y, Rostami A, Li X. Potential roles of extracellular vesicles in the pathophysiology, diagnosis, and treatment of autoimmune diseases. *Int J Biol Sci* (2020) **16**:620–632. doi:10.7150/ijbs.39629

132. Piazza N, Dehghani M, Gaborski TR, Wuertz-Kozak K. Therapeutic Potential of Extracellular Vesicles in Degenerative Diseases of the Intervertebral Disc. *Front Bioeng Biotechnol* (2020) **8**: doi:10.3389/fbioe.2020.00311

133. Shaimardanova AA, Solovyeva VV, Chulpanova DS, James V, Kitaeva KV, Rizvanov AA. Extracellular vesicles in the diagnosis and treatment of central nervous system diseases. *Neural Regen Res* (2020) **15**:586–596. doi:10.4103/1673-5374.266908

134. Boere J, Malda J, van de Lest CHA, van Weeren PR, Wauben MHM. Extracellular Vesicles in Joint Disease and Therapy. *Front Immunol* (2018) **9**: doi:10.3389/fimmu.2018.02575

135. Alcaraz MJ, Compañ A, Guillén MI. Extracellular Vesicles from Mesenchymal Stem Cells as Novel Treatments for Musculoskeletal Diseases. *Cells* (2020) **9**:98. doi:10.3390/cells9010098

136. Ali M, Pham A, Wang X, Wolfram J, Pham S. Extracellular vesicles for treatment of solid organ ischemia–reperfusion injury. *Am J Transplant* **n/a**: doi:10.1111/ajt.16164

137. Wang J, Huang R, Xu Q, Zheng G, Qiu G, Ge M, Shu Q, Xu J. Mesenchymal Stem Cell–Derived Extracellular Vesicles Alleviate Acute Lung Injury Via Transfer of miR-27a-3p*. *Crit Care Med* (2020) **48**:e599. doi:10.1097/CCM.0000000000004315

138. Yang L, Zhu J, Zhang C, Wang J, Yue F, Jia X, Liu H. Stem cell-derived extracellular vesicles for myocardial infarction: a meta-analysis of controlled animal studies. *Aging* (2019) **11**:1129–1150. doi:10.18632/aging.101814

139. Chong SY, Lee CK, Huang C, Ou YH, Charles CJ, Richards AM, Neupane YR, Pavon MV, Zharkova O, Pastorin G, et al. Extracellular Vesicles in Cardiovascular Diseases: Alternative Biomarker Sources, Therapeutic Agents, and Drug Delivery Carriers. *Int J Mol Sci* (2019) **20**: doi:10.3390/ijms20133272

140. Baylón K, Rodríguez-Camarillo P, Elías-Zúñiga A, Díaz-Elizondo JA, Gilkerson R, Lozano K. Past, Present and Future of Surgical Meshes: A Review. *Membranes* (2017) **7**: doi:10.3390/membranes7030047

141. Pulikkottil BJ, Pezeshk RA, Daniali LN, Bailey SH, Mapula S, Hoxworth RE. Lateral Abdominal Wall Defects: The Importance of Anatomy and Technique for a Successful Repair. *Plast Reconstr Surg Glob Open* (2015) **3**:e481. doi:10.1097/GOX.0000000000000439

142. Finan KR, Kilgore ML, Hawn MT. Open suture versus mesh repair of primary incisional hernias: a cost-utility analysis. *Hernia J Hernias Abdom Wall Surg* (2009) **13**:173–182. doi:10.1007/s10029-008-0462-1

143. Rastegarpour A, Cheung M, Vardhan M, Ibrahim MM, Butler CE, Levinson H. Surgical mesh for ventral incisional hernia repairs: Understanding mesh design. *Plast Surg* (2016) **24**:41–50.

144. Vorst AL, Kaoutzanis C, Carbonell AM, Franz MG. Evolution and advances in laparoscopic ventral and incisional hernia repair. *World J Gastrointest Surg* (2015) **7**:293–305. doi:10.4240/wjgs.v7.i11.293

145. Majumder A, Neupane R, Novitsky YW. Antibiotic Coating of Hernia Meshes: The Next Step Toward Preventing Mesh Infection. *Surg Technol Int* (2015) **27**:147–153.

146. Bredikhin M, Gil D, Rex J, Cobb W, Reukov V, Vertegel A. Anti-inflammatory coating of hernia repair meshes: a 5-rabbit study. *Hernia J Hernias Abdom Wall Surg* (2020) doi:10.1007/s10029-020-02122-9

147. Poppas DP, Sung JJ, Magro CM, Chen J, Toyohara JP, Ramshaw BJ, Felsen D. Hydrogel coated mesh decreases tissue reaction resulting from polypropylene mesh implant: implication in hernia repair. *Hernia J Hernias Abdom Wall Surg* (2016) **20**:623–632. doi:10.1007/s10029-016-1481-y

148. Lyons M, Mohan H, Winter DC, Simms CK. Biomechanical abdominal wall model applied to hernia repair. *BJS Br J Surg* (2015) **102**:e133–e139. doi:https://doi.org/10.1002/bjs.9687

149. Blázquez R, Sánchez-Margallo FM, Álvarez V, Usón A, Marinaro F, Casado JG. Fibrin glue mesh fixation combined with mesenchymal stem cells or exosomes modulates the inflammatory reaction in a murine model of incisional hernia. *Acta Biomater* (2018) **71**:318–329. doi:10.1016/j.actbio.2018.02.014

150. Monteiro GA, Delossantos AI, Rodriguez NL, Patel P, Franz MG, Wagner CT. Porcine incisional hernia model: Evaluation of biologically derived intact extracellular matrix repairs. *J Tissue Eng* (2013) **4**: doi:10.1177/2041731413508771

151. Grindflek E, Hansen MHS, Lien S, van Son M. Genome-wide association study reveals a QTL and strong candidate genes for umbilical hernia in pigs on SSC14. *BMC Genomics* (2018) **19**:412. doi:10.1186/s12864-018-4812-9

152. Atkinson M, Amezcua R, DeLay J, Widowski T, Friendship R. Evaluation of the effect of umbilical hernias on play behaviors in growing pigs. *Can Vet J Rev Veterinaire Can* (2017) **58**:1065–1072.

153. Bassols A, Costa C, Eckersall PD, Osada J, Sabrià J, Tibau J. The pig as an animal model for human pathologies: A proteomics perspective. *PROTEOMICS - Clin Appl* (2014) **8**:715–731. doi:10.1002/prca.201300099

154. Schook LB, Collares TV, Darfour-Oduro KA, De AK, Rund LA, Schachtschneider KM, Seixas FK. Unraveling the Swine Genome: Implications for Human Health. *Annu Rev Anim Biosci* (2015) **3**:219–244. doi:10.1146/annurev-animal-022114-110815

155. Gonzalez LM, Moeser AJ, Blikslager AT. Porcine models of digestive disease: the future of large animal translational research. *Transl Res J Lab Clin Med* (2015) **166**:12–27. doi:10.1016/j.trsl.2015.01.004

156. Kemppainen BW ed. *Methods for skin absorption*. Boca Raton, Fl.: CRC Press (1990).

157. Avon SL, Wood RE. Porcine skin as an in-vivo model for ageing of human bite marks. *J Forensic Odontostomatol* (2005) **23**:30–39.

158. Debeer S, Le Luduec J-B, Kaiserlian D, Laurent P, Nicolas J-F, Dubois B, Kanitakis J. Comparative histology and immunohistochemistry of porcine versus human skin. *Eur J Dermatol* (2013) **23**:456–466. doi:10.1684/ejd.2013.2060

159. Wei JCJ, Edwards GA, Martin DJ, Huang H, Crichton ML, Kendall MAF. Allometric scaling of skin thickness, elasticity, viscoelasticity to mass for micro-medical device translation: from mice, rats, rabbits, pigs to humans. *Sci Rep* (2017) **7**:15885. doi:10.1038/s41598-017-15830-7

160. Fossum TW, Duprey LP eds. *Small animal surgery*. Fifth edition. Philadelphia, PA: Elsevier (2019).

161. Marinaro F, Sánchez-Margallo FM, Álvarez V, López E, Tarazona R, Brun MV, Blázquez R, Casado JG. Meshes in a mess: Mesenchymal stem cell-based therapies for soft tissue reinforcement. *Acta Biomater* (2019) **85**:60–74. doi:10.1016/j.actbio.2018.11.042

162. Ong S-B, Hernández-Reséndiz S, Crespo-Avilan GE, Mukhametshina RT, Kwek X-Y, Cabrera-Fuentes HA, Hausenloy DJ. Inflammation following acute myocardial infarction: Multiple players, dynamic roles, and novel therapeutic opportunities. *Pharmacol Ther* (2018) **186**:73–87. doi:10.1016/j.pharmthera.2018.01.001

163. Hausenloy DJ, Yellon DM. Myocardial ischemia-reperfusion injury: a neglected therapeutic target. *J Clin Invest* (2013) **123**:92–100. doi:10.1172/JCI62874

164. Braunwald E. The treatment of acute myocardial infarction: the Past, the Present, and the Future. *Eur Heart J Acute Cardiovasc Care* (2012) **1**:9–12. doi:10.1177/2048872612438026

165. Roth GA, Abate D, Abate KH, Abay SM, Abbafati C, Abbasi N, Abbastabar H, Abd-Allah F, Abdela J, Abdelalim A, et al. Global, regional, and national age-sex-specific mortality for 282 causes of death in 195 countries and territories, 1980–2017: a systematic analysis for the Global Burden of Disease Study 2017. *The Lancet* (2018) **392**:1736–1788. doi:10.1016/S0140-6736(18)32203-7

166. Huang S, Frangogiannis NG. Anti-inflammatory therapies in myocardial infarction: failures, hopes and challenges. *Br J Pharmacol* (2018) **175**:1377–1400. doi:10.1111/bph.14155

167. Munir H, Ward LSC, McGettrick HM. Mesenchymal Stem Cells as Endogenous Regulators of Inflammation. *Adv Exp Med Biol* (2018) **1060**:73–98. doi:10.1007/978-3-319-78127-3_5

168. Regulski MJ. Mesenchymal Stem Cells: "Guardians of Inflammation." *Wounds Compend Clin Res Pract* (2017) **29**:20–27.

169. van der Spoel TIG, Jansen of Lorkeers SJ, Agostoni P, van Belle E, Gyöngyösi M, Sluijter JPG, Cramer MJ, Doevendans PA, Chamuleau SAJ. Human relevance of pre-clinical studies in stem cell therapy:

systematic review and meta-analysis of large animal models of ischaemic heart disease. *Cardiovasc Res* (2011) **91**:649–658. doi:10.1093/cvr/cvr113

170. Heusch G, Skyschally A, Schulz R. The in-situ pig heart with regional ischemia/reperfusion - ready for translation. *J Mol Cell Cardiol* (2011) **50**:951–963. doi:10.1016/j.yjmcc.2011.02.016

171. Crisóstomo V, Maestre J, Maynar M, Sun F, Báez-Díaz C, Usón J, Sánchez-Margallo FM. Development of a Closed Chest Model of Chronic Myocardial Infarction in Swine: Magnetic Resonance Imaging and Pathological Evaluation. *ISRN Cardiol* (2013) **2013**: doi:10.1155/2013/781762

172. Koudstaal S, Jansen of Lorkeers SJ, Gho JMIH, van Hout GPJ, Jansen MS, Gründeman PF, Pasterkamp G, Doevendans PA, Hoefer IE, Chamuleau SAJ. Myocardial Infarction and Functional Outcome Assessment in Pigs. *J Vis Exp JoVE* (2014) **86**:e51269. doi:10.3791/51269

173. Babuin L, Jaffe AS. Troponin: the biomarker of choice for the detection of cardiac injury. *CMAJ Can Med Assoc J J Assoc Medicale Can* (2005) **173**:1191–1202. doi:10.1503/cmaj/051291

174. Blázquez R, Álvarez V, Antequera-Barroso JA, Báez-Díaz C, Blanco V, Maestre J, Moreno-Lobato B, López E, Marinaro F, Casado JG, et al. Altered hematological, biochemical and immunological parameters as predictive biomarkers of severity in experimental myocardial infarction. *Vet Immunol Immunopathol* (2018) **205**:49–57. doi:10.1016/j.vetimm.2018.10.007

175. Zhang Y, Mignone J, MacLellan WR. Cardiac Regeneration and Stem Cells. *Physiol Rev* (2015) **95**:1189–1204. doi:10.1152/physrev.00021.2014

176. Miao C, Lei M, Hu W, Han S, Wang Q. A brief review: the therapeutic potential of bone marrow mesenchymal stem cells in myocardial infarction. *Stem Cell Res Ther* (2017) **8**:242. doi:10.1186/s13287-017-0697-9

177. Inhorn MC, Patrizio P. Infertility around the globe: new thinking on gender, reproductive technologies and global movements in the 21st century. *Hum Reprod Update* (2015) **21**:411–426. doi:10.1093/humupd/dmv016

178. Sun H, Gong T-T, Jiang Y-T, Zhang S, Zhao Y-H, Wu Q-J. Global, regional, and national prevalence and disability-adjusted life-years for infertility in 195 countries and territories, 1990–2017: results from a global burden of disease study, 2017. *Aging* (2019) **11**:10952–10991. doi:10.18632/aging.102497

179. Campo-Engelstein L. For the Sake of Consistency and Fairness: Why Insurance Companies Should Cover Fertility Preservation Treatment for Iatrogenic Infertility. *Cancer Treat Res* (2010) **156**:381–388. doi:10.1007/978-1-4419-6518-9_29

180. Ubaldi FM, Cimadomo D, Vaiarelli A, Fabozzi G, Venturella R, Maggiulli R, Mazzilli R, Ferrero S, Palagiano A, Rienzi L. Advanced Maternal Age in IVF: Still a Challenge? The Present and the Future of Its Treatment. *Front Endocrinol* (2019) **10**: doi:10.3389/fendo.2019.00094

181. Liu J, Zheng J, Lei Y, Wen X. Effects of endometrial preparations and transferred embryo types on pregnancy outcome from patients with advanced maternal age. *Syst Biol Reprod Med* (2019) **65**:181–186. doi:10.1080/19396368.2018.1501114

182. De Geyter C, Calhaz-Jorge C, Kupka MS, Wyns C, Mocanu E, Motrenko T, Scaravelli G, Smeenk J, Vidakovic S, Goossens V, et al. ART in Europe, 2015: results generated from European registries by ESHRE. *Hum Reprod Open* (2020) **2020**: doi:10.1093/hropen/hoz038

183. Farhi J, Farhi J, Ben-Haroush A, Dresler H, Pinkas H, Sapir O, Fisch B. Male factor infertility, low fertilisation rate following ICSI and low number of high-quality embryos are associated with high order recurrent implantation failure in young IVF patientsa. *Acta Obstet Gynecol Scand* (2008) **87**:76–80. doi:10.1080/00016340701743074

184. Cagnone G, Sirard M-A. The embryonic stress response to in vitro culture: insight from genomic analysis. *Reproduction* (2016) **152**:R247–R261. doi:10.1530/REP-16-0391

185. Sunde A, Brison D, Dumoulin J, Harper J, Lundin K, Magli MC, Van den Abbeel E, Veiga A. Time to take human embryo culture seriously. *Hum Reprod* (2016) **31**:2174–2182. doi:10.1093/humrep/dew157

186. Highet AR, Bianco-Miotto T, Pringle KG, Peura A, Bent S, Zhang J, Nottle MB, Thompson JG, Roberts CT. A novel embryo culture media supplement that improves pregnancy rates in mice. *Reprod Camb Engl* (2017) **153**:327–340. doi:10.1530/REP-16-0517

187. Fazeli Z, Abedindo A, Omrani MD, Ghaderian SMH. Mesenchymal Stem Cells (MSCs) Therapy for Recovery of Fertility: a Systematic Review. *Stem Cell Rev Rep* (2018) **14**:1–12. doi:10.1007/s12015-017-9765-x

188. Malard PF, Peixer MAS, Grazia JG, Brunel H dos SS, Feres LF, Villarroel CL, Siqueira LGB, Dode MAN, Pogue R, Viana JHM, et al. Intraovarian injection of mesenchymal stem cells improves oocyte yield and in vitro embryo production in a bovine model of fertility loss. *Sci Rep* (2020) **10**:8018. doi:10.1038/s41598-020-64810-x

189. Domnina A, Novikova P, Obidina J, Fridlyanskaya I, Alekseenko L, Kozhukharova I, Lyublinskaya O, Zenin V, Nikolsky N. Human mesenchymal stem cells in spheroids improve fertility in model animals with damaged endometrium. *Stem Cell Res Ther* (2018) **9**:50. doi:10.1186/s13287-018-0801-9

190. Gervasi MG, Soler AJ, González-Fernández L, Alves MG, Oliveira PF, Martín-Hidalgo D. Extracellular Vesicles, the Road toward the Improvement of ART Outcomes. *Anim Open Access J MDPI* (2020) **10**: doi:10.3390/ani10112171

191. Greening DW, Nguyen HPT, Elgass K, Simpson RJ, Salamonsen LA. Human Endometrial Exosomes Contain Hormone-Specific Cargo Modulating Trophoblast Adhesive Capacity: Insights into Endometrial-Embryo Interactions. *Biol Reprod* (2016) **94**:38. doi:10.1095/biolreprod.115.134890

192. Homer H, Rice GE, Salomon C. Review: Embryo- and endometrium-derived exosomes and their potential role in assisted reproductive treatments-liquid biopsies for endometrial receptivity. *Placenta* (2017) **54**:89–94. doi:10.1016/j.placenta.2016.12.011

193. Bozorgmehr M, Gurung S, Darzi S, Nikoo S, Kazemnejad S, Zarnani A-H, Gargett CE. Endometrial and Menstrual Blood Mesenchymal Stem/Stromal Cells: Biological Properties and Clinical Application. *Front Cell Dev Biol* (2020) **8**: doi:10.3389/fcell.2020.00497

194. Mor G, Cardenas I, Abrahams V, Guller S. Inflammation and pregnancy: the role of the immune system at the implantation site. *Ann N Y Acad Sci* (2011) **1221**:80–87. doi:10.1111/j.1749-6632.2010.05938.x

195. Carter AM. Animal models of human pregnancy and placentation: alternatives to the mouse. *Reproduction* (2020) **160**:R129–R143. doi:10.1530/REP-20-0354

196. Rabadán-Diehl C, Nathanielsz P. From Mice to Men: research models of developmental programming. *J Dev Orig Health Dis* (2013) **4**:3–9. doi:10.1017/S2040174412000487

197. Klosterhalfen B, Klinge U, Schumpelick V. Functional and morphological evaluation of different polypropylene-mesh modifications for abdominal wall repair. *Biomaterials* (1998) **19**:2235–2246.

198. Klinge U, Schumpelick V, Klosterhalfen B. Functional assessment and tissue response of short- and long-term absorbable surgical meshes. *Biomaterials* (2001) **22**:1415–1424.

199. Leber GE, Garb JL, Alexander AI, Reed WP. Long-term complications associated with prosthetic repair of incisional hernias. *Arch Surg Chic Ill 1960* (1998) **133**:378–382.

200. SCENIHR (Scientific Committee on Emerging and Newly Identified Health Risks). Opinion on the safety of surgical meshes used in urogynecological surgery. (2015) Available at: https://ec.europa.eu/health/sites/health/files/scientific_committees/emerging/docs/scenihr_o_049.pdf [Accessed September 7, 2018]

201. Center for Devices and Radiological Health. Urogynecologic Surgical Mesh Implants - Urogynecologic Surgical Mesh Implants: Reporting Problems to the FDA. Available at:

https://www.fda.gov/MedicalDevices/ProductsandMedicalProcedures/ImplantsandProsthetics/UroGynSurgicalMesh/ucm262304.htm [Accessed September 7, 2018]

202. Administration AGD of HTG. TGA actions after review into urogynaecological surgical mesh implants. *Ther Goods Adm TGA* (2018) Available at: https://www.tga.gov.au/alert/tga-actions-after-review-urogynaecological-surgical-mesh-implants [Accessed November 5, 2018]

203. Zhao Y, Zhang Z, Wang J, Yin P, Zhou J, Zhen M, Cui W, Xu G, Yang D, Liu Z. Abdominal hernia repair with a decellularized dermal scaffold seeded with autologous bone marrow-derived mesenchymal stem cells. *Artif Organs* (2012) **36**:247–255. doi:10.1111/j.1525-1594.2011.01343.x

204. Zhang Y, Zhou Y, Zhou X, Zhao B, Chai J, Liu H, Zheng Y, Wang J, Wang Y, Zhao Y. Preparation of a nano- and micro-fibrous decellularized scaffold seeded with autologous mesenchymal stem cells for inguinal hernia repair. *Int J Nanomedicine* (2017) **12**:1441–1452. doi:10.2147/IJN.S125409

205. Spelzini F, Manodoro S, Frigerio M, Nicolini G, Maggioni D, Donzelli E, Altomare L, Farè S, Veneziano F, Avezza F, et al. Stem cell augmented mesh materials: an in vitro and in vivo study. *Int Urogynecology J* (2015) **26**:675–683. doi:10.1007/s00192-014-2570-z

206. Jankovičová J, Sečová P, Michalková K, Antalíková J. Tetraspanins, More than Markers of Extracellular Vesicles in Reproduction. *Int J Mol Sci* (2020) **21**: doi:10.3390/ijms21207568

207. Li Y, Meng H, Liu Y, Lee BP. Fibrin Gel as an Injectable Biodegradable Scaffold and Cell Carrier for Tissue Engineering. *Sci World J* (2015) **2015**:1–10. doi:10.1155/2015/685690

208. Spotnitz WD. Fibrin Sealant: The Only Approved Hemostat, Sealant, and Adhesive—a Laboratory and Clinical Perspective. *ISRN Surg* (2014) **2014**:e203943. doi:10.1155/2014/203943

209. Wolberg AS. Determinants of fibrin formation, structure, and function. *Curr Opin Hematol* (2012) **19**:349–356. doi:10.1097/MOH.0b013e32835673c2

210. Topart P, Vandenbroucke F, Lozac'h P. Tisseel versus tack staples as mesh fixation in totally extraperitoneal laparoscopic repair of groin hernias: a retrospective analysis. *Surg Endosc* (2005) **19**:724–727. doi:10.1007/s00464-004-8812-2

211. Katkhouda N, Mavor E, Friedlander MH, Mason RJ, Kiyabu M, Grant SW, Achanta K, Kirkman EL, Narayanan K, Essani R. Use of fibrin sealant for prosthetic mesh fixation in laparoscopic extraperitoneal inguinal hernia repair. *Ann Surg* (2001) **233**:18–25.

212. Lo Sicco C, Reverberi D, Balbi C, Ulivi V, Principi E, Pascucci L, Becherini P, Bosco MC, Varesio L, Franzin C, et al. Mesenchymal Stem Cell-Derived Extracellular Vesicles as Mediators of Anti-Inflammatory Effects:

Endorsement of Macrophage Polarization. *Stem Cells Transl Med* (2017) **6**:1018–1028. doi:10.1002/sctm.16-0363

213. Gnecchi M, Danieli P, Malpasso G, Ciuffreda MC. "Paracrine Mechanisms of Mesenchymal Stem Cells in Tissue Repair," in *Mesenchymal Stem Cells: Methods and Protocols* Methods in Molecular Biology., ed. M. Gnecchi (New York, NY: Springer), 123–146. doi:10.1007/978-1-4939-3584-0_7

214. Henriksen NA, Yadete DH, Sorensen LT, Ågren MS, Jorgensen LN. Connective tissue alteration in abdominal wall hernia. *Br J Surg* (2011) **98**:210–219. doi:10.1002/bjs.7339

215. Calaluce R, Davis JW, Bachman SL, Gubin MM, Brown JA, Magee JD, Loy TS, Ramshaw BJ, Atasoy U. Incisional hernia recurrence through genomic profiling: a pilot study. *Hernia* (2013) **17**:193–202. doi:10.1007/s10029-012-0923-4

216. HerniaSurge Group. International guidelines for groin hernia management. *Hernia J Hernias Abdom Wall Surg* (2018) **22**:1–165. doi:10.1007/s10029-017-1668-x

217. Bellafiore M, Battaglia G, Bianco A, Farina F, Palma A, Paoli A. The involvement of MMP-2 and MMP-9 in heart exercise-related angiogenesis. *J Transl Med* (2013) **11**:283. doi:10.1186/1479-5876-11-283

218. Bergers G, Brekken R, McMahon G, Vu TH, Itoh T, Tamaki K, Tanzawa K, Thorpe P, Itohara S, Werb Z, et al. Matrix metalloproteinase-9 triggers the angiogenic switch during carcinogenesis. *Nat Cell Biol* (2000) **2**:737–744. doi:10.1038/35036374

219. Muller M, Trocme C, Lardy B, Morel F, Halimi S, Benhamou PY. Matrix metalloproteinases and diabetic foot ulcers: the ratio of MMP-1 to TIMP-1 is a predictor of wound healing. *Diabet Med J Br Diabet Assoc* (2008) **25**:419–426. doi:10.1111/j.1464-5491.2008.02414.x

220. Altman AM, Abdul Khalek FJ, Alt EU, Butler CE. Adipose tissue-derived stem cells enhance bioprosthetic mesh repair of ventral hernias. *Plast Reconstr Surg* (2010) **126**:845–854. doi:10.1097/PRS.0b013e3181e6044f

221. Iyyanki TS, Dunne LW, Zhang Q, Hubenak J, Turza KC, Butler CE. Adipose-Derived Stem-Cell-Seeded Non-Cross-Linked Porcine Acellular Dermal Matrix Increases Cellular Infiltration, Vascular Infiltration, and Mechanical Strength of Ventral Hernia Repairs. *Tissue Eng Part A* (2015) **21**:475–485. doi:10.1089/ten.tea.2014.0235

222. van Steenberghe M, Schubert T, Guiot Y, Goebbels RM, Gianello P. Improvement of mesh recolonization in abdominal wall reconstruction with adipose vs. bone marrow mesenchymal stem cells in a rodent model. *J Pediatr Surg* (2017) **52**:1355–1362. doi:10.1016/j.jpedsurg.2016.11.041

223. Hansen SG, Taskin MB, Chen M, Wogensen L, Vinge Nygaard J, Axelsen SM. Electrospun nanofiber mesh with fibroblast growth factor and stem cells for pelvic floor repair. *J Biomed Mater Res B Appl Biomater* (2020) **108**:48–55. doi:10.1002/jbm.b.34364

224. Marinaro F, Casado JG, Blázquez R, Brun MV, Marcos R, Santos M, Duque FJ, López E, Álvarez V, Usón A, et al. Laparoscopy for the Treatment of Congenital Hernia: Use of Surgical Meshes and Mesenchymal Stem Cells in a Clinically Relevant Animal Model. *Front Pharmacol* (2020) **11**:01332. doi:10.3389/fphar.2020.01332

225. Prudente A, Favaro WJ, Latuf P, Riccetto CLZ. Host inflammatory response to polypropylene implants: insights from a quantitative immunohistochemical and birefringence analysis in a rat subcutaneous model. *Int Braz J Urol Off J Braz Soc Urol* (2016) **42**:585–593. doi:10.1590/S1677-5538.IBJU.2015.0289

226. DiPietro LA. Angiogenesis and wound repair: when enough is enough. *J Leukoc Biol* (2016) **100**:979–984. doi:10.1189/jlb.4MR0316-102R

227. Karvinen H, Pasanen E, Rissanen TT, Korpisalo P, Vähäkangas E, Jazwa A, Giacca M, Ylä-Herttuala S. Long-term VEGF-A expression promotes aberrant angiogenesis and fibrosis in skeletal muscle. *Gene Ther* (2011) **18**:1166–1172. doi:10.1038/gt.2011.66

228. Palini GM, Morganti L, Paratore F, Coccolini F, Crescentini G, Nardi M, Veneroni L. Challenging abdominal incisional hernia repaired with platelet-rich plasma and bone marrow-derived mesenchymal stromal cells. A case report. *Int J Surg Case Rep* (2017) **37**:145–148. doi:10.1016/j.ijscr.2017.06.005

229. Mahapatra DSK, Hembrom DP, Mohanty DJA, Singh DP. Cell coated mesh in Lichtenstein hernia repair: An open label trial. *Int J Surg Sci* (2020) **4**:214–217. doi:10.33545/surgery.2020.v4.i2d.419

230. Sakorafas GH, Halikias I, Nissotakis C, Kotsifopoulos N, Stavrou A, Antonopoulos C, Kassaras GA. Open tension free repair of inguinal hernias; the Lichtenstein technique. *BMC Surg* (2001) **1**:3. doi:10.1186/1471-2482-1-3

231. Day RO, Williams KM. Open-label extension studies: do they provide meaningful information on the safety of new drugs? *Drug Saf* (2007) **30**:93–105. doi:10.2165/00002018-200730020-00001

232. Beyer-Westendorf J, Büller H. External and internal validity of open label or double-blind trials in oral anticoagulation: better, worse or just different? *J Thromb Haemost* (2011) **9**:2153–2158. doi:https://doi.org/10.1111/j.1538-7836.2011.04507.x

233. Torabi A, Cleland JG, Rigby AS, Sherwi N. Development and course of heart failure after a myocardial infarction in younger and older people. *J Geriatr Cardiol JGC* (2014) **11**:1–12. doi:10.3969/j.issn.1671-5411.2014.01.002

234. Chicco D, Jurman G. Machine learning can predict survival of patients with heart failure from serum creatinine and ejection fraction alone. *BMC Med Inform Decis Mak* (2020) **20**:16. doi:10.1186/s12911-020-1023-5

235. Ponikowski P, Voors AA, Anker SD, Bueno H, Cleland JGF, Coats AJS, Falk V, Ramon Gonzalez-Juanatey J, Harjola V-P, Jankowska EA, et al. 2016 ESC Guidelines for the diagnosis and treatment of acute and chronic heart failure. *Eur Heart J* (2016) **37**:2129-U130. doi:10.1093/eurheartj/ehw128

236. de Waard GA, Hollander MR, Teunissen PFA, Jansen MF, Eerenberg ES, Beek AM, Marques KM, van de Ven PM, Garrelds IM, Danser AHJ, et al. Changes in Coronary Blood Flow After Acute Myocardial Infarction: Insights From a Patient Study and an Experimental Porcine Model. *JACC Cardiovasc Interv* (2016) **9**:602–613. doi:10.1016/j.jcin.2016.01.001

237. Ishikawa K, Ladage D, Takewa Y, Yaniz E, Chen J, Tilemann L, Sakata S, Badimon JJ, Hajjar RJ, Kawase Y. Development of a preclinical model of ischemic cardiomyopathy in swine. *Am J Physiol Heart Circ Physiol* (2011) **301**:H530-537. doi:10.1152/ajpheart.01103.2010

238. López E, Sánchez-Margallo FM, Álvarez V, Blázquez R, Marinaro F, Abad A, Martín H, Báez C, Blanco V, Crisóstomo V, et al. Identification of very early inflammatory markers in a porcine myocardial infarction model. *BMC Vet Res* (2019) **15**:91. doi:10.1186/s12917-019-1837-5

239. Reinstadler SJ, Reindl M, Feistritzer H-J, Klug G, Mayr A, Kofler M, Tu AM-D, Huybrechts L, Mair J, Franz W-M, et al. Prognostic significance of transaminases after acute ST-elevation myocardial infarction: insights from a cardiac magnetic resonance study. *Wien Klin Wochenschr* (2015) **127**:843–850. doi:10.1007/s00508-015-0868-6

240. Engström G, Melander O, Hedblad B. Leukocyte count and incidence of hospitalizations due to heart failure. *Circ Heart Fail* (2009) **2**:217–222. doi:10.1161/CIRCHEARTFAILURE.108.827071

241. Sager HB, Hulsmans M, Lavine KJ, Moreira MB, Heidt T, Courties G, Sun Y, Iwamoto Y, Tricot B, Khan OF, et al. Proliferation and Recruitment Contribute to Myocardial Macrophage Expansion in Chronic Heart Failure. *Circ Res* (2016) **119**:853–864. doi:10.1161/CIRCRESAHA.116.309001

242. Gao M, Cheng Y, Zheng Y, Zhang W, Wang L, Qin L. Association of serum transaminases with short- and long-term outcomes in patients with ST-elevation myocardial infarction undergoing primary

percutaneous coronary intervention. *BMC Cardiovasc Disord* (2017) **17**:43. doi:10.1186/s12872-017-0485-6

243. Ferrari JP, Lueneberg ME, da Silva RL, Fattah T, Gottschall CAM, Moreira DM. Correlation between leukocyte count and infarct size in ST segment elevation myocardial infarction. *Arch Med Sci Atheroscler Dis* (2016) **1**:e44–e48. doi:10.5114/amsad.2016.60759

244. Men M, Zhang L, Li T, Mi B, Wang T, Fan Y, Chen Y, Shen G, Liang L, Ma A. Prognostic Value of the Percentage of Neutrophils on Admission in Patients with ST-elevated Myocardial Infarction Undergoing Primary Percutaneous Coronary Intervention. *Arch Med Res* (2015) **46**:274–279. doi:10.1016/j.arcmed.2015.05.002

245. Greenberg G, Assali A, Vaknin-Assa H, Brosh D, Teplitsky I, Fuchs S, Battler A, Kornowski R, Lev EI. Hematocrit level as a marker of outcome in ST-segment elevation myocardial infarction. *Am J Cardiol* (2010) **105**:435–440. doi:10.1016/j.amjcard.2009.10.016

246. Paul GK, Sen B, Bari MA, Rahman Z, Jamal F, Bari MS, Sazidur SR. Correlation of platelet count and acute ST-elevation in myocardial infarction. *Mymensingh Med J MMJ* (2010) **19**:469–473.

247. Ly HQ, Kirtane AJ, Murphy SA, Buros J, Cannon CP, Braunwald E, Gibson CM, TIMI Study Group. Association of platelet counts on presentation and clinical outcomes in ST-elevation myocardial infarction (from the TIMI Trials). *Am J Cardiol* (2006) **98**:1–5. doi:10.1016/j.amjcard.2006.01.046

248. Yan W, Song Y, Zhou L, Jiang J, Yang F, Duan Q, Che L, Shen Y, Song H, Wang L. Immune Cell Repertoire and Their Mediators in Patients with Acute Myocardial Infarction or Stable Angina Pectoris. *Int J Med Sci* (2017) **14**:181–190. doi:10.7150/ijms.17119

249. Hofmann U, Frantz S. Role of T-cells in myocardial infarction. *Eur Heart J* (2016) **37**:873–879. doi:10.1093/eurheartj/ehv639

250. Emoto T, Sasaki N, Yamashita T, Kasahara K, Yodoi K, Sasaki Y, Matsumoto T, Mizoguchi T, Hirata K. Regulatory/Effector T-Cell Ratio Is Reduced in Coronary Artery Disease. *Circ J* (2014) **78**:2935–2941. doi:10.1253/circj.CJ-14-0644

251. Szkodzinski J, Hudzik B, Osuch M, Romanowski W, Szygula-Jurkiewicz B, Polonski L, Zubelewicz-Szkodzinska B. Serum concentrations of interleukin-4 and interferon-gamma in relation to severe left ventricular dysfunction in patients with acute myocardial infarction undergoing percutaneous coronary intervention. *Heart Vessels* (2011) **26**:399–407. doi:10.1007/s00380-010-0076-2

252. Kawaguchi H, Mori T, Kawano T, Kono S, Sasaki J, Arakawa K. Band neutrophil count and the presence and severity of coronary atherosclerosis. *Am Heart J* (1996) **132**:9–12. doi:10.1016/S0002-8703(96)90384-1

253. Omran MM, Zahran FM, Kadry M, Belal AAM, Emran TM. Role of myeloperoxidase in early diagnosis of acute myocardial infarction in patients admitted with chest pain. *J Immunoassay Immunochem* (2018) **39**:337–347. doi:10.1080/15321819.2018.1492423

254. Swirski FK, Nahrendorf M, Etzrodt M, Wildgruber M, Cortez-Retamozo V, Panizzi P, Figueiredo J-L, Kohler RH, Chudnovskiy A, Waterman P, et al. Identification of Splenic Reservoir Monocytes and Their Deployment to Inflammatory Sites. *Science* (2009) **325**:612–616. doi:10.1126/science.1175202

255. Smith RR, Barile L, Cho HC, Leppo MK, Hare JM, Messina E, Giacomello A, Abraham MR, Marbán E. Regenerative Potential of Cardiosphere-Derived Cells Expanded From Percutaneous Endomyocardial Biopsy Specimens. *Circulation* (2007) **115**:896–908. doi:10.1161/CIRCULATIONAHA.106.655209

256. Ashur C, Frishman WH. Cardiosphere-Derived Cells and Ischemic Heart Failure. *Cardiol Rev* (2018) **26**:8–21. doi:10.1097/CRD.0000000000000173

257. Blázquez R, Sánchez-Margallo FM, Crisóstomo V, Báez C, Maestre J, Álvarez V, Casado JG. Intrapericardial Delivery of Cardiosphere-Derived Cells: An Immunological Study in a Clinically Relevant Large Animal Model. *PloS One* (2016) **11**:e0149001. doi:10.1371/journal.pone.0149001

258. Gallet R, de Couto G, Simsolo E, Valle J, Sun B, Liu W, Tseliou E, Zile MR, Marbán E. Cardiosphere-derived cells reverse heart failure with preserved ejection fraction (HFpEF) in rats by decreasing fibrosis and inflammation. *JACC Basic Transl Sci* (2016) **1**:14–28. doi:10.1016/j.jacbts.2016.01.003

259. Nana-Leventaki E, Nana M, Poulianitis N, Sampaziotis D, Perrea D, Sanoudou D, Rontogianni D, Malliaras K. Cardiosphere-Derived Cells Attenuate Inflammation, Preserve Systolic Function, and Prevent Adverse Remodeling in Rat Hearts With Experimental Autoimmune Myocarditis. *J Cardiovasc Pharmacol Ther* (2019) **24**:70–77. doi:10.1177/1074248418784287

260. Ishigami S, Ohtsuki S, Tarui S, Ousaka D, Eitoku T, Kondo M, Okuyama M, Kobayashi J, Baba K, Arai S, et al. Intracoronary autologous cardiac progenitor cell transfer in patients with hypoplastic left heart syndrome: the TICAP prospective phase 1 controlled trial. *Circ Res* (2015) **116**:653–664. doi:10.1161/CIRCRESAHA.116.304671

261. Makkar RR, Smith RR, Cheng K, Malliaras K, Thomson LE, Berman D, Czer LS, Marbán L, Mendizabal A, Johnston PV, et al. Intracoronary cardiosphere-derived cells for heart regeneration after myocardial

infarction (CADUCEUS): a prospective, randomised phase 1 trial. *Lancet Lond Engl* (2012) **379**:895–904. doi:10.1016/S0140-6736(12)60195-0

262. Makkar RR, Kereiakes DJ, Aguirre F, Kowalchuk G, Chakravarty T, Malliaras K, Francis GS, Povsic TJ, Schatz R, Traverse JH, et al. Intracoronary ALLogeneic heart STem cells to Achieve myocardial Regeneration (ALLSTAR): a randomized, placebo-controlled, double-blinded trial. *Eur Heart J* (2020) **41**:3451–3458. doi:10.1093/eurheartj/ehaa541

263. Sano T, Ousaka D, Goto T, Ishigami S, Hirai K, Kasahara S, Ohtsuki S, Sano S, Oh H. Impact of Cardiac Progenitor Cells on Heart Failure and Survival in Single Ventricle Congenital Heart Disease. *Circ Res* (2018) **122**:994–1005. doi:10.1161/CIRCRESAHA.117.312311

264. Tarui S, Ishigami S, Ousaka D, Kasahara S, Ohtsuki S, Sano S, Oh H. Transcoronary infusion of cardiac progenitor cells in hypoplastic left heart syndrome: Three-year follow-up of the Transcoronary Infusion of Cardiac Progenitor Cells in Patients With Single-Ventricle Physiology (TICAP) trial. *J Thorac Cardiovasc Surg* (2015) **150**:1198–1207, 1208.e1–2. doi:10.1016/j.jtcvs.2015.06.076

265. Masterson CH, Curley GF, Laffey JG. Modulating the distribution and fate of exogenously delivered MSCs to enhance therapeutic potential: knowns and unknowns. *Intensive Care Med Exp* (2019) **7**:41. doi:10.1186/s40635-019-0235-4

266. Ibrahim AG-E, Cheng K, Marbán E. Exosomes as critical agents of cardiac regeneration triggered by cell therapy. *Stem Cell Rep* (2014) **2**:606–619. doi:10.1016/j.stemcr.2014.04.006

267. Namazi H, Mohit E, Namazi I, Rajabi S, Samadian A, Hajizadeh-Saffar E, Aghdami N, Baharvand H. Exosomes secreted by hypoxic cardiosphere-derived cells enhance tube formation and increase pro-angiogenic miRNA. *J Cell Biochem* (2018) **119**:4150–4160. doi:10.1002/jcb.26621

268. Tseliou E, Fouad J, Reich H, Slipczuk L, de Couto G, Aminzadeh M, Middleton R, Valle J, Weixin L, Marbán E. Fibroblasts Rendered Antifibrotic, Antiapoptotic, and Angiogenic by Priming With Cardiosphere-Derived Extracellular Membrane Vesicles. *J Am Coll Cardiol* (2015) **66**:599–611. doi:10.1016/j.jacc.2015.05.068

269. López E, Blázquez R, Marinaro F, Álvarez V, Blanco V, Báez C, González I, Abad A, Moreno B, Sánchez-Margallo FM, et al. The Intrapericardial Delivery of Extracellular Vesicles from Cardiosphere-Derived Cells Stimulates M2 Polarization during the Acute Phase of Porcine Myocardial Infarction. *Stem Cell Rev Rep* (2020) **16**:612–625. doi:10.1007/s12015-019-09926-y

270. Mayer A, Lee S, Jung F, Grütz G, Lendlein A, Hiebl B. CD14+ CD163+ IL-10+ monocytes/macrophages: Pro-angiogenic and non pro-inflammatory isolation, enrichment and long-term secretion profile. *Clin Hemorheol Microcirc* (2010) **46**:217–223. doi:10.3233/CH-2010-1348

271. Martinez FO, Helming L, Gordon S. Alternative activation of macrophages: an immunologic functional perspective. *Annu Rev Immunol* (2009) **27**:451–483. doi:10.1146/annurev.immunol.021908.132532

272. Yang Z, Ming X-F. Functions of arginase isoforms in macrophage inflammatory responses: impact on cardiovascular diseases and metabolic disorders. *Front Immunol* (2014) **5**:533. doi:10.3389/fimmu.2014.00533

273. Ben-Mordechai T, Palevski D, Glucksam-Galnoy Y, Elron-Gross I, Margalit R, Leor J. Targeting macrophage subsets for infarct repair. *J Cardiovasc Pharmacol Ther* (2015) **20**:36–51. doi:10.1177/1074248414534916

274. López E, Marinaro F, de Pedro M de LÁ, Sánchez-Margallo FM, Gómez-Serrano M, Ponath V, Pogge von Strandmann E, Jorge I, Vázquez J, Fernández-Pereira LM, et al. The Immunomodulatory Signature of Extracellular Vesicles From Cardiosphere-Derived Cells: A Proteomic and miRNA Profiling. *Front Cell Dev Biol* (2020) **8**:321. doi:10.3389/fcell.2020.00321

275. The interleukin-6 receptor as a target for prevention of coronary heart disease: a mendelian randomisation analysis. *The Lancet* (2012) **379**:1214–1224. doi:10.1016/S0140-6736(12)60110-X

276. Carroll MB. Tocilizumab in the treatment of myocardial infarction. *Mod Rheumatol* (2018) **28**:733–735. doi:10.1080/14397595.2018.1427457

277. Group RC, Horby PW, Pessoa-Amorim G, Peto L, Brightling CE, Sarkar R, Thomas K, Jeebun V, Ashish A, Tully R, et al. Tocilizumab in patients admitted to hospital with COVID-19 (RECOVERY): preliminary results of a randomised, controlled, open-label, platform trial. *medRxiv* (2021)2021.02.11.21249258. doi:10.1101/2021.02.11.21249258

278. Fuster JJ, Walsh K. The good, the bad, and the ugly of interleukin-6 signaling. *EMBO J* (2014) **33**:1425–1427. doi:10.15252/embj.201488856

279. Xing Z, Gauldie J, Cox G, Baumann H, Jordana M, Lei XF, Achong MK. IL-6 is an antiinflammatory cytokine required for controlling local or systemic acute inflammatory responses. *J Clin Invest* (1998) **101**:311–320. doi:10.1172/JCI1368

280. Mauer J, Chaurasia B, Goldau J, Vogt MC, Ruud J, Nguyen KD, Theurich S, Hausen AC, Schmitz J, Brönneke HS, et al. Signaling by IL-6 promotes alternative activation of macrophages to limit endotoxemia and obesity-associated resistance to insulin. *Nat Immunol* (2014) **15**:423–430. doi:10.1038/ni.2865

281. Wang X, Ha T, Zou J, Ren D, Liu L, Zhang X, Kalbfleisch J, Gao X, Williams D, Li C. MicroRNA-125b protects against myocardial ischaemia/reperfusion injury via targeting p53-mediated apoptotic signalling and TRAF6. *Cardiovasc Res* (2014) **102**:385–395. doi:10.1093/cvr/cvu044

282. Bayoumi AS, Park K-M, Wang Y, Teoh J-P, Aonuma T, Tang Y, Su H, Weintraub NL, Kim I-M. A carvedilol-responsive microRNA, miR-125b-5p protects the heart from acute myocardial infarction by repressing pro-apoptotic bak1 and klf13 in cardiomyocytes. *J Mol Cell Cardiol* (2018) **114**:72–82. doi:10.1016/j.yjmcc.2017.11.003

283. Álvarez V, Sánchez-Margallo FM, Macías-García B, Gómez-Serrano M, Jorge I, Vázquez J, Blázquez R, Casado JG. The immunomodulatory activity of extracellular vesicles derived from endometrial mesenchymal stem cells on CD4+ T cells is partially mediated by TGFbeta. *J Tissue Eng Regen Med* (2018) **12**:2088–2098. doi:10.1002/term.2743

284. Marinaro F, Gómez-Serrano M, Jorge I, Silla-Castro JC, Vázquez J, Sánchez-Margallo FM, Blázquez R, López E, Álvarez V, Casado JG. Unraveling the Molecular Signature of Extracellular Vesicles From Endometrial-Derived Mesenchymal Stem Cells: Potential Modulatory Effects and Therapeutic Applications. *Front Bioeng Biotechnol* (2019) **7**:431. doi:10.3389/fbioe.2019.00431

285. Chen L, Wang S, Wang Y, Zhang W, Ma K, Hu C, Zhu H, Liang S, Liu M, Xu N. IL-6 influences the polarization of macrophages and the formation and growth of colorectal tumor. *Oncotarget* (2018) **9**:17443–17454. doi:10.18632/oncotarget.24734

286. Barragan F, Irwin JC, Balayan S, Erikson DW, Chen JC, Houshdaran S, Piltonen TT, Spitzer TLB, George A, Rabban JT, et al. Human Endometrial Fibroblasts Derived from Mesenchymal Progenitors Inherit Progesterone Resistance and Acquire an Inflammatory Phenotype in the Endometrial Niche in Endometriosis1. *Biol Reprod* (2016) **94**: doi:10.1095/biolreprod.115.136010

287. Spitzer TLB, Rojas A, Zelenko Z, Aghajanova L, Erikson DW, Barragan F, Meyer M, Tamaresis JS, Hamilton AE, Irwin JC, et al. Perivascular Human Endometrial Mesenchymal Stem Cells Express Pathways Relevant to Self-Renewal, Lineage Specification, and Functional Phenotype. *Biol Reprod* (2012) **86**: doi:10.1095/biolreprod.111.095885

288. Gargett CE, Gurung S. Endometrial Mesenchymal Stem/Stromal Cells, Their Fibroblast Progeny in Endometriosis, and More. *Biol Reprod* (2016) **94**:129. doi:10.1095/biolreprod.116.141325

289. Gargett CE, Schwab KE, Deane JA. Endometrial stem/progenitor cells: the first 10 years. *Hum Reprod Update* (2016) **22**:137–163. doi:10.1093/humupd/dmv051

290. Nikoo S, Ebtekar M, Jeddi-Tehrani M, Shervin A, Bozorgmehr M, Kazemnejad S, Zarnani AH. Effect of menstrual blood-derived stromal stem cells on proliferative capacity of peripheral blood mononuclear cells in allogeneic mixed lymphocyte reaction. *J Obstet Gynaecol Res* (2012) **38**:804–809. doi:10.1111/j.1447-0756.2011.01800.x

291. Nikoo S, Ebtekar M, Jeddi-Tehrani M, Shervin A, Bozorgmehr M, Vafaei S, Kazemnejad S, Zarnani A-H. Menstrual blood-derived stromal stem cells from women with and without endometriosis reveal different phenotypic and functional characteristics. *Mol Hum Reprod* (2014) **20**:905–918. doi:10.1093/molehr/gau044

292. Peron JPS, Jazedje T, Brandão WN, Perin PM, Maluf M, Evangelista LP, Halpern S, Nisenbaum MG, Czeresnia CE, Zatz M, et al. Human endometrial-derived mesenchymal stem cells suppress inflammation in the central nervous system of EAE mice. *Stem Cell Rev* (2012) **8**:940–952. doi:10.1007/s12015-011-9338-3

293. Du X, Yuan Q, Qu Y, Zhou Y, Bei J. Endometrial Mesenchymal Stem Cells Isolated from Menstrual Blood by Adherence. *Stem Cells Int* (2016) **2016**:3573846. doi:10.1155/2016/3573846

294. Marinaro F, Gómez-Serrano M, Jorge I, Silla-Castro JC, Vázquez J, Sánchez-Margallo FM, Blázquez R, López E, Álvarez V, Casado JG. Unraveling the Molecular Signature of Extracellular Vesicles From Endometrial-Derived Mesenchymal Stem Cells: Potential Modulatory Effects and Therapeutic Applications. *Front Bioeng Biotechnol* (2019) **7**:431. doi:10.3389/fbioe.2019.00431

295. Blázquez R, Sánchez-Margallo FM, Álvarez V, Matilla E, Hernández N, Marinaro F, Gómez-Serrano M, Jorge I, Casado JG, Macías-García B. Murine embryos exposed to human endometrial MSCs-derived extracellular vesicles exhibit higher VEGF/PDGF AA release, increased blastomere count and hatching rates. *PloS One* (2018) **13**:e0196080. doi:10.1371/journal.pone.0196080

296. Marinaro F, Pericuesta E, Sánchez-Margallo FM, Casado JG, Álvarez V, Matilla E, Hernández N, Blázquez R, González-Fernández L, Gutiérrez-Adán A, et al. Extracellular vesicles derived from endometrial human mesenchymal stem cells improve IVF outcome in an aged murine model. *Reprod Domest Anim* (2018) **53**:46–49. doi:10.1111/rda.13314

297. Marinaro F, Macías-García B, Sánchez-Margallo FM, Blázquez R, Álvarez V, Matilla E, Hernández N, Gómez-Serrano M, Jorge I, Vázquez J, et al. Extracellular vesicles derived from endometrial human mesenchymal stem cells enhance embryo yield and quality in an aged murine model. *Biol Reprod* (2019) **100**:1180–1192. doi:10.1093/biolre/ioy263

298. Lopera-Vásquez R, Hamdi M, Fernandez-Fuertes B, Maillo V, Beltrán-Breña P, Calle A, Redruello A, López-Martín S, Gutierrez-Adán A, Yañez-Mó M, et al. Extracellular Vesicles from BOEC in In Vitro Embryo Development and Quality. *PloS One* (2016) **11**:e0148083. doi:10.1371/journal.pone.0148083

299. Almiñana C, Corbin E, Tsikis G, Alcântara-Neto AS, Labas V, Reynaud K, Galio L, Uzbekov R, Garanina AS, Druart X, et al. Oviduct extracellular vesicles protein content and their role during oviduct-embryo cross-talk. *Reprod Camb Engl* (2017) **154**:153–168. doi:10.1530/REP-17-0054

300. Liu C, Yin H, Jiang H, Du X, Wang C, Liu Y, Li Y, Yang Z. Extracellular Vesicles Derived from Mesenchymal Stem Cells Recover Fertility of Premature Ovarian Insufficiency Mice and the Effects on their Offspring. *Cell Transplant* (2020) **29**:963689720923575. doi:10.1177/0963689720923575

301. Griffith OW, Chavan AR, Protopapas S, Maziarz J, Romero R, Wagner GP. Embryo implantation evolved from an ancestral inflammatory attachment reaction. *Proc Natl Acad Sci* (2017) **114**:E6566–E6575. doi:10.1073/pnas.1701129114

302. Sung BH, Ketova T, Hoshino D, Zijlstra A, Weaver AM. Directional cell movement through tissues is controlled by exosome secretion. *Nat Commun* (2015) **6**:7164. doi:10.1038/ncomms8164

303. Mu W, Rana S, Zöller M. Host Matrix Modulation by Tumor Exosomes Promotes Motility and Invasiveness. *Neoplasia N Y N* (2013) **15**:875.

304. Hoshino A, Costa-Silva B, Shen T-L, Rodrigues G, Hashimoto A, Tesic Mark M, Molina H, Kohsaka S, Di Giannatale A, Ceder S, et al. Tumour exosome integrins determine organotropic metastasis. *Nature* (2015) **527**:329–335. doi:10.1038/nature15756

305. Sedgwick AE, Clancy JW, Balmert MO, D'Souza-Schorey C. Extracellular microvesicles and invadopodia mediate non-overlapping modes of tumor cell invasion. *Sci Rep* (2015) **5**: doi:10.1038/srep14748

306. Majumdar R, Tameh AT, Parent CA. Exosomes Mediate LTB4 Release during Neutrophil Chemotaxis. *PLoS Biol* (2016) **14**: doi:10.1371/journal.pbio.1002336

307. Wang J, Xia J, Huang R, Hu Y, Fan J, Shu Q, Xu J. Mesenchymal stem cell-derived extracellular vesicles alter disease outcomes via endorsement of macrophage polarization. *Stem Cell Res Ther* (2020) **11**:424. doi:10.1186/s13287-020-01937-8

308. Domenis R, Cifù A, Quaglia S, Pistis C, Moretti M, Vicario A, Parodi PC, Fabris M, Niazi KR, Soon-Shiong P, et al. Pro inflammatory stimuli enhance the immunosuppressive functions of adipose mesenchymal stem cells-derived exosomes. *Sci Rep* (2018) **8**:13325. doi:10.1038/s41598-018-31707-9

309. An J-H, Li Q, Bhang D-H, Song W-J, Youn H-Y. TNF-α and INF-γ primed canine stem cell-derived extracellular vesicles alleviate experimental murine colitis. *Sci Rep* (2020) **10**:2115. doi:10.1038/s41598-020-58909-4

310. Witwer KW, Théry C. Extracellular vesicles or exosomes? On primacy, precision, and popularity influencing a choice of nomenclature. *J Extracell Vesicles* (2019) **8**: doi:10.1080/20013078.2019.1648167

311. Somiya M. Where does the cargo go?: Solutions to provide experimental support for the "extracellular vesicle cargo transfer hypothesis." *J Cell Commun Signal* (2020) **14**:135–146. doi:10.1007/s12079-020-00552-9

312. D'Arrigo D, Roffi A, Cucchiarini M, Moretti M, Candrian C, Filardo G. Secretome and Extracellular Vesicles as New Biological Therapies for Knee Osteoarthritis: A Systematic Review. *J Clin Med* (2019) **8**: doi:10.3390/jcm8111867

313. Gandham S, Su X, Wood J, Nocera AL, Alli SC, Milane L, Zimmerman A, Amiji M, Ivanov AR. Technologies and Standardization in Research on Extracellular Vesicles. *Trends Biotechnol* (2020) **38**:1066–1098. doi:10.1016/j.tibtech.2020.05.012

314. Coolidge HJ, Lord RH. *Archibald Cary Coolidge: Life and Letters*. Books for Libraries Press (1932).

# Appendix 1: Publications forming part of this Thesis

## Publications

Acta Biomaterialia 71 (2018) 318–329

Contents lists available at ScienceDirect

Acta Biomaterialia

journal homepage: www.elsevier.com/locate/actabiomat

Full length article

# Fibrin glue mesh fixation combined with mesenchymal stem cells or exosomes modulates the inflammatory reaction in a murine model of incisional hernia

Rebeca Blázquez [a,b,1], Francisco Miguel Sánchez-Margallo [a,b,1], Verónica Álvarez [a], Alejandra Usón [a], Federica Marinaro [a], Javier G. Casado [a,b,c,*]

[a] Stem Cell Therapy Unit, 'Jesús Usón' Minimally Invasive Surgery Centre, Cáceres 10071, Spain
[b] CIBER de Enfermedades Cardiovasculares, Spain
[c] Immunology Unit, Department of Physiology, University of Extremadura, 10071 Caceres, Spain

ARTICLE INFO

*Article history:*
Received 6 November 2017
Received in revised form 9 February 2018
Accepted 12 February 2018
Available online 17 February 2018

*Keywords:*
Surgical meshes
Fibrin glue
Mesenchymal stem cells
Exosomes
Murine model

ABSTRACT

Surgical meshes are effective and frequently used to reinforce soft tissues. Fibrin glue (FG) has been widely used for mesh fixation and is also considered an optimal vehicle for stem cell delivery. The aim of this preclinical study was to evaluate the therapeutic effect of MSCs and their exosomes combined with FG for the treatment of incisional hernia.

A murine incisional hernia model was used to implant surgical meshes and different treatments with FG, MSCs and *exo*-MSCs were applied. The implanted meshes were evaluated at day 7 by anatomopathology, cellular analysis of infiltrating leukocytes and gene expression analysis of TH1/TH2 cytokines, MMPs, TIMPs and collagens.

Our results demonstrated a significant increase of anti-inflammatory M2 macrophages and TH2 cytokines when MSCs or *exo*-MSCs were used. Moreover, the analysis of MMPs, TIMPs and collagen exerted significant differences in the extracellular matrix and in the remodeling process.

Our *in vivo* study suggests that the fixation of surgical meshes with FG and MSCs or *exo*-MSCs will have a beneficial effect for the treatment of incisional hernia in terms of improved outcomes of damaged tissue, and especially, in the modulation of inflammatory responses towards a less aggressive and pro-regenerative profile.

**Statement of Significance**

The implantation of surgical meshes is the standard procedure to reinforce tissue defects such as hernias. However, an exacerbated and persistent inflammatory response secondary to this implantation is frequently observed, leading to a strong discomfort and chronic pain in the patients. In many cases, an additional surgical intervention is needed to remove the mesh.

This study shows that mesenchymal stem cells and their exosomes, combined with a fibrin sealant, can be used for the successful fixation of these meshes. This new therapeutic approach, assayed in a murine model of incisional hernia, favors the modulation of the inflammatory response towards a less aggressive and pro-regenerative profile.

© 2018 Acta Materialia Inc. Published by Elsevier Ltd. All rights reserved.

## 1. Introduction

An incisional hernia is a protrusion of tissue which occurs through a defect in the site of a surgical scar that has failed to heal properly. It may occur immediately following surgery and may not become apparent for months to years. Surgical meshes are effective and frequently used to reinforce soft tissues providing a support for tissue reconstruction, organ prolapse repair and closure of large wounds. The majority of surgical meshes are produced with synthetic material such as polypropylene, polyester, expanded polytetrafluoroethylene (ePTFE) or Polyvinylidene fluoride (PVDF). From these, polypropylene is the most commonly used

* Corresponding author at: Ctra. N-521, km 41.8, 10071 Cáceres, Spain.
*E-mail address:* jgarcia@ccmijesususon.com (J.G. Casado).
[1] These authors equally contributed and should be regarded as co-first authors.

https://doi.org/10.1016/j.actbio.2018.02.014
1742-7061/© 2018 Acta Materialia Inc. Published by Elsevier Ltd. All rights reserved.

due to its versatility, mechanical stability and strength, demonstrating to be an inert and hydrophobic material resistant to biologic degradation [1]. All these synthetic components can be combined with a wide range of additional materials (i.e. titanium, omega 3, hyaluronate or extracellular matrix) [2,3].

Regarding to mesh fixation methods, different procedures and materials are currently used. Briefly, the fixation can be performed by sutures, staples or tacks [4], but also by cyanoacrylate which has been proved to be a simple and effective method for fixation [5]. The use of fibrin glue (also called fibrin sealant) was introduced in 1909 and used for skin graft fixation in the 40's. In the last two decades, fibrin glue has been widely used for mesh fixation. In fact, in a systematic review with 5993 recruited patients undergoing surgical mesh fixation with Tisseel/Tissucol (brand names of fibrin glue), it was demonstrated that this procedure does not increase the risks associated to inguinal hernia (recurrence and complications such as hematoma or bleeding) and decreases the risk compared with tissue-penetrating fixation methods. Additionally, the use of fibrin glue in the repair of incisional hernias significantly decreased both postoperative morbidity and duration of hospital stay [6].

Another systematic review including twelve randomized clinical trials demonstrated that, in three out of twelve clinical trials, significantly lower rates of chronic pain were observed using fibrin glue compared to sutures. Moreover, a significant reduction in operative time was reported in five out of twelve clinical trials [7]. In the last years, several reviews have been also focused in the comparison of biologic adhesives with tacking. Most of published results suggest that, there is less pain when using biologic adhesives than with tacking [8]. Additionally, in a rat animal model for incisional hernia, Petter-Puchner *et al.* demonstrated that fibrin sealant yielded excellent fixation when compared to stapling, and histology revealed good tissue integration and neovascularization in all groups. The biomechanical investigations also revealed that fibrin sealant in combination with meshes provided a remarkably high initial tensile strength and no dislocation occurred [9].

Apart from the adhesive properties of fibrin sealants, the biological role of fibrin clots has been studied from different perspectives. Basically, fibrin clots are rapidly formed in response to injuries to any part of the vascular system but artificial clots can be formed by mixing purified fibrinogen and thrombin. *In vivo* experiments for colonic anastomosis demonstrated the presence of infiltrating neutrophils into the fibrin sealants [10] and *in vitro* experiments have demonstrated that the composition of these fibrin clots has a significant effect on neutrophils migration and influence the wound healing process [11].

In the last 20 years, fibrin sealants combined with cells have been successfully used for tissue engineering applications [12]. One of the first published reports demonstrated that fibrin sealants can be used as a cell vehicle for human dermal fibroblasts in the treatment of chronic wounds [13]. More recently, the fibrin sealant has become the preferred scaffold for stem cell transplantation and different types of stem cells have been combined with fibrin glue for cell delivery: bone marrow mononuclear cells [14], bone marrow-derived mesenchymal stem cells [15], adipose tissue stem cells [16], embryonic stem-like [17] and Bone Mesenchymal Stem Cells [18]. These stem cells, together with fibrin glue, have been successfully used for osteochondral repair [17], neuroprotection [14], bone repair [18], enhancement of nerve regeneration [16], wound healing [15] and myocardial infarction repair [19].

Our research group has recently demonstrated that surgical meshes coated with mesenchymal stem cells (MSCs) provide an anti-inflammatory environment to reduce the exacerbated and persistent inflammatory processes commonly observed after surgical mesh implantation [20]. Based on that, and considering that fibrin glue is widely used for mesh fixation as well as an optimal vehicle for stem cell delivery, here we aimed to evaluate the biological and therapeutic effect of fibrin glue and mesenchymal stem cells in the setting of incisional hernia. Moreover, as the therapeutic effect of MSCs is thought to be mediated by a paracrine effect, the exosomes released from these cells have been proposed as a main player in their immunomodulatory activity. The potential of these microvesicles has been described in different *in vitro* and *in vivo* studies with promising results [21]. Taking into account the advantages that a cell-free based therapy offers with respect to a cell-based therapy, we decided to study the effect of these microvesicles conveyed in fibrin glue in our incisional hernia model.

Our *in vivo* study was evaluated from different points of view: histological, tissue-infiltrated leukocytes, macrophage polarization and gene expression analyses on explanted meshes (TH1/TH2 cytokines, matrix metalloproteinases or MMPs, tissue inhibitor of metalloproteinases or TIMPs and collagens I/III). In summary, here we show that, the characterization of tissue infiltrated leukocytes is in agreement with our previous studies where MSC-coated surgical meshes were used [20]. Moreover, this preliminary *in vivo* study suggests that the fixation of surgical meshes with fibrin glue and mesenchymal stem cells or exosomes will have a beneficial effect for the treatment of incisional hernia in terms of changes in the extracellular matrix structure, reduction of inflammatory responses and control of foreign body reactions.

## 2. Materials and methods

### *2.1. Isolation, expansion and characterization of murine mesenchymal stem cells for in vivo assays*

Murine bone marrow-derived MSCs were isolated from femurs of three euthanized B6D2 mice aged between 2 and 6 months and weighted between 20 and 25 g. The cells were flushed via needle and syringe. Cell suspension was filtered through a 40 μm nylon mesh and mononuclear cells were isolated by centrifugation over Histopaque-1077 (Sigma, St. Louis, MO). Mononuclear cells were recovered and washed twice with PBS. Finally, mononuclear cells were resuspended in DMEM containing 10% FBS, seeded onto tissue culture flasks and expanded at 37 °C and 5% $CO_2$. Following 48 h in culture, non-adherent hematopoietic cells were removed. Adhered cells were passaged at 80–90% confluence by 0.25% trypsin solution (Lonza Walkersville, Inc., Walkersville, MD) and seeded onto new culture flask at a density of 5000–6000 cells/$cm^2$. Culture medium was changed every 3–4 days. The murine MSCs were used at passages 10–15 for *in vivo* experiments.

For phenotypic analysis $2 \times 10^5$ cells were stained with murine monoclonal antibodies (mAbs) against CD29, CD44, CD90, CD105, MHC class I and MHC class II and incubated for 30 min at 4 °C with an appropriate concentration of mAbs in the presence of PBS containing 2% FBS. The cells were washed and re-suspended in PBS. The flow cytometric analysis was performed on a FACScalibur cytometer (BD Biosciences, CA, USA) after acquisition of $10^5$ events. Viable cells were selected using forward and side scatter characteristics and analyzed using CellQuest software (BD Biosciences, CA, USA). Isotype-matched negative control antibodies were used in the experiments. The mean relative fluorescence intensity (MRFI) was calculated by dividing the mean fluorescent intensity (MFI) by the MFI of its negative control.

Additionally, the differentiation potential of MSCs was assayed using standard protocols to promote osteogenic, adipogenic and chondrogenic differentiation. Cells were cultured for 21 days with differentiation specific media (Gibco Life Sciences, Rockville, MD, USA), which was replaced every three days. Oil Red O, Alcian Blue

and Alizarin Red S stainings were performed to evidence adipogenic, chondrogenic and osteogenic differentiation, respectively.

### 2.2. Isolation, purification and characterization of mesenchymal stem cell-derived exosomes

Mesenchymal stem cells-derived exosomes (*exo*-MSCs) were obtained from murine bone marrow-derived MSCs cultured in 175 $cm^2$ flasks. When cells reached a confluence of 80%, culture medium (DMEM containing 10% FBS) was replaced by exosome isolation medium (DMEM containing 1% insulin-transferrin-selenium). Supernatants were collected every 3–4 days. To eliminate death cells and debris, the supernatants were centrifuged at 1000×*g* for 10 min and 5000×*g* for 20 min at 4 °C, and passed through a 0.22 μm filter. About 15 ml of these supernatants were ultra-filtered through 3 kDa MWCO Amicon® Ultra devices (Merck-Millipore, MA, USA). Samples were spun at 4000×*g* for 60 min and 200–300 μl of concentrated supernatant were collected and stored at −20 °C.

Prior to *in vivo* experiments, the concentrated supernatants were characterized by total protein quantification, nanoparticle tracking analysis and flow cytometry. First, exosome concentrations were indirectly measured by protein quantification in a Bradford assay. To quantify protein concentration, 20 μl of exosomes sample were incubated with 180 μl of Bradford reagent (Bio Rad Laboratories, Hercules, CA) at RT. Absorbance was read 5 min after at 595 nm, and protein concentration was extrapolated from a standard concentration curve of Bovine Serum Albumin. The concentration and size of the particles were measured by nanoparticle tracking analysis (NanoSight Ltd, Amesbury, UK) that relates the rate of Brownian motion to particle size. Results were analyzed using the nanoparticle tracking analysis software package version 2.2.

For flow cytometric analysis, exosomes were conjugated with latex beads. Briefly, 5 μg of exosomes were incubated overnight at 4 °C with 10 μl of aldehyde/Sulfate latex beads (4μm) (Molecular probes, Life Technologies, Carlsbad, CA, USA). A total of 110 μl of 1 M glycine was added and after 30 min of incubation, samples were centrifuged, washed and re-suspended in a final volume of 0.5 ml PBS/0.5% BSA. These exosome-coated beads were incubated for 30 min at 4 °C with anti-CD9 murine mAb (BD Biosciences, San Jose, CA, USA). After incubation, the exosome-coated beads were washed and re-suspended in PBS/0.5% BSA. The flow cytometry analysis was performed on a FACScalibur cytometer (BD Biosciences, San Jose, CA, USA). Isotype-matched control antibodies were used as negative controls.

### 2.3. Fibrin glue preparation

The fibrin glue was prepared using thrombin (500 IU/ml) and fibrinogen (80 mg/ml). These compounds were mixed at a ratio 1:1 using a fibrin glue applicator. This fibrin glue applicator was based on a dual syringe (dual-plunger with a joining Y-piece and an application cannula). Every mesh was fixed with a total volume of 400 μl of fibrin glue.

### 2.4. Mesenchymal stem cells and fibrin glue admixture

The MSCs were detached from flasks with 0.25% trypsin solution, counted and adjusted at $4 \times 10^6$ cells/ml. A total of $1.6 \times 10^6$ cells in 400 μl of DMEM were mixed in thrombin (500 IU/ml) at 1:1 ratio. The cell suspension was then mixed at a ratio 1:1 with fibrinogen (80 mg/ml) using a fibrin glue applicator. A final volume of 400 μl of the final solution was used for every mesh fixation, containing $4 \times 10^5$ cells.

The viability of MSCs in fibrin glue was measured in terms of metabolic activity by a CCK-8 assay according to manufacturer's instruction. Briefly, MSCs were admixed with fibrin glue and cultured for 2 days in DMEM. MSCs cultured under standard conditions were used as controls. Additionally, MSCs admixed with fibrin glue shape was examined under a microscope at 20X magnification.

### 2.5. Exosomes from mesenchymal stem cells and fibrin glue admixture

Exosomes from mesenchymal stem cells (*exo*-MSCs) were slowly thawed prior to be mixed with fibrin glue solution. A total of 200 μl of exosomal proteins at 20,000 μg/ml was admixed 1:1 with thrombin (500 IU/ml) and 1:1 with fibrinogen (80 mg/ml). Finally, the thrombin-exosomes dilution was mixed with fibrinogen-exosomes dilution using a fibrin glue applicator. A final volume of 400 μl containing 4000 μg of exosomal proteins were used for mesh fixation.

### 2.6. Incisional hernia model and surgical procedures

Animal care and all experimental procedures were approved by the Committee on the Ethics of Animal Experiments of Minimally Invasive Surgery Centre and fully complied with recommendations outlined by the local government. 16 ICR mice aged 3–5 months and weighted 35–40 g were used in this study. The animals were divided into four groups. In the first group (n = 4), surgical meshes were fixed with simple stitches (−/−). In the second group (n = 4), the surgical meshes were fixed with fibrin glue (FG/−). In the third group (n = 4), the surgical meshes where fixed with fibrin glue admixed with MSCs (FG/MSCs). In the fourth group (n = 4), the surgical meshes where fixed with fibrin glue admixed with *exo*-MSCs (FG/*exo*-MSCs).

The murine incisional hernia model performed bilaterally using a method inspired on a model reported in previous studies [22]. Briefly, once the animals were anesthetized, the abdomen was trichotomized. A small incision of 0.7–0.8 cm length was made on the skin at each side of the abdomen. A muscular and aponeurotic fragment with a diameter of 0.6 cm was removed from the abdominal wall below each incision. Polypropylene surgical meshes (Assumesh, Assut Europe, Rome, Italy) were implanted in the preperitoneal space, covering each of the defects (Fig. 1). The surgical meshes (1 $cm^2$) were fixed with simple stitches or 400 μl of FG, FG/MSCs or FG/*exo*-MSCs. Finally, the skin incisions were sutured with a 5–0 polydioxanone monofilament absorbable suture (PDSII ™, Ethicon, Johnson & Johnson, NJ, USA) by 4–5 simple stitches.

### 2.7. Anesthesia and analgesia procedures

Animals were pre-medicated intraperitoneally with 2 mg/kg meloxicam (Metacam®, Boehringer Ingelheim, Ingelheim am Rhein, Germany) and 0.06 mg/kg buprenorphine (Buprex®, Schering-Plough, NJ, USA). Inhalant anesthesia was induced in a chamber with 3% isoflurane and maintained with 1.5–2.0% isoflurane through a nosecone. Oxygen flow was maintained at 0.5–1.0 l/min during all the procedure. Once the mesh was implanted, during the first three days from surgery, 10 mg/ml paracetamol (Apiretal®, ERN, Barcelona, Spain) were administered in drinking water and 0.1 mg/kg buprenorphine were injected subcutaneously each 12 h. Euthanasia was performed by carbon dioxide asphyxiation at day seven following surgery.

### 2.8. Histological analysis in explanted meshes

Surgically implanted meshes were excised from euthanized animals. The excised meshes were used for flow cytometry analysis, quantitative real-time PCR (qRT-PCR) and histological analysis. For histological analyses, the whole layer composed by the skin, mesh

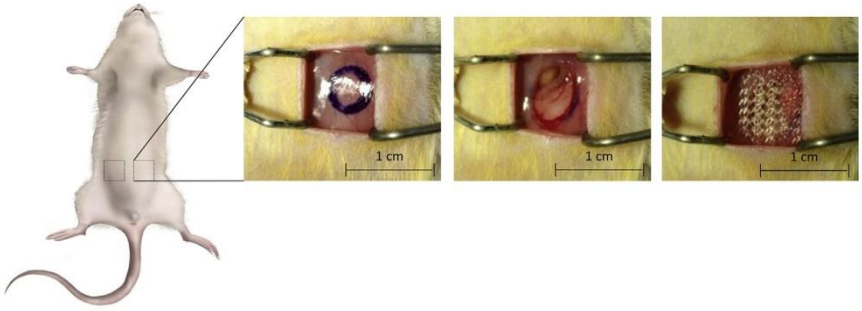


**Fig. 1.** Murine incisional hernia model and surgical mesh implantation. The incisional hernia was bilaterally created in study groups. Non-absorbable polypropylene-made surgical meshes (1 $cm^2$) were implanted and fixed with simple stitches, FG, FG/MSCs or FG/exo-MSCs.

and muscular-peritoneum was fixed in paraformaldehyde 4%, paraffin-embedded and sliced in 5–8 μm thickness. Histological samples were stained for Hematoxylin-Eosin and Masson Trichrome.

### 2.9. qRT-PCR studies in explanted meshes

For transcriptional analysis studies, total RNA from the cells retained in the excised meshes was purified using TRI-Reagent (Sigma, St. Louis, MO, USA) according to the manufacturer's instructions.

cDNA was synthesized in reverse transcription reaction using Superscript III reverse transcriptase (Invitrogen). For PCR amplification, commercial gene expression assay kits were used (Life Technologies, Thermo Fisher Scientific Inc.) (Table 1). The qRT-PCR was performed using TaqMan probes in a 7300 Real-Time PCR System (Applied Biosystems, Thermo Fisher Scientific Inc.). The qRT-PCR products were quantified by fluorescent method and the expression of each gene was calculated using the $2^{-\Delta\Delta Ct}$ expression as described by Livak and Schmittgen [23]. Gene ratios were calculated using $2^{-\Delta Ct}$ values. All samples (n = 4 per group) were analyzed separately and normalized using Glyceraldehyde 3-phosphate dehydrogenase (GAPDH) as a housekeeping control gene. For $2^{-\Delta\Delta Ct}$ calculation, −/− group was used as calibrator.

### 2.10. Phenotypic analysis of tissue-infiltrating leukocytes in explanted meshes

Phenotypic analysis of infiltrating leukocytes in explanted meshes was performed by flow cytometry. Briefly, explanted meshes were submerged in PBS and cells were detached with a 0.25% trypsin solution. $2 \times 10^5$ cells were incubated for 30 min at 4 °C with appropriate concentrations of mAbs in the presence of PBS containing 2% FBS. Cells were stained with murine FITC-conjugated anti-Ly6C (Miltenyi Biotec) and murine PerCP-conjugated anti-CD45 (Miltenyi Biotec). The percentage of CD45 + cells was quantified on total infiltrating cells. Additionally, CD45 + gated cells were used to quantify the percentage of M1 and M2 macrophages. For that, macrophages were gated according to FSC, SSC, CD45 expression and the expression of Ly6Chigh was used to identify distinct macrophage subsets. Although it is a very simplistic way to categorize M1 and M2 macrophage, the CD45+/Ly6C high population could be defined as M1 macrophages and predominantly inflammatory. On the contrary, the CD45+/Ly6C low population correspond to M2 macrophages with anti-inflammatory characteristics.

**Table 1**
Gene ID and commercial references for gene expression assays.

| Gene (Gene ID) | Life Technologies Assay ID |
|---|---|
| GAPDH (14433) | Mm99999915_g1 |
| MMP2 (17390) | Mm00439498_m1 |
| MMP8 (17394) | Mm00439509_m1 |
| MMP9 (17395) | Mm00442991_m1 |
| MMP13 (17386) | Mm00439491_m1 |
| TIMP1 (21857) | Mm01341361_m1 |
| TIMP2 (21858) | Mm00441825_m1 |
| TIMP3 (21859) | Mm00441826_m1 |
| TIMP4 (110595) | Mm01184417_m1 |
| COL1a1 (12842) | Mm00801666_g1 |
| COL3a1 (12825) | Mm01254476_m1 |
| IFN-g (15978) | Mm00801778_m1 |
| TNF-a (21926) | Mm00443258_m1 |
| IL-12a (16159) | Mm00434165_m1 |
| IL-10 (16153) | Mm00439616_m1 |
| IL-4 (16189) | Mm00445259_m1 |
| IL-13 (16163) | Mm00434204_m1 |

### 2.11. Statistical analysis

Data were statistically analyzed with SPSS-21 software (SPSS, Chicago, IL, USA) using the one-way ANOVA test followed by a *post-hoc* Tukey test for variables with a parametric distribution. For non-parametric variables, a Kruskal-Wallis test was performed, followed by a Mann-Whitney U test to evidence differences between groups. Those p-values $\leq 0.05$ were considered statistically significant.

## 3. Results

### 3.1. Phenotypic analysis and multipotentiality of murine-derived mesenchymal stem cells

The stemness markers expression profile of MSCs was CD29+/CD44+/CD90+/CD105+/HLA class I+/HLA class II− (Fig. 2A) and the differentiation assays towards adipogenic, chondrogenic and osteogenic lineages demonstrated their multipotentiality (Fig. 2B). Moreover, these cells, when cultured in the presence of fibrin glue, showed a fusiform morphology after 2 days under standard culture conditions and revealed an optimal viability (Fig. 2C).

### 3.2. Size distribution and exosome specific markers in exosomes derived from MSCs

The cell culture supernatants from MSCs were enriched up to 50 times with centrifugal filter concentration devices. Protein

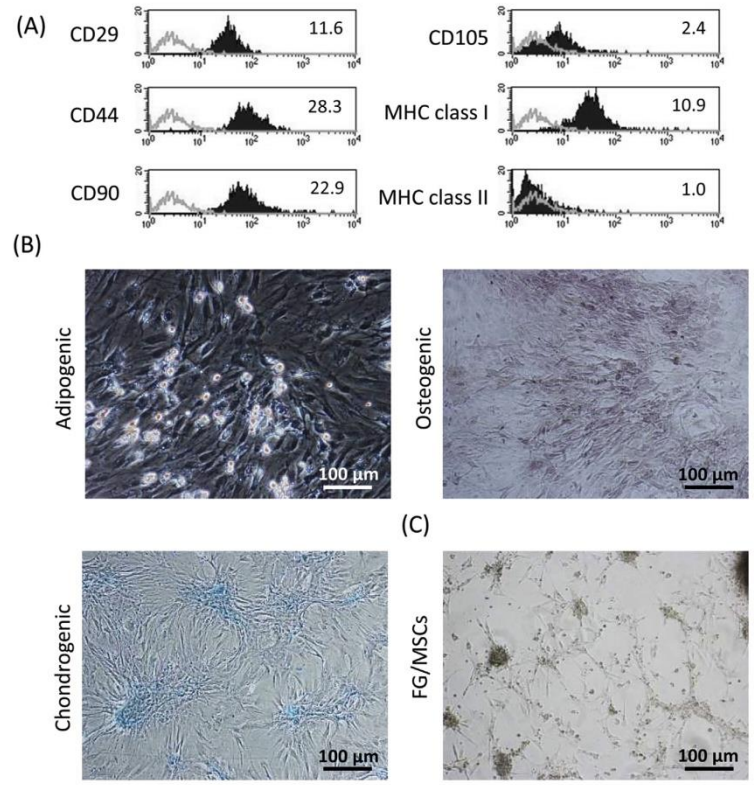


**Fig. 2.** Characterization and morphology of MSCs. A) Phenotypic analysis of MSCs was performed by multicolor flow cytometry. Representative histograms are shown. The expression level of cell surface markers (CD29, CD44, CD90, CD105, MHC class I and MHC class II) is represented as Normalized Mean Relative Fluorescence Intensity (MRFI) which is calculated by dividing the Mean Fluorescent Intensity (black filled histograms) by its isotype control (gray lined histogram). The MRFI values are included in the upper right corner of the histograms. B) Adipogenic, osteogenic and chondrogenic differentiation of MSCs stained with Oil Red O, Alizarin Red S and Alcian Blue 8GX and confirmed by microscopic examination at 20× magnification. C) Morphology and shape of MSCs admixed with fibrin glue at 20× magnification.

quantification in exosome-enriched supernatants was performed by Bradford assay. The resulting protein concentration in exosome-enriched supernatants was 20,000 µg/ml.

Additionally, a nanoparticle tracking analysis was performed in order to fully characterize these exosomes (size distribution and particle concentration were quantified). Fig. 3A shows a representative analysis of nanoparticle tracking with a mean size and standard deviation of isolated vesicles between 150 and 200 nm. Finally, CD9 (an exosomal marker) expression was found to be positive in these vesicles (Fig. 3B).

### 3.3. Surgical mesh implantation in an incisional hernia model

No mortality or bleeding complications were observed in mice during the surgical procedure or during the follow up period (7 days). The duration of the surgical procedure was 63 ± 21 min *per* animal. Our results demonstrated that the surgical procedure, fixation method and treatments were safe, well tolerated and simple to perform.

Additionally, considering that safety aspects is one of the major issues in stem cell-based therapies, this animal model was useful to determine the hypothetical adverse effects of MSCs and *exo*-MSCs admixed with FG. Seven days after implantation, the macroscopic evaluation of incisional hernia and implanted meshes showed a normal conformation of tissues. Surgical adhesions, effusions or tissue fibrosis were not observed in any of the groups (data not shown).

### 3.4. Histological evaluation at the implantation site and phenotype of infiltrating leukocytes

Microscopic alterations in the different study groups were evaluated in surgically implanted meshes as well as in the adjacent tissues. As shown in Fig. 4A, the H/E staining demonstrated an increased infiltration of leukocytes in all surgical meshes fixed with FG. However, no visual differences were found when FG, FG/MSCs and FG/*exo*-MSCs were compared. No differences between study groups were found in terms of hemorrhage, necrosis or neovascularization. The MT stain demonstrated that there were no significant differences in collagen depositions around implanted meshes (Fig. 4A).

Apart from histological findings, our study was also focused on the identification and characterization of tissue-infiltrating leukocytes. This analysis was performed by flow cytometry in explanted surgical meshes at day 7. The percentage of infiltrating leukocytes (CD45 + cells), M1 macrophages (CD45+/Ly6C high) and M2 macrophages (CD45+/Ly6C low) was quantified and compared between study groups. Our results demonstrated that, the percent-

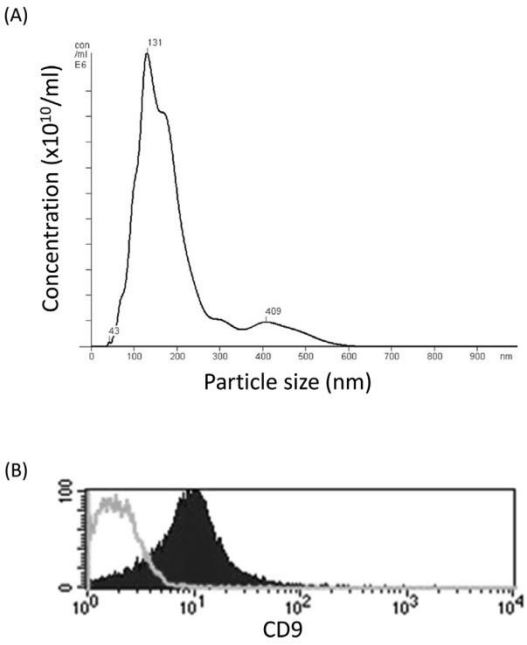


**Fig. 3.** Characterization of exo-MSCs. A) Frequency size distribution graph of exo-MSCs. The nanoparticle tracking analysis was performed to quantify size distribution and particle concentration. B) Representative histogram of CD9 expression (black filled histograms) in exosome-coated latex beads together with the negative control (gray lined histogram).

age of infiltrated leukocytes (CD45 + cells among total cells) was significantly increased when explanted meshes from control group (−/−) were compared with meshes fixed with FG, FG/MSCs and FG/*exo*-MSCs (Fig. 4B). No differences were found in the percentage of infiltrated leukocytes when FG, FG/MSCs and FG/*exo*-MSCs were compared (Fig. 4B). Additionally, the distribution of macrophages subsets in explanted surgical meshes was also analyzed by flow cytometry. The statistical analysis demonstrated a significant decrease of CD45 + Ly6C high cells, in the explanted meshes from groups FG/MSCs and FG/*exo*-MSCs when compared to FG. Similarly, a significant decrease was found when FG/MSCs were compared to −/− group (Fig. 4C). Regarding to CD45 + Ly6C low, our results demonstrated a significant increase of these cells in the explanted meshes from groups FG/MSCs and FG/*exo*-MSCs when compared to FG/−. Moreover, a significant difference was found when compared −/− and FG/*exo*-MSCs groups (Fig. 4D).

### *3.5. Gene expression analysis in explanted surgical meshes: inflammation-related cytokines*

TH1/TH2 cytokines (IFN-γ, TNF-α, IL-12a, IL-10, IL-4 and IL-13) gene expression was quantified in explanted meshes and compared between groups. In this analysis, the gene expression from MSCs and *exo*-MSCs are also shown. No significant differences were observed for IFN-γ, TNF-α, IL-12a (TH1 cytokines) and IL-10. However a significant increase in IL-4 and IL-13 (TH2 cytokines) was found in FG/MSCs when compared to FG/− and −/−. Furthermore, a statistically significant increase of IL-13 was found in FG/*exo*-MSCs when compared to −/− group (Fig. 5).

### *3.6. Gene expression analysis in explanted surgical meshes: MMPs and TIMPs*

Regarding to MMPs, the results obtained in the transcriptional analysis revealed a significant decrease of MMP2 in FG, FG/MSCs and FG/*exo*-MSCs groups when compared to −/− group (Fig. 6A). No differences were found in MMP8 (Fig. 6B) and MMP13 (Fig. 6D). Moreover, a significant increase of MMP9 was found in FG/MSCs groups when compared to −/− and FG/− groups (Fig. 6C). Regarding to TIMPs, we only found a significant decrease of TIMP2 in FG/− group when compared to −/− group (Fig. 6A-D). On the other hand, the MMPs/TIMPs ratios were calculated and different groups were also compared. It is interesting to note that, statistically significant differences were observed in MMP2/TIMPs and MMP9/TIMPs ratios (Fig. 6A and C, respectively) but not in the MMP8/TIMPs and MMP13/TIMPs ratios (Fig. 6B and 6D, respectively). In the case of MMP2/TIMPs ratio (Fig. 6A), a significant decrease of MMP2/TIMP1 was observed for FG/MSCs when compared to −/−. Similarly, a significant decrease was observed in MMP2/TIMP2 when FG/−, FG/MSCs and FG/*exo*-MSCs groups were compared to −/−. Moreover, a significant decrease of MMP2/TIMP3 was found in FG/− when compared to −/− and several differences were also found in the MMP2/TIMP4 ratio (Fig. 6A). Regarding to MMP9/TIMPs ratio a significant increase of MMP9/TIMP1 and MMP2/TIMP2 was found in FG/MSCs when compared to −/− and FG/− groups (Fig. 6C).

### *3.7. Gene expression analysis in explanted surgical meshes: Collagen I and III*

The expression of COL1A1 and COL3A1 genes (which encode the major component of type I collagen and type III collagen respectively) was quantified in explanted meshes from different groups at day 7. Our results demonstrated that COL1A1 and COL3A1 expression was significantly reduced in FG/−, FG/MSCs and FG/*exo*-MSCs when compared to −/− group. Moreover the COL1A1/COL3A1 gene expression ratio was also analyzed showing a significant decrease in the FG/MSCs group when compared to FG/− (Fig. 7).

## 4. Discussion

Synthetic surgical meshes have been used for over 5 decades for the treatment of hernias. This material provides an additional support to weakened or damaged tissue such inguinal hernia (the most common), femoral hernia or incisional hernia. In the case of incisional hernia, it occurs when abdominal wounds are unable to heal properly and the implantation of prosthetic meshes seems to be the ideal treatment for the reinforcement of soft abdominal tissue. Unfortunately, several adverse effects such as pain and patient discomfort are reported, but new materials and new designs have been developed to reduce adverse inflammatory reaction, chronic pain or mesh erosion [24]. In the last decades, surgical mesh improvements have been focused on the biocompatibility of materials and the mechanisms to permit the transmigration and localization of beneficial host cells [25]. Moreover, different coatings have been clinically tested in propylene meshes to reduce foreign body reaction and increase biocompatibility [26,27]. More recently, pre-seeding of acellular implants with stem cells from different sources demonstrated an improvement of tissue integration and vascularization as well as an accelerated healing process in comparison with their inert counterparts [28,29]. In relation to this, the combination of surgical meshes with adult stem cells has been tested by our group in preclinical settings demonstrating an anti-inflammatory effect of MSCs-coated meshes which is mediated through the polarization of macrophages towards M2 phenotype [20].

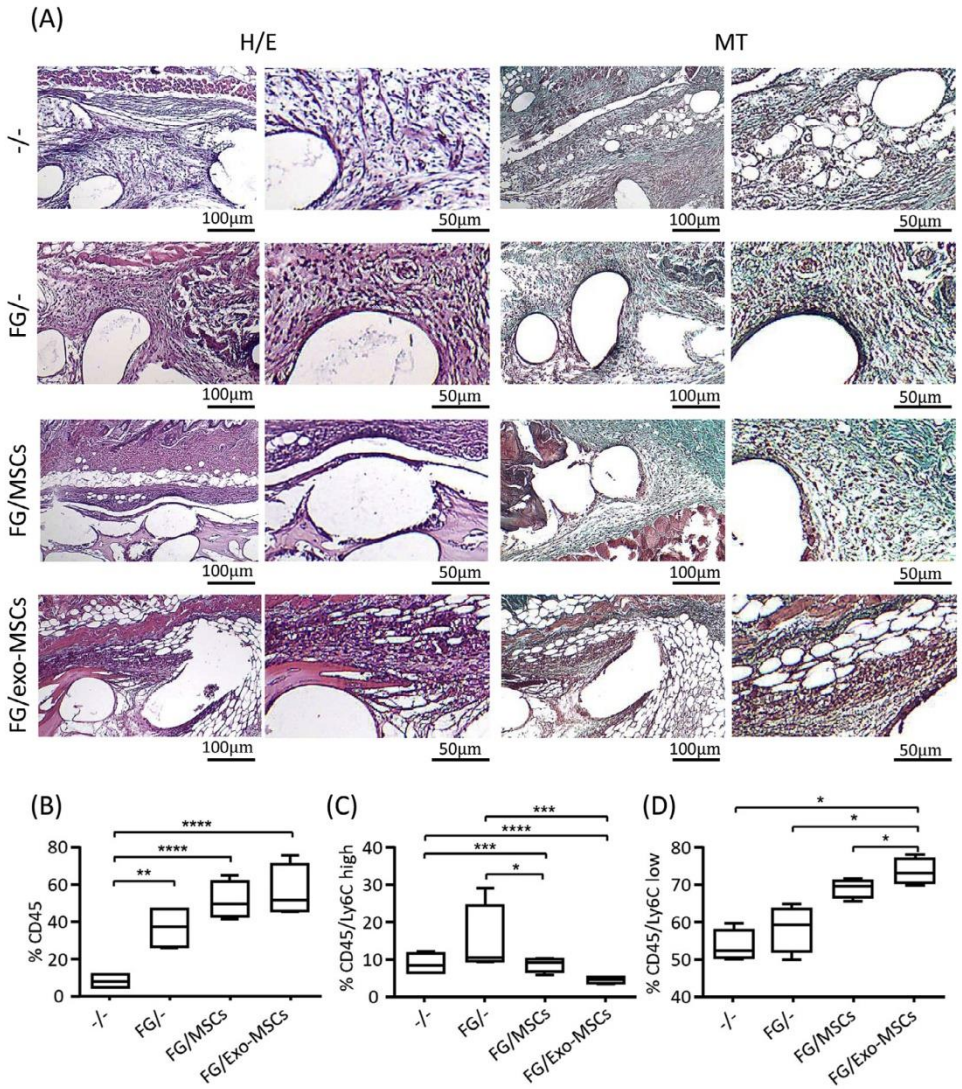


**Fig. 4.** Histological evaluation and characterization of tissue-infiltrating leukocytes. A) At day 7 post-implantation, the whole layer composed by the skin, mesh and muscular-peritoneum of euthanized animals was fixed in paraformaldehyde 4%, paraffin-embedded, sliced in 5–8 µm thickness and stained for hematoxylin-eosin (H/E) and Masson Trichrome (MT). B) Flow cytometry analysis of CD45+ cells among total cells in explanted surgical meshes at day 7. C) Percentage of Ly6C high cells among CD45+ leukocytes in explanted surgical meshes at day 7. D) Percentage of Ly6C low cells among CD45+ leukocytes in explanted surgical meshes at day 7. Graphs represent the mean ± SD of 4 independently performed experiments. Data were statistically analysed using a one-way ANOVA test followed by a post-hoc Tukey test for variables with a parametric distribution (%CD45 and %CD45/Ly6C high). For non-parametric variables (%CD45/Ly6C low), a Kruskal-Wallis test was performed, followed by a Mann-Whitney U test to evidence differences between groups. Horizontal bar represents statistically significant differences ($^{*}p \leq 0.05$, $^{**}p \leq 0.01$, $^{***}p \leq 0.001$, $^{****}p \leq 0.0001$).

On the other hand, fixation methods for surgical mesh implantation are a matter of debate. Absorbable or non-absorbable sutures with tacks as well as double crown without sutures have been compared in a clinical trial [30]. In animal models, mesh fixations have been compared between non-absorbable sutures, fibrin glue, non-absorbable spiral tacks and absorbable screw-type tacks suggesting that the best fixation method may be achieved using a combination of the studied materials [31].

This paper aimed to evaluate the dual role of fibrin glue, as a surgical mesh fixation method and as a cell and exosome vehicle for the treatment of incisional hernia. The usage of fibrin glue as a scaffold for stem cell transplantation has been previously tested in multiple scenarios for tissue engineering [12] and more especially in osteochondral repair [32] and myocardial infarction [19]. However, the innovative aspect of this study has been to evaluate the biological effect of MSCs and *exo*-MSCs co-administered with fibrin glue in an incisional hernia model.

To implement cell based therapies in clinical settings, one important aspect to be considered, together with the regulatory issues, is the feasibility of this implementation. Recently, numer-

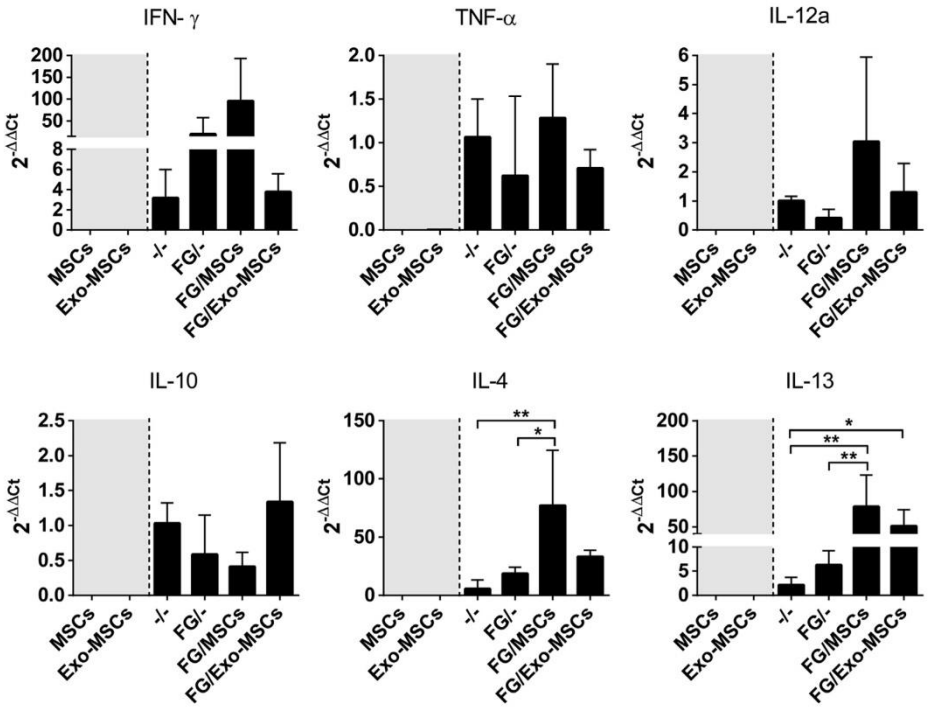


**Fig. 5.** Gene expression of immune-related soluble factors on surgically implanted meshes. At day 7 post-implantation, total RNA from explanted meshes was isolated and qRT-PCR products were quantified by the $2^{-\Delta\Delta Ct}$ method using GAPDH as housekeeping gene and −/− as calibrator group. Graph represents the mean ± SD of 4 independently performed experiments. Data were statistically analysed using a one-way ANOVA test followed by a post-hoc Tukey test. Horizontal bars represents statistically significant differences ($^{*}p \leq 0.05$, $^{**}p \leq 0.01$).

ous Advanced-therapy Medicinal Products (ATMP) achieved market authorization but failed to secure reimbursement (e.g., Glybera, Provenge, ChondroCelect, MACI) [33]. For this reason, it is important to ensure that the incremental benefit of the novel ATMP is proportionate to its incremental cost above current therapeutic approaches [34]. Finally, regarding to market access for cell therapies, and in agreement with Rémuzat et al., we consider that a high manufacturing costs and price of FG/MSCs or FG/*exo*-MSCs treatments will be compensated only if this product leads to important additional patient benefits compared to available treatment options [35].

It is important to note that, although MSCs have been previously tested in combination with surgical meshes [20,36] and more recently in decellularized scaffolds seeded with autologous MSCs for the treatment of inguinal hernia rabbit models [37], to our knowledge, this is the first report where exosomes derived from MSCs have been combined with surgical meshes.

In our first *in vitro* studies, the isolated, expanded and characterized murine bone marrow-derived MSCs were demonstrated to be positive for stemness markers with multipotent lineage potential. Additionally, our *in vitro* results of viability and proliferation (data not shown) demonstrated that the FG composition should be carefully tested prior to be used as a stem cell vehicle. Here we report that, the concentration of fibrinogen and thrombin (80 mg/ml and 500 IU/ml respectively) was found to be optimal for cell delivery and the pH of fibrinogen and thrombin solutions should range between 6.5 and 7.5 to maintain the viability of FG-admixed cells. These results are similar to those obtained by Ho *et al.* who demonstrated that fibrinogen and thrombin solutions may vary the proliferation rates of hMSCs [38].

Our next set of experiments was driven to isolate and characterize the exosomes derived from murine bone marrow-derived MSCs. The concentration, size and expression of exosomal markers demonstrated that the isolation protocol was simple and reproducible for using these vesicles as a therapeutic product. Actually, our characterization of murine bone marrow-derived MSCs was very similar to previous publications using human and porcine-derived exosomes [39,40].

Our *in vivo* assays were performed in a murine incisional hernia model. Although incisional hernia model has been previously described for pigs, rabbits and rats, the murine model offers several advantages, especially in terms of availability of laboratory reagents and consumables. Certainly, this animal model allowed us a better understanding of local inflammatory reaction and the identification of infiltrated inflammatory cells.

The anatomopathological analysis of surgical meshes at day 7 revealed an infiltration of leukocytes in surgical meshes with FG (independently of the co-administration with *exo*-MSCs or MSCs). Previous reports had already demonstrated an increase of infiltrated cells, mainly leukocytes, into the fibrin network [41] subjected to the regulation by chemo-attractant factors such as fibrinopeptides, fibronectin or enzymatically active thrombin [42]. Similarly, in previous studies using surgical meshes mixed with fibrin glue, the histological examinations revealed that fibrin glue was capable of triggering a stronger fibrous reaction and inflammatory response [43]. It is important to consider that, the inflammatory reaction might also be a specie-related phenomenon because of the allogeneic reaction against human-derived fibrinogen/thrombin in the animal model [44] and according to this author, this inflammation may be advantageous for surgical mesh

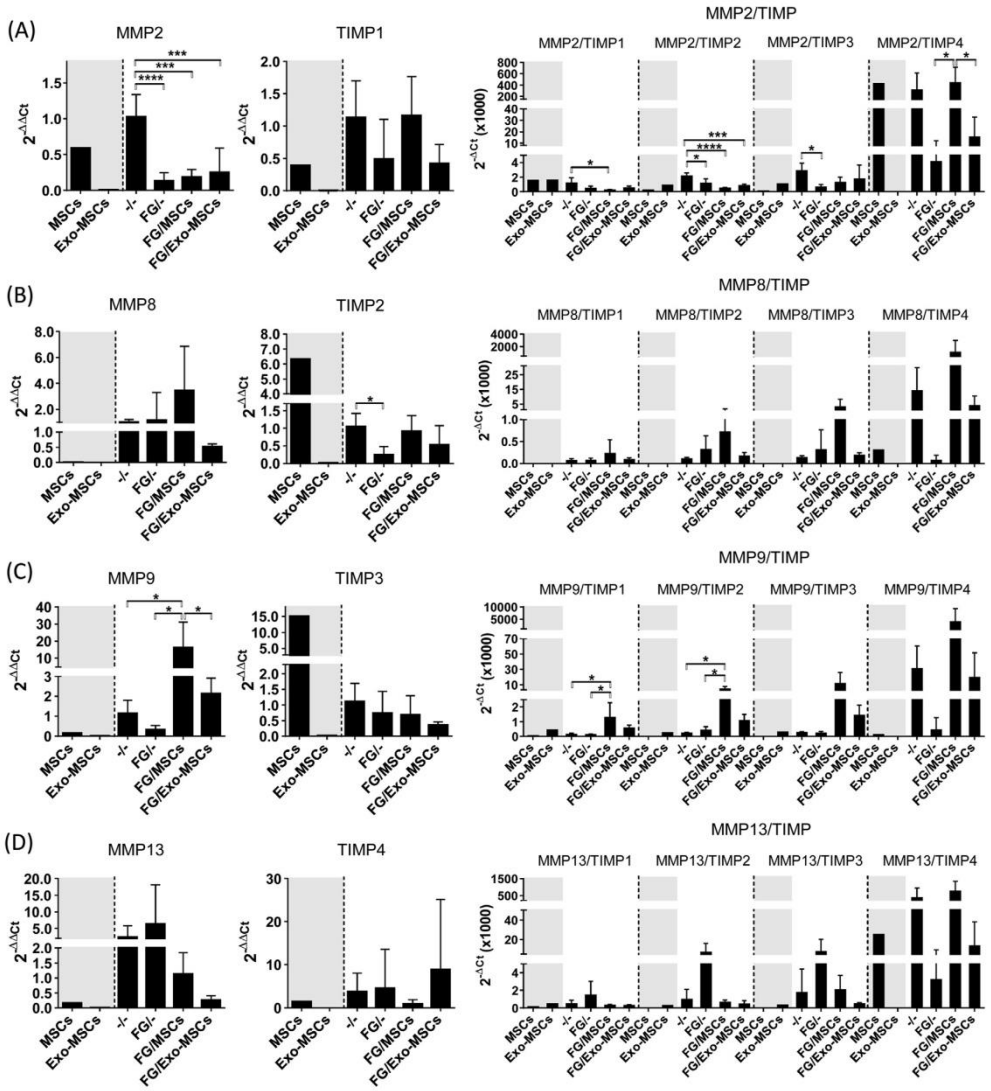


**Fig. 6.** Gene expression of MMPs and TIMPs on surgically implanted meshes. At day 7 postimplantation, total RNA from explanted meshes was isolated and qRT-PCR products were quantified by the $2^{-\Delta\Delta Ct}$ method using GAPDH as a housekeeping gene and −/− as calibrator group. Gene ratios were expressed as $2^{-\Delta Ct}$ values. Graph represents the mean ± SD of 4 independently performed experiments. Data were statistically analysed using a one-way ANOVA test followed by a post-hoc Tukey test. Horizontal bars represents statistically significant differences (*$p \leq 0.05$, ***$p \leq 0.001$, ****$p \leq 0.0001$).

implantation as it may improve tissue incorporation. Indeed, the reinforcement given by these prosthesis does not occur due to the material itself but by the tissue produced around the mesh fibers [45]. In relation to this, the use of FG for the fixation of polypropylene meshes has been previously related to a reduction of postoperative pain in comparison with sutures or cyanoacrylate [46,47], and to a marked fibroblastic ingrowth into the grafts when compared to staples [44], being suggested as a more suitable method for mesh fixation than conventional ones.

Once the histological sections of implanted surgical meshes were evaluated, our analysis of infiltrated leukocytes by flow cytometry corroborated the histological findings showing an increase of leukocyte cells (CD45+) in all the groups receiving FG. When compared to FG/− and −/− group, our results demonstrated a decrease of infiltrated M1-inflammatory macrophages together with an increase of M2 macrophages in surgical meshes when MSCs were co-administered. These results are similar and confirm our previous studies using MSCs-coated meshes [20]. Interestingly, the decrease of inflammatory macrophages was also observed when *exo*-MSCs were co-administered. Regarding the group with exosomes, we found a significant decrease of M1 macrophages when compared to −/− and FG/− groups as well as an increase of M2 macrophages when compared to FG/− group. The immunomodulatory effect of these exosomes has been previously

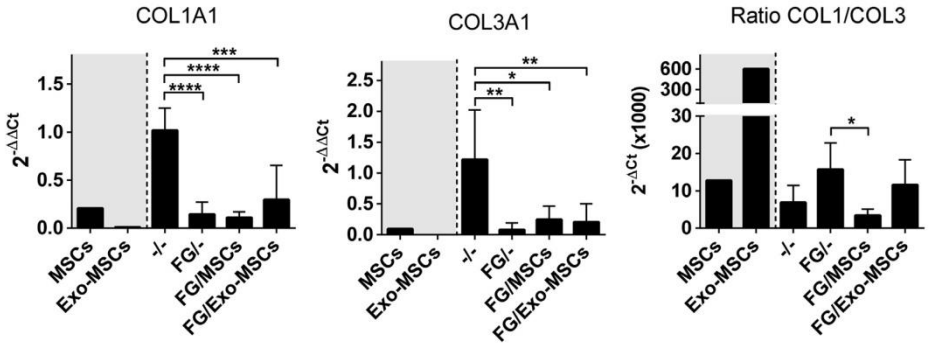


**Fig. 7.** Gene expression of Collagen Type I Alpha 1 and Collagen Type III Alpha 1 on surgically implanted meshes. At day 7 post-implantation, total RNA from explanted meshes was isolated and qRT-PCR products were quantified by the $2^{-\Delta\Delta Ct}$ method using GAPDH as a housekeeping gene and −/− as calibrator group. Gene ratios were expressed as $2^{-\Delta Ct}$ values. Graph represents the mean±SD of 4 independently performed experiments. Data were statistically analysed using a one-way ANOVA test followed by a post-hoc Tukey test. Horizontal bars represents statistically significant differences ($^{*}p \leq 0.05$, $^{**}p \leq 0.01$, $^{***}p \leq 0.001$, $^{****}p \leq 0.0001$).

described under *in vitro* conditions against T cell activation [40] and in animal models in the setting of synovitis [40] and cardiovascular diseases [48]. More recently, Lo Sicco *et al.* have also demonstrated *in vitro* that extracellular vesicles released by MSCs induced a shift in the balance of macrophages towards a M2 phenotype [49], which is coincident with our *in vivo* results.

In order to fully characterize the local inflammatory response, gene expression analysis of TH1/TH2 cytokines was analyzed. Our results demonstrated a significant increase of TH2 cytokines (IL-4 and IL-13) in surgical meshes where FG was co-administered with MSCs or *exo*-MSCs. These results sustain our previous analysis of infiltrated M1/M2 macrophages, suggesting that M2 macrophages may promote this TH2 response. This hypothesis is based on previous studies which demonstrated that MSCs induce the increase of IL-4 secretion by TH2 cells [50].

Altogether, these results indicate that, although MSCs and *exo*-MSCs did not show any decrease of the inflammatory response in terms of CD45 + cells –a response that, as stated before, could be beneficial for tissue incorporation–, they were able to modulate this response towards a less aggressive and pro-regenerative profile, which could have an impact in the prevention of the development of a foreign body reaction without decreasing the ability to incorporate new tissue to reinforce the weakened tissue. The gene expression analysis was also analyzed in the therapeutic products (MSCs and *exo*-MSCs) and considered as reference parameters. In the analysis of TH1/TH2 and MMPs and TIMPS, when compared MSCs and *exo*-MSCs, our results showed statistically significant differences (3 out of 16 analyzed genes), so according to Ekström et al., mRNAs could be specifically packed into the exosomes by a specific mechanism [51].

Finally, this study was also focused in the analysis of MMPs, TIMP and collagens which have been closely related with the development of inguinal hernia [52] and incisional hernia [53]. Regarding to MMPs and TIMPs our first set of results demonstrated a very high expression of MMP2, TIMP2 and TIMP3 in MSCs control samples (*in vitro* cultured MSCs under standard conditions), which is coincident with previous reports that demonstrated how these molecules were involved in the invasive capacity of MSCs [54].

Regarding to the analysis of MMPs and TIMPs in explanted meshes, the most relevant results were found in MMP9 expression evaluation. Based on a previous publication from Ben David et al., here we hypothesize that the increase of MMP9 in the tissue could be the consequence of MMP9 secretion by implanted MSCs [55]. Moreover, as suggested by this publication, the MMP9 release could also be induced by inflammatory cytokines. Supporting this idea, other authors have also demonstrated that umbilical cord-derived MSCs secrete MMP9 enabling collagen degradation [56]. On the other hand, according to a publication from Lolmede *et al.* a second hypothesis may explain our findings [57] and the high levels of MMP-9 in surgically implanted meshes could be the consequence of MMP-9 release from M2 polarized macrophages. Independently of MMP9 source, the high expression of this molecule in surgical meshes may be associated with an early process of neovascularization and angiogenesis [58,59].

Apart from MMPs and TIMPs expression, MMPs/TIMPs ratios were also analyzed. The alteration of these ratios has been reported in human incisional hernia tissues [53] and the increase of MMP9/TIMP1 and MMP9/TIMP2 in surgical meshes fixed with FG and MSCs may indicate alterations in the microstructure and loss of extracellular matrix. In contrast, the decrease of MMP2/TIMP1 and MMP2/TIMP2 may reflect a successful wound-healing [60] in our murine incisional hernia model.

Finally, type I and type III collagen gene expression showed a significant decrease in all surgical meshes fixed with FG. Moreover, the type I and type III ratio was significantly different when compared FG/− and FG/MSCs. Taking into account that hernia formation and recurrence is associated with a decreased type I/III collagen ratio [61], these results may indicate that fixation methods using FG would improve the biomechanical strength of surgical meshes having thick collagen fibers in the surrounding tissue.

## 5. Conclusions

To our knowledge this is the first preclinical study where MSCs and exosomes derived from MSCs have been used in combination with surgical meshes for the treatment of incisional hernia. Here, we firstly demonstrated that FG can be used as a stem cell vehicle for surgical mesh fixation. The histological and cellular identification of infiltrated leukocytes demonstrated that MSCs and exosomes reduce M1 inflammatory macrophages infiltration. The gene expression analysis of TH1/TH2 corroborated this observation showing a predominance of TH2 cytokines in those meshes where MSCs or exosomes were used. Finally, the gene expression analysis of MMPs, TIMPs and collagen I/II ratio showed significant differences, suggesting changes in the extracellular matrix structure.

This study demonstrates the potential beneficial effect of MSCs and *exo*-MSCs on the modulation of the immune response and healing process after mesh implantation. To corroborate the results obtained, further studies need to be performed concerning differ-

ent aspects. Firstly, *in vivo* assays in a clinically relevant animal model will be performed to extrapolate the preclinical results to the clinical scenario. Secondly, the therapeutic effect of MSCs and *exo*-MSCs should be further evaluated with other mesh structures and materials.

**Acknowledgements**

*In vitro* experiments were performed by the ICTS Nanbiosis (Unit 14. Cell therapy at CCMIJU). Exosomes characterization was performed by the ICTS Nanbiosis (Unit 6: Biomaterial processing and Nanostructuring Unit). *In vivo* experiments were performed by the ICTS Nanbiosis (Unit 22. Animal housing at CCMIJU). Technical and human support provided by Facility of Bioscience Applied Techniques of SAIUEx (financed by UEX, Junta de Extremadura, MICINN, FEDER and FSE).

**Funding**

This work was supported in part by ISCIII (CP17/00021), co-funded by ERDF/ESF, "Investing in your future". One grant from Junta de Extremadura (Ayuda a grupos catalogados de la Junta de Extremadura, GR15175) and two grants from Junta de Extremadura to JGC (TA13042 and IB16168 co-funded by ERDF/ESF). The funders had no role in study designs, data collection and analysis, decision to publish or preparation of the manuscript.

**Disclosure**

The authors declare that they have no competing interests.

**References**

[1] S. Todros, P.G. Pavan, A.N. Natali, Synthetic surgical meshes used in abdominal wall surgery: Part I-materials and structural conformation, J. Biomed. Mater. Res. Part B Appl. Biomater. 105 (2017) 689–699, https://doi.org/10.1002/jbm.b.33586.
[2] C. Brown, J. Finch, Which mesh for hernia repair?, Ann R. Coll. Surg. Engl. 92 (2010) 272–278, https://doi.org/10.1308/003588410X12664192076296.
[3] M.T. Wolf, C.A. Carruthers, C.L. Dearth, P.M. Crapo, A. Huber, O.A. Burnsed, R. Londono, S.A. Johnson, K.A. Daly, E.C. Stahl, J.M. Freund, C.J. Medberry, L.E. Carey, A. Nieponice, N.J. Amoroso, S.F. Badylak, Polypropylene surgical mesh coated with extracellular matrix mitigates the host foreign body response, J. Biomed. Mater. Res. A 102 (2014) 234–246, https://doi.org/10.1002/jbm.a.34671.
[4] C.M.P. Claus, G.M. Rocha, A.C.L. Campos, E.A. Bonin, D. Dimbarre, M.P. Loureiro, J.C.U. Coelho, Prospective, randomized and controlled study of mesh displacement after laparoscopic inguinal repair: fixation versus no fixation of mesh, Surg. Endosc. 30 (2016) 1134–1140, https://doi.org/10.1007/s00464-015-4314-7.
[5] L. Garcia-Vallejo, I. Couto-Gonzalez, P. Concheiro-Coello, B. Brea-Garcia, A. Taboada-Suarez, Cyanoacrylate surgical glue for mesh fixation in laparoscopic total extraperitoneal hernia repair, Surg. Laparosc. Endosc. Percutan Tech. 24 (2014) 240–243, https://doi.org/10.1097/SLE.0b013e3182a2f008.
[6] R.H. Fortelny, A.H. Petter-Puchner, K.S. Glaser, H. Redl, Use of fibrin sealant (Tisseel/Tissucol) in hernia repair: a systematic review, Surg. Endosc. 26 (2012) 1803–1812, https://doi.org/10.1007/s00464-012-2156-0.
[7] D.L. Sanders, S. Waydia, A systematic review of randomised control trials assessing mesh fixation in open inguinal hernia repair, Hernia 18 (2014) 165–176, https://doi.org/10.1007/s10029-013-1093-8.
[8] B.S. Powell, G.R. Voeller, Current developments in hernia repair; meshes, adhesives, and tacking, Surg. Technol. Int. 20 (2010) 175–181.
[9] A.H. Petter-Puchner, R. Fortelny, R. Mittermayr, W. Ohlinger, H. Redl, Fibrin sealing versus stapling of hernia meshes in an onlay model in the rat, Hernia 9 (2005) 322–329, https://doi.org/10.1007/s10029-005-0009-7.
[10] A.C. van der Ham, W.J. Kort, I.M. Weijma, H.F. van den Ingh, J. Jeekel, Effect of fibrin sealant on the healing colonic anastomosis in the rat, Br. J. Surg. 78 (1991) 49–53.
[11] A.J. Hanson, M.T. Quinn, Effect of fibrin sealant composition on human neutrophil chemotaxis, J. Biomed. Mater. Res. 61 (2002) 474–481, https://doi.org/10.1002/jbm.10196.
[12] T.A.E. Ahmed, E.V. Dare, M. Hincke, Fibrin: a versatile scaffold for tissue engineering applications, Tissue Eng. Part B Rev. 14 (2008) 199–215, https://doi.org/10.1089/ten.teb.2007.0435.
[13] S. Cox, M. Cole, B. Tawil, Behavior of human dermal fibroblasts in three-dimensional fibrin clots: dependence on fibrinogen and thrombin concentration, Tissue Eng. 10 (2004) 942–954, https://doi.org/10.1089/1076327041348392.
[14] R. Barbizan, M.V. Castro, B. Barraviera, R.S. Ferreira, A.L.R. Oliveira, Influence of delivery method on neuroprotection by bone marrow mononuclear cell therapy following ventral root reimplantation with fibrin sealant, PLoS ONE 9 (2014) e105712, https://doi.org/10.1371/journal.pone.0105712.
[15] R.A. Mehanna, I. Nabil, N. Attia, A.A. Bary, K.A. Razek, T.A.E. Ahmed, F. Elsayed, The effect of bone marrow-derived mesenchymal stem cells and their conditioned media topically delivered in fibrin glue on chronic wound healing in rats, Biomed. Res. Int. 2015 (2015) 846062, https://doi.org/10.1155/2015/846062.
[16] M.A. Reichenberger, W. Mueller, J. Hartmann, Y. Diehm, U. Lass, E. Koellensperger, U. Leimer, G. Germann, S. Fischer, ADSCs in a fibrin matrix enhance nerve regeneration after epineural suturing in a rat model, Microsurgery 36 (2016) 491–500, https://doi.org/10.1002/micr.30018.
[17] A.F. Manunta, P. Zedde, S. Pilicchi, S. Rocca, R.R. Pool, M. Dattena, G. Masala, L. Mara, S. Casu, D. Sanna, M.L. Manunta, E.S. Passino, The use of embryonic cells in the treatment of osteochondral defects of the knee: an ovine in vivo study, Joints 4 (2016) 70–79, https://doi.org/10.11138/jts/2016.4.2.070.
[18] C. Hao, Y. Wang, L. Shao, J. Liu, L. Chen, Z. Zhao, Local Injection of Bone Mesenchymal Stem Cells and Fibrin Glue Promotes the Repair of Bone Atrophic Nonunion In Vivo, Adv. Ther. 33 (2016) 824–833, https://doi.org/10.1007/s12325-016-0329-2.
[19] S. Roura, C. Gálvez-Montón, A. Bayes-Genis, Fibrin, the preferred scaffold for cell transplantation after myocardial infarction? An old molecule with a new life, J. Tissue Eng. Regen. Med. 11 (2017) 2304–2313, https://doi.org/10.1002/term.2129.
[20] R. Blázquez, F.M. Sánchez-Margallo, V. Álvarez, A. Usón, J.G. Casado, Surgical meshes coated with mesenchymal stem cells provide an anti-inflammatory environment by a M2 macrophage polarization, Acta Biomater. 31 (2016) 221–230, https://doi.org/10.1016/j.actbio.2015.11.057.
[21] R.C. Lai, T.S. Chen, S.K. Lim, Mesenchymal stem cell exosome: a novel stem cell-based therapy for cardiovascular disease, Regen. Med. 6 (2011) 481–492, https://doi.org/10.2217/rme.11.35.
[22] Mde L. Biondo-Simões, P.A.P. Moura, K. Colla, A.F.Z. Tocchio, C.G. de Morais, R. A. de Miranda, R.R. Robes, S.O. Ioshii, Inflammatory reaction and tensile strength of the abdominal wall after an implant of polypropylene mesh and polypropylene/poliglecaprone mesh for abdominal wall defect treatment in rats, Acta Cir Bras. 29 (Suppl 1) (2014) 45–51.
[23] K.J. Livak, T.D. Schmittgen, Analysis of relative gene expression data using real-time quantitative PCR and the 2(-Delta Delta C(T)) Method, Methods 25 (2001) 402–408, https://doi.org/10.1006/meth.2001.1262.
[24] B. Klosterhalfen, U. Klinge, V. Schumpelick, Functional and morphological evaluation of different polypropylene-mesh modifications for abdominal wall repair, Biomaterials 19 (1998) 2235–2246.
[25] D. Barski, H. Gerullis, E. Georgas, A. Bär, B. Lammers, A. Ramon, D. Ysebaert, B. Klosterhalfen, M. Boros, T. Otto, Coating of mesh grafts for prolapse and urinary incontinence repair with autologous plasma: exploration stage of a surgical innovation, Biomed. Res. Int. 2014 (2014) 296498, https://doi.org/10.1155/2014/296498.
[26] H. Gerullis, E. Georgas, C. Eimer, C. Arndt, D. Barski, B. Lammers, B. Klosterhalfen, M. Borós, T. Otto, Coating with autologous plasma improves biocompatibility of mesh grafts in vitro: development stage of a surgical innovation, Biomed. Res. Int. 2013 (2013) 536814, https://doi.org/10.1155/2013/536814.
[27] K. Junge, R. Rosch, U. Klinge, M. Saklak, B. Klosterhalfen, C. Peiper, V. Schumpelick, Titanium coating of a polypropylene mesh for hernia repair: effect on biocompatibilty, Hernia 9 (2005) 115–119, https://doi.org/10.1007/s10029-004-0292-8.
[28] S. Kalaba, E. Gerhard, J.S. Winder, E.M. Pauli, R.S. Haluck, J. Yang, Design strategies and applications of biomaterials and devices for Hernia repair, Bioact. Mater. 1 (2016) 2–17, https://doi.org/10.1016/j.bioactmat.2016.05.002.
[29] O. Guillaume, A.H. Teuschl, S. Gruber-Blum, R.H. Fortelny, H. Redl, A. Petter-Puchner, Emerging trends in abdominal wall reinforcement: bringing bio-functionality to meshes, Adv Healthc Mater. 4 (2015) 1763–1789, https://doi.org/10.1002/adhm.201500201.
[30] E. Wassenaar, E. Schoenmaeckers, J. Raymakers, J. van der Palen, S. Rakic, Mesh-fixation method and pain and quality of life after laparoscopic ventral or incisional hernia repair: a randomized trial of three fixation techniques, Surg. Endosc. 24 (2010) 1296–1302, https://doi.org/10.1007/s00464-009-0763-1.
[31] G. Chatzimavroudis, S. Kalaitzis, N. Voloudakis, S. Atmatzidis, S. Kapoulas, I. Koutelidakis, B. Papaziogas, E.C. Christoforidis, Evaluation of four mesh fixation methods in an experimental model of ventral hernia repair, J. Surg. Res. 212 (2017) 253–259, https://doi.org/10.1016/j.jss.2017.01.013.
[32] M.T. Berninger, G. Wexel, E.J. Rummeny, A.B. Imhoff, M. Anton, T.D. Henning, S. Vogt, Treatment of osteochondral defects in the rabbit's knee joint by implantation of allogeneic mesenchymal stem cells in fibrin clots, J. Vis. Exp. (2013) e4423, https://doi.org/10.3791/4423.
[33] D. Driscoll, S. Farnia, P. Kefalas, R.T. Maziarz, Concise review: the high cost of high tech medicine: planning ahead for market access, Stem Cells Transl. Med. 6 (2017) 1723–1729, https://doi.org/10.1002/sctm.16-0487.
[34] J. Jørgensen, P. Kefalas, Reimbursement of licensed cell and gene therapies across the major European healthcare markets, J. Mark Access Health Policy 3 (2015), https://doi.org/10.3402/jmahp.v3.29321.

[35] C. Rémuzat, M. Toumi, J. Jørgensen, P. Kefalas, Market access pathways for cell therapies in France, J. Mark Access Health Policy 3 (2015), https://doi.org/10.3402/jmahp.v3.29094.
[36] L.C. Schon, N. Gill, M. Thorpe, J. Davis, J. Nadaud, J. Kim, J. Molligan, Z. Zhang, Efficacy of a mesenchymal stem cell loaded surgical mesh for tendon repair in rats, J. Transl. Med. 12 (2014) 110, https://doi.org/10.1186/1479-5876-12-110.
[37] Y. Zhang, Y. Zhou, X. Zhou, B. Zhao, J. Chai, H. Liu, Y. Zheng, J. Wang, Y. Wang, Y. Zhao, Preparation of a nano- and micro-fibrous decellularized scaffold seeded with autologous mesenchymal stem cells for inguinal hernia repair, Int. J. Nanomedicine 12 (2017) 1441–1452, https://doi.org/10.2147/IJN.S125409.
[38] W. Ho, B. Tawil, J.C.Y. Dunn, B.M. Wu, The behavior of human mesenchymal stem cells in 3D fibrin clots: dependence on fibrinogen concentration and clot structure, Tissue Eng. 12 (2006) 1587–1595, https://doi.org/10.1089/ten.2006.12.1587.
[39] R. Blazquez, F.M. Sanchez-Margallo, O. de la Rosa, W. Dalemans, V. Alvarez, R. Tarazona, J.G. Casado, Immunomodulatory potential of human adipose mesenchymal stem cells derived exosomes on in vitro stimulated T cells, Front. Immunol. 5 (2014) 556, https://doi.org/10.3389/fimmu.2014.00556.
[40] J.G. Casado, R. Blázquez, F.J. Vela, V. Álvarez, R. Tarazona, F.M. Sánchez-Margallo, Mesenchymal stem cell-derived exosomes: immunomodulatory evaluation in an antigen-induced synovitis porcine model, Front. Vet. Sci. 4 (2017) 39, https://doi.org/10.3389/fvets.2017.00039.
[41] A.S. Wolberg, Determinants of fibrin formation, structure, and function, Curr. Opin. Hematol. 19 (2012) 349–356, https://doi.org/10.1097/MOH.0b013e32835673c2.
[42] N. Laurens, P. Koolwijk, M.P.M. de Maat, Fibrin structure and wound healing, J. Thromb. Haemost. 4 (2006) 932–939, https://doi.org/10.1111/j.1538-7836.2006.01861.x.
[43] P. Topart, F. Vandenbroucke, P. Lozac'h, Tisseel versus tack staples as mesh fixation in totally extraperitoneal laparoscopic repair of groin hernias: a retrospective analysis, Surg. Endosc. 19 (2005) 724–727, https://doi.org/10.1007/s00464-004-8812-2.
[44] N. Katkhouda, E. Mavor, M.H. Friedlander, R.J. Mason, M. Kiyabu, S.W. Grant, K. Achanta, E.L. Kirkman, K. Narayanan, R. Essani, Use of fibrin sealant for prosthetic mesh fixation in laparoscopic extraperitoneal inguinal hernia repair, Ann. Surg. 233 (2001) 18–25.
[45] L. Zogbi, The Use of Biomaterials to Treat Abdominal Hernias, in: R. Pignatello (Ed.), Biomaterials Applications for Nanomedicine, InTech, 2011. http://www.intechopen.com/books/biomaterials-applications-for-nanomedicine/the-use-of-biomaterials-to-treat-abdominal-hernias (accessed September 23, 2017).
[46] A. Odobasic, G. Krdzalic, M. Hodzic, S. Hasukic, A. Sehanovic, A. Odobasic, The role of fibrin glue polypropylene mesh fixation in open inguinal hernia repair, Med. Arch. 68 (2014) 90–93, https://doi.org/10.5455/medarh.2014.68.90-93.
[47] M. Canziani, F. Frattini, M. Cavalli, S. Agrusti, F. Somalvico, G. Campanelli, Sutureless mesh fibrin glue incisional hernia repair, Hernia 13 (2009) 625–629, https://doi.org/10.1007/s10029-009-0555-5.
[48] E. Suzuki, D. Fujita, M. Takahashi, S. Oba, H. Nishimatsu, Stem cell-derived exosomes as a therapeutic tool for cardiovascular disease, World J. Stem. Cells. 8 (2016) 297–305, https://doi.org/10.4252/wjsc.v8.i9.297.
[49] C. Lo Sicco, D. Reverberi, C. Balbi, V. Ulivi, E. Principi, L. Pascucci, P. Becherini, M.C. Bosco, L. Varesio, C. Franzin, M. Pozzobon, R. Cancedda, R. Tasso, Mesenchymal stem cell-derived extracellular vesicles as mediators of anti-inflammatory effects: endorsement of macrophage polarization, Stem. Cells Transl. Med. 6 (2017) 1018–1028, https://doi.org/10.1002/sctm.16-0363.
[50] S. Aggarwal, M.F. Pittenger, Human mesenchymal stem cells modulate allogeneic immune cell responses, Blood 105 (2005) 1815–1822, https://doi.org/10.1182/blood-2004-04-1559.
[51] K. Ekström, H. Valadi, M. Sjöstrand, C. Malmhäll, A. Bossios, M. Eldh, J. Lötvall, Characterization of mRNA and microRNA in human mast cell-derived exosomes and their transfer to other mast cells and blood CD34 progenitor cells, J. Extracell Vesicles 1 (2012), https://doi.org/10.3402/jev.v1i0.18389.
[52] A. Isik, C. Gursul, K. Peker, M. Aydın, D. Fırat, İ. Yılmaz, Metalloproteinases and their inhibitors in patients with inguinal hernia, World J. Surg. 41 (2017) 1259–1266, https://doi.org/10.1007/s00268-016-3858-6.
[53] J. Guillen-Marti, R. Diaz, M.T. Quiles, M. Lopez-Cano, R. Vilallonga, P. Huguet, S. Ramon-y-Cajal, A. Sanchez-Niubo, J. Reventós, M. Armengol, M.A. Arbos, MMPs/TIMPs and inflammatory signalling de-regulation in human incisional hernia tissues, J. Cell Mol. Med. 13 (2009) 4432–4443, https://doi.org/10.1111/j.1582-4934.2008.00637.x.
[54] C. Ries, V. Egea, M. Karow, H. Kolb, M. Jochum, P. Neth, MMP-2, MT1-MMP, and TIMP-2 are essential for the invasive capacity of human mesenchymal stem cells: differential regulation by inflammatory cytokines, Blood 109 (2007) 4055–4063, https://doi.org/10.1182/blood-2006-10-051060.
[55] D. Ben David, A.Z. Reznick, S. Srouji, E. Livne, Exposure to pro-inflammatory cytokines upregulates MMP-9 synthesis by mesenchymal stem cells-derived osteoprogenitors, Histochem. Cell Biol. 129 (2008) 589–597, https://doi.org/10.1007/s00418-008-0391-1.
[56] L. Xu, L. Ding, L. Wang, Y. Cao, H. Zhu, J. Lu, X. Li, T. Song, Y. Hu, J. Dai, Umbilical cord-derived mesenchymal stem cells on scaffolds facilitate collagen degradation via upregulation of MMP-9 in rat uterine scars, Stem Cell Res. Ther. 8 (2017) 84, https://doi.org/10.1186/s13287-017-0535-0.
[57] K. Lolmede, L. Campana, M. Vezzoli, L. Bosurgi, R. Tonlorenzi, E. Clementi, M.E. Bianchi, G. Cossu, A.A. Manfredi, S. Brunelli, P. Rovere-Querini, Inflammatory and alternatively activated human macrophages attract vessel-associated stem cells, relying on separate HMGB1- and MMP-9-dependent pathways, J. Leukoc. Biol. 85 (2009) 779–787, https://doi.org/10.1189/jlb.0908579.
[58] M. Bellafiore, G. Battaglia, A. Bianco, F. Farina, A. Palma, A. Paoli, The involvement of MMP-2 and MMP-9 in heart exercise-related angiogenesis, J Transl Med. 11 (2013) 283, https://doi.org/10.1186/1479-5876-11-283.
[59] G. Bergers, R. Brekken, G. McMahon, T.H. Vu, T. Itoh, K. Tamaki, K. Tanzawa, P. Thorpe, S. Itohara, Z. Werb, D. Hanahan, Matrix metalloproteinase-9 triggers the angiogenic switch during carcinogenesis, Nat. Cell Biol. 2 (2000) 737–744, https://doi.org/10.1038/35036374.
[60] M. Muller, C. Trocme, B. Lardy, F. Morel, S. Halimi, P.Y. Benhamou, Matrix metalloproteinases and diabetic foot ulcers: the ratio of MMP-1 to TIMP-1 is a predictor of wound healing, Diabet. Med. 25 (2008) 419–426, https://doi.org/10.1111/j.1464-5491.2008.02414.x.
[61] N.A. Henriksen, D.H. Yadete, L.T. Sorensen, M.S. Agren, L.N. Jorgensen, Connective tissue alteration in abdominal wall hernia, Br. J. Surg. 98 (2011) 210–219, https://doi.org/10.1002/bjs.7339.

Acta Biomaterialia 85 (2019) 60–74

Contents lists available at ScienceDirect

Acta Biomaterialia

journal homepage: www.elsevier.com/locate/actabiomat

Review article

# Meshes in a mess: Mesenchymal stem cell-based therapies for soft tissue reinforcement

F. Marinaro [a,1], F.M. Sánchez-Margallo [a,b,1], V. Álvarez [a], E. López [a], R. Tarazona [c], M.V. Brun [d], R. Blázquez [a,b,*], J.G. Casado [a,b,1]

[a] Stem Cell Therapy Unit, Jesús Usón Minimally Invasive Surgery Centre, Ctra. N-521, km 41.8, 10071 Cáceres, Spain
[b] CIBER de Enfermedades Cardiovasculares, Avenida Monforte de Lemos, 3-5. Pabellón 11. Planta 0, 28029 Madrid, Spain
[c] Immunology Unit, Department of Physiology, University of Extremadura, 10071 Caceres, Spain
[d] Department of Small Animal Medicine, Federal University of Santa Maria (UFSM), Av. Roraima, 1000 – 7 – Camobi, Santa Maria, 97105-900 Rio Grande do Sul, Brazil

ARTICLE INFO

*Article history:*
Received 28 June 2018
Received in revised form 21 November 2018
Accepted 26 November 2018
Available online 27 November 2018

*Keywords:*
Surgical meshes
Mesenchymal stem cells
Foreign body reaction
Hernia

ABSTRACT

Surgical meshes are frequently used for the treatment of abdominal hernias, pelvic organ prolapse, and stress urinary incontinence. Though these meshes are designed for tissue reinforcement, many complications have been reported. Both differentiated cell- and mesenchymal stem cell-based therapies have become attractive tools to improve their biocompatibility and tissue integration, minimizing adverse inflammatory reactions. However, current studies are highly heterogeneous, making it difficult to establish comparisons between cell types or cell coating methodologies. Moreover, only a few studies have been performed in clinically relevant animal models, leading to contradictory results. Finally, a thorough understanding of the biological mechanisms of mesenchymal stem cells in the context of foreign body reaction is lacking. This review aims to summarize *in vitro* and *in vivo* studies involving the use of differentiated and mesenchymal stem cells in combination with surgical meshes. According to preclinical and clinical studies and considering the therapeutic potential of mesenchymal stem cells, it is expected that these cells will become valuable tools in the treatment of pathologies requiring tissue reinforcement.

**Statement of Significance**

The implantation of surgical meshes is the standard procedure to reinforce tissue defects such as hernias. However, an adverse inflammatory response secondary to this implantation is frequently observed, leading to a strong discomfort and chronic pain in the patients. In many cases, an additional surgical intervention is needed to remove the mesh.

Both differentiated cell- and stem cell-based therapies have become attractive tools to improve biocompatibility and tissue integration, minimizing adverse inflammatory reactions. However, current studies are incredibly heterogeneous and it is difficult to establish a comparison between cell types or cell coating methodologies. This review aims to summarize *in vitro* and *in vivo* studies where differentiated and stem cells have been combined with surgical meshes.

© 2018 Acta Materialia Inc. Published by Elsevier Ltd. All rights reserved.

**Contents**

1. Introduction . . . 61
2. Differentiated cell-based applications for surgical mesh implantation. . . . 62
   2.1. Fibroblast-based therapy . . . 62
   2.2. Blood cell-based therapy. . . . 62
   2.3. Final remarks about differentiated cell-based applications for surgical mesh implantation . . . 64

* Corresponding author at: Ctra. N-521, km 41.8, 10071 Cáceres, Spain.
*E-mail address:* rblazquez@ccmijesususon.com (R. Blázquez).
[1] These authors equally contributed and should be regarded as co-first authors.

https://doi.org/10.1016/j.actbio.2018.11.042
1742-7061/© 2018 Acta Materialia Inc. Published by Elsevier Ltd. All rights reserved.

3. Mesenchymal stem cell-based applications for surgical mesh implantation . . . 64
3.1. Application of surgical mesh with adipose-derived mesenchymal stem cells. . . . 66
3.2. Application of surgical mesh with bone marrow-derived mesenchymal stem cells . . . 67
3.3. Application of surgical mesh with endometrial-derived mesenchymal stem cells . . . 68
3.4. Final remarks about mesenchymal stem cell-based applications for surgical mesh implantation . . . 68
4. Foreign body reaction and MSC activity during surgical mesh implantation . . . 69
4.1. MSCs in phase I of foreign body reaction: protein adsorption process . . . 69
4.2. MSCs in phase II of foreign body reaction: acute inflammation process . . . 69
4.3. MSCs in phase III of foreign body reaction: chronic inflammation process. . . . 69
4.4. MSCs in phase IV of foreign body reaction: wound-healing process . . . 71
5. Future perspectives for mesenchymal stem cell-based therapies in surgical meshes . . . 71
Acknowledgement . . . 71
Funding . . . 71
Disclosure . . . 71
References . . . 71

## 1. Introduction

Surgical meshes are medical devices designed to reinforce and stabilize weakened tissue, frequently used for the treatment of incisional hernia, pelvic organ prolapse, and stress urinary incontinence [1–3]. The implantation of surgical meshes by open surgery or laparoscopy is a common procedure. According to bioengineering parameters, the "ideal mesh" should be inert, resistant to infections, and flexible, with long-term tensile strength and rapid mesh-tissue integration [4]. It is important to note that the concept of "ideal mesh" is closely related to the pathology to be treated. In this sense, urogynecologic meshes (for stress urinary incontinence and pelvic organ prolapse) are implanted in tissues which are mechanically, anatomically, and biologically different from abdominal or inguinal hernias. Currently, non-absorbable meshes are the most widely-used implants for tissue reinforcement in hernia-related complications; their successful integration involves histopathological and immunological changes providing long-term strength, stability, and durability [5].

The majority of non-absorbable surgical meshes are made of polypropylene, polyester, expanded polytetrafluoroethylene (ePTFE), or polyvinylidene fluoride (PVDF). Out of these materials, polypropylene is the most commonly used due to its versatility, mechanical stability, strength, lower risk of bacterial infections, and resistance to biological degradation [6]. These synthetic meshes have been combined with a wide range of compounds to improve their biological properties [7,8]. Several studies have demonstrated that the physical-mechanical properties of implanted meshes are closely related to the pore size, weight, and elasticity of the mesh. They can also be divided into ultralight, light, standard, or heavy categories [9] and classified in terms of tensile strength ($N/cm^2$, MPa). Animal models have demonstrated that multifilament hydrophobic meshes exhibit an increased bacterial persistence when compared to monofilament polypropylene [10]; furthermore the risk of infection is inversely correlated with the pore size of surgical meshes [11–13].

It is important to note that these non-absorbable meshes can lead to pathological changes such as adherence to visceral organs, hardening, shrinking, fibrosis, calcification, thrombosis, and infections, all of which are related to clinical symptoms such as chronic pain and discomfort [14–16]. These adverse effects are frequently reported in patients with urogynecological disorders where tissue erosion at the implantation site is particularly common [17–19]. At present, the unacceptable failure rate of surgical interventions is a matter of debate in the FDA (Food and Drug Administration) and EMA (European Medicines Agency) [20,21]. In October 2008, after a review of adverse events, the FDA supplied a Public Health Notification about the safety and effectiveness concerns over the use of surgical meshes for the transvaginal repair of pelvic organ prolapse [22]. Given the high number of reports of injury, death, and malfunction, in 2011 the FDA issued an Update on the Safety and Effectiveness of Transvaginal Placement for Pelvic Organ Prolapse [23] as well as a Safety Communication [24] to inform patients and health care providers about the risks associated with urogynecologic meshes. In light of these warnings, many devices were removed from urogynecological use [25].

In hernia-related disorders, several complications are possible after mesh implantation [26]; however compared to pelvic organ prolapse or stress urinary incontinence, the failure rates are significantly lower [27].

Apart from non-absorbable meshes, both absorbable and biological meshes are being used to decrease post-operative complications. Absorbable meshes are gradually absorbed over time to minimize the amount of foreign material remaining. In theory, these meshes should be capable of reducing the intense foreign body reaction and immune response encountered with non-absorbable meshes [5]. Biological meshes are composed of decellularized tissue with a dense network of collagen and biological factors which positively influence wound healing. In comparison to synthetic materials, biological meshes increase the safety of mesh implantation in contaminated areas [5]. They can be crosslinked to delay degradation and increase their stability; however, crosslinking seems to decrease the biocompatibility of the material as well as the strength of incorporation into host tissue [28,29]. It is important to note that also patient-specific factors may differently influence the wound-healing response to the same biological mesh, modifying the implantation environment and mesh degradation [30].

In the last decade, cell-based therapies have become attractive tools for improving host tissue infiltration and integration of surgical meshes. In the case of mesenchymal stem cell (MSC) based therapies, these cells have been found to exhibit an anti-inflammatory effect and a pro-regenerative potential thus enhancing wound healing and tissue repair [31,32]. An autologous approach to MSC therapy (i.e., using cells from the patient's own body) may be safer in that it avoids unwanted immune responses, yet it presents obvious drawbacks in the time frame for treatments and clinical costs. Allogeneic therapies offer the possibility of administering cells as an "off-the-shelf" product that can be subjected to more stringent quality control than autologous products [33]. Recent studies demonstrate that allogeneic MSCs are not immunoprivileged, exhibiting both cell- and humoral-mediated immune responses to major histocompatibility complex (MHC)-mismatched MSCs [34–36]. In any case, under the authors' point of view, both autologous and allogeneic MSCs may provide safe and clinically applicable therapies in the field of surgical meshes.

Therefore, the purpose of this review is as follows: (I) to provide an overview of *in vitro* and *in vivo* studies where differentiated cells have been combined with surgical meshes; (II) to summarize current research on surgical meshes and mesenchymal stem cell-based therapies; and (III) to describe and classify the sequential mechanisms that occur after surgical-mesh implantation and the role of MSCs in these mechanisms.

## 2. Differentiated cell-based applications for surgical mesh implantation

### *2.1. Fibroblast-based therapy*

One of the main disadvantages of non-absorbable materials is the induction of adverse foreign body reactions [37]. To ameliorate this problem, various studies have been conducted attempting to enhance the biocompatibility of these materials. As shown in Table 1, autologous differentiated cells have been combined with biomaterials and *in vitro* and *in vivo* assays have been performed to assess tissue regeneration.

A number of *in vitro* studies have been conducted to assess the feasibility of combining non-absorbable surgical meshes and fibroblasts. One of the first studies was developed by Kapischke et al., who analyzed cell adherence, proliferation, and collagen deposition in human foreskin fibroblasts co-cultured with three different polypropylene meshes (commonly used for abdominal wall repair). This study demonstrated that fibroblasts were able to colonize the meshes within 4–6 weeks and produce collagen deposits, suggesting that cells may modify the biomaterial surface by the deposition of extracellular matrix components prior to colonization [38]. Similarly, four years later, Skala et al. performed an *in vitro* study to determine a suitable technique for fibroblast-coating of different meshes (commonly used for urinary incontinence and pelvic organ prolapse). The authors reported that the best coating was achieved with xenograft-based meshes. Moreover, they concluded that polypropylene meshes showed an acceptable fibroblast-coating rate and that the poorest coating was observed with polyester and modified polypropylene meshes. Interestingly, small-pore polypropylene meshes showed higher coating rates than those with larger pores [39].

To decrease tissue ingrowth and adhesions to the viscera, Canuto et al. designed a two-layer polypropylene mesh for hernia repair composed of a macroporous light mesh (parietal side) and a thin, transparent, nonporous film (visceral side). The authors incubated BJ fibroblast (a human-derived fibroblast cell line) with the two-layer mesh for 7, 14, and 21 days. They observed that the formation of the cell coating on the macroporous layer was successful, while no cell growth occurred on the film. The production of type I collagen by fibroblasts, was significantly increased during the experimental time frame. Finally, an increase in proinflammatory factors at day 7, followed by a decrease at days 14 and 21, was shown [40]. These results highlight the fact that not only the composition of the mesh, but also its design, is a determinant for tissue integration and host response.

A recent report from Guillaume et al. used self-manufactured silk meshes combined with lectin (wheat germ agglutinin). In this study, the authors aimed to enhance the cytoadhesion and cytocompatibility of surgical meshes by testing lectin pretreatment. Their results demonstrated that NIH3T3 fibroblast (a mouse-derived fibroblast cell line) had a significantly higher binding affinity to the lectin-treated silk when compared to untreated silk. Also, after 4 days of culture, the fibroblasts were able to colonize silk meshes (with a higher number of cells in lectin-treated meshes), but not the polypropylene meshes used as a control. Moreover, they demonstrated that the presence of the lectin did not have a negative effect on either the proliferative behavior of fibroblasts nor the immunogenicity of the mesh. In fact, when they compared the release of Il-6 and IL-8 from peripheral blood lymphocytes co-cultured with untreated or lectin-treated silk meshes, no significant differences were found. Additionally, when polypropylene meshes were compared with silk meshes, the cytokine levels were lower on silk meshes [41]. It is important to note that although silk is known to degrade completely within approximately two years [42], it is usually classified as a non-absorbable material due to its prolonged persistence in the body [43–45].

In summary, all fibroblast-based therapies have a common objective: to improve mesh-tissue integration, especially on materials with a hydrophobic surface and low cell adhesion rate such as polypropylene [6]. Coating these materials with fibroblasts results in a superior biocompatibility, as these cells secrete extracellular matrix components that modify the mesh surface [38]. Taking into account the low adhesion properties of non-absorbable meshes while considering that the coating of cells is difficult when macroporous meshes are used [39], pretreatments with hydrophilic substances may help to attain a better proliferation rate, achieving the coating of fibroblasts in a shorter period of time.

### *2.2. Blood cell-based therapy*

One component that has acquired importance in the field of regenerative medicine is platelet-rich plasma (PRP). Although its use has largely been focused on osteoarticular diseases, the promising results obtained in other clinical situations have made of PRP a valuable tool for tissue healing and regeneration. In 2015, Medel et al. used PRP to promote human vaginal fibroblast attachment to synthetic meshes, thus increasing the healing potential of the material in pelvic organ prolapse. In comparison to meshes without PRP, pre-incubation with PRP significantly increased fibroblast adhesion to polypropylene and polyglactin meshes [46]. The importance of PRP in this study is relative, as it was used strictly as a "supplement" to improve the adhesion of fibroblasts to meshes, being these cells the therapeutic agent.

PRP was also used to improve mesh biocompatibility in two related preclinical studies. In the first one, the authors implanted a PRP-coated polypropylene mesh in the abdomen of female rabbits, evaluating the production of types I and III collagen and the inflammatory infiltrate at 7, 30, and 90 days. No significant differences were found at 7 and 30 days; the authors stated that the absence of difference at day 7 provided evidence that PRP does not alter the initial inflammatory response. Additionally, a significant increase in type I and type III collagen in the PRP group at 7 days was reported, suggesting a possible acceleration of the healing process mediated by PRP. To the contrary, there was a significantly higher inflammatory cell infiltration in the PRP group at day 90 when compared to control meshes. Assuming that the continued migration of these cells (mainly macrophages and lymphocytes) favors wound healing and repair, the authors suggested that this increase might help to consolidate late phase tissue repair [47]. In opposition to this hypothesis, several reports suggest that a prolonged inflammatory reaction after mesh implantation is commonly related to a long-lasting and adverse foreign body reaction [37,48,49]. It is likely that the characterization of the inflammatory infiltrate observed at day 90 would help to elucidate the biological implication of this reaction.

The results of the second study showed important differences when compared with the first one, even though the methodology was similar in terms of animal model, type of mesh, time points, and determinations. In this case, the meshes were implanted between the vaginal epithelium and the rectovaginal fascia. This difference in the implantation site mandates the consideration of certain experimental conditions to evaluate the results of each

**Table 1**
Cell-coating methodology performed in the different studies using synthetic materials.

| | Study | Type of study | Cell type | Cell dose | Mesh (material) | Coating methodology | Main outcomes |
|---|---|---|---|---|---|---|---|
| Fibroblast-based therapy | Kapische et al., 2005 [38] | *In vitro* | Human foreskin fibroblasts | 300 000 cells/ml on drop form on a 0.5 × 0.5 cm mesh fragment | SurgiPro® (PP)<br>Parietene3 PP1510® (PP)<br>VIPRO II® (PP) | Cells seeded on top of the mesh with a low volume of culture medium. Addition of fresh culture medium 12 h later. Evaluation at 1, 4, and 6 weeks. | Fibroblasts proliferated and produced collagen deposits on PP meshes. Cells may modify the hydrophobic surface by deposition of ECM components before colonization. |
| | Skala et al., 2009 [39] | *In vitro* | Human vaginal fibroblasts | $10^7$ cells in 1 ml seeded onto 2 × 3 cm mesh | Monarc® (PP)<br>Obtape® (PP)<br>Timesh® (Titanized PP)<br>Pelvitex® (coated PP with hydrophilic porcine collagen)<br>Mersilene® (PE)<br>Surgisis® (Porcine intestinal submucosa)*<br>Pelvicol® (Acellular collagen matrix)* | Cells seeded on top of the mesh with a low volume of culture medium. Addition of fresh culture medium 5 h later. Evaluation at 5 h and 5 weeks. | The best coating rate was achieved by Surgisis® and Pelvicol®. PP meshes had an intermediate outcome (better in meshes with smaller pores) and the worst results were obtained with PE and modified PP. |
| | Canuto et al., 2013 [40] | *In vitro* | BJ human fibroblasts | Not indicated | ClearMesh Composite (PP) | Cells seeded on wells with the meshes. Evaluation at 7, 14, and 21 days. | Fibroblasts proliferated on the macroporous layer but not on the film. Collagen deposition increased with time. Inflammatory cytokines increased at 7 days and decreased at 14 and 21 days. |
| | Guillaume et al., 2016 [41] | *In vitro* | NIH3T3 fibroblasts | 700 000 cells/well (24 well plate) on a mesh held by a cell crown | Optilene® (PP)<br>Self-manufactured (Silk)<br>Self-manufactured (Silk treated with lectin WGA) | Lectin WGA pretreatment and incubation of meshes with cell suspension for 4 days. | Lectin pretreatment improved binding affinity and cell number growing on meshes. PP mesh presented worse outcomes than silk meshes. |
| Blood cell-based therapy | Medel et al., 2015 [46] | *In vitro* | PRP + Human vaginal fibroblasts | 5 × 5 mm mesh coated with 0.2 ml of PRP.<br>50 000 cells in 500 µl seeded onto each mesh. | Vicryl® (PG)*<br>Restorelle® (PP) | Pre-incubation of meshes + PRP for 30 min followed by co-culture of meshes + cells for 2 h. | Fibroblasts showed better attachment to mesh when treated with PRP. |
| | Ávila et al., 2016 [47]<br>Parizzi et al., 2017 [50] | *In vivo* (rabbit) | PRP | PRP gel obtained from 10 ml of blood on 1 × 1 cm mesh | PP | Placement of PRP gel (PRP + calcium gluconate) covering the mesh after its implantation. Evaluation at 7, 30, and 90 days. | Abdominal location: increased inflammatory infiltrate at 90 days and collagen I and III deposition at 7 days in PRP-coated meshes.<br>Vaginal location: decreased inflammatory infiltrate at day 30 and increased collagen III deposition at 90 days in PRP-coated meshes. |
| | Gerullis et al., 2013a [51] | *In vitro* | PBMCs/plasma/platelets | 12 ml of blood component on 2 × 2 cm mesh | VitaMesh™ (PP)<br>DynaMesh® (PVDF)<br>MotifMesh™ (PTFT)<br>TVT PP (PP)<br>UltraPro® (PP reinforced with PC)<br>Proceed® (PP encapsulated with PDS)<br>Mersilene® (PET) | Incubation of mesh + blood component for 12 h. Evaluation after co-culture with expanded tissue probes for 6 weeks and 4 months. | Coating with plasma and platelets increased the adherence score in all meshes tested. |
| | Gerullis et al., 2013b [52]<br>Gerullis et al., 2014 [53] | *In vivo* (sheep) | Autologous plasma | Not indicated | Dynamesh® (PVDF)<br>UltraPro® (PP reinforced with PC)<br>TVT PP (PP) | Incubation of mesh + autologous plasma for 12 h prior to implantation. Evaluation after 3, 6, 12, and 24 months, or 5, 20, 60, and 120 min. | Autologous plasma-coated meshes showed better biocompatibility in terms of thickness of inflammatory tissue, connective tissue, and macrophage infiltration than non-coated meshes at later time points. At early time points, no differences were found. |

(*continued on next page*)

**Table 1** (*continued*)

| Study | Type of study | Cell type | Cell dose | Mesh (material) | Coating methodology | Main outcomes |
|---|---|---|---|---|---|---|
| Barski et al., 2014 [54] | Clinical study | Autologous plasma | Not indicated | Seratim® PA (PP, PGA and CL) Vitamesh™ (PP) UltraPro® (PP reinforced with PC) TVT PP (PP) | Incubation of mesh + autologous plasma for 30 min prior to implantation. The remaining plasma was spilled over the implantation site. Evaluation after implantation and at 6–8 weeks. | The implantation of autologous plasma-coated meshes was safe and improved functional outcome and quality of life regardless of the mesh type. |

* Absorbable materials; CL: caprolactone; ECM: extracellular matrix; PBMC: peripheral blood mononuclear cells; PC: poliglecaprone; PDS: polydioxanone; PE: polyester; PET: polyethylene terephthalate; PG: polyglactin 910; PGA: polyglycolic acid; POP: pelvic organ prolapse; PP: polypropylene; PRP: platelet-rich plasma; PTFT: polytetrafluoroethylene; PVDF: polyvinylidene fluoride; WGA: wheat germ agglutinin.

study. Vaginal and abdominal tissues have different biomechanical properties, moreover, as the authors state, abdominal implants are placed in a sterile environment, while vaginal implants are placed in a potentially contaminated environment. In this study, the group without PRP showed a significant increase in the inflammatory infiltrate at 30 days that was not reported in the PRP group. Moreover, there was a significant increase of type III collagen in the PRP group at day 90 [50]. It is important to highlight that the evaluation of these two studies was based on histological analysis without quantitative determinations of inflammatory cells; therefore, reliable conclusions cannot be drawn.

Similarly, Gerullis et al. developed a series of studies evaluating the combination of surgical meshes and autologous plasma. In the first *in vitro* approach, the authors analyzed tissue ingrowth on seven commercial meshes used for different surgical purposes and coated with peripheral blood mononuclear cells (PBMCs), platelets, or plasma. They concluded that plasma and platelet coating improved *in vitro* biocompatibility and that the PVDF mesh exhibited the best cell-adherence score [51]. In the next study, three meshes (previously scored as good, intermediate, and poor in terms of tissue ingrowth) were coated with autologous plasma and intraperitoneally implanted in sheep. After 3, 6, 12, and 24 months, foreign body reaction, scar formation, and inflammatory reactions were evaluated. The best outcomes were obtained with PVDF meshes, again suggesting a beneficial effect of autologous plasma coating [52]. An equivalent study was subsequently performed to monitor the acute inflammatory response at shorter time points (5, 20, 60, and 120 min); however, no remarkable differences were observed between study groups [53].

Preclinical studies using autologous plasma and meshes reached the clinical phase in 2014 in a clinical study that used four different synthetically coated-meshes. These meshes were implanted in 20 patients with pelvic organ prolapse or stress urinary incontinence. Functional outcome and quality of life were evaluated before surgery and 3 months post-surgery, showing significant improvement in all groups, not reporting intraoperative problems or complications associated with the mesh coating [54]. However, the absence of a control group in this study makes it impossible to evaluate the beneficial outcomes of this treatment in relation to non-coated meshes. Further conclusions will require a randomized, placebo-controlled trial.

Despite the significant number of studies addressing the use of PRP and autologous plasma to improve mesh biocompatibility, robust *in vitro* results were only achieved on cell adhesion assays performed by Medel et al. and Gerullis et al. These studies demonstrated optimal adhesion in meshes pretreated with blood derivatives [46,51]. With the exception of the paper from Gerullis et al. which showed a prolonged positive effect when using surgical meshes coated with autologous plasma [52], to date, no concluding results support a direct effect of autologous plasma or PRP-coated meshes on biocompatibility.

### *2.3. Final remarks about differentiated cell-based applications for surgical mesh implantation*

Along with the previously described studies, some preclinical studies have been conducted to appraise the combination of different cells with biological meshes. Biological matrices such as small intestine submucosa [55,56], muscle acellular matrix [57,58], and bovine tunica vaginalis [59] were coated with fibroblasts or myoblasts and implanted in rat [55–58] or rabbit [59] models. The cell-treated groups showed better infiltration and mechanical performance [55], abundant blood vessels and myoblasts [57], better disposition of newly formed collagen with neovascularization [59], and/or increased vascular regeneration and mechanical strength [56].

In summary, several studies demonstrate the beneficial effects of cell-coated meshes in neovascularization and foreign body reaction. However, the heterogeneity of these different studies renders the comparison between cell types challenging. First, it is clear that there are strong differences in coating efficiency with regard to mesh material. The use of an intermediate treatment has been found to improve cell adhesion in those materials with poor adhesion outcomes. Second, the variability in methodological procedures for cell coating is almost as high as the number of studies, since each group developed its own methodology (see Table 1). Finally, although many *in vitro* studies have been performed to assess the feasibility of the combinations, little is known from *in vivo* studies. Moreover, some of the studies using laboratory animal models seem to be contradictory and only a few were performed in clinically relevant models such as sheep or pig, which afford a more appropriate extrapolation of results for human clinical settings.

## 3. Mesenchymal stem cell-based applications for surgical mesh implantation

The use of MSCs with surgical meshes represents a new option in the field of abdominal wall repair when soft tissue reinforcement is necessary. Their differentiation, immunomodulatory effect, and anti-inflammatory properties can be combined with the physical-mechanical support provided by the surgical mesh itself. However, few studies have thoroughly investigated the optimal source of MSCs and their participation in tissue remodeling and inflammation.

Based on a bibliographic search, it can be stated that two types of MSCs have been most frequently used for stem cell therapy in

**Table 2**
Mesenchymal stem cell-coating methodology performed in the different studies using synthetic materials.

| Study | Type of study | Cell type | Cell dose | Mesh (material) | Coating methodology | Main outcomes |
|---|---|---|---|---|---|---|
| Altman et al., 2010 [61] | *In vivo* (rat) | Rat ASCs | $0.5 \times 10^6$ cells per side of a $3 \times 1$ cm ellipse of mesh | Strattice® (porcine ADM)* | Meshes seeded with cells under standard culture conditions immediately before surgery. | ASCs migrated, proliferated and enhanced the vascularity at the musculofascial/graft interface, improving the incorporation of the mesh into the abdominal wall. |
| Iyyanki et al., 2015 [62] | *In vivo* (rat) | Rat ASCs | $2.5 \times 10^4$ cells/cm$^2$ onto scaffolds of 6 mm diameter | Strattice® (porcine ADM)* | Cells seeded on meshes and cultured for 0.5, 1, and 2 h. | ASCs improved tissue remodeling by increasing cellular infiltration and vascularization of the mesh and improving the mechanical properties of the mesh at the mesh-tissue interface. |
| Ochoa et al., 2011 [63] | *In vitro* | Human ASCs | 30 000 cell/cm$^2$ | Porcine dermal tissue* | Cells seeded on meshes and cultured for 1 to 7 days. | "The cross-linking treatment increased cell adhesion and the mechanical properties of the collagen meshes after seeding." |
| Mestak et al, 2014 [28] | *In vivo* (rat) | Rat ASCs | $3 \times 10^5$ cells seeded on $2 \times 3$ cm mesh then cultured for 4 days | Non-crosslinked ECM* Permacol® (crosslinked porcine-derived ECM)* | Cells seeded on meshes and cultured for 4 days. | ASCs-meshes did not improve capsule thickness, foreign body reaction, cellularization, or vascularization compared with acellular meshes. The strength of incorporation was increased by ASC seeding but only in the non-crosslinked ECM. |
| Cheng et al., 2017 [64] | *In vivo* (rabbit) | Rabbit ASCs | Not indicated | PP | Cells seeded on meshes prior to implantation. | ADSC-fixed PP mesh was less corroded, induced a milder chronic inflammatory response, had lower scores for inflammation, and higher scores for neovascularization and fibroblastic proliferation than the PP mesh alone. |
| Li et al., 2013 [66] | *In vivo* (rat) | Rat ASCs | $2 \times 10^5$ cells/ml in 500 µl seeded onto a 20 mm × 20 mm scaffold | Self-manifactured (Silk) | Cell suspension dripped onto the meshes. Incubation for 30 min, then addition of culture medium. Incubation under standard culture conditions for 7 days with medium replacement every day. | ASCs adhered and proliferated on silk fibroin scaffolds. These constructs possessed favorable mechanical properties and biocompatibility and promoted autologous tissue formation. |
| Blázquez et al., 2016 [65] | *In vitro* *In vivo* (mouse) | Human ASCs Murine BM-MSCs | 2, 4, and $8 \times 10^6$ cells in 2 ml of medium placed in a vial together with a $2 \times 2$ cm mesh | Surgimesh® (PP) | Co-culture of meshes pre-coated with gelatin from porcine skin or poly-L-lysine hydrobromide + cells for 1, 2, or 4 h at 37 °C. | MSC-coated surgical meshes could be cryopreserved and did not trigger adverse effects when compared to acellular meshes. MSCs exerted an immunomodulatory effect mediated by anti-inflammatory macrophages. |
| Zhao et al., 2012 [67] | *In vivo* (rabbit) | Rabbit BM-MSCs | 1.5 ml cellular suspension ($2 \times 10^5$ cells/ml) per gram of mesh ($3 \times 4$ cm) | Porcine ADM* | Cells seeded on meshes three times. Constructs cultured for 7 days prior to implantation. | BM-MSCs prevented hernia recurrence and improved the gross and histological appearance of the implants, as well as improving angiogenesis. |
| Zhang et al., 2017[68] | *In vivo* (rabbit) | Rabbit BM-MSCs | $1 \times 10^7$ cells/ml in 2 ml of collagen I gel + medium seeded and injected 4 times | Sheep decellularized aorta* | Cells suspended in a collagen-medium solution and seeded onto and injected into the mesh four times in a week. | BM-MSCs prevented hernia recurrence, increasing cell infiltration, tissue regeneration, and neovascularization. |
| Majumder et al., 2016 [69] | *In vivo* (rat) | Rat BM-MSCs | Not indicated | Parietex® (PE) TIGR® (PGA and PLA composite)* Strattice® (porcine ADM)* | Cell-coating achieved by placing mesh on top of a monolayer of cells. Medium refreshed every 2 days. | MSC-coating improved collagen deposition and ingrowth, especially in the biologic mesh when implanted in the subcutaneous onlay position. |
| Palini et al., 2017 [70] | *In vivo* (human) | Human autologous BM-MSCs + PRP | $72 \times 10^6$/ml bone marrow nucleated cells (20 ml) + $1.2 \times 10^9$/ml autologous PRP (5 ml) spread over a $20 \times 30$ cm mesh | Crosslinked acellular porcine dermal collagen* | Cells mixed with a platelet gel (autologous PRP, plasma, thrombin, gluconate calcium) and spread over the mesh. | PRP and BM-MSCs improved mesh biocompatibility, reducing inflammation and adhesion formation. |
| Gao et al., 2014a [71] | *In vitro* | Rat MSCs Human dermal fibroblasts Rat kidney fibroblast | Not indicated | Soft Mesh® (light weight PP) Parietex®-TET (PE) TIGR® (PGA and PLA composite)* Marlex® (heavy weight PP) Strattice® (porcine ADM)* | Mesh placed on top of a confluent monolayer cell culture. Glass beads to hold the mesh in place. Addition of new cells every 2 days, until complete coating of the meshes was achieved. | MSCs covered the entire meshes in only 2 weeks, regardless of the material. The highest cell densities were produced on Parietex and TIGR. |

(*continued on next page*)

**Table 2** (*continued*)

| Study | Type of study | Cell type | Cell dose | Mesh (material) | Coating methodology | Main outcomes |
|---|---|---|---|---|---|---|
| Gao et al., 2014b [72] | | Rat MSCs<br>Human dermal fibroblasts | | Soft Mesh® (light weight PP)<br>Parietex®-TET (PE)<br>TIGR® (PGA and PLA composite)<br>Strattice® (porcine ADM)* | | "MSC coating blunted the immunogenic effect of both synthetic and biologic meshes *in vitro*." |
| Spelzini et al., 2015 [73] | *In vivo* (rat) | Rat BM-MSCs | $25 \times 10^6$ cells seeded onto 20 × 20 mm meshes, then cultured 7 days | Surgisis® (porcine SIS)*<br>Pelvicol® (porcine ADM)*<br>Gynemesh® (PP)<br>Pelvitex® (PP coated with porcine collagen)* | Suspension of cells poured onto the PP meshes through pipetting. Drop seeding with a 25-gauge needle on SIS mesh. Medium changed after 4 h, then every 3–4 days. | "MSCs reduced the systemic inflammatory response on synthetic implants and improved collagen characteristics at the interface between biological grafts and native tissues. MSCs enhanced the stripping force on biological explants". |
| Blázquez et al., 2018 [74] | *In vivo* (mouse) | Murine BM-MSCs and exo-MSCs | $4 \times 10^5$ cells or 4000 µg of exosomal proteins in 400 µl onto a 1 $cm^2$ mesh | Assumesh® (PP) | Meshes fixed with fibrin glue admixed with MSCs or exo-MSCs | MSCs and their exosomes modulated the inflammatory responses toward a less aggressive and pro-regenerative profile. |
| Su et al., 2014 [76] | *In vitro* | Human endMSCs | 50 000 cells/$cm^{-2}$ | PA<br>PA coated with gelatin | Cells seeded onto the scaffold. Culture of the constructs under standard conditions, refreshing the medium every 2 days. | PA + G scaffolds allow endMSC delivery, proliferation and differentiation into smooth muscle cells and fibroblasts. |
| Ulrich et al., 2014 [77] | *In vivo* (rat) | Human endMSCs | 250 000 cells in 100 µl of medium onto a 10 × 25 mm mesh and cultured for 24–48 h | PA coated with gelatin | Cells seeded on top of the 12% porcine gelatin-coated meshes. Incubation for 24–48 h with regular evaluation. | "Seeding with endMSC exerts an anti-inflammatory effect and promotes wound repair with new tissue growth and minimal fibrosis, and produces mesh with greater extensibility". |
| Edwards et al., 2015 [78] | *In vivo* (rat) | Human endMSCs | 250 000 cells onto a 10 × 25 mm mesh and cultured for 24–48 h | PA coated with gelatin | Cells seeded on meshes coated with human fibronectin. Incubation for 24–48 h prior to implantation. | "The endMSCs were associated with altered collagen growth and organization around the mesh filaments". |
| Darzi et al., 2018 [79] | *In vivo* (mouse) | Human endMSCs | 500 000 cells seeded onto 1 × 1 cm mesh | PA coated with gelatin | 125 000 cells/$cm^2$ seeded on meshes coated with fibronectin, then cultured for 48–72 h. Additional 125 000 cells/mesh added to the mesh before surgery. | Reduced inflammatory cytokine secretion in both groups of mice with endMSC-meshes. Reduced M1 macrophage and increased M2 macrophage markers in immunocompetent mice and delayed increase in expression of M2 macrophage markers in immunocompromised mice with endMSC-meshes. |

* Absorbable materials; ADM: acellular dermal matrix; ASCs: adipose-derived mesenchymal stem cells; BM-MSCs: bone marrow-derived mesenchymal stem cells; ECM: extracellular matrix; endMSCs: endometrial-derived mesenchymal stem cells; exo-MSCs: exosomes from bone marrow mesenchymal stem cells; PA: polyamide; PE: polyester; PGA: polyglycolic acid; PLA: polylactide; PP: polypropylene; PRP: platelet rich plasma; SIS: small intestinal submucosa.

soft tissue reinforcement: bone marrow-derived and adipose tissue-derived MSCs. Moreover, few studies have been focused on adult MSCs derived from endometrial tissue (see Table 2). At present, it is impossible to discern the best source of MSCs for surgical mesh implants in terms of safety and therapeutic efficacy.

It is important to note that regulatory aspects of MSCs-based treatments are complex. To date, no major adverse events have been reported following local administration of MSCs and systematic reviews suggest that MSC-based therapy appears to be safe in clinical trials [60]. Autologous therapies might be safer than allogeneic therapies, but their clinical application in surgical meshes would be expensive and complex. On the contrary, allogeneic therapies have several advantages in terms of production and logistics, but cellular and humoral immune responses against donor human leukocyte antigen (HLA) following administration of these cells may occur [34–36]. The prospective use of MSCs in the field of surgical meshes remains under basic, preclinical investigation and require substantial time and effort before achieving clinical clearance and regulatory approval from the appropriate governmental agencies.

### *3.1. Application of surgical mesh with adipose-derived mesenchymal stem cells*

The first study of adipose-derived mesenchymal stem cells (ASCs) application on surgical mesh was carried out by Altman et al. using rats with surgically-induced ventral hernias. In this study, rat ASCs were pre-seeded onto a porcine acellular dermal matrix (Strattice®, LifeCell Corp., Branchburg, NJ, USA) or injected locally into the implanted mesh. The authors observed an increase in leukocyte and vascular infiltration in the abdominal defects 2 weeks post-implantation [61]. Similarly, lyyanki et al. seeded ASCs onto Strattice® meshes for 24 h, before repairing the induced ventral hernia defects in rat models. In agreement with Altman et al. [61], lyyanki et al. demonstrated that vascular infiltration was greater in the ASC-seeded group 4 weeks after surgery, while only one week was adequate to increase cellular infiltration. Additionally, given the increase in elastic modulus, it can be claimed that mesh elasticity was improved by ASCs at 4 weeks. On the contrary, ultimate tensile strength was unaffected [62].

ASCs have also been evaluated in other biological meshes. Ochoa I. et al. evaluated the mechanical and biological behaviors

of ASCs combined with collagen meshes (derived from porcine dermis). This study demonstrated that ASCs increased the mechanical properties of the meshes (tangent modulus, secant modulus, ultimate strength, and ultimate strain) in direct correlation to the degree of crosslinking. According to the authors, the positive effect of ASCs may be due to their increased production of extracellular matrix protein when seeded on crosslinked meshes [63].

It is interesting to note that preclinical studies using autologous ASCs cultured on crosslinked and non-crosslinked porcine extracellular matrices did not demonstrate any benefits for the use of ASCs. In this study, Mestak et al. did not find any significant differences in capsule thickness, foreign body reaction, cellularization, and vascularization when comparing these ASC-enriched grafts with the acellular ones. According to the authors' opinion, the extracellular matrix mesh itself improves hernia repair, regardless of the presence of MSCs [28].

Positive results were obtained by Cheng et al. using non-absorbable meshes, leading to the idea that MSC-coated meshes may have a potential use in clinical practice. These authors allotransplanted ASCs combined with polypropylene meshes into the abdomens of rabbits. After 4 weeks, the ASCs induced a higher degree of angiogenesis. Similarly, the ASC-treated rabbits showed an increased fibroblastic proliferation coupled with a lower degree of fibrosis, as well as a weaker inflammatory response [64].

Human ASCs were used by our group to study the anti-inflammatory and immunomodulatory properties of MSCs in non-absorbable meshes [65]. First, polypropylene meshes were pretreated to improve ASC adhesion and cryopreservability. We then conducted *in vitro* tests to determine lymphocyte proliferation, IFN-γ production, and macrophage polarization. The presence of ASCs on the polypropylene mesh significantly decreased the proliferation rate of stimulated T cells *in vitro*. Moreover, intracellular IFN-γ was lower in CD8+ T cells co-cultured with MSC-coated meshes. For macrophage polarization, when ASC-coated meshes were co-cultured *in vitro* with a macrophage-like cell line (U937) for 7 days, the differentiation of macrophages toward M1 was prevented and the percentage of M2 macrophages increased [65].

Finally, although most preclinical studies using surgical meshes and ASCs have been focused on hernia repair, these cells have also been evaluated for pelvic reconstruction. In a recent paper from Li et al., silk fibroin scaffolds were fabricated with ASCs and surgically implanted in a rat animal model. This study demonstrated an increase in angiogenesis and collagen matrix production when ASCs were co-administered. Moreover, silk fibroin scaffolds exhibited favorable biocompatibility and optimal mechanical properties for pelvic floor reconstruction [66].

In this section, we reported various evidence of the potentially beneficial effect of the ASC-mesh combination. ASCs contributed to improved tissue remodeling after mesh implantation by increasing neovascularization [61,62,64,66], fibroblastic proliferation [64], and collagen matrix production [66]. In addition, inflammatory response was modulated by ASCs [64,65]. It is important to note that the physical-mechanical properties of mesh were also improved by ASC seeding [62–64]. Contrary to these results, the study from Mestak et al. found neither beneficial nor adverse effects related to the use of ASCs [28]. Given the current levels of understanding, further preclinical studies are warranted to investigate adipose tissue as a suitable source for cell-mesh coupled therapies.

### *3.2. Application of surgical mesh with bone marrow-derived mesenchymal stem cells*

In a work published by Zhao in 2012, rabbit autologous bone marrow MSCs (BM-MSCs) were seeded onto decellularized dermal scaffolds for the treatment of abdominal wall defects in New Zealand white rabbits. Animals with surgical meshes co-administered with MSCs were compared with other animals treated with acellular meshes. Gross examination revealed no abdominal hernia recurrence and fewer adhesions in the presence of MSCs. Moreover, histological analysis showed better tissue regeneration and cellular infiltration, together with enhanced angiogenesis [67]. Similarly, Zhang et al. implanted a decellularized aorta combined with autologous BM-MSCs in inguinal hernia in rabbits. As in the previously cited study [67], these authors reported no hernia recurrence and the presence of neovascularization in the cellularized meshes. In addition, Zhang et al. observed fewer adhesions, higher mechanical strength, and better cell infiltration and tissue regeneration than in the acellular meshes [68].

More recently, Majumder et al. used rat BM-MSCs or rat kidney fibroblasts to coat a non-absorbable polyester mesh (Parietex®, Covidien, Mansfield, MA, USA), a copolymer composite resorbable mesh (TIGR®, Novus Scientific, San Diego, CA, USA), or a porcine skin mesh (Strattice®) and compared these cell-mesh constructs. Independent of the position of implantation (subcutaneous onlay or intraperitoneal underlay) and the type of mesh, MSC-coating resulted in thicker collagen deposition compared to control surgical meshes. Even though this result may be beneficial for wound healing in the short term, no tests were performed to evaluate the negative effects of the excessive collagen deposition (such as pain and tissue stiffening) in the long term [69].

Palini et al. used a slightly different approach in their 2017 case-report in which a 71-year old woman presenting an abdominal incisional hernia, complicated by an enterocutaneous fistula, was treated with a crosslinked acellular porcine dermal collagen mesh associated with autologous BM-MSCs and PRP. The authors claimed that this treatment significantly prevented hernia relapse and adhesion formation, improving mesh biocompatibility in this particularly complex patient [70].

BM-MSCs were evaluated by Gao et al. to assess inflammation/immunomodulation. A preliminary study compared the coating efficacy of rat MSCs on four different synthetic meshes and one biologic mesh. *In vitro* studies showed that MSCs did not exhibit special substrate-preference and fully covered the mesh surface in 2 weeks [71]. The authors completed this work by analyzing the *in vitro* effect of this coating on the immunogenic potential of the meshes. When rat MSC-coated meshes were co-cultured with macrophages, their production of IL-1β, IL-6, and VEGF significantly decreased in comparison to non-coated meshes [72].

Spelzini et al. instead fixed the meshes Surgisis® (purified porcine small intestine submucosa, Cook Ireland, Limerick, Ireland) and Pelvitex® (polypropylene, Bard), coated or not, with rat BM-MSCs over the muscular abdominal wall of Sprague-Dawley rats. Macroscopic evaluation, hemochromocytometric tests, histological assessment, and mechanical tensile tests were then performed to compare the tissue response and mechanical properties of MSC-implants with acellular implants. The presence of the BM-MSCs, regardless of the type of mesh, improved the conditions of the surrounding tissue, especially with regard to both systemic and local inflammatory responses. Furthermore, when the biologic mesh Surgisis® was seeded with the cells, it exhibited a higher breaking force and stiffness, leading to an improvement in collagen characteristics at the interface between the biological grafts and native tissues [73].

The research of Blázquez et al. considered the use of murine BM-MSCs for *in vivo* studies. As described previously, polypropylene meshes were pre-coated with cells and subcutaneously implanted in a mouse model. The *in vivo* studies demonstrated a polarization of infiltrated macrophages toward the M2 phenotype. Moreover, transcriptional analysis of surgically implanted MSC-coated meshes was evaluated by qPCR showing a significant increase in MIP-1a, IL-1b, IL-4, IL-13, Arg-1, and iNOS gene

expression, as well as a significant decrease in the expression of MCP-1 and FGF-1 [65].

A recent preclinical study published in 2018 by our research group [74], compared four different types of implants in a murine incisional hernia model: polypropylene meshes fixed with simple stitches; with fibrin glue; with fibrin glue admixed with murine BM-MSCs; and with fibrin glue admixed with MSC-derived exosomes. The comparative assays were performed at day 7 post-implantation. The histological analysis showed an increased leukocyte infiltration in all surgical meshes fixed with fibrin glue, regardless of the presence of MSCs or exosomes. Factors like hemorrhage, necrosis, neovascularization, and collagen deposition around implanted meshes seemed not to be affected by the use of fibrin glue, MSCs, or exosomes. Flow cytometry showed that the use of fibrin glue fixation, without considering the absence/presence of MSCs or exosomes, increased the percentage of infiltrated leukocytes (CD45+ cells), M1 macrophages, and M2 macrophages. However, the presence of MSCs or their exosomes produced a significant decrease in infiltrated M1 inflammatory macrophages, together with an increase in M2 macrophages, when compared with the meshes fixed with stitches or fibrin glue only. Transcriptional analysis revealed that the presence of MSCs produced an increase in IL-4 and IL-13 (TH2 cytokines) when compared with the other groups, while the exosomes induced IL-13 increase only. An analysis of wound-healing related to matrix metalloproteinases (MMPs) and tissue inhibitors of metalloproteinases (TIMPs) was also performed. As a result, a significant increase in MMP9 associated with neovascularization and angiogenesis was found in the presence of the BM-MSCs. Additionally, taking into account that hernia development seems to be triggered by variations in the MMP/TIMP balance, which increase net proteolytic activity on the extracellular matrix network [75], Blázquez et al. detected some variations in the MMP/TIMP ratios, demonstrating alterations in the microstructure and successful wound-healing when MSCs or their exosomes were applied to the surgical meshes. More importantly, this was the first study that investigated the use of MSC-derived exosomes coupled to surgical meshes for the treatment of incisional hernia. These microvesicles are known to be paracrine mediators of MSC immunomodulatory activity and their potential use as a cell-free based therapy is promising [74].

BM-MSCs, when associated to surgical meshes for the treatment of injured soft tissues, had diverse but favorable consequences, including prevention of hernia relapse [67,68,70] and improved mesh properties [68,70]. The tissues showed enhanced angiogenesis [67,68,74], thicker collagen deposition [69], and increased cell [67,68] and leukocyte infiltration [74]. An overall reduction of the inflammatory response was observed [73], with lower pro-inflammatory cytokine levels [72] and macrophage polarization toward M2 induced by BM-MSCs [65,74]. None of the studies revealed adverse effects associated with the use of BM-MSCs.

### *3.3. Application of surgical mesh with endometrial-derived mesenchymal stem cells*

In 2014, an *in vitro* study by Su et al. demonstrated the feasibility and biocompatibility of endometrial-derived MSCs (endMSC)-mesh constructs for pelvic organ prolapse. Polyamide meshes were optimized with a gelatin-coating and compared with standard polyamide meshes after seeding with endMSCs. The optimized meshes not only positively influenced the growth rate of endMSCs, but also proved to be an appropriate platform for endMSC differentiation into smooth muscle cells and fibroblast-like cells. This study initiated subsequent preclinical trials aimed at validating endMSC-seeded meshes in natural hernia/prolapse models [76].

In 2014, Ulrich et al. evaluated the adherence of endMSCs to gelatin/polyamide meshes for subcutaneous wound repair. The study was carried out in a rat model 7, 30, 60, and 90 days post-implantation. At day 7, the authors noted a superior organization of the connective tissue together with a greater number of thin collagen fibers and a significant neovascularization when endMSCs were applied along with the meshes. Additionally, the highest accumulation of CD68+ macrophages was observed in rats treated with endMSCs. At 30 days post-implantation, M2 macrophages became the most predominant cells when the engineered meshes were applied. At 90 days, the rats implanted with endMSCs instead showed very low macrophage concentration and less inflammatory cells present around the mesh filaments in the cell-treated group. In conclusion, seeding with endMSCs improved mesh biocompatibility while reducing inflammation, promoting neovascularization, and stimulating wound repair [77].

In 2015, Edwards et al. covered gelatin-coated polyamide scaffolds with human endMSCs to evaluate their effect in a subcutaneous rat model of wound repair. By analyzing the removed scaffolds 7, 30, 60, and 90 days after implantation, they described not only more physiological crimped collagen deposition and organization, but also improved biomechanical properties in the endMSC-scaffolds in comparison with the controls [78].

Darzi et al. in 2018 coated polyamide/gelatin composite meshes with human endMSCs to repair abdominal subcutaneous wounds in C57BL6 immunocompetent mice. These cells showed significant immunomodulatory and anti-inflammatory properties in their effect on macrophages. Specifically, the endMSCs seeded on the meshes triggered a reduction in inflammatory M1 macrophages (3 days after implantation) as well as a reduction in the secretion of IL-1β and TNFα cytokines (7 days). At later time-points (14–30 days), even *Il-1β* and *Tnfα* gene expression levels were reduced, while the M2 macrophage mRNA markers *Arg1*, *Mrc1*, and *Il10* were upregulated. The authors went on to consider whether the endMSC immunomodulatory effect is different in the absence of an adaptive immune system and NK cells. To answer the question, they implanted the endMSC-coated meshes in NSG immunocompromised mice, obtaining a similar though delayed response, when compared with the immunocompetent mice. Here, the endMSCs triggered a prolonged elevation of M2 macrophages and an increase in *Mrc1* and *Arg1* levels (day 30), as well as a reduction in pro-inflammatory cytokine secretion and mRNA expression. Consequently, it was demonstrated that endMSCs triggered the induction of macrophage polarization regardless of the immune status of the animals; however, the survival of the xenogeneic endMSCs was a key regulator of the short-term or long-term macrophage responses detected in the immunocompetent and immunocompromised mice, respectively [79].

In summary, it is widely accepted that the endometrium is a source of MSCs with angiogenic, anti-apoptotic, and immunosuppressive activity. These cells are emerging in recent years for use in MSC-based therapies and, when used in combination with surgical meshes, exhibit improved mesh biocompatibility [76] and mechanical properties [78]. These endMSCs induced intensified angiogenesis [77] as well as greater collagen deposition and organization [77,78]. Moreover, endMSCs reduced the infiltration of inflammatory cells [77] and M1 macrophages [79] and increased M2 macrophages [77] and TH2 cytokines [79]. Considering these promising preclinical results, endMSCs are encouraging prospects for clinical translation. However, further preclinical work is required, especially in clinically relevant animal models.

### *3.4. Final remarks about mesenchymal stem cell-based applications for surgical mesh implantation*

According to the relevant bibliography, preclinical studies have demonstrated that the combined use of surgical meshes with MSCs may improve the healing outcome of damaged tissues by reducing

adverse inflammatory reactions, providing a pro-regenerative environment. Most of the studies were performed by coating surgical meshes with MSCs purified from bone marrow [65,67,68,70,73,74], adipose tissue [28,61–63,65,66] or endometrial biopsies [77–79]. Unfortunately, even when different authors used similar cell types, the methodological variability of *in vitro* and *in vivo* assays makes it impossible to compare their results. However, the most prevalent effects shared by MSCs and differentiated cells are neovascularization induction [56,57,61,62,64,66–68,74,77], increased collagen deposition [40,47,50,59,66,69,77,78], and inflammatory cell infiltration [47,67,68], leading to improved physical-mechanical mesh properties [55,56,62–64,68,70,78].

A key conundrum in MSC-based therapies is the duration of MSC survival in patients. It is therefore useful to apply tracking of *in vivo* MSCs in preclinical models to answer this question. Unfortunately, only a few studies have focused on this aspect: Altman et al. [61], Iyyanki et al. [62], and Darzi et al. [79] transfected their cells with fluorescent proteins; Zhang et al. [68] and Zhao et al. [67] used fluorescent dyes; and Ulrich et al. [77] labeled MSCs with the carbocyanine dye DiO. Darzi et al. [79] did not detect fluorescent cells in immunocompetent mice 3 or 7 days after implantation, while the fluorescent cells were around the mesh filaments and in the gelatin layer. Labeled cells were found up to 2 weeks post-implantation in three studies [61,62,77] and two authors found labeled cells in the engineered meshes up to two months post-implantation [67,68]. It seems clear that this aspect is controversial and it might influence the putative roles attributed to MSCs for soft tissue reinforcement.

As to the mechanism of action of MSCs, it is important to note that in recent years, MSC efficacy has shifted toward the "paracrine hypothesis." It is currently well known that MSC-based therapies are related to soluble factors released by MSCs which enhance tissue regeneration and angiogenesis while reducing inflammation, fibrosis, and apoptosis. Nearly all of the studies using surgical meshes and MSCs have linked their beneficial effects to paracrine mechanisms: enhancing vascularization [61,70,73,77,79], improving collagen deposition and features [73,77], promoting neotissue formation [76,77,79], influencing macrophage migration, activation and differentiation [65,77,79], and promoting wound healing [79]. Interestingly, other studies have conferred the therapeutic effect of MSCs to the trans-differentiation potential of these cells in the healing microenvironment. In this sense, some authors report that MSC differentiation occurs toward smooth muscle cells [76], fibroblast-like cells [73,76,77], and endothelial cells [67,68].

Finally, we should point out that all preclinical studies included in this review varied widely in terms of animal models (mice, rats, and rabbits) and that no studies have been performed in animal models whose anatomy and physiology resemble the human patient most (dogs, goats, non-human primates and pigs) [80–82]. As a result, some contradictory results have been obtained and further preclinical trials that follow the guidelines for experimental hernia research [80] are necessary to completely and safely translate this strategy to the clinical setting.

## 4. Foreign body reaction and MSC activity during surgical mesh implantation

Foreign body reaction is the host response to implanted biomaterials which, after inflammation and wound healing, leads to fibrous encapsulation of the implant. In this fibrous capsule, macrophages and giant cells surrounded by lymphocytes and plasma cells are accumulated around the biomaterial. In this section, we summarize the different phases of this sequential process together with the biological mechanisms in which the MSCs may simultaneously participate during tissue integration of surgical meshes (see Table 3).

### *4.1. MSCs in phase I of foreign body reaction: protein adsorption process*

Once the surgical mesh is implanted for tissue reinforcement, the first step in foreign body reaction involves the adsorption of blood-derived proteins into the material. As reviewed by Klopfleisch et al., protein adsorption depends on the characteristics of the biomaterial [83]. This provisional blood clot is a fibrin-predominant matrix that facilitates platelet adhesion. Platelets adhere to the protein coagulum, mainly composed of fibrin, albumin, plasminogen, or complement factors (see Table 3). The adhered platelets release chemoattractants such as IL-1β, platelet-derived growth factor (PDGF), and leukotriene for the recruitment of polymorphonuclear neutrophils (PMNs) and macrophages to initiate the inflammatory phases and wound healing (reviewed in [83–87]).

The simultaneous implantation of MSCs and surgical meshes first requires the cellular adhesion of MSCs to adsorbed proteins. This adhesion might be mediated by fibrin binding. In support of this idea, it has previously been reported that BM-MSCs can be cultured in fibrin, thereby increasing the angiogenic behavior of these cells [88]. It is important to note that the local release of chemoattractants in this first step have a clear impact on the migratory behavior of MSCs. Actually, PDGF-D (released by adhered platelets) has been found to play a pivotal role in the growth and migration of MSCs [89]. Finally, although this is not known with certainty, since protein adsorption and platelet adhesion depend on the characteristics of the biomaterial, the implantation of MSC-coated meshes might initially reduce the adsorption of blood plasma proteins. If this were to occur in actuality, the dynamic sequence of foreign body reaction would be different from the one observed after implantation of conventional meshes.

### *4.2. MSCs in phase II of foreign body reaction: acute inflammation process*

In the second phase of surgical mesh implantation, new platelets and PMNs migrate from the blood vessels to the implantation site. These infiltrating cells are attracted to the surface of the prosthetic and remain infiltrated around the prosthetic for a short period of time (from hours to a few days). Due to the size of the implanted material, phagocytosis by PMNs is usually impossible; during this period, the cells release proteases and granular components. PMNs and mast cells trigger the subsequent inflammatory response through IL-8, MCP-1, MIP1β, IL-4, IL-13, and histamine, attracting more leukocytes (reviewed in [83–87]).

When MSCs are simultaneously implanted with surgical meshes, the participation of these cells as "invited actors" in this phase would be related to MSC and PMN crosstalk. In support of this, *in vitro* experiments have demonstrated that MSCs improve the viability and activity of neutrophils [90,91]. Additionally, *in vivo* experiments have demonstrated that resident MSCs increase the inflammatory activity on neutrophils in the early phases of pathogen challenge [92]. Finally, it is important to note that in animal models, the crosstalk between neutrophils and MSCs has been found to be crucial for the treatment of bacterial infections. In fact, the beneficial effects of MSCs in sepsis are related to the ability of MSCs to enhance the phagocytic activity of neutrophils [93]. Whether MSCs in combination with prosthetics or implants might prevent postoperative infections remains an open question to be addressed [94,95].

### *4.3. MSCs in phase III of foreign body reaction: chronic inflammation process*

In the third phase of foreign body reaction, migrated monocytes differentiate toward macrophages and colonize the area. This

**Table 3**
Role of mesenchymal stem cells in foreign body reaction.

| | Foreign Body Reaction | | Mesenchymal Stem Cells |
|---|---|---|---|
| Phase I: Protein adsorption [83–87] | Predominant cells<br>Soluble factors | • Platelets<br>• Albumin<br>• Complement factors<br>• Fibrinogen Fibronectin<br>• IL-1β<br>• Leukotriene<br>• Plasminogen<br>• Thrombin<br>• Vibronectin<br>• PDGF<br>• • PF4 | Migration and adhesion of MSCs [88,89,109]<br>• MSCs migration toward chemoattractants<br>• MSCs adhesion to fibrin |
| Phase II: Acute inflammation [83–87] | Predominant cells<br><br><br>Soluble factors | • Platelets<br>• Mast cells<br>• PMNs<br>• Coagulation factors VII, XI<br>• Histamine<br>• IL-1<br>• IL4<br>• IL-8<br>• IL-13<br>• MCP-1<br>• MIP1β<br>• P-selectin<br>• TGF-β<br>• TNFα<br>• vWF | PMNs and MSCs crosstalk [90–93,110,111]<br>• ↑ viability of neutrophils<br>• ↑ activity of neutrophils<br>• ↑ phagocytic activity of neutrophils |
| Phase III: Chronic inflammation [83–87] | Predominant cells<br><br>Soluble factors | • Macrophages<br>• FBGCs<br>• G-CSF<br>• GM-CSF<br>• IL4<br>• IL-6<br>• IL-13<br>• MCP-1<br>• MCP-4<br>• MIP1β<br>• PDGF<br>• TGF-β<br>• TNFα | Macrophage and MSC crosstalk [65,74,83,96–98]<br>• Chemoattractive response to macrophage-derived cytokines:<br>- PDGF<br>- TNFα<br>• Immunosuppression of MSCs<br>- ↑ M2 macrophages<br>- IL-4/IL-13 independent |
| Phase IV: Wound healing [83–87] | Predominant cells<br><br>Soluble factors | • Macrophages<br>• Fibroblasts<br>• MMPs<br>• TIMP<br>• Angiogenic factors<br>• Pro-fibrogenic factors | Fibroblast and MSC crosstalk [74,103–105]<br>• ↑ Proliferation/activity of fibroblasts<br>• ↑Angiogenesis<br>• ↑ Collagen deposition<br>• ↑ Healing and remodeling |

FBGCs: foreign body giant cells; G-CSF: granulocyte-colony stimulating factor; GM-CSF: granulocyte-macrophage colony-stimulating factor; IL: interleukin; MCP-1: monocyte chemoattractant protein-1; MCP-4: monocyte chemoattractant protein-4; MIP-1β: macrophage inflammatory protein-1β; MMPs: matrix metalloproteinases; PDGF: platelet-derived growth factor; PF4: platelet factor 4; PMNs: polymorphonuclear neutrophils; TGF-β: tumor growth factor beta; TIMPs: tissue inhibitors of metalloproteinases; TNFα: tumor necrosis factor alpha; vWF: von Willebrand factor.

phase is defined as the "chronic inflammation phase" and is characterized by the presence of mononuclear cells around the biomaterial. Macrophages migrate toward the implantation area and become "activated" macrophages. *In vitro* studies have demonstrated that initial cell adhesion is mediated by β2 integrins and adsorbed proteins. These adhered macrophages release chemoattractants (i.e., PDGF, TNFα, IL-6, G-CSF, and GM-CSF) to recruit macrophages to the biomaterial-tissue interface. These macrophages release not only cytokines, but also chemokines such as MCP-1, MCP-4, and MIP1β for sustained recruitment. The tissue-infiltrated macrophages fuse to form foreign body giant cells (FBGCs) around the implanted biomaterial. In this process, IL-4 and IL-13 as well as the expression of mannose receptors are absolutely necessary to induce this fusion. Other proteins such as CD44, CD47, DC-STAMP, and CCL2 are known to be positively correlated with the formation of FBGCs (reviewed in [83–87]).

The presence of MSCs in the biomaterial-tissue interface exerts an immunomodulatory effect against tissue-infiltrated macrophages, macrophage fusion/FBGC formation, and subsequently on the chronic inflammatory reaction. First, regarding the chemoattraction mediated by macrophages, soluble factors released by these cells (especially PDGF and TNFα) are known to be involved in the migratory behavior and chemoattractive response of MSCs [96]. In the case of IL-4 and IL-13 (inductors of macrophage fusion and necessary for the formation of FBGCs), it has been demonstrated that the immunosuppressive activity of MSCs is IL-4 independent [97,98]. Moreover, a previous report from Freytes et al. using MSCs co-cultured with different M1 and M2 cytokines suggested that the IL-4 and IL-13 environment did not interfere with the viability and growth of MSCs [99]. Finally, our group has demonstrated that MSCs adhered to surgical meshes provide an anti-inflammatory environment by triggering an M2 polarization [65] as well as an increase in TH2 cytokines [74]. To summarize, MSCs are involved in phase III through the crosstalk between MSCs and tissue-infiltrated macrophages. The anti-inflammatory and pro-regenerative ability of MSCs favors the immunomodulation of infiltrating macrophages toward a less aggressive and pro-regenerative profile [65,74]. It is interesting to note that the

prolonged presence of M2 macrophages may lead to the formation of detrimental FBGCs [85], but this question remains unanswered in the field of surgical meshes.

### 4.4. MSCs in phase IV of foreign body reaction: wound-healing process

Usually, the wound-healing phase is achieved within a few weeks after biomaterial implantation. It is characterized by the secretion of extracellular matrix and collagen deposition. The conformational changes in extracellular proteins such as collagen improve wound repair and tissue integration of the implanted mesh. In this step, fibroblasts become the predominant cell subset, playing a key role in promoting tissue repair through the synthesis of collagen. In this process, the macrophages are also involved in tissue remodeling, secreting growth factors, angiogenic factors, and pro-fibrogenic factors. Adhered macrophages surrounding the material secrete MMPs and TIMPs (especially MMP8 and TIMP-1) which are critical for remodeling the extracellular matrix (reviewed in [83–87]).

The beneficial effects of MSCs in wound healing have been extensively reviewed [31,100–102]. The combination of MSCs with biomaterials such as polycaprolactone/gelatin has been found to accelerate wound healing by promoting angiogenesis [103]. Our group has demonstrated that MSC-coated sutures enhanced collagen deposition in sutured tissues [104]. Regarding macrophage-MSC crosstalk in the wound healing phase, Chen et al. suggested that soluble factors released by MSCs (especially MIP-1 and 2 and MCP-5) increase the recruitment of macrophages, enhancing wound healing [105]. Similarly, Zhang et al. demonstrated that MSCs elicit M2 polarization in macrophages, improving wound-healing [106]. In the field of surgical mesh implantation, our group has also demonstrated that surgically implanted meshes combined with MSCs participate in tissue remodeling, modifying the composition of the extracellular matrix [74]. Finally, the bibliographic references describing the crosstalk between MSCs and fibroblasts are extensive. For instance, a recent report demonstrated that exosomes derived from MSCs stimulate the proliferation and migration of fibroblasts [107] and optimize wound-healing through the activation of fibroblasts [108].

## 5. Future perspectives for mesenchymal stem cell-based therapies in surgical meshes

According to the preclinical studies described above and the therapeutic potential of MSCs, it is expected that these cells will become a valuable tool in the treatment of diseases requiring tissue reinforcement. From a surgical point of view, future studies should be conducted to develop medical devices and surgical procedures to optimize MSC delivery at the implantation site. In the field of stem cell biology, such studies should focus on determining the optimal source for MSC-based therapies as well as the ideal therapeutic dose. Moreover, engineered cell-vehicles (i.e., biomaterial, hydrogel, or biological glue) might be necessary to ensure the viability and tissue implantation efficacy of these cells. Our experience in preclinical models, surgery, and cell-based therapies suggests that multidisciplinary and collaborative studies will lead to the successful application of this therapy in clinical settings. Finally, considering the economic aspects and market access for MSC-based therapies in the field of surgical meshes, the manufacturing costs of such therapy will only be compensated if this product leads to significantly improved patient outcomes compared to available treatments. To this end, the proper balance between costs and benefits associated with this therapy must be evaluated further in clinical trials.

## Acknowledgement

Special thanks to Nuria Gónzalez Trejo for graphical abstract design and to Beatriz Macías for reviewing the manuscript.

## Funding

This work was supported in part by ISCIII (CP17/00021), co-funded by ERDF/ESF, "Investing in Your Future," a grant from Junta de Extremadura (Ayuda a grupos catalogados de la Junta de Extremadura, GR15175), a grant from Junta de Extremadura to JGC (IB16168) co-funded by ERDF/ESF, a grant from MAFRESA S.L. to FM and grants to MVB as Researcher at the National Council for Science and Technological Development – CNPq, Brazil (308019/2015-6 and 200346/2017-2).

## Disclosure

The authors declare that they have no competing interests.

## References

[1] Y. Bilsel, I. Abci, The search for ideal hernia repair; mesh materials and types, Int. J. Surg. 10 (2012) 317–321, https://doi.org/10.1016/j.ijsu.2012.05.002.
[2] A.C. Kirby, C.W. Nager, Indications, contraindications, and complications of mesh in the surgical treatment of urinary incontinence, Clin. Obstet. Gynecol. 56 (2013) 257–275, https://doi.org/10.1097/GRF.0b013e31828563d2.
[3] L. Rogo-Gupta, Current trends in surgical repair of pelvic organ prolapse, Curr. Opin. Obstet. Gynecol. 25 (2013) 395–398, https://doi.org/10.1097/GCO.0b013e3283648cfb.
[4] A.S. Pandit, J.A. Henry, Design of surgical meshes – an engineering perspective, Technol. Health Care Off. J. Eur. Soc. Eng. Med. 12 (2004) 51–65.
[5] O. Guillaume, A.H. Teuschl, S. Gruber-Blum, R.H. Fortelny, H. Redl, A. Petter-Puchner, Emerging trends in abdominal wall reinforcement: bringing biofunctionality to meshes, Adv. Healthc. Mater. 4 (2015) 1763–1789, https://doi.org/10.1002/adhm.201500201.
[6] S. Todros, P.G. Pavan, A.N. Natali, Synthetic surgical meshes used in abdominal wall surgery: part I-materials and structural conformation, J. Biomed. Mater. Res. B Appl. Biomater. 105 (2017) 689–699, https://doi.org/10.1002/jbm.b.33586.
[7] C. Brown, J. Finch, Which mesh for hernia repair?, Ann R. Coll. Surg. Engl. 92 (2010) 272–278, https://doi.org/10.1308/003588410X12664192076296.
[8] M.T. Wolf, C.A. Carruthers, C.L. Dearth, P.M. Crapo, A. Huber, O.A. Burnsed, R. Londono, S.A. Johnson, K.A. Daly, E.C. Stahl, J.M. Freund, C.J. Medberry, L.E. Carey, A. Nieponice, N.J. Amoroso, S.F. Badylak, Polypropylene surgical mesh coated with extracellular matrix mitigates the host foreign body response, J. Biomed. Mater. Res. A. 102 (2014) 234–246, https://doi.org/10.1002/jbm.a.34671.
[9] A. Coda, R. Lamberti, S. Martorana, Classification of prosthetics used in hernia repair based on weight and biomaterial, Hernia J. Hernias Abdom. Wall Surg. 16 (2012) 9–20, https://doi.org/10.1007/s10029-011-0868-z.
[10] A.F. Engelsman, G.M. van Dam, H.C. van der Mei, H.J. Busscher, R.J. Ploeg, In vivo evaluation of bacterial infection involving morphologically different surgical meshes, Ann. Surg. 251 (2010) 133–137, https://doi.org/10.1097/SLA.0b013e3181b61d9a.
[11] P.K. Amid, Classification of biomaterials and their related complications in abdominal wall hernia surgery, Hernia 1 (1997) 15–21, https://doi.org/10.1007/BF02426382.
[12] K. Bury, M. Śmietański, B. Justyna, P. Gumiela, A.I. Śmietańska, R. Owczuk, Ł. Naumiuk, A. Samet, J. Paradziej-Łukowicz, Effects of macroporous monofilament mesh on infection in a contaminated field, Langenbecks Arch. Surg. 399 (2014) 873–877, https://doi.org/10.1007/s00423-014-1225-3.
[13] M. Kelly, K. Macdougall, O. Olabisi, N. McGuire, In vivo response to polypropylene following implantation in animal models: a review of biocompatibility, Int. Urogynecol. J. 28 (2017) 171–180, https://doi.org/10.1007/s00192-016-3029-1.
[14] B. Klosterhalfen, U. Klinge, V. Schumpelick, Functional and morphological evaluation of different polypropylene-mesh modifications for abdominal wall repair, Biomaterials 19 (1998) 2235–2246.
[15] U. Klinge, V. Schumpelick, B. Klosterhalfen, Functional assessment and tissue response of short- and long-term absorbable surgical meshes, Biomaterials 22 (2001) 1415–1424.
[16] G.E. Leber, J.L. Garb, A.I. Alexander, W.P. Reed, Long-term complications associated with prosthetic repair of incisional hernias, Arch. Surg. Chic. Ill 1960 (133) (1998) 378–382.
[17] S.L. García, D.L. Ramírez, J.R. Rey, J.F. Calvo, B.R. Iglesias, A.O. Calvo, Complications of polypropylene mesh for the treatment of female pelvic floor disorders, Arch. Esp. Urol. 64 (2011) 620–628.

[18] L. Zhang, L. Zhu, J. Chen, T. Xu, J.-H. Lang, Tension-free polypropylene mesh-related surgical repair for pelvic organ prolapse has a good anatomic success rate but a high risk of complications, Chin. Med. J. (Engl.) 128 (2015) 295–300, https://doi.org/10.4103/0366-6999.150088.

[19] H.N. Shah, G.H. Badlani, Mesh complications in female pelvic floor reconstructive surgery and their management: a systematic review, Indian J. Urol. IJU J. Urol. Soc. India 28 (2012) 129–153, https://doi.org/10.4103/0970-1591.98453.

[20] SCENIHR (Scientific Committee on Emerging and Newly Identified Health Risks), Opinion on the safety of surgical meshes used in urogynecological surgery, (2015). https://ec.europa.eu/health/sites/health/files/scientific_committees/emerging/docs/scenihr_o_049.pdf (accessed September 7, 2018).

[21] Center for Devices and Radiological Health, Urogynecologic Surgical Mesh Implants – Urogynecologic Surgical Mesh Implants: Reporting Problems to the FDA, (n.d.). https://www.fda.gov/MedicalDevices/ProductsandMedicalProcedures/ImplantsandProsthetics/UroGynSurgicalMesh/ucm262304.htm (accessed September 7, 2018).

[22] C. for D. and R. Health, Public Health Notifications (Medical Devices) – FDA Public Health Notification: Serious Complications Associated with Transvaginal Placement of Surgical Mesh in Repair of Pelvic Organ Prolapse and Stress Urinary Incontinence, (n.d.). http://wayback.archive-it.org/7993/20170111190506/http://www.fda.gov/MedicalDevices/Safety/AlertsandNotices/PublicHealthNotifications/ucm061976.htm (accessed November 5, 2018).

[23] Center for Devices and Radiological Health, Urogynecologic Surgical Mesh: Update on the Safety and Effectiveness of Transvaginal Placement for Pelvic Organ Prolapse, Https://Www.Fda.Gov/Downloads/MedicalDevices/Safety/AlertsandNotices/UCM262760.Pdf. (2011). http://wayback.archive-it.org/7993/20170111231227/http://www.fda.gov/downloads/MedicalDevices/Safety/AlertsandNotices/UCM262760.pdf (accessed November 5, 2018).

[24] Center for Devices and Radiological Health, Safety Communications – Surgical Mesh: FDA Safety Communication, (n.d.). http://wayback.archive-it.org/7993/20170723125456/https://www.fda.gov/MedicalDevices/Safety/AlertsandNotices/ucm142636.htm (accessed November 5, 2018).

[25] A.G.D. of H.T.G. Administration, TGA actions after review into urogynaecological surgical mesh implants, Ther. Goods Adm. TGA. (2018). https://www.tga.gov.au/alert/tga-actions-after-review-urogynaecological-surgical-mesh-implants (accessed November 5, 2018).

[26] M. Śmietański, I.A. Śmietańska, A. Modrzejewski, M.P. Simons, T.J. Aufenacker, Systematic review and meta-analysis on heavy and lightweight polypropylene mesh in Lichtenstein inguinal hernioplasty, Hernia J. Hernias Abdom. Wall Surg. 16 (2012) 519–528, https://doi.org/10.1007/s10029-012-0930-5.

[27] HerniaSurge Group, International guidelines for groin hernia management, Hernia J. Hernias Abdom. Wall Surg. 22 (2018) 1–165, https://doi.org/10.1007/s10029-017-1668-x.

[28] O. Mestak, E. Matouskova, Z. Spurkova, K. Benkova, P. Vesely, J. Mestak, M. Molitor, A. Pombinho, A. Sukop, Mesenchymal stem cells seeded on cross-linked and noncross-linked acellular porcine dermal scaffolds for long-term full-thickness hernia repair in a small animal model, Artif. Organs. 38 (2014) 572–579, https://doi.org/10.1111/aor.12224.

[29] L. Melman, E.D. Jenkins, N.A. Hamilton, L.C. Bender, M.D. Brodt, C.R. Deeken, S. C. Greco, M.M. Frisella, B.D. Matthews, Early biocompatibility of crosslinked and non-crosslinked biologic meshes in a porcine model of ventral hernia repair, Hernia J. Hernias Abdom. Wall Surg. 15 (2011) 157–164, https://doi.org/10.1007/s10029-010-0770-0.

[30] A.H. Annor, M.E. Tang, C.L. Pui, G.C. Ebersole, M.M. Frisella, B.D. Matthews, C. R. Deeken, Effect of enzymatic degradation on the mechanical properties of biological scaffold materials, Surg. Endosc. 26 (2012) 2767–2778, https://doi.org/10.1007/s00464-012-2277-5.

[31] W.U. Hassan, U. Greiser, W. Wang, Role of adipose-derived stem cells in wound healing, Wound Repair Regen, Off. Publ. Wound Heal. Soc. Eur. Tissue Repair Soc. 22 (2014) 313–325, https://doi.org/10.1111/wrr.12173.

[32] S. Kariminekoo, A. Movassaghpour, A. Rahimzadeh, M. Talebi, K. Shamsasenjan, A. Akbarzadeh, Implications of mesenchymal stem cells in regenerative medicine, Artif. Cells Nanomedicine Biotechnol. 44 (2016) 749–757, https://doi.org/10.3109/21691401.2015.1129620.

[33] V. Crisostomo, C. Baez-Diaz, J. Maestre, M. Garcia-Lindo, F. Sun, J.G. Casado, R. Blazquez, J.L. Abad, I. Palacios, L. Rodriguez-Borlado, F.M. Sanchez-Margallo, Delayed administration of allogeneic cardiac stem cell therapy for acute myocardial infarction could ameliorate adverse remodeling: experimental study in swine, J. Transl. Med. 13 (2015) 156, https://doi.org/10.1186/s12967-015-0512-2.

[34] A.K. Berglund, L.A. Fortier, D.F. Antczak, L.V. Schnabel, Immunoprivileged no more: measuring the immunogenicity of allogeneic adult mesenchymal stem cells, Stem Cell Res. Ther. 8 (2017) 288, https://doi.org/10.1186/s13287-017-0742-8.

[35] J.A. Ankrum, J.F. Ong, J.M. Karp, Mesenchymal stem cells: immune evasive, not immune privileged, Nat. Biotechnol. 32 (2014) 252–260, https://doi.org/10.1038/nbt.2816.

[36] P. Lohan, O. Treacy, M.D. Griffin, T. Ritter, A.E. Ryan, Anti-donor immune responses elicited by allogeneic mesenchymal stem cells and their extracellular vesicles: are we still learning?, Front Immunol. 8 (2017) 1626, https://doi.org/10.3389/fimmu.2017.01626.

[37] U. Klinge, B. Klosterhalfen, M. Müller, V. Schumpelick, Foreign body reaction to meshes used for the repair of abdominal wall hernias, Eur. J. Surg. Acta Chir. 165 (1999) 665–673, https://doi.org/10.1080/11024159950189726.

[38] M. Kapischke, K. Prinz, J. Tepel, J. Tensfeldt, T. Schulz, Precoating of alloplastic materials with living human fibroblasts–a feasibility study, Surg. Endosc. 19 (2005) 791–797, https://doi.org/10.1007/s00464-004-9222-1.

[39] C.E. Skala, I.B. Petry, S. Gebhard, J.G. Hengstler, S.B. Albrich, T. Maltaris, G. Naumann, H. Koelbl, Isolation of fibroblasts for coating of meshes for reconstructive surgery: differences between mesh types, Regen. Med. 4 (2009) 197–204, https://doi.org/10.2217/17460751.4.2.197.

[40] R.A. Canuto, S. Saracino, M. Oraldi, V. Festa, F. Festa, G. Muzio, A. Chiaravalloti, Colonization by human fibroblasts of polypropylene prosthesis in a composite form for hernia repair, Hernia J. Hernias Abdom. Wall Surg. 17 (2013) 241–248, https://doi.org/10.1007/s10029-012-0996-0.

[41] O. Guillaume, J. Park, X. Monforte, S. Gruber-Blum, H. Redl, A. Petter-Puchner, A.H. Teuschl, Fabrication of silk mesh with enhanced cytocompatibility: preliminary in vitro investigation toward cell-based therapy for hernia repair, J. Mater. Sci. Mater. Med. 27 (2016) 37, https://doi.org/10.1007/s10856-015-5648-3.

[42] G.H. Altman, F. Diaz, C. Jakuba, T. Calabro, R.L. Horan, J. Chen, H. Lu, J. Richmond, D.L. Kaplan, Silk-based biomaterials, Biomaterials 24 (2003) 401–416.

[43] E. Karaca, A.S. Hockenberger, Analysis of the fracture morphology of polyamide, polyester, polypropylene, and silk sutures before and after implantation in vivo, J. Biomed. Mater. Res. B Appl. Biomater. 87 (2008) 580–589, https://doi.org/10.1002/jbm.b.31136.

[44] K.B. Kelly, D.M. Krpata, J.A. Blatnik, T.A. Ponsky, Suture choice matters in rabbit model of laparoscopic, preperitoneal, inguinal hernia repair, J. Laparoendosc. Adv. Surg. Tech. A. 24 (2014) 428–431, https://doi.org/10.1089/lap.2013.0352.

[45] G. Sakman, F. Kaya, C.K. Parsak, A. Kuvvetli, G. Seydaoglu, T. Akcam, I. Sungur, Comparison of different operation techniques and suture materials in pyloric exclusion, in an animal model, Surg. Today 38 (2008) 826–832, https://doi.org/10.1007/s00595-007-3710-6.

[46] S. Medel, M. Alarab, H. Kufaishi, H. Drutz, O. Shynlova, Attachment of primary vaginal fibroblasts to absorbable and nonabsorbable implant materials coated with platelet-rich plasma: potential application in pelvic organ prolapse surgery, Female Pelvic Med. Reconstr. Surg. 21 (2015) 190–197, https://doi.org/10.1097/SPV.0000000000000178.

[47] O.R. Ávila, N.G. Parizzi, A.P.M. Souza, D.S. Botini, J.Y. Alves, S.H.M. Almeida, Histological response to platelet-rich plasma added to polypropylene mesh implemented in rabbits, Int. Braz. J. Urol. Off. J. Braz. Soc. Urol. 42 (2016) 993–998.

[48] K. Junge, M. Binnebösel, K.T. von Trotha, R. Rosch, U. Klinge, U.P. Neumann, P. Lynen Jansen, Mesh biocompatibility: effects of cellular inflammation and tissue remodelling, Langenbecks Arch. Surg. Dtsch. Ges. Für Chir. 397 (2012) 255–270, https://doi.org/10.1007/s00423-011-0780-0.

[49] G. Sternschuss, D.R. Ostergard, H. Patel, Post-implantation alterations of polypropylene in the human, J. Urol. 188 (2012) 27–32, https://doi.org/10.1016/j.juro.2012.02.2559.

[50] N.G. Parizzi, O.Á. Rubini, S.H.M. de Almeida, L.C. Ireno, R.M. Tashiro, V.H.T. de Carvalho, Effect of platelet-rich plasma on polypropylene meshes implanted in the rabbit vagina: histological analysis, Int. Braz. J. Urol. Off. J. Braz. Soc. Urol. 43 (2017) 746–752, https://doi.org/10.1590/S1677-5538.IBJU.2016.0177.

[51] H. Gerullis, E. Georgas, C. Eimer, C. Arndt, D. Barski, B. Lammers, B. Klosterhalfen, M. Borós, T. Otto, Coating with autologous plasma improves biocompatibility of mesh grafts in vitro: development stage of a surgical innovation, BioMed. Res. Int. 2013 (2013), https://doi.org/10.1155/2013/536814 536814.

[52] H. Gerullis, B. Klosterhalfen, M. Borós, B. Lammers, C. Eimer, E. Georgas, T. Otto, IDEAL in meshes for prolapse, urinary incontinence, and hernia repair, Surg. Innov. 20 (2013) 502–508, https://doi.org/10.1177/1553350612472987.

[53] H. Gerullis, E. Georgas, M. Borós, B. Klosterhalfen, C. Eimer, C. Arndt, S. Otto, D. Barski, D. Ysebaert, A. Ramon, T. Otto, Inflammatory reaction as determinant of foreign body reaction is an early and susceptible event after mesh implantation, BioMed Res. Int. 2014 (2014), https://doi.org/10.1155/2014/510807 510807.

[54] D. Barski, H. Gerullis, E. Georgas, A. Bär, B. Lammers, A. Ramon, D. Ysebaert, B. Klosterhalfen, M. Boros, T. Otto, Coating of mesh grafts for prolapse and urinary incontinence repair with autologous plasma: exploration stage of a surgical innovation, BioMed Res. Int. 2014 (2014), https://doi.org/10.1155/2014/296498 296498.

[55] J.-Y. Lai, P.-Y. Chang, J.-N. Lin, Body wall repair using small intestinal submucosa seeded with cells, J. Pediatr. Surg. 38 (2003) 1752–1755.

[56] Z. Song, Z. Peng, Z. Liu, J. Yang, R. Tang, Y. Gu, Reconstruction of abdominal wall musculofascial defects with small intestinal submucosa scaffolds seeded with tenocytes in rats, Tissue Eng. Part A 19 (2013) 1543–1553, https://doi.org/10.1089/ten.TEA.2011.0748.

[57] M.T. Conconi, P. De Coppi, S. Bellini, G. Zara, M. Sabatti, M. Marzaro, G.F. Zanon, P.G. Gamba, P.P. Parnigotto, G.G. Nussdorfer, Homologous muscle acellular matrix seeded with autologous myoblasts as a tissue-engineering approach to abdominal wall-defect repair, Biomaterials 26 (2005) 2567–2574, https://doi.org/10.1016/j.biomaterials.2004.07.035.

[58] P. De Coppi, S. Bellini, M.T. Conconi, M. Sabatti, E. Simonato, P.G. Gamba, G.G. Nussdorfer, P.P. Parnigotto, Myoblast-acellular skeletal muscle matrix

constructs guarantee a long-term repair of experimental full-thickness abdominal wall defects, Tissue Eng. 12 (2006) 1929–1936, https://doi.org/10.1089/ten.2006.12.1929.
[59] T. Ayele, A.B.Z. Zuki, B.M.A. Noorjahan, M.M. Noordin, Tissue engineering approach to repair abdominal wall defects using cell-seeded bovine tunica vaginalis in a rabbit model, J. Mater. Sci. Mater. Med. 21 (2010) 1721–1730, https://doi.org/10.1007/s10856-010-4007-7.
[60] M.M. Lalu, L. McIntyre, C. Pugliese, D. Fergusson, B.W. Winston, J.C. Marshall, J. Granton, D.J. Stewart, Canadian Critical Care Trials Group, Safety of cell therapy with mesenchymal stromal cells (SafeCell): a systematic review and meta-analysis of clinical trials, PloS One 7 (2012), https://doi.org/10.1371/journal.pone.0047559 e47559.
[61] A.M. Altman, F.J. Abdul Khalek, E.U. Alt, C.E. Butler, Adipose tissue-derived stem cells enhance bioprosthetic mesh repair of ventral hernias, Plast. Reconstr. Surg. 126 (2010) 845–854, https://doi.org/10.1097/PRS.0b013e3181e6044f.
[62] T.S. Iyyanki, L.W. Dunne, Q. Zhang, J. Hubenak, K.C. Turza, C.E. Butler, Adipose-derived stem-cell-seeded non-cross-linked porcine acellular dermal matrix increases cellular infiltration, vascular infiltration, and mechanical strength of ventral hernia repairs, Tissue Eng. Part A 21 (2015) 475–485, https://doi.org/10.1089/ten.TEA.2014.0235.
[63] I. Ochoa, E. Peña, E.J. Andreu, M. Pérez-Ilzarbe, J.E. Robles, C. Alcaine, T. López, F. Prósper, M. Doblaré, Mechanical properties of cross-linked collagen meshes after human adipose derived stromal cells seeding, J. Biomed. Mater. Res. A 96 (2011) 341–348, https://doi.org/10.1002/jbm.a.32988.
[64] H. Cheng, Y. Zhang, B. Zhang, J. Cheng, W. Wang, X. Tang, P. Teng, Y. Li, Biocompatibility of polypropylene mesh scaffold with adipose-derived stem cells, Exp. Ther. Med. 13 (2017) 2922–2926, https://doi.org/10.3892/etm.2017.4338.
[65] R. Blázquez, F.M. Sánchez-Margallo, V. Álvarez, A. Usón, J.G. Casado, Surgical meshes coated with mesenchymal stem cells provide an anti-inflammatory environment by a M2 macrophage polarization, Acta Biomater. 31 (2016) 221–230, https://doi.org/10.1016/j.actbio.2015.11.057.
[66] Q. Li, J. Wang, H. Liu, B. Xie, L. Wei, Tissue-engineered mesh for pelvic floor reconstruction fabricated from silk fibroin scaffold with adipose-derived mesenchymal stem cells, Cell Tissue Res. 354 (2013) 471–480, https://doi.org/10.1007/s00441-013-1719-2.
[67] Y. Zhao, Z. Zhang, J. Wang, P. Yin, J. Zhou, M. Zhen, W. Cui, G. Xu, D. Yang, Z. Liu, Abdominal hernia repair with a decellularized dermal scaffold seeded with autologous bone marrow-derived mesenchymal stem cells, Artif. Organs 36 (2012) 247–255, https://doi.org/10.1111/j.1525-1594.2011.01343.x.
[68] Y. Zhang, Y. Zhou, X. Zhou, B. Zhao, J. Chai, H. Liu, Y. Zheng, J. Wang, Y. Wang, Y. Zhao, Preparation of a nano- and micro-fibrous decellularized scaffold seeded with autologous mesenchymal stem cells for inguinal hernia repair, Int. J. Nanomed. 12 (2017) 1441–1452, https://doi.org/10.2147/IJN.S125409.
[69] A. Majumder, Y. Gao, E.E. Sadava, J.M. Anderson, Y.W. Novitsky, Cell-coating affects tissue integration of synthetic and biologic meshes: comparative analysis of the onlay and underlay mesh positioning in rats, Surg. Endosc. 30 (2016) 4445–4453, https://doi.org/10.1007/s00464-016-4764-6.
[70] G.M. Palini, L. Morganti, F. Paratore, F. Coccolini, G. Crescentini, M. Nardi, L. Veneroni, Challenging abdominal incisional hernia repaired with platelet-rich plasma and bone marrow-derived mesenchymal stromal cells. A case report, Int. J. Surg. Case Rep. 37 (2017) 145–148, https://doi.org/10.1016/j.ijscr.2017.06.005.
[71] Y. Gao, L.-J. Liu, J.A. Blatnik, D.M. Krpata, J.M. Anderson, C.N. Criss, N. Posielski, Y.W. Novitsky, Methodology of fibroblast and mesenchymal stem cell coating of surgical meshes: a pilot analysis, J. Biomed. Mater. Res. B Appl. Biomater. 102 (2014) 797–805, https://doi.org/10.1002/jbm.b.33061.
[72] Y. Gao, D.M. Krpata, C.N. Criss, L. Liu, N. Posielski, M.J. Rosen, Y.W. Novitsky, Effects of mesenchymal stem cell and fibroblast coating on immunogenic potential of prosthetic meshes in vitro, Surg. Endosc. 28 (2014) 2357–2367, https://doi.org/10.1007/s00464-014-3470-5.
[73] F. Spelzini, S. Manodoro, M. Frigerio, G. Nicolini, D. Maggioni, E. Donzelli, L. Altomare, S. Farè, F. Veneziano, F. Avezza, G. Tredici, R. Milani, Stem cell augmented mesh materials: an in vitro and in vivo study, Int. Urogynecol. J. 26 (2015) 675–683, https://doi.org/10.1007/s00192-014-2570-z.
[74] R. Blázquez, F.M. Sánchez-Margallo, V. Álvarez, A. Usón, F. Marinaro, J.G. Casado, Fibrin glue mesh fixation combined with mesenchymal stem cells or exosomes modulates the inflammatory reaction in a murine model of incisional hernia, Acta Biomater. 71 (2018) 318–329, https://doi.org/10.1016/j.actbio.2018.02.014.
[75] J. Guillen-Marti, R. Diaz, M.T. Quiles, M. Lopez-Cano, R. Vilallonga, P. Huguet, S. Ramon-y-Cajal, A. Sanchez-Niubo, J. Reventós, M. Armengol, M.A. Arbos, MMPs/TIMPs and inflammatory signalling de-regulation in human incisional hernia tissues, J. Cell. Mol. Med. 13 (2009) 4432–4443, https://doi.org/10.1111/j.1582-4934.2008.00637.x.
[76] K. Su, S.L. Edwards, K.S. Tan, J.F. White, S. Kandel, J.A.M. Ramshaw, C.E. Gargett, J.A. Werkmeister, Induction of endometrial mesenchymal stem cells into tissue-forming cells suitable for fascial repair, Acta Biomater. 10 (2014) 5012–5020, https://doi.org/10.1016/j.actbio.2014.08.031.
[77] D. Ulrich, S.L. Edwards, K. Su, K.S. Tan, J.F. White, J.A.M. Ramshaw, C. Lo, A. Rosamilia, J.A. Werkmeister, C.E. Gargett, Human endometrial mesenchymal stem cells modulate the tissue response and mechanical behavior of polyamide mesh implants for pelvic organ prolapse repair, Tissue Eng. Part A 20 (2014) 785–798, https://doi.org/10.1089/ten.TEA.2013.0170.
[78] S.L. Edwards, D. Ulrich, J.F. White, K. Su, A. Rosamilia, J.a.M. Ramshaw, C.E. Gargett, J.A. Werkmeister, Temporal changes in the biomechanical properties of endometrial mesenchymal stem cell seeded scaffolds in a rat model, Acta Biomater. 13 (2015) 286–294, https://doi.org/10.1016/j.actbio.2014.10.043.
[79] S. Darzi, J.A. Deane, C.A. Nold, S.E. Edwards, D.J. Gough, S. Mukherjee, S. Gurung, K.S. Tan, A.V. Vashi, J.A. Werkmeister, C.E. Gargett, Endometrial mesenchymal stem/stromal cells modulate the macrophage response to implanted polyamide/gelatin composite mesh in immunocompromised and immunocompetent mice, Sci. Rep. 8 (2018) 6554, https://doi.org/10.1038/s41598-018-24919-6.
[80] R.R.M. Vogels, R. Kaufmann, L.C.L. van den Hil, S. van Steensel, M.H.F. Schreinemacher, J.F. Lange, N.D. Bouvy, Critical overview of all available animal models for abdominal wall hernia research, Hernia J. Hernias Abdom. Wall Surg. 21 (2017) 667–675, https://doi.org/10.1007/s10029-017-1605-z.
[81] J. Harding, R.M. Roberts, O. Mirochnitchenko, Large animal models for stem cell therapy, Stem Cell Res. Ther. 4 (2013) 23, https://doi.org/10.1186/scrt171.
[82] M. Mapara, B.S. Thomas, K.M. Bhat, Rabbit as an animal model for experimental research, Dent. Res. J. 9 (2012) 111–118, https://doi.org/10.4103/1735-3327.92960.
[83] R. Klopfleisch, F. Jung, The pathology of the foreign body reaction against biomaterials, J. Biomed. Mater. Res. A. 105 (2017) 927–940, https://doi.org/10.1002/jbm.a.35958.
[84] J.M. Anderson, Biological responses to materials, Annu. Rev. Mater. Res. 31 (2001) 81–110, https://doi.org/10.1146/annurev.matsci.31.1.81.
[85] J.M. Anderson, A. Rodriguez, D.T. Chang, Foreign body reaction to biomaterials, Semin. Immunol. 20 (2008) 86–100, https://doi.org/10.1016/j.smim.2007.11.004.
[86] W. Kenneth Ward, A review of the foreign-body response to subcutaneously-implanted devices: the role of macrophages and cytokines in biofouling and fibrosis, J. Diabetes Sci. Technol. 2 (2008) 768–777, https://doi.org/10.1177/193229680800200504.
[87] Z. Sheikh, P.J. Brooks, O. Barzilay, N. Fine, M. Glogauer, Macrophages, foreign body giant cells and their response to implantable biomaterials, Mater. Basel Switz. 8 (2015) 5671–5701, https://doi.org/10.3390/ma8095269.
[88] N.F. Huang, A. Lam, Q. Fang, R.E. Sievers, S. Li, R.J. Lee, Bone marrow-derived mesenchymal stem cells in fibrin augment angiogenesis in the chronically infarcted myocardium, Regen. Med. 4 (2009) 527–538, https://doi.org/10.2217/rme.09.32.
[89] J. Hye Kim, S. Gyu Park, W.-K. Kim, S.U. Song, J.-H. Sung, Functional regulation of adipose-derived stem cells by PDGF-D, Stem Cells Dayt. Ohio 33 (2015) 542–556, https://doi.org/10.1002/stem.1865.
[90] M. Maqbool, S. Vidyadaran, E. George, R. Ramasamy, Human mesenchymal stem cells protect neutrophils from serum-deprived cell death, Cell Biol. Int. 35 (2011) 1247–1251, https://doi.org/10.1042/CBI20110070.
[91] Y.S. Park, G.-W. Lim, K.-A. Cho, S.-Y. Woo, M. Shin, E.-S. Yoo, J. Chan Ra, K.-H. Ryu, Improved viability and activity of neutrophils differentiated from HL-60 cells by co-culture with adipose tissue-derived mesenchymal stem cells, Biochem. Biophys. Res. Commun. 423 (2012) 19–25, https://doi.org/10.1016/j.bbrc.2012.05.049.
[92] S. Brandau, M. Jakob, H. Hemeda, K. Bruderek, S. Janeschik, F. Bootz, S. Lang, Tissue-resident mesenchymal stem cells attract peripheral blood neutrophils and enhance their inflammatory activity in response to microbial challenge, J. Leukoc. Biol. 88 (2010) 1005–1015, https://doi.org/10.1189/jlb.0410207.
[93] S.R.R. Hall, K. Tsoyi, B. Ith, R.F. Padera, J.A. Lederer, Z. Wang, X. Liu, M.A. Perrella, Mesenchymal stromal cells improve survival during sepsis in the absence of heme oxygenase-1: the importance of neutrophils, Stem Cells Dayt. Ohio 31 (2013) 397–407, https://doi.org/10.1002/stem.1270.
[94] E.T. Criman, W.E. Kurata, K.W. Matsumoto, H.T. Aubin, C.E. Campbell, L.M. Pierce, Bone marrow-derived mesenchymal stem cells enhance bacterial clearance and preserve bioprosthetic integrity in a model of mesh infection, Plast. Reconstr. Surg. Glob. Open 4 (2016), https://doi.org/10.1097/GOX.0000000000000765 e751.
[95] A. Ha, E.T. Criman, W.E. Kurata, K.W. Matsumoto, L.M. Pierce, Evaluation of a novel hybrid viable bioprosthetic mesh in a model of mesh infection, Plast. Reconstr. Surg. Glob. Open 5 (2017), https://doi.org/10.1097/GOX.0000000000001418 e1418.
[96] Y. Naaldijk, A.A. Johnson, S. Ishak, H.J. Meisel, C. Hohaus, A. Stolzing, Migrational changes of mesenchymal stem cells in response to cytokines, growth factors, hypoxia, and aging, Exp. Cell Res. 338 (2015) 97–104, https://doi.org/10.1016/j.yexcr.2015.08.019.
[97] V. Holan, B. Hermankova, P. Bohacova, J. Kossl, M. Chudickova, M. Hajkova, M. Krulova, A. Zajicova, E. Javorkova, Distinct immunoregulatory mechanisms in mesenchymal stem cells: role of the cytokine environment, Stem Cell Rev. 12 (2016) 654–663, https://doi.org/10.1007/s12015-016-9688-y.
[98] Y.-M. Liou, Y.-H. Chuang, In vitro immunosuppressive effects of mesenchymal stem cells on allergic asthma, J. Immunol. 53 (3-53) (196 2016,) 3.
[99] D.O. Freytes, J.W. Kang, I. Marcos-Campos, G. Vunjak-Novakovic, Macrophages modulate the viability and growth of human mesenchymal stem cells, J. Cell. Biochem. 114 (2013) 220–229, https://doi.org/10.1002/jcb.24357.
[100] N. Bertozzi, F. Simonacci, M.P. Grieco, E. Grignaffini, E. Raposio, The biological and clinical basis for the use of adipose-derived stem cells in the field of wound healing, Ann. Med. Surg. 2012 (20) (2017) 41–48, https://doi.org/10.1016/j.amsu.2017.06.058.

[101] M. Cherubino, J.P. Rubin, N. Miljkovic, A. Kelmendi-Doko, K.G. Marra, Adipose-derived stem cells for wound healing applications, Ann. Plast. Surg. 66 (2011) 210–215, https://doi.org/10.1097/SAP.0b013e3181e6d06c.
[102] Y. Shingyochi, H. Orbay, H. Mizuno, Adipose-derived stem cells for wound repair and regeneration, Expert Opin. Biol. Ther. 15 (2015) 1285–1292, https://doi.org/10.1517/14712598.2015.1053867.
[103] Y. Fu, J. Guan, S. Guo, F. Guo, X. Niu, Q. Liu, C. Zhang, H. Nie, Y. Wang, Human urine-derived stem cells in combination with polycaprolactone/gelatin nanofibrous membranes enhance wound healing by promoting angiogenesis, J. Transl. Med. 12 (2014) 274, https://doi.org/10.1186/s12967-014-0274-2.
[104] J.G. Casado, R. Blazquez, I. Jorge, V. Alvarez, G. Gomez-Mauricio, M. Ortega-Muñoz, J. Vazquez, F.M. Sanchez-Margallo, Mesenchymal stem cell-coated sutures enhance collagen depositions in sutured tissues, Wound Repair, Regen. Off. Publ. Wound Heal. Soc. Eur. Tissue Repair Soc. 22 (2014) 256–264, https://doi.org/10.1111/wrr.12153.
[105] L. Chen, E.E. Tredget, P.Y.G. Wu, Y. Wu, Paracrine factors of mesenchymal stem cells recruit macrophages and endothelial lineage cells and enhance wound healing, PloS One 3 (2008), https://doi.org/10.1371/journal.pone.0001886 e1886.
[106] Q.-Z. Zhang, W.-R. Su, S.-H. Shi, P. Wilder-Smith, A.P. Xiang, A. Wong, A.L. Nguyen, C.W. Kwon, A.D. Le, Human gingiva-derived mesenchymal stem cells elicit polarization of m2 macrophages and enhance cutaneous wound healing, Stem Cells Dayt. Ohio 28 (2010) 1856–1868, https://doi.org/10.1002/stem.503.
[107] E.W. Choi, M.K. Seo, E.Y. Woo, S.H. Kim, E.J. Park, S. Kim, Exosomes from human adipose-derived stem cells promote proliferation and migration of skin fibroblasts, Exp. Dermatol. (2017), https://doi.org/10.1111/exd.13451.
[108] L. Hu, J. Wang, X. Zhou, Z. Xiong, J. Zhao, R. Yu, F. Huang, H. Zhang, L. Chen, Exosomes derived from human adipose mensenchymal stem cells accelerates cutaneous wound healing via optimizing the characteristics of fibroblasts, Sci. Rep. 6 (2016) 32993, https://doi.org/10.1038/srep32993.
[109] W.-S. Kim, H.-S. Park, J.-H. Sung, The pivotal role of PDGF and its receptor isoforms in adipose-derived stem cells, Histol. Histopathol. 30 (2015) 793–799, https://doi.org/10.14670/HH-11-598.
[110] C.B. Sullivan, R.M. Porter, C.H. Evans, T. Ritter, G. Shaw, F. Barry, J.M. Murphy, TNFα and IL-1β influence the differentiation and migration of murine MSCs independently of the NF-κB pathway, Stem Cell Res. Ther. 5 (2014) 104, https://doi.org/10.1186/scrt492.
[111] S.-J. Zhang, X.-Y. Song, M. He, S.-B. Yu, Effect of TGF-β1/SDF-1/CXCR4 signal on BM-MSCs homing in rat heart of ischemia/perfusion injury, Eur. Rev. Med. Pharmacol. Sci. 20 (2016) 899–905.

frontiers in Pharmacology

ORIGINAL RESEARCH
published: 25 September 2020
doi: 10.3389/fphar.2020.01332

# Laparoscopy for the Treatment of Congenital Hernia: Use of Surgical Meshes and Mesenchymal Stem Cells in a Clinically Relevant Animal Model

*Federica Marinaro[1]*, Javier G. Casado[1,2]*, Rebeca Blázquez[1,2], Mauricio Veloso Brun[3], Ricardo Marcos[4], Marta Santos[4], Francisco Javier Duque[5], Esther López[1], Verónica Álvarez[1], Alejandra Usón[1] and Francisco Miguel Sánchez-Margallo[2,6]*

[1] Stem Cell Therapy Unit, Jesús Usón Minimally Invasive Surgery Centre, Cáceres, Spain, [2] CIBER de Enfermedades Cardiovasculares, Madrid, Spain, [3] Department of Small Animal Clinics, Center of Rural Science, Federal University of Santa Maria (UFSM), Santa Maria, Brazil, [4] Laboratory of Histology and Embryology, Department of Microscopy, Abel Salazar Institute of Biomedical Sciences, University of Porto, Porto, Portugal, [5] Animal Medicine Department, Faculty of Veterinary Medicine, University of Extremadura, Cáceres, Spain, [6] Scientific Direction, Jesús Usón Minimally Invasive Surgery Centre, Cáceres, Spain

OPEN ACCESS

**Edited by:**
*Vivian Capilla-González, Andalusian Center of Molecular Biology and Regenerative Medicine (CABIMER), Spain*

**Reviewed by:**
*Ulises Gomez-Pinedo, Instituto de Investigación Sanitaria del Hospital Clínico San Carlos, Spain*
*Alexander H. Petter-Puchner, Institute for Experimental and Clinical Traumatology (LBG), Austria*

***Correspondence:**
*Federica Marinaro*
*fmarinaro@ccmijesususon.com*
*Javier G. Casado*
*jgarcia@ccmijesususon.com*

**Specialty section:**
*This article was submitted to Integrative and Regenerative Pharmacology, a section of the journal Frontiers in Pharmacology*

**Received:** *09 June 2020*
**Accepted:** *11 August 2020*
**Published:** *25 September 2020*

**Citation:**
*Marinaro F, Casado JG, Blázquez R, Brun MV, Marcos R, Santos M, Duque FJ, López E, Álvarez V, Usón A and Sánchez-Margallo FM (2020) Laparoscopy for the Treatment of Congenital Hernia: Use of Surgical Meshes and Mesenchymal Stem Cells in a Clinically Relevant Animal Model. Front. Pharmacol. 11:01332. doi: 10.3389/fphar.2020.01332*

More than a century has passed since the first surgical mesh for hernia repair was developed, and, to date, this is still the most widely used method despite the great number of complications it poses. The purpose of this study was to combine stem cell therapy and laparoscopy for the treatment of congenital hernia in a swine animal model. Porcine bone marrow-derived mesenchymal stem cells (MSCs) were seeded on polypropylene surgical meshes using a fibrin sealant solution as a vehicle. Meshes with (cell group) or without (control group) MSCs were implanted through laparoscopy in Large White pigs with congenital abdominal hernia after the approximation of hernia borders (implantation day). A successive laparoscopic biopsy of the mesh and its surrounding tissues was performed a week after implantation, and surgical meshes were excised a month after implantation. Ultrasonography was used to measure hernia sizes. Flow cytometry, histological, and gene expression analyses of the biopsy and necropsy samples were performed. The fibrin sealant solution was easy to prepare and preserved the viability of MSCs in the surgical meshes. Ultrasonography demonstrated a significant reduction in hernia size 1 week after implantation in the cell group relative to that on the day of implantation ($p < 0.05$). Flow cytometry of the mesh-infiltrated cells showed a non-significant increase of M2 macrophages when the cell group was compared with the control group 1 week after implantation. A significant decrease in the gene expression of *VEGF* and a significant increase in *TNF* expression were determined in the cell group 1 month after implantation compared with gene expressions in the control group ($p < 0.05$). Here, we propose an easy and feasible method to combine stem cell therapy and minimally invasive surgical techniques for hernia repair. In this study, stem cell therapy did not show a great immunomodulatory or

regenerative effect in overcoming hernia-related complications. However, our clinically relevant animal model with congenital hernia closely resembles the clinical human condition. Further studies should be focused on this valuable animal model to evaluate stem cell therapies in hernia surgery.

**Keywords: mesh, congenital hernia, mesenchymal stem cells, animal model, hernia repair, stem cell therapy, abdominal hernia, laparoscopy**

## INTRODUCTION

Internal organs can move from their normal position in the body and slip or protrude through weakened muscles and connective tissue, thereby resulting in hernias and pelvic organ prolapses (Baylón et al., 2017). The abdominal wall is particularly vulnerable to weaknesses, defects, or holes that may be due to iatrogenic causes, trauma, or congenital defects (Pulikkottil et al., 2015); these vulnerabilities may lead to the herniation of internal viscera. The physical location of the protrusion outward from the anterior abdominal wall is usually used to classify hernias according to type: inguinal hernias are protrusions outward of soft tissues through the inguinal canal; umbilical hernias occur in correspondence with the umbilicus; epigastric hernias are situated between the umbilicus and chest cavity; and incisional hernias occur through a previously made incision in the abdominal wall (Wales and Holloway, 2019). Many hernias are not accompanied by symptoms, except for the presence of a bulge in the abdomen. When a hernia opening in the abdominal wall is too narrow, it is defined as "incarcerated" and causes pain and obstruction of the intestines. Incarcerated hernias, in which the blood supply to hernia tissues is compromised, are defined as "strangulated" and can be associated with symptoms of pain, nausea, vomiting, peritonitis, septicemia, and circulatory failure (Kavic, 2005; Birindelli et al., 2017).

Repairing irregularities in the abdominal wall is necessary but challenging. For hernia repair, surgeons usually resort to an open suturing technique and/or mesh implantation through open surgery procedures or laparoscopic approaches. However, in the treatment of abdominal hernias, the application of surgical meshes has proved to be more effective than suturing (Finan et al., 2009). Surgical meshes are sterile, chemically and physically inert prosthetic materials that guarantee the reinforcement of the abdominal wall such that hernia recurrence is prevented when they are used (López-Cano et al., 2018). Nevertheless, implantation of a prosthetic material, despite its inertness, can lead to bacterial growth and infection that can delay wound healing. Concurrently, surgical meshes can trigger an exacerbated and chronic inflammatory reaction, leading to wound healing but also to foreign body reaction and the formation of scar tissues. A high proliferation of fibroblasts during the wound-healing phase has been linked to inflammation and fibrosis, which thereby cause contraction and shrinkage of the mesh (Baylón et al., 2017). Wound-healing-related issues, together with surgical complications, may result in paresthesia, pain, adhesions, fistulas, scar entrapment of nerves, infection, mesh migration, erosion, and rejection; these require consequent excision (Baylón et al., 2017; Klinge and Klosterhalfen, 2018). Researchers, physicians, and surgeons have been fighting a two-front war for many years, trying to improve surgical meshes and their applications. Regarding progress in surgical implantation, the laparoscopic approach for hernia repair was proposed as an alternative to traditional open surgery in the early 1990s (Eker et al., 2013). Although there remains a debate in defining whether open surgery or laparoscopy is the "gold standard" for hernia repair (Al Chalabi et al., 2015), surgeons have recently pointed toward the use of robot-assisted surgery (Carbonell et al., 2018). Additionally, advances in hernia surgery deal with primary defect closure, retrorectus mesh placement, and concomitant component separation (Vorst et al., 2015).

On the other hand, the improvement in surgical meshes has been focused on identifying and making use of the most appropriate material. More than 200 types of meshes were reported in 2013 (Klinge et al., 2013); these meshes have different mechanical properties, pore sizes, weight, density, constitution (monofilament or twisted), manufacturing processes (extrusion or knitting), anisotropy, and type of material (synthetic non-absorbable, mixed or composite, and biological) (Rastegarpour et al., 2016). Moreover, many biocompatible coatings have been developed to modify surgical mesh surfaces and are aimed at protecting the prosthesis from degradation, decreasing postsurgical inflammation, minimizing foreign body reaction, reducing the risk of infections, and decreasing adhesions (Majumder et al., 2015; Baylón et al., 2017; Bredikhin et al., 2020). Because of their huge therapeutic potential, stem cells have been one of the focuses of biomedical researchers in the last 20 years. Stem cells have a wide range of applications in many different diseases (Sánchez et al., 2012; Reisman and Adams, 2014; Rajabzadeh et al., 2019) and are now the targets of a multitude of clinical trials[1] aimed at treating pathological conditions such as Crohn's disease, urinary incontinence, multiple sclerosis, diabetes, rheumatoid arthritis, glioblastoma, and myocardial infarction. Stem cell therapy has also been applied to mesh-aided hernia repair to improve the healing outcome of damaged tissues. However, contradictory results have been obtained (Marinaro et al., 2019).

Previous studies from our group have demonstrated that mesenchymal stem cells (MSCs) reduce adverse inflammation following surgical mesh application in a murine incisional hernia model (Blázquez et al., 2018) by promoting macrophage polarization towards an anti-inflammatory and pro-regenerative M2 phenotype (Blázquez et al., 2016). In the present study, we have investigated a new approach for the treatment of abdominal hernias. Here, we propose the combined use of surgical meshes with MSCs for controlling an adverse inflammatory response

[1] https://stemcellsportal.com/stem-cells-translational-medicine-clinical-trials-portal

following the implantation of mesh. In addition, this study was performed in a clinically relevant animal model (swine model of congenital abdominal hernia) by using minimally invasive procedures (laparoscopic approach). In this animal model, we have investigated: (i) the use of fibrin sealant as a vehicle to favor the adhesion of MSCs onto surgical meshes; (ii) the optimization and application of laparoscopic surgical procedures for the implantation of surgical meshes in a swine model of congenital abdominal hernia; and (iii) the evaluation of the effects of MSCs on mesh-repaired hernias. We demonstrated that fibrin sealants allow the adhesion of stem cells onto surgical meshes. Laparoscopy is a feasible approach for the successful implantation of stem cell-coated meshes. Our animal model with congenital hernia, which closely resembles the conditions of human patients with the same hernia, should be used for further preclinical studies. Although stem cell-based therapies have demonstrated a therapeutic potential in murine models (and under *in vitro* conditions), our experimental approach in this large animal model did not reveal any important contribution of stem cell therapy. It is important to note that further research is necessary to optimize the implantation of these cells in a real surgical context.

## MATERIALS AND METHODS

### Ethical Considerations

The Ethics Committee on Animal Experiments of the Jesús Usón Minimally Invasive Surgery Centre (JUMISC), Cáceres, Spain, validated all the experimental procedures according to the recommendations outlined by the local government (Junta de Extremadura) and EU Directive 2010/63/EU of the European Parliament on the protection of animals used for scientific purposes. Housing, care, and husbandry of all the animals used throughout the study were carried out in the animal facility of the JUMISC.

### Isolation, Expansion, and Characterization of Allogeneic Porcine Bone Marrow-Derived Mesenchymal Stem Cells

A Large White pig (3 months old and 25 kg) was euthanized, and allogeneic bone marrow-derived MSCs (BM-MSCs) were obtained from its femurs by using a needle and syringe. BM-MSCs were isolated and characterized as previously described (Casado et al., 2012). Briefly, the mononuclear cells were collected from the cell suspension by filtration through a 40 μm nylon mesh (Fisher Scientific, Leicestershire, UK) and centrifugation in Histopaque-1077 solution (Sigma-Aldrich, St. Louis, MO). After washing with phosphate-buffered saline (PBS), the mononuclear cells were resuspended in complete cell culture medium, prepared with Dulbecco's modified Eagle's medium, 10% fetal bovine serum (FBS) (Sigma-Aldrich), 5 μl/ml amphotericin B (Fungizone), 1% glutamine, and 1% penicillin/streptomycin (Lonza, Basel, Switzerland), seeded into tissue culture flasks, and incubated at 37°C and 5% $CO_2$. The non-adherent hematopoietic cells were removed after 48 h of incubation, whereas the adherent cells were passaged upon 80–90% confluence. The phenotypic characterization of BM-MSCs at passages 4–6 was performed by using a FACSCalibur™ Flow Cytometry System (BD Biosciences, CA, USA). Approximately $2 \times 10^5$ cells were incubated for 30 min at 4°C with adequate concentrations of porcine fluorescein isothiocyanate-conjugated monoclonal antibodies against Integrin beta-1 (CD29), CD44 antigen (CD44), Thy-1 antigen (CD90), Endoglin (CD105), CD45 antigen (CD45), Swine leukocyte antigen class 1 (SLA-1), and Swine leukocyte antigen class 2 (SLA-2) (Bio-Rad, CA, USA), according to the manufacturer's instructions. Isotype-matched negative control antibodies were used in the experiments. The CellQuest software (BD Biosciences, CA, USA) was used to analyze viable cells after the acquisition of $10^5$ events by using forward and side scatter characteristics. The mean fluorescence intensity (MFI) was determined relative to the MFI of its negative control to obtain the mean relative fluorescence intensity. As performed in our previous study (Casado et al., 2012), BM-MSCs were cultured for 21 days with differentiation medium (Gibco Life Sciences, Rockville, MD, USA) and stained with Oil Red O, Alcian Blue, and Alizarin Red S for the assessment of their potential toward adipogenic, chondrogenic, and osteogenic differentiation, respectively (Mok et al., 2008).

### Fibrin Sealant Admixture, Fibrin Clotting, and Cell Viability Assay of Mesenchymal Stem Cells

A fibrin sealant vehicle for allogeneic MSCs was prepared by using commercially available fibrin sealant Tisseel® (Baxter, USA; product number 1504516). This product consists of two separated components: a "thrombin solution" (500 IU/ml thrombin) and a "sealer protein solution" (91 mg/ml fibrinogen and synthetic aprotinin). These solutions are mixed in a ratio of 1:1 to prepare a ready-to-use fibrin solution. To determine the optimal mixture for mesh coating, BM-MSCs were detached from flasks with 0.25% trypsin solution and counted. Around $5 \times 10^4$ cells were resuspended in 0, 25, 50, 75, or 100 μl of complete cell culture medium and mixed with 100, 75, 50, 25, or 0 μl thrombin solution (pH 7.2, from Tisseel®; product number 1504516), respectively. Afterwards, these suspensions were mixed in a 1:1 ratio with the sealer protein solution (from Tisseel®; product number 1504516) (**Table 1**) and tested according to clotting capability and cell viability. Clotting capability was visually assessed, comparing clotted and gelatinous fibrin hydrogels against the unclotted liquid

**TABLE 1** | Composition of the culture medium (Dulbecco's modified Eagle's medium) and fibrin sealant mixtures for clotting capability assessment and cell viability assays.

| Culture medium + fibrin sealant mixtures | | |
|---|---|---|
| **Complete cell culture medium (μl)** | **Thrombin solution (thrombin 500 UI/ml) (μl)** | **Sealer protein solution (fibrinogen 91 mg/ml) (μl)** |
| 0 | 100 | 100 |
| 25 | 75 | 100 |
| 50 | 50 | 100 |
| 75 | 25 | 100 |
| 100 | 0 | 100 |

solutions for each mixture of thrombin solution, cell culture medium, and "sealer protein solution."

The Cell Counting Kit-8 (CCK-8) assay (Merck KGaA, Darmstadt, Germany) was used according to the manufacturer's instructions to determine cell viability. BM-MSCs were resuspended in the above-mentioned volumes of thrombin solution, cell culture medium, and sealer protein solution and cultured for 2 days at 37°C under 5% $CO_2$. Concurrently, BM-MSCs under standard culture conditions served as a positive control of cell viability, whereas the mixture of thrombin solution and "sealer protein solution," in combination, was used as the negative control.

## Animals, Experimental Design, Anesthesia, Analgesia, and Ultrasonography

The experimental approach that we used is shown in **Figure 1**. The number of animals for our pilot study was defined and approved by the Ethics Committee on Animal Experiments of JUMISC. All the experimental surgical procedures were performed on 10 Large White pigs that initially weighed 38.9 ± 11.2 kg and had a congenital abdominal non-incarcerated hernia. These animals were randomly divided into control ($n$ = 5) and cell ($n$ = 5) groups and underwent three surgeries at different times: mesh implantation (day 0), biopsy (day 6 or 7, hereinafter referred to as 1 week after implantation), and euthanasia and necropsy (days 28–31, hereinafter referred to as 1 month after implantation). Prior to the surgical procedures, all animals were administered with 0.3 mg/kg diazepam and 20 mg/kg ketamine intramuscularly. Anesthesia induction was achieved with 2–3 mg/kg propofol administered intravenously and maintained with 2.3–2.5% sevoflurane. After each surgery, all animals were administered with 0.01 mg/kg buprenorphine, 0.2 mg/kg meloxicam, and 15 mg/kg amoxicillin. One month after the implantation, anesthesia was induced in all animals as previously mentioned; they were then euthanized with intravenous administration of 1 mEq/kg of KCl.

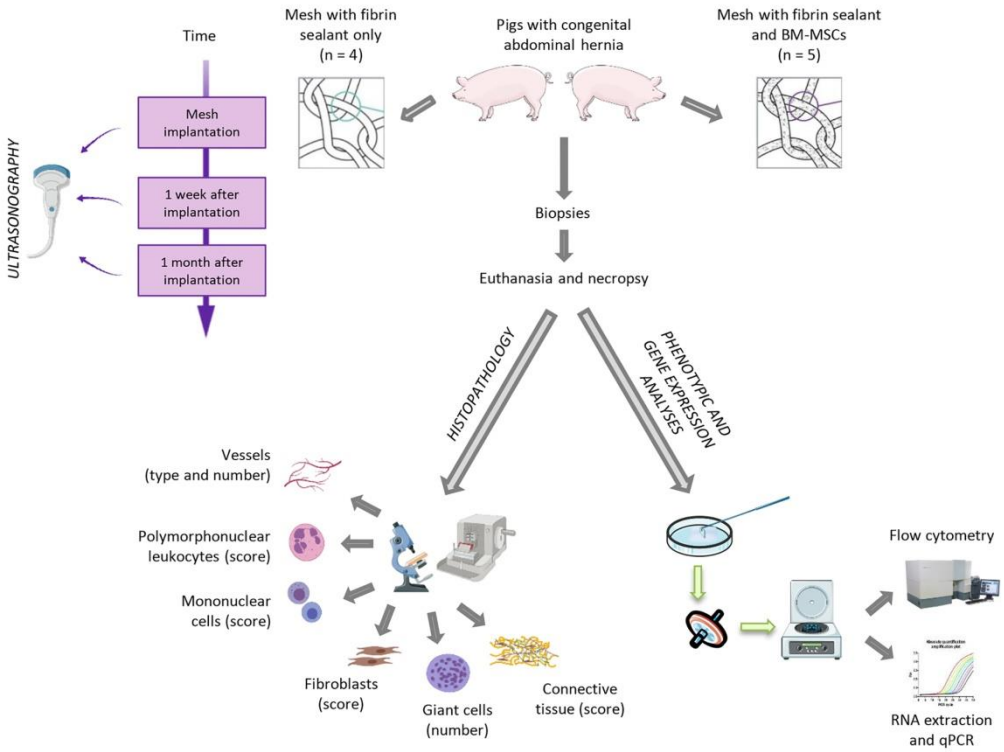


**FIGURE 1** | Overview of the experimental approach. Large White pigs with a congenital abdominal non-incarcerated hernia were randomly divided into "control" and "cell" groups. Polypropylene surgical meshes were covered with a fibrin sealant solution (control group) or with porcine bone marrow-derived mesenchymal stem cells (BM-MSCs) (cell group) and were implanted into the animals by laparoscopy. All animals were then biopsied (1 week after implantation) and euthanized prior to the excision of the surgical mesh (1 month after implantation). Prior to all surgeries, an ultrasonographic examination of the hernia was carried out to record the maximal diameter of the hernia orifice. Flow cytometry and histological and gene expression analyses of the biopsy and necropsy samples were performed. qPCR, quantitative real-time polymerase chain reaction. Mesh images are taken from Marinaro et al., 2019. The entire figure has been created with BioRender (https://app.biorender.com/) and Smart Servier Medical Art (https://smart.servier.com/).

Prior to all the implantation surgeries, an ultrasonographic examination of the hernia was performed on each animal by an experienced operator (FD), and the maximal diameter of the hernia orifice was recorded according to the short-axis view (**Figure 2**). To describe the evolution of the ultrasonographic findings and the hernia measurements after mesh implantation surgery, an ultrasonographic assessment was performed 1 week and 1 month after implantation. The results are presented in terms of percent reduction.

## Mesh Preparation and Laparoscopic Surgery Procedures for Hernia Repair

Monofilament polypropylene (PP) meshes (90 g/m$^2$ weight; Assumesh®, Assut Europe, Italy) were cut into 6 × 6 cm pieces and used for the surgical repair of abdominal hernias in both groups. For the cell group, allogeneic BM-MSCs were detached from flasks with 0.25% trypsin solution and stained with Trypan Blue stain (0.4%) (Thermo Fisher Scientific, Waltham, MA, USA) and counted with a Countess® Automated Cell Counter (Thermo Fisher Scientific, Waltham, MA, USA). A Trypan Blue dye exclusion test showed a viability of more than 95%. A total of $9 \times 10^6$ cells were resuspended in 3 ml of a 3:1 ratio of complete cell culture medium to thrombin solution (according to the results of the previous clotting and cell viability assays). This cell suspension was then mixed with 3 ml sealer protein solution and applied on the top of each PP mesh by using the fibrin sealant Tisseel® applicator.[2] As previously stated, the thrombin solution (500 IU/ml thrombin) and sealer protein solution (91 mg/ml fibrinogen) were provided with the commercially available fibrin sealant Tisseel® (Baxter). Cell dose was based on one of our previous studies (Blázquez et al., 2018) and optimized according to mesh size, the minimum volume of fibrin sealant to obtain complete coverage of the mesh surface, and the potential cell loss due to laparoscopic handling.

For the control group, the same volumes of complete cell culture medium, thrombin solution, and sealer protein solution without cells were mixed and spread on top of the PP meshes by using the fibrin sealant Tisseel® applicator. The approximation of hernia borders was performed through intracorporeal suturing by expert laparoscopic surgeons (FS-M and MB). The previously prepared meshes for the control and cell groups were carefully rolled inside a trocar for laparoscopic implantation. The surgical implantation was performed through laparoscopy by using 8–10 helicoidal staples.

A week after implantation, laparoscopic inspections were performed and small biopsy samples of the mesh with its surrounding muscle–peritoneum were collected with Metzenbaum scissors for further analyses. A month after implantation, the animals were euthanized and macroscopically evaluated. The surgically implanted meshes were excised from the euthanized animals and samples were taken for histology, flow cytometry, and gene expression analyses. Representative images of the surgical procedures are shown in **Figure 3**.

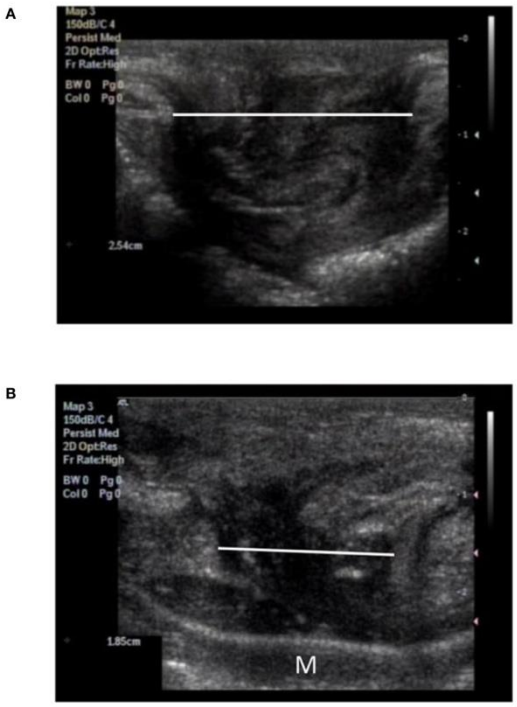


**FIGURE 2** | Appearance of the congenital hernia using ultrasonographic imaging before and after mesh implantation surgery. **(A)** Ultrasonographic evaluation before surgical mesh implantation (maximal diameter of the hernia 2.54 cm). **(B)** Ultrasonographic findings 1 month after mesh implantation surgery. A decrease in the diameter of the hernia can be observed (maximal diameter of the hernia 1.85 cm). Implanted mesh (M) appears as a linear echogenic interface.

## Histological Analysis

The samples obtained 1 week and 1 month after implantation were washed with PBS to remove excess blood, and histological analysis of the whole layer composed of the mesh and muscle–peritoneum was performed. All the histological samples were fixed in 4% formaldehyde, embedded in paraffin, sliced into 5–8 μm thick sections for histological analysis, and stained with hematoxylin and eosin (HE) and Masson's trichrome (MT). The microscopic evaluation of the specimens was performed on the tissue area where the mesh was implanted (clear circular areas representing mesh fibers) except for the connective tissue, which was also assessed below the mesh (**Figure 4**). The histological features, except the number of giant cells, were evaluated and counted in five fields distributed along the length of the specimen (oil immersion objective). Each specimen was first evaluated under low magnification in order to exclude necrotic or less preserved areas. Mononuclear and polymorphonuclear cells and fibroblasts were counted and assigned scores (**Table 2**) according to their mean number in the five fields of the HE specimens. Vessels (HE specimens) and connective tissue (MT specimens) were grouped according to their appearance and assigned scores (**Table 2**). The scores (**Table 2**) were assigned according to a

[2]https://baxterpi.com/pi-pdf/Tisseel_PI.pdf

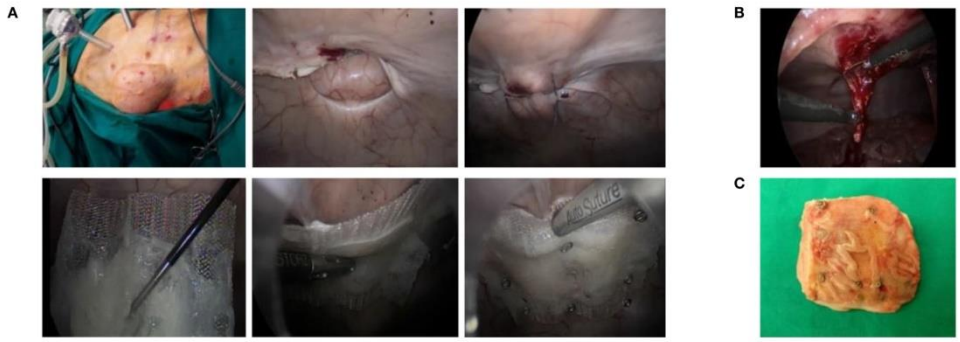


**FIGURE 3** | Surgical approach. **(A)** The abdomen of the pig was insufflated with $CO_2$ and the hernia orifice was visualized from the outside and from the inside with a laparoscopic camera. Hernia borders were approximated by intracorporeal suturing. The rolled surgical meshes (prepared as shown in **Supplementary Figure 1**) were inserted into a trocar and placed in contact with the hernia. Then the mesh was fixed with helicoidal staples. **(B)** Small biopsy samples of the mesh and its surrounding tissues were collected with Metzenbaum scissors 1 week after implantation surgery. **(C)** The meshes were excised following euthanasia of the animals 1 month after the implantation.

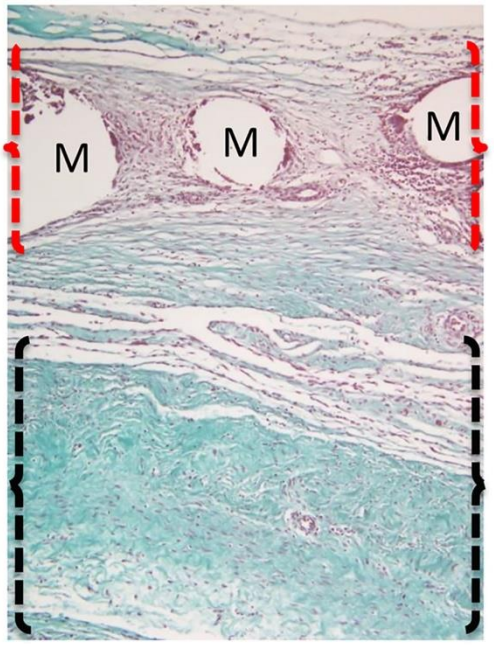


**FIGURE 4** | Representative image of a surgically implanted mesh and its surrounding tissue. The assessment of cellular characteristics was performed in the mesh (M) area (indicated by red brackets), whereas the connective tissue was evaluated in the area below the mesh (indicated by black brackets). The image represents a tissue sample stained with Masson's trichome stain.

previously published score system (Badylak et al., 2002). Vessels and giant cells (HE specimens) were counted and recorded according to their mean number in the five oil immersion magnification fields. Moreover, the average number of giant cells around mesh fibers was also determined under high-power field (×40 objective) and recorded.

## Flow Cytometry and Quantitative Polymerase Chain Reaction Studies

Phenotypic and gene expression analyses were performed on the infiltrating cells in the implanted surgical meshes. To collect these cells, the samples obtained 1 week and 1 month after implantation were washed with PBS to remove blood and other residues, and the muscle–peritoneum was removed. The meshes were moved to Petri dishes, submerged in PBS, and scraped with a blade to collect the outer layer of cells. The PBS containing the scraped cells was collected and filtered through a 40 μm filter (Fisher Scientific, Leicestershire, UK) to remove debris and the PP filaments. Afterwards, the infiltrating cells were detached twice from the scraped meshes with 0.25% trypsin solution.

For phenotypic analysis, $2 \times 10^5$ cells were resuspended in PBS containing 2% FBS and stained with the appropriate concentrations (according to the manufacturer's instructions) of fluorescence-labeled monoclonal antibodies against extracellular porcine surface markers T-cell surface antigen T4/Leu-3 (CD4), T-cell surface glycoprotein CD8 alpha chain (CD8α), CD45, Neural cell adhesion molecule 1 (CD56), Scavenger receptor cysteine-rich type 1 protein M130 (CD163) (BD Pharmingen, CA, USA), Monocyte differentiation antigen CD14 (CD14), Low affinity immunoglobulin gamma Fc region receptor III (CD16), CD27, CD45 antigen isoform RA (CD45RA), and SLA-II (Bio-Rad, CA, USA) for 30 min at 4°C (**Table 3**). The cells were washed, resuspended in PBS, and analyzed by using a FACSCalibur™ Flow Cytometry System (BD Biosciences, San Jose, CA, USA).

**TABLE 2** | Scoring system for histological evaluation of the tissue surrounding and infiltrating the surgical meshes 1 week and 1 month after implantation.

| Parameter | Score | | | | |
|---|---|---|---|---|---|
| | 0 | 1 | 2 | 3 | 4 |
| Polymorphonuclear leukocytes | No cells | Between 0 and 5 cells | Between 6 and 10 cells | Greater than 10 cells | |
| Mononuclear cells | No cells | Between 0 and 5 cells | Between 6 and 10 cells | Greater than 10 cells | |
| Vessels | No vessels | 1–3 blood vessels | 4–10 blood vessels | Greater than 10 blood vessels | |
| Vessel type | No vessels | Small arterioles and/or small venules and/or capillaries | Arterioles and/or venules | Both types | |
| Fibroblasts | No cells | Between 0 and 5 cells | Between 6 and 10 cells | Greater than 10 cells | |
| Connective tissue | No connective tissue | Loose (areolar) connective tissue with sparse and random arrangement of fibers | Moderately dense connective tissue with increased number of collagen fibers | Dense irregular (non-organized) connective tissue enriched with collagen fibers but the fibers are randomly arranged | Dense regular or organized connective tissue enriched with collagen fibers and the fibers tend to be organized in parallel bundles |

*The scores were adapted from a previously published score system (Badylak et al., 2002). The score for each parameter was evaluated per oil immersion field (×100 objective).*

After the acquisition of $10^5$ events, cells were selected according to forward and side scatter characteristics, and fluorescence was analyzed by using CellQuest software (BD Biosciences). Appropriate isotype-matched negative control antibodies were used in all experiments.

The gene expression of cells that infiltrated the surgical meshes 1 week and 1 month after implantation was analyzed by using quantitative real-time polymerase chain reaction (qPCR). The total RNA from scraped and detached cell samples was isolated by using a mirVana™ miRNA Isolation Kit (Invitrogen, Thermo Fisher Scientific Inc., Waltham, MA, USA) according to the manufacturer's instructions. RNA quality and concentration were spectrophotometrically evaluated by using a Synergy™ Mx Microplate Reader (Biotek, Winooski, VT, USA). Only the RNA samples with a 260/280 nm absorbance ratio between 1.8 and 2.1 were retrotranscribed to complementary DNA (cDNA) and amplified by qPCR. The amount of total RNA required for the reverse transcription reaction was calculated according to their concentrations after isolation such that the same starting cDNAs for qPCR amplifications of the compared study groups was guaranteed (control and cell groups 1 week after implantation; and control and cell groups 1 month after implantation). To this aim, 300 ng cDNA for the 1 week after implantation samples and 700 ng cDNA for the 1 month after implantation samples were synthesized from total RNAs in reverse transcription reactions by using iScript Reverse Transcription Supermix (BioRad, Hercules, CA, USA) with a reaction set-up and thermal cycling protocol according to the manufacturer's instructions. qPCR was performed by using TaqMan® Gene Expression Assays (Applied Biosystems, Thermo Fisher Scientific Inc., **Supplementary Table 1**) in combination with TaqMan Fast Advanced Master Mix (Applied Biosystems, Thermo Fisher Scientific Inc.). The thermal cycling conditions were as follows: 50°C for 2 min, 95°C for 2 min, and then 40 cycles of 95°C for 1 s and 60°C for 20 s. The amplification of cDNAs was performed by using a QuantStudio 3 System (Applied Biosystems, Thermo Fisher Scientific) and the qPCR products were quantified by a fluorescent method using the $2^{-\Delta Ct}$ expression (Livak and Schmittgen, 2001). The duplicates of all samples were analyzed separately and normalized against the *HRPT1* gene. Duplicate no-template control samples were prepared for each gene and showed no DNA contamination.

**TABLE 3** | Combination of antibodies used for phenotypic analysis by flow cytometry of the infiltrated cells inside the surgical mesh.

| Flow cytometry: combination of antibodies | |
|---|---|
| Percentage of lymphocyte subpopulations | CD4, CD8, CD16, CD56 |
| Lymphocyte differentiation | CD4, CD8, CD27, CD45RA |
| Lymphocyte subsets: activation markers | CD4, CD8, CD16, CD56, SLAII |
| Macrophage infiltration and activation | SLAII, CD14, CD163 |

## Statistical Analysis

The data were statistically analyzed using SPSS-21 software (SPSS, Chicago, IL, USA). For ultrasonographic data, ANOVA and the Tukey test were applied. The normal distribution of variables was assessed with the Shapiro–Wilk test, and the Levene test was used to assess homoscedasticity. For variables with normal distribution and homogeneity of variances, we used Student's *t*-test, and the Mann–Whitney *U*-test was used for non-parametric and heteroscedastic variables. A $p < 0.05$ was considered statistically significant.

# RESULTS

## Phenotypic Analysis and Multipotentiality of Mesenchymal Stem Cells, Admixture With Fibrin Sealant, Fibrin Clotting, and Cell Viability Assay

The stemness markers expression profile of BM-MSCs was $CD29^+$/$CD44^+$/$CD45^-$/$CD90^+$/$CD105^+$/SLA-$1^+$/SLA-$2^-$. Moreover, the differentiation assays assessing adipogenic, chondrogenic, and osteogenic lineages demonstrated the multipotentiality of BM-MSCs; this is consistent with a previously published study (Casado et al., 2012).

Assessment of the clotting capability of the solutions prepared by mixing complete cell culture medium, thrombin solution, and

sealer protein solution revealed that clotting took place with any mixture containing thrombin solution with volumes up to 25 µl. Less liquid leakage was observed with higher volumes of thrombin solution (data not shown).

The cell viability CCK-8 assay demonstrated the highest cell viability when the complete cell culture medium-to-thrombin solution ratio was 3:1 (data not shown). Hence, the latter ratio of complete cell culture medium-to-thrombin solution was: (i) mixed with the same volume of sealer protein solution and used to coat the PP mesh before implantation surgery (control group) or (ii) used to prepare the MSC suspension, mixed with the same volume of sealer protein solution, and used to coat the PP mesh (cell group).

## Evaluation of Congenital Hernia Size

Ultrasonographic assessment of hernia size is presented in terms of percent reduction of the mean hernia size 1 week and 1 month after implantation and compared with the hernia size before the suturing of hernia borders and mesh implantation (implantation day). The mean size of the congenital hernias before mesh implantation was 2.49 ± 0.99 cm (0%). As shown in **Figure 5**, the approximation of the hernia borders by suturing reduced the hernia size by 29.49 ± 25.72% 1 week after implantation and increased the same by 9.58 ± 43.15% 1 month after implantation in the control group, with reference to the size on implantation day. The cell group had a reduction of 46.01 ± 34.69% 1 week after implantation and a further reduction of 26.61 ± 28.79% 1 month after implantation, with reference to the size on implantation day. The decrease in the mean size of the hernia 1 week after implantation in the cell-treated group compared with the mean size of the hernia on implantation day was statistically significant ($p < 0.05$).

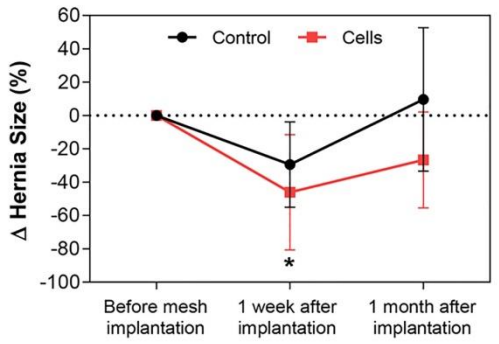


**FIGURE 5** | Evaluation of hernia size by ultrasonography. The maximum diameter of the hernia orifice was recorded by ultrasonography before, 1 week after, and 1 month after hernia border approximation and mesh implantation surgery in all animals in the two groups: control (black line) and cell group (red line). Changes in hernia size are presented as percent reduction at different time points, with the initial size of the hernia pertaining to the size before mesh implantation. A statistically significant decrease in the size of the hernias was observed 1 week after implantation in the cell group compared with the size recorded before mesh implantation surgery. All data are presented as mean ± standard deviation. The graph was created with GraphPad Prism. *$p < 0.05$ refers to the size of the hernia before mesh implantation.

## Surgical Mesh Implantation by Laparoscopic Surgery

The laparoscopic procedures allowed successful mesh implantation in all animals. In most cases (7 out of 10 animals), the implantation site did not show excessive inflammation or tissue adhesions except for three pigs that had adherence of the omentum, spleen, and small intestine to the surgical mesh. One animal showed hernia maintenance and another had *Escherichia coli* infection of the peritoneum and implant site. One pig manifested anorexia and vomiting 2 days after mesh implantation and died 4 days after implantation. Unfortunately, it was not possible to determine whether the cause of death was associated with mesh implantation surgery. The mean duration of the surgical procedure for hernia implantation was 41.27 ± 15.18 min per animal. Our results demonstrated that the surgical procedure, fixation method, and treatments were well tolerated and feasible to perform in this animal model. Additionally, considering that safety is one of the major issues in stem cell-based therapies, this animal model was useful in determining the hypothetical adverse effects of MSCs admixed with a fibrin sealant. Macroscopic evaluation of the incisional hernia and implanted meshes 1 week and 1 month after implantation showed a normal morphology of the tissues. Surgical adhesions, effusions, or tissue fibrosis were not observed in any of the groups.

## Histological Evaluation of the Mesh Implant Site

Histological evaluation of the cellular characteristics in the mesh area was performed. Connective tissue was observed also below the mesh area (**Figure 4**). Histological samples from the control group 1 month after implantation showed the presence of polymorphonuclear and inflammatory giant cells around the mesh area, whereas samples from the cell group 1 month after implantation showed a mononuclear infiltrate with few polymorphonuclear cells around the mesh. Regarding the connective tissue, the control group showed highly cellular connective tissue between the mesh threads, with few collagen fibers below the mesh area 1 month after implantation. In contrast, a moderately dense connective tissue enriched in blood vessels with some organization of the collagen fibers could be observed in the mesh area in the cell group. Additionally, a dense organized connective tissue with parallel bundles of fibers was seen below the mesh in the cell group 1 month after implantation (**Figure 6**). Nevertheless, when the histological features were counted and their scores were compared, no statistically significant differences were observed among the groups. The tissue and cellular characteristics underneath and between the mesh fibers did not seem to be affected by the presence of BM-MSCs at either 1 week or 1 month after implantation (**Figure 7**).

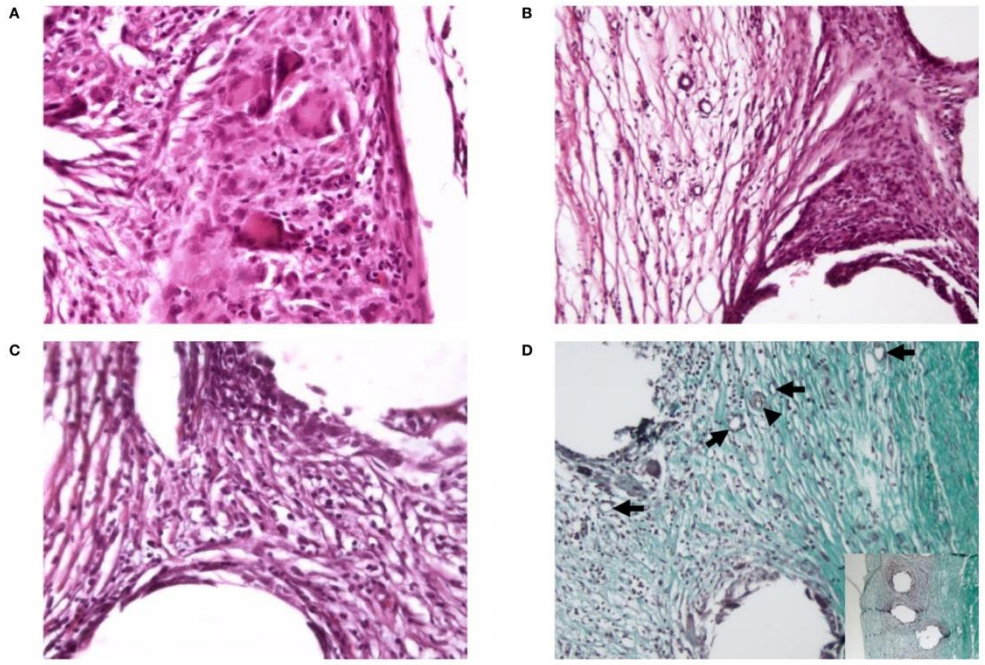


**FIGURE 6** | Representative figures of the histology of a control case and a cell case 1 month after implantation. **(A)** Polymorphonuclear cells around the mesh, along with inflammatory giant cells in a control case. Hematoxylin–eosin, ×40 objective. **(B)** Highly cellular connective tissue between the mesh with few collagen fibers below the mesh area in a control case. Hematoxylin–eosin, ×20 objective. **(C)** Presence of mononuclear infiltrate with few polymorphonuclear cells around the mesh in a cell case. Hematoxylin–eosin, ×40 objective. **(D)** Moderately dense connective tissue-enriched blood vessels (*arrows*; including arteriole, *arrowhead*) with some organization of the collagen fibers is present between the mesh fibers in a cell case. Note the dense organized connective tissue with parallel bundles of fibers below the mesh (*inset*). Masson Trichrome, ×20 objective and ×10 objective (*inset*).

## Phenotypic Evaluation of Cells Infiltrating the Surgical Mesh

Apart from the histological findings, our study also identified and characterized mesh-infiltrated cells. This analysis was performed by using flow cytometry of tissue obtained by biopsy 1 week after implantation and in explanted surgical meshes 1 month after implantation. Flow cytometry of the mesh-infiltrated cells showed an increase in tissue-infiltrated $CD14^{+}CD163^{+}$ (M2 macrophages) when the cell group was compared with the control group 1 week after implantation, but this change was not significant. The geometric mean of the activated macrophages in the cell group (52.96 ± 5.42%) significantly decreased 1 month after implantation ($p < 0.05$) compared with that of the control group (80.39 ± 19.55%). The results of the phenotypic analysis by flow cytometry are reported in **Tables 4**, **5**.

## Gene Expression Analysis of Cells Infiltrating the Surgical Mesh

The expression of 32 genes by the cells that infiltrated the surgical meshes was quantified 1 week and 1 month after implantation. **Figures 8**, **9** represent the analysis of gene expression when consistent amplifications were obtained with qPCR at both time points. The decrease in the expression of vascular endothelial growth factor A (*VEGFA*) (control group 0.427 ± 0.033 versus cell group 0.265 ± 0.108, $p = 0.0483$) and the increase in tumor necrosis factor (*TNF*) expression (control group 0.046 ± 0.025 versus cell group 0.188 ± 0.106, $p = 0.0357$) were statistically significant in the cell group 1 month after implantation ($p < 0.05$).

## DISCUSSION

Hernia remains a notable problem in human and veterinary medicine despite the fact that its conventional treatment was proposed for the first time in 1890 (Baylón et al., 2017). As a matter of fact, if surgical meshes had become the standard procedure for repairing abdominal hernias, an adverse inflammatory response would usually be observed after implantation, producing a multitude of complications and side effects.

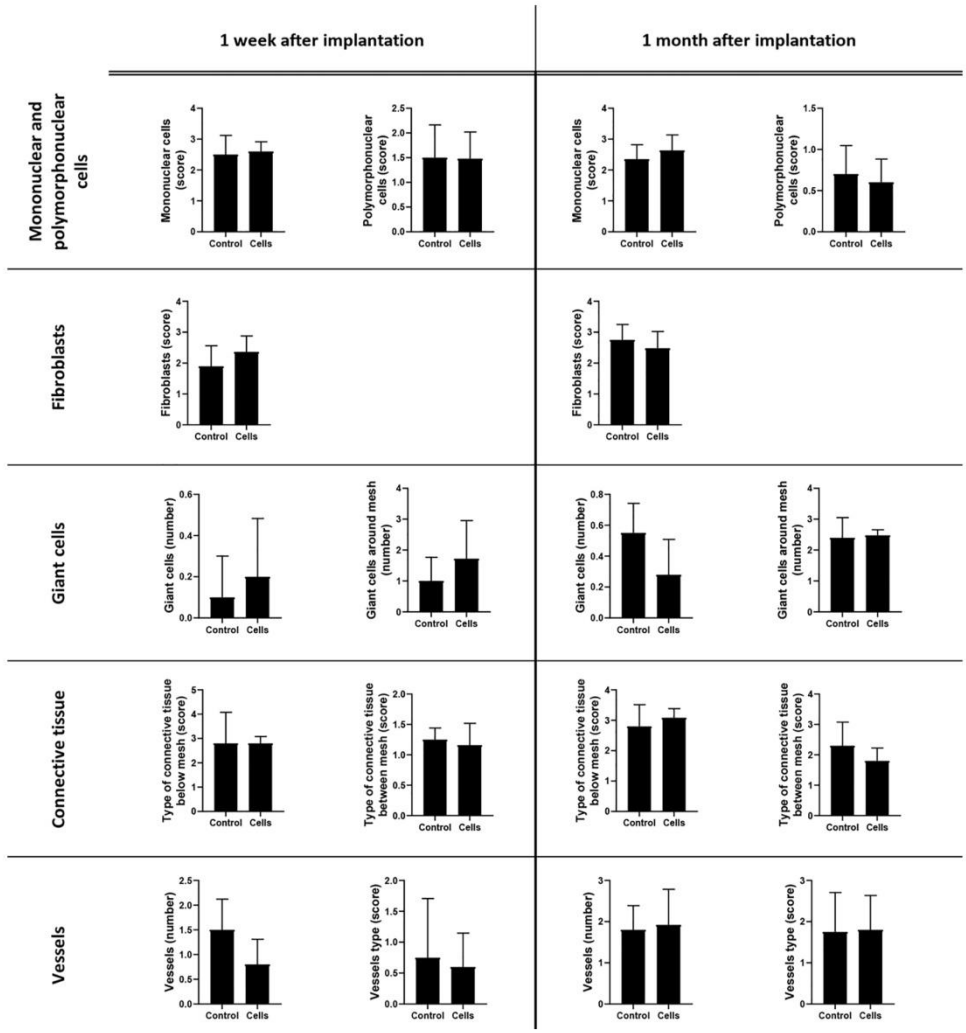


**FIGURE 7** | Histological evaluation of surgical meshes and surrounding tissues 1 week and 1 month after mesh implantation. The microscopic appearance of the tissue surrounding the surgical mesh was examined in the hematoxylin–eosin (HE) and Masson's trichome-stained specimens. Polymorphonuclear leukocytes (score), mononuclear cells (score), vessels (type and number), giant cells (number), and fibroblasts (score) between the mesh area were evaluated in five oil immersion fields. The type and organization of the connective tissue presented between and below the mesh were also scored. The average number of giant cells (number around the mesh fibers) was evaluated under a high-power field (×40 objective field). The scoring criteria are shown in **Table 2**. All the data are presented as mean ± standard deviation. The graphs were created with GraphPad Prism 8.

Adult stem cells can differentiate into a wide variety of cell types (Pittenger, 1999) and can be isolated from different tissues such as liver, lung, adipose tissue, skeletal muscle, amniotic fluid, bone marrow, skin, and heart (Mushahary et al., 2018). They have regenerative properties owing to their ability to differentiate and secrete factors that locally activate progenitor cells (Uccelli et al., 2008). Bearing these properties in mind, different cell-based treatments have been proposed to reduce the adverse inflammation and to improve tissue integration and regeneration after surgical mesh implantation (Marinaro et al., 2019). Nevertheless, it is important to consider that some clinical trials involving stem cell therapy have successfully reached the

**TABLE 4 |** Results of the phenotypic analysis by flow cytometry of the infiltrated lymphocytes and macrophages inside the surgical meshes 1 week and 1 month after implantation surgery.

| | | | | 1 week after implantation | | 1 month after implantation | |
|---|---|---|---|---|---|---|---|
| | | | | Control | Cells | Control | Cells |
| Tissue-infiltrating lymphocyte subsets | T-helper cells | Differentiation phenotype | Effector-memory cells (%CD45RA$^-$/CD27$^-$on CD4$^+$ CD8α$^-$) | 87.4 ± 3 | 88.42 ± 8.83 | 84.23 ± 3.37 | 83.49 ± 5.11 |
| | | | Naive cells (%CD45RA$^+$ or CD27$^+$ on CD4$^+$ CD8α$^-$) | 12.59 ± 3 | 11.58 ± 8.83 | 15.76 ± 3.37 | 16.5 ± 5.11 |
| | | Activation markers | NK-related receptor (%CD56/CD16$^+$ on CD4$^+$ CD8α$^-$) | 23.48 ± 13.37 | 12.18 ± 8.63 | 16.17 ± 10.3 | 9.08 ± 2.39 |
| | | | SLA-2 receptor (%SLA-2$^+$ on CD4$^+$ CD8α$^-$) | 37.28 ± 22.77 | 24 ± 14.25 | 23.07 ± 11.39 | 18.2 ± 4.77 |
| | T-cytotoxic cells | Differentiation phenotype | Effector-memory cells (%CD45RA$^-$/CD27$^-$ on CD4$^-$ CD8α$^+$) | 44.55 ± 19.99 | 68.65 ± 13.18 | 51.61 ± 12.53 | 60.78 ± 9.09 |
| | | | Naive cells (%CD45RA$^+$ or CD27$^+$ on CD4$^-$ CD8α$^+$) | 55.44 ± 19.99 | 31.34 ± 13.18 | 48.39 ± 12.53 | 39.21 ± 9.09 |
| | | Activation markers | NK-related receptor (%CD56/CD16$^+$ on CD4$^-$ CD8α$^+$) | 17.98 ± 11.83 | 15.05 ± 5.89 | 16.43 ± 11.48 | 13.67 ± 12.13 |
| | | | SLA-2 receptor (%SLA-2$^+$ on CD4$^-$ CD8α$^+$) | 56.59 ± 25.61 | 51 ± 18.33 | 19.79 ± 11.81 | 22.37 ± 19.01 |
| Tissue-infiltrating macrophage subsets | M1/M2 phenotype | | M2 macrophages (%CD163$^+$ on CD14$^+$) | 67.3 ± 11.72 | 72.56 ± 4.22 | 82.42 ± 14.93 | 83.82 ± 5.99 |
| | | | M1 macrophages (%CD163$^-$ on CD14$^+$) | 32.69 ± 11.72 | 27.44 ± 4.22 | 17.57 ± 14.93 | 16.17 ± 5.99 |
| | Activation markers | | SLA-2 expression (SLA-2 geometric mean on CD14$^+$) | 73.49 ± 20.07 | 77.41 ± 22.79 | 80.39 ± 19.55 | 52.96 ± 5.42* |

*All data are presented as the mean ± standard deviation. *p < 0.05 refers to the control group. CD4, T-cell surface antigen T4/Leu-3; CD8α, T-cell surface glycoprotein CD8 alpha chain; CD14, Monocyte differentiation antigen CD14; CD16, Low affinity immunoglobulin gamma Fc region receptor III; CD45RA, CD45 antigen isoform RA; CD56, Neural cell adhesion molecule 1; CD163, Scavenger receptor cysteine-rich type 1 protein M130; SLA-2, Swine leukocyte antigen class 2.*

**TABLE 5 |** Results of the phenotypic analysis by flow cytometry of the infiltrated leukocytes inside the surgical meshes 1 week and 1 month after mesh implantation.

| | | 1 week after implantation | | 1 month after implantation | |
|---|---|---|---|---|---|
| | | Control | Cells | Control | Cells |
| Tissue-infiltrating leukocytes | T-helper cells (% CD4$^+$ CD8α$^-$) | 4.39 ± 2.73 | 15.67 ± 11.01 | 12.71 ± 12.31 | 2.25 ± 1.65 |
| | T-cytotoxic cells (% CD4$^-$ CD8α$^+$) | 10.71 ± 6.51 | 28.48 ± 15.08 | 17.46 ± 18.42 | 2.38 ± 1.17 |
| | Ratio CD4$^+$:CD8α | 1.16 ± 0.96 | 0.55 ± 0.2 | 0.95 ± 0.55 | 0.88 ± 0.26 |
| | NK cells (% CD8α$^-$ CD16$^+$/CD56$^+$) | 5.04 ± 4.68 | 17.86 ± 14.96 | 8.69 ± 7.49 | 4.11 ± 0.49 |
| | Macrophages (% CD14$^+$) | 14.41 ± 22.45 | 16.32 ± 12.19 | 10.23 ± 9.01 | 5.56 ± 1 |

*All data are presented as mean ± standard deviation.*

third phase, where long-term benefits and side effects are evaluated. However, many of them have not yielded the desired results (Trounson and McDonald, 2015) and their number has dropped over the years. This decline may be due to the fact that these preclinical and clinical trials are too heterogeneous: MSCs from different sources, different cell preparation protocols, and different cell passage numbers have been used over time (Kabat et al., 2020). Under these circumstances, the application of stem cell therapy to the surgical implantation of meshes for hernia treatment remains challenging. Even in this particular field, there is a lack of standardization in preclinical trials. Hence, creating a consensus about surgical procedures, the type of surgical meshes to use, and the effectiveness of stem cells in the pathophysiology of hernia is difficult (Marinaro et al., 2019).

First, there is a lack of uniformity regarding the use of animal models in preclinical trials (Vogels et al., 2017). Even the most recent studies that have investigated the use of stem cells on surgical meshes have been performed *in vitro* (Gao et al., 2014; Vozzi et al., 2017) or in small animal models, especially in mice (Darzi et al., 2018; Paul et al., 2019; Mukherjee et al., 2020), rats (Altman et al., 2010a; Altman et al., 2010b; Edwards et al., 2015; Iyyanki et al., 2015; Klinger et al., 2016; van Steenberghe et al., 2017; Hansen et al., 2020), and rabbits (Zhao et al., 2012; Cheng et al., 2017). Only a few preclinical studies have been performed in sheep (Gerullis et al., 2013; Gerullis et al., 2014). However, this animal model has only been used for the study of surgical meshes in the case of pelvic organ prolapse (Emmerson et al., 2019), owing to similarities between the ovine and human urogenital tracts. To date, and to our knowledge, only one clinical case involving a human patient has been published (Palini et al., 2017).

Second, stem cell-based therapies for the treatment of hernia have been developed by using different stem cell sources such as placenta-derived stem cells (Zhang et al., 2016), endometrium-derived MSCs (Su et al., 2014; Ulrich et al., 2014; Edwards et al., 2015; Darzi et al., 2018), and adipose-derived MSCs (Melman et al., 2011; Li et al., 2013; Iyyanki et al., 2015; Blázquez et al., 2016; Cheng et al., 2017).

Third, surgical meshes can be used to reinforce tissues in pelvic prolapses or hernias, but these two conditions are quite different. The most recent and relevant studies investigating the use of stem cells on surgical meshes are focused towards reinforcement of the pelvic floor (Emmerson et al., 2019; Paul et al., 2019; Mukherjee et al., 2020) rather than of the abdominal wall; however, it is necessary to consider the fundamental

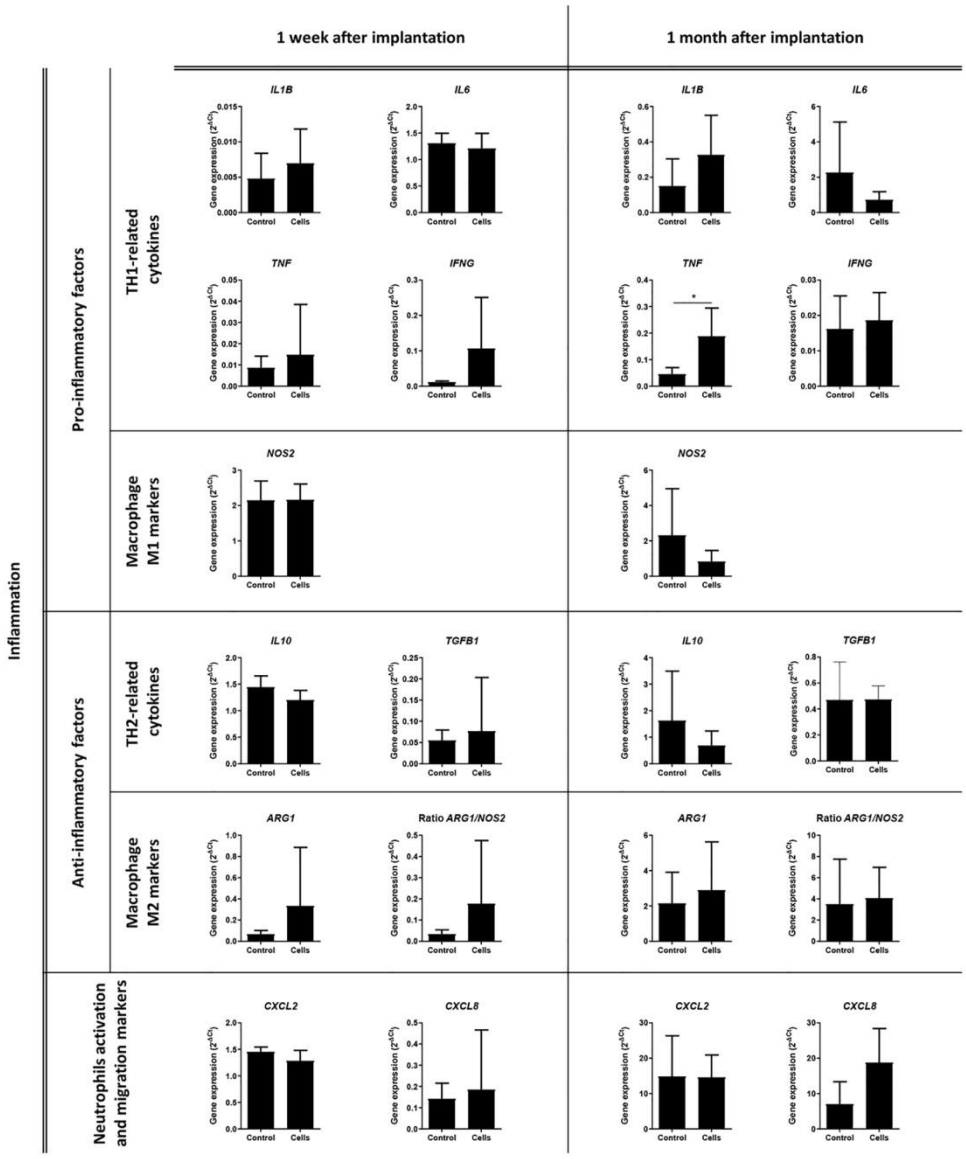


**FIGURE 8** | Analysis of the expression of inflammation-related genes. Quantitative real-time polymerase chain reaction was performed on the infiltrated cells within the surgical meshes 1 week and 1 month after mesh implantation. All the data are presented as mean ± standard deviation. The graphs were created with GraphPad Prism. *$p < 0.05$ refers to the control group. ARG1, Arginase 1; CXCL2, C-X-C Motif Chemokine Ligand 2; CXCL8, C-X-C Motif Chemokine Ligand 8; IFNG, Interferon Gamma; IL1B, Interleukin 1 Beta; IL6, Interleukin 6; IL10, Interleukin 10; NOS2, Nitric Oxide Synthase 2; TGFB1, Transforming Growth Factor Beta 1; TNF, Tumor Necrosis Factor.

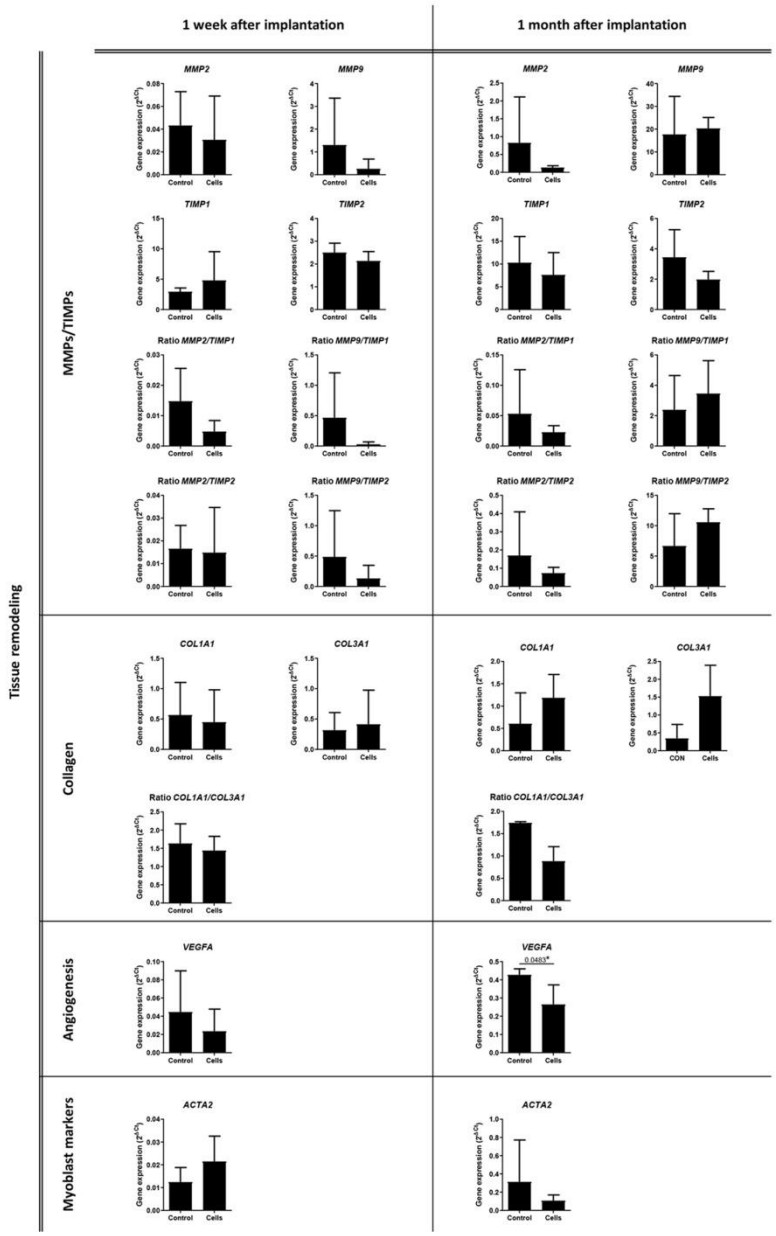


**FIGURE 9** | Analysis of the expression of tissue remodeling-related genes. Quantitative real-time polymerase chain reaction was performed on the infiltrated cells within the surgical meshes 1 week and 1 month after mesh implantation. All the data are presented as mean ± standard deviation. The graphs were created with GraphPad Prism. *$p < 0.05$ refers to the control group. ACTA2, Actin Alpha 2, Smooth Muscle; COL1A1, Collagen Type I Alpha 1 Chain; COL3A1, Collagen Type III Alpha 1 Chain; MMP2, Matrix Metallopeptidase 2; MMP9, Matrix Metallopeptidase 9; TIMP1, TIMP Metallopeptidase Inhibitor 1; TIMP2, TIMP Metallopeptidase Inhibitor 2; VEGFA, Vascular Endothelial Growth Factor A.

differences between the two pathological conditions in the evaluation of preclinical trials.

Fourth, even though standardization and reproducibility are very important to obtain consistent results in research, the clinical setting is characterized by a huge variability in patients, with a variety of body masses and type, position, and size of hernias. Preclinical trials should involve animal models resembling the variability of human and veterinary patients to guarantee the safety, feasibility, effectiveness, and applicability of the preclinical results. Most of the studies investigating stem cell-aided surgical mesh hernia repair are performed after a ventral incision (Altman et al., 2010a; Iyyanki et al., 2015; van Steenberghe et al., 2017; Hansen et al., 2020), which may be an appropriate model for incisional hernias following laparotomies but not for other kinds of hernias.

A plethora of different surgical meshes are commercially available; however, they can be generally categorized under three groups: synthetic non-absorbable, synthetic absorbable, and biological meshes (FitzGerald and Kumar, 2014). Each type of mesh may produce different effects on a human or veterinary patient according to its intrinsic characteristics such as material, absorbability, and biocompatibility.

Many surgical meshes for urogynecological use[3] and for abdominal wall repair[4] have been withdrawn from the market because of safety concerns. One of the reasons for the recall of surgical meshes may be the lack of thorough understanding in hernia research.

We developed an experimental approach to test whether the use of stem cells for abdominal hernia treatment is viable in a clinically relevant animal model. To the best of our knowledge, this is the first preclinical study where pigs with congenital abdominal hernias were treated with surgical meshes seeded with adult stem cells. Additionally, the surgical approach was performed with minimally invasive procedures to avoid complications related to open surgery. An exhaustive follow-up was performed at different time points using different evaluation methods: ultrasonography, gene expression analysis, complete histological evaluation, and cellular characterization by flow cytometry of infiltrated leukocytes.

Our experimental study was initially focused on the selection of the best animal model. We chose the swine model for different reasons. First, pigs are comparable to humans in terms of body mass, metabolism, organ size, omnivorous diet (Bassols et al., 2014; Schook et al., 2015), and gastrointestinal anatomy (Gonzalez et al., 2015). Second, porcine skin is similar to human skin in different histological and anatomical aspects; for example, the sparse and simple hair coat, epidermal thickness and turnover kinetics, the presence of adipose tissue at the hypodermis, and the presence of musculocutaneous vessels that run perpendicular to the skin's surface are similar between humans and pigs (Kemppainen, 1990; Avon and Wood, 2005; Debeer et al., 2013; Wei et al., 2017; Fossum and Duprey, 2019). Third, abdominal and inguinal hernias are relatively common in pigs; the incidence of these hernias range from 1.7% to 6.7% in different swine breeds (Atkinson et al., 2017). Piglets frequently present an incomplete closure of the umbilical ring after birth as a result of genetic causes (Grindflek et al., 2018) and are usually rejected by farmers as they have slower growth and higher mortality (Yun et al., 2017).

Hence, in order to evaluate the therapeutic effect of adult stem cells combined with surgical meshes, we chose Large White pigs with congenital abdominal hernias, and two study groups were established: a control group and a cell group. For the application of stem cells in surgical meshes, we considered the synthetic polymer PP as it is chemically inert and does not support cell adhesion. Fibrin sealants allow cell adhesion, viability, migration, and proliferation, and allow cells to execute their paracrine action locally. Moreover, fibrin sealants are rarely related to inflammation and foreign body reaction; hence, they are widely used in tissue engineering (Li et al., 2015). We used a commercially available fibrin sealant to aid cell adhesion on the PP surgical mesh and to aid the compatibility of this cell-seeded mesh with the laparoscopic instrumentation. Finally, we used MSCs that were previously characterized in terms of phenotype, gene expression, and differentiation capacity (Casado et al., 2012; Álvarez et al., 2016) and that were used in preclinical studies without adverse effects (Blázquez et al., 2015). It is important to note that, even though we did not evaluate their clonic capacity, the MSCs used in this study fulfill the "minimal criteria for defining multipotent mesenchymal stromal cells" defined by the International Society for Cellular Therapy (Dominici et al., 2006). Additionally, we proposed the administration of heterologous cells, as they can be safer than autologous cells (Crisostomo et al., 2015). Under these circumstances, all the steps from cell preparation and seeding on the top of the surgical mesh to rolling and insertion within the laparoscopic trocar are easy and quick; the cell-seeded material can be cryopreserved (Blázquez et al., 2018), offering a safe and bioactive off-the-shelf product for hernia repair.

The first aim of this paper was to evaluate the reduction in hernia size after the approximation of hernia borders and the implantation of the surgical mesh by laparoscopy. Additionally, we aimed to test the effect of the stem cells that we seeded on the surgical meshes in the cell group.

Ultrasonography was performed prior to surgical mesh implantation and 1 week and 1 month after mesh implantation surgery. It is important to note that the mean diameter of the congenital hernias in the experimental groups was 2.49 ± 0.99 cm; however, these sizes were heterogeneous and ranged from 0.74 cm to 4.15 cm in diameter. In order to normalize hernia sizes, we presented our results in terms of percent reduction. There was a statistically significant reduction in terms of mean hernia size when surgical meshes were combined with stem cells 1 week after implantation (–46.01 ± 34.69). Obviously, we cannot simply state that this reduction is a cell-mediated effect only as it can be associated with inherent differences in the surgical procedures (different suture closures in different kinds of hernias and subsequent mesh fixation) and with the heterogeneous range of size and weight of the animals in the study.

[3]https://www.fda.gov/medical-devices/implants-and-prosthetics/urogynecologic-surgical-mesh-implants

[4]https://www.fda.gov/medical-devices/implants-and-prosthetics/hernia-surgical-mesh-implants

In both groups, the repair of the hernias and mesh fixation were performed by laparoscopy. Although a systematic review and meta-analysis has revealed that the recurrence rate, infection, hospital stay, and operation time are similar between open surgery and laparoscopy (Al Chalabi et al., 2015), there has not yet been a consensus about the best method to repair ventral hernias (Van Veenendaal et al., 2015). There are reviews and meta-analyses wherein the laparoscopic repair of umbilical hernias was reported to be associated with a lower risk of infections, a lower recurrence rate, and a shorter hospitalization stay (Hajibandeh et al., 2017); based on these and considering that laparoscopy is widely used for hernia surgery, our results have revealed that this surgical procedure is suitable and safe in a swine model. An important advantage of using laparoscopy in the proposed model (animal with hernia congenital disease) is the possibility of evaluating the macroscopic status of internal tissues. Our surgical procedures consisted in the removal of previous adhesions (if present), followed by the closure of the hernial ring with sutures and placement of the mesh. The surgical techniques were successfully executed, even though a reduced number of animals presented some complications. We observed an incomplete closure of the hernial ring in one animal, with no leakage or protrusion of hernial contents. This recurrence of the hernia may have been due to loose sutures or to the intraperitoneal fixation of the mesh with helicoidal staples. We think that the implantation of the helicoidal clips could be insufficient to guarantee deep aponeurotic fixation to support the displacement of tissues during pig growth. We also stated that there was an *E. coli* contamination, which could have been caused by bacterial contamination from a contaminated pneumoperitoneum needle, trocar, or tweezers or by an ineffective antibiotic therapy protocol. Additionally, three animals presented tissue adherences. It is important to note that intraperitoneal implantation places the mesh in direct contact with the visceral peritoneum. This kind of implant *per se* can cause post-surgical adhesions (Farmer et al., 1998). Laparoscopy also allowed us to perform biopsies of the implanted meshes and their surrounding tissues at intermediate time points. In our study, the follow-up was conducted after 1 month, and the biopsies 1 week after implantation allowed us to analyze early histological and genetic changes as well as leukocyte infiltrations at short intervals.

The third aim of this study was to characterize the inflammatory response of the abdominal tissues to surgically implanted PP meshes with or without stem cells. Thus, we evaluated the expression of TH1/TH2 markers and M1/M2 markers in mesh-infiltrated cells by qPCR. We also analyzed mesh-infiltrating leukocytes by flow cytometry and assessed the inflammatory status of the tissue surrounding the surgical meshes through a histopathological examination. Even though previous observations in murine models using MSC-coated meshes (Blázquez et al., 2016; Blázquez et al., 2018) have demonstrated an M2 polarization within the tissue and around the mesh fibers, we did not find any significant change in the expression of M1/M2 markers. Surprisingly, our comparative analyses in 10 different TH1/TH2 cytokines revealed a significant increase in the expression of *TNF* in the cell group 1 month after implantation. An increase in TNF production has already been linked to the implantation of PP meshes in one study (Prudente et al., 2016). Although a reduction in *TNF* gene expression in the cell group was expected (Yan et al., 2018) we hypothesized that the short survival and paracrine activity *in vivo* of stem cells for tissue engineering applications (Dash et al., 2018) was not effective in counteracting the strong inflammatory response induced by the PP mesh. This hypothesis can be confirmed by the fact that even our histological evaluation did not present significant differences in the infiltration of mononuclear/polymorphonuclear leukocytes in mesh that surrounded tissues at any time point.

The surgical implantation of non-absorbable meshes is associated with a foreign body reaction that leads to fibrous encapsulation of the implant. In the initial host response, proteins and platelets favor the recruitment and adhesion of macrophages and neutrophils; these are followed by lymphocyte infiltration (Klopfleisch and Jung, 2017). We performed a phenotypic characterization of the different leukocyte subsets that infiltrated the surgical mesh and determined the activation status of T helper cells, T-cytotoxic cells, and macrophages. This analysis (performed 1 week and 1 month after mesh implantation surgery) did not reveal any significant differences in the T-cell subsets. We were expecting a macrophage polarization toward M2 cells owing to the immunomodulatory effect of BM-MSCs, according to our previous studies in murine models (Blázquez et al., 2016; Blázquez et al., 2018). The increase in the percentage of tissue-infiltrated $CD14^+$ $CD163^+$ (M2 cells) in the cell group 1 week after implantation with reference to the control group (**Table 4**), together with the decrease in the expression of the *NOS2* gene (a M1 marker) in the cell group 1 month after implantation, may suggest an M2 polarization by MSCs. However, these changes were not statistically significant. The macrophage analysis also demonstrated a significant decrease in SLA-II expression (SLA-II geometric mean on $CD14^+$) in the cell group 1 month after implantation with reference to the control group; nevertheless, the biological significance of this decrease remains uncertain. Hence it is difficult to assert that MSCs triggered an M2 differentiation under these experimental conditions.

The last aim of our study was to evaluate the effects of mesh implantation on connective tissue and vascularization, with or without stem cells. Connective tissue is known to be altered in hernia patients (Henriksen et al., 2011), who thereby present with a low collagen 1/collagen 3 ratio, poor quality collagen, and increased collagen breakdown (Henriksen et al., 2011; Calaluce et al., 2013; HerniaSurge Group, 2018). Moreover, collagen metabolism is strictly related to matrix metalloproteinase (MMP) proteolytic activity in healthy individuals; however, this balance is altered in hernia patients (Henriksen et al., 2011). Stem cells have already been demonstrated to trigger connective tissue remodeling throughout the induction of collagen synthesis and reorganization (Ku et al., 2006; Casado et al., 2014; Liu et al., 2017) and MMP release (Ding et al., 2009; Clarke et al., 2015). For this reason, we performed gene expression analysis of collagens, MMPs, and tissue inhibitors of metalloproteinases (TIMPs) by qPCR and evaluated the histology of connective tissue between and below the mesh areas. However, we found no significant statistical differences

in the gene expression of either collagens, MMPs, and TIMPs or their ratios and nor in the histological analysis. Regarding vascularization and angiogenesis, we did not observe any significant changes in vascularization. However, we found a slight, but significant, reduction in *VEGF* expression in the cell group 1 month after mesh implantation. It is true that stem cells have been associated with enhanced angiogenesis in wounds through the release and induction of VEGF (King et al., 2014); however, a high level of angiogenesis has been associated with hypertrophic scarring and fibrosis (DiPietro, 2016), especially in the long term (Karvinen et al., 2011). We hypothesized that stem cells, 1 month after implantation, contributed to the slight reduction in *VEGF*, which thereby minimized severe scarring of the wound.

Altogether, our histological, phenotypic, and gene expression analyses did not reveal any important contribution of stem cell therapy to the implantation of surgical meshes. Nevertheless, this study has established that there remains a lack of knowledge about how to correctly repair hernias with surgical meshes that would guarantee the safety of patients and pose a small risk of adverse effects for them. We recognize that this study has some important limitations. First, our insight led us to rely on a large animal model rather than on small animal models such as rodents, as the large animal model we used is more similar to humans in terms of metabolic requirements, anatomical size, and skin histology. Small animal models with artificially induced abdominal wall defects guarantee the standardization of experimental practices (in this case, similar body mass, sex, and hernia size) and fewer ethical concerns. However, they remain far from clinical practice. Our animal model, in contrast, did not allow the use of large sample sizes and homogeneity: this led to poor significant results in the histological, phenotypic, and gene expression analyses and it is the most important limitation of our study. Second, excluding all the related advantages, laparoscopy has a long learning curve (Hopper et al., 2007) and even expert surgeons need time to practice and standardize this innovative type of surgery. Third, some tests, such as biodistribution or teratogenicity tests, should have been performed to guarantee the safety of the stem cell therapy. We believe that stem cells are not meritless, especially when combined with surgical meshes for hernia repair, but a much larger number of animals, more standardization, and further analyses are required to guarantee reliable results.

To our knowledge, this is the first preclinical study evaluating the use of stem cell therapy in the field of abdominal hernias in a clinically relevant swine model with congenital hernia. According to our study, pigs with congenital hernia closely resemble hernia patients and can be used for further preclinical studies. However, a large number of animals, with similar body masses and hernia sizes, are required to provide consistent results; fibrin sealants can be used to allow cell adhesion on the surgical mesh surface. Moreover, laparoscopy can be used for hernia repair by suturing and it allows for the implantation of surgical meshes seeded with cells. The combined use of meshes and MSCs may allow the creation of bioinert products intended for future clinical applications. This product might have an immediate economic impact by reducing the recurrence of the aforementioned pathologies, hospitalization, and casualties; this product might also have an important impact in the quality of life of patients with hernias. To achieve these aims, extensive and standardized preclinical studies assessing safety and feasibility must be established with urgency.

## DATA AVAILABILITY STATEMENT

The datasets presented in this study can be found in online repositories. The names of the repository/repositories and accession number(s) can be found below: https://figshare.com/, https://doi.org/10.6084/m9.figshare.12287288.v2.

## ETHICS STATEMENT

The animal study was reviewed and approved by Ethics Committee on Animal Experiments of the Jesús Usón Minimally Invasive Surgery Centre, in compliance with the recommendations outlined by the local government (Junta de Extremadura), and the EU Directive 2010/63/EU of the European Parliament on the protection of animals used for scientific purposes.

## AUTHOR CONTRIBUTIONS

FM, JC, RB, and FS-M conceived and designed the experiments. FD performed the ultrasonography. MB and FS-M performed all the surgical procedures. FM, JC, RB, VÁ, and EL isolated and characterized the cells, prepared the meshes for surgical procedures, and performed molecular and phenotypic analyses. AU prepared histological samples. MS and RM performed the histological evaluations. FM, JC, and RB analyzed the data. FM and JC wrote the article. All authors contributed to the article and approved the submitted version.

## FUNDING

JUMISC is supported by CIBERCV (CB16/11/00494) and a grant from Junta de Extremadura, Consejería de Economía, Ciencia y Agenda Digital: Ayuda a Grupos Catalogados de la Junta de Extremadura (GR18199) co-financed by European Regional Development Fund (ERDF). This study was also supported by competitive grants, such as: "Miguel Servet I" grant (CP17/00021 and MS17/00021) and project PI18/0911 from Instituto de Salud Carlos III to JC (co-financed by ERDF/ESF); MAFRESA S.L. (Grupo Jorge) grant (promoted by Jesús Usón Gargallo) to FM; Consejería de Economía e Infraestructuras – Junta de Extremadura grant to JC (IB16168 co-financed by ERDF/ESF "Investing in your future"); Sara Borrell grant from Instituto de Salud Carlos III to EL (CD19/00048); CNPqBrazil fellowship (305876/2018-0) to MB. Surgical procedures and imaging diagnoses were performed at

the ICTS Nanbiosis (Unit 21, Operating rooms). The funders had no role in study designs, data collection and analysis, decision to publish, or preparation of the article.

## ACKNOWLEDGMENTS

First of all, we are extremely thankful for the invisible but very hard work of all the veterinarians and technicians working in our animal facilities (Luis Dávila, María Isabel Higuero, Victor Pérez, and Jorge Mateos), in anesthesia (Juan Rafael Lima, Ana Abad, Jenifer Bermejo, David Mariscal, and Patricia Arévalo), in our surgery theaters (María Borrega, Vanesa García, Jesús González, Helena Martín, María Ángeles Pámpano, and Rocío Román), and in laboratories (Juan Antonio Samino) throughout the study. Thanks to Julia de la Cruz and Beatriz Macías for their help in the ultrasonographic procedures and to Verónica Crisóstomo for helping us with statistical analysis. Last but not least, we want to acknowledge Dr Jesús Usón, for constantly supporting and motivating all researchers, especially the youngest ones, and for his tireless and countless attempts to introduce the values of research to the business world, which is usually foreign to the world of research. Thanks to Alfonzo Rodríguez and Sergio Samper, on behalf of the companies Mafresa S.L. and Grupo Jorge, who believe in research and are supporting us, asking nothing in return.

## SUPPLEMENTARY MATERIAL

The Supplementary Material for this article can be found online at: https://www.frontiersin.org/articles/10.3389/fphar.2020.01332/full#supplementary-material

## REFERENCES

Al Chalabi, H., Larkin, J., Mehigan, B., and McCormick, P. (2015). A systematic review of laparoscopic versus open abdominal incisional hernia repair, with meta-analysis of randomized controlled trials. *Int. J. Surg.* 20, 65–74. doi: 10.1016/j.ijsu.2015.05.050

Altman, A. M., Abdul Khalek, F. J., Alt, E. U., and Butler, C. E. (2010a). Adipose tissue-derived stem cells enhance bioprosthetic mesh repair of ventral hernias. *Plast. Reconstr. Surg.* 126, 845–854. doi: 10.1097/PRS.0b013e3181e6044f

Altman, A. M., Khalek, F. J. A., Alt, E. U., and Butler, C. E. (2010b). Adipose Tissue–Derived Stem Cells Enhance Bioprosthetic Mesh Repair of Ventral Hernias. *Plast. Reconstr. Surg.* 126, 845–854. doi: 10.1097/PRS.0b013e3181e6044f

Álvarez, V., Sánchez-Margallo, F.-M., Blázquez, R., Tarazona, R., and Casado, J. G. (2016). Comparison of mesenchymal stem cells and leukocytes from Large White and Göttingen Minipigs: Clues for stem cell-based immunomodulatory therapies. *Vet. Immunol. Immunopathol.* 179, 63–69. doi: 10.1016/j.vetimm.2016.08.002

Atkinson, M., Amezcua, R., DeLay, J., Widowski, T., and Friendship, R. (2017). Evaluation of the effect of umbilical hernias on play behaviors in growing pigs. *Can. Vet. J.* 58, 1065–1072.

Avon, S. L., and Wood, R. E. (2005). Porcine skin as an in-vivo model for ageing of human bite marks. *J. Forensic Odontostomatol.* 23, 30–39.

Badylak, S., Kokini, K., Tullius, B., Simmons-Byrd, A., and Morff, R. (2002). Morphologic study of small intestinal submucosa as a body wall repair device. *J. Surg. Res.* 103, 190–202. doi: 10.1006/jsre.2001.6349

Bassols, A., Costa, C., Eckersall, P. D., Osada, J., Sabrià, J., and Tibau, J. (2014). The pig as an animal model for human pathologies: A proteomics perspective. *Prot. Clin. Appl.* 8, 715–731. doi: 10.1002/prca.201300099

Baylón, K., Rodríguez-Camarillo, P., Elías-Zúñiga, A., Díaz-Elizondo, J. A., Gilkerson, R., and Lozano, K. (2017). Past, Present and Future of Surgical Meshes: A Review. *Membr. (Basel)* 7. doi: 10.3390/membranes7030047

Birindelli, A., Sartelli, M., Di Saverio, S., Coccolini, F., Ansaloni, L., van Ramshorst, G. H., et al. (2017). 2017 update of the WSES guidelines for emergency repair of complicated abdominal wall hernias. *World J. Emerg. Surg.* 12, 37. doi: 10.1186/s13017-017-0149-y

Blázquez, R., Sánchez-Margallo, F. M., Crisóstomo, V., Báez, C., Maestre, J., García-Lindo, M., et al (2016). Intrapericardial administration of mesenchymal stem cells in a large animal model: a bio-distribution analysis. *PLoS ONE* 10, e0122377. doi: 10.1371/journal.pone.0122377

Blázquez, R., Sánchez-Margallo, F. M., Álvarez, V., Usón, A., and Casado, J. G. (2016). Surgical meshes coated with mesenchymal stem cells provide an anti-inflammatory environment by a M2 macrophage polarization. *Acta Biomater.* 31, 221–230. doi: 10.1016/j.actbio.2015.11.057

Blázquez, R., Sánchez-Margallo, F. M., Álvarez, V., Usón, A., Marinaro, F., and Casado, J. G. (2018). Fibrin glue mesh fixation combined with mesenchymal stem cells or exosomes modulates the inflammatory reaction in a murine model of incisional hernia. *Acta Biomater.* 71, 318–329. doi: 10.1016/j.actbio.2018.02.014

Bredikhin, M., Gil, D., Rex, J., Cobb, W., Reukov, V., and Vertegel, A. (2020). Anti-inflammatory coating of hernia repair meshes: a 5-rabbit study. *Hernia* 1–9. doi: 10.1007/s10029-020-02122-9

Calaluce, R., Davis, J. W., Bachman, S. L., Gubin, M. M., Brown, J. A., Magee, J. D., et al. (2013). Incisional hernia recurrence through genomic profiling: a pilot study. *Hernia* 17, 193–202. doi: 10.1007/s10029-012-0923-4

Carbonell, A. M., Warren, J. A., Prabhu, A. S., Ballecer, C. D., Janczyk, R. J., Herrera, J., et al. (2018). Reducing Length of Stay Using a Robotic-assisted Approach for Retromuscular Ventral Hernia Repair: A Comparative Analysis From the Americas Hernia Society Quality Collaborative. *Ann. Surg.* 267, 210–217. doi: 10.1097/SLA.0000000000002244

Casado, J. G., Gomez-Mauricio, G., Alvarez, V., Mijares, J., Tarazona, R., Bernad, A., et al. (2012). Comparative phenotypic and molecular characterization of porcine mesenchymal stem cells from different sources for translational studies in a large animal model. *Vet. Immunol. Immunopathol.* 147, 104–112. doi: 10.1016/j.vetimm.2012.03.015

Casado, J. G., Blazquez, R., Jorge, I., Alvarez, V., Gomez-Mauricio, G., Ortega-Muñoz, M., et al. (2014). Mesenchymal stem cell-coated sutures enhance collagen depositions in sutured tissues. *Wound Repair Regener.* 22, 256–264. doi: 10.1111/wrr.12153

Cheng, H., Zhang, Y., Zhang, B., Cheng, J., Wang, W., Tang, X., et al. (2017). Biocompatibility of polypropylene mesh scaffold with adipose-derived stem cells. *Exp. Ther. Med.* 13, 2922–2926. doi: 10.3892/etm.2017.4338

Clarke, M. R., Imhoff, F. M., and Baird, S. K. (2015). Mesenchymal stem cells inhibit breast cancer cell migration and invasion through secretion of tissue inhibitor of metalloproteinase-1 and -2: MESENCHYMAL STEM CELLS ARE ANTI-TUMORIGENIC. *Mol. Carcinog.* 54, 1214–1219. doi: 10.1002/mc.22178

Crisostomo, V., Casado, J. G., Baez-Diaz, C., Blazquez, R., and Sanchez-Margallo, F. M. (2015). Allogeneic cardiac stem cell administration for acute myocardial infarction. *Expert Rev. Cardiovasc. Ther.* 13, 285–299. doi: 10.1586/14779072.2015.1011621

Darzi, S., Deane, J. A., Nold, C. A., Edwards, S. E., Gough, D. J., Mukherjee, S., et al. (2018). Endometrial Mesenchymal Stem/Stromal Cells Modulate the Macrophage Response to Implanted Polyamide/Gelatin Composite Mesh in Immunocompromised and Immunocompetent Mice. *Sci. Rep.* 8, 6554. doi: 10.1038/s41598-018-24919-6

Dash, B. C., Xu, Z., Lin, L., Koo, A., Ndon, S., Berthiaume, F., et al. (2018). Stem Cells and Engineered Scaffolds for Regenerative Wound Healing. *Bioeng. (Basel)* 5. doi: 10.3390/bioengineering5010023

Debeer, S., Le Luduec, J.-B., Kaiserlian, D., Laurent, P., Nicolas, J.-F., Dubois, B., et al. (2013). Comparative histology and immunohistochemistry of porcine versus human skin. *Eur. J. Dermatol.* 23, 456–466. doi: 10.1684/ejd.2013.2060

Ding, Y., Xu, D., Feng, G., Bushell, A., Muschel, R. J., and Wood, K. J. (2009). Mesenchymal Stem Cells Prevent the Rejection of Fully Allogenic Islet Grafts

by the Immunosuppressive Activity of Matrix Metalloproteinase-2 and -9. *Diabetes* 58, 1797–1806. doi: 10.2337/db09-0317

DiPietro, L. A. (2016). Angiogenesis and wound repair: when enough is enough. *J. Leukoc. Biol.* 100, 979–984. doi: 10.1189/jlb.4MR0316-102R

Dominici, M., Blanc, K. L., Mueller, I., Slaper-Cortenbach, I., Marini, F. C., Krause, D. S., et al (2006). Minimal criteria for defining multipotent mesenchymal stromal cells. The International Society for Cellular Therapy position statement. *Cytotherapy* 8, 315–317. doi: 10.1080/14653240600855905

Edwards, S. L., Ulrich, D., White, J. F., Su, K., Rosamilia, A., Ramshaw, J., et al. (2015). Temporal changes in the biomechanical properties of endometrial mesenchymal stem cell seeded scaffolds in a rat model. *Acta Biomater.* 13, 286–294. doi: 10.1016/j.actbio.2014.10.043

Eker, H. H., Hansson, B. M. E., Buunen, M., Janssen, I. M. C., Pierik, R. E. G. J. M., Hop, W. C., et al. (2013). Laparoscopic vs. open incisional hernia repair: a randomized clinical trial. *JAMA Surg.* 148, 259–263. doi: 10.1001/jamasurg.2013.1466

Emmerson, S., Mukherjee, S., Melendez-Munoz, J., Cousins, F., Edwards, S. L., Karjalainen, P., et al. (2019). Composite mesh design for delivery of autologous mesenchymal stem cells influences mesh integration, exposure and biocompatibility in an ovine model of pelvic organ prolapse. *Biomaterials* 225, 119495. doi: 10.1016/j.biomaterials.2019.119495

Farmer, L., Ayoub, M., Warejcka, D., Southerland, S., Freeman, A., and Solis, M. (1998). Adhesion formation after intraperitoneal and extraperitoneal implantation of polypropylene mesh. *Am. Surg.* 64, 144–146.

Finan, K. R., Kilgore, M. L., and Hawn, M. T. (2009). Open suture versus mesh repair of primary incisional hernias: a cost-utility analysis. *Hernia* 13, 173–182. doi: 10.1007/s10029-008-0462-1

FitzGerald, J., and Kumar, A. (2014). Biologic versus Synthetic Mesh Reinforcement: What are the Pros and Cons? *Clinics Colon Rectal Surg.* 27, 140–148. doi: 10.1055/s-0034-1394155

Fossum, T. W., and Duprey, L. P. (2019). *Small animal surgery. Fifth edition* (Philadelphia, PA: Elsevier). eds.

Gao, Y., Liu, L.-J., Blatnik, J. A., Krpata, D. M., Anderson, J. M., Criss, C. N., et al. (2014). Methodology of fibroblast and mesenchymal stem cell coating of surgical meshes: A pilot analysis: Cell Coating Of Surgical Meshes: A Pilot Analysis. *J. Biomed. Mater. Res.* 102, 797–805. doi: 10.1002/jbm.b.33061

Gerullis, H., Klosterhalfen, B., Borós, M., Lammers, B., Eimer, C., Georgas, E., et al. (2013). IDEAL in meshes for prolapse, urinary incontinence, and hernia repair. *Surg. Innov.* 20, 502–508. doi: 10.1177/1553350612472987

Gerullis, H., Georgas, E., Borós, M., Klosterhalfen, B., Eimer, C., Arndt, C., et al. (2014). Inflammatory reaction as determinant of foreign body reaction is an early and susceptible event after mesh implantation. *BioMed. Res. Int.* 2014, 510807. doi: 10.1155/2014/510807

Gonzalez, L. M., Moeser, A. J., and Blikslager, A. T. (2015). Porcine models of digestive disease: the future of large animal translational research. *Transl. Res.* 166, 12–27. doi: 10.1016/j.trsl.2015.01.004

Grindflek, E., Hansen, M. H. S., Lien, S., and van Son, M. (2018). Genome-wide association study reveals a QTL and strong candidate genes for umbilical hernia in pigs on SSC14. *BMC Genomics* 19, 412. doi: 10.1186/s12864-018-4812-9

Hajibandeh, S., Hajibandeh, S., Sreh, A., Khan, A., Subar, D., and Jones, L. (2017). Laparoscopic versus open umbilical or paraumbilical hernia repair: a systematic review and meta-analysis. *Hernia* 21, 905–916. doi: 10.1007/s10029-017-1683-y

Hansen, S. G., Taskin, M. B., Chen, M., Wogensen, L., Vinge Nygaard, J., and Axelsen, S. M. (2020). Electrospun nanofiber mesh with fibroblast growth factor and stem cells for pelvic floor repair. *J. Biomed. Mater. Res. Part B Appl. Biomater.* 108, 48–55. doi: 10.1002/jbm.b.34364

Henriksen, N. A., Yadete, D. H., Sorensen, L. T., Agren, M. S., and Jorgensen, L. N. (2011). Connective tissue alteration in abdominal wall hernia. *Br. J. Surg.* 98, 210–219. doi: 10.1002/bjs.7339

HerniaSurge Group (2018). International guidelines for groin hernia management. *Hernia* 22, 1–165. doi: 10.1007/s10029-017-1668-x

Hopper, A. N., Jamison, M. H., and Lewis, W. G. (2007). Learning curves in surgical practice. *Postgrad. Med. J.* 83, 777–779. doi: 10.1136/pgmj.2007.057190

Iyyanki, T. S., Dunne, L. W., Zhang, Q., Hubenak, J., Turza, K. C., and Butler, C. E. (2015). Adipose-derived stem-cell-seeded non-cross-linked porcine acellular dermal matrix increases cellular infiltration, vascular infiltration, and mechanical strength of ventral hernia repairs. *Tissue Eng. Part A* 21, 475–485. doi: 10.1089/ten.TEA.2014.0235

Kabat, M., Bobkov, I., Kumar, S., and Grumet, M. (2020). Trends in mesenchymal stem cell clinical trials 2004-2018: Is efficacy optimal in a narrow dose range? *Stem Cells Transl. Med.* 9, 17–27. doi: 10.1002/sctm.19-0202

Karvinen, H., Pasanen, E., Rissanen, T. T., Korpisalo, P., Vähäkangas, E., Jazwa, A., et al. (2011). Long-term VEGF-A expression promotes aberrant angiogenesis and fibrosis in skeletal muscle. *Gene Ther.* 18, 1166–1172. doi: 10.1038/gt.2011.66

Kavic, M. S. (2005). Hernias as a source of abdominal pain: a matter of concern to general surgeons, gynecologists, and urologists. *JSLS* 9, 249–251.

Kemppainen, B. W. (1990). *Methods for skin absorption* (Boca Raton, Fl: CRC Press).

King, A., Balaji, S., Keswani, S. G., and Crombleholme, T. M. (2014). The Role of Stem Cells in Wound Angiogenesis. *Adv. Wound Care (New Rochelle)* 3, 614–625. doi: 10.1089/wound.2013.0497

Klinge, U., and Klosterhalfen, B. (2018). Mesh implants for hernia repair: an update. *Expert Rev. Med. Devices* 15, 735–746. doi: 10.1080/17434440.2018.1529565

Klinge, U., Park, J.-K., and Klosterhalfen, B. (2013). "The ideal mesh?" *Pathobiology* 80, 169–175. doi: 10.1159/000348446

Klinger, A., Kawata, M., Villalobos, M., Jones, R. B., Pike, S., Wu, N., et al. (2016). Living scaffolds: surgical repair using scaffolds seeded with human adipose-derived stem cells. *Hernia* 20, 161–170. doi: 10.1007/s10029-015-1415-0

Klopfleisch, R., and Jung, F. (2017). The pathology of the foreign body reaction against biomaterials. *J. BioMed. Mater. Res. A* 105, 927–940. doi: 10.1002/jbm.a.35958

Ku, C.-H., Johnson, P. H., Batten, P., Sarathchandra, P., Chambers, R. C., Taylor, P. M., et al. (2006). Collagen synthesis by mesenchymal stem cells and aortic valve interstitial cells in response to mechanical stretch. *Cardiovasc. Res.* 71, 548–556. doi: 10.1016/j.cardiores.2006.03.022

Li, Q., Wang, J., Liu, H., Xie, B., and Wei, L. (2013). Tissue-engineered mesh for pelvic floor reconstruction fabricated from silk fibroin scaffold with adipose-derived mesenchymal stem cells. *Cell Tissue Res.* 354, 471–480. doi: 10.1007/s00441-013-1719-2

Li, Y., Meng, H., Liu, Y., and Lee, B. P. (2015). Fibrin Gel as an Injectable Biodegradable Scaffold and Cell Carrier for Tissue Engineering. *Sci. World J.* 2015, 1–10. doi: 10.1155/2015/685690

Liu, Z., Hu, G.-D., Luo, X.-B., Yin, B., Shu, B., Guan, J.-Z., et al. (2017). Potential of bone marrow mesenchymal stem cells in rejuvenation of the aged skin of rats. *Biomed. Rep.* 6, 279–284. doi: 10.3892/br.2017.842

Livak, K. J., and Schmittgen, T. D. (2001). Analysis of relative gene expression data using real-time quantitative PCR and the 2(-Delta Delta C(T)) Method. *Methods* 25, 402–408. doi: 10.1006/meth.2001.1262

López-Cano, M., Martin-Dominguez, L. A., Pereira, J. A., Armengol-Carrasco, M., and García-Alamino, J. M. (2018). Balancing mesh-related complications and benefits in primary ventral and incisional hernia surgery. A meta-analysis and trial sequential analysis. *PloS One* 13, e0197813. doi: 10.1371/journal.pone.0197813

Majumder, A., Neupane, R., and Novitsky, Y. W. (2015). Antibiotic Coating of Hernia Meshes: The Next Step Toward Preventing Mesh Infection. *Surg. Technol. Int.* 27, 147–153.

Marinaro, F., Sánchez-Margallo, F. M., Álvarez, V., López, E., Tarazona, R., Brun, M. V., et al. (2019). Meshes in a mess: Mesenchymal stem cell-based therapies for soft tissue reinforcement. *Acta Biomater.* 85, 60–74. doi: 10.1016/j.actbio.2018.11.042

Melman, L., Jenkins, E. D., Hamilton, N. A., Bender, L. C., Brodt, M. D., Deeken, C. R., et al. (2011). Early biocompatibility of crosslinked and non-crosslinked biologic meshes in a porcine model of ventral hernia repair. *Hernia* 15, 157–164. doi: 10.1007/s10029-010-0770-0

Mok, P. L., Cheong, S. K., and Leong, C. F. (2008). In-vitro differentiation study on isolated human mesenchymal stem cells. *Malays J. Pathol.* 30, 11–19.

Mukherjee, S., Darzi, S., Paul, K., Cousins, F. L., Werkmeister, J. A., and Gargett, C. E. (2020). Electrospun Nanofiber Meshes With Endometrial MSCs Modulate Foreign Body Response by Increased Angiogenesis, Matrix Synthesis, and Anti-Inflammatory Gene Expression in Mice: Implication in Pelvic Floor. *Front. Pharmacol.* 11, 353. doi: 10.3389/fphar.2020.00353

Mushahary, D., Spittler, A., Kasper, C., Weber, V., and Charwat, V. (2018). Isolation, cultivation, and characterization of human mesenchymal stem cells: hMSC. *Cytometry* 93, 19–31. doi: 10.1002/cyto.a.23242

Palini, G. M., Morganti, L., Paratore, F., Coccolini, F., Crescentini, G., Nardi, M., et al. (2017). Challenging abdominal incisional hernia repaired with platelet-rich plasma and bone marrow-derived mesenchymal stromal cells. A case report. *Int. J. Surg. Case Rep.* 37, 145–148. doi: 10.1016/j.ijscr.2017.06.005

Paul, K., Darzi, S., McPhee, G., Del Borgo, M. P., Werkmeister, J. A., Gargett, C. E., et al. (2019). 3D bioprinted endometrial stem cells on melt electrospun poly ϵ-caprolactone mesh for pelvic floor application promote anti-inflammatory responses in mice. *Acta Biomater.* 97, 162–176. doi: 10.1016/j.actbio.2019.08.003

Pittenger, M. F. (1999). Multilineage Potential of Adult Human Mesenchymal Stem Cells. *Science* 284, 143–147. doi: 10.1126/science.284.5411.143

Prudente, A., Favaro, W. J., Latuf, P., and Riccetto, C. L. Z. (2016). Host inflammatory response to polypropylene implants: insights from a quantitative immunohistochemical and birefringence analysis in a rat subcutaneous model. *Int. Braz. J. Urol.* 42, 585–593. doi: 10.1590/S1677-5538.IBJU.2015.0289

Pulikkottil, B. J., Pezeshk, R. A., Daniali, L. N., Bailey, S. H., Mapula, S., and Hoxworth, R. E. (2015). Lateral Abdominal Wall Defects: The Importance of Anatomy and Technique for a Successful Repair. *Plast. Reconstr. Surg. Glob. Open* 3, e481. doi: 10.1097/GOX.0000000000000439

Rajabzadeh, N., Fathi, E., and Farahzadi, R. (2019). Stem cell-based regenerative medicine. *Stem Cell Invest.* 6:19. doi: 10.21037/sci.2019.06.04

Rastegarpour, A., Cheung, M., Vardhan, M., Ibrahim, M. M., Butler, C. E., and Levinson, H. (2016). Surgical mesh for ventral incisional hernia repairs: Understanding mesh design. *Plast. Surg. (Oakv)* 24, 41–50. doi: 10.4172/plastic-surgery.1000955

Reisman, M., and Adams, K. T. (2014). Stem cell therapy: a look at current research, regulations, and remaining hurdles. *P T* 39, 846–857.

Sánchez, A., Schimmang, T., and García-Sancho, J. (2012). Cell and tissue therapy in regenerative medicine. *Adv. Exp. Med. Biol.* 741, 89–102. doi: 10.1007/978-1-4614-2098-9_7

Schook, L. B., Collares, T. V., Darfour-Oduro, K. A., De, A. K., Rund, L. A., Schachtschneider, K. M., et al. (2015). Unraveling the Swine Genome: Implications for Human Health. *Annu. Rev. Anim. Biosci.* 3, 219–244. doi: 10.1146/annurev-animal-022114-110815

Su, K., Edwards, S. L., Tan, K. S., White, J. F., Kandel, S., Ramshaw, J. A. M., et al. (2014). Induction of endometrial mesenchymal stem cells into tissue-forming cells suitable for fascial repair. *Acta Biomater.* 10, 5012–5020. doi: 10.1016/j.actbio.2014.08.031

Trounson, A., and McDonald, C. (2015). Stem Cell Therapies in Clinical Trials: Progress and Challenges. *Cell Stem Cell* 17, 11–22. doi: 10.1016/j.stem.2015.06.007

Uccelli, A., Moretta, L., and Pistoia, V. (2008). Mesenchymal stem cells in health and disease. *Nat. Rev. Immunol.* 8, 726–736. doi: 10.1038/nri2395

Ulrich, D., Edwards, S. L., Su, K., Tan, K. S., White, J. F., Ramshaw, J. A. M., et al. (2014). Human endometrial mesenchymal stem cells modulate the tissue response and mechanical behavior of polyamide mesh implants for pelvic organ prolapse repair. *Tissue Eng. Part A* 20, 785–798. doi: 10.1089/ten.TEA.2013.0170

van Steenberghe, M., Schubert, T., Guiot, Y., Goebbels, R. M., and Gianello, P. (2017). Improvement of mesh recolonization in abdominal wall reconstruction with adipose vs. bone marrow mesenchymal stem cells in a rodent model. *J. Pediatr. Surg.* 52, 1355–1362. doi: 10.1016/j.jpedsurg.2016.11.041

Van Veenendaal, N., Poelman, M., and Bonjer, J. (2015). Controversies in laparoscopic ventral hernia repair. *Minerva Chir.* 70, 481–492.

Vogels, R. R. M., Kaufmann, R., van den Hil, L. C. L., van Steensel, S., Schreinemacher, M. H. F., Lange, J. F., et al. (2017). Critical overview of all available animal models for abdominal wall hernia research. *Hernia* 21, 667–675. doi: 10.1007/s10029-017-1605-z

Vorst, A. L., Kaoutzanis, C., Carbonell, A. M., and Franz, M. G. (2015). Evolution and advances in laparoscopic ventral and incisional hernia repair. *World J. Gastrointest. Surg.* 7, 293–305. doi: 10.4240/wjgs.v7.i11.293

Vozzi, F., Guerrazzi, I., Campolo, J., Cozzi, L., Comelli, L., Cecchettini, A., et al. (2017). Biological and proteomic characterization of a composite mesh for abdominal wall hernia treatment: Reference Study: Cell response to not absorbable polypropylene composite mesh. *J. Biomed. Mater. Res.* 105, 2045–2052. doi: 10.1002/jbm.b.33749

Wales, E., and Holloway, S. (2019). The use of prosthetic mesh for abdominal wall repairs: A semi-systematic-literature review. *Int. Wound J.* 16, 30–40. doi: 10.1111/iwj.12977

Wei, J. C. J., Edwards, G. A., Martin, D. J., Huang, H., Crichton, M. L., and Kendall, M. A. F. (2017). Allometric scaling of skin thickness, elasticity, viscoelasticity to mass for micro-medical device translation: from mice, rats, rabbits, pigs to humans. *Sci. Rep.* 7, 15885. doi: 10.1038/s41598-017-15830-7

Yan, L., Zheng, D., and Xu, R.-H. (2018). Critical Role of Tumor Necrosis Factor Signaling in Mesenchymal Stem Cell-Based Therapy for Autoimmune and Inflammatory Diseases. *Front. Immunol.* 9, 1658. doi: 10.3389/fimmu.2018.01658

Yun, J., Olkkola, S., Hänninen, M.-L., Oliviero, C., and Heinonen, M. (2017). The effects of amoxicillin treatment of newborn piglets on the prevalence of hernias and abscesses, growth and ampicillin resistance of intestinal coliform bacteria in weaned pigs. *PloS One* 12, e0172150. doi: 10.1371/journal.pone.0172150

Zhang, K., Guo, X., Li, Y., Fu, Q., Mo, X., Nelson, K., et al. (2016). Electrospun nanoyarn seeded with myoblasts induced from placental stem cells for the application of stress urinary incontinence sling: An in vitro study. *Colloids Surf. B Biointerf.* 144, 21–32. doi: 10.1016/j.colsurfb.2016.03.083

Zhao, Y., Zhang, Z., Wang, J., Yin, P., Zhou, J., Zhen, M., et al. (2012). Abdominal hernia repair with a decellularized dermal scaffold seeded with autologous bone marrow-derived mesenchymal stem cells. *Artif. Organs* 36, 247–255. doi: 10.1111/j.1525-1594.2011.01343.x

**Conflict of Interest:** The authors declare that the research was conducted in the absence of any commercial or financial relationships that could be construed as a potential conflict of interest.

*Copyright © 2020 Marinaro, Casado, Blázquez, Brun, Marcos, Santos, Duque, López, Álvarez, Usón and Sánchez-Margallo. This is an open-access article distributed under the terms of the Creative Commons Attribution License (CC BY). The use, distribution or reproduction in other forums is permitted, provided the original author(s) and the copyright owner(s) are credited and that the original publication in this journal is cited, in accordance with accepted academic practice. No use, distribution or reproduction is permitted which does not comply with these terms.*

López et al. BMC Veterinary Research (2019) 15:91
https://doi.org/10.1186/s12917-019-1837-5

BMC Veterinary Research

RESEARCH ARTICLE Open Access

# Identification of very early inflammatory markers in a porcine myocardial infarction model

Esther López[1], Francisco Miguel Sánchez-Margallo[1,2*], Verónica Álvarez[1], Rebeca Blázquez[1,2], Federica Marinaro[1], Ana Abad[1], Helena Martín[1], Claudia Báez[1,2], Virginia Blanco[1,2], Verónica Crisóstomo[1,2] and Javier García Casado[1,2]

## Abstract

**Background:** Acute myocardial infarction (AMI) is one of the most deleterious conditions leading to cardiovascular diseases and mortality. The importance of an early and accurate diagnosis assures immediate medical treatments, which are fundamental to reduce mortality and improve prognoses. AMI is associated to an inflammatory response which includes the increase of circulating inflammatory cytokines, chemokines and immune cell activation. This study aimed to identify which are the very early immune-related biomarkers that may be used as predictors of myocardial infarction severity. In order to mimic the pathophysiological events involved in human myocardial infarction, a temporary occlusion (90 min) of the mid-left anterior descending coronary artery was performed in a swine animal model.

**Results:** Lymphocyte subsets analysis in peripheral blood revealed significant alterations in CD4+/CD8+ ratio and naïve and effector/memory T cell percentages at 1 h post-myocardial infarction. Changes in TH1/TH2-related cytokine, monocyte and neutrophil markers gene expression were observed in peripheral blood lymphocytes, as well. Additionally, significant correlations between cardiac parameters (cardiac enzymes, left ventricular ejection fraction and % infarct) and blood-derived parameters (cytokine expression and lymphocyte subset distribution) were found.

**Conclusions:** Peripheral blood lymphocyte alterations are easily and swiftly detectable, so they may be good biomarkers for a very early prognosis and to predict myocardial infarction severity.

**Keywords:** Acute myocardial infarction, Porcine model, Early biomarkers

## Background

Acute myocardial infarction (AMI) is one of the main death causes in the world. Only in the United States, over 795,000 myocardial infarctions occur each year [1]. Consequently, an early and accurate diagnosis would guarantee immediate medical intervention, leading to reduced mortality and improved AMI prognosis.

Myocardial infarction results from the occlusion of a coronary artery and the subsequent myocardial ischemia. The generated ischemia results in cell death, initiating an inflammatory response ultimately resulting in scar formation [2]. During the inflammatory phase, chemokine and cytokine cascades activation results in leukocytes recruitment into the infarcted area. While neutrophils and macrophages are involved in removing dead cells and matrix debris from the wound site, activated macrophages release cytokines and growth factors, leading to granulation tissue formation [3]. These events, therefore, may be used as predictive biomarkers for early myocardial infarction detection.

Preclinical studies in cardiovascular research are necessary for the translation of basic research to the clinic. Animal models are widely used in the research of cardiovascular disease pathogenesis and drug therapy [4]. Swine are reliable animal models in the field of cardiovascular diseases, due to their similarity in cardiac

* Correspondence: msanchez@ccmijesususon.com
[1]Stem Cell Therapy Unit, Jesús Usón Minimally Invasive Surgery Centre, 10071 Cáceres, Spain
[2]CIBER de Enfermedades Cardiovasculares, 28029 Madrid, Spain

© The Author(s). 2019 **Open Access** This article is distributed under the terms of the Creative Commons Attribution 4.0 International License (http://creativecommons.org/licenses/by/4.0/), which permits unrestricted use, distribution, and reproduction in any medium, provided you give appropriate credit to the original author(s) and the source, provide a link to the Creative Commons license, and indicate if changes were made. The Creative Commons Public Domain Dedication waiver (http://creativecommons.org/publicdomain/zero/1.0/) applies to the data made available in this article, unless otherwise stated.

function and anatomy with the human heart. As a matter of fact, cardiomyocyte metabolism, electrophysiological properties and response to an ischemic insult, such as AMI, have been reported to be closely similar to the human [5]. Among all the different surgical procedures developed to mimic acute or chronic myocardial infarction, minimally invasive approaches, like the closed-chest model, have been successfully developed using different coronary occlusion times [6]. The standardized endovascular model of 90 min balloon occlusion exhibits great similarities with AMI in humans [7].

Several evaluation methods and follow up procedures have been established for the swine myocardial infarction model. Biomarker tests combined with electrocardiographic analysis are the most used procedures for AMI diagnosis. Moreover, echocardiography and cardiac magnetic resonance imaging are commonly performed for the non-invasive detection of myocardial and scar mass, left ventricular volumes, geometric remodelling, scar reduction, contractility, myocardial perfusion and viable myocardial mass regeneration. On the other hand, cardiac enzymes can be detected in plasma at 4–6 h post-infarction and are the currently preferred diagnosis biomarkers for AMI [8]. The aim of this study was to identify the most significant alterations occurring during the very early phase of AMI in terms of cytokine expression and lymphocyte subset distribution in peripheral blood. So, tracing the first symptoms, together with detecting some biological biomarkers, could be useful to predict and monitor the pathogenic process of AMI. Here we propose some easily and rapidly accessible immunological markers that could provide early information for the diagnosis of AMI.

## Results

### Phenotypic analysis of peripheral blood lymphocytes

The phenotypic analysis of peripheral blood lymphocytes (PBLs) in the animal model was analyzed by flow cytometry before and 1 h after myocardial infarction model creation. Statistically significant differences were found in peripheral blood T-cell subsets. The percentage of CD4+ T cells (gated as CD4+ CD8–) was significantly increased, while CD8+ T cells (gated CD4- CD8+) percentage decreased 1 h after myocardial infarction, in comparison to pre-AMI levels. Consequently, the CD4/CD8 ratio was significantly raised at 1 h after model creation. No statistically significant difference was found in NK cells (gated as CD3- CD8- CD4- CD16+) percentage (Fig. 1a).

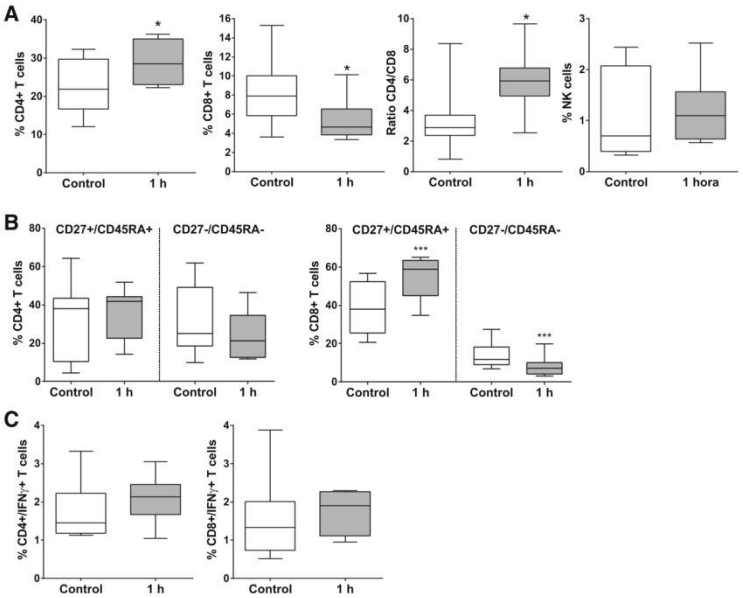


**Fig. 1** Lymphocyte subsets distribution in peripheral blood. Peripheral blood lymphocytes were isolated from blood samples collected before acute myocardial infarction model creation (control) and 1 h after it. The blood lymphocytes subsets (**a**). differentiation/activation T cell subsets (**b**) and IFNγ+ cells (**c**) were analyzed by flow cytometry. Paired comparisons were performed using a Student t-test for parametric data. Graphs show the mean ± SD (n = 11) of subpopulation subsets. * ≤ 0.05. ** ≤ 0.01. *** ≤ 0.001

A deep analysis of activation/differentiation markers was also performed on CD4+ and CD8+ T cell subsets. CD45RA and CD27 co-expression was analyzed on peripheral lymphocytes and the percentages of naïve T cells (CD45RA+ CD27+) and effector/memory T cells (CD45RA−CD27−) were compared before and 1 h after myocardial infarction. No significant changes were observed in CD4+ T cells. Nevertheless, the percentage of CD8+ naïve T cells and CD8+ effector/memory T cells exhibited substantial statistically significant differences ($p<0.001$). While the CD8+ naïve T cell subsets significantly increased 1 h after myocardial infarction, the CD8 + effector/memory T cell subsets had a substantial decrease (Fig. 1b). Interferon γ (IFNγ) + T cells did not suffer significant changes 1 h after myocardial infarction, when compared to the control (Fig. 1c).

### Gene expression analysis of peripheral blood lymphocytes

Cytokines and soluble factors gene expression of PBLs was evaluated by qPCR. The transcriptional analysis revealed that the most studied TH1-related cytokines (Interleukin (IL)2, IFNγ, Tumor Necrosis Factor α (TNFα), IL12) decreased 1 h after myocardial infarction, but only IFNγ showed significant differences ($p<0.01$) (Fig. 2a). Regarding TH2-related cytokines, only IL4 gene expression changed significantly, showing a decrease 1 h after AMI (Fig. 2b).

Markers related with monocytes and neutrophils were also evaluated in this study. Among monocyte-related markers, a significant increase in Arg-1 was found (Fig. 2c). Surprisingly, gene expression of CELA and BPI (neutrophil markers), was significantly decreased at 1 h post-infarction (Fig. 2d).

### Cardiac function parameters and cardiac enzymes in myocardial infarction animal model

Myocardial infarction was successfully induced in all animals. A significant increase of cardiac enzymes (Creatine kinase-myocardial band (CK-MB) and Troponin I) was found at 24 h when compared to baseline levels. Cardiac Magnetic Resonance at day 7 after myocardial

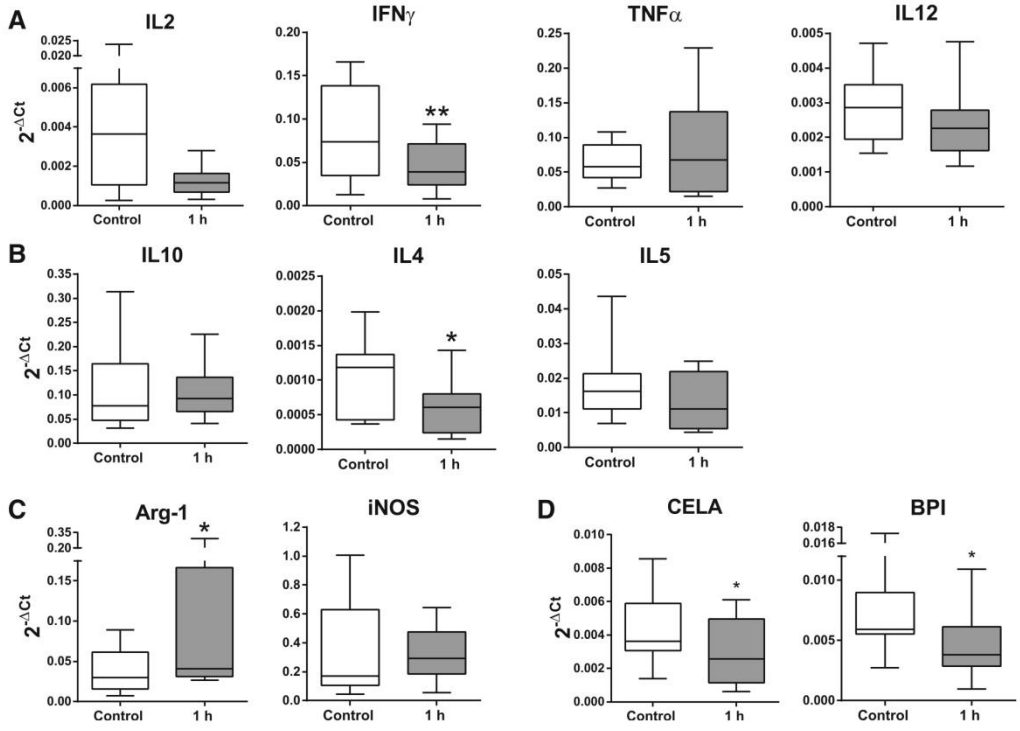


**Fig. 2** Cytokines gene expression in peripheral blood lymphocytes. TH1-related cytokines (**a**). TH2-related cytokines (**b**). monocyte markers (**c**) and neutrophil markers (**d**) were analyzed by qPCR. using GAPDH as a reference gene. Data were compared between control and 1 h after myocardial infarction. The statistical analysis was performed using a Student t-test for parametric data. Graphs show the mean ± SD ($n = 11$) of $2^{-\Delta Ct}$. * ≤ 0.05. ** ≤ 0.01

infarct induction showed a significant decrease of Left Ventricular Ejection Fraction (% LVEF) as well as a significant increase of myocardial infarction (Table 1).

### Correlation analysis between cardiac function and blood-derived parameters

Correlation analysis between cardiac parameters (cardiac enzymes, % LVEF, % Infarct) and immunological markers (T cell subsets and gene expression) was performed since it may be useful for the evaluation and follow-up of myocardial infarction in this animal model.

The analysis showed a strong positive correlation between the percentage of CD4+ IFNγ+ T cells 1 h after AMI and the levels of Troponin I at 7 days post-infarction ($r = 0.7847$; $p = 0.0367$) (Fig. 3a). More significant correlations were found between gene expression results and cardiac function parameters. In particular, CK-MB at 7 days and iNOS at 1 h ($r = 0.6660$; $p = 0.0253$) were found to be strongly and positively correlated, as well as CK-MB at 7 days and CELA at 1 h ($r = 0.7074$; $p = 0.0149$). Contrarily, strong negative correlations were identified between Troponin I at 24 h and IL2 at 1 h ($r = -0.6380$; $p = 0.0472$), CK-MB at 7 days and IFNγ at 1 h ($r = -0.6373$; $p = 0.0349$) and % LVEF at 7 d and IL5 at 1 h ($r = -0.6855$; $p = 0.0199$) (Fig. 3b).

## Discussion

An earlier diagnosis of patients with symptoms suggestive of myocardial infarction might possibly reduce their morbidity and mortality. AMI is a life-threatening disorder and its rapid identification is important for the early initiation of appropriate, evidence-based and effective therapy. Diagnosis of AMI is usually based on electrocardiogram data and detection of biomarkers of myocardial injury, like cardiac enzymes. Although troponin assays have a good sensitivity, they have a low specificity due to troponin elevations in the absence of cardiac failure [9]. Consequently, it is necessary to identify early, effective and specific biomarkers for a rapid diagnosis of AMI.

Large animal models, such as swine, are widely accepted for studies of AMI and ischemic cardiomyopathy. They allow the identification of biomarkers under controlled conditions, avoiding the intrinsic variability of clinical studies: atherosclerosis, coronary arterial inflammation, myocardial inflammation and other associated pathologies. The homogeneity and repeatability of using an animal model under controlled conditions could also be considered a limitation because AMI in human medicine is frequently associated with risk factors and comorbidities (i.e. smoking, hypertension, diabetes or obesity).

AMI is defined as myocardial necrosis after a marked ischemia. Tissue injury generates endogenous signals that activate the innate immune system. The immune cells identify these signals and induce molecular pathways that lead to the recruitment of inflammatory cells in the healing infarct [10]. Our results have demonstrated that, 1 h after myocardial infarction, peripheral blood lymphocytes can "identify" these alarms showing alterations in lymphocyte subsets and cytokine expression.

More precisely, we have found that the ratio CD4+/CD8+ T cells increases due to an increase of percentage of CD4+ T cells and a decrease of CD8+ T cells. These findings are consistent with the results found in AMI patients diagnosed no more than 12 h from the onset of symptoms [11]. In this study, an analogous T cells-related gene expression was observed; however, the

**Table 1** Data of cardiac function in terms of percentage of myocardial infarction and left ventricular ejection fraction and cardiac enzymes blood levels (Troponin I and CK-MB) in μg/l for the different animals

| | Cardiac function | | Troponin I (μg/l) | | | CK-MB (μg/l) | | |
|---|---|---|---|---|---|---|---|---|
| Animal | % Infarct | % LVEF | Control | 24 h | 7 days | Control | 24 h | 7 days |
| #1 | 18 | 30 | 0 | 26 | 0.2 | 3.3 | 9.7 | 3 |
| #2 | 24 | 38 | 0.018 | 18 | 0.8 | 2.2 | 7.9 | 3.5 |
| #3 | 25 | 34 | 0.037 | 31 | 0.71 | 3.7 | 26 | 2.7 |
| #4 | 28 | 22 | 0.071 | 22 | 0.29 | 5.5 | 15 | 4.4 |
| #5 | 20 | 17 | 0.022 | 41 | 0.66 | 4.4 | 20 | 4.4 |
| #6 | 25 | 26 | 0.017 | 18 | 0.13 | 4.3 | 19 | 3.4 |
| #7 | 16 | 24 | 0.027 | 23 | 0.28 | 3 | 14 | 4.1 |
| #8 | 23 | 18 | 0 | 17 | 0.039 | 2.8 | 6.6 | 2.3 |
| #9 | 25 | 18 | 0 | 29 | 0.69 | 5.1 | 6.8 | 3.1 |
| #10 | 26 | 14 | 0.024 | 52 | 0.71 | 2 | 6 | 2 |
| #11 | 25 | 27 | 0 | 36 | 1.4 | 2.1 | 10 | 2 |
| #12 | 20 | 19 | 0.013 | 44 | 0.78 | 2.6 | 21 | 4.5 |

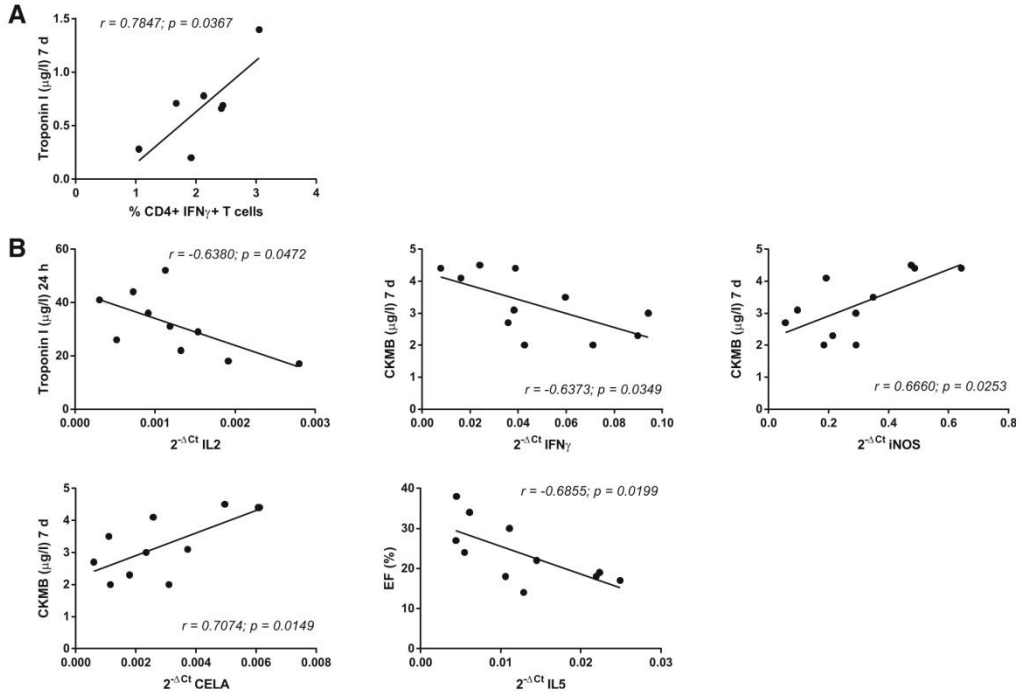


**Fig. 3** Correlation analysis between cardiac function parameters (cardiac enzymes. Left ventricular ejection fraction) and blood-derived parameters. Correlations were calculated using the Pearson coefficient correlation. Graphs show significant correlations observed between cardiac function parameters (blood levels of cardiac enzymes and percentage of left ventricular ejection fraction) and blood-derived parameters (lymphocytes subsets (**a**) and cytokine gene expression (**b**))

number of NK cells was reported as significantly decreased, while, in our animal model, NK cell subpopulations seemed not to be affected in the early stage of AMI.

Regarding lymphocyte differentiation/activation status, an increase in naïve T cells (CD8+ CD45+ CD27+) and a decrease in the effector/memory T cells (CD8+ CD45- CD27-) could be detected at 1 h post-infarction. The loss in peripheral blood CD8+ memory T-cell subsets may be caused by entrapment in the coronary microcirculation early after the onset of reperfusion, as shown in myocardial infarction patients [12]. Moreover, Emoto and cols. Related the regulatory T cells/effector T cells ratio with the pathophysiology of coronary atherosclerosis, suggesting that this ratio could be a useful marker for the evaluation of severity of atherosclerosis [13].

Cytokines are secreted as cellular signalling proteins that can mediate effector and regulatory effects on the immune response playing an essential role during T cell differentiation. Cytokine levels have been used as biomarkers for the diagnosis of multiple diseases such as rheumatoid arthritis [14], multiple sclerosis [15] or liver toxicity [16]. In this study, we have demonstrated that the gene expression of cytokines produced by Th1 lymphocytes (IFNγ) and Th2 lymphocytes (IL4) was altered at 1 h post-infarction. Clinical studies have demonstrated that both cytokines have a diagnostic value of success of percutaneous coronary intervention in patients with AMI [17].

Regarding peripheral blood monocytes, these cells migrate to the site of injure and infiltrate as macrophages. Using the coronary ligation technique in mice, it was observed that a large proportion of these newly recruited monocytes were provided by the spleen, increasing the blood monocytes before the recruitment into infarcted cardiac tissue [18]. This theory may explain, at least in part, the increased expression of Arg-1 in our animal model. Neutrophils are also used as predictive cells in coronary heart diseases [19] and their specific marker, myeloperoxidase (MPO), is reliable when used for discriminating AMI patients [20]. Our results have demonstrated a deficient expression of neutrophil marker BPI

which, together with Arg-1, IFNγ and IL4, could contribute to the diagnosis and prognosis of AMI.

Additionally, in order to correlate lymphocyte subset distribution and gene expression levels with "classical" cardiac parameters, a correlation analysis was performed with the data from cardiac magnetic resonance imaging (% LVEF and Infarct area) and cardiac enzymes (Troponin I and CK-MB). In our analysis, serum Troponin I levels at 7 days post-infarction showed a positive correlation with CD4 + IFNγ+ lymphocytes, suggesting that patients with a high percentage of CD4 + IFNγ+ lymphocytes at 1 h post-infarction may have higher circulating Troponin I levels at 7 days. The correlation between IL2 and Troponin I levels indicates that a low expression level of IL2 at 1 h after infarction could be associated with a higher Troponin I level at 24 h. On the other hand, IFNγ, iNOS and CELA expression levels were also related with the serum levels of CK-MB at 7 days. Additionally, high expression levels of IL5 detected at 1 h post-infarction could be associated with a lower % LVEF at 7 days in patients.

## Conclusions

Although it is well known that cardiac enzymes are relevant and predictive biomarkers for the diagnosis of AMI, our swine myocardial infarction model -performed under controlled conditions- suggests that early inflammatory biomarkers may be useful in the follow-up of patients who have suffered an AMI. These biomarkers are easily and swiftly detectable, which means they could be candidates for early prognosis, predicting the severity of myocardial infarction in a clinical scenario. It is important to note that the usefulness of these biomarkers in AMI patients with concomitant immune-mediated diseases may be compromised, since immune biomarkers may be masked in patients with pre-existing immune disorders.

## Methods

### Animals and experimental design

Young female Large White pigs ($n = 12$) weighting 30–35 kg at the beginning of the study, were used for all experimental procedures. These animals were provided and housed by the Animal facility of the Jesús Usón Minimally Invasive Surgery Centre. At the end of experiments all animals were euthanatized by intravenous administration of 2 mmol/kg of potassium chloride. All experimental protocols were approved by the Ethics Committee on Animal Experiments of the Jesús Usón Minimally Invasive Surgery Centre, in accordance with the recommendations outlined by the local government (Junta de Extremadura) and the Directive 2010/63/EU of the European Parliament on the protection of animals used for scientific purposes.

### Myocardial infarction model creation

A closed chest reperfused myocardial infarction was created in the operating theaters of the Jesús Usón Minimally Invasive Surgery Centre as previously described [21]. Briefly, anesthetized animals were subjected to a percutaneous femoral access using a 7 Fr Introducer sheath (Terumo, Tokyo, Japan). A Hockey Stick 6 Fr guiding catheter (Mach 1, Boston Scientific Corporation, Natick, MA, USA) was navigated under fluoroscopic guidance to the origin of the left coronary artery. Coronary angiograms were obtained in the 40° left anterior oblique projection to better demonstrate the length of the left anterior descending artery. Subsequently, a coronary balloon catheter (typically 3 mm × 8 mm, Ryujin Plus, Terumo, Tokio, Japan) was inserted over a 0.014″ coronary guidewire and advanced to below the origin of the first diagonal branch, where it was inflated to occlude blood flow to the distal myocardium. Occlusion was maintained for 90 min to assure infarct creation. Upon balloon deflation, the coronary artery was checked for patency by repeating the angiogram. During the procedure, animals were fully monitored, including blood pressure, electrocardiogram, $O_2$ saturation, and end tidal $CO_2$ determinations. Continuous infusion of lidocaine at a rate of 1 mg/kg/h (Lidocaine, Braun Medical, Barcelona, Spain) was used throughout the procedure. Systemic heparin (Heparina Rovi 5%, Laboratorios farmacéuticos Rovi, Madrid, Spain) was intravenously injected (150 UI/kg) prior to percutaneous sheath placement.

### Phenotypic characterization of peripheral blood lymphocytes

Blood samples were drawn by puncture of the cranial vena cava before myocardial infarct induction and 1 h after the balloon deflation and collected in EDTA containing tubes for further analysis.

The PBLs were isolated by centrifugation over Histopaque-1077 (Sigma, St. Louis, MO). $1 \times 10^6$ PBLs were stained with fluorescent-labeled monoclonal antibodies against extracellular porcine CD4, CD8α, CD14, CD16, CD27, CD45RA, CD56 and SLAII (AbD Serotec, Kidlington, United Kingdom). For the detection of intracellular antigen IFNγ, PBLs were fixed and permeabilized using Fix&Perm (Life technologies, Thermo Fisher Scientific Inc., Waltham, MA USA) and stained with the appropriate antibody (AbD Serotec). The cells were washed and re-suspended in PBS.

Flow cytometric analysis was performed in a FACScalibur cytometer (BD Biosciences, San Jose, CA, USA) after acquisition of $10^5$ events. Cells were primarily selected using forward and side scatter characteristics and fluorescence was analyzed using CellQuest software (BD

Biosciences). Appropriate isotype-matched negative control antibodies were used in all the experiments.

### Gene expression analysis

For transcriptional analysis studies, total RNA from isolated lymphocytes was extracted and purified by using the mirVana miRNA Isolation Kit (Life technologies, Thermo Fisher Scientific Inc.), following the manufacturer's instructions. RNA quality was evaluated through spectrophotometry and cDNA was synthesized from 1 μg of RNA in reverse transcription reaction with the iScript Reverse Transcription Supermix (BioRad, Hercules, California, USA). qPCR was performed with commercial gene expression assays (Life Technologies, Thermo Fisher Scientific Inc.) (Table 2), using TaqMan Fast Advance Master Mix in a QuantStudio 3 System (Applied Biosystems, Thermo Fisher Scientific). The qPCR products were quantified by fluorescent method using the $2^{-\Delta Ct}$ expression. Duplicates of all samples were analyzed separately and normalized using GAPDH as a reference gene.

### Cardiac magnetic resonance

Cardiac Magnetic Resonance studies (Intera 1.5 T, Philips Medical Systems. Best, The Netherlands) were performed at day 7 post-infarction. Retrospective cardiac triggering was used. A 4 elements phase array coil was placed around the animals' chest. Images were acquired in the intrinsic cardiac planes: short axis, vertical long axis and horizontal long axis views. In order to measure left ventricular function and mass breath hold gradient, echo cine images were obtained over the entire left ventricle. For infarct size measurements, short axis images were acquired 5 to 15 min after the injection of 0.2 mmol/kg of a gadolinium-based contrast agent (Gadobutrol. Gadovist 1.1 mmol/l, Bayer Schering Pharma AG, Berlin, Germany) using a breath-hold 3D gradient-echo inversion-recovery sequence.

**Table 2** Gene and commercial references from gene expression assays

| Gene | Life Techonologies Assay ID |
|---|---|
| IL-2 | Ss03392428_m1 |
| IFN-γ | Ss03391054_m1 |
| TNF-α | Ss03391318_g1 |
| IL-12A | Ss03391176_m1 |
| IL-10 | Ss03382372_u1 |
| IL-4 | Ss03394125_m1 |
| IL-5 | Ss03394369_m1 |
| FOXP3 | Ss03376695_u1 |
| Nos2 | Ss03374608_u1 |
| Arg1 | Ss03391394_m1 |
| CELA1 | Ss03392393_m1 |
| BPI | Ss04321426_m1 |
| GAPDH | Ss03375629_u1 |

### Statistical analysis

Data were statistically analyzed with SPSS-21 software (SPSS, Chicago, IL, USA). Normality was assessed using a Shapiro-Wilk test. Paired comparisons were performed using a Student t-test for parametric data or Wilcoxon sign test for non-parametric data. Correlations were calculated using the Pearson coefficient correlation and "r" value was interpreted as follows: – 1.0 to – 0.5 or 0.5 to 1.0: Strong correlation, – 0.5 to – 0.3 or 0.3 to 0.5: Moderate correlation, – 0.3 to – 0.1 or 0.1 to 0.3: Weak correlation, – 0.1 to 0.1: None or very weak correlation. All *p*-values ≤0.05 were considered statistically significant.

#### Abbreviations

AMI: Acute myocardial infarction; CK-MB: Creatine kinase-myocardial band; IFNγ: Interferon γ; IL: Interleukin; LVEF: Left ventricular ejection fraction; PBLs: Peripheral blood lymphocytes; TNFα: Tumor Necrosis Factor α

#### Acknowledgements

Thanks to all people of ICTS Nanbiosis specially, Clinical test lab, animal housing, experimental operating room and medical imaging technicians.

#### Funding

This work was supported in part by CIBER-CV (CB16/11/00494 to F.M.S.M.). One grant from Junta de Extremadura (Ayuda a grupos catalogados de la Junta de Extremadura, GR15175). Two grants from Junta de Extremadura (IB16168 to J.G.C) and (IB16201 to V.C.) co-funded by FEDER/FSE. Four grants from ISCIII (CP17/00021, MS17/00021 and PI18/0911 to JGC) and (PI16/01172 to V.C.) co-funded by FEDER/FSE, "Investing in your future". One predoctoral grant from Grupo Jorge-Mafresa to F.M. Experimental studies have been conducted by the ICTS "NANBIOSIS", in the Units 14, 21, 22 and 24 of the CCMIJU. The funders had no role in study design, data collection, interpretation and analysis, decision to publish or preparation of the manuscript.

#### Availability of data and materials

The datasets used and/or analysed during the current study are available from the corresponding author on reasonable request.

#### Authors' contributions

E.L. contributed as first author. E.L., R.B., F.M.S.M. and J.G.C. conceived and designed the experiments. R.B., F.M.S.M., V.A., C.B., V.B., J.M., B.M., E.L., F.M., V.C., H.M., A.A. and J.G.C. performed the experiments and analyzed the data. E.L., R.B., F.M.S.M. and J.G.C. wrote the manuscript. All authors read and approved the final manuscript.

#### Ethics approval and consent to participate

All experimental protocols were approved by the Ethics Committee on Animal Experiments of Jesús Usón Minimally Invasive Surgery Centre, in accordance with the recommendations outlined by the local government (Junta de Extremadura) and the Directive 2010/63/EU of the European Parliament on the protection of animals used for scientific purposes. Verbal informed consent was obtained from all the participants for publication of this manuscript.

#### Consent for publication

Not applicable.

#### Competing interests

The authors declare that they have no competing interests.

## Publisher's Note

Springer Nature remains neutral with regard to jurisdictional claims in published maps and institutional affiliations.

Received: 20 November 2018 Accepted: 5 March 2019
Published online: 12 March 2019

### References

1. Benjamin EJ, Blaha MJ, Chiuve SE, Cushman M, Das SR, Deo R, et al. Heart disease and stroke statistics—2017 update: a report from the American Heart Association. Circulation. 2017;135(10):e146–603.
2. Frangogiannis NG. The mechanistic basis of infarct healing. Antioxid Redox Signal. 2006;8(11–12):1907–39.
3. van Zuylen V, den Haan MC, Geutskens SB, Roelofs H, Fibbe WE, Schalij MJ, et al. Post-myocardial infarct inflammation and the potential role of cell therapy. Cardiovasc Drugs Ther. 2015;29(1):59–73.
4. Chen Y, Shao D-B, Zhang F-X, Zhang J, Yuan W, Man Y-L, et al. Establishment and evaluation of a swine model of acute myocardial infarction and reperfusion–ventricular fibrillation–cardiac arrest using the interventional technique. J Chin Med Assoc. 2013;76(9):491–6.
5. Heusch G, Skyschally A, Schulz R. The in-situ pig heart with regional ischemia/reperfusion — ready for translation. J Mol Cell Cardiol. 2011;50(6):951–63.
6. McCall FC, Telukuntla KS, Karantalis V, Suncion VY, Heldman AW, Mushtaq M, et al. Myocardial infarction and intramyocardial injection models in swine. Nat Protoc. 2012;7(8):1479–96.
7. Koudstaal S, Jansen of Lorkeers S, Gho JMIH, van Hout GP., Jansen MS, Gründeman PF, et al. Myocardial Infarction and Functional Outcome Assessment in Pigs. J Vis Exp [Internet]. 2014 Apr 25 [cited 2018 Sep 10];(86). Available from: http://www.jove.com/video/51269/myocardial-infarction-and-functional-outcome-assessment-in-pigs
8. Babuin L, Jaffe AS. Troponin: the biomarker of choice for the detection of cardiac injury. CMAJ Can Med Assoc J. 2005;173(10):1191–202.
9. Čolak T, Mikulić I, Landeka K, Sesar A, Vranješ M, Mikulić I. Predictive value of high sensitive troponin I assay in acute coronary syndrome compared to classic biochemical markers. Psychiatr Danub. 2017 Suppl 4(Suppl 4):823–829.
10. Frangogiannis NG. The inflammatory response in myocardial injury, repair, and remodelling. Nat Rev Cardiol. 2014;11(5):255–65.
11. Yan W, Song Y, Zhou L, Jiang J, Yang F, Duan Q, et al. Immune cell repertoire and their mediators in patients with acute myocardial infarction or stable angina pectoris. Int J Med Sci. 2017;14(2):181–90.
12. Hofmann U, Frantz S. Role of T-cells in myocardial infarction. Eur Heart J. 2016;37(11):873–9.
13. Emoto T, Sasaki N, Yamashita T, Kasahara K, Yodoi K, Sasaki Y, et al. Regulatory/effector T-cell ratio is reduced in coronary artery disease. Circ J. 2014;78(12):2935–41.
14. Burska A, Boissinot M, Ponchel F. Cytokines as biomarkers in rheumatoid arthritis. Mediat Inflamm. 2014;2014:1–24.
15. Tomioka R, Matsui M. Biomarkers for multiple sclerosis. Intern Med. 2014;53(5):361–5.
16. Lacour S, Gautier J-C, Pallardy M, Roberts R. Cytokines as potential biomarkers of liver toxicity. Cancer Biomark Sect Dis Markers. 2005;1(1):29–39.
17. Szkodzinski J, Hudzik B, Osuch M, Romanowski W, Szygula-Jurkiewicz B, Polonski L, et al. Serum concentrations of interleukin-4 and interferon-gamma in relation to severe left ventricular dysfunction in patients with acute myocardial infarction undergoing percutaneous coronary intervention. Heart Vessel. 2011;26(4):399–407.
18. Swirski FK, Nahrendorf M, Etzrodt M, Wildgruber M, Cortez-Retamozo V, Panizzi P, et al. Identification of splenic reservoir monocytes and their deployment to inflammatory sites. Science. 2009;325(5940):612–6.
19. Kawaguchi H, Mori T, Kawano T, Kono S, Sasaki J, Arakawa K. Band neutrophil count and the presence and severity of coronary atherosclerosis. Am Heart J. 1996;132(1):9–12.
20. Omran MM, Zahran FM, Kadry M, Belal AAM, Emran TM. Role of myeloperoxidase in early diagnosis of acute myocardial infarction in patients admitted with chest pain. J Immunoassay Immunochem. 2018;39(3):337–47.
21. Crisóstomo V, Maestre J, Maynar M, Sun F, Báez-Díaz C, Usón J, et al. Development of a closed chest model of chronic myocardial infarction in swine: magnetic resonance imaging and pathological evaluation. ISRN Cardiol. 2013;2013:781762.

**Ready to submit your research? Choose BMC and benefit from:**

- fast, convenient online submission
- thorough peer review by experienced researchers in your field
- rapid publication on acceptance
- support for research data, including large and complex data types
- gold Open Access which fosters wider collaboration and increased citations
- maximum visibility for your research: over 100M website views per year

**At BMC, research is always in progress.**

**Learn more** biomedcentral.com/submissions

BMC

Veterinary Immunology and Immunopathology 205 (2018) 49–57

Contents lists available at ScienceDirect

Veterinary Immunology and Immunopathology

journal homepage: www.elsevier.com/locate/vetimm

# Altered hematological, biochemical and immunological parameters as predictive biomarkers of severity in experimental myocardial infarction

Rebeca Blázquez[a,b], Verónica Álvarez[a], Juan Antonio Antequera-Barroso[c], Claudia Báez-Díaz[b,d], Virginia Blanco[b,d], Juan Maestre[b,d], Beatriz Moreno-Lobato[e], Esther López[a], Federica Marinaro[a], Javier G. Casado[a,b,*], Verónica Crisóstomo[b,d,1], Francisco Miguel Sánchez-Margallo[a,b,1]

[a] Stem Cell Therapy Unit, Jesús Usón Minimally Invasive Surgery Centre, Cáceres, 10071, Spain
[b] CIBER de Enfermedades Cardiovasculares, Madrid, 28029, Spain
[c] Mathematics and Experimental Sciences Department, University of Extremadura, Cáceres, 10003, Spain
[d] Endoluminal Therapy and Diagnosis Unit, Jesús Usón Minimally Invasive Surgery Centre, Cáceres, 10071, Spain
[e] Animal Modelling Service, Jesús Usón Minimally Invasive Surgery Centre, Cáceres, 10071, Spain

ARTICLE INFO

*Keywords:*
Myocardial infarction
Porcine model
Biomarkers

ABSTRACT

Preclinical studies in cardiovascular medicine are necessary to translate basic research to the clinic. The porcine model has been widely used to understand the biological mechanisms involved in cardiovascular disorders for which purpose different closed-chest models have been developed in the last years to mimic the pathophysiological events seen in human myocardial infarction.

In this work, we studied hematological, biochemical and immunological parameters, as well as Magnetic resonance derived cardiac function measurements obtained from a swine myocardial infarction model. We identified some blood parameters which were significantly altered after myocardial infarction induction. More importantly, these parameters (gamma-glutamyl transferase, glutamic pyruvic transaminase, red blood cell counts, hemoglobin concentration, hematocrit, platelet count and plateletcrit) correlated positively with cardiac function, infarct size and/or cardiac enzymes (troponin I and creatine kinase-MB).

Thus several blood-derived parameters have allowed us to predict the severity of myocardial infarction in a clinically relevant animal model. Therefore, here we provide a simple, affordable and reliable way that could prove useful in the follow up of myocardial infarction and in the evaluation of new therapeutic strategies in this animal model.

## 1. Introduction

Preclinical studies in cardiovascular medicine are mandatory in order to effect the translation of basic research to clinical practice (bench to beside. There are many anatomical and physiological differences between small animal models and humans limit the extrapolation of research results to the clinical scenario. In contrast, large animal models such as swine display similarities to humans in terms of anatomy, physiology and biochemical parameters (van der Spoel et al., 2011). In the field of cardiovascular medicine, the porcine model has been widely accepted by researchers and regulatory agencies as representative of the human disease, and is considered mandatory for understanding the biological mechanisms involved in cardiovascular disorders and to evaluate new therapies. In the setting of myocardial

*Abbreviations:* CRP, C-reactive protein; EF, ejection fraction; GGT, gamma-glutamyl transferase; GOT, glutamic oxaloacetic transaminase; GPT, glutamic pyruvic transaminase; HCT, hematocrit; HGB, hemoglobin concentration; MCH, mean corpuscular hemoglobin; MCHC, mean corpuscular hemoglobin concentration; MCV, mean corpuscular volume; MPV, mean platelet volume; MR, magnetic resonance; PCT, plateletcrit; PDW, platelet distribution width; PLT, platelet count; RBC, red blood cell count; RDW-CV, red blood cell distribution width coefficient of variation; RDW-SD, red blood cell distribution width standard deviation; WBC, total white blood cells count

* Corresponding author at: Stem Cell Therapy Unit, Jesús Usón Minimally Invasive Surgery Centre, Ctra. N-521, km 41.8, 10071, Cáceres, Spain.
*E-mail addresses:* rblazquez@ccmijesususon.com (R. Blázquez), valvarez@ccmijesususon.com (V. Álvarez), jaab@unex.es (J.A. Antequera-Barroso), cbaez@ccmijesususon.com (C. Báez-Díaz), vblanco@ccmijesususon.com (V. Blanco), jmaestre@ccmijesususon.com (J. Maestre), bmorenolobato@ccmijesususon.com (B. Moreno-Lobato), elopez@ccmijesususon.com (E. López), fmarinaro@ccmijesususon.com (F. Marinaro), jgarcia@ccmijesususon.com (J.G. Casado), crisosto@ccmijesususon.com (V. Crisóstomo), msanchez@ccmijesususon.com (F.M. Sánchez-Margallo).
[1] These authors are co-senior authors.

https://doi.org/10.1016/j.vetimm.2018.10.007
Received 21 March 2018; Received in revised form 9 October 2018; Accepted 19 October 2018
0165-2427/ © 2018 Elsevier B.V. All rights reserved.

infarction, clinically-relevant animal models have permitted the identification of pathophysiological changes with clinical relevance. Additionally, these animal models are a valuable tool in the evaluation of safety aspects and efficacy of new therapeutic approaches and ideas prior to clinical application.

The vast majority of swine animal models have been used to mimic myocardial ischemia, either acute or chronic (Qu et al., 2012; Varga-Szemes et al., 2014), but they have also prooved useful for studying tachycardia and the anatomical substrate of arrhythmias (Tschabrunn et al., 2016).

Different surgical procedures have been developed in the last 40 years to model acute or chronic myocardial infarction. Early studies used open chest surgery ligating left anterior descending coronary artery (Lichtig et al., 1975). This surgical procedure has been used recently to study the effects of the ligation at different levels and diagonal branches (Huang et al., 2010). This approach, however, presents several disadvantages, mostly related to its invasive nature, that adversely affect the homogeneity of the injury obtained between animals. Moreover, cardiac parameters are influenced by the thoracotomy and high mortality rate and complications related to the surgical trauma are common (Munz et al., 2011).

In the last 20–30 years, the closed-chest model of myocardial infarction has been widely described in swine (Biondi-Zoccai et al., 2013; Crisóstomo et al., 2013; Pérez de Prado et al., 2009) and it is widely recognized as a more appropriate approach for cardiovascular research as it mimics the pathophysiological events in human myocardial infarction in absence of surgical influences (de Waard et al., 2016; Ishikawa et al., 2011). Variations of this model using different occlusion times that range from 40 min (Fernández-Jiménez et al., 2017), 60 min (McCall et al., 2012), 90 min (Koudstaal et al., 2014) or 150 min (Sasano et al., 2009) have been successfully developed in the last years.

Conventional evaluation methods such as electrocardiography and cardiac enzymes have been widely used in large animal model. New techniques developed in the last years include: modified electrocardiograms such as epicardial electrograms and body surface electrocardiograms in dogs subjected to occlusion of coronary artery (Mor-Avi et al., 1987), endocardial electromechanical mapping in a porcine acute infarction model (Odenstedt et al., 2003) and PET imaging in canine myocardial infarction models (Zalutsky et al., 1992). Although very different methods have been proposed to evaluate and monitor myocardial infarction, the anatomopathological analysis using different histological staining such as tetrazolium chloride (TTC) is still considered the most accurate approach for measuring infarct size.

To the best of our knowledge, there is a lack of immunological, hematological and biochemical studies in swine myocardial infarction models. In the present study, we aimed to identify any significant changes to commonly measured parameters that occur during the acute phase of myocardial infarction. Moreover, hematological/biochemical parameters were correlated with biomarkers widely used to quantify myocardial infarction such as cardiac enzymes (troponin I and creatine kinase-MB) and cardiac magnetic resonance-derived data (ejection fraction and infarct area).

The novelty of this work relies on the identification of biochemical or cellular parameters altered after myocardial infarction in the porcine model. We have identified several biomarkers useful for the assessment of myocardial infarction. These biomarkers are closely correlated with cardiac function or cardiac enzymes and may provide a simple, fast and accurate quantification of myocardial infarction in this animal model.

## 2. Materials and methods

### 2.1. Animals and experimental design

Nineteen Large White pigs were housed in the animal facility at the Jesús Usón Minimally Invasive Surgery Centre and used for all experimental procedures. Animals aged 3 months and weighing 30–35 kg at the beginning of the study were used. All experimental protocols were approved by the Animal Welfare Ethical Committee of the Jesús Usón Minimally Invasive Surgery Centre and fully complied with recommendations outlined by the local government (Junta de Extremadura) and by the Directive 2010/63/EU of the European Parliament on the protection of animals used for scientific purposes.

Blood sampling was performed before myocardial infarction model creation, at 24 h and 7 days after myocardial infarction.

### 2.2. Myocardial infarction model creation

A closed chest reperfused myocardial infarction was created as previously described (Crisóstomo et al., 2013). Briefly, anesthetized animals were subjected to a percutaneous right femoral access using a 7 Fr Introducer sheath (Terumo, Tokyo, Japan), and a Hockey Stick 6 Fr guiding catheter (Mach 1, Boston Scientific Corporation, Natick, MA, USA) was navigated under fluoroscopic guidance to the origin of the left coronary artery. Coronary angiograms were obtained in the 40° left anterior oblique projection to better demonstrate the length of the left anterior descending artery. A coronary balloon catheter (typically 3 mm x 8 mm, Ryujin Plus, Terumo, Tokio, Japan) was inserted over a 0.014″ coronary guidewire and advanced to below the origin of the first diagonal branch, where it was inflated to occlude flow to the distal myocardium. Occlusion was maintained for 90 min to assure transmural infarct creation. Upon balloon deflation, the coronary artery was checked for patency by repeating the angiogram. During the procedure, animals were fully monitored, including blood pressure, electrocardiogram, $O_2$ saturation, and end tidal $CO_2$. Continuous infusion of lidocaine at rate of 1 mg/kg/h (Lidocaine, Braun Medical, Barcelona, Spain) was used through the procedure. Systemic heparin (Heparina Rovi 5%, Laboratorios farmaceuticos Rovi, Madrid, Spain) was injected intravenously (150 UI/kg) prior to percutaneous sheath placement.

### 2.3. Biochemical analysis

Blood samples were collected, centrifuged to eliminate cellular debris and processed in the random access clinical analyzer Metrolab 2300 (Metrolab S.A., Buenos Aires, Argentina) to determine their biochemical composition (bilirubin, creatinine, glucose, urea, gamma-glutamyl transferase or GGT, glutamic oxaloacetic transaminase or GOT, glutamic pyruvic transaminase or GPT and C-reactive protein or CRP).

### 2.4. Hematological analysis and phenotypic characterization of peripheral blood lymphocytes

Blood samples were collected in EDTA containing tubes and leukocyte, red blood cells and platelets-related parameters were determined in an automatic hematology analyzer (Mindray BC-5300 Vet, Hamburg, Germany). Total white blood cells (WBC) were counted: neutrophils, lymphocytes, monocytes, eosinophils and basophils. Red blood cells (RBC) were also counted and additional parameters were also determined: hemoglobin concentration (HGB), hematocrit (HCT), mean corpuscular volume (MCV), mean corpuscular hemoglobin (MCH), mean corpuscular hemoglobin concentration (MCHC), red blood cell distribution width coefficient of variation (RDW-CV), red blood cell distribution width standard deviation (RDW-SD). Finally, platelets count (PLT) was also quantified together with mean platelet volume (MPV), platelet distribution width (PDW) and plateletcrit (PCT).

For flow cytometry analysis, peripheral blood lymphocytes were isolated by centrifugation over Histopaque-1077 (Sigma, St. Louis, MO). The cells were washed twice with DMEM containing 10% FBS and stained with fluorescent-labelled monoclonal antibodies against porcine CD3 (Clone: CD3-12), CD8α (Clone: MIL12), CD16 (Clone: G7), CD27 (Clone: B30C7) and CD45RA (Clone: MIL13) from AbD Serotec

(Kidlington, UK) and CD4 (Clone: 74-12-4) from BD Biosciences (San Jose, CA, USA). For cytometric analysis, $2 \times 10^5$ cells were incubated for 30 min at 4 °C with appropriate concentrations of monoclonal antibodies and were then washed and re-suspended in PBS. The flow cytometric analysis was performed in a FACScalibur cytometer (BD Biosciences) after acquisition of $10^5$ events. Cells were primarily selected using forward and side scatter characteristics. Multiparametric flow cytometry was performed on CD4 + T cells and CD8 + T cells (gated as CD4+ CD8α– and CD4- CD8α+ respectively). The co-expression of CD27 and CD45RA on CD4 + T cells and CD8 + T cells allowed us to distinguish three different T cell subsets with distinct functional properties: naïve T cells (CD45RA + CD27+), effector T cells (CD45RA–CD27+) and effector/memory T cells (CD45RA–CD27–). Fluorescence was analyzed using CellQuest software (BD Biosciences, San Jose, CA, USA) and isotype-matched negative control antibodies were used in all the experiments.

### 2.5. Cardiac enzyme analysis

Blood samples were collected in EDTA containing tubes for troponin I and creatine kinase-MB immunoassay (AQT90 Flex, Radiometer Iberica SL, Madrid, Spain). Results are given as μg/l.

### 2.6. Cardiac magnetic resonance

Cardiac MR studies (Intera 1.5 T, Philips Medical Systems. Best, The Netherlands) were performed 7 days after infarction. Retrospective cardiac triggering was used. A 4 elements phase array coil was placed around the animals' chest. Images were acquired in the intrinsic cardiac planes: short axis, vertical long axis and horizontal long axis views. For measurement of left ventricular function and mass breath hold gradient echo cine images were obtained over the entire left ventricle. For infarct size measurements, short axis images were acquired 5–15 min after the injection of 0.2 mmol/kg of a gadolinium-based contrast agent (Gadobutrol. Gadovist 1.1 mmol/l, Bayer Schering Pharma AG, Berlin, Germany) using a breath-hold 3D gradient-echo inversion-recovery sequence.

### 2.7. Statistical analysis

Statistical analysis was performed using the SPSS-21 software (SPSS, Chicago, IL, USA). Normality was assessed using a Shapiro-Wilk test. Paired comparisons were performed using a Student *t*-test for parametric data or Wilcoxon sign test for non-parametric data. Correlations were calculated using the Pearson coefficient correlation and "r" value was interpreted as follows: -1.0 to -0.5 or 0.5–1.0: Strong correlation, -0.5 to -0.3 or 0.3 to 0.5: Moderate correlation, -0.3 to -0.1 or 0.1 to 0.3: Weak correlation, -0.1 to 0.1: None or very weak correlation. All *p*-values $\leq 0.05$ were considered statistically significant.

## 3. Results

### 3.1. Biochemical parameters in peripheral blood from infarcted swine

A total of 19 animals were used for this study. Two animals died from refractory arrhythmias during infarct creation. Peripheral blood samples were collected from the remaining 17 pigs before model creation (basal), at 24 h and 7 days after myocardial infarction. Biochemical parameters are shown in Fig. 1. Our results firstly demonstrated a significant decrease in bilirubin ($p \leq 0.001$) at 24 h and 7 d when compared to basal. In the case of urea, a significant decrease ($p \leq 0.05$) was found at day 7 when compared to 24 h. Interestingly, highly significant increases ($p \leq 0.001$) both in GOT and GPT were found at 24 h when compared to basal or 7 d. Moreover, significant increases were also observed on GOT ($p \leq 0.05$) and GPT ($p \leq 0.001$) at day 7 when compared to baseline. Finally, significant differences were also found on CRP showing a decrease at day 7 when compared to 24 h ($p \leq 0.05$) and basal ($p \leq 0.05$). Variations seen in creatinine, glucose and GGT, did not reach statistical significance.

### 3.2. Hematological parameters in peripheral blood from infarcted swine

The analysis of hematological parameters was performed on the same peripheral blood samples as above, collected before myocardial infarction (basal), and post-myocardial infarction at 24 h and 7 days.

We performed the quantitative analysis of different leukocyte subsets (lymphoid and myeloid). Leukocyte subsets were counted in an automatic hematology analyzer. Results are shown in Fig. 2. Fig. 2A shows a highly significant increase ($p \leq 0.001$) in WBC at 24 h when compared to basal and 7 d. Regarding neutrophils, a significant increase was also observed at 24 h when compared to basal and 7 d ($p \leq 0.001$ and $p \leq 0.01$, respectively). In the case of lymphocytes, a significant increase ($p \leq 0.05$) was only found at 7 d when compared to basal. Monocytes showed a significant increase at 24 h ($p \leq 0.05$) when compared to basal. Eosinophils displayed a significant increase at 24 h ($p \leq 0.01$) and 7 d ($p \leq 0.01$) when compared to basal. Finally, basophils showed a significant increase at 24 h and 7 days ($p \leq 0.001$ and $p \leq 0.05$, respectively) when compared to basal.

On the other hand, the hematological analysis was also focused on red blood cells and hemoglobin. This analysis, represented in Fig. 2B showed a significant decrease ($p \leq 0.01$) in RBC, HGB and HCT when comparing 7 d to 24 h. In terms of MCV, a significant decrease was found at 24 h ($p \leq 0.05$) and 7 d ($p \leq 0.05$) when compared to basal. No differences were found in MCH but a significant decrease was found in MCHC at 24 h and 7 d when compared to basal ($p \leq 0.05$). Regarding RDW-CV, several changes were found, with the highest significant difference ($p \leq 0.001$) seen between 7 d and basal. Finally, RDW-SD was significantly reduced at day 7 ($p \leq 0.05$) when compared to basal.

The hematologic analysis was completed with the evaluation of different platelet parameters. This analysis, represented in Fig. 2C, showed only a significant decrease in PLT ($p \leq 0.05$) and PCT ($p \leq 0.05$) at 24 h when compared to basal.

### 3.3. Phenotypic analysis of peripheral blood lymphocytes from swine myocardial infarction model

Lymphocytes from the 17 study pigs were isolated from blood samples by gradient centrifugation and phenotypically analyzed by flow cytometry at pre-specified time points: before myocardial infarction (basal) and at 24 h and 7 days post-infarction. The percentage of CD4 + T cells (gated as CD4+ CD8α–), CD8 + T cells (gated CD4-CD8α+), NK cells (gated as CD3-CD8α-CD4-CD16+) as well as the CD4/CD8 ratio was determined. This analysis of lymphocyte subsets, shown in Fig. 3, did not reveal any statistically significant difference. Only, a slight but not significant decrease in the percentage of NK cells was observed at 7d when compared to 24 h and basal samples.

Regarding the activation/differentiation status of lymphocytes after myocardial infarction, a deep analysis of activation/differentiation markers was performed on CD4+ and CD8 + T cell subsets. The CD45RA and CD27 co-expression was analyzed on peripheral lymphocytes and the percentages of naïve T cells (CD45RA + CD27+), effector T cells (CD45RA–CD27+) and effector/memory T cells (CD45RA–CD27–) were compared at different time points. No significant change was observed between different time points.

### 3.4. Myocardial infarction model assessment

Infarction was successfully induced in all surviving animals as demonstrated by a significant increase ($p \leq 0.001$) in cardiac enzymes at 24 h post-infarction (troponin I 27.41 ± 10.46 μg/l and CK-MB 15.02 ± 7.96 μg/l), compared to basal levels (troponin I 0.02 ± 0.02 μg/l and CK-MB 3.80 ± 1.34 μg/l) (Supplementary File 1).

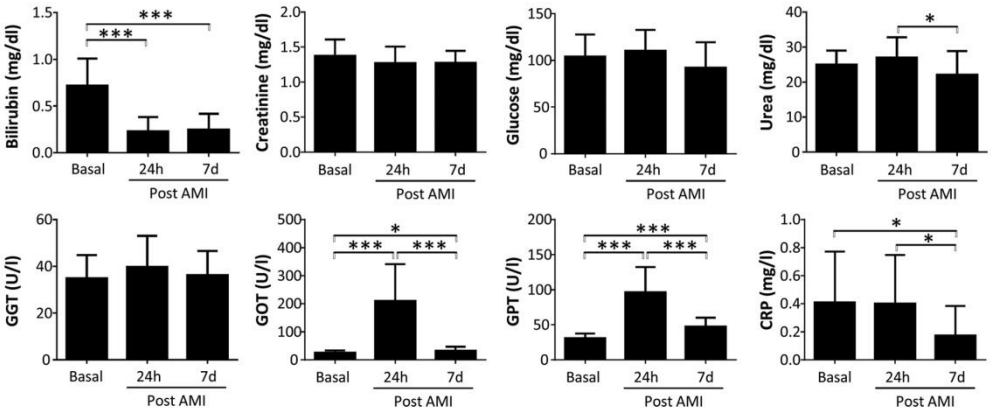


**Fig. 1.** Levels of biochemical parameters in peripheral blood. Blood samples were collected before acute myocardial infarction model creation (basal) 24 h and 7 d after. Blood samples were collected, centrifuged and processed to determine their biochemical composition. Normality was assessed using a Shapiro-Wilk test. Paired comparisons were performed using a Student *t*-test for parametric data or Wilcoxon sign test for non-parametric data. Graphs show the mean ± SD (n = 17). Horizontal lines show significant differences. *p ≤ 0.05; ***p ≤ 0.001.

Cardiac function was evaluated by Cardiac Magnetic Resonance at day 7 after myocardial experimental myocardial infarction. Ejection Fraction (% EF) as well as the size of myocardial infarction expressed as percentage of the Left Ventricle (% Infarct) were calculated from the MR studies. As shown in Table 1, EF ranged from 14% to 38% with a mean ± SD of 23.5% ± 8.1%. The % Infarct ranged from 14% to 33% with a mean ± SD of 23.2% ± 5.5%. Fig. 4 shows the individual MR analysis in the study group (n = 17) with the myocardial infarct area depicted on a selected representative short axis image.

### *3.5. Correlation analysis between cardiac function and blood-derived parameters*

In order to identify biochemical and hematological biomarkers that could be useful for the evaluation and follow-up of myocardial infarction in this animal model, we performed a correlation analysis between MR-derived % EF and % Infarct at day 7 and blood-derived parameters (biochemical and hematological) obtained 24 h and 7 d post-infarction. This paired sample correlation was also evaluated on cardiac enzymes obtained at 24 h and day 7 post-infarction.

As expected, most of the blood-derived parameters analyzed did not show any significant correlation with cardiac function parameters and cardiac enzymes (Supplementary File 2). Fig. 5A shows the only significant correlations observed on biochemical parameters: strong positive correlation between GGT and % EF ($r = 0.529$; $p = 0.029$) and strong positive correlation between GPT and troponin I ($r = 0.545$; $p = 0.024$).

Similarly, Fig. 5B represents the significant correlations observed on red blood cells or hemoglobin: strong positive correlation between RBC and % Infarct ($r = 0.514$; $p = 0.035$), strong positive correlation between HGB and % Infarct ($r = 0.536$; $p = 0.027$) and moderate positive correlation between HCT and % Infarct ($r = 0.482$; $p = 0.050$).

Finally, regarding platelet parameters, Fig. 5C shows the correlations found between PLT and % Infarct ($r = -0.504$; $p = 0.039$), PLT and troponin I ($r = -0.554$; $p = 0.021$) and PCT and % Infarct ($r = -0.493$; $p = 0.044$).

Additionally, as expected, significant correlations were observed for cardiac enzymes and % EF ($r = -0.482$; $p = 0.050$ for CK-MB at 24 h) as well as between cardiac enzymes and % Infarct ($r = -0.563$; $p = 0.019$ and $r = 0.623$; $p = 0.008$ for troponin I at 24 h and 7 d, respectively).

## 4. Discussion

Clinically relevant animal models are essential to evaluate new therapeutic strategies in myocardial infarction. It is widely accepted that the anatomical and physiological parallelism between humans and pigs makes this animal model a valuable tool to mimic biological and adverse events that occur during myocardial ischemia and reperfusion. This paper aimed to analyze biochemical parameters, hematological values and lymphocyte subsets parameters during the acute phase of myocardial infarction in a closed chest porcine model. Additionally, changes in these blood-derived parameters were correlated to cardiac function measurements obtained by MRI.

Our biochemical analysis firstly demonstrated a significant decrease of bilirubin (heme oxygenase-1 metabolite) within 24 h post-infarction, which is normal considering that animals were fasted for 48 h prior to infarct induction, which causes an important physiological increase in this parameter (Baetz and Mengeling, 1971). The significant decrease observed after infarction corresponds to the normalization of bilirubin levels after the fasting period.

We also evidenced highly significant changes in GOT and GPT 24 h post-infarction as well as a direct correlation between GPT–troponin I and GGT–EF. These results are in agreement with recent clinical studies which demonstrated a correlation between serum transaminases and cardiac parameters (Killip classification, infarct-related coronary artery and troponin I) in patients with ST-segment elevation myocardial infarction (Gao et al., 2017). Additionally, in another study, transaminases quantified in 167 patients during the acute phase of percutaneous coronary intervention demonstrated a direct correlation with systolic dysfunction detected by MRI (Reinstadler et al., 2015). As in those clinical observations, in our animal model the correlation between hepatic enzymes and MRI was observed at day 7 post-infarction.

In terms of hematological parameters quantified in our preclinical infarct model, we observed a significant increase of WBC, neutrophils, eosinophils, monocytes and basophils at 24 h post-infarction when compared to basal samples. This leukocytosis is triggered by myocardial infarction through the activation of bone marrow, hematopoietic cells and leukocyte production (Dutta et al., 2015). In our animal model, the increase of myeloid cells at 24 h exhibits strong similarities with results previously described in patients (Engström et al., 2009; Sager et al., 2016). Moreover, Ferrari et al. have recently demonstrated that WBC counts in hospitalized patients at 72 h post-admission are predictive biomarkers that correlate with the size of ST segment elevation

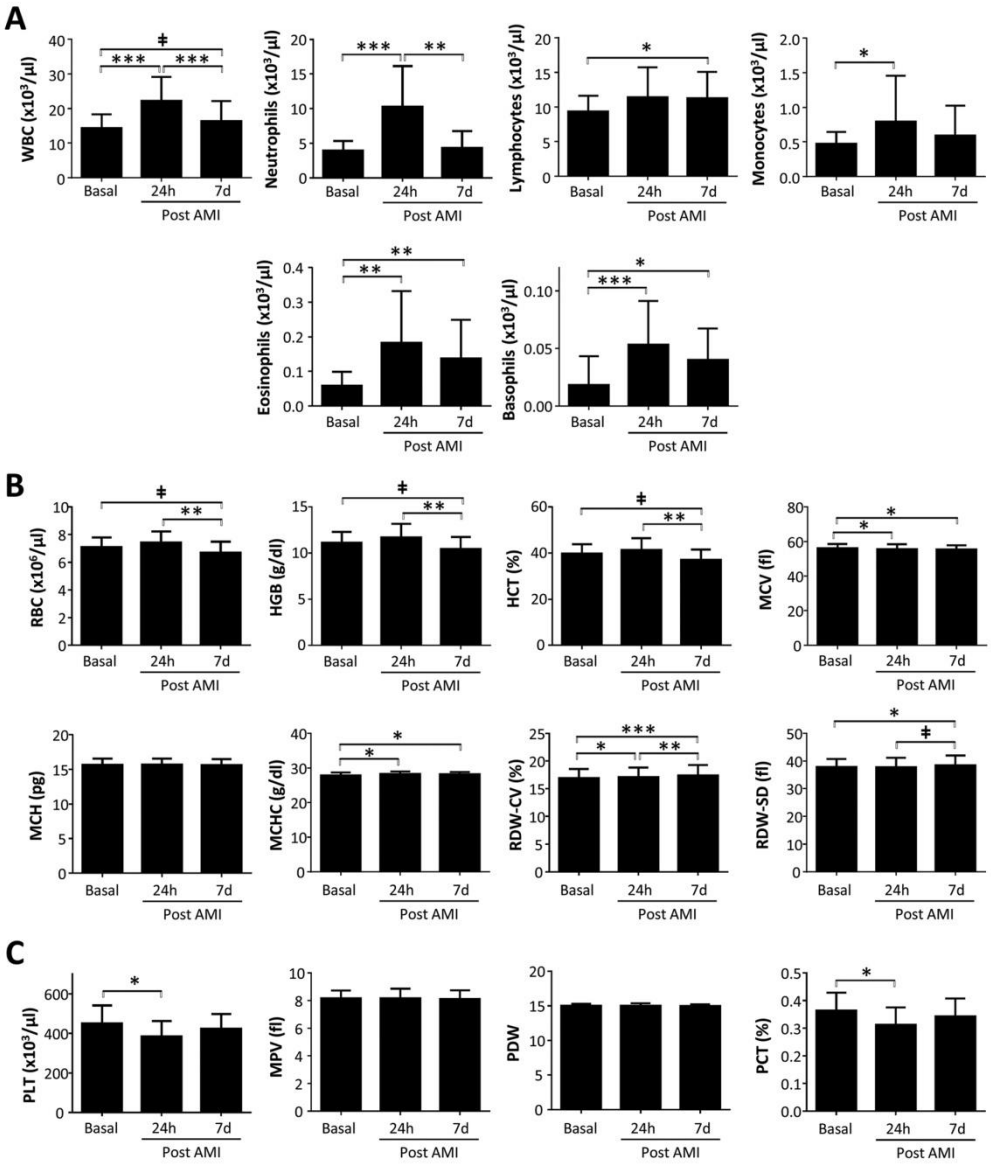


**Fig. 2.** Levels of hematological parameters in peripheral blood. Blood samples were collected before acute myocardial infarction model creation (basal) 24 h and 7 d after. Blood samples were collected in EDTA containing tubes and leukocyte subsets (A), red blood cells (B) and platelets (C) were counted in an automated hematology analyzer. Normality was assessed using a Shapiro-Wilk test. Paired comparisons were performed using a Student *t*-test for parametric data or Wilcoxon sign test for non-parametric data. Graphs show the mean ± SD (n = 17). Horizontal lines show significant differences. ǂp ≤ 0.1; *p ≤ 0.05; **p ≤ 0.01; ***p ≤ 0.001.

myocardial infarction (Ferrari et al., 2016).

Among the different subsets of WBC, neutrophils play a key role in myocardial infarction. A recent paper in neutrophil-depleted mice has demonstrated that neutrophils are involved in macrophages polarization towards an anti-inflammatory and reparative phenotype (Horckmans et al., 2017). Moreover, a clinical study with 701 patients showed that the percentage of neutrophils in patients with ST-segment elevated myocardial infarction was a predictor for long-term mortality (Men et al., 2015).

Our hematological characterization of porcine myocardial infarction model was also focused on RBC, HGB and HCT and platelets. Our results showed a significant decrease of RBC, HGB and HCT at day 7 when compared to 24 h. Interestingly, our analyses revealed not only significant differences but also a positive correlation between RBC, HGB and HCT with the percentage of infarcted area. Our results are related with clinical studies where the hematocrit has been used as a prognostic

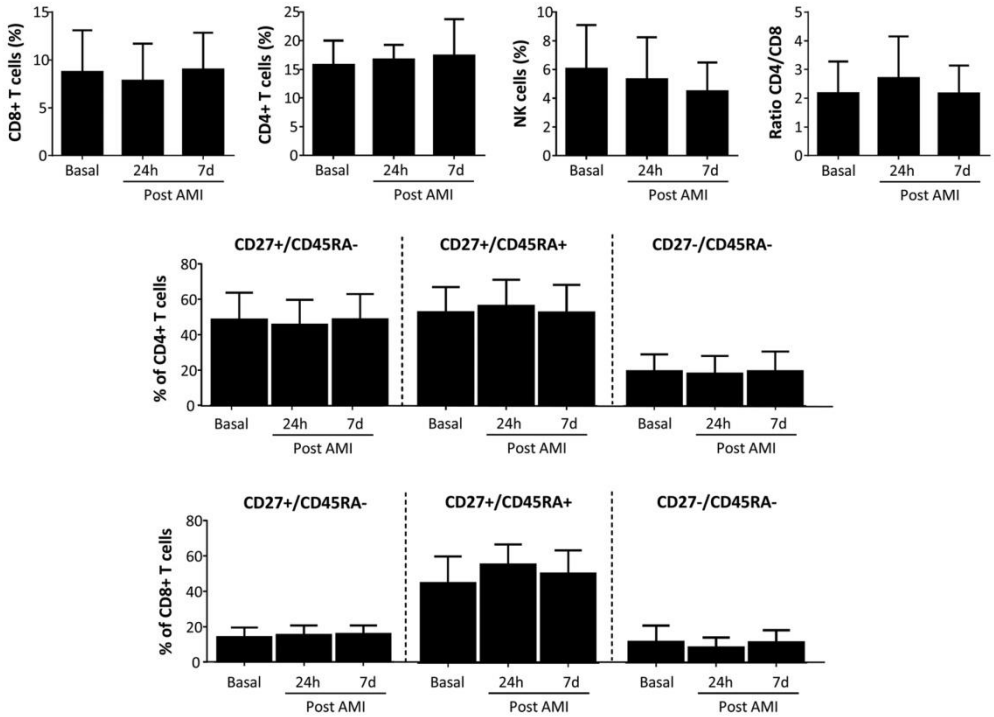


**Fig. 3.** Lymphocyte subsets distribution in peripheral blood. Peripheral blood lymphocytes were isolated from blood samples collected before acute myocardial infarction model creation (basal) 24 h and 7 d after. Peripheral blood lymphocytes were stained with fluorescent-labelled monoclonal antibodies against porcine CD3, CD4, CD8α, CD16, CD27 and CD45RA and different lymphocyte subpopulation were analyzed by flow cytometry. Normality was assessed using a Shapiro-Wilk test. Paired comparisons were performed using a Student *t*-test for parametric data or Wilcoxon sign test for non-parametric data. Graphs show the mean ± SD (n = 17). No significant differences ($p \leq 0.05$) were found.

**Table 1**
Cardiac assessment parameters derived from Magnetic Resonance in terms of percentage of myocardial infarction and ejection fraction for the different animals included in the study.

| | CARDIAC ASSESSMENT | |
|---|---|---|
| Animal number | MI (%) | EF (%) |
| #1 | 33 | 23 |
| #2 | 28 | 22 |
| #3 | 25 | 34 |
| #4 | 31 | 38 |
| #5 | 18 | 16 |
| #6 | 14 | 26 |
| #7 | 24 | 38 |
| #8 | 18 | 30 |
| #9 | 23 | 18 |
| #10 | 20 | 19 |
| #11 | 16 | 24 |
| #12 | 26 | 14 |
| #13 | 27 | 15 |
| #14 | 25 | 18 |
| #15 | 20 | 17 |
| #16 | 25 | 26 |
| #17 | 25 | 27 |

biomarker in patients with ST-segment elevation myocardial infarction (Greenberg et al., 2010). Based on that, here we suggest that these blood parameters (RBC, HGB and HCT) could be considered as early biomarkers to predict the severity of surgically-induced myocardial infarction.

In the case of platelets, a significant decrease was observed 24 h post-infarction when compared to basal measurements. Platelets level has been considered a very helpful tool for the classification and monitoring of patients with ST-segment elevation (Paul et al., 2010). Additionally, platelet count has been associated with the outcomes of ST-elevation myocardial infarction (Ly et al., 2006) and unstable angina (Mueller et al., 2006). In our animal model, the significant decrease in platelets was accompanied by a significant increase in inflammatory cells which is in agreement with clinical results published by Järemo et al. who described that patients with acute myocardial infarction displayed an elevated inflammatory response associated to lower platelet counts (Järemo et al., 2000). Additionally, the correlation analysis in our animal model demonstrated that PLT counts and PCT at 24 h post-infarction were inversely correlated with the size of myocardial infarction at day 7. These findings support the use of PLT and PCT at 24 h as blood derived biomarkers which are inversely correlated with the severity of induced myocardial infarction. Moreover, the correlation observed between troponin I and PLT counts further supports the usefulness of this parameter in the follow-up of this animal model.

Finally, considering that myocardial infarction is an inflammatory process (acute or chronic depending on the etiology), here we analyzed the different lymphocyte subsets and differentiation/activation markers on CD4 + and CD8 + T cells. Although clinical studies monitoring these T cell subsets are somewhat ambiguous, it seems that there is a significant decrease of CD4 + /CCR7 + T cells after myocardial infarction (Hoffmann et al., 2012). The reason behind this change is still unclear in patients: redistribution of CD4 + T cells in periphery vs accumulation in myocardium. Experimental animal models are providing very

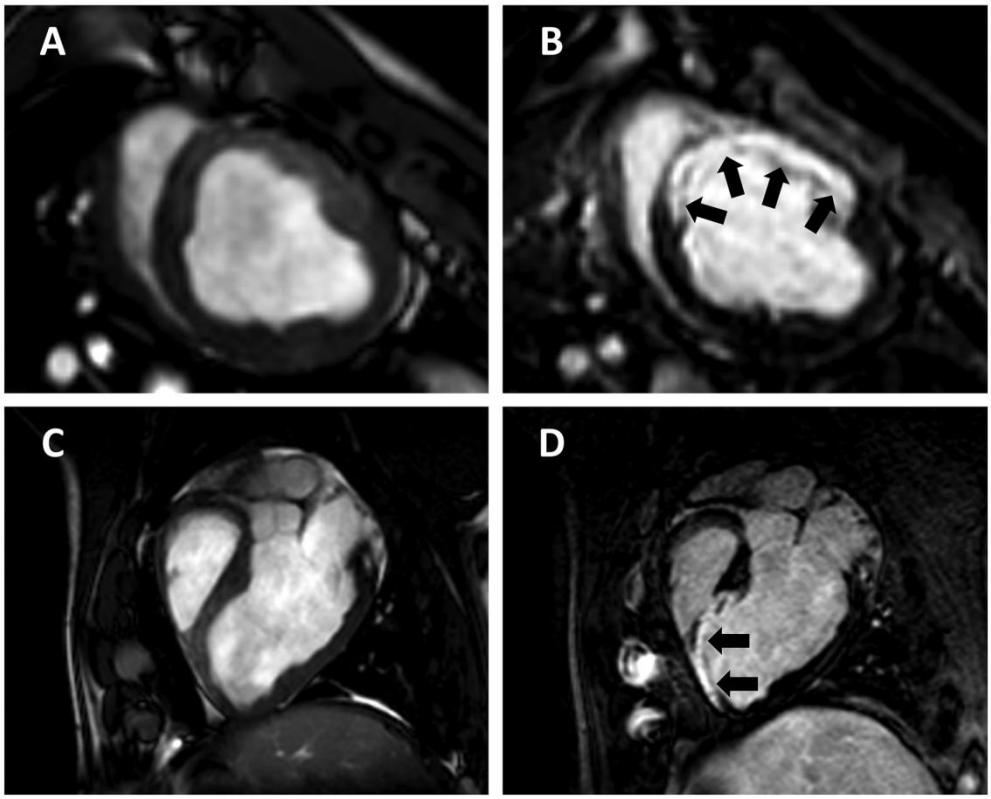


**Fig. 4.** Representative images of Cardiac Magnetic Resonance. Cardiac Magnetic Resonance studies were acquired at day 7 after myocardial infarction. Representative images were obtained from animal #12. A and B: short axis images. C and D: Four-chamber views. B and D depict delayed enhancement images obtained 10–15 min after gadolinium administration. The infarcted area is shown in white (arrows) and healthy myocardium in black.

relevant information regarding the role of CD4 + T cells. Firstly, a significant decrease in myocardial infarct size has been observed in CD4-depleted mice (Yang et al., 2006). Secondly, CD4+ regulatory T cells could reduce the pro-inflammatory environment shifting it towards a pro-healing phenotype in a rat myocardial infarction model (Tang et al., 2012). In the case of circulating CD8 + T cells in myocardial infarction, animal studies have demonstrated that CD8-deficiency did not result in any significant clinical phenotype after experimental myocardial infarction (Hofmann and Frantz, 2016).

In our study, no significant difference was observed when comparing different time points. However we should not discard hypothetical differences at short term follow-up. Indeed, our current studies are being focused in the very acute phase of myocardial infarction which have shown significant differences in the CD4/CD8 ratio and percentage of CD4+ and CD8 + T cells (manuscript in preparation).

Here we hypothesize that the absence of differences in CD4+ and CD8 + T cells after myocardial infarction may be related to the immunological status of our animal model. This idea is supported by clinical studies in cytomegalovirus-infected patients. These patients have an early and long-term decrease of terminally differentiated effector-memory CD8 + T cells after myocardial infarction (Hoffmann et al., 2015) and a direct relation between CD8 + T cell activation status and the pathophysiology of myocardial infarction has been suggested (Savva et al., 2013). Obviously, the immunological status and T-cell activation status of patients with acute coronary syndromes is completely different to the immunological status of young animals housed under pathogen-controlled conditions and without any co-morbidities. Based on that, we consider that the non-significant decrease of CD8 + T cells at 24 h post-AMI could be the consequence of using an animal model with an immune system under a naïve or resting state. However, we should highlight that studies performed under controlled conditions and in a homogeneous experimental group may provide a valuable tool to identify immunologically relevant biomarkers following the onset of ischemia.

In summary, we have performed a hematological, biochemical and immunological characterization of acute myocardial infarction in a clinically relevant animal model. We have identified blood derived parameters which are significantly altered after myocardial induction, and more importantly, which are significantly correlated with cardiac functional parameters and/or cardiac enzymes. For that reason, the *in vitro* determination of these parameters could be used as early markers to predict the severity of myocardial infarction. Moreover, it is a simple affordable and reliable way for the follow up of myocardial infarction and the evaluation of therapeutic products in preclinical settings.

## 5. Conclusions

The novelty of this paper lies in the identification of blood-derived biomarkers in a large animal model that closely resembles the pathophysiological progression of myocardial infarction. The identification of biomarkers is very useful for bridging the gap between preclinical studies in large animal models and clinical trials. It provides relevant

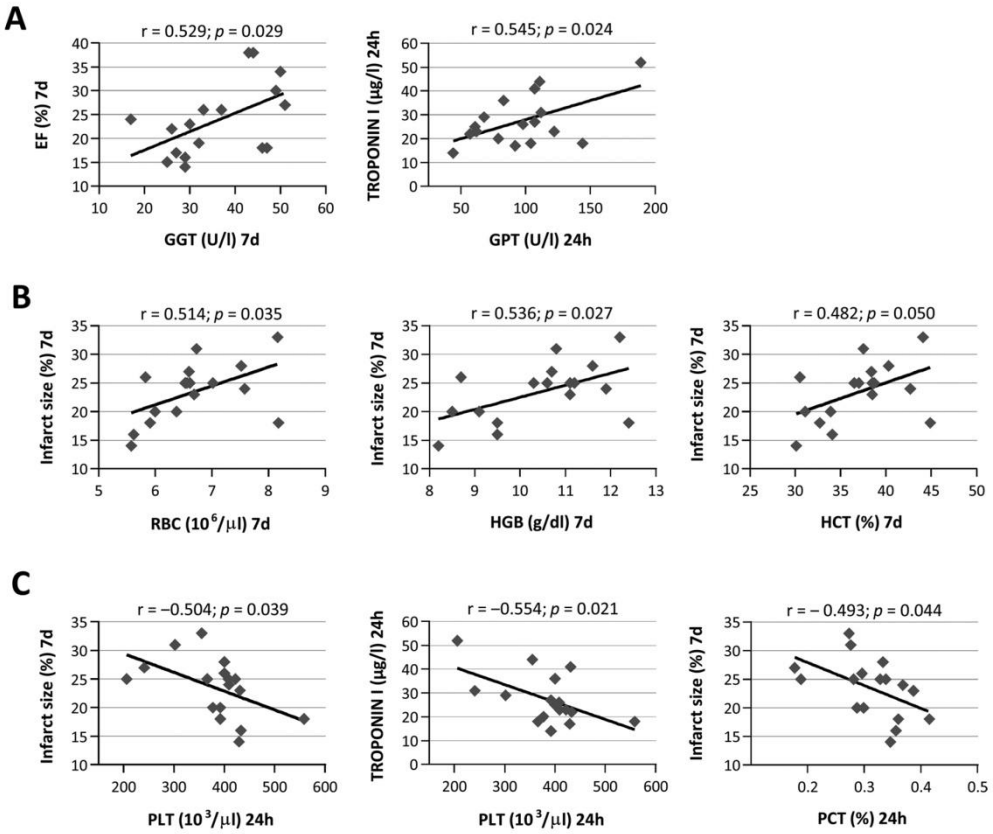


**Fig. 5.** Correlation analysis between cardiac assessment and blood-derived parameters. Correlations were calculated using the Pearson coefficient correlation. Graphs show significant correlations observed between cardiac assessment (percentage of ejection fraction and infarct area) and biochemical parameters (A) red blood cells (B) and platelets (C).

information in the evaluation of new therapeutic strategies for the treatment of myocardial infarction.

## Declarations of interest

None.

## Funding

This work was supported in part by CIBER-CV (CB16/11/00494), one grant from Junta de Extremadura (Ayuda a grupos catalogados de la Junta de Extremadura, GR15175), two grants from Junta de Extremadura to J.G.C. (IB16168) and V.C. (IB16201) co-financed by FEDER/FSE, two grants from ISCIII to J.G.C. (CP17/00021) and V.C. (PI16/01172) co-funded by ERDF/ESF, "Investing in your future", and one predoctoral grant from Grupo Jorge-Mafresa to F.M. The funders had no role in study design, data collection, interpretation and analysis, decision to publish or preparation of the manuscript.

## Acknowledgements

Biochemical and hematological determinations were performed by the ICTS Nanbiosis (Unit 19. Clinical test lab at CCMIJU). Flow cytometry analyses were performed by the ICTS Nanbiosis (Unit 14. Cell therapy at CCMIJU). Blood sampling and maintenance of animals were performed by the ICTS Nanbiosis (Unit 22. Animal housing at CCMIJU). Myocardial infarction induction and Magnetic Resonance studies waere performed by the ICTS Nanbiosis (Unit 21. Experimental operating rooms and Unit 24. Medical imaging at CCMIJU).

Special thanks to our students Iria Diaz Trigo and Eva Alegre Cortés for data management.

## References

Baetz, A.L., Mengeling, W.L., 1971. Blood constituent changes in fasted swine. Am. J. Vet. Res. 32, 1491–1499.

Biondi-Zoccai, G., De Falco, E., Peruzzi, M., Cavarretta, E., Mancone, M., Leoni, O., Caristo, M.E., Lotrionte, M., Marullo, A.G.M., Amodeo, A., Pacini, L., Calogero, A., Petrozza, V., Chimenti, I., D'Ascenzo, F., Frati, G., 2013. A novel closed-chest porcine model of chronic ischemic heart failure suitable for experimental research in cardiovascular disease. Biomed. Res. Int. 2013, 410631. https://doi.org/10.1155/2013/410631.

Crisóstomo, V., Maestre, J., Maynar, M., Sun, F., Báez-Díaz, C., Usón, J., Sánchez-Margallo, F.M., 2013. Development of a closed chest model of chronic myocardial infarction in swine: magnetic resonance imaging and pathological evaluation. ISRN Cardiol. 2013, 781762. https://doi.org/10.1155/2013/781762.

de Waard, G.A., Hollander, M.R., Teunissen, P.F.A., Jansen, M.F., Eerenberg, E.S., Beek, A.M., Marques, K.M., van de Ven, P.M., Garrelds, I.M., Danser, A.H.J., Duncker, D.J., van Royen, N., 2016. Changes in coronary blood flow after acute myocardial infarction: insights from a patient study and an experimental porcine model. JACC Cardiovasc. Interv. 9, 602–613. https://doi.org/10.1016/j.jcin.2016.01.001.

Dutta, P., Sager, H.B., Stengel, K.R., Naxerova, K., Courties, G., Saez, B., Silberstein, L., Heidt, T., Sebas, M., Sun, Y., Wojtkiewicz, G., Feruglio, P.F., King, K., Baker, J.N., van

der Laan, A.M., Borodovsky, A., Fitzgerald, K., Hulsmans, M., Hoyer, F., Iwamoto, Y., Vinegoni, C., Brown, D., Di Carli, M., Libby, P., Hiebert, S.W., Scadden, D.T., Swirski, F.K., Weissleder, R., Nahrendorf, M., 2015. Myocardial infarction activates CCR2(+) hematopoietic stem and progenitor cells. Cell Stem Cell 16, 477–487. https://doi.org/10.1016/j.stem.2015.04.008.

Engström, G., Melander, O., Hedblad, B., 2009. Leukocyte count and incidence of hospitalizations due to heart failure. Circ Heart Fail. 2, 217–222. https://doi.org/10.1161/CIRCHEARTFAILURE.108.827071.

Fernández-Jiménez, R., Galán-Arriola, C., Sánchez-González, J., Agüero, J., López-Martín, G.J., Gomez-Talavera, S., Garcia-Prieto, J., Benn, A., Molina-Iracheta, A., Barreiro-Pérez, M., Martin-García, A., García-Lunar, I., Pizarro, G., Sanz, J., Sánchez, P.L., Fuster, V., Ibanez, B., 2017. Effect of ischemia duration and protective interventions on the temporal dynamics of tissue composition after myocardial infarction. Circ. Res. 121, 439–450. https://doi.org/10.1161/CIRCRESAHA.117.310901.

Ferrari, J.P., Lueneberg, M.E., da Silva, R.L., Fattah, T., Gottschall, C.A.M., Moreira, D.M., 2016. Correlation between leukocyte count and infarct size in ST segment elevation myocardial infarction. Arch. Med. Sci. Atheroscler. Dis. 1, e44–e48. https://doi.org/10.5114/amsad.2016.60759.

Gao, M., Cheng, Y., Zheng, Y., Zhang, W., Wang, L., Qin, L., 2017. Association of serum transaminases with short- and long-term outcomes in patients with ST-elevation myocardial infarction undergoing primary percutaneous coronary intervention. BMC Cardiovasc. Disord. 17 (43). https://doi.org/10.1186/s12872-017-0485-6.

Greenberg, G., Assali, A., Vaknin-Assa, H., Brosh, D., Teplitsky, I., Fuchs, S., Battler, A., Kornowski, R., Lev, E.I., 2010. Hematocrit level as a marker of outcome in ST-segment elevation myocardial infarction. Am. J. Cardiol. 105, 435–440. https://doi.org/10.1016/j.amjcard.2009.10.016.

Hoffmann, J., Fiser, K., Weaver, J., Dimmick, I., Loeher, M., Pircher, H., Martin-Ruiz, C., Veerasamy, M., Keavney, B., von Zglinicki, T., Spyridopoulos, I., 2012. High-throughput 13-parameter immunophenotyping identifies shifts in the circulating T-cell compartment following reperfusion in patients with acute myocardial infarction. PLoS One 7, e47155. https://doi.org/10.1371/journal.pone.0047155.

Hoffmann, J., Shmeleva, E.V., Boag, S.E., Fiser, K., Bagnall, A., Murali, S., Dimmick, I., Pircher, H., Martin-Ruiz, C., Egred, M., Keavney, B., von Zglinicki, T., Das, R., Todryk, S., Spyridopoulos, I., 2015. Myocardial ischemia and reperfusion leads to transient CD8 immune deficiency and accelerated immunosenescence in CMV-seropositive patients. Circ. Res. 116, 87–98. https://doi.org/10.1161/CIRCRESAHA.116.304393.

Hofmann, U., Frantz, S., 2016. Role of T-cells in myocardial infarction. Eur. Heart J. 37, 873–879. https://doi.org/10.1093/eurheartj/ehv639.

Horckmans, M., Ring, L., Duchene, J., Santovito, D., Schloss, M.J., Drechsler, M., Weber, C., Soehnlein, O., Steffens, S., 2017. Neutrophils orchestrate post-myocardial infarction healing by polarizing macrophages towards a reparative phenotype. Eur. Heart J. 38, 187–197. https://doi.org/10.1093/eurheartj/ehw002.

Huang, Z., Ge, J., Sun, A., Wang, Y., Zhang, Shaoheng, Cui, J., Zhang, Suning, Qian, J., Zou, Y., 2010. Ligating LAD with its whole length rather than diagonal branches as coordinates is more advisable in establishing stable myocardial infarction model of swine. Exp. Anim. 59, 431–439.

Ishikawa, K., Ladage, D., Takewa, Y., Yaniz, E., Chen, J., Tilemann, L., Sakata, S., Badimon, J.J., Hajjar, R.J., Kawase, Y., 2011. Development of a preclinical model of ischemic cardiomyopathy in swine. Am. J. Physiol. Heart Circ. Physiol. 301, H530–537. https://doi.org/10.1152/ajpheart.01103.2010.

Järemo, P., Hansson, G., Nilsson, O., 2000. Elevated inflammatory parameters are associated with lower platelet density in acute myocardial infarctions with ST-elevation. Thromb. Res. 100, 471–478.

Koudstaal, S., Jansen of Lorkeers, S.J., Gho, J.M.I.H., van Hout, G.P., Jansen, M.S., Gründeman, P.F., Pasterkamp, G., Doevendans, P.A., Hoefer, I.E., Chamuleau, S.A.J., 2014. Myocardial infarction and functional outcome assessment in pigs. J. Vis. Exp. 86, e51269. https://doi.org/10.3791/51269.

Lichtig, C., Brooks, H., Chassagne, G., Glagov, S., Wissler, R.W., 1975. Basic fuchsin picric acid method to detect acute myocardial ischemia. An experimental study in swine. Arch. Pathol. 99, 158–161.

Ly, H.Q., Kirtane, A.J., Murphy, S.A., Buros, J., Cannon, C.P., Braunwald, E., Gibson, C.M., Study Group, T.I.M.I., 2006. Association of platelet counts on presentation and clinical outcomes in ST-elevation myocardial infarction (from the TIMI trials). Am. J. Cardiol. 98, 1–5. https://doi.org/10.1016/j.amjcard.2006.01.046.

McCall, F.C., Telukuntla, K.S., Karantalis, V., Suncion, V.Y., Heldman, A.W., Mushtaq, M., Williams, A.R., Hare, J.M., 2012. Myocardial infarction and intramyocardial injection models in swine. Nat. Protoc. 7, 1479–1496. https://doi.org/10.1038/nprot.2012.075.

Men, M., Zhang, L., Li, T., Mi, B., Wang, T., Fan, Y., Chen, Y., Shen, G., Liang, L., Ma, A., 2015. Prognostic value of the percentage of neutrophils on admission in patients with ST-elevated myocardial infarction undergoing primary percutaneous coronary intervention. Arch. Med. Res. 46, 274–279. https://doi.org/10.1016/j.arcmed.2015.05.002.

Mor-Avi, V., Shargorodsky, B., Abboud, S., Laniado, S., Akselrod, S., 1987. Effects of coronary occlusion on high-frequency content of the epicardial electrogram and body surface electrocardiogram. Circulation 76, 237–243.

Mueller, C., Neumann, F.-J., Hochholzer, W., Trenk, D., Zeller, T., Perruchoud, A.P., Buettner, H.J., 2006. The impact of platelet count on mortality in unstable angina/non-ST-segment elevation myocardial infarction. Am. Heart J. 151 (1214), e1–e7. https://doi.org/10.1016/j.ahj.2006.03.011.

Munz, M.R., Faria, M.A., Monteiro, J.R., Aguas, A.P., Amorim, M.J., 2011. Surgical porcine myocardial infarction model through permanent coronary occlusion. Comp. Med. 61, 445–452.

Odenstedt, J., Månsson, C., Jansson, S.-O., Grip, L., 2003. Endocardial electromechanical mapping in a porcine acute infarct and reperfusion model evaluating the extent of myocardial ischemia. J. Invasive Cardiol. 15, 497–501.

Paul, G.K., Sen, B., Bari, M.A., Rahman, Z., Jamal, F., Bari, M.S., Sazidur, S.R., 2010. Correlation of platelet count and acute ST-elevation in myocardial infarction. Mymensingh Med. J. 19, 469–473.

Pérez de Prado, A., Cuellas-Ramón, C., Regueiro-Purriños, M., Gonzalo-Orden, J.M., Pérez-Martínez, C., Altónaga, J.R., García-Iglesias, M.J., Orden-Recio, M.A., García-Marín, J.F., Fernández-Vázquez, F., 2009. Closed-chest experimental porcine model of acute myocardial infarction-reperfusion. J. Pharmacol. Toxicol. Methods 60, 301–306. https://doi.org/10.1016/j.vascn.2009.05.007.

Qu, X., Fang, W., Ye, J., Koh, A.S., Xu, Y., Guan, S., Li, R., Shen, Y., 2012. Acute and chronic myocardial infarction in a pig model: utility of multi-slice cardiac computed tomography in assessing myocardial viability and infarct parameters. Eur. J. Radiol. 81, e431–437. https://doi.org/10.1016/j.ejrad.2011.03.062.

Reinstadler, S.J., Reindl, M., Feistritzer, H.-J., Klug, G., Mayr, A., Kofler, M., Tu, A.M.-D., Huybrechts, L., Mair, J., Franz, W.-M., Metzler, B., 2015. Prognostic significance of transaminases after acute ST-elevation myocardial infarction: insights from a cardiac magnetic resonance study. Wien Klin Wochenschr 127, 843–850. https://doi.org/10.1007/s00508-015-0868-6.

Sager, H.B., Hulsmans, M., Lavine, K.J., Moreira, M.B., Heidt, T., Courties, G., Sun, Y., Iwamoto, Y., Tricot, B., Khan, O.F., Dahlman, J.E., Borodovsky, A., Fitzgerald, K., Anderson, D.G., Weissleder, R., Libby, P., Swirski, F.K., Nahrendorf, M., 2016. Proliferation and recruitment contribute to myocardial macrophage expansion in chronic heart failure. Circ. Res. 119, 853–864. https://doi.org/10.1161/CIRCRESAHA.116.309001.

Sasano, T., Kelemen, K., Greener, I.D., Donahue, J.K., 2009. Ventricular tachycardia from the healed myocardial infarction scar: validation of an animal model and utility of gene therapy. Heart Rhythm. 6, S91–S97. https://doi.org/10.1016/j.hrthm.2009.03.048.

Savva, G.M., Pachnio, A., Kaul, B., Morgan, K., Huppert, F.A., Brayne, C., Moss, P.A.H., Medical Research Council Cognitive Function and Ageing Study, 2013. Cytomegalovirus infection is associated with increased mortality in the older population. Aging Cell 12, 381–387. https://doi.org/10.1111/acel.12059.

Tang, T.-T., Yuan, J., Zhu, Z.-F., Zhang, W.-C., Xiao, H., Xia, N., Yan, X.-X., Nie, S.-F., Liu, J., Zhou, S.-F., Li, J.-J., Yao, R., Liao, M.-Y., Tu, X., Liao, Y.-H., Cheng, X., 2012. Regulatory T cells ameliorate cardiac remodeling after myocardial infarction. Basic Res. Cardiol. 107 (232). https://doi.org/10.1007/s00395-011-0232-6.

Tschabrunn, C.M., Roujol, S., Nezafat, R., Faulkner-Jones, B., Buxton, A.E., Josephson, M.E., Anter, E., 2016. A swine model of infarct-related reentrant ventricular tachycardia: electroanatomic, magnetic resonance, and histopathological characterization. Heart Rhythm. 13, 262–273. https://doi.org/10.1016/j.hrthm.2015.07.030.

van der Spoel, T.I.G., Jansen of Lorkeers, S.J., Agostoni, P., van Belle, E., Gyöngyösi, M., Sluijter, J.P.G., Cramer, M.J., Doevendans, P.A., Chamuleau, S.A.J., 2011. Human relevance of pre-clinical studies in stem cell therapy: systematic review and meta-analysis of large animal models of ischaemic heart disease. Cardiovasc. Res. 91, 649–658. https://doi.org/10.1093/cvr/cvr113.

Varga-Szemes, A., Simor, T., Lenkey, Z., van der Geest, R.J., Kirschner, R., Toth, L., Brott, B.C., Elgavish, A., Elgavish, G.A., 2014. Infarct density distribution by MRI in the porcine model of acute and chronic myocardial infarction as a potential method transferable to the clinic. Int. J. Cardiovasc. Imaging 30, 937–948. https://doi.org/10.1007/s10554-014-0408-x.

Yang, Z., Day, Y.-J., Toufektsian, M.-C., Xu, Y., Ramos, S.I., Marshall, M.A., French, B.A., Linden, J., 2006. Myocardial infarct-sparing effect of adenosine A2A receptor activation is due to its action on CD4+ T lymphocytes. Circulation 114, 2056–2064. https://doi.org/10.1161/CIRCULATIONAHA.106.649244.

Zalutsky, M.R., Garg, P.K., Johnson, S.H., Utsunomiya, H., Coleman, R.E., 1992. Fluorine-18-antimyosin monoclonal antibody fragments: preliminary investigations in a canine myocardial infarct model. J. Nucl. Med. 33, 575–580.

frontiers in Cell and Developmental Biology

ORIGINAL RESEARCH
published: 09 June 2020
doi: 10.3389/fcell.2020.00321

# The Immunomodulatory Signature of Extracellular Vesicles From Cardiosphere-Derived Cells: A Proteomic and miRNA Profiling

*Esther López[1†], Federica Marinaro[1†], María de los Ángeles de Pedro[1], Francisco Miguel Sánchez-Margallo[1,2]*, María Gómez-Serrano[2,3,4]*, Viviane Ponath[5,6], Elke Pogge von Strandmann[5,6], Inmaculada Jorge[2,3], Jesús Vázquez[2,3], Luis Miguel Fernández-Pereira[7], Verónica Crisóstomo[1,2], Verónica Álvarez[1] and Javier G. Casado[1,2]*

[1] Stem Cell Therapy Unit, Jesús Usón Minimally Invasive Surgery Centre, Cáceres, Spain, [2] CIBER de Enfermedades Cardiovasculares (CIBERCV), Madrid, Spain, [3] Laboratory of Cardiovascular Proteomics, Centro Nacional de Investigaciones Cardiovasculares (CNIC), Madrid, Spain, [4] Institute of Molecular Biology and Tumor Research (IMT), Center for Tumor Biology and Immunology (ZTI), Philipps University, Marburg, Germany, [5] Institute for Tumor Immunology, Center for Tumor Biology and Immunology (ZTI), Philipps University, Marburg, Germany, [6] Clinic for Hematology, Oncology, and Immunology, Philipps University, Marburg, Germany, [7] Immunology Department, Hospital San Pedro de Alcántara, Cáceres, Spain

Experimental data demonstrated that the regenerative potential and immunomodulatory capacity of cardiosphere-derived cells (CDCs) is mediated by paracrine mechanisms. In this process, extracellular vesicles derived from CDCs (EV-CDCs) are key mediators of their therapeutic effect. Considering the future applicability of these vesicles in human diseases, an accurate preclinical-to-clinical translation is needed, as well as an exhaustive molecular characterization of animal-derived therapeutic products. Based on that, the main goal of this study was to perform a comprehensive characterization of proteins and miRNAs in extracellular vesicles from porcine CDCs as a clinically relevant animal model. The analysis was performed by identification and quantification of proteins and miRNA expression profiles. Our results revealed the presence of clusters of immune-related and cardiac-related molecular biomarkers in EV-CDCs. Additionally, considering that priming stem cells with inflammatory stimuli may increase the therapeutic potential of released vesicles, here we studied the dynamic changes that occur in the extracellular vesicles from IFNγ-primed CDCs. These analyses detected statistically significant changes in several miRNAs and proteins. Notably, the increase in interleukin 6 (IL6) protein, as well as the increase in mir-125b (that targets IL6 receptor) was especially relevant. These results suggest a potential involvement of EV-CDCs in the regulation of the IL6/IL6R axis, with implications in inflammatory-mediated diseases.

**Keywords: cardiosphere-derived cells, cardiac stem cells, proteomic analyses, quantitative polymerase chain reaction, interferon-γ, extracellular vesicles, miRNA–microRNA, priming**

**Abbreviations:** CDCs, cardiosphere-derived cells; DMEM, Dulbecco's modified Eagle's medium; EV-CDCs, extracellular vesicles from cardiosphere-derived cells; EVs, extracellular vesicles; FDR, false discovery rate; IFNγ, interferon gamma; IFNγ/EV-end MSCs, extracellular vesicles from IFNγ-primed cardiosphere-derived cells; IPA, ingenuity pathway analysis; iTRAQ, isobaric Tags for Relative and Absolute Quantitation; LC-MS/MS, liquid chromatography-tandem mass spectrometry; MSCs, mesenchymal stem cells; Np, number of peptides; PBS, phosphate-buffered saline; PCA, principal component analysis; SBT, Systems Biology Triangle; WSPP, weighted spectrum, peptide, protein.

OPEN ACCESS

**Edited by:**
*Mahmood Khan, The Ohio State University, United States*

**Reviewed by:**
*Lucio Barile, University of Zurich, Switzerland*
*Venkata Naga Srikanth Garikipati, Temple University, United States*

***Correspondence:**
*Francisco Miguel Sánchez-Margallo msanchez@ccmijesususon.com*
*María Gómez-Serrano maria.gomezserrano@imt.uni-marburg.de*

*[†]These authors have contributed equally to this work and share first authorship*

**Specialty section:**
*This article was submitted to Stem Cell Research, a section of the journal Frontiers in Cell and Developmental Biology*

**Received:** *29 November 2019*
**Accepted:** *15 April 2020*
**Published:** *09 June 2020*

**Citation:**
*López E, Marinaro F, de Pedro MÁ, Sánchez-Margallo FM, Gómez-Serrano M, Ponath V, Pogge von Strandmann E, Jorge I, Vázquez J, Fernández-Pereira LM, Crisóstomo V, Álvarez V and Casado JG (2020) The Immunomodulatory Signature of Extracellular Vesicles From Cardiosphere-Derived Cells: A Proteomic and miRNA Profiling. Front. Cell Dev. Biol. 8:321. doi: 10.3389/fcell.2020.00321*

## INTRODUCTION

Cardiac-derived stem cells have been considered as one of the most promising therapeutic options for myocardial regeneration (Zhang et al., 2015; Lader et al., 2017). However, more than 30 top-cited articles have been retracted in the last year (Chien et al., 2019). In the early years of stem cell-based therapies, several disappointing results were reported after the administration of MSCs in myocardial infarction (Miao et al., 2017). Some years later, clinical trials were focused on the administration of cardiac stem cells, and 5 years ago, the clinical trial CADUCEUS (ClinicalTrials.gov Identifier: NCT00893360) opened an optimistic scenario in cardiology, demonstrating the regenerative potential of autologous CDCs (Malliaras et al., 2014).

Nowadays, accumulating pieces of evidence have demonstrated that paracrine mechanisms have a major impact on immunomodulation and tissue regeneration capacity of stem cells (Epstein, 2018). In this sense, exosomes derived from CDCs have demonstrated a therapeutic effect (Ibrahim et al., 2014). This was further confirmed in a clinically relevant animal model of acute and chronic myocardial infarction, where exosomes also demonstrated a relevant clinical outcome (Gallet et al., 2016).

Considering these results, different groups have tried to unravel the molecular mechanisms underlying the therapeutic effects of CDCs and their EVs. In this sense, *in vitro* and *in vivo* studies in murine models using EV-CDCs and their most abundant small RNA constituent, the Y RNA fragment YF1, produced an increase in the anti-inflammatory cytokine IL10 levels, inducing cardioprotection and attenuating hypertension-associated damage (Cambier et al., 2017, 2018).

*In vivo* studies in rats and pigs have also demonstrated that exosomes from CDCs reduce the presence of infiltrating macrophages in the infarcted tissue and mediate macrophage polarization through miRNAs, such as mir-181b (de Couto et al., 2017). Furthermore, the analysis of miRNAs in exosomes from CDCs cultured under hypoxic conditions increased pro-angiogenic miRNAs (mir-126, mir-130a, and mir-210) (Namazi et al., 2018a) as well as helped in the release of exosomes with anti-apoptotic properties (Namazi et al., 2018b).

Taking together the therapeutic effect of CDC-derived EVs and their promising application in different diseases, such as Duchenne muscular dystrophy (Aminzadeh et al., 2018), the first goal of this study was to identify biomarkers, or clusters of biomarkers, that might be associated with the therapeutic efficacy of EV-CDCs. A detailed characterization and classification of the proteome was performed by high-throughput proteomic screening, followed by bioinformatic analyses.

Furthermore, an innovative aspect of our study lies in the characterization of EVs isolated from IFNγ-primed CDCs (IFNγ/EV-CDCs). The idea of priming adult stem cells with IFNγ to increase their immunomodulatory or pro-regenerative effect is not new, and this effect has been experimentally demonstrated in MSCs from umbilical cord blood (Oh et al., 2008) and human adipose tissue (DelaRosa et al., 2009). More recently, several studies have been focused on *in vitro* stimulation protocols to trigger the release of vesicles loaded with therapeutic agents. In this regard, primed MSCs (exposed to hypoxia and serum deprivation) released exosomes with increase in the immunomodulatory potential (Showalter et al., 2019), inflammation-primed MSCs amplified EVs' immunosuppression against T-cell proliferation (Di Trapani et al., 2016), and interleukin-1β-primed MSCs produced exosomes with an increased expression of mir-146a with immunomodulatory properties (Song et al., 2017). It is important to note that the inflammatory priming of MSCs has been recently used for donor selection using miRNAs as biomarkers (Ragni et al., 2019).

Apart from protein characterization and considering that miRNA cargo has a key role in the effector function of EVs (Qiu et al., 2018), this study has been also focused on the characterization of a large panel of miRNAs. These miRNAs were selected for their involvement in cardiac regeneration, immune response, and expression in EVs derived from adult stem cells.

To our knowledge, this is the first study describing the proteomic and miRNA profiling of IFNγ/EV-CDCs from a clinically relevant animal model. Here, we show the identification, quantification, and classification of proteins according to immune-related and cardiac-related categories. The presence of interleukin 6 (IL6) in the proteomic analysis is especially relevant, as well as the expression of different miRNAs targeting interleukin 6 receptor (IL6R). Altogether, these results highlight a critical role for IL6/IL6R axis in the therapeutic effect of EV-CDCs.

## MATERIALS AND METHODS

### Isolation and Characterization of CDCs

CDCs were isolated from cardiac explants of four euthanized healthy large white pigs. This procedure was authorized by the Animal Welfare and Ethics Committee of the Jesús Usón Minimally Invasive Surgery Centre, in accordance with the recommendations outlined by the local government (Junta de Extremadura), and the EU Directive 2010/63/EU of the European Parliament on the protection of animals used for scientific purposes.

Briefly, explants were mechanically disaggregated and subjected to three successive enzymatic digestions with a solution of 0.2% trypsin (Lonza, Basel, Switzerland) and 0.2% collagenase IV (Sigma, St. Louis, MO, United States). Cell culture, isolation, and *in vitro* expansion were performed as previously described by our group (Blázquez et al., 2016).

### IFNγ Treatment, Isolation, and Characterization of EV-CDCs

EV-CDCs were isolated from expanded CDCs at passages 12–15 and 80% confluence. For preconditioning, cells were treated with 3 ng/ml swine IFN gamma Recombinant Protein (IFNγ, catalog number RP0126S-025; Kingfisher Biotech, Saint Paul, MN, United States) for 3 days in standard culture medium. Controls and preconditioned cells were washed with PBS and incubated with DMEM containing 1% insulin–transferrin–selenium (product code: 41400045; Thermo Fisher Scientific, Waltham, MA, United States). This conditioned

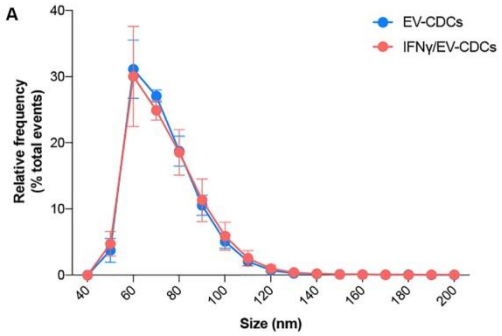


| Final concentration (No. Particles E+08/mL) | Median size (nm) | |
|---|---|---|
| 4.69 ± 1.20 | 71.00 ± 2.19 | EV-CDCs |
| 3.53 ± 1.80 | 72.50 ± 5.45 | IFNγ/EV-CDCs |

**FIGURE 1 |** High-sensitivity flow cytometry analysis of extracellular vesicles derived from CDCs (EV-CDCs) at the single-particle level. **(A)** Histogram of particle size with a bin width of 10 nm for control EV-CDCs (blue, $n = 4$) and EVs isolated from IFNγ-primed CDCs (IFNγ/EV-CDCs) (red, $n = 4$) analyzed by NanoFCM. Data show average (±SD) of the relative frequency of total events from representative technical replicates. **(B)** Concentration and median size values of EV-CDC ($n = 4$) and IFNγ/EV-CDC ($n = 4$) samples characterized in this study. Dilution range was tested for every sample, and two technical replicates were recorded for at least 3,000 and up to 12,000 events. Data show the average (±SD) of group samples.

medium was collected at day 4 and centrifuged first at 1,000 × *g* for 10 min at 4°C, and then 5,000 × *g* for 20 min at 4°C. Supernatants were filtered through a 0.22-μm mesh to eliminate dead cells and debris. The filtrate was used to concentrate the EV-CDCs through a 3-kDa MWCO Amicon® Ultra device (Merck-Millipore, MA, United States) by centrifugation at 4,000 × *g* for 1 h at 4°C. Concentrate samples were recovered from the device and stored at −20°C until further analyses.

The characterization of EV-CDCs was performed by high-throughput proteomic analysis, and proteins were classified following the MISEV2018 guidelines of the International Society for Extracellular Vesicles (ISEV) (Théry et al., 2018). In compliance with ISEV recommendations, EV preparations should be characterized by at least three positive protein markers. Accordingly, a total of 88 proteins from our EV-CDCs were grouped in the following categories: "Transmembrane or GPI-anchored proteins associated to plasma membrane and/or endosomes", "Cytosolic proteins recovered in EVs", "Major components of non-EV co-isolated structures", "Transmembrane, lipid-bound, and soluble proteins associated to other intracellular compartments than PM/endosomes", and "Secreted proteins recovered with EVs". **Supplementary Table S1** shows the classification of proteins according to these categories.

In addition to proteomics, a Flow NanoAnalyzer (NanoFCM INC., United Kingdom) was used for the multiparameter analysis of EV-CDCs samples. The Flow NanoAnalyzer platform enables quantitative and multiparameter analysis of single EVs down to 40 nm, which is distinctively sensitive and high throughput. All experiments were performed in compliance with the NanoFCM system's recommendations (more information on http://www.nanofcm.com/). Briefly, dilution of all samples was individually tested in order to record a total number of events in between 3,000 and 12,000. Concentrated DMEM 1% insulin–transferrin–selenium medium was used for threshold setting and as a blank. Monodisperse silica nanoparticles cocktail (68–155 nm. Cat. No. S16M-Exo; NanoFCM INC.) were employed as the reference to calibrate the size of EVs and polystyrene 210 nm beads (QC Beads; Cat. No. S08210; NanoFCM INC.) at 1:100 dilution for particle concentration estimation. Light scattering was used for the measurement of nanoparticle size and size distributions. The EV size range was set at 40-200 nm. All samples were measured with at least two technical replicates.

## Protein Identification by High-Resolution Liquid Chromatography Coupled to Mass Spectrometry

Protein characterization of EV-CDCs and their comparison with IFNγ/EV-CDCs was performed by a high-throughput multiplexed quantitative proteomic approach according to previously described protocols (Jorge et al., 2009; Navarro and Vázquez, 2009; Bonzon-Kulichenko et al., 2011; Navarro et al., 2014; García-Marqués et al., 2016). Protein extracts were incubated with trypsin using the Filter Aided Sample Preparation (FASP) digestion kit (Expedeon, San Diego, CA, United States), as previously described (Wiśniewski et al., 2011). The resulting peptides were labeled using 8plex-iTRAQ reagents, according to the manufacturer's instructions, and desalted on OASIS HLB extraction cartridges (Waters Corporation, Milford, MA, United States). Half of the tagged peptides were directly analyzed by liquid chromatography tandem mass spectrometry (LC-MS/MS) in different acquisition runs, and the remaining peptides were separated into three fractions using the high pH reversed-phase peptide fractionation kit (Thermo Fisher Scientific). Samples were analyzed using an Easy nLC 1000 nano-HPLC coupled to a Q Exactive mass spectrometer (Thermo Fisher Scientific). Peptides were injected onto a C18 reversed-phase nano-column (75 μm I.D. and 50 cm; Acclaim PepMap100 from Thermo Fisher Scientific) in buffer A [0.1% formic acid (v/v)] and eluted with a 300-min lineal gradient of buffer B [90% acetonitrile, 0.1% formic acid (v/v)], at 200 nl/min. Mass spectrometry (MS) runs consisted of 140,000 enhanced FT-resolution spectra in the 390 to 1,500-m/z wide range and separated 390–700 m/z (range 1), 650–900 m/z (range 2), and 850–1500 m/z (range 3) followed by data-dependent MS/MS spectra of the 15 most intense parent ions acquired along the chromatographic run. HCD fragmentation was performed at 30% of normalized collision energy. A total of 14 MS

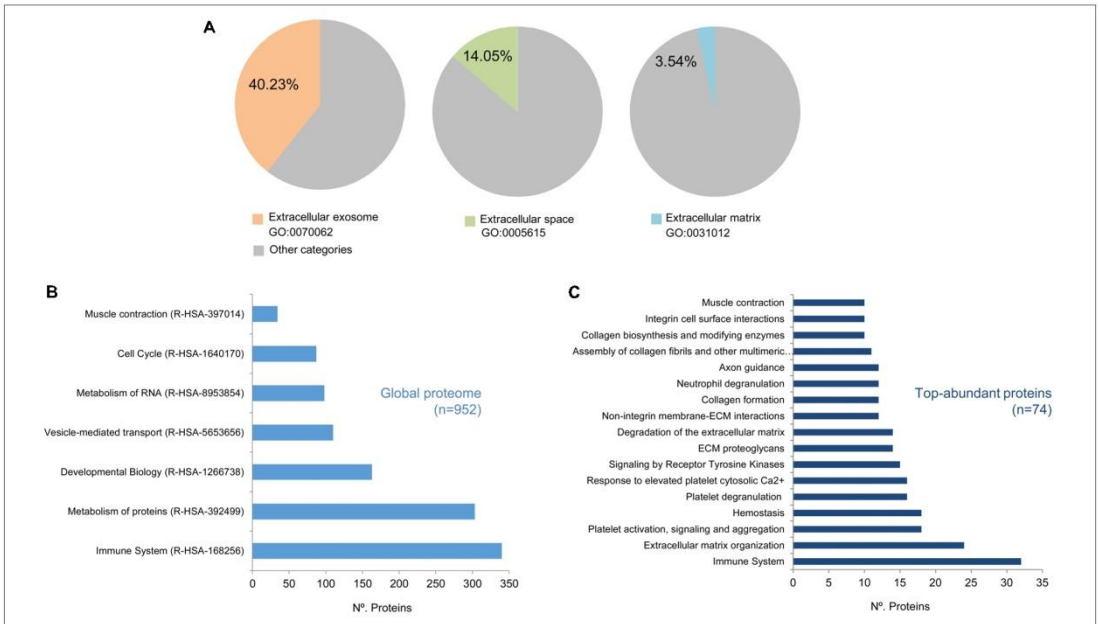


**FIGURE 2 |** High-throughput proteomic analysis on EV-CDCs. Protein extracts from EV-CDCs ($n$ = 4) and IFNγ/EV-CDCs ($n$ = 4) were processed by high-resolution liquid chromatography coupled to tandem mass spectrometry analyses. Those proteins were identified by at least two peptides ($n$ = 952) and were classified according to their biological function using annotations from the Gene Ontology **(A)** or Reactome **(B,C)** databases. **(A)** Pie charts representing the percentage of proteins (% of total pig annotated proteins) classified as *Extracellular exosome* (GO:0070062, orange), *Extracellular space* (GO:0005615, green), and *Extracellular matrix* (GO:0031012, blue) proteins. Significantly enriched Reactome top-level pathways [enrichment value of $p < 0.01$, 5% false discovery rate (FDR)] including **(B)** the global EV-CDC proteome ($n$ = 952, Np ≥ 2) and **(C)** particular most abundant proteins ($n$ = 74, Np ≥ 20).

data sets, eight from unfractionated material and six from the corresponding fractions, were registered with 80 h total acquisition time.

## Peptide Identification, Protein Quantification, and Statistical Analysis

For peptide identification, MS/MS scans were searched as previously described by Binek et al. (2017) using a combined pig and human database (UniProtKB/Swiss-ProtUniProtKB/Swiss-Prot 20147_02 07 Release). *Sus scrofa* gene and protein annotation is not complete; hence, pig proteins were given priority when they shared peptides with human proteins. The Proteome Discoverer 2.1 software (Thermo Fisher) was used for database searching with the following parameters: trypsin digestion with two maximum missed cleavage sites, precursor mass tolerance of 800 ppm, fragment mass tolerance of 0.02 Da. Variable methionine oxidation (+15.994915 Da) and fixed cysteine carbamidomethylation (+57.021 Da), and 8plex-iTRAQ labeling at lysine and N-terminal modification (+304.2054) were chosen.

For peptide identification, the MS/MS spectra were searched using the probability ratio method (Martínez-Bartolomé et al., 2008), and the FDR of peptide identification was calculated based on the search results against a decoy database using the refined method (Navarro and Vázquez, 2009). Peptide and scan counting were performed assuming as positive events those with an FDR equal or lower than 1%.

Quantitative information of 8plex-iTRAQ reporter ions was extracted from MS/MS spectra using an in-house developed program (SanXoT) as already described (Trevisan-Herraz et al., 2019), and protein abundance changes were analyzed using the WSPP statistical model (Navarro et al., 2014).

Briefly, the $\log_2$-ratio of concentration in the two samples being compared, A and B, determined by spectrum $s$ of peptide $p$ derived from protein $q$ in experiment $e$ is expressed as $X_{eqps} = \log_2(A/B)$. The $\log_2$-ratio value associated with each peptide, $X_{eqp}$, is then calculated as a weighted average of the spectra used to quantify the peptide, and the value associated with each protein, $X_{eq}$, is similarly the weighted average of its peptides. In addition, a grand mean, $X_e$, is calculated in each experiment as a weighted average of the protein values. In this study, we calculated $X_e$ by the integration of the four biological replicates, both from control and IFNγ samples, and determined $\log_2$ -($X_e$IFNγ/$X_e$ control). WSSP was applied in the SBT workflow that detects significant protein abundance by performing the protein to category integration and taking into account the protein outliers within each category (García-Marqués et al.,

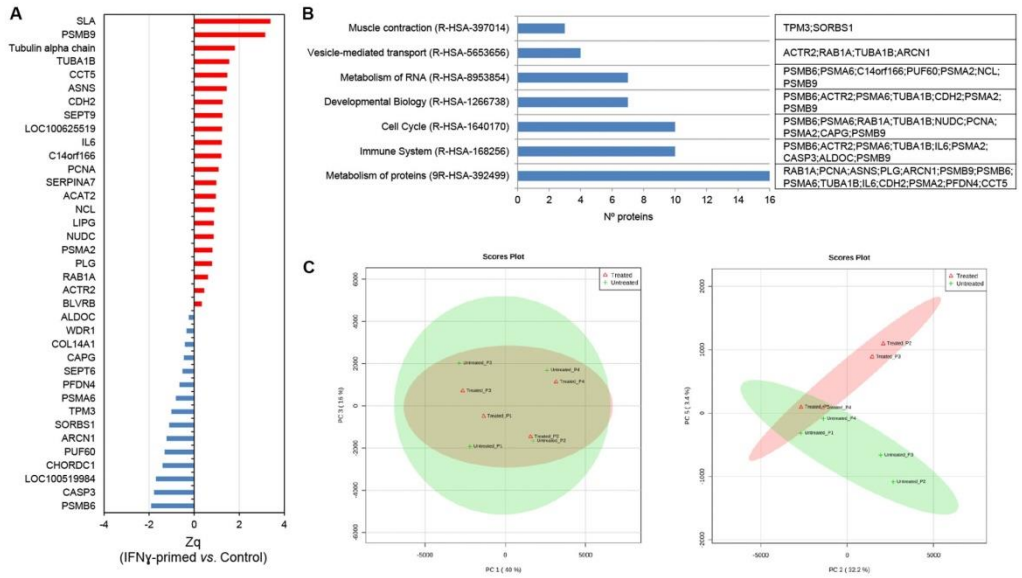


**FIGURE 3 |** Quantitative proteomic analysis of IFNγ/EV-CDCs. **(A)** Quantitative proteomic results. Protein profile changes were analyzed by the WSPP model (Navarro et al., 2014) to identify significantly altered proteins comparing IFNγ/EV-CDCs and EV-CDCs samples. Since a combined database (human and pig) for peptide searching was used, data were integrated at the gene coding level. Protein (gene) values (Zq) are reported as the standardized variable, which is defined as the mean corrected $\log_2$-ratio expressed in units of standard deviation. The protein ratio of each sample was calculated against an internal standard (IS) based on the average of iTRAQ reporters from EV-CDCs control samples. Statistical differences between Zq values of sample groups were evaluated by paired *t*-test. Significant protein abundance change was set at a value of $p < 0.05$. Plots show the integrated Zq values from the sample groups for those proteins significantly up- (red) or down-regulated (blue) in IFNγ/EV-CDCs vs. EV-CDCs. **(B)** Significantly changed proteins were classified and annotated by Reactome in the top level pathways. **(C)** A total of 952 proteins (number of peptides, Np ≥ 2 at 1% FDR) quantified by iTRAQ-based proteomics were subjected to PCA. Left: Score plot for PC1 (40% variance explained) vs. PC3 (16% variance explained). Right: Score plot for PC2 (32.2% variance explained) vs. PC5 (3.4% variance explained). Data display 95% confidence regions. Animal origin ($n = 4$) is indicated on the plots as p1–p4. IFNγ/EV-CDCs (treated) and EV-CDCs (untreated, control) samples are indicated in red and green, respectively.

2016). For that, proteins were previously annotated based on Gene Ontology database (The Gene Ontology Consortium, 2017). The algorithm provides a standardized variable, $Z_q$, defined as the mean-corrected $\log_2$(A/B) expressed in units of standard deviation at the protein level. Student *t*-test was used to compare $Z_q$ values from EV-CDCs and IFNγ/EV-CDCs, and the statistical significance was set at a value of $p < 0.05$. Enrichment analysis of proteins was performed by DAVID functional annotation database[1] (Huang et al., 2009a,b) and Benjamini–Hochberg FDR was used for multiple test correction (FDR < 0.05). For biological data interpretation, proteins were classified using the Reactome pathway database[2] (Fabregat et al., 2018). The mass spectrometry proteomics data have been deposited to the ProteomeXchange Consortium via the PRIDE (Perez-Riverol et al., 2019) partner repository with the dataset identifier PXD016434.

Additionally, PCA was performed on proteins with two or more peptides (number of peptides or Np ≥ 2) quantified after iTRAQ proteomic analysis and at 1% FDR. For PCA, Metaboanalyst software version 4.0[3] (Chong et al., 2018) was used.

To validate the differential expression patterns shown by proteomic analysis, the expression of IL6 in EV-CDCs and IFNγ/EV-CDCs from three pigs was determined using Porcine IL6 DuoSet ELISA kit (R&D SYSTEMS, Minneapolis, MN, United States). EV samples were normalized by total particle concentration measured by NanoFCM system. ELISA protocol was performed following the manufacturer's instructions. IL6 concentrations between EV-CDCs and IFNγ/EV-CDCs were compared through a paired *t*-test.

## miRNAs Expression in EV-CDCs and Target Interactions

Expression of the selected miRNAs in EV-CDCs was evaluated by real-time quantitative PCR (qPCR). Total RNAs from EV-CDCs were isolated using mirVANA miRNA isolation

[1]https://david.ncifcrf.gov/home.jsp

[2]https://reactome.org/

[3]https://www.metaboanalyst.ca/

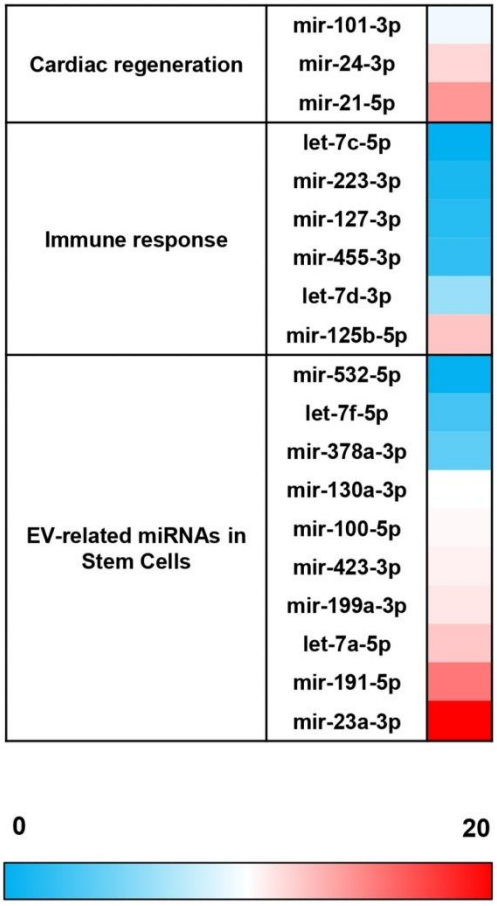


**FIGURE 4 |** miRNA expression abundance in EV-CDCs. miRNA expression was analyzed by qPCR. Total RNA was isolated from EV-CDCs, and the amplification products were analyzed by the $2^{-\Delta Ct}$ method using the most stable miRNAs as endogenous controls. The statistical analysis was performed using a Thermo Fisher Cloud Analysis version 1.1. The figure shows the abundance of miRNAs in terms of $2^{-\Delta Ct}$, from less (blue) to more abundant (red), grouped by our selected miRNA panel.

kit (Applied Biosystems, Foster City, CA, United States), following the manufacturer's protocol for total RNA extraction. Quality and concentration of total RNAs were evaluated by spectrophotometry. For reverse transcription, 10 ng of total RNA was used to synthesize miRNAs' cDNA using TaqMan® Advanced miRNA cDNA Synthesis kit (Cat. No. A28007; Thermo-Fisher Scientific Inc., Waltham, MA, United States), according to the manufacturer's instructions. Five microliters of diluted cDNA (1:100) was then employed as template for qPCR amplification with the TaqMan™ Fast Advanced Master Mix (Cat. No. 4444964; Thermo-Fisher Scientific Inc., Waltham, MA, United States). Commercial TaqMan® Gene Expression Assays probes (Thermo-Fisher Scientific Inc., Waltham, MA, United States) were used, according to the manufacturer's recommendations, to evaluate the relative expression of 44 miRNAs (**Supplementary Table S2**). qPCR reactions were performed in duplicate, and molecular biology-grade water replaced cDNA in no template control reactions. Data from individual TaqMan Assays were acquired by QuantStudio 3 Real-Time PCR System (Applied Biosystems, Thermo Fisher Scientific Inc.) and quantified with the Relative Quantification Application (Thermo Fisher) tool in the Thermo Fisher Cloud software. Levels of each miRNA were normalized to three endogenous controls selected by their score variation. The quantification of miRNAs was performed by $2^{-\Delta Ct}$ calculation. Moreover, EV-CDC and IFNγ/EV-CDC differences were compared through paired *t*-test and $2^{-\Delta\Delta Ct}$ calculation (Livak and Schmittgen, 2001).

The miRNet web tool[4] (Fan and Xia, 2018), that integrates *Sus scrofa* database, was used for miRNA target interaction analysis. Subsequently, Reactome was used to classify the targeted genes according to their biological function.

## *In vitro* Differentiation and Activation of Peripheral Blood Lymphocytes (PBLs), Co-culture With EV-CDCs and IFNγ/EV-CDCs, and Flow Cytometry Analysis

Extracellular vesicles from cardiosphere-derived cells and IFNγ/EV-CDCs were co-cultured *in vitro* with peripheral blood lymphocytes (PBLs) in order to evaluate their immunomodulatory effect. Peripheral blood from one large white pig was collected in EDTA-containing tubes. The blood was diluted in PBS, layered over Histopaque-1077 (Sigma, St. Louis, MO, United States), centrifuged, washed twice with PBS, and seeded in V-bottom 96 well plates at a total density of 200,000 cells per well in RPMI medium. EV-CDCs ($n$ = 4) and IFNγ/EV-CDCs ($n$ = 4) from four different animals were added to different wells at different concentrations (50, 100, and 200 μg/ml), and analyzed at day 3 by flow cytometry. PBLs without EVs were used as negative control.

For flow cytometry analyses, cells were incubated for 30 min at 4°C with fluorescence-labeled porcine monoclonal antibodies against porcine CD4, CD8α, CD14, CD16, CD27, CD45RA, and Swine Leukocyte Antigen class II (SLAII; AbD Serotec, Kidlington, United Kingdom). Cells were then washed and re-suspended in PBS. Analyses were performed in a FACScalibur cytometer (BD Biosciences, San Jose, CA, United States) after acquisition of 10,000 events. Cells were primarily selected using forward and side scatter characteristics, and fluorescence was analyzed using CellQuest software (BD Biosciences). Appropriate isotype-matched negative control antibodies were used in all the experiments. Paired *t*-test

[4]https://www.mirnet.ca/miRNet/home.xhtml

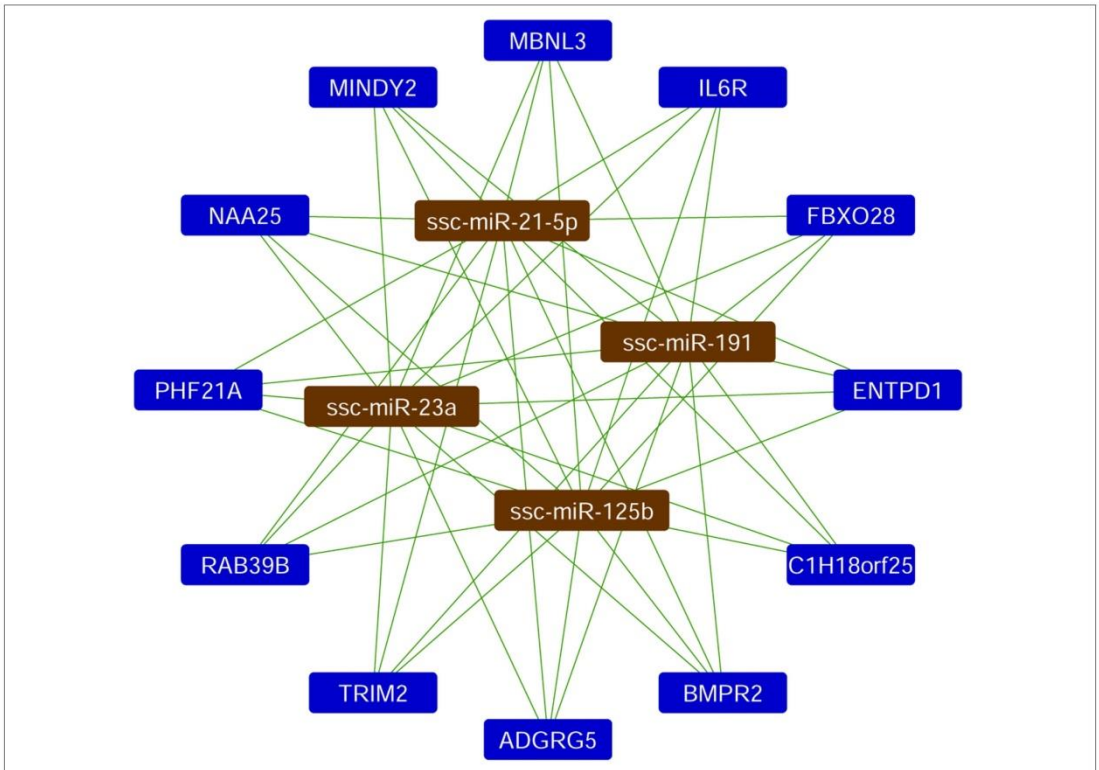


**FIGURE 5 |** Analysis of miRNA target network. The miRNet analysis was performed in the four top-abundant expression analyzed miRNAs. The network shows the interactions with the *Sus scrofa* target genes.

was used to compare each EV dose to the corresponding negative control.

## RESULTS

### High-Throughput Analysis of EV-CDCs and IFNγ/EV-CDCs

Proteomic profiling provides a global view of subcellular fractions, offering a better understanding of protein abundance. Moreover, quantitative proteomics is a valuable technique for a better characterization of biological products, such as stem cells or stem cell-derived vesicles. In this work, the identification and quantification of EV-CDCs proteins were performed by high-throughput quantitative proteomics using multiplex peptide stable isotope labeling, a useful technique for the characterization of these vesicles (Cypryk et al., 2014). Additionally, high-sensitivity flow cytometry analyses on EV-CDCs samples were performed. Sizing profile of the samples demonstrated that preparations were enriched in small EVs (ranging from 40 to 200 nm) (**Figure 1**). Median size and concentration of the released EVs showed no significant differences between EV-CDCs and IFNγ-primed CDCs. Besides, nano-FCM analyses performed on non-concentrated conditioned media did not show significant differences in particle releasing between CDCs and IFNγ/CDCs (*data not shown*).

Unfortunately, protein and gene annotation databases for *Sus scrofa* are not as complete as databases for *Homo sapiens*. Thus, MS/MS scans were searched against a combined pig and human database, giving priority to pig identifications when peptide sequences were identified in both (Binek et al., 2017). Quantification of each protein was calculated at the gene-coding level. Of note, 1,205 protein identifications were retrieved only from the pig database. This combined strategy allowed us to increase the depth of the study, depicting around 30% of the identifications (remarkably, 369 identifications were retrieved exclusively from the human database).

Our study was limited to those proteins represented by at least two peptides (Np $\geq$ 2). Using this cut-off value, a total of $n$ = 952 proteins were analyzed and classified by the DAVID

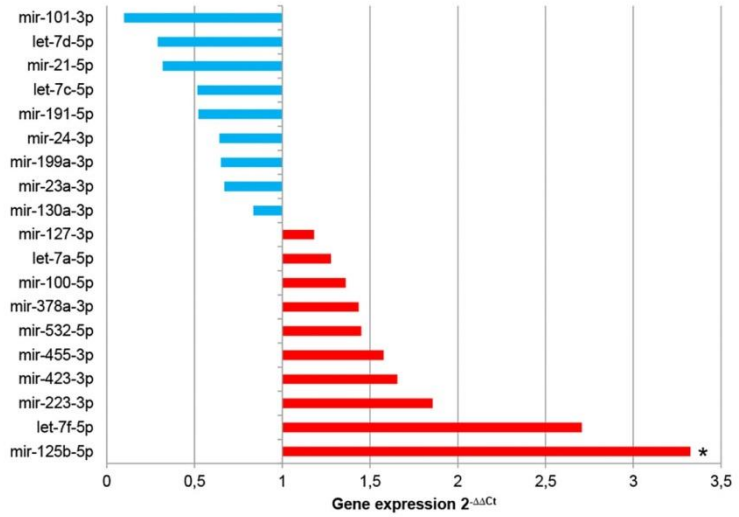


**FIGURE 6 |** Comparative analysis of miRNA expression between EV-CDCs and IFNγ/EV-CDCs. The comparative analysis of miRNA expression was performed by qPCR. Total RNA was isolated from EV-CDCs and IFNγ/EV-CDCs, and amplification products were compared by the $2^{-\Delta\Delta Ct}$ method using the most stable miRNAs as endogenous controls. The statistical analysis was performed using a Thermo Fisher Cloud Analysis version 1.1. Graphs show $2^{-\Delta\Delta Ct}$, $^{*}p \leq 0.05$.

software[5] (**Supplementary Table S3**) (Huang et al., 2009a,b). As shown in **Figure 2A**, this classification revealed that $n = 375$ annotations (40.23% from total annotations) were comprised in the *extracellular exosome* category (GO:0070062), $n = 131$ (14.05%) were comprised in the *extracellular space* category (GO:0005615), and $n = 33$ (3.54%) in the *extracellular matrix* category (GO:0031012). Additionally, the EV-CDCs proteome included 75 proteins from the 100 top-identified proteins in ExoCarta database[6] (Keerthikumar et al., 2016).

The 952 proteins were then classified according to the Reactome database (Fabregat et al., 2018) to elucidate the functional pathways. Reactome is a hierarchically classified database divided in 24 top-level pathways (such as *Metabolism of Proteins*, *Signal Transduction*, *Immune System*) that serve as "roots" for thousands of more specific pathways. **Figure 2B** represents the number of proteins classified in the following top-level pathways: *Metabolism of Proteins* (R-HSA-392499), *Signal Transduction* (R-HSA-162582), *Immune System* (R-HSA-168256), *Cell Cycle* (R-HSA-1640170), *Metabolism* (R-HSA-1430728), *Developmental Biology* (R-HSA-1266738), *Metabolism of RNA* (R-HSA-8953854), *Transport of Small Molecules* (R-HSA-382551), *Vesicle-Mediated Transport* (R-HSA-5653656), and *Muscle Contraction* (R-HSA-397014). It is important to note that the number of proteins included in these top-level pathways is directly correlated with the total amount of proteins pre-classified in the Reactome database. Taking into account this observation, an enrichment analysis of the top-abundant proteins ($n = 74$, Np $\geq 20$) was performed to identify over-represented pathways (enrichment analyses were calculated using a value (−Log) adjusted by Benjamini–Hochberg FDR correction of $p \leq 0.05$). Our analysis for the global EV-CDC proteome ($n = 952$, Np $\geq 2$) demonstrated an enrichment of several top-level pathways: *Immune System*, *Vesicle Transport*, and *Muscle Contraction* (**Figure 2B**). The identification of more than 300 proteins in the *immune system* pathway was especially relevant. Additionally, the enrichment analysis of top-abundant proteins highlighted several subcategories, such as *Neutrophil Degranulation*, *Platelet Activation*, *Signaling and Aggregation*, and *Degradation of the Extracellular Matrix*, among others (**Figure 2C**).

Once the EV-CDC protein cargo was classified, we resorted to a multiplexed quantitative proteomic approach, which offers an extensive dynamic range and great proteome coverage, allowing the simultaneous identification and quantification of hundreds of proteins in the same experiment. This methodology offers an important advantage for the analysis of limited sample amounts (Edwards and Haas, 2016; Jylhä et al., 2018), as in EV-CDC case. In this analysis, protein abundance changes in the IFNγ/EV-CDCs were calculated in relation to the average values of each protein quantified in EV-CDCs (log2-ratio) and expressed in units of standard deviation (Zq). Our results showed that a total of 37 proteins were differentially expressed when EV-CDCs and IFNγ/EV-CDCs were compared ($p \leq 0.05$). Among the significantly increased proteins in IFNγ/EV-CDCs, we identified SLA, PSMB9, Tubulin alpha chain, TUBA1B, CCT5, ASNS, CDH2, SEPT9, COC100625519, IL6, C14orf166, PCNA, SERPINA7, ACAT2, NCL, LIPG, NUDC, PSMA2, PLG, RAB1A,

[5]http://david.abcc.ncifcrf.gov
[6]http://www.exocarta.org/

ACTR2, and BLVRB ($n = 22$). Conversely, among the significantly decreased proteins in IFNγ/EV-CDCs, we identified ALDOC, WDR1, COL14A1, CAPG, SEPT6, PFDN4, PSMA6, TPM3, SORBS1, ARCN1, PUF60, CHORDC1, LOC100519984, CASP3, and PSMB6 ($n = 15$) (**Figure 3A**).

In order to validate these proteomic results, ELISA tests were performed in EV-CDCs and IFNγ/EV-CDCs. Unfortunately, there are few available reagents for swine protein detection, and this study was limited to the validation of IL6 expression in EVs from three pigs by ELISA. According to proteomic analysis, ELISA tests showed an increase in IL6 in IFNγ/EV-CDCs samples: $9.52 \times 10^{-8} \pm 4.68 \times 10^{-8}$ ng/particle in EV-CDCs ($n = 3$) and $1.37 \times 10^{-7} \pm 8.43 \times 10^{-8}$ in IFNγ/EV-CDCs ($n = 3$). It is important to note that the number of samples did not allow a proper statistical analysis, and further validations are required.

The differentially expressed proteins were then classified according to top-level Reactome pathways (**Figure 3B**). Of note, proteins such as PSMB6, ACTR2, PSMA6, TUBA1B, IL6, PSMA2, CASP3, ALDOC, and PSMB9 were classified in the pathway *Immune System* where six of them were found to be increased (PSMB6, ACTR2, TUBA1B, IL6, PSMA2, and PSMB9) and three decreased (PSMA6, CASP3, and ALDOC) in IFNγ/EV-CDCs vs. control EV-CDCs.

Finally, the unsupervised evaluation of proteomic results through principal component analyses (PCA) showed considerable differences between EV-CDCs and IFNγ/EV-CDCs (**Figure 3C**). Additionally, PCA analyses revealed that the distribution of main protein components (PC1 vs. PC2) from the same animal under both treatments behaved similarly, highlighting a distinctive individual EV-CDC proteome background regardless of IFNγ priming (**Figure 3C**, left). Despite individual differences among animals, IFNγ-priming of CDCs caused an important effect on the EV proteome (**Figure 3C**, right).

These proteomic results prompted us to complete the characterization of EV-CDCs and IFNγ/EV-CDCs based on miRNA analysis.

## Real-Time Quantification of miRNAs on EV-CDCs and IFNγ/EV-CDCs

The comparative analysis of miRNAs was performed in a selected panel of cardiac-related miRNAs, immune-related miRNAs, and miRNAs associated to EVs from adult/mesenchymal and stem/stromal cells. The evaluation of miRNAs by qPCR revealed that 25 of 44 total evaluated miRNAs were not expressed (or expressed below the detection limit) in EV-CDCs (**Table 1**). Interestingly, mir-23a-3p, mir-191-5p, mir-21-5p, mir-125b-5p, and let-7a-5p were abundantly expressed ($2^{-\Delta Ct} > 4$) in EV-CDCs (**Figure 4**).

Based on the quantification of miRNAs, the top four most abundant miRNAs in EV-CDCs (mir-23a-3p, mir-191-5p, mir-21-5p, and mir-125b-5p) were further analyzed using a *Sus scrofa* database with the miRNet tool. As shown in **Figure 5**, this analysis revealed that the following genes could be targeted by each of these top-abundant miRNAs: *IL6R*, *ADGRG5*, *C1H18orf25*, *NAA25*, *PHF21A*, *MINDY2*, *RAB39B*, *TRIM2*, *MBNL3*, *ENTPD1*, *FBXO28*, and *BMPR2*.

**TABLE 1 |** Panel of miRNA transcriptomic analysis of extracellular vesicles derived from CDCs (EV-CDCs).

| | miRNAs | | References |
|---|---|---|---|
| | **Expressed in EV-CDCs** | **Not expressed in EV-CDCs** | |
| **Cardiac-related miRNAs** | mir-101-3p<br>mir-21-5p<br>mir-24-3p | mir-133a-5p<br>mir-15b-5p<br>mir-208b-3p<br>mir-29b-3p<br>mir-29c-3p<br>mir-34a-5p<br>mir-34c-5p<br>mir-92a-3p | Bernardo et al., 2015; Chistiakov et al., 2016; Zhu et al., 2016 |
| **Immune-related miRNAs** | let-7c-5p<br>let-7d-3p<br>mir-125b-5p<br>mir-127-3p<br>mir-223-3p<br>mir-455-3p | let-7d-3p<br>mir-126-3p<br>mir-126-5p<br>mir-132-3p<br>mir-137-3p<br>mir-139-3p<br>mir-142-5p<br>mir-145-3p<br>mir-150-5p<br>mir-487b-5p | O'Neill et al., 2011; Marques-Rocha et al., 2015 |
| **EV-MSCs-related miRNAs** | let-7a-5p<br>let-7f-5p<br>mir-100-5p<br>mir-130a-3p<br>mir-191-5p<br>mir-199a-3p<br>mir-23a-3p<br>mir-378a-3p<br>mir-423-3p<br>mir-532-5p | let-7i-3p<br>mir-146a-5p<br>mir-148a-3p<br>mir-148a-5p<br>mir-29a-5p<br>mir-424-5p<br>mir-451a | Eirin et al., 2014; Fernández-Messina et al., 2015; Fafián-Labora et al., 2017; Zhao et al., 2017; Ferguson et al., 2018; Namazi et al., 2018a |

*A deep bibliographic research was performed to select a list of miRNAs for transcriptomic analysis of EV-CDCs. These miRNAs were classified into different groups: cardiac-related miRNAs, immune-related miRNAs, and miRNAs associated with extracellular vesicles from adult/mesenchymal and stem/stromal cells. Real-time quantitative PCR (qPCR) was carried out to analyze miRNA expression. The table shows miRNA classification according to their expression in EV-CDCs.*

The analysis of miRNA expression levels was also used to compare EV-CDCs and IFNγ/EV-CDCs. With this aim, $2^{-\Delta\Delta Ct}$ calculation was performed using EV-CDCs as the "control group." Paired *t*-test analysis demonstrated a significant increase in mir-125b-5p in IFNγ/EV-CDCs. Additionally, this analysis showed an increase (although non-significant) in IFNγ/EV-CDCs of let-7f-5p, mir-223-3p, mir-423-3p, mir-455-3p, mir-532-5p, mir-378a-3p, mir-100-5p, let-7a-5p, and mir-127-3p, together with a non-significant decrease in mir-130a-3p, mir-23a-3p, mir-199a-3p, mir-24-3p, mir-191-5p, let-7c-5p, mir-21-5p, and let-7d-5p, and mir-101-3p (**Figure 6**).

Finally, miRNet analysis was carried out for the differentially expressed mir-125b. This analysis revealed a total of 1,367 interactions with *Sus scrofa* target genes. The 510 genes with more than 150 *experiment scores* were further classified by the webserver g:Profiler in the Reactome pathways (**Figure 7**). This classification showed that 59 targeted genes were categorized in *Metabolism*; 51 targeted genes were categorized in *Immune*

*System*; 22 targeted genes in *Transport of Small Molecules*; 20 targeted genes in *Cytokine Signaling in Immune System*; 17 targeted genes in *Signaling by Interleukins*, 12 targeted genes in *Extracellular Matrix Organization*; and 8 targeted genes in *Toll-Like Receptor 4 (TLR4) Cascade.*

### *In vitro* Effect of EV-CDCs and IFNγ/EV-CDCs in Lymphocyte Differentiation and Activation

The flow cytometry analysis of PBLs co-cultured with EV-CDCs and IFNγ/EV-CDCs was performed on day 3. Activation/differentiation markers were analyzed on CD4+ and CD8+ T-cell subsets. The first analysis was focused on CD45RA and CD27 expression. The percentages of naïve CD8+ T cells (CD45RA+/CD27+) and naïve CD4+ T cells (CD45RA+) were compared in a paired *t*-test using PBLs without EVs as negative controls. Our results demonstrated that EV-CDCs at 200 μg/ml counteracted the *in vitro* differentiation of CD4+ T cells and CD8+ T cells toward effector/memory cells. The percentages of naïve CD4+ T cells and CD8+ T cells were significantly higher than the negative controls (PBLs without EVs) (**Figures 8A,B**, respectively). Similarly, IFNγ/EV-CDCs partially counteracted the *in vitro* differentiation of CD4+ T cells and CD8+ T cells. However, the differences of percentage of naïve T cells between EV-CDCs and IFNγ/EV-CDCs were not statistically significant (**Figures 8A,B**).

The second analysis was focused on Swine Leukocyte Antigen class II (SLAII) expressed in CD4+ and CD8+ T-cell subsets. The surface expression of MHC class II can be defined as an activation marker on T-cell subsets (Revenfeld et al., 2017). In this study, we quantified the percentages of CD4+ SLAII+ T cells and CD8+ SLAII+ T cells on PBLs co-cultured with EVs. Our results showed a significant decrease in activated CD4+ T cells in PBLs co-cultured with EV-CDCs and IFNγ/EV-CDCs at 200 μg/ml (**Figure 8C**). Additionally, PBLs co-cultured with different EVs showed a decrease in CD8+ SLAII+ T cells (**Figure 8D**), although no significant difference was found when EV-CDCs and IFNγ/EV-CDCs were compared.

## DISCUSSION

Large animal models in preclinical research are essential for a successful clinical translation of advanced therapies. Porcine models have been widely used in cardiovascular research to evaluate different administration routes (McCall et al., 2012), stem cell-based therapies (Bolli et al., 2013; Ye et al., 2014; Crisostomo et al., 2015), and to identify biomarkers under controlled experimental conditions (Koudstaal et al., 2014; Blázquez et al., 2018; López et al., 2019). Obviously, the translation of preclinical results to clinical trials is an arduous and challenging process. First, animal models cannot fully represent human disease, where risk factors and comorbidities play important roles. Second, therapeutic products (such as stem cells) are usually different in animal studies and clinical trials. For this reason, an exhaustive analysis of animal-derived therapeutic products is necessary prior to be used in preclinical models.

Nowadays, human-derived EVs from adult stem cells are very well studied; however, animal-derived EVs are poorly characterized, and this characterization is mandatory for a successful translation from animal models to humans. Based on that, the first goal of this study was to perform a deep proteomic and genomic analysis of porcine-derived EV-CDCs. Additionally, we hypothesized that priming *in vitro* cultured CDCs with inflammatory stimuli (such as IFNγ) may increase the therapeutic potential (immunomodulatory and/or pro-regenerative) of released vesicles. This hypothesis is based on previous studies in which primed MSCs with hypoxia, serum deprivation, or inflammatory cytokines produced soluble factors with immunomodulatory and pro-angiogenic properties (Oh et al., 2008; DelaRosa et al., 2009; Di Trapani et al., 2016; Song et al., 2017; Ragni et al., 2019; Showalter et al., 2019).

Our first set of results has demonstrated that *in vitro* culture conditions for CDCs and vesicle isolations were optimal and provided a satisfactory enrichment of EV-CDCs. The nano flow-cytometry analyses led us to demonstrate that our EV-CDC preparations were enriched in small EVs (ranging from 40 to 200 nm). Of note, high-sensitivity nano-flow cytometry has recently demonstrated to be comparable to electron microscopy, notably reducing costs, sample preparation time, and increasing statistical power of analysis (Tian et al., 2018). In our case, although the isolation protocols demonstrated significant enrichment of *extracellular exosome* proteins, this methodology did not exclude the co-purification of extracellular matrix proteins, such as collagens, and other proteins, such as Vinculin, Filamin A, or Fibronectin 1.

The enrichment analysis of top-abundant protein ($Np \geq 20$) in EV-CDCs by Reactome revealed an over-representation in three top-level categories: *Immune System*, *Homeostasis*, and *Muscle Contraction*. This enrichment analysis highlights the hypothetical involvement of proteins and clusters of proteins in the therapeutic effect of these vesicles. For example, HSP90 (classified in *Immune System*) has been found to be involved in the modulation of cardiac ventricular hypertrophy (Tamura et al., 2019), and SPARC (classified in *Hemostasis*) has been found to be involved in the improvement of cardiac function after myocardial infarction (Deckx et al., 2019).

This study was also focused on the comparative analysis between EVs released from *in vitro* cultured CDCs and EVs from IFNγ-primed CDCs. NanoFCM results did not show significant differences between IFNγ-primed and control EV-CDCs in terms of size profile, nor particle concentration (**Figure 1**). The idea of inflammatory priming to increase the immunomodulatory effect of cells has been first described to generate anti-inflammatory cells and, more recently, to generate anti-inflammatory vesicles (Di Trapani et al., 2016; Song et al., 2017; Showalter et al., 2019). Our matched-paired comparative analysis revealed significant differences in 37 proteins and, although many of these proteins may deserve a proper discussion, we focused our interest in some of the proteins categorized in the *Immune System* pathway by Reactome.

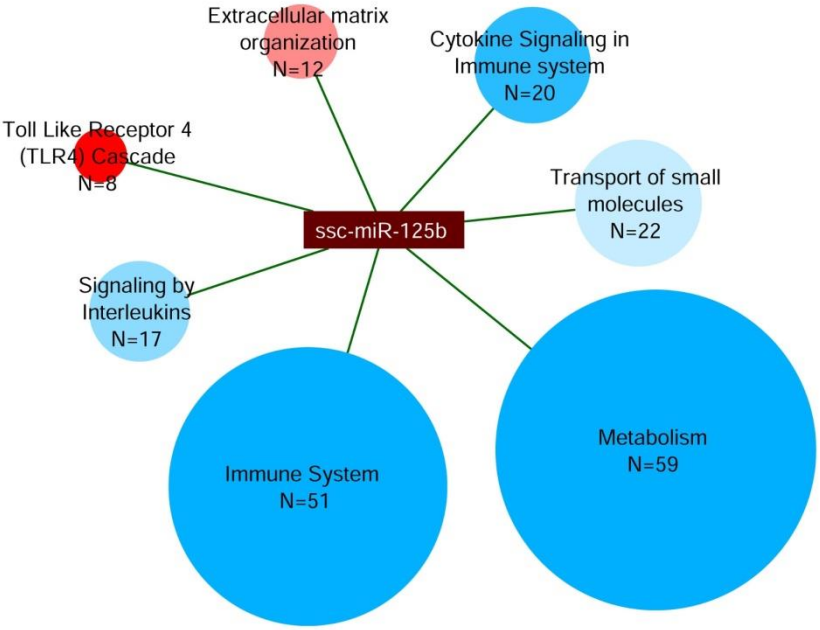


**FIGURE 7 |** Analysis of miRNA target network of mir-125b. The miRNet analysis was performed on the up-regulated mir-125b in IFNγ/EV-CDCs vs. EV-CDCs. Targeted genes were classified by g:Profiler in Reactome pathways. The network shows the interactions between mir-125b and the Reactome terms (ellipses). Ellipsis size represents the number of proteins in each category (N), while their color represents the significance level of each category, from less (blue) to more statistically significant (red).

Our results showed differential expressions in four different proteasome subunits: PSMA2, PSMB9 (increased), PSMB6, and PSMA6 (decreased). It is well known that IFNγ and other pro-inflammatory signals are involved in the formation of immunoproteasome, which is derived from the constitutive proteasome (Strehl et al., 2005). Moreover, the presence of co-purified proteasome subunits has been described in exosomes derived from MSCs, and the authors suggested that these proteasome subunits "*could synergize with other constituents to ameliorate tissue damage*" (Lai et al., 2012).

Apart from proteasome subunits, the comparative analysis showed a significant increase in ACTR2 (actin-related protein 2) in IFNγ/EV-CDCs. This protein is also classified in the *Immune System* pathway (*R-SSC-168256*) and is a key component of the Arp2/3 complex, which is involved in actin polymerization (Suetsugu and Takenawa, 2003). According to Exocarta (Mathivanan and Simpson, 2009), this protein was previously described in very different tissues and cell types. Moreover, Reactome pathway analysis demonstrated that this protein is functionally classified in very different pathways, such as *EPHB-Mediated Forward Signaling*, *Regulation of Actin Dynamics for Phagocytic Cup Formation*, and *RHO GTPases Activate WASPs and WAVEs* (Mathivanan and Simpson, 2009). Unfortunately, it is difficult to elucidate the consequences of this change, and the functional relevance of this protein requires further investigations.

Among the significantly increased proteins in IFNγ/EV-CDCs classified in the *Immune System* pathway, the increase in IL6 is especially relevant. The biological role of this cytokine has always been contradictory. On the one hand, IL6 has been considered as a pro-inflammatory cytokine, participating in the development of coronary heart disease, obesity or diabetes (Fuster and Walsh, 2014). In contrast, it has been associated with the alternative activation of macrophages (Mauer et al., 2014) and with an atheroprotective effect against inflammatory vascular disorders (Elhage et al., 2001; Schieffer et al., 2004). Additionally, it was defined as a "myokine" with anti-inflammatory effects during exercise (Pedersen, 2006). In the context of inflammatory-primed MSCs, IL6 secretion has been considered as an anti-inflammatory molecule (Xing et al., 1998). So, here, we hypothesize that the presence of IL6 in EV-CDCs, as well as the increase in IFNγ/EV-CDCs, may have a therapeutic effect in the control of acute inflammatory responses in myocardial infarction. However, we should also keep in mind that many different studies have experimentally demonstrated that IL6R signaling has an adverse effect and a key role in the development of stroke (IL6R Genetics Consortium Emerging Risk Factors Collaboration et al., 2012; Schuett et al., 2012).

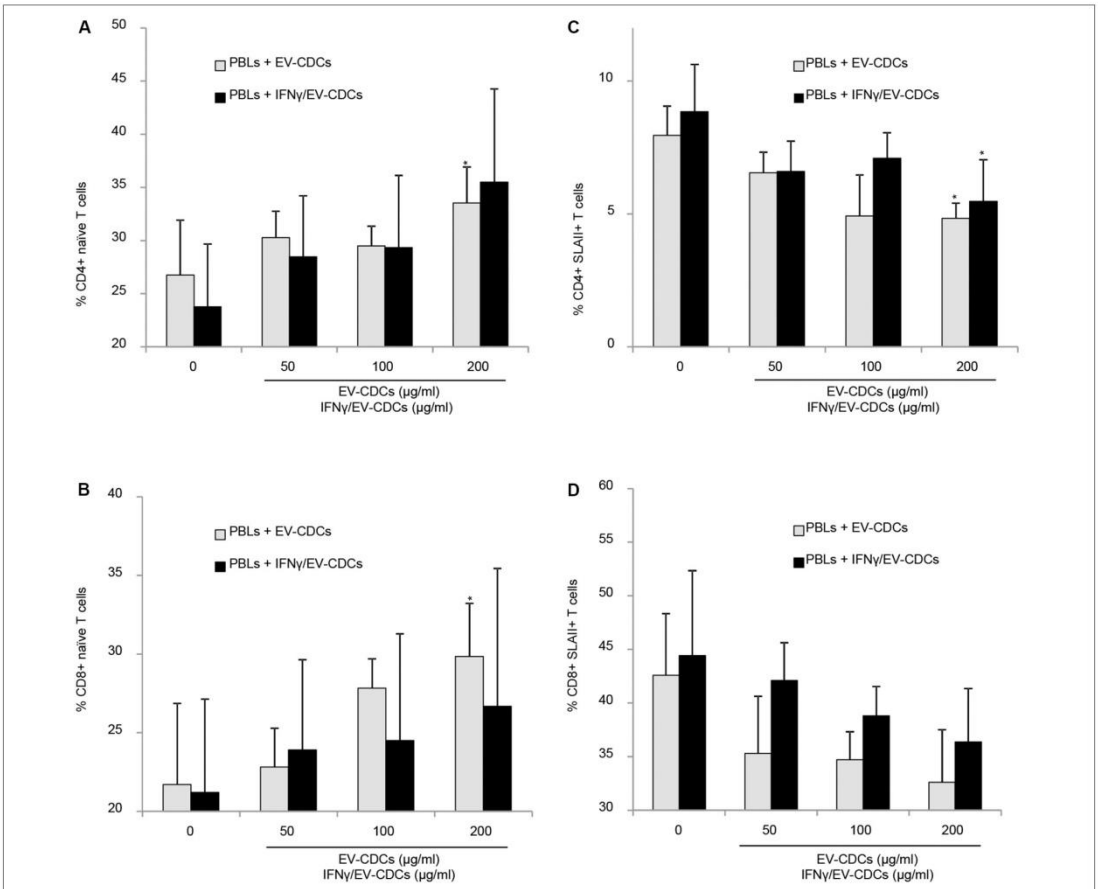


**FIGURE 8 |** *In vitro* peripheral blood lymphocyte (PBL) activation and differentiation assays in co-culture with EV-CDCs and IFNγ/EV-CDCs. Peripheral blood lymphocytes (PBLs) were isolated from blood samples by density gradient and co-cultured with 0 (control), 50, 100, and 200 µg/ml of EV-CDC (gray bars) and IFNγ/EV-CDC (black bars) protein for 3 days. Lymphocyte activation/differentiation was analyzed by flow cytometry on CD4+ **(A,C)** and CD8+ T-cell subpopulations **(B,D)**, using naïve T-cell markers (CD45RA+, CD27+) and activation marker (SLAII). Paired *t*-test was used to compare doses of EVs to negative controls (*$p < 0.05$).

In short, the proteomic analysis of EV-CDCs and IFNγ/EV-CDCs showed a myriad of different proteins with different functions. The bioinformatic and biostatistical analyses in top-abundant proteins (Np $\geq$ 20) suggest the contribution of clusters of proteins in immune-related and cardiac-related process. Once the proteomic profile of vesicles was identified, and considering that the therapeutic effect of exosomes from CDCs is also mediated by miRNAs (Namazi et al., 2018b), here, we performed a quantitative and comparative analysis in a panel of miRNAs. This panel was selected for their association with cardiac regeneration, immune response, and expression in EVs.

In this analysis, mir-23a-3p, mir-191-5p, mir-21-5p, mir-125b-5p, and let-7a-5p were identified as the top-abundant miRNAs in EV-CDCs. Although further experimental validations are needed to assess the impact of these miRNAs, the *in silico* analysis by miRNet revealed that *IL6R* is a target gene of the four top-abundant miRNAs.

The comparative analysis of miRNAs in EV-CDCs and IFNγ/EV-CDCs showed a statistically significant difference in the expression of mir-125b-5p. Previous studies demonstrated that the presence of this miRNA is positively correlated with circulating inflammatory cytokines in patients with chronic obstructive pulmonary disease (Hu et al., 2017). This may explain, at least in part, the increased release of mir-125b-5p under IFNγ stimuli. Additionally, mir-125b has been described as a cardioprotective miRNA that participates in cardiac regeneration after myocardial infarction (Wang et al., 2014), having a key role in the regulation of cardiomyocyte survival during acute myocardial

infarction (Bayoumi et al., 2018). So, the local administration of IFNγ-primed vesicles may have increased therapeutic potential in infarcted patients.

The target network for mir-125b-5p was finally analyzed by miRNet. This analysis identified 1,367 miRNA–gene target interactions. Although this *in silico* study needs to be corroborated by functional studies, the 510 genes with the highest *experiment score* (>150) were categorized by Reactome. Most of the targeted genes were classified in the terms of *Metabolism* and *Immune System*.

Our *in silico* analysis also suggested the hypothetical involvement of the four top-abundant miRNAs in EV-CDCs, including mir-125b-5p (differentially expressed between EV-CDCs and IFNγ/EV-CDCs), in the regulation of the *IL6R* gene. According to the Interleukin-6 Receptor Mendelian Randomisation Consortium, *IL6R* has been considered a target for coronary heart disease: "*IL6R blockade could provide a novel therapeutic approach to prevention of coronary heart disease.*" Nowadays, monoclonal antibodies against IL6R, such as tocilizumab, have been considered as a therapeutic strategy for prevention of coronary heart disease (Carroll, 2018). Based on that, the optimization of *in vitro* culture conditions for EV-CDC isolation may have a therapeutic relevance for targeting IL6R and subsequently in inflammatory-mediated diseases. Moreover, it would be interesting to analyze additional miRNA targeting *IL6R* in EV-CDCs (i.e., mir-34b-3p, mir-124-3p).

Our proteomic and genomic analysis was finally completed with an *in vitro* study to determine the immunomodulatory effect of EV-CDCs and IFNγ/EV-CDCs on lymphocyte subsets. Owing to the limited availability of reagents for this animal model, this study was focused on CD4+ and CD8+ T-cell subsets. The *in vitro* differentiation and activation markers were analyzed in PBLs co-cultured with EV-CDCs and IFNγ/EV-CDCs. Our results demonstrated that EV-CDCs counteracted the *in vitro* differentiation of CD4+ and CD8+ T-cells toward an effector memory phenotype and reduced the expression of activation markers. This result agrees with our previous studies using EVs derived from endometrial stem cells (Álvarez et al., 2018; Marinaro et al., 2019). In fact, similar to Álvarez et al. (2018) here, we could also assert that EV-CDCs have an "*inhibitory effect against CD4+ T cell activation.*" It is important to note that, under these experimental conditions, paired *t*-test did not reveal significant differences between control EV-CDCs and IFNγ/EV-CDCs.

In summary, here, we demonstrate that *in vitro* cultured CDCs release vesicles that are enriched in immune-related proteins. On the one hand, the content of these EV-CDCs can modify *in vitro* the immunomodulatory status of PBLs. Within the protein content, the abundance and the increased expression of IL6 in IFNγ/EV-CDCs are especially relevant. According to preclinical models, which demonstrated an IL6-dependent M2b polarization using IFNγ pre-conditioned MSCs (Philipp et al., 2018), here, we hypothesize that IL6 expression in EV-CDCs may have a key role in the regulation of macrophage and/or neutrophil polarization. On the other hand, miRNA analyses pinpoint the abundance and the differential expression of mir-125b-5p, which target genes involved in the *Immune System* process, including *IL6R*. Altogether, the proteomic and genomic results point out the hypothetical involvement of these vesicles in the regulation of IL6/IL6R axis and, subsequently, in inflammatory-mediated diseases.

## DATA AVAILABILITY STATEMENT

The mass spectrometry proteomics data can be found in ProteomeXchange (http://www.proteomexchange.org/) with identifier PXD016434.

## ETHICS STATEMENT

The animal study was reviewed and approved by the Animal Welfare and Ethics Committee of the Jesús Usón Minimally Invasive Surgery Centre, in accordance with the recommendations outlined by the local government (Junta de Extremadura), and the EU Directive 2010/63/EU of the European Parliament on the protection of animals used for scientific purposes.

## AUTHOR CONTRIBUTIONS

EL, FM, MP, MG-S, FS-M, IJ, and JC conceived and designed the experiments. EL, FM, MP, MG-S, IJ, JV, VÁ, VC, LF-P, VP, EP, and JC performed the experiments and analyzed the data. EL, FM, MG-S, IJ, and JC wrote the manuscript.

## FUNDING

For this study, EL received a funding from the National Institute of Health Carlos III (ISCIII) through the "Sara Borrell" grant (CD19/00048); FM received a MAFRESA S.L. grant (promoted by Jesús Usón Gargallo); a "PFIS" contract (FI19/00041), 2019 Call Strategic Action in Health 2019 (Acción Estratégica en Salud 2017-2020) to MP; Grant "CB16/11/00494" from CIBER-CV (CB16/11/00494) and Ayuda Grupos de Investigación de Extremadura (GR18199) from Consejería de Economía, Ciencia y Agenda Digital (co-funded by European Regional Development Fund – ERDF) to FS-M; a Postgraduate Scholarship for Foreign Studies (Fundación Ramón Areces, XXXI Edition) to MG-S; grants of the Deutsche Forschungsgemeinschaft (KFO325, 1408/14-1, and GRK2573/1) to EP; JV received funding from CIBER-CV (grant "CB16/11/00277"); Spanish Ministry of Science, Innovation and Universities (grants "BIO2015-67580-P" and "PGC2018-097019-B-I00"), ISCIII – Fondo de Investigación Sanitaria

(PRB3 grant "IPT17/0019-ISCIII-SGEFI/ERDF", ProteoRed), Fundació Marató TV3 (grant "122/C/2015"), and "la Caixa" Banking Foundation (project "HR17-00247"); JC received funding by ISCIII through a "Miguel Servet I" grant "MS17/00021" [co-funded by ERDF/European Social Fund (ESF) "A way to make Europe"/"Investing in your future"], the projects "CP17/00021" and "PI18/0911" (co-funded by ERDF/ESF), and by Junta de Extremadura through a "IB16168" grant (co-funded by ERDF/ESF). CNIC is supported by Instituto de Salud Carlos III (ISCIII), Ministerio de Ciencia, Innovación y Universidades (MCNU) and the Pro CNIC Foundation, and it is a Severo Ochoa Center of Excellence (SEV-2015-0505). Cell culture and in vitro studies were performed at the ICTS Nanbiosis (Unit 14, Stem Cell Therapy). The funders had no role in study designs, data collection and analysis, decision to publish, or preparation of the manuscript.

## ACKNOWLEDGMENTS

The authors acknowledge the support, inspiration, and motivation of Dr. Jesús Usón. He spread enthusiasm at work demonstrating exemplary qualities, character, and devotion to scientific research. The authors are thankful for the invisible but hard work of our surgery, anesthesia, and animal facilities technicians. The authors would also like to thank Alejandro, the baby of their co-author VÁ, who made their days happier since he was just an embryo.

## SUPPLEMENTARY MATERIAL

The Supplementary Material for this article can be found online at: https://www.frontiersin.org/articles/10.3389/fcell.2020.00321/full#supplementary-material

## REFERENCES

Álvarez, V., Sánchez-Margallo, F. M., Macías-García, B., Gómez-Serrano, M., Jorge, I., Vázquez, J., et al. (2018). The immunomodulatory activity of extracellular vesicles derived from endometrial mesenchymal stem cells on CD4+ T cells is partially mediated by TGFbeta. *J. Tissue Eng. Regen. Med.* 12, 2088–2098. doi: 10.1002/term.2743

Aminzadeh, M. A., Rogers, R. G., Fournier, M., Tobin, R. E., Guan, X., Childers, M. K., et al. (2018). Exosome-Mediated benefits of cell therapy in mouse and human models of duchenne muscular dystrophy. *Stem Cell Rep.* 10, 942–955. doi: 10.1016/j.stemcr.2018.01.023

Bayoumi, A. S., Park, K. M., Wang, Y., Teoh, J. P., Aonuma, T., Tang, Y., et al. (2018). A carvedilol-responsive microRNA, miR-125b-5p protects the heart from acute myocardial infarction by repressing pro-apoptotic bak1 and klf13 in cardiomyocytes. *J. Mol. Cell. Cardiol.* 114, 72–82. doi: 10.1016/j.yjmcc.2017.11.003

Bernardo, B. C., Ooi, J. Y., Lin, R. C., and McMullen, J. R. (2015). miRNA therapeutics: a new class of drugs with potential therapeutic applications in the heart. *Future Med. Chem.* 7, 1771–1792. doi: 10.4155/fmc.15.107

Binek, A., Fernández-Jiménez, R., Jorge, I., Camafeita, E., López, J. A., Bagwan, N., et al. (2017). Proteomic footprint of myocardial ischemia/reperfusion injury: Longitudinal study of the at-risk and remote regions in the pig model. *Sci. Rep.* 7:12343. doi: 10.1038/s41598-017-11985-5

Blázquez, R., Álvarez, V., Antequera-Barroso, J. A., Báez-Díaz, C., Blanco, V., Maestre, J., et al. (2018). Altered hematological, biochemical and immunological parameters as predictive biomarkers of severity in experimental myocardial infarction. *Vet. Immunol. Immunopathol.* 205, 49–57. doi: 10.1016/j.vetimm.2018.10.007

Blázquez, R., Sánchez-Margallo, F. M., Crisóstomo, V., Báez, C., Maestre, J., Álvarez, V., et al. (2016). Intrapericardial delivery of cardiosphere-derived cells: an immunological study in a clinically relevant large animal model. *PLoS One* 11:e0149001. doi: 10.1371/journal.pone.0149001

Bolli, R., Tang, X. L., Sanganalmath, S. K., Rimoldi, O., Mosna, F., Abdel-Latif, A., et al. (2013). Intracoronary delivery of autologous cardiac stem cells improves cardiac function in a porcine model of chronic ischemic cardiomyopathy. *Circulation* 128, 122–131. doi: 10.1161/CIRCULATIONAHA.112.001075

Bonzon-Kulichenko, E., Pérez-Hernández, D., Núñez, E., Martínez-Acedo, P., Navarro, P., Trevisan-Herraz, M., et al. (2011). A robust method for quantitative high-throughput analysis of proteomes by 18O labeling. *Mol. Cell Proteom.* 10:M110.003335. doi: 10.1074/mcp.M110.003335

Cambier, L., de Couto, G., Ibrahim, A., Echavez, A. K., Valle, J., Liu, W., et al. (2017). Y RNA fragment in extracellular vesicles confers cardioprotection via modulation of IL-10 expression and secretion. *EMBO Mol. Med.* 9, 337–352. doi: 10.15252/emmm.201606924

Cambier, L., Giani, J. F., Liu, W., Ijichi, T., Echavez, A. K., Valle, J., et al. (2018). Angiotensin II-induced end-organ damage in mice is attenuated by human exosomes and by an exosomal Y RNA fragment. *Hypertension* 72, 370–380. doi: 10.1161/HYPERTENSIONAHA.118.11239

Carroll, M. B. (2018). Tocilizumab in the treatment of myocardial infarction. *Mod. Rheumatol.* 28, 733–735. doi: 10.1080/14397595.2018.1427457

Chien, K. R., Frisén, J., Fritsche-Danielson, R., Melton, D. A., Murry, C. E., and Weissman, I. L. (2019). Regenerating the field of cardiovascular cell therapy. *Nat. Biotechnol.* 37, 232–237. doi: 10.1038/s41587-019-0042-1

Chistiakov, D., Orekhov, A., and Bobryshev, Y. (2016). cardiac extracellular vesicles in normal and infarcted heart. *Intern. J. Mol. Sci.* 17:63. doi: 10.3390/ijms17010063

Chong, J., Soufan, O., Li, C., Caraus, I., Li, S., Bourque, G., et al. (2018). MetaboAnalyst 4.0: towards more transparent and integrative metabolomics analysis. *Nucleic Acids Res.* 46, W486–W494. doi: 10.1093/nar/gky310

Crisostomo, V., Baez-Diaz, C., Maestre, J., Garcia-Lindo, M., Sun, F., Casado, J. G., et al. (2015). Delayed administration of allogeneic cardiac stem cell therapy for acute myocardial infarction could ameliorate adverse remodeling: experimental study in swine. *J. Transl. Med.* 13:156. doi: 10.1186/s12967-015-0512-2

Cypryk, W., Öhman, T., Eskelinen, E. L., Matikainen, S., and Nyman, T. A. (2014). Quantitative proteomics of extracellular vesicles released from human monocyte-derived macrophages upon β-Glucan stimulation. *J. Proteom. Res.* 13, 2468–2477. doi: 10.1021/pr4012552

de Couto, G., Gallet, R., Cambier, L., Jaghatspanyan, E., Makkar, N., Dawkins, J. F., et al. (2017). Exosomal MicroRNA transfer into macrophages mediates cellular postconditioning. *Circulation* 136, 200–214. doi: 10.1161/CIRCULATIONAHA.116.024590

Deckx, S., Johnson, D. M., Rienks, M., Carai, P., Van Deel, E., Van der Velden, J., et al. (2019). Extracellular SPARC increases cardiomyocyte contraction during health and disease. *PLoS One* 14:e0209534. doi: 10.1371/journal.pone.0209534

DelaRosa, O., Lombardo, E., Beraza, A., Mancheño-Corvo, P., Ramirez, C., Menta, R., et al. (2009). Requirement of IFN-gamma-mediated indoleamine 2,3-dioxygenase expression in the modulation of lymphocyte proliferation by human adipose-derived stem cells. *Tissue Eng. Part A* 15, 2795–2806. doi: 10.1089/ten.TEA.2008.0630

Di Trapani, M., Bassi, G., Midolo, M., Gatti, A., Kamga, P. T., Cassaro, A., et al. (2016). Differential and transferable modulatory effects of mesenchymal stromal cell-derived extracellular vesicles on T, B and NK cell functions. *Sci. Rep.* 6:24120. doi: 10.1038/srep24120

Edwards, A., and Haas, W. (2016). Multiplexed quantitative proteomics for high-throughput comprehensive proteome comparisons of human cell lines. *Methods Mol. Biol.* 1394, 1–13. doi: 10.1007/978-1-4939-3341-9_1

Eirin, A., Riester, S. M., Zhu, X.-Y., Tang, H., Evans, J. M., O'Brien, D., et al. (2014). MicroRNA and mRNA cargo of extracellular vesicles from porcine adipose

tissue-derived mesenchymal stem cells. *Gene* 551, 55–64. doi: 10.1016/j.gene.2014.08.041

Elhage, R., Clamens, S., Besnard, S., Mallat, Z., Tedgui, A., Arnal, J., et al. (2001). Involvement of interleukin-6 in atherosclerosis but not in the prevention of fatty streak formation by 17beta-estradiol in apolipoprotein E-deficient mice. *Atherosclerosis* 156, 315–320. doi: 10.1016/s0021-9150(00)00682-1

Epstein, J. A. (2018). A time to press reset and regenerate cardiac stem cell biology. *JAMA Cardiol.* 4, 95–96. doi: 10.1001/jamacardio.2018.4435

Fabregat, A., Jupe, S., Matthews, L., Sidiropoulos, K., Gillespie, M., Garapati, P., et al. (2018). The reactome pathway knowledgebase. *Nucleic Acids Res.* 46, D649–D655. doi: 10.1093/nar/gkx1132

Fafián-Labora, J., Lesende-Rodriguez, I., Fernández-Pernas, P., Sangiao-Alvarellos, S., Monserrat, L., Arntz, O. J., et al. (2017). Effect of age on pro-inflammatory miRNAs contained in mesenchymal stem cell-derived extracellular vesicles. *Sci. Rep.* 7:23. doi: 10.1038/srep43923

Fan, Y., and Xia, J. (2018). "miRNet—functional analysis and visual exploration of mirna–target interactions in a network context," in *Computational Cell Biology*, eds L. von Stechow and A. Santos Delgado (New York, NY: Springer), 215–233. doi: 10.1007/978-1-4939-8618-7_10

Ferguson, S. W., Wang, J., Lee, C. J., Liu, M., Neelamegham, S., Canty, J. M., et al. (2018). The microRNA regulatory landscape of MSC-derived exosomes: a systems view. *Sci. Rep.* 8:581. doi: 10.1038/s41598-018-19581-x

Fernández-Messina, L., Gutiérrez-Vázquez, C., Rivas-García, E., Sánchez-Madrid, F., and de la Fuente, H. (2015). Immunomodulatory role of microRNAs transferred by extracellular vesicles: Immunomodulatory role of EV-delivered miRNAs. *Biol. Cell* 107, 61–77. doi: 10.1111/boc.201400081

Fuster, J. J., and Walsh, K. (2014). The good, the bad, and the ugly of interleukin-6 signaling. *EMBO J.* 33, 1425–1427. doi: 10.15252/embj.201488856

Gallet, R., Dawkins, J., Valle, J., Simsolo, E., de Couto, G., Middleton, R., et al. (2016). Exosomes secreted by cardiosphere-derived cells reduce scarring, attenuate adverse remodelling, and improve function in acute and chronic porcine myocardial infarction. *Eur. Heart J.* 38, 201–211. doi: 10.1093/eurheartj/ehw240

García-Marqués, F., Trevisan-Herraz, M., Martínez-Martínez, S., Camafeita, E., Jorge, I., Lopez, J. A., et al. (2016). A Novel Systems-Biology Algorithm for the Analysis of Coordinated Protein Responses Using Quantitative Proteomics. *Mol. Cell Proteomics* 15, 1740–1760. doi: 10.1074/mcp.M115.055905

Hu, H. L., Nie, Z. Q., Lu, Y., Yang, X., Song, C., Chen, H., et al. (2017). Circulating miR-125b but not miR-125a correlates with acute exacerbations of chronic obstructive pulmonary disease and the expressions of inflammatory cytokines. *Medicine* 96:e9059. doi: 10.1097/MD.0000000000009059

Huang, D. W., Sherman, B. T., and Lempicki, R. A. (2009a). Bioinformatics enrichment tools: paths toward the comprehensive functional analysis of large gene lists. *Nucleic Acids Res.* 37, 1–13. doi: 10.1093/nar/gkn923

Huang, D. W., Sherman, B. T., and Lempicki, R. A. (2009b). Systematic and integrative analysis of large gene lists using DAVID bioinformatics resources. *Nat Protoc* 4, 44–57. doi: 10.1038/nprot.2008.211

Ibrahim, A. G.-E., Cheng, K., and Marbán, E. (2014). Exosomes as critical agents of cardiac regeneration triggered by cell therapy. *Stem Cell Rep.* 2, 606–619. doi: 10.1016/j.stemcr.2014.04.006

IL6R Genetics Consortium Emerging Risk Factors Collaboration, Sarwar, N., Butterworth, A. S., Freitag, D. F., Gregson, J., Willeit, P., et al. (2012). Interleukin-6 receptor pathways in coronary heart disease: a collaborative meta-analysis of 82 studies. *Lancet* 379, 1205–1213. doi: 10.1016/S0140-6736(11)61931-4

Jorge, I., Navarro, P., Martínez-Acedo, P., Núñez, E., Serrano, H., Alfranca, A., et al. (2009). Statistical model to analyze quantitative proteomics data obtained by 18O/16O labeling and linear ion trap mass spectrometry: application to the study of vascular endothelial growth factor-induced angiogenesis in endothelial cells. *Mol. Cell Proteom.* 8, 1130–1149. doi: 10.1074/mcp.M800260-MCP200

Jylhä, A., Nättinen, J., Aapola, U., Mikhailova, A., Nykter, M., Zhou, L., et al. (2018). Comparison of iTRAQ and SWATH in a clinical study with multiple time points. *Clin Proteom.* 15:9201. doi: 10.1186/s12014-018-9201-5

Keerthikumar, S., Chisanga, D., Ariyaratne, D., Al Saffar, H., Anand, S., Zhao, K., et al. (2016). ExoCarta: a web-based compendium of exosomal cargo. *J. Mol. Biol.* 428, 688–692. doi: 10.1016/j.jmb.2015.09.019

Koudstaal, S., Lorkeers, S. J., Gho, J. M. I. H., van Hout, G. P., Jansen, M. S., Gründeman, P. F., et al. (2014). Myocardial infarction and functional outcome assessment in pigs. *J. Vis. Exp.* 86:e51269. doi: 10.3791/51269

Lader, J., Stachel, M., and Bu, L. (2017). Cardiac stem cells for myocardial regeneration: promising but not ready for prime time. *Curr. Opin. Biotechnol.* 47, 30–35. doi: 10.1016/j.copbio.2017.05.009

Lai, R. C., Tan, S. S., Teh, B. J., Sze, S. K., Arslan, F., de Kleijn, D. P., et al. (2012). Proteolytic potential of the MSC exosome proteome: implications for an exosome-mediated delivery of therapeutic proteasome. *Intern. J. Proteom.* 2012:971907. doi: 10.1155/2012/971907

Livak, K. J., and Schmittgen, T. D. (2001). Analysis of relative gene expression data using real-time quantitative PCR and the 2(-Delta Delta C(T)) Method. *Methods* 25, 402–408. doi: 10.1006/meth.2001.1262

López, E., Sánchez-Margallo, F. M., Álvarez, V., Blázquez, R., Marinaro, F., Abad, A., et al. (2019). Identification of very early inflammatory markers in a porcine myocardial infarction model. *BMC Vet. Res.* 15:91. doi: 10.1186/s12917-019-1837-5

Malliaras, K., Makkar, R. R., Smith, R. R., Cheng, K., Wu, E., Bonow, R. O., et al. (2014). Intracoronary cardiosphere-derived cells after myocardial infarction: evidence of therapeutic regeneration in the final 1-year results of the CADUCEUS trial (CArdiosphere-Derived aUtologous stem CElls to reverse ventricULar dySfunction). *J. Am. Coll. Cardiol.* 63, 110–122. doi: 10.1016/j.jacc.2013.08.724

Marinaro, F., Gómez-Serrano, M., Jorge, I., Silla-Castro, J. C., Vázquez, J., Sánchez-Margallo, F. M., et al. (2019). Unraveling the molecular signature of extracellular vesicles from endometrial-derived mesenchymal stem cells: potential modulatory effects and therapeutic applications. *Front. Bioeng. Biotechnol.* 7:431. doi: 10.3389/fbioe.2019.00431

Marques-Rocha, J. L., Samblas, M., Milagro, F. I., Bressan, J., Martínez, J. A., and Marti, A. (2015). Noncoding RNAs, cytokines, and inflammation-related diseases. *FASEB J.* 29, 3595–3611. doi: 10.1096/fj.14-260323

Martínez-Bartolomé, S., Navarro, P., Martín-Maroto, F., López-Ferrer, D., Ramos-Fernández, A., Villar, M., et al. (2008). Properties of average score distributions of SEQUEST: the probability ratio method. *Mol. Cell Proteom.* 7, 1135–1145. doi: 10.1074/mcp.M700239-MCP200

Mathivanan, S., and Simpson, R. J. (2009). ExoCarta: a compendium of exosomal proteins and RNA. *Proteomics* 9, 4997–5000. doi: 10.1002/pmic.200900351

Mauer, J., Chaurasia, B., Goldau, J., Vogt, M. C., Ruud, J., Nguyen, K. D., et al. (2014). Signaling by IL-6 promotes alternative activation of macrophages to limit endotoxemia and obesity-associated resistance to insulin. *Nat. Immunol.* 15, 423–430. doi: 10.1038/ni.2865

McCall, F. C., Telukuntla, K. S., Karantalis, V., Suncion, V. Y., Heldman, A. W., Mushtaq, M., et al. (2012). Myocardial infarction and intramyocardial injection models in swine. *Nat. Protoc.* 7, 1479–1496. doi: 10.1038/nprot.2012.075

Miao, C., Lei, M., Hu, W., Han, S., and Wang, Q. (2017). A brief review: the therapeutic potential of bone marrow mesenchymal stem cells in myocardial infarction. *Stem Cell Res. Ther.* 8:242. doi: 10.1186/s13287-017-0697-9

Namazi, H., Mohit, E., Namazi, I., Rajabi, S., Samadian, A., Hajizadeh-Saffar, E., et al. (2018a). Exosomes secreted by hypoxic cardiosphere-derived cells enhance tube formation and increase pro-angiogenic miRNA. *J. Cell. Biochem.* 119, 4150–4160. doi: 10.1002/jcb.26621

Namazi, H., Namazi, I., Ghiasi, P., Ansari, H., Rajabi, S., Hajizadeh-Saffar, E., et al. (2018b). Exosomes Secreted by Normoxic and Hypoxic Cardiosphere-derived Cells Have Anti-apoptotic Effect. *Iran J. Pharm. Res.* 17, 377–385.

Navarro, P., Trevisan-Herraz, M., Bonzon-Kulichenko, E., Núñez, E., Martínez-Acedo, P., Pérez-Hernández, D., et al. (2014). General statistical framework for quantitative proteomics by stable isotope labeling. *J. Proteome Res.* 13, 1234–1247. doi: 10.1021/pr4006958

Navarro, P., and Vázquez, J. (2009). A refined method to calculate false discovery rates for peptide identification using decoy databases. *J. Proteome Res.* 8, 1792–1796. doi: 10.1021/pr800362h

Oh, W., Kim, D. S., Yang, Y. S., and Lee, J. K. (2008). Immunological properties of umbilical cord blood-derived mesenchymal stromal cells. *Cell. Immunol.* 251, 116–123. doi: 10.1016/j.cellimm.2008.04.003

O'Neill, L. A., Sheedy, F. J., and McCoy, C. E. (2011). MicroRNAs: the fine-tuners of Toll-like receptor signalling. *Nat. Rev. Immunol.* 11, 163–175. doi: 10.1038/nri2957

Pedersen, B. K. (2006). The anti-inflammatory effect of exercise: its role in diabetes and cardiovascular disease control. *Essays Biochem.* 42, 105–117. doi: 10.1042/bse0420105

Perez-Riverol, Y., Csordas, A., Bai, J., Bernal-Llinares, M., Hewapathirana, S., Kundu, D. J., et al. (2019). The PRIDE database and related tools and resources in 2019: improving support for quantification data. *Nucleic Acids Res.* 47, D442–D450. doi: 10.1093/nar/gky1106

Philipp, D., Suhr, L., Wahlers, T., Choi, Y.-H., and Paunel-Görgülü, A. (2018). Preconditioning of bone marrow-derived mesenchymal stem cells highly strengthens their potential to promote IL-6-dependent M2b polarization. *Stem Cell. Res. Ther.* 9:286. doi: 10.1186/s13287-018-1039-2

Qiu, G., Zheng, G., Ge, M., Wang, J., Huang, R., Shu, Q., et al. (2018). Mesenchymal stem cell-derived extracellular vesicles affect disease outcomes via transfer of microRNAs. *Stem Cell. Res. Ther.* 9:320. doi: 10.1186/s13287-018-1069-9

Ragni, E., De Luca, P., Perucca Orfei, C., Colombini, A., Viganò, M., Lugano, G., et al. (2019). Insights into inflammatory priming of adipose-derived mesenchymal stem cells: validation of extracellular vesicles-embedded mirna reference genes as a crucial step for donor selection. *Cells* 8:369. doi: 10.3390/cells8040369

Revenfeld, A. L. S., Bæk, R., Jørgensen, M. M., Varming, K., and Stensballe, A. (2017). Induction of a regulatory phenotype in CD3+ CD4+ HLA-DR+ T cells after allogeneic mixed lymphocyte culture; indications of both contact-dependent and -independent activation. *Int. J. Mol. Sci.* 18:1603. doi: 10.3390/ijms18071603

Schieffer, B., Selle, T., Hilfiker, A., Hilfiker-Kleiner, D., Grote, K., Tietge, U. J. F., et al. (2004). Impact of interleukin-6 on plaque development and morphology in experimental atherosclerosis. *Circulation* 110, 3493–3500. doi: 10.1161/01.CIR.0000148135.08582.97

Schuett, H., Oestreich, R., Waetzig, G. H., Annema, W., Luchtefeld, M., Hillmer, A., et al. (2012). Transsignaling of interleukin-6 crucially contributes to atherosclerosis in mice. *Arterioscler. Thromb. Vasc. Biol.* 32, 281–290. doi: 10.1161/ATVBAHA.111.229435

Showalter, M. R., Wancewicz, B., Fiehn, O., Archard, J. A., Clayton, S., Wagner, J., et al. (2019). Primed mesenchymal stem cells package exosomes with metabolites associated with immunomodulation. *Biochem. Biophys. Res. Commun.* 512, 729–735. doi: 10.1016/j.bbrc.2019.03.119

Song, Y., Dou, H., Li, X., Zhao, X., Li, Y., Liu, D., et al. (2017). Exosomal miR-146a contributes to the enhanced therapeutic efficacy of interleukin-1β-primed mesenchymal stem cells against sepsis. *Stem Cells* 35, 1208–1221. doi: 10.1002/stem.2564

Strehl, B., Seifert, U., Krüger, E., Heink, S., Kuckelkorn, U., and Kloetzel, P. M. (2005). Interferon-gamma, the functional plasticity of the ubiquitin-proteasome system, and MHC class I antigen processing. *Immunol. Rev.* 207, 19–30. doi: 10.1111/j.0105-2896.2005.00308.x

Suetsugu, S., and Takenawa, T. (2003). Regulation of cortical actin networks in cell migration. *Int. Rev. Cytol.* 229, 245–286. doi: 10.1016/s0074-7696(03)29006-9

Tamura, S., Marunouchi, T., and Tanonaka, K. (2019). Heat-shock protein 90 modulates cardiac ventricular hypertrophy via activation of MAPK pathway. *J. Mol. Cell. Cardiol.* 127, 134–142. doi: 10.1016/j.yjmcc.2018.12.010

The Gene Ontology Consortium (2017). Expansion of the gene ontology knowledgebase and resources. *Nucleic Acids Res.* 45, D331–D338. doi: 10.1093/nar/gkw1108

Théry, C., Witwer, K. W., Aikawa, E., Alcaraz, M. J., Anderson, J. D., Andriantsitohaina, R., et al. (2018). Minimal information for studies of extracellular vesicles 2018 (MISEV2018): a position statement of the international society for extracellular vesicles and update of the MISEV2014 guidelines. *J. Extracell. Ves.* 7:750. doi: 10.1080/20013078.2018.1535750

Tian, Y., Ma, L., Gong, M., Su, G., Zhu, S., Zhang, W., et al. (2018). Protein profiling and sizing of extracellular vesicles from colorectal cancer patients via flow cytometry. *ACS Nano* 12, 671–680. doi: 10.1021/acsnano.7b07782

Trevisan-Herraz, M., Bagwan, N., García-Marqués, F., Rodriguez, J. M., Jorge, I., Ezkurdia, I., et al. (2019). SanXoT: a modular and versatile package for the quantitative analysis of high-throughput proteomics experiments. *Bioinformatics* 35, 1594–1596. doi: 10.1093/bioinformatics/bty815

Wang, X., Ha, T., Zou, J., Ren, D., Liu, L., Zhang, X., et al. (2014). MicroRNA-125b protects against myocardial ischaemia/reperfusion injury via targeting p53-mediated apoptotic signalling and TRAF6. *Cardiovasc. Res.* 102, 385–395. doi: 10.1093/cvr/cvu044

Wiśniewski, J. R., Ostasiewicz, P., and Mann, M. (2011). High recovery FASP applied to the proteomic analysis of microdissected formalin fixed paraffin embedded cancer tissues retrieves known colon cancer markers. *J. Proteome Res.* 10, 3040–3049. doi: 10.1021/pr200019m

Xing, Z., Gauldie, J., Cox, G., Baumann, H., Jordana, M., Lei, X. F., et al. (1998). IL-6 is an antiinflammatory cytokine required for controlling local or systemic acute inflammatory responses. *J. Clin. Invest.* 101, 311–320. doi: 10.1172/JCI1368

Ye, L., Chang, Y.-H., Xiong, Q., Zhang, P., Zhang, L., Somasundaram, P., et al. (2014). Cardiac repair in a porcine model of acute myocardial infarction with human induced pluripotent stem cell-derived cardiovascular cells. *Cell Stem Cell* 15, 750–761. doi: 10.1016/j.stem.2014.11.009

Zhang, Y., Mignone, J., and MacLellan, W. R. (2015). Cardiac regeneration and stem cells. *Physiol. Rev.* 95, 1189–1204. doi: 10.1152/physrev.00021.2014

Zhao, A., Xie, H., Lin, S., Lei, Q., Ren, W., Gao, F., et al. (2017). Interferon-γ alters the immune-related miRNA expression of microvesicles derived from mesenchymal stem cells. *J. Huazhong Univer. Sci. Technol.* 37, 179–184. doi: 10.1007/s11596-017-1712-1

Zhu, K., Liu, D., Lai, H., Li, J., and Wang, C. (2016). Developing miRNA therapeutics for cardiac repair in ischemic heart disease. *J. Thorac. Dis.* 8, E918–E927. doi: 10.21037/jtd.2016.08.93

**Conflict of Interest:** The authors declare that the research was conducted in the absence of any commercial or financial relationships that could be construed as a potential conflict of interest.

*Copyright © 2020 López, Marinaro, de Pedro, Sánchez-Margallo, Gómez-Serrano, Ponath, Pogge von Strandmann, Jorge, Vázquez, Fernández-Pereira, Crisóstomo, Álvarez and Casado. This is an open-access article distributed under the terms of the Creative Commons Attribution License (CC BY). The use, distribution or reproduction in other forums is permitted, provided the original author(s) and the copyright owner(s) are credited and that the original publication in this journal is cited, in accordance with accepted academic practice. No use, distribution or reproduction is permitted which does not comply with these terms.*

Stem Cell Reviews and Reports (2020) 16:612–625
https://doi.org/10.1007/s12015-019-09926-y

# The Intrapericardial Delivery of Extracellular Vesicles from Cardiosphere-Derived Cells Stimulates M2 Polarization during the Acute Phase of Porcine Myocardial Infarction

Esther López[1] · Rebeca Blázquez[1,2] · Federica Marinaro[1] · Verónica Álvarez[1] · Virginia Blanco[1,2] · Claudia Báez[1,2] · Irene González[1] · Ana Abad[1] · Beatriz Moreno[1] · Francisco Miguel Sánchez-Margallo[1,2] · Verónica Crisóstomo[1,2] · Javier García Casado[1,2]

Published online: 21 December 2019
© The Author(s) 2019, corrected publication 2020

**Abstract**
Acute myocardial infarction triggers a strong inflammatory response in the affected cardiac tissue. New therapeutic tools based on stem cell therapy may modulate the unbalanced inflammation in the damaged cardiac tissue, contributing to the resolution of this pathological condition. The main goal of this study was to analyze the immunomodulatory effects of cardiosphere-derived cells (CDCs) and their extracellular vesicles (EV-CDCs), delivered by intrapericardial administration in a clinically relevant animal model, during the initial pro-inflammatory phase of an induced myocardial infarction. This effect was assessed in peripheral blood and pericardial fluid leukocytes from infarcted animals. Additionally, cardiac functional parameters, troponin I, hematological and biochemical components were also analyzed to characterize myocardial infarction-induced changes, as well as the safety aspects of these procedures. Our preclinical study demonstrated a successful myocardial infarction induction in all animals, without any reported adverse effect related to the intrapericardial administration of CDCs or EV-CDCs. Significant changes were observed in biochemical and immunological parameters after myocardial infarction. The analysis of peripheral blood leukocytes revealed an increase of M2 monocytes in the EV-CDCs group, while no differences were reported in other lymphocyte subsets. Moreover, arginase-1 (M2-differentiation marker) was significantly increased in pericardial fluids 24 h after EV-CDCs administration. In summary, we demonstrate that, in our experimental conditions, intrapericardially administered EV-CDCs have an immunomodulatory effect on monocyte polarization, showing a beneficial effect for counteracting an unbalanced inflammatory reaction in the acute phase of myocardial infarction. These M2 monocytes have been defined as "pro-regenerative cells" with a pro-angiogenic and anti-inflammatory activity.

**Keywords** Extracellular vesicles · Cardiosphere-derived cells · Acute myocardial infarction · Intrapericardial administration · Inflammation

## Introduction

Cardiac heart failure is one of the main death causes worldwide [1]. In acute myocardial infarction (AMI), the cardiac tissue injury triggers a strong inflammatory process where immune cells and soluble mediators are involved. This inflammatory process has been extensively studied, characterized and sequenced. An initial pro-inflammatory phase occurs at days 1–3 after myocardial infarction, and is followed by an anti-inflammatory phase at days 4–7, to achieve tissue repair [2]. During the pro-inflammatory phase, cell death and tissue injury trigger the release of "danger signals" (i.e. activation of complement cascade, reactive oxygen species production, Toll-like receptor activation), which induce cytokine/chemokine production for the recruitment of leukocytes, such

Esther López and Rebeca Blázquez equally contributed and should be regarded as co-first authors.
Verónica Crisóstomo and Javier García Casado are co-senior authors

**Electronic supplementary material** The online version of this article (https://doi.org/10.1007/s12015-019-09926-y) contains supplementary material, which is available to authorized users.

✉ Francisco Miguel Sánchez-Margallo
msanchez@ccmijesususon.com

[1] Stem Cell Therapy Unit, Jesus Uson Minimally Invasive Surgery Centre, Cáceres, Spain

[2] CIBER de Enfermedades Cardiovasculares (CIBERCV), Madrid, Spain

as neutrophils, monocytes, and T cells, to the myocardial infarction area. After myocardial infarction, the bone marrow initiates the activation of hematopoietic cells and leukocyte production which are mobilized into the blood [3].

Nowadays, many different anti-inflammatory therapies, aimed to modulate an adverse and unbalanced inflammation, are under evaluation [4]. Among them, cell therapy has become a valuable tool since stem cells have proved to exert an immunomodulatory effect on different immune mediated diseases [5, 6]. In relation to myocardial infarction, the intracoronary delivery of cardiosphere-derived cells (CDCs) has already been found to attenuate myocardial inflammation in a murine model of autoimmune myocarditis [7], and to reverse inflammation and fibrosis in hypertensive rats [8]. The intramyocardial injection of CDCs in a myocardial porcine model have demonstrated an inverse correlation between doses and engraftment, together with an increase of left ventricular ejection fraction [9]. Few years later, these authors could also demonstrate that cardioprotection was safe and effective using $7.5 \times 10^6$ to $10 \times 10^6$ allogeneic CDCs [10]. More recently, exosomes secreted by CDCs were evaluated in an acute and chronic porcine myocardial infarction models, demonstrating that intramyocardial administration (but not intracoronary) decreased scarring, and improved cardiac function [11]. These exosomes have also demonstrated an immunomodulatory effect [12], an anti-apoptotic protection under in vitro conditions [13], as well as favorable effects on hearts from aged rats [14].

In stem cell-based therapies, the administration routes are key factors for the treatment success. Our previous studies have demonstrated that the intrapericardial administration of mesenchymal stem/stromal cells (MSCs) in a porcine model of myocardial infarction provided an optimal retention and implantation of MSCs in the infarcted heart [15]. A similar work using CDCs showed that these cells exert changes in pericardial fluid lymphocytes after intrapericardial administration [16]. Based on these observations, here we hypothesize that CDCs and/or their extracellular vesicles (EV-CDCs) may counterbalance an exacerbated inflammatory reaction during the acute phase of myocardial infarction.

For understanding the immunological mechanisms involved in AMI after the therapies, the present study has been carried out in a porcine model. This clinically relevant animal model has been widely accepted by researchers and regulatory agencies as a valuable tool in the evaluation of safety aspects and efficacy of new therapeutic products [17].

Our preclinical study has demonstrated a successful myocardial infarction induction in all animals and no adverse effect was seen for intrapericardial administration of CDCs or EV-CDCs. As expected, significant changes were observed in biochemical and immunological parameters after myocardial infarction. A complete and exhaustive analysis of peripheral blood leukocytes revealed an increase of M2 monocytes at 24 h after EV-CDCs administration, while no differences were reported in other lymphocyte subsets. Moreover, arginase-1 (a classical M2-differentiation marker) was significantly increased in pericardial fluid at 24 h after EV-CDCs administration.

In summary, here we demonstrate that, in our experimental conditions, intrapericardially administered EV-CDCs have an immunomodulatory effect, enhancing M2 monocyte polarization. These M2 monocytes have been defined as "pro-regenerative cells" with a pro-angiogenic and anti-inflammatory activity which may counteract an unbalanced inflammatory reaction in the acute phase of myocardial infarction.

## Methods

### Animals and Experimental Design

Female Large White pigs ($n = 18$), weighting $36.68 \pm 5.18$ kg at the beginning of the study, were used for all experimental procedures. Fifteen animals were randomly divided into three groups: Placebo ($n = 5$), CDCs (n = 5), and EV-CDCs (n = 5). Three additional animals were used to evaluate the effect of EV-CDCs on the pericardial fluid leukocytes. The time points for myocardial infarction induction, blood sampling, magnetic resonance imaging, and intrapericardial administration are schematized in Fig. 1. Animals were housed in the animal facility of the Jesús Usón Minimally Invasive Surgery Centre. The final destination of all animals was the euthanasia, performed with an intravenous administration of 2 mmol/kg of KCl, applied under deep anesthesia. The experimental procedures were validated by the Ethics Committee on Animal Experiments of the Jesús Usón Minimally Invasive Surgery Centre, in accordance with the recommendations outlined by the local government (Junta de Extremadura), and the EU Directive 2010/63/EU of the European Parliament on the protection of animals used for scientific purposes.

### Isolation and Characterization of CDCs

CDCs were isolated from cardiac explants of experimental Large White pigs. Briefly, explants were mechanically disaggregated and digested three times with a solution of 0.2% trypsin (Lonza, Basel, Switzerland), and 0.2% collagenase IV (Sigma, St. Louis, MO). The cell culture isolation and in vitro expansion were performed as previously described by our group [16].

### Isolation and Characterization of EV-CDCs

EV-CDCs were obtained from cell lines cultured at a confluence of 80% at passages 12–15. Culture medium (DMEM with 10% Penicillin/Streptomycin, and 10% Fetal Bovine

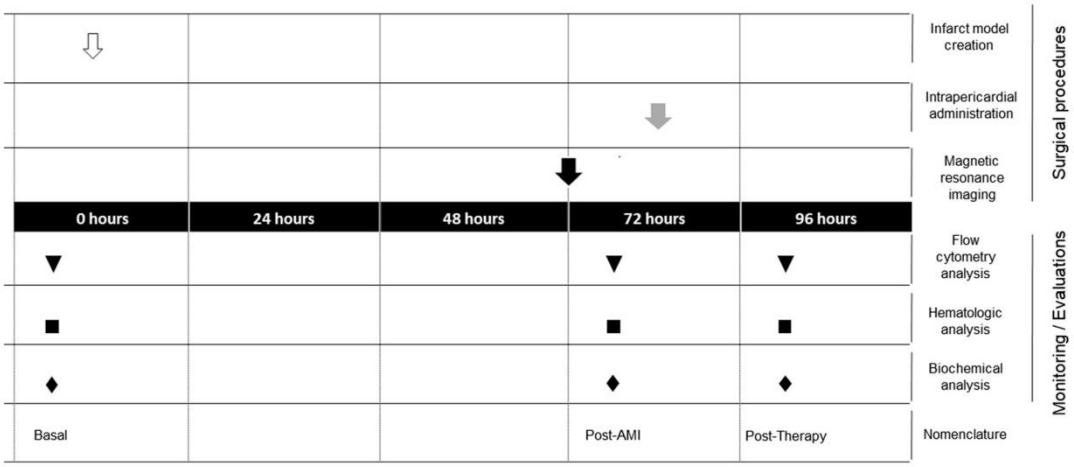


**Fig. 1** Experimental design. At day 0, infarct model was created (white arrow). At 72 h, magnetic resonance imaging was performed (black arrow). Placebo, EV-CDCs or CDCs were intrapericardially administered at 72 h (grey arrow). Blood samples were collected at day 0 (Basal), 72 h (post-AMI) and 24 h after intrapericardial administration (post-therapy). Blood samples were used for flow cytometry analysis (triangles), hematology (squares) and biochemical analysis (rhombus)

Serum) was replaced by exosome isolation medium (1% insulin-transferrin-selenium in DMEM with 10% Penicillin/Streptomycin). The supernatants were collected at day 4 and centrifuged in two steps: first at 1000 x g for 10 min, and then 5000 x g for 20 min at 4 °C. Supernatants were filtered through a 0.22 μM filter to eliminate dead cells and debris, and ultra-filtered through a 3 kDa MWCO Amicon® Ultra device (Merck-Millipore, MA, USA). EV-CDCs were firstly characterized by Field-Flow Fractionation carried out with a regenerated cellulose membrane (cut off 10 kDa), and with a spacer of 350 mm. Finally, a high throughput proteomic analysis was performed on EV-CDCs using high-resolution liquid chromatography coupled to mass spectrometry-based proteomic analyses, as described in our previous studies [18, 19]. The detected proteins were classified according to the Gene Ontology term GO:0070062 (*Extracellular exosome*). For the intrapericardial administrations, protein quantifications were performed by Bradford assay, and the resulting protein concentration was diluted in Sodium Chloride 0.9% (*w*/*v*) to 1.832 mg/ml. Finally, 9.16 mg of exosomal proteins were intrapericardially administered in 5 mL of Sodium Chloride 0.9%.

## Myocardial Infarction Model Creation

The animal model was created by a closed chest reperfused myocardial infarction technics, as previously described [20]. Briefly, animals were anesthetized and subjected to coronary angiograms in the 40° left anterior oblique projection. The occlusion of blood flow to the distal myocardium was carried out with the insertion of a coronary balloon catheter (typically 3 mm × 8 mm, Ryujin Plus, Terumo, Tokio, Japan) over a 0.014″ coronary guidewire until reach the origin of the first diagonal branch. The balloon was inflated for 90 min and after balloon deflation, coronary patency was evaluated by another angiogram. Animals were monitored during the procedure, evaluating different parameters like blood pressure, electrocardiogram, $O_2$ saturation, and end tidal $CO_2$. Lidocaine (Lidocaine, Braun Medical, Barcelona, Spain) was perfused during the procedure at a rate of 1 mg/kg/h and heparin (Heparina Rovi 5%, Laboratorios farmacéuticos Rovi, Madrid, Spain) was intravenously injected at 150 UI/kg before of the intervention.

## Cardiac Magnetic Resonance

Cardiac Magnetic Resonance studies (Intera 1.5 T, Philips Medical Systems. Best, The Netherlands) were acquired at 72 h after myocardial infarction. A dedicated cardiac coil was used. Acquisitions were performed in the intrinsic cardiac view: short axis, two- and four-chamber views. For morphological and functional studies, gradient echo cine exams, including the entire left ventricle, were performed during apneas. Scar sizes were computed in short axis delayed enhancement studies performed 5–15 min after contrast administration at a dose of 0.2 mmol/kg of gadolinium (Gadobutrol. Gadovist 1.1 mmol/l, Bayer Schering Pharma AG, Berlin, Germany) with a breath-hold 3D gradient-echo inversion-recovery sequence. Typical inversion time determined with the Look and Locker sequence was 150 to 190 ms to obtain the best myocardial nulling. A slice thickness of 8 mm without gap, a FOV: 330 × 330 × 50, matrix: 224 × 200, flip angle: 15°

and TR/TE: 4.9/1.67 were used for imaging. Post-processing was done using the scanner's own software (IntelliSpace Portal 7.0.2.20700 Philips Medical Systems, Best, The Netherlands) by a blinded researcher. Automatically detected endo and epicardial borders were carefully reviewed, and corrected when necessary to compute left ventricular function in terms of indexed End Diastolic (EDVi) and Systolic (ESVi) volumes and Ejection Fraction (% LVEF). To calculate infarct size, the percentage of left ventricular mass in normal conditions, and in the infarcted myocardium were identified (% Infarct) in short axis delayed enhancement views, with dark areas corresponding to hemorrhage or microvascular obstruction included.

### Intrapericardial Administration

72 h after myocardial infarction induction, animals were premedicated with diazepam 0.3 mg/kg and ketamine 10 mg/kg intramuscularly. Anesthesia induction was achieved with 2 mg/kg of propofol and maintained with 1.8%–2% sevofluorane. Auricular vein were catheterized to perfuse normal saline to preserve hydration. During this procedure, animals' parameters were monitored, as in the previous section.

A total of 5 animals received an intrapericardial injection of $30 \times 10^6$ allogeneic CDCs in 5 ml of sodium chloride 0.9% (w/v). Animals treated with EV-CDCs (n = 8) received a total of 9.16 mg EV-CDCs proteins per animal in 5 ml of sodium chloride 0.9% (w/v). The placebo group (n = 5) received 5 ml of sodium chloride 0.9% (w/v). The administration was achieved via mini-thoracotomy and placebo, EV-CDCs, or CDCs were administered using an Abbocath®-T 20G catheter (Hospira, Lake Forest, IL, USA). The incision was closed layer by layer and the animals were let to recover.

### Troponin I Analysis

Blood samples were collected in EDTA tubes, and used for Troponin I analyses at 72 h after myocardial infarction. Concentration of Troponin I was quantified in terms of μg/l by immunoassay (AQT90 Flex, Radiometer Iberica SL, Madrid, Spain).

### Biochemical Analyses

Biochemical analyses of peripheral blood samples were performed in the clinical analyzer Metrolab 2300 (Metrolab S.A., Buenos Aires, Argentina). The following serum parameters were determined: bilirubin, creatinine, glucose, urea, gamma-glutamyl transferase (GGT), glutamic oxaloacetic transaminase (GOT), glutamic pyruvic transaminase (GPT), and total proteins.

### Hematological Analysis

Hematological analyses were assessed in an automatic hematology analyzer (Mindray BC-5300 Vet, Hamburg, Germany). The blood parameters determined were: white blood cell count (WBC), neutrophils, lymphocytes, monocytes, eosinophils, basophils, red blood cell count (RBC), hemoglobin concentration (HGB), hematocrit (HCT), mean corpuscular volume (MCV), mean corpuscular hemoglobin (MCH), mean corpuscular hemoglobin concentration (MCHC), red blood cell distribution width coefficient of variation (RDW-CV), red blood cell distribution width standard deviation (RDW-SD), platelets (PLT), mean platelet volume (MPV), platelet distribution width (PDW), and plateletcrit (PCT).

### Phenotypic Characterization of Peripheral Blood Leukocytes

Peripheral blood leukocytes were isolated by centrifugation over Histopaque-1077 (Sigma, St. Louis, MO), and washed twice with PBS. Cells were labelleded with fluorescent-dye anti-porcine monoclonal antibodies for the following surface molecules: CD4 (clone 74–12-4, BD Pharmingen, CA, USA), CD8α (clone 76–2-11, BD Pharmingen, CA, USA), CD14 (clone TÜK4, Bio-Rad, CA, USA), CD16 (clone G7, Bio-Rad, CA, USA), CD27 (clone B30C7, Bio-Rad, CA, USA), CD45RA (clone MIL13, Bio-Rad, CA, USA), CD107a (clone 4E9/11, Bio-Rad, CA, USA), CD163 (clone 2A10/11, BD Pharmingen, CA, USA), and SLA-II (clone 2E9/13, Bio-Rad, CA, USA).

$2 \times 10^5$ cells were incubated for 30 min at 4 °C with adequate concentrations of monoclonal antibodies and the washed and re-suspended in PBS. The analysis was performed in a FACScalibur cytometer (BD Biosciences) after acquisition of $10^5$ events. First, cells were selected using forward and side scatter parameters, and then, were characterize by their fluorescence using CellQuest software (BD Biosciences, CA, USA). In all experiments, appropriate isotype-matched negative controls were included.

### Pericardial Fluid Analysis

Before intrapericardial administration of EV-CDCs and 24 h post-therapy, pericardial fluid samples were collected with an Abbocath®-T 20G catheter and then centrifuged for 5 min at 450 x g. The pellet was used for relative gene expression analysis with real time quantitative PCR (qPCR). Total RNA from pellets was purified using mirVANA miRNA isolation kit (Applied Biosystems, Foster City, CA), following the manufacturer's protocol for total RNA extraction. Quality and concentration of total RNAs were evaluated by spectrophotometry. For each RNA sample, 1 μg of the corresponding cDNA was synthesized using iScript Reverse Transcription

Supermix (BioRad, Hercules, CA, USA), according to manufacturer's instructions. 1 μl of cDNA for each sample was then employed as template for the qPCR amplification with the TaqMan™ Fast Advanced Master Mix (Catalogue number 4444964, Thermo-Fisher Scientific Inc., MA, USA). Commercial TaqMan® Gene Expression Assays probes (Thermo-Fisher Scientific Inc., MA, USA) were used, according to manufacturer's recommendations, to evaluate the relative expression of the following genes: IFN-γ (Ss03391054_m1), TNF (Ss03391318_g1), IL-2 (Ss03392428_m1), IL-12 (Ss03391176_m1), IL-4 (Ss03394125_m1), IL-5 (Ss03394369_m1), IL-10 (Ss03382372_u1), Arg1 (Ss03391394_m1), NOS2 (Ss03374608_u1), BPI (Ss04321426_m1) and CELA (Ss03392393_m1). Samples were evaluated in triplicate and 1 μl of water was substituted to templates to perform three negative controls for each probe. The qPCR reaction was performed in a QuantStudio 3 Real-Time PCR System (Applied Biosystems, Thermo Fisher Scientific Inc.), and the products were quantified by fluorescent method using $2^{-\Delta Ct}$ expression [21] with GAPDH (Ss03375629_u1) as endogenous control. All data were analyzed in the Thermo Fisher Cloud (also called Thermo Fisher Connect).

### Statistical Analysis

Data were statistically analyzed with SigmaPlot for Windows version 14 software (Systat Software, IL, USA). A Shapiro-Wilk test was used to assess normality. Paired comparisons were determined using a Student t-test for parametric data or a Wilcoxon signed rank test with the Yates continuity correction for non-parametric variables. qPCR data were analyzed using a Thermo Fisher Cloud Analysis version 1.0. Data are shown as mean ± standard deviation (SD). All $p$-values $<0.05$ were considered statistically significant.

## Results

Prior to animal studies, allogeneic CDCs from a single donor were isolated and characterized as previously described [16]. The dosage ($30 \times 10^6$ CDCs/animal) was selected on the basis of previous studies using allogeneic cardiac stem cells [16, 20]. Additionally, EV-CDCs were collected and isolated as previously described our group [18]. These vesicles showed a mean diameter of 198 nm and the proteomic analysis demonstrated a purity of 98% (percentage of proteins classified in the *Extracellular exosome* term by Gene Ontology) [22]. The supplementary fig. 1 shows the Field-Flow Fractionation and the classification of proteins by Gene Ontology. Moreover, according to MISEV2018 guidelines [23], our results demonstrated the expression of CD63, LAMP2, CD81 and CD9 molecules which are classified as "Transmembrane or GPI-anchored proteins associated to plasma membrane and/or endosomes". Additionally, the proteomic analysis identified HSP90AB1 and HSPA1A proteins which are classified by MISEV2018 guidelines as "Cytosolic proteins recovered in EVs".

In this study, CDCs and EV-CDCs were intrapericardially delivered in a closed chest porcine myocardial infarction model and the follow-up was constrained to the acute phase of myocardial infarction (Fig. 1). Cardiac function parameters and troponin I levels at 72 h after myocardial infarction evidenced that the myocardial infarction was successfully induced in all animals. The percentage of myocardial infarction ranged from 14% to 38% (21.93 ± 6.49) and left ventricular ejection fraction ranged from 20% to 45% (28.07 ± 6.08). It is important to note that, no significant difference was observed between randomized groups (Table 1).

The in vivo monitoring was firstly focused on different biochemical parameters (Table 2). These biochemical parameters were determined before myocardial infarction (Basal) and 72 h after (Post-AMI). This analysis demonstrated that total proteins and urea were significantly reduced (Table 2). The analysis of biochemical parameters was also performed to compare the different study groups: Placebo, CDCs and EV-CDCs. In spite of the intrinsic variability between animals, the three groups showed an increase (although non-significant) in the GOT and GPT after treatments (Table 3).

Our determinations also included the quantification of hematological parameters. The hematological analysis before myocardial infarction and 72 h after did not show any significant difference (Fig. 2a). However, White Blood Cells (WBC) and neutrophils were significantly increased after EV-CDC treatment (Fig. 2b). Taking into account that WBC quantification is the sum of all leukocytes, the increase of WBC is reflecting this neutrophils increase.

Apart from the biochemical and hematological analyses, the main goal of this study was to perform a deep characterization of peripheral blood lymphocyte subsets to determine the hypothetical immunomodulatory effect of these therapies. Although the scarce commercial availability of reagents for the porcine model is a limiting factor in these studies, here we could quantify CD4+ T cells (also called helper T cells), CD8+ T cells (also called cytotoxic T cells), NK cells (here defined as CD4-/CD16+) and double positive cells (CD4+/CD8+), which are considered by other authors as T helper memory cells [24, 25]. Additionally, the analysis of CD4+ T cells and CD8+ T cells was also focused on their differentiation/activation status using CD27 and CD45RA markers. The co-expression analysis of these two markers allowed us to identify naïve T cells (CD27+ CD45RA+) and effector/memory T cells (CD27- CD45RA-). Not only peripheral blood lymphocytes were analyzed, but also monocyte counts, as well as the percentage of circulating M2 monocytes (here defined as CD14 + CD163+).

**Table 1** Data of cardiac function. Cardiac function parameters were determined 72 h after myocardial infarction induction in terms of: percentage of myocardial infarction (% Infarction), Left Ventricular Ejection Fraction (% LVEF), End Diastolic Volume index (EDVi), End Systolic Volume index (ESVi), heart rate and troponin I levels

| Animal | % Infarction | % LVEF | EDVi | ESVi | Heart rate (bpm) | Troponin I (μg/l) |
|---|---|---|---|---|---|---|
| #1 | 28 | 25 | 79.8 | 60 | 103 | 5.5 |
| #2 | 28 | 23 | 80.4 | 61.6 | 102 | 4.1 |
| #3 | 18 | 28 | 69.7 | 50.4 | 89 | 8.9 |
| #4 | 38 | 31 | 106.9 | 74.1 | 83 | 5 |
| #5 | 19 | 25 | 105.89 | 79.66 | 100 | 1.5 |
| #6 | 29 | 24 | 101.7 | 77.2 | 74 | 3.8 |
| #7 | 26 | 23 | 75.9 | 58.8 | 81 | 3.2 |
| #8 | 19 | 24 | 68.5 | 52 | 95 | 3.8 |
| #9 | 18 | 33 | 89.9 | 60.3 | 68 | 7.5 |
| #10 | 19 | 33 | 77.4 | 51.7 | 89 | 1 |
| #11 | 18 | 29 | 74.6 | 52.6 | 85 | 0.6 |
| #12 | 14 | 45 | 67.9 | 37.6 | 79 | 0.7 |
| #13 | 20 | 20 | 73.9 | 59 | 88 | 6.3 |
| #14 | 20 | 30 | 88.8 | 62.2 | 110 | 2.5 |
| #15 | 15 | 28 | 99.9 | 72.1 | 89 | 1.8 |
| Mean | 21.93 | 28.07 | 84.08 | 60.62 | 89.00 | 3.75 |
| SD | 6.49 | 6.08 | 13.79 | 11.38 | 11.48 | 2.53 |

As expected, significant changes were observed when compared T cell subsets before myocardial infarction and 72 h after. The CD4/CD8 ratio was significantly higher, as a consequence of CD8 + T cells decrease, and CD4+ T cells increase (Fig. 3a).

Not only CD4 + T cells and CD8+ T cells were altered after myocardial infarction. In our lymphocyte analysis, the CD4+/CD8+ double positive cells and NK cells were also significantly decreased after myocardial infarction (Fig. 3a). Unfortunately, the analysis of these lymphocyte subsets at 24 h post-therapy did not show any relevant difference in the different study groups. Uniquely, the CD4/CD8 ratio was significantly reduced in all groups when compared to post-AMI.

In the comparative analysis of naïve and effector memory cells (performed in CD4 + T cells and CD8+ T cells) significant differences were found when compared basal and post-AMI (Fig. 4a). These changes were reverted after placebo, EV-CDCs and CDCs treatments (Fig. 4b).

The multiparametric flow cytometry analysis was finally focused in the percentage of circulating CD14 + CD163+ cells. Our results demonstrated that EV-CDCs treatment significantly increased the percentage of these cells in peripheral blood (Fig. 5b). This difference was not observed in the placebo, or in the CDCs group and any significant difference was found in terms of monocyte counts.

In order to extend our results from peripheral blood to heart tissue, pericardial fluids were collected to determine the inflammatory environment before and after EV-CDCs administration. A Real-time quantitative PCR was performed to quantify the expression of TH1 cytokines (IFN-γ, TNF-α, IL-2 and IL-12), TH2 cytokines (IL-4, IL-5 and IL-10), M1/M2 markers (Arg1 and NOS2), as well as neutrophils markers (BPI and CELA). Arg1, NOS2, IFN-γ, and IL-10 were successfully amplified and detected in all individuals, showing a significant increase of Arg1 at 24 h post-therapy, as well as a non-significant increase of NOS2, IFN-γ, and IL-10 (Fig. 6a). Unfortunately, the cDNA amplification was unsuccessful for the other TH1 and TH2 cytokines, probably due to the limited amount of pericardial leukocytes. Arg1 is a classical M2 marker for monocytes [26] and neutrophils [27], so the increase of Arg1/NOS2 ratio after EV-CDCs administration (Fig. 6b) confirmed the M2 polarization observed by flow cytometry.

## Discussion

There is extensive literature describing the therapeutic potential of CDCs in myocardial infarction [28], which has been extended to other diseases such as Duchenne muscular dystrophy [29] and aging [14]. Nowadays, although the therapeutic effect of CDCs in aging mouse hearts is a matter of debate [30, 31], it is widely accepted that CDCs attenuate the inflammation during myocardial injury [7, 8, 16]. In vitro studies using CDCs have also demonstrated that the anti-inflammatory, anti-apoptotic, and pro-angiogenic effects of are mediated, at least in part, through the release of extracellular vesicles [32–34]. These CDCs-derived exosomes have been recently evaluated in a clinically relevant animal model of myocardial infarction demonstrating a therapeutic effect in adverse remodeling and scarring [11]. This therapeutic effect was solely observed after intramyocardial delivery while the

**Table 2** Biochemical parameters in basal conditions and after myocardial infarction induction. Blood samples were collected before acute myocardial infarction model creation (basal) and 72 h after (post-AMI). Normality was assessed using a Shapiro-Wilk test. Paired comparisons were performed using a Student t-test for parametric data or a Wilcoxon signed rank test with the Yates continuity correction for non-parametric variables. Values show the mean ± SD (n = 15). Numbers in bold show significant differences at $p \leq 0.05$

| | Basal (n = 15) | Post-AMI (n = 15) |
|---|---|---|
| Bilirubin (mg/dl) | 0.35 ± **0.04** | **0.14 ± 0.04** |
| Creatinine (mg/dl) | 1.65 ± 0.24 | 1.66 ± 0.24 |
| GGT (U/l) | 50.86 ± 7.07 | 39.80 ± 7.07 |
| Glucose (mg/dl) | 108.50 ± 12.83 | 88.40 ± 12.83 |
| GOT (U/l) | **32.21 ± 19.18** | **56.80 ± 19.18** |
| GPT (U/l) | **31.00 ± 19.68** | 75.80 ± **19.68** |
| Proteins (g/dl) | 6.20 ± 0.39 | 5.22 ± 0.39 |
| Urea (mg/l) | 25.79 ± 4.62 | 22.42 ± 33.30 |

intracoronary administration was ineffective and very similar to placebo.

In this study, we aimed to evaluate the immunomodulatory effect of intrapericardially delivered CDCs and EV-CDCs in a clinically relevant myocardial infarction model. The intrapericardial delivery is considered a safe and effective route for stem cell-based therapies [15, 16]. Our group has previously demonstrated that, the pericardial fluid preserve the viability of BM-MSCs favoring the adhesion and homogeneous distribution of administered cells without adverse effects [15]. Moreover, the intrapericardial administration of CDCs altered immunological parameters in a myocardial infarction model [16]. An important advantage of using our animal model (a close chest experimental porcine model of myocardial infarction), is the repeatability and homogeneity of study groups. However, this fact could also be considered a drawback as myocardial infarction in humans is frequently related with other complications.

In our preclinical study, we demonstrated that the intrapericardial administration of $30 \times 10^6$ CDCs/animal was simple and safe, which is in agreement with our previous studies [15]. Similarly, any adverse reaction was observed after EV-CDCs administration. In the follow-up period, our first set of determinations was focused on the quantification of biochemical parameters. The three groups showed a non-significant increase of GOT and GPT at 24 h after treatments which is in agreement with our own findings [35]. The alterations of biochemical parameters during cardiac failure is a very common event and associated with a hepatic dysfunction due to an increase in hepatic veins pressure [36]. Moreover, surgical approaches such as laparoscopy could also increase serum transaminase levels [37].

In the hematological analysis, our results showed a significant increase in neutrophils after EV-CDC treatment. It is well known that neutrophils are recruited into the infarcted area during the inflammatory phase, being attracted by cell debris and inflammatory signals. These cells have been usually considered as pro-inflammatory cells and according to clinical outcomes in myocardial disease, the increase of circulating neutrophils after EV-CDCs administration could be correlated with an aggravated outcome [38]. On the contrary, there are evidences for the pro-regenerative and anti-inflammatory capacity of these cells in myocardial infarction [27, 39]. Considering this duality, the increase of circulating neutrophils after EV-CDCs treatment deserves further investigation and a full characterization of these neutrophils.

In order to determine the hypothetical immunomodulatory effect of these therapies, peripheral blood lymphocytes were characterized by multiparametric flow cytometry. In this analysis, the CD4/CD8 ratio was significantly reduced in all

**Table 3.** Biochemical parameters after myocardial infarction induction and 24 h after treatment. Blood samples were collected 72 h after myocardial infarction model creation (post-AMI) and 24 h after intrapericardial administrations of Placebo, EV-CDCs and CDCs. Normality was assessed using a Shapiro-Wilk test. Paired comparisons were performed using a Student t-test for parametric data or a Wilcoxon signed rank test with the Yates continuity correction for non-parametric variables. Numbers in bold show significant differences ($p \leq 0.05$) for each study group comparing post-AMI and 24 h after treatment. Table shows the mean ± SD (n = 5)

| | PLACEBO GROUP | | CDCs GROUP | | EV-CDCs GROUP | |
|---|---|---|---|---|---|---|
| | Post-AMI (n = 5) | Post-therapy (n = 5) | Post-AMI (n = 5) | Post-therapy (n = 5) | Post-AMI (n = 5) | Post-therapy (n = 5) |
| Bilirubin (mg/dl) | 0.19 ± 0.05 | 0.12 ± 0.05 | 0.14 ± 0.04 | 0.28 ± 0.30 | 0.13 ± 0.04 | 0.12 ± 0.03 |
| Creatinine (mg/dl) | 1.54 ± 0.34 | 1.48 ± 0.26 | 1.71 ± 0.19 | 1.52 ± 0.09 | 1.42 ± 0.30 | 1.46 ± 0.11 |
| GGT (U/l) | 41.80 ± 6.87 | 59.40 ± 21.52 | 36.00 ± 5.10 | 39.00 ± 5.10 | 44.00 ± 10.30 | 59.00 ± 22.73 |
| Glucose (mg/dl) | 93.60 ± 19.89 | 95.20 ± 20.97 | 86.20 ± 9.60 | 109.75 ± 16.11 | 78.20 ± 19.07 | 89.00 ± 23.82 |
| GOT (U/l) | **61.00 ± 22.12** | **95.00 ± 13.17** | 54.60 ± 20.27 | 116.50 ± 71.59 | 47.60 ± 17.62 | 89.40 ± 43.47 |
| GPT (U/l) | 75.00 ± 25.81 | 83.00 ± 20.94 | 70.20 ± 19.75 | 88.00 ± 19.61 | 68.60 ± 21.98 | 74.20 ± 14.29 |
| Proteins (g/dl) | **5.33 ± 0.45** | **6.35 ± 0.52** | 5.24 ± 0.37 | 5.61 ± 0.40 | 5.60 ± 0.30 | 6.51 ± 0.36 |
| Urea (mg/l) | 21.56 ± 5.66 | 28.14 ± 3.95 | 21.78 ± 7.61 | 24.46 ± 8.85 | 21.78 ± 7.61 | 24.46 ± 8.85 |

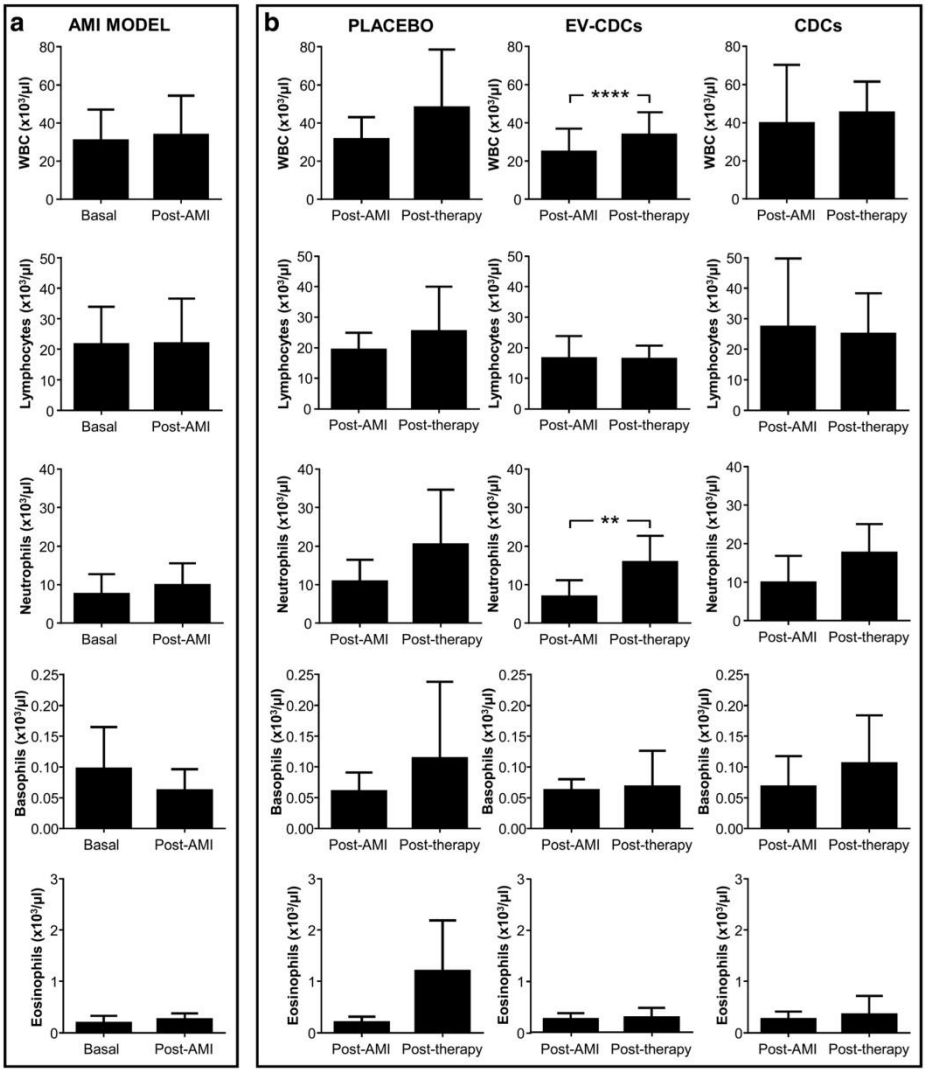


**Fig. 2** White blood cell analysis in peripheral blood. Blood samples were collected in EDTA containing tubes before acute myocardial infarction model creation (Basal), 72 h after (Post-AMI) and 24 h after the treatment (Post-therapy) and white blood cells were counted in an automated hematology analyzer. Normality was assessed using a Shapiro-Wilk test. Paired comparisons of the AMI model (**a**)($n = 15$) and paired comparisons of the administered therapies (**b**) ($n = 5$) were performed using a Student t-test for parametric data or a Wilcoxon signed rank test with the Yates continuity correction for non-parametric variables. Graphs show the mean ± SD of cell populations. $^{**}p \leq 0.01$. $^{****}p \leq 0.0001$

groups when compared to post-AMI. Most probably, this change could be the consequence of leukocytes redistribution from blood to the inflammation site or homeostasis-restoring mechanisms to basal conditions. Our second hypothesis is that, the surgical approach itself may initiate a post-operative immunosuppression. Supporting this idea, a previous study comparing laparoscopy and thoracotomy approaches demonstrated that CD4 + T cells and lymphocyte numbers were significantly reduced in the thoracotomy group, suggesting a post-operative immunosuppression after thoracotomy approach [40].

The immunomodulatory analysis of CDCs and EV-CDCs therapies was completed with the quantification of CD14 + CD16+ cells in peripheral blood. These cells correspond to pro-angiogenic and immunomodulatory subsets of monocytes (also defined as "M2 monocytes") [41]. Taking into account

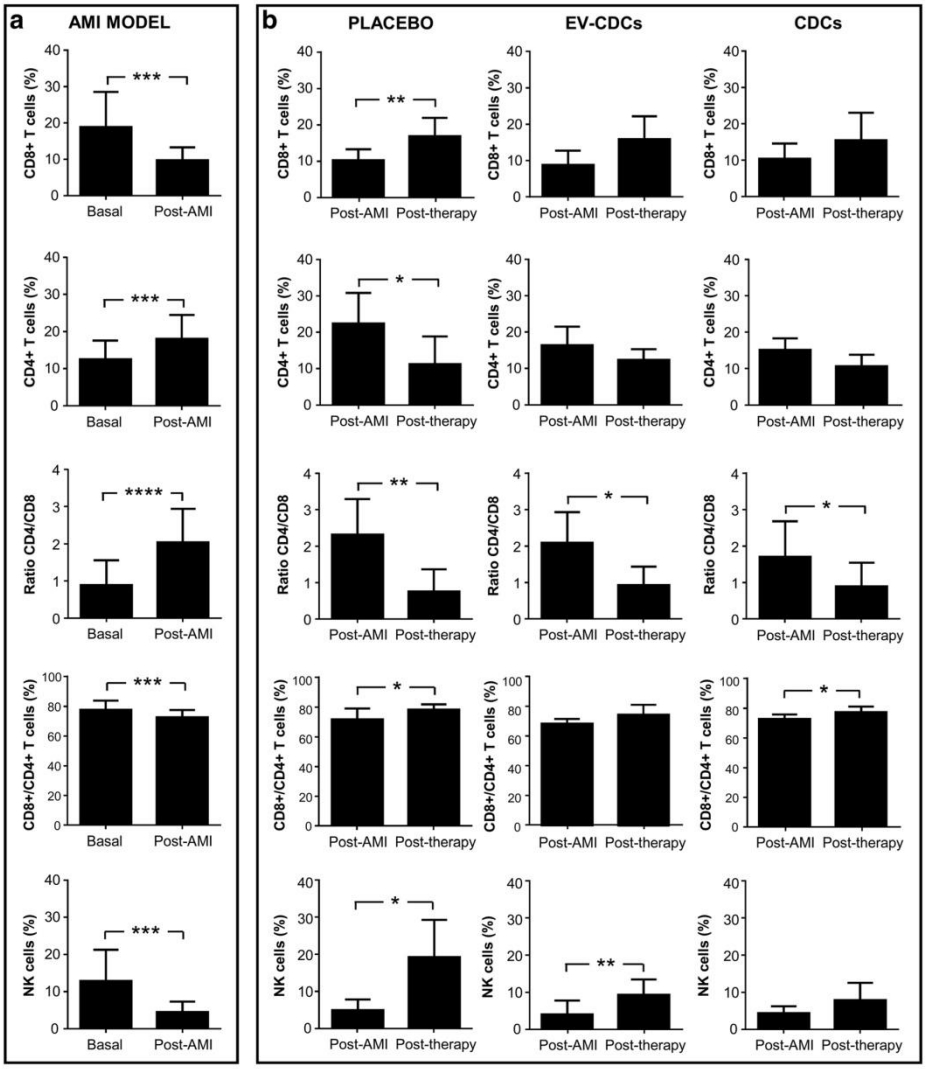


**Fig. 3** Lymphocyte subsets distribution in peripheral blood. Peripheral blood lymphocytes were isolated from blood samples before acute myocardial infarction model creation (Basal), 72 h after (Post-AMI) and 24 h after the treatment (Post-therapy). Lymphocyte subsets distribution was analyzed by flow cytometry. Normality was assessed using a Shapiro-Wilk test. Paired comparisons of the AMI model (**a**)(n = 15) and paired comparisons of the administered therapies (**b**) (n = 5) were performed using a Student t-test for parametric data or a Wilcoxon signed rank test with the Yates continuity correction for non-parametric variables. Graphs show the mean ± SD of cell populations. *$p \leq 0.05$. **p ≤ 0.01. ***$p \leq 0.001$. ****p ≤ 0.0001

that M2 polarization contributes to resolution of inflammation promoting tissue repair [42–44], here we hypothesize that the increase of M2 monocytes after EV-CDCs treatment might counteract the exacerbated inflammatory response in the acute phase of myocardial infarction. A similar hypothesis was proposed by Sekerkova et al., where these cells "might play a protective role in the early phase after kidney transplantation" [45]. It is important to note that the increase of M2 monocytes was solely observed in EV-CDCs, but not in CDCs. Taking into account that, the concentration of paracrine factors released by $30 \times 10^6$ allogeneic CDCs must be significantly lower than the average of paracrine factors in EV-CDCs, we consider that there may be a dose-response relationship between these factors and M2 differentiation.

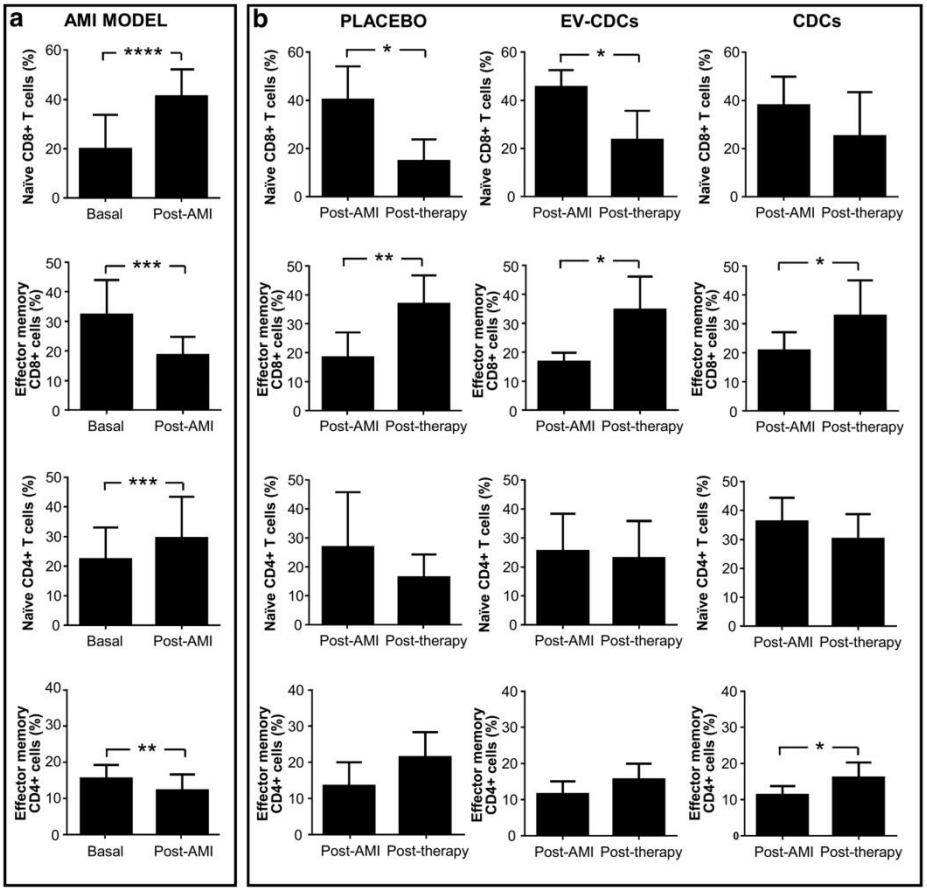


**Fig. 4** Differentiation/activation T cell subsets status in peripheral blood. Peripheral blood lymphocytes were isolated from blood samples before acute myocardial infarction model creation (Basal), 72 h after (Post-AMI) and 24 h after the treatment (Post-therapy). T cell subset status was analyzed by flow cytometry using CD27 and CD45RA markers. The co-expression analysis of these two markers allowed us to identify naïve T cells (CD27+ CD45RA+) and effector/memory T cells (CD27-CD45RA-). Normality was assessed using a Shapiro-Wilk test. Paired comparisons of the AMI model (**a**) (n = 15) and paired comparisons of the administered therapies (**b**) (n = 5) were performed using a Student t-test for parametric data or a Wilcoxon signed rank test with the Yates continuity correction for non-parametric variables. Graphs show the mean ± SD of cell populations. *$p \leq 0.05$. **$p \leq 0.01$. ***$p \leq 0.001$. ****$p \leq 0.0001$

A significant and innovative aspect of our study lies in the use of a different administration route. In this sense, and in agreement with de Couto et al. [12], our results have demonstrated the immunomodulatory effects of EV-CDCs in a clinically relevant animal model of myocardial infarction. While previous in vivo experiments have been performed by open-chest intramyocardial injection, here we demonstrate that intrapericardial administration was a safe and efficient alternative for reducing the adverse or unbalanced inflammatory reaction triggering the M2 polarization in circulating monocytes and pericardial leukocytes.

Although it was not the purpose of the study, the long-term effect of these treatments (in terms of cardiac functionality) could be determined at 10 weeks. Unfortunately these results were not conclusive, more especially since these healthy and young animal models are characterized by an early regenerative potential which could mask the therapeutic effect of the treatments [46]. In any case, our results did not show any significant difference between groups (Ejection Fraction: 29.6 ± 8.0 in Placebo, 29.8 ± 17.2 in EV-CDCs, 32.0 ± 6.7 in CDCs; % Infarct: 12.4 ± 3.5 in Placebo, 10.6 ± 1.7 in EV-CDCs, 9.2 ± 4.0 in CDCs).

Obviously, one of the limitations of the study is related to the identification of molecular mechanisms involved in M2 polarization. The group of E. Marban has already demonstrated that Y RNA fragment [47] and miR-181b [12] are directly

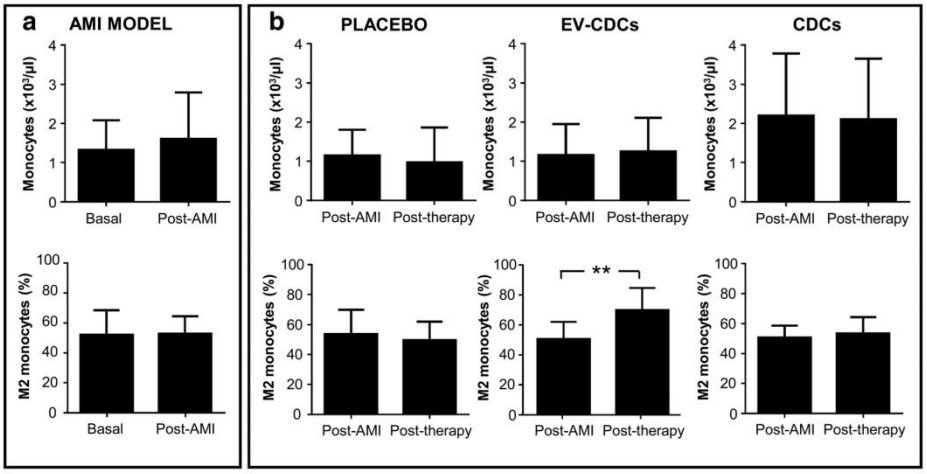


**Fig. 5** Monocyte populations in peripheral blood. Blood samples were collected in EDTA containing tubes before acute myocardial infarction model creation (Basal), 72 h after (Post-AMI) and 24 h after the treatment (Post-therapy). Monocyte count was performed in an automated hematology analyzer and its phenotype characterization was evaluated by flow cytometry, defining circulating M2 monocytes as CD14 + CD163+. Normality was assessed using a Shapiro-Wilk test. Paired comparisons of the AMI model (**a**)(n = 15) and paired comparisons of the administered therapies (**b**) (n = 5) were performed using a Student t-test for parametric data or a Wilcoxon signed rank test with the Yates continuity correction for non-parametric variables. Graphs show the mean ± SD of cell populations. **p ≤ 0.01

implicated in the immunomodulatory effect of EV-CDCs. In this sense, our research group is currently focused in "OMICS" studies, analyzing miRNA profiles by Next Generation Sequencing and proteins by high throughput proteomic analysis. Our preliminary results from these studies are showing an abundant expression of immune-related proteins and miRNAs (manuscript in preparation).

In conclusion, this is the first report where stem cell-derived extracellular vesicles have been intrapericardially administered in a clinically relevant animal model of myocardial infarction. In our experimental conditions and dose, EV-CDCs stimulate a M2 polarization during the acute phase of porcine myocardial infarction. Moreover, the immunomodulatory effects of EV-CDCs,

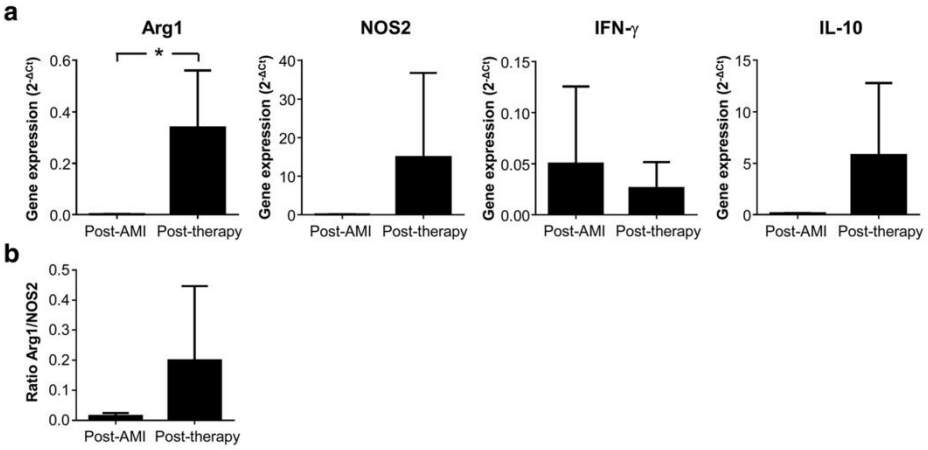


**Fig. 6** Cytokines gene expression in pericardial fluid cells. Pericardial fluids were compiled before and 24 h after EV-CDCs administration. Total RNA was isolated from pericardial fluid cells and qPCR products were quantified by the $2^{-\Delta Ct}$ method using GAPDH as an endogenous control. The statistical analysis was performed using a Thermo Fisher Cloud Analysis version 1.0. Graphs show the mean ± SD ($n = 3$). *p ≤ 0.05

after intrapericardial administration, were comparable to previous studies using the open-chest intramyocardial injections. Finally, the intrapericardial administration route offers the possibility of a minimally invasive surgical approach and could be more advantageous from a clinical perspective.

**Acknowledgements** Thanks to all people of ICTS Nanbiosis: Clinical test lab, animal housing, experimental operating room and medical imaging technicians. Finally, especial thanks to Dr. Simona Sapino and Marina Gallarate from Università degli Studi di Torino for the FFF analysis.

**Availability of Data and Materials** The datasets used and/or analyzed during the current study are available from the corresponding author on reasonable request.

**Authors' Contributions** E.L. contributed as first author. E.L., R.B., F.M.S.M. and J.G.C. conceived and designed the experiments. R.B., F.M.S.M., V.A., C.B., V.B., B.M., E.L., F.M., V.C., H.M., A.A. and J.G.C. performed the experiments and analyzed the data. E.L., R.B., F.M.S.M. and J.G.C. wrote the manuscript. All authors read and approved the final manuscript.

**Funding Information** CIBER-CV (CB16/11/00494 grant) and Ayuda Grupos de Investigación de Extremadura, Consejería de Economía, Ciencia y Agenda Digital (GR18199 co-financed by FEDER) to Francisco Miguel Sánchez-Margallo. "Miguel Servet I" grant from Instituto de Salud Carlos III (CP17/00021, and MS17/00021 co-financed by FEDER and FSE); Instituto de Salud Carlos III grant (PI18/0911 669 co-financed by FEDER); Junta de Extremadura (IB16168 grant ) co-financed by FEDER to Javier G Casado. Sara Borrell grant (CD1900048 co-financed by FSE) to Esther López. Mafresa S.L. grant to Federica Marinaro.

## Compliance with Ethical Standards

**Conflict of Interests** The authors declare that they have no conflict of interest.

**Ethics Approval** All experimental protocols were approved by the Ethics Committee on Animal Experiments of Jesús Usón Minimally Invasive Surgery Centre, in accordance with the recommendations outlined by the local government (Junta de Extremadura) and the EU Directive 2010/63/EU of the European Parliament on the protection of animals used for scientific purposes.

**Informed Consent** Informed consent was obtained from all individual participants included in the study.

**Open Access** This article is licensed under a Creative Commons Attribution 4.0 International License, which permits use, sharing, adaptation, distribution and reproduction in any medium or format, as long as you give appropriate credit to the original author(s) and the source, provide a link to the Creative Commons licence, and indicate if changes were made. The images or other third party material in this article are included in the article's Creative Commons licence, unless indicated otherwise in a credit line to the material. If material is not included in the article's Creative Commons licence and your intended use is not permitted by statutory regulation or exceeds the permitted use, you will need to obtain permission directly from the copyright holder. To view a copy of this licence, visit http://creativecommons.org/licenses/by/4.0/.

## References

1. Dokainish, H., Teo, K., Zhu, J., Roy, A., AlHabib, K. F., ElSayed, A., et al. (2017). Global mortality variations in patients with heart failure: Results from the international congestive heart failure (INTER-CHF) prospective cohort study. *The Lancet Global Health, 5*(7), e665–e672. https://doi.org/10.1016/S2214-109X(17)30196-1.
2. Ong, S.-B., Hernández-Reséndiz, S., Crespo-Avilan, G. E., Mukhametshina, R. T., Kwek, X.-Y., Cabrera-Fuentes, H. A., & Hausenloy, D. J. (2018). Inflammation following acute myocardial infarction: Multiple players, dynamic roles, and novel therapeutic opportunities. *Pharmacology & Therapeutics, 186*, 73–87. https://doi.org/10.1016/j.pharmthera.2018.01.001.
3. Dutta, P., Sager, H. B., Stengel, K. R., Naxerova, K., Courties, G., Saez, B., et al. (2015). Myocardial infarction activates CCR2(+) hematopoietic stem and progenitor cells. *Cell Stem Cell, 16*(5), 477–487. https://doi.org/10.1016/j.stem.2015.04.008.
4. Huang, S., & Frangogiannis, N. G. (2018). Anti-inflammatory therapies in myocardial infarction: Failures, hopes and challenges. *British Journal of Pharmacology, 175*(9), 1377–1400. https://doi.org/10.1111/bph.14155.
5. Munir, H., Ward, L. S. C., & McGettrick, H. M. (2018). Mesenchymal stem cells as endogenous regulators of inflammation. *Advances in Experimental Medicine and Biology, 1060*, 73–98. https://doi.org/10.1007/978-3-319-78127-3_5.
6. Regulski, M. J. (2017). Mesenchymal Stem Cells: "Guardians of Inflammation.". *Wounds: A Compendium of Clinical Research and Practice, 29*(1), 20–27.
7. Nana-Leventaki, E., Nana, M., Poulianitis, N., Sampaziotis, D., Perrea, D., Sanoudou, D., et al. (2019). Cardiosphere-derived cells attenuate inflammation, preserve systolic function, and prevent adverse remodeling in rat hearts with experimental autoimmune myocarditis. *Journal of Cardiovascular Pharmacology and Therapeutics, 24*(1), 70–77. https://doi.org/10.1177/1074248418784287.
8. Gallet, R., de Couto, G., Simsolo, E., Valle, J., Sun, B., Liu, W., et al. (2016). Cardiosphere-derived cells reverse heart failure with preserved ejection fraction (HFpEF) in rats by decreasing fibrosis and inflammation. *JACC. Basic to Translational Science, 1*(1–2), 14–28. https://doi.org/10.1016/j.jacbts.2016.01.003.
9. Lee, S.-T., White, A. J., Matsushita, S., Malliaras, K., Steenbergen, C., Zhang, Y., et al. (2011). Intramyocardial injection of autologous cardiospheres or cardiosphere-derived cells preserves function and minimizes adverse ventricular remodeling in pigs with heart failure post-myocardial infarction. *Journal of the American College of Cardiology, 57*(4), 455–465. https://doi.org/10.1016/j.jacc.2010.07.049.
10. Kanazawa, H., Tseliou, E., Malliaras, K., Yee, K., Dawkins, J. F., De Couto, G., et al. (2015). Cellular postconditioning: Allogeneic cardiosphere-derived cells reduce infarct size and attenuate microvascular obstruction when administered after reperfusion in pigs with acute myocardial infarction. *Circulation. Heart Failure, 8*(2), 322–332. https://doi.org/10.1161/CIRCHEARTFAILURE.114.001484.
11. Gallet, R., Dawkins, J., Valle, J., Simsolo, E., de Couto, G., Middleton, R., et al. (2016). Exosomes secreted by cardiosphere-derived cells reduce scarring, attenuate adverse remodelling, and improve function in acute and chronic porcine myocardial infarction. *European Heart Journal*. https://doi.org/10.1093/eurheartj/ehw240.
12. de Couto, G., Gallet, R., Cambier, L., Jaghatspanyan, E., Makkar, N., Dawkins, J. F., et al. (2017). Exosomal MicroRNA transfer into macrophages mediates cellular Postconditioning. *Circulation,*

*136*(2), 200–214. https://doi.org/10.1161/CIRCULATIONAHA.116.024590.
13. Namazi, H., Namazi, I., Ghiasi, P., Ansari, H., Rajabi, S., Hajizadeh-Saffar, E., et al. (2018). Exosomes secreted by normoxic and hypoxic Cardiosphere-derived cells have anti-apoptotic effect. *Iranian Journal of Pharmaceutical Research: IJPR, 17*(1), 377–385.
14. Grigorian-Shamagian, L., Liu, W., Fereydooni, S., Middleton, R. C., Valle, J., Cho, J. H., & Marbán, E. (2017). Cardiac and systemic rejuvenation after cardiosphere-derived cell therapy in senescent rats. *European Heart Journal, 38*(39), 2957–2967. https://doi.org/10.1093/eurheartj/ehx454.
15. Blázquez, R., Sánchez-Margallo, F. M., Crisóstomo, V., Báez, C., Maestre, J., García-Lindo, M., Usón, A., Álvarez, V., & Casado, J. G. (2015). Intrapericardial administration of mesenchymal stem cells in a large animal model: A bio-distribution analysis. *PLoS One, 10*(3), e0122377. https://doi.org/10.1371/journal.pone.0122377.
16. Blázquez, R., Sánchez-Margallo, F. M., Crisóstomo, V., Báez, C., Maestre, J., Álvarez, V., & Casado, J. G. (2016). Intrapericardial delivery of Cardiosphere-derived cells: An immunological study in a clinically relevant large animal model. *PLoS One, 11*(2), e0149001. https://doi.org/10.1371/journal.pone.0149001.
17. van der Spoel, T. I. G., Jansen of Lorkeers, S. J., Agostoni, P., van Belle, E., Gyongyosi, M., Sluijter, J. P. G., et al. (2011). Human relevance of pre-clinical studies in stem cell therapy: Systematic review and meta-analysis of large animal models of ischaemic heart disease. *Cardiovascular Research, 91*(4), 649–658. https://doi.org/10.1093/cvr/cvr113.
18. Álvarez, V., Sánchez-Margallo, F. M., Macías-García, B., Gómez-Serrano, M., Jorge, I., Vázquez, J., et al. (2018). The immunomodulatory activity of extracellular vesicles derived from endometrial mesenchymal stem cells on CD4+ T cells is partially mediated by TGFbeta. *Journal of Tissue Engineering and Regenerative Medicine, 12*(10), 2088–2098. https://doi.org/10.1002/term.2743.
19. Marinaro, F., Macías-García, B., Sánchez-Margallo, F. M., Blázquez, R., Álvarez, V., Matilla, E., et al. (2018). Extracellular vesicles derived from endometrial human mesenchymal stem cells enhance embryo yield and quality in an aged murine model. *Biology of Reproduction*. https://doi.org/10.1093/biolre/ioy263.
20. Crisostomo, V., Baez-Diaz, C., Maestre, J., Garcia-Lindo, M., Sun, F., Casado, J. G., et al. (2015). Delayed administration of allogeneic cardiac stem cell therapy for acute myocardial infarction could ameliorate adverse remodeling: Experimental study in swine. *Journal of Translational Medicine, 13*, 156–116. https://doi.org/10.1186/s12967-015-0512-2.
21. Livak, K. J., & Schmittgen, T. D. (2001). Analysis of relative gene expression data using real-time quantitative PCR and the 2(−Delta Delta C(T)) method. *Methods, 25*(4), 402–408. https://doi.org/10.1006/meth.2001.1262.
22. Garcia-Casado, J., Lopez, E., Alvarez, V., Blazquez, R., Marinaro, F., Gomez-Serrano, M., et al. (2018). Isolation and proteomics analysis of microvesicles from cardiosphere-derived cells for cardiac repair therapy. *European Journal of Clinical Investigation, 48*, 132–132.
23. Théry, C., Witwer, K. W., Aikawa, E., Alcaraz, M. J., Anderson, J. D., Andriantsitohaina, R. … Zuba-Surma, E. K. (2018). Minimal information for studies of extracellular vesicles 2018 (MISEV2018): A position statement of the International Society for Extracellular Vesicles and update of the MISEV2014 guidelines. *Journal of Extracellular Vesicles*, 7(1). https://doi.org/10.1080/20013078.2018.1535750.
24. Summerfield, A., Rziha, H. J., & Saalmüller, A. (1996). Functional characterization of porcine CD4+CD8+ extrathymic T lymphocytes. *Cellular Immunology, 168*(2), 291–296. https://doi.org/10.1006/cimm.1996.0078.
25. Zuckermann, F. A. (1999). Extrathymic CD4/CD8 double positive T cells. *Veterinary Immunology and Immunopathology, 72*(1–2), 55–66. https://doi.org/10.1016/S0165-2427(99)00118-X.
26. Italiani, P., & Boraschi, D. (2014). From monocytes to M1/M2 macrophages: Phenotypical vs. Functional Differentiation. *Frontiers in Immunology, 5*, 514. https://doi.org/10.3389/fimmu.2014.00514.
27. Horckmans, M., Ring, L., Duchene, J., Santovito, D., Schloss, M. J., Drechsler, M., et al. (2017). Neutrophils orchestrate post-myocardial infarction healing by polarizing macrophages towards a reparative phenotype. *European Heart Journal, 38*(3), 187–197. https://doi.org/10.1093/eurheartj/ehw002.
28. Ashur, C., & Frishman, W. H. (2018). Cardiosphere-derived cells and ischemic heart failure. *Cardiology in Review, 26*(1), 8–21. https://doi.org/10.1097/CRD.0000000000000173.
29. Aminzadeh, M. A., Rogers, R. G., Fournier, M., Tobin, R. E., Guan, X., Childers, M. K., et al. (2018). Exosome-mediated benefits of cell therapy in mouse and human models of Duchenne muscular dystrophy. *Stem Cell Reports, 10*(3), 942–955. https://doi.org/10.1016/j.stemcr.2018.01.023.
30. Ibrahim, A., Grigorian-Shamagian, L., Rogers, R. G., & Marbán, E. (2018). Letter by Ibrahim et al Regarding Article, "Lack of Cardiac Improvement After Cardiosphere-Derived Cell Transplantation in Aging Mouse Hearts.". *Circulation Research, 123*(12), e65–e66. https://doi.org/10.1161/CIRCRESAHA.118.314147.
31. Zhao, Z.-A., Han, X., Lei, W., Li, J., Yang, Z., Wu, J., et al. (2018). Lack of cardiac improvement after Cardiosphere-derived cell transplantation in aging mouse hearts. *Circulation Research, 123*(10), e21–e31. https://doi.org/10.1161/CIRCRESAHA.118.313005.
32. Ibrahim, A. G.-E., Cheng, K., & Marbán, E. (2014). Exosomes as critical agents of cardiac regeneration triggered by cell therapy. *Stem Cell Reports, 2*(5), 606–619. https://doi.org/10.1016/j.stemcr.2014.04.006.
33. Namazi, H., Mohit, E., Namazi, I., Rajabi, S., Samadian, A., Hajizadeh-Saffar, E., et al. (2018). Exosomes secreted by hypoxic cardiosphere-derived cells enhance tube formation and increase pro-angiogenic miRNA. *Journal of Cellular Biochemistry, 119*(5), 4150–4160. https://doi.org/10.1002/jcb.26621.
34. Tseliou, E., Fouad, J., Reich, H., Slipczuk, L., de Couto, G., Aminzadeh, M., et al. (2015). Fibroblasts rendered Antifibrotic, Antiapoptotic, and Angiogenic by priming with Cardiosphere-derived extracellular membrane vesicles. *Journal of the American College of Cardiology, 66*(6), 599–611. https://doi.org/10.1016/j.jacc.2015.05.068.
35. Blázquez, R., Álvarez, V., Antequera-Barroso, J. A., Báez-Díaz, C., Blanco, V., Maestre, J., et al. (2018). Altered hematological, biochemical and immunological parameters as predictive biomarkers of severity in experimental myocardial infarction. *Veterinary Immunology and Immunopathology, 205*, 49–57. https://doi.org/10.1016/j.vetimm.2018.10.007.
36. Alvarez, A., & Mukherjee, D. (2011). Liver abnormalities in cardiac diseases and heart failure. *International Journal of Angiology, 20*(03), 135–142. https://doi.org/10.1055/s-0031-1284434.
37. Tan, M. (2003). Changes in the level of serum liver enzymes after laparoscopic surgery. *World Journal of Gastroenterology, 9*(2), 364. https://doi.org/10.3748/wjg.v9.i2.364.
38. Men, M., Zhang, L., Li, T., Mi, B., Wang, T., Fan, Y., et al. (2015). Prognostic value of the percentage of neutrophils on admission in patients with ST-elevated myocardial infarction undergoing primary percutaneous coronary intervention. *Archives of Medical Research, 46*(4), 274–279. https://doi.org/10.1016/j.arcmed.2015.05.002.
39. Puhl, S.-L., & Steffens, S. (2019). Neutrophils in post-myocardial infarction inflammation: Damage vs. resolution? *Frontiers in Cardiovascular Medicine*, *6*. https://doi.org/10.3389/fcvm.2019.00025.

40. Ng, C. S. H., Lee, T. W., Wan, S., Wan, I. Y. P., Sihoe, A. D. L., Arifi, A. A., & Yim, A. P. C. (2005). Thoracotomy is associated with significantly more profound suppression in lymphocytes and natural killer cells than video-assisted thoracic surgery following major lung resections for cancer. *Journal of Investigative Surgery: The Official Journal of the Academy of Surgical Research, 18*(2), 81–88. https://doi.org/10.1080/08941930590926320.
41. Mayer, A., Lee, S., Jung, F., Grütz, G., Lendlein, A., & Hiebl, B. (2010). CD14+ CD163+ IL-10+ monocytes/macrophages: Pro-angiogenic and non pro-inflammatory isolation, enrichment and long-term secretion profile. *Clinical Hemorheology and Microcirculation, 46*(2–3), 217–223. https://doi.org/10.3233/CH-2010-1348.
42. Martinez, F. O., Helming, L., & Gordon, S. (2009). Alternative activation of macrophages: An immunologic functional perspective. *Annual Review of Immunology, 27*, 451–483. https://doi.org/10.1146/annurev.immunol.021908.132532.
43. Yang, Z., & Ming, X.-F. (2014). Functions of arginase isoforms in macrophage inflammatory responses: Impact on cardiovascular diseases and metabolic disorders. *Frontiers in Immunology, 5*, 533. https://doi.org/10.3389/fimmu.2014.00533.
44. Ben-Mordechai, T., Palevski, D., Glucksam-Galnoy, Y., Elron-Gross, I., Margalit, R., & Leor, J. (2015). Targeting macrophage subsets for infarct repair. *Journal of Cardiovascular Pharmacology and Therapeutics, 20*(1), 36–51. https://doi.org/10.1177/1074248414534916.
45. Sekerkova, A., Krepsova, E., Brabcova, E., Slatinska, J., Viklicky, O., Lanska, V., & Striz, I. (2014). CD14+CD16+ and CD14+ CD163+ monocyte subpopulations in kidney allograft transplantation. *BMC Immunology, 15*, 4. https://doi.org/10.1186/1471-2172-15-4.
46. Crisóstomo, V., Maestre, J., Maynar, M., Sun, F., Báez-Díaz, C., Usón, J., & Sánchez-Margallo, F. M. (2013). Development of a closed chest model of chronic myocardial infarction in swine: Magnetic resonance imaging and pathological evaluation. *ISRN cardiology, 2013*, 781762. https://doi.org/10.1155/2013/781762.
47. Cambier, L., de Couto, G., Ibrahim, A., Echavez, A. K., Valle, J., Liu, W., et al. (2017). Y RNA fragment in extracellular vesicles confers cardioprotection via modulation of IL-10 expression and secretion. *EMBO Molecular Medicine, 9*(3), 337–352. https://doi.org/10.15252/emmm.201606924.


**Publisher's Note** Springer Nature remains neutral with regard to jurisdictional claims in published maps and institutional affiliations.

frontiers in Bioengineering and Biotechnology

ORIGINAL RESEARCH
published: 20 December 2019
doi: 10.3389/fbioe.2019.00431

# Unraveling the Molecular Signature of Extracellular Vesicles From Endometrial-Derived Mesenchymal Stem Cells: Potential Modulatory Effects and Therapeutic Applications

*Federica Marinaro[1†], María Gómez-Serrano[2,3,4†], Inmaculada Jorge[2,3*], Juan Carlos Silla-Castro[5], Jesús Vázquez[2,3], Francisco Miguel Sánchez-Margallo[1,2*], Rebeca Blázquez[1,2], Esther López[1], Verónica Álvarez[1] and Javier G. Casado[1,2]*

[1] Stem Cell Therapy Unit, Jesús Usón Minimally Invasive Surgery Centre, Cáceres, Spain, [2] CIBER de Enfermedades Cardiovasculares, Madrid, Spain, [3] Laboratory of Cardiovascular Proteomics, Centro Nacional de Investigaciones Cardiovasculares, Madrid, Spain, [4] Center for Tumor Biology and Immunology, Institute of Molecular Biology and Tumor Research, Philipps University, Marburg, Germany, [5] Bioinformatics Unit, Centro Nacional de Investigaciones Cardiovasculares, Madrid, Spain

OPEN ACCESS

**Edited by:**
*Wolfgang Holnthoner, Ludwig Boltzmann Institute for Experimental and Clinical Traumatology, Austria*

**Reviewed by:**
*Benedetta Bussolati, University of Turin, Italy*
*Michela Pozzobon, University of Padova, Italy*

***Correspondence:**
*Inmaculada Jorge*
*inmaculada.jorge@cnic.es*
*Francisco Miguel Sánchez-Margallo*
*msanchez@ccmijesususon.com*

*†These authors have contributed equally to this work and share first authorship*

**Specialty section:**
*This article was submitted to Tissue Engineering and Regenerative Medicine, a section of the journal Frontiers in Bioengineering and Biotechnology*

**Received:** *20 September 2019*
**Accepted:** *05 December 2019*
**Published:** *20 December 2019*

**Citation:**
*Marinaro F, Gómez-Serrano M, Jorge I, Silla-Castro JC, Vázquez J, Sánchez-Margallo FM, Blázquez R, López E, Álvarez V and Casado JG (2019) Unraveling the Molecular Signature of Extracellular Vesicles From Endometrial-Derived Mesenchymal Stem Cells: Potential Modulatory Effects and Therapeutic Applications. Front. Bioeng. Biotechnol. 7:431. doi: 10.3389/fbioe.2019.00431*

Endometrial-derived Mesenchymal Stem Cells (endMSCs) are involved in the regeneration and remodeling of human endometrium, being considered one of the most promising candidates for stem cell-based therapies. Their therapeutic effects have been found to be mediated by extracellular vesicles (EV-endMSCs) with pro-angiogenic, anti-apoptotic, and immunomodulatory effects. Based on that, the main goal of this study was to characterize the proteome and microRNAome of these EV-endMSCs by proteomics and transcriptomics approaches. Additionally, we hypothesized that inflammatory priming of endMSCs may contribute to modify the therapeutic potential of these vesicles. High-throughput proteomics revealed that 617 proteins were functionally annotated as *Extracellular exosome* (GO:0070062), corresponding to the 70% of the EV-endMSC proteome. Bioinformatics analyses allowed us to identify that these proteins were involved in adaptive/innate immune response, complement activation, antigen processing/presentation, negative regulation of apoptosis, and different signaling pathways, among others. Of note, multiplexed quantitative proteomics and Systems Biology analyses showed that IFNγ priming significantly modulated the protein profile of these vesicles. As expected, proteins involved in antigen processing and presentation were significantly increased. Interestingly, immunomodulatory proteins, such as CSF1, ERAP1, or PYCARD were modified. Regarding miRNAs expression profile in EV-endMSCs, Next-Generation Sequencing (NGS) showed that the preferred site of microRNAome targeting was the nucleus ($n = 371$ microTargets), significantly affecting *signal transduction* (GO:0007165), *cell proliferation* (GO:0008283), and *apoptotic processes* (GO:0006915), among others. Interestingly, NGS analyses highlighted that several miRNAs, such as hsa-miR-150-5p or hsa-miR-196b-5p, were differentially expressed in IFNγ-primed EV-endMSCs. These miRNAs have a functional involvement in glucocorticoid receptor signaling, IL-6/8/12 signaling, and in the role of macrophages.

In summary, these results allowed us to understand the complexity of the molecular networks in EV-endMSCs and their potential effects on target cells. To our knowledge, this is the first comprehensive study based on proteomic and genomic approaches to unravel the therapeutic potential of these extracellular vesicles, that may be used as immunomodulatory effectors in the treatment of inflammatory conditions.

**Keywords: mesenchymal stem cells, endometrial, proteomic analyses, next generation sequencing-NGS, interferon-γ, extracellular vesicles (EV), miRNA-microRNA, priming**

## INTRODUCTION

Mesenchymal Stem Cells (MSCs) obtained from endometrial tissue have become one of the most promising candidates in the field of stem cell therapies. They are involved in the dynamic remodeling and regeneration of human endometrium, being necessary for normal tissue self-renewal. In bibliography, different populations of endometrial stem cells have been described (Chan et al., 2004) and different names have been used for these cells, such as menstrual blood-derived stromal/mesenchymal cells, or endometrial-derived stromal/mesenchymal stem cells (endMSCs) (Kyurkchiev et al., 2010; Gargett et al., 2016). Additionally, different laboratory procedures have been established for *in vitro* isolation and expansion (Schüring et al., 2011; Wang et al., 2012; Rossignoli et al., 2013). Nowadays, menstrual blood-derived endMSCs can be easily isolated by a non-invasive method, without any painful procedure and their *in vitro* expansion can be achieved by simple, and reproducible methods (Sun et al., 2019).

The therapeutic potential of endMSCs have been described and reviewed for different diseases, such as myocardial infarction (Liu et al., 2019), and Parkinson disease (Bagheri-Mohammadi et al., 2019). Recent preclinical studies have also evaluated their therapeutic effects in murine models of pulmonary fibrosis (Zhao et al., 2018), and experimental colitis (Lv et al., 2014). In addition, a recent clinical trial using autologous menstrual blood-derived stromal cells have shown satisfactory results for the treatment of severe Asherman's syndrome (Tan et al., 2016).

The biological mechanisms underlying endMSCs function have been associated to their immunomodulatory capacity (Nikoo et al., 2012), which is mediated—at least in part—by indoleamine 2,3-dioxygenase-1, cyclooxygenase-2, IL-10, and IL-27 (Peron et al., 2012; Nikoo et al., 2014). Moreover, these cells have demonstrated a potent pro-angiogenic and anti-apoptotic effect mediated by HGF, IGF-1, and VEGF (Du et al., 2016). Similarly to other MSCs, such as adipose-derived MSCs, or bone marrow-derived MSCs, the therapeutic effect of endMSCs is mediated by the paracrine action of extracellular vesicles (EVs). EVs (including microvesicles, exosomes, and apoptotic bodies) act as carriers of bioactive molecules, such as proteins, microRNAs (miRNAs), and lipids (Doyle and Wang, 2019). In this sense, our group has recently revealed the presence of TGF-β in EVs derived from endMSCs (EV-endMSCs). The functional studies performed by TGF-β blockade demonstrated that this molecule is partially involved in the immunomodulatory effect of these vesicles (Álvarez et al., 2018). Apart from their immunomodulatory effects, EV-endMSCs have been used as co-adjuvants to improve the *in vitro* fertilization outcomes in murine models (Blázquez et al., 2018), and the proteomic analysis of these EVs revealed an abundant expression of proteins involved in embryo development (Marinaro et al., 2019).

These preliminary results opened several questions about the hypothetical biological mechanisms that may mediate the therapeutic effect of EV-endMSCs. In this regard, a profound characterization of proteins and miRNAs, as regulatory elements, may help us to identify protein or gene targets for the treatment of specific diseases, increasing the translational impact of this research.

On the other hand, an important issue in the field of EVs derived from MSCs relies in the enhancement of their therapeutic effect. Basically, the main goal is to get vesicles with more biologically relevant effector molecules. During the last years, the protocols for MSCs priming (also called "MSCs licensing"), to generate more immunosuppressive MSCs, are gaining interest. This idea has been studied by using Interferon gamma (IFNγ)-priming (DelaRosa et al., 2009; Chinnadurai et al., 2014; Liang et al., 2018), Toll-like receptors priming (Sangiorgi and Panepucci, 2016; Najar et al., 2017), and other inflammatory stimuli (Kim and Cho, 2016). This concept has been recently reviewed by Yin et al. (2019) and the idea of MSCs priming has been extrapolated to the production of licensed EVs. Several examples can be found in bibliography: exosomes from Interleukin 1β-primed MSCs expressed miR-146a to induce M2 polarization (Song et al., 2017); EVs from TNFα/IFNγ-primed MSCs were found to enhance the immunomodulatory activity of MSCs by altering the COX2/PGE2 pathway (Harting et al., 2018); furthermore, it was proved that exosomes from MSCs under low oxygen conditions produced exosomes with a higher pro-mitotic effect (Yuan et al., 2019), and immunomodulatory potential (Showalter et al., 2019).

**Abbreviations:** DMEM, Dulbecco's Modified Eagle's medium; endMSCs, Endometrial-derived stromal/Mesenchymal Stem Cells; EV-endMSCs, Extracellular Vesicles from Endometrial-derived stromal/Mesenchymal Stem Cells; EVs, Extracellular Vesicles; FDR, False Discovery Rate; GO, Gene Ontology; IFNγ/EV-endMSCs, Extracellular Vesicles from IFNγ-primed Endometrial-derived stromal/Mesenchymal Stem Cells; IFNγ, Interferon gamma; IPA, Ingenuity Pathway Analysis; iTRAQ, Isobaric Tags for Relative and Absolute Quantitation; LC-MS/MS, Liquid chromatographytandem mass spectrometry; MS, Mass spectrometry; MSCs, Mesenchymal Stem Cells; NGS, Next Generation Sequencing; PBS, Phosphate buffered saline; PCA, Principal Component Analysis; SBT, Systems Biology Triangle; TMM, Trimmed mean of M-values; TPM, Tags Per Million; UMI, Unique Molecular Index; WSPP, Weighted Spectrum, Peptide, Protein.

In this work, we hypothesized that IFNγ-primed endMSCs may produce EVs (IFNγ/EV-endMSCs) with therapeutic effects that may be applicable in different clinical settings. In order to explore this idea, a large-scale analysis of proteins and miRNAs was performed using high throughput proteomic screening and Next Generation Sequencing (NGS), respectively. Our results revealed the existence of a wide range of proteins and miRNAs involved in the immune process, apoptosis, or cell signaling, among others. Nowadays, bioinformatics resources, such as DAVID (https://david.ncifcrf.gov/), miRTargetLink (https://ccb-web.cs.uni-saarland.de/mirtargetlink/), and Ingenuity Pathway Analysis (IPA) (https://www.qiagenbioinformatics.com/products/ingenuity-pathway-analysis/) are available and effective tools to handle and filter the massive amount of data at the basis of *in silico* functional analyses. In our study, these tools allowed us to classify proteins and miRNAs according to their biological roles. In the case of high throughput proteomic analysis, some of the most significant differences were observed on immune-related proteins, being the increase of CSF-1 in IFNγ/EV-endMSCs especially relevant. Additionally, NGS for miRNA expression identified relevant miRNAs whose target genes are implicated in the functionality of macrophages, and IL6/IL8/IL12 signaling. These results suggest that IFNγ/EV-endMSCs may serve as important carriers for miRNAs and proteins with immunomodulatory effects.

## MATERIALS AND METHODS

### Human endMSCs Isolation, Culture, and Characterization

This study was performed in agreement with the ethical guidelines of the Minimally Invasive Surgery Centre Research Ethics Committee, which approved the study (approval number: 017/16). All menstrual blood donors provided written informed consent to participate in the study. The endMSCs were obtained from menstrual blood collected by four healthy pre-menopausal women (30–34 years of age). Cells were isolated according to previously described protocols (Álvarez et al., 2018; Marinaro et al., 2019). Briefly, the menstrual blood was diluted 1:2 in phosphate buffered saline (PBS) and centrifuged at 450 × g for 10 min. The pellets of cells were resuspended in Dulbecco's Modified Eagle's medium (DMEM) (containing 10% fetal bovine serum (Gibco, Thermo Fisher Scientific, Bremen, Germany), 1% penicillin/streptomycin, and 1% glutamine) and cultured at 37°C and 5% $CO_2$. Cell culture medium was removed after 24 h to eliminate non-adherent cells. The adherent endMSCs were cultured to 80% confluency, then detached using PBS containing 0.25% trypsin (Lonza, Gaithersburg, MD, USA) and seeded again into 175 $cm^2$ culture flasks at a density of 5,000 cells/$cm^2$, changing the cell culture medium every 4 days. endMSCs characterization was carried out by flow cytometry and differentiation assay, as previously mentioned (Álvarez et al., 2018; Marinaro et al., 2019). Briefly, the phenotypic analysis by flow cytometry was performed on 2 × $10^5$ cells (passages 3–4), stained with human monoclonal antibodies against CD14, CD20, CD34, CD44, CD45, CD73, CD80, CD90, CD117, and HLA-DR, using the isotype-matched antibodies as negative controls. A FACScalibur cytometer (BD Biosciences, San Jose, CA, USA) and the CellQuest software (BD Biosciences) were used to analyze the cells. The differentiation of endMSCs toward the adipogenic, chondrogenic, and osteogenic lineages was carried out on cells at passages 3–4. After 21 days of culture in differentiation specific media (Gibco, Thermo Fisher Scientific), adipogenic, chondrogenic, and osteogenic differentiation were evidenced by Oil Red O, Alcian Blue, and Alizarin Red S stainings, respectively.

### Human endMSCs Treatment With IFNγ and EV-endMSCs Purification and Characterization

*in vitro* expanded endMSCs at passages 5–6 were treated with 3 ng/ml human IFNγ Recombinant Protein (Invitrogen, Thermo Fisher Scientific) for 6 days. For EV-endMSCs isolation, the standard culture medium (for control EV-endMSCs), or the culture medium containing IFNγ (for IFNγ/EV-endMSCs) were removed, and replaced by DMEM containing 1% insulin–transferrin–selenium (ThermoFisher Scientific), after rinsing with PBS. After 4 days, the supernatants were collected and EVs isolated according to a previous optimized protocol (Álvarez et al., 2018; Marinaro et al., 2019). Briefly, supernatants were centrifuged at 1,000 × g for 10 min and 5,000 × g for 20 min at 4°C to eliminate dead cells and debris. The supernatants were then filtered using firstly 450 nm pore size sterile cellulose acetate filters, followed by 200 nm pore size filters (Corning, NY, USA). 3 kDa MWCO Amicon® Ultra devices (Merck-Millipore, MA, USA) were used to concentrate up to 15 ml filtered supernatants, by centrifugation at 4,000 × g for 60 min at 4°C. The obtained concentrated supernatants were collected, characterized, and stored at −20°C for the subsequent analyses. EV-endMSCs characterization was carried out as previously described our group (Álvarez et al., 2018). Briefly, the protein content of EV-endMSCs was quantified by a Bradford assay (BioRad Laboratories, CA, USA); the size of EV-endMSCs was determined by nanoparticle tracking analysis (Malvern Panalytical Ltd., Malvern, UK), and the particle-tracking analysis software package version 2.2 (Malvern Panalytical Ltd.); EV-endMSCs surface marker analysis was performed by flow cytometry in a FACScalibur cytometer (BD Biosciences) and with the CellQuest software (BD Biosciences), after incubation with aldehyde/sulfate latex beads (Molecular probes, Life Technologies, Thermo Fisher Scientific), and human monoclonal antibodies against CD9 and CD63 (BD Biosciences, San Jose, CA, USA).

### Protein Analysis by High-Resolution Liquid Chromatography Coupled to Mass Spectrometry-Based Proteomics

The characterization of EV-endMSCs proteome from three different donors was performed by high-throughput multiplexed quantitative proteomics approach according to previously described protocols (Jorge et al., 2009; Navarro and Vázquez, 2009; Bonzon-Kulichenko et al., 2011; Navarro et al., 2014; García-Marqués et al., 2016). Protein extracts were incubated

with trypsin using the Filter Aided Sample Preparation (FASP) digestion kit (Expedeon, San Diego, CA), as previously described (Wiśniewski et al., 2011). The resulting peptides were labeled using 8plex-iTRAQ (isobaric Tags for Relative and Absolute Quantitation) reagents, according to manufacturer's instructions, and desalted on OASIS HLB extraction cartridges (Waters Corporation, Milford, MA, USA). Half of the tagged peptides were directly analyzed by liquid chromatography tandem mass spectrometry (LC-MS/MS) in different acquisition runs, and the remaining peptides were separated into three fractions using the high pH reversed-phase peptide fractionation kit (Thermo Fisher Scientific). Samples were analyzed using an Easy nLC 1000 nano-HPLC coupled to a QExactive mass spectrometer (Thermo Fisher Scientific). Peptides were injected onto a C18 reversed phase nano-column (75 μm I.D. and 50 cm, Acclaim PepMap100 from Thermo Fisher Scientific) in buffer A [0.1% formic acid (v/v)] and eluted with a 180 min lineal gradient of buffer B [90% acetonitrile, 0.1% formic acid (v/v)], at 200 nl/min. Mass spectrometry (MS) runs consisted of 140,000 enhanced FT-resolution spectra in the 390–1,500 m/z wide range and separated 390–700 m/z (range 1), 650–900 m/z (range 2), and 850–1,500 m/z (range 3) followed by data-dependent MS/MS spectra of the 15 most intense parent ions acquired along the chromatographic run. HCD fragmentation was performed at 30% of normalized collision energy. A total of 14 MS data sets, eight from unfractionated material and six from the corresponding fractions, were registered with 42 h total acquisition time. For peptide identification the MS/MS spectra were searched with the SEQUEST HT algorithm implemented in Thermo Fisher Proteome Discoverer version 2.1 using a Uniprot database containing human protein sequences (Dec-2017). For database searching, parameters were selected as follows: trypsin digestion with two maximum missed cleavage sites, precursor mass tolerance of 800 ppm, fragment mass tolerance of 0.02 Da. Variable methionine oxidation (+15.994915 Da) and fixed cysteine carbamidomethylation (+57.021 Da), and iTRAQ 8-plex labeling at lysine and N-terminal modification (+304.2054) were chosen.

## Peptide Identification, Protein Quantification, and Statistical Analysis

Peptide identification from MS/MS data was performed using the probability ratio method (Martínez-Bartolomé et al., 2008) and the false discovery rate (FDR) of peptide identification was calculated based on the search results against a decoy database using the refined method (Navarro and Vázquez, 2009). Peptide and scan counting were performed assuming as positive events those with a FDR equal or lower than 1%.

Quantitative information of iTRAQ-8plex reporter ions was extracted from MS/MS spectra using an in-house developed program (SanXoT), as described (Trevisan-Herraz et al., 2019), and protein abundance changes were analyzed using the weighted spectrum, peptide and protein (WSPP) statistical model (Navarro et al., 2014). This model provides a standardized variable, Zq, defined as the mean-corrected $\log_2$-ratio expressed in units of standard deviation at the protein level. For the protein functional analysis, proteins were annotated based on Gene Ontology database (The Gene Ontology Consortium, 2017) and Systems Biology Triangle (SBT) model (García-Marqués et al., 2016). This algorithm estimates weighted functional category averages (Zc) from the protein values by performing the protein to category integration. Student *t*-test was used to compare Zq and Zc values from EV-endMSCs and IFNγ/EV-endMSCs, and the statistical significance was set at $p$-value $< 0.05$. Enrichment analysis of proteins was performed by DAVID bioinformatics tool (Huang et al., 2009a,b) and Benjamini-Hochberg FDR was used for multiple test correction (FDR $< 0.05$).

Principal Component Analysis (PCA) was performed on Zq values of 895 selected proteins (number of peptides, Np, >2 at 1% FDR) quantified after iTRAQ proteomics analysis, using Metaboanalyst software version 4.0 (https://www.metaboanalyst.ca/) (Chong et al., 2018).

## Human M-CSF ELISA

Considering the biological relevance of M-CSF, the changes observed for this protein were analyzed by ELISA. The quantification of M-CSF (also called CSF-1) was performed using the Human M-CSF Pre-Coated ELISA Kit (Peprotech, UK) according to the manufacturer's instructions. Briefly, the EV-endMSCs and IFNγ/EV-endMSCs from four different donors were diluted 1:10 in dilution buffer and quantified. Median, mean, 25th percentile, and 75th percentile were calculated and paired *t*-test was used to compare the two groups.

## miRNA Analysis by Next Generation Sequencing

All experiments, except IPA, PCA, miRTargetLink, and DAVID analyses, were performed at QIAGEN Genomic Services (Hilden, Germany). Total RNA was isolated from aliquots of 3–4 ml of concentrated EV-endMSCs, with an exoRNeasy Serum/Plasma Kit (QIAGEN) according to manufacturer's instructions. For NGS, the miRNA NGS library was generated by fragmentation and reverse transcription to cDNA, starting with 5 μl total RNA for each sample, and with the use of the QIAseq miRNA Library Kit (QIAGEN). Each individual RNA molecule was tagged with adapters containing a Unique Molecular Index (UMI), aimed to detect, quantify, and sequence unique RNA transcripts with high-resolution. The obtained cDNAs were amplified in 22 cycles of PCR and purified. Bioanalyzer 2100 or TapeStation 4200 (both from Agilent Technologies, Santa Clara, CA, USA) were used for library preparation QC. The libraries were pooled in equimolar ratios, according to quality and concentration of the inserts, and were submitted to qPCR for quantification. Next, the library pools were sequenced on a NextSeq500 sequencing instrument in accordance with manufacturer's indications. The bcl2fastq software (Illumina, San Diego, CA, USA) was used to obtain FASTQ files from raw data, and the FastQC tool (http://www.bioinformatics.babraham.ac.uk/projects/fastqc/) was adopted the check FASTQ data.

As previously mentioned, adapters and 12 nt-long UMI sequences were ligated to RNA molecules during processing.

Therefore, trimming and UMI correction were required before moving to the mapping of detected sequences. Cutadapt (1.11) (https://cutadapt.readthedocs.io/en/stable/) was used to rid the raw reads of adapter sequences and UMIs. Briefly, the raw FASTQ data were screened to detect adapters and UMI, filtering only the reads containing adapters and insert sequence length equal or larger than minimal insert length (default 16 nt). Raw data with UMI sequences shorter than 10 nt were discarded, while reads containing UMI (equal or longer than 10 nt) were classified in partial-UMI reads (equal or longer than 10 nt), and full-UMI reads (equal or longer than 12 nt). The last reads were combined and were submitted to the quality control (FastQC) and to the mapping process, that was carried out with the software Bowtie2 (2.2.2) in order to evaluate the quality of the samples. Reads were aligned to spike-ins, abundant sequence and miRBase_20 (http://www.mirbase.org/) (Kozomara et al., 2019) taking into consideration, as mapping criterion, the perfect match of the reads to the reference sequences. To map to the genome, not more than one mismatch was allowed in the first 32 bases of the read. No INDELs (small insertions and deletions) were allowed in mapping. Bowtie2 (2.2.2) was used to map the reads. UMI-corrected reads whose length was around 18–23 nucleotides and that were associated to relevant entries in mirbase_20, were selected for further analyses.

Mapped miRNAs with Tags Per Million (TPM) $\geq$ 10, belonging to EV-endMSCs samples, were processed by IPA (QIAGEN Inc.) (Ngwa et al., 2011) to determine the human targeted genes with *Experimentally observed* annotations. Enrichment analysis of EV-endMSCs microTargets was performed using DAVID bioinformatics tool. Only terms with $p$-value $< 0.05$ were considered statistically significant. For multiple test correction, Benjamini-Hochberg approach was used to control the FDR (FDR $< 0.05$).

PCA was performed on log-fold and absolute gene-wise changes in expression levels between samples (TMM normalization) (Robinson and Oshlack, 2010) of the 225 miRNAs, considering that each miRNA was detected in at least three of the four replicates from one group (EV-endMSCs and IFNγ/EV-endMSCs), and using Metaboanalyst software (version 4.0) (https://www.metaboanalyst.ca/) (Chong et al., 2018).

Differential expression analysis was performed using the EdgeR statistical software package (http://bioconductor.org/). For normalization, the trimmed mean of M-values method based on log-fold and absolute gene-wise changes in expression levels between samples (TMM normalization) was used. Using Benjamini-Hochberg FDR corrected $p$-values, miRNAs were considered differentially expressed at a significance level of 0.05 (FDR). IPA was performed to determine the microTargets of the significantly altered miRNAs between EV-endMSCs and IFNγ/EV-endMSCs samples.

In order to identify multiple query nodes among miRNAs in EV-endMSCs, the top-abundant miRNAs ($\geq$200 TPMs), were submitted to a miRTargetLink analysis. Only results with a strong experimental evidence were taken into consideration.

## Macrophage Polarization Assay

Human monocytes from one healthy donor were isolated from peripheral blood collected in EDTA containing tubes. Blood was diluted in PBS, layered over Histopaque-1077 (Sigma, St. Louis, MO) and centrifuged at 900 × g for 20 min at room temperature. The peripheral blood mononuclear cells were carefully aspirated and washed twice with PBS. The peripheral blood mononuclear cells were resuspended in RPMI-1640 supplemented with 10% FBS. The cells were seeded in tissue culture plates and incubated for 3 h at 37°C and 5% $CO_2$. Non-adherent cells were removed by four washes with PBS. Adherent monocytes were stimulated with 50 ng/ml of Macrophages Colony-Stimulating Factor (M-CSF) (Gibco, Thermo Fisher Scientific) to promote the cell differentiation from monocytes to M2 macrophages. Simultaneously, adherent monocytes were stimulated with 50 ng/ml of Granulocyte-Macrophages Colony-Stimulating Factor (GM-CSF) (Gibco, Thermo Fisher Scientific) to promote cell differentiation from monocytes to M1 macrophages (Gao et al., 2018). Finally, EV-endMSCs and IFNγ/EV-endMSCs from four different donors were added to the adherent monocytes. At day 6, adherent cells were trypsinized with a 0.25% trypsin solution, washed, and counted for flow cytometry analysis.

For flow cytometry, adherent cells co-cultured with M-CSF, GM-CSF, EV-endMSCs, and IFNγ/EV-endMSCs were incubated for 30 min at 4°C with the following human monoclonal antibodies from BD Biosciences. PE-conjugated anti-CD14 was used as macrophage marker and APC-conjugated anti-CD206 was used as a M2-differentiation marker. Cells were analyzed on a FACScalibur cytometer (BD Biosciences) using FSC/SSC characteristics. Fluorescence was analyzed with CellQuest Pro software (BD Biosciences), using isotype-matched antibodies as negative controls. The percentage of CD206-positive cells on gated CD14 macrophages was represented. Median, mean, 25th percentile, and 75th percentile were calculated and paired $t$-test was used to compare EV-endMSCs and IFNγ/EV-endMSCs with GM-CSF.

For transcriptional analysis studies, total RNA from adherent cells co-cultured with EV-endMSCs ($n = 3$) and IFNγ/EV-endMSCs ($n = 3$) was isolated at day 6 using mirVana miRNA isolation kit (ThermoFisher Scientific), following the manufacturer's protocol for total RNA extraction. Quality and concentration of total RNAs were evaluated by spectrophotometry. The cDNA was synthesized from 55 ng of RNA in reverse transcription reactions performed with the iScript Reverse Transcription Supermix (BioRad, Hercules, CA, USA), according to manufacturer's instructions. 5.5 ng of cDNA for each sample were then amplified in qPCR reactions using TaqMan™ Fast Advanced Master Mix (Catalog number 4444964, ThermoFisher Scientific) and TaqMan® Gene Expression Assays probes (ThermoFisher Scientific) for the genes *TBP* (Assay ID: Hs00427620_m1), *IL1B* (Hs01555410_m1), *TNF* (Hs00174128_m1), *NOS2* (Hs01075529_m1), and *TGFB* (Hs00998133_m1). Samples were evaluated in triplicate and 2 µl of water replaced the cDNA templates in the three negative controls for each probe. All the reaction mixtures were prepared

following manufacturer's protocol, and the suggested thermal profile was used to carry out templates amplification in a QuantStudio 3 Real-Time PCR System (Applied Biosystems, Thermo Fisher Scientific Inc.). The qRT-PCR products were quantified by fluorescent method using the $2^{-\Delta Ct}$ expression. All samples were analyzed separately and normalized using TATA-Box Binding Protein (*TBP)* as endogenous control (Saleh et al., 2011).

## RESULTS

### Characterization of endMSCs and EV-endMSCs

The phenotypic analysis of endMSCs was performed by flow cytometry. The endMSCs ($n = 4$) were negative for CD14, CD20, CD34, CD45, CD80, and HLA-DR, while CD44, CD73, CD90, and CD117 markers were positively expressed. Microscopic analysis of Oil Red O, Alcian Blue, and Alizarin Red S stainings on endMSCs cultured in differentiation specific media proved their multipotency toward the adipogenic, chondrogenic, and osteogenic lineages. The nanoparticle tracking analysis of EV-endMSCs showed that their mean size was 153.5 ± 63.05 nm. Furthermore, CD9 and CD63 exosomal markers were positively expressed, in accordance with the Minimal information for studies of extracellular vesicles 2018 (MISEV2018) guidelines (Théry et al., 2018) (**Supplementary Figure 1**). An accurate explanation and the characterization of cells and vesicles can be found in our previous studies (Álvarez et al., 2018; Blázquez et al., 2018; Marinaro et al., 2019).

### Characterization of EV-endMSCs Molecular Cargo

In order to elucidate the modulation of protein composition suffered by EV-endMSCs under IFNγ priming, we have resorted to a high-throughput quantitative proteomic approach performed using multiplex peptide stable isotope labeling (**Figure 1**). The datasets generated and analyzed for this study are available via ProteomeXchange (http://www.proteomexchange.org/) with identifier PXD015465 (https://www.ebi.ac.uk/pride/archive/projects/PXD015465). This strategy of data discovery gave us a reliable identification of 895 proteins (number of peptides, Np, >2 at 1% FDR) corresponding to 866 human genes (**Supplementary Table 1**). Of note, 71 proteins were included in the 100 top-identified proteins of ExoCarta database (http://www.exocarta.org/) (Keerthikumar et al., 2016), and 617 proteins were annotated as *Extracellular exosome* proteins (GO:0070062) in the Gene Ontology (GO) database ($p$-value < 0.001, 1% FDR) (**Figure 1**, **Supplementary Table 2**). These exosomal proteins corresponded to about 80% of the EV-endMSCs proteome composition in terms of absolute quantification (**Supplementary Table 1**). Regarding the subcellular origin of EV-endMSCs identified proteins, *Extracellular matrix* (GO:0031012), *Cytosol* (GO:0005829), and *Membrane* (GO:0016020) were the most representative categories (**Figure 2A**, **Supplementary Table 2**). *Mitochondrion* (GO:0005739), and *Cytoskeleton* (GO:0005856) terms were also significantly enriched ($p$-value < 0.001, 1% FDR). In contrast, no significant results were found for nuclear, or ribosomal proteins. Interestingly, *Immunological synapse* (GO:0001772) related proteins were also significantly represented in the EV-endMSCs proteome (enrichment $p$-value < 0.001, 1% FDR) (**Figure 2B**, **Supplementary Table 2**).

Since RNA species are also essential components of EV cargo (Abels and Breakefield, 2016), we performed NGS analysis to identify and quantify the presence of miRNAs in EV-endMSCs and IFNγ/EV-endMSCs (**Figure 1**). The datasets generated and analyzed for this study can be found in the European Nucleotide Archive (https://www.ebi.ac.uk/ena) with accession number PRJEB34442. On average 6.6 million UMI-corrected reads were obtained for each sample and the average percentage of mappable reads was 79.5%. Nearly 54% (on average) corresponded mostly to small RNA species (**Supplementary Figure 2**).

After mapping the data using miRBase 20 database, a total of 225 miRNAs were identified in at least three of the four replicates from each group (EV-endMSCs and IFNγ/EV-endMSCs). In order to predict the potential effects that these miRNAs may have on a target cell, we performed an Ingenuity Pathway Analysis (IPA). This analysis allowed us to elucidate a detailed regulatory network to identify those genes targeted by identified miRNAs (Ngwa et al., 2011). The microTargets with *Experimentally observed* annotations for these microRNAs were analyzed (**Supplementary Table 3**). A total of 48 miRNAs identified in EV-endMSCs (≥10 TPM) targeted 937 genes (**Supplementary Table 3A**). Of note, key intracellular signaling nodes, such as *PTEN* or *MYC* were highly targeted (8 and 4 miRNAs targeted these genes, respectively) (**Supplementary Table 3B**). In contrast to protein cargo, enrichment analysis showed that the preferred site for miRNAs targeting is the nucleus ($n$ = 371 microTargets) (**Figure 2C**). Other over-represented subcellular targets were cytosol ($n$ = 296 microTargets), plasma membrane ($n$ = 250), and mitochondrion ($n = 101$), among others (**Figures 2C,D** and **Supplementary Table 4**). The miRTargetLink analysis (Wong and Wang, 2015; Liu and Wang, 2019) was performed to identify multiple query nodes among those miRNAs with more than or equal to 200 TPMs, on average: hsa-let-7a-5p, hsa-miR-143-3p, hsa-miR-21-5p, hsa-let-7b-5p, hsa-let-7f-5p, hsa-miR-16-5p, and hsa-miR-199a-3p (see **Supplementary Table 3A**). Our results revealed that *PTGS2*, *BCL2*, *KRAS*, *HRAS*, *EGFR*, *HMGA2*, *HMGA1*, *CDK6*, *TNFRSF10B*, *CCND1*, and *PRDM1* genes were targeted by at least three of these miRNAs with a strong experimental evidence and that *IGF1R* was the target of four out of seven top-abundant miRNAs in EV-endMSCs (hsa-miR-143-3p, hsa-miR-16-5p, hsa-miR-21-5p, and hsa-let-7b-5p) (**Supplementary Figure 3**).

Interestingly, enrichment analyses also showed the potential effect of molecular cargo on different biological processes (**Figure 3**). EV-endMSCs proteins were shown to be involved in several processes as the *extracellular matrix organization* (GO:0030198), the *unfolded protein response* (GO:0006986), and the *cell redox homeostasis* (GO:0045454) ($p$-value < 0.001, 1% FDR, **Figure 3A**, **Supplementary Table 2**). Besides, the

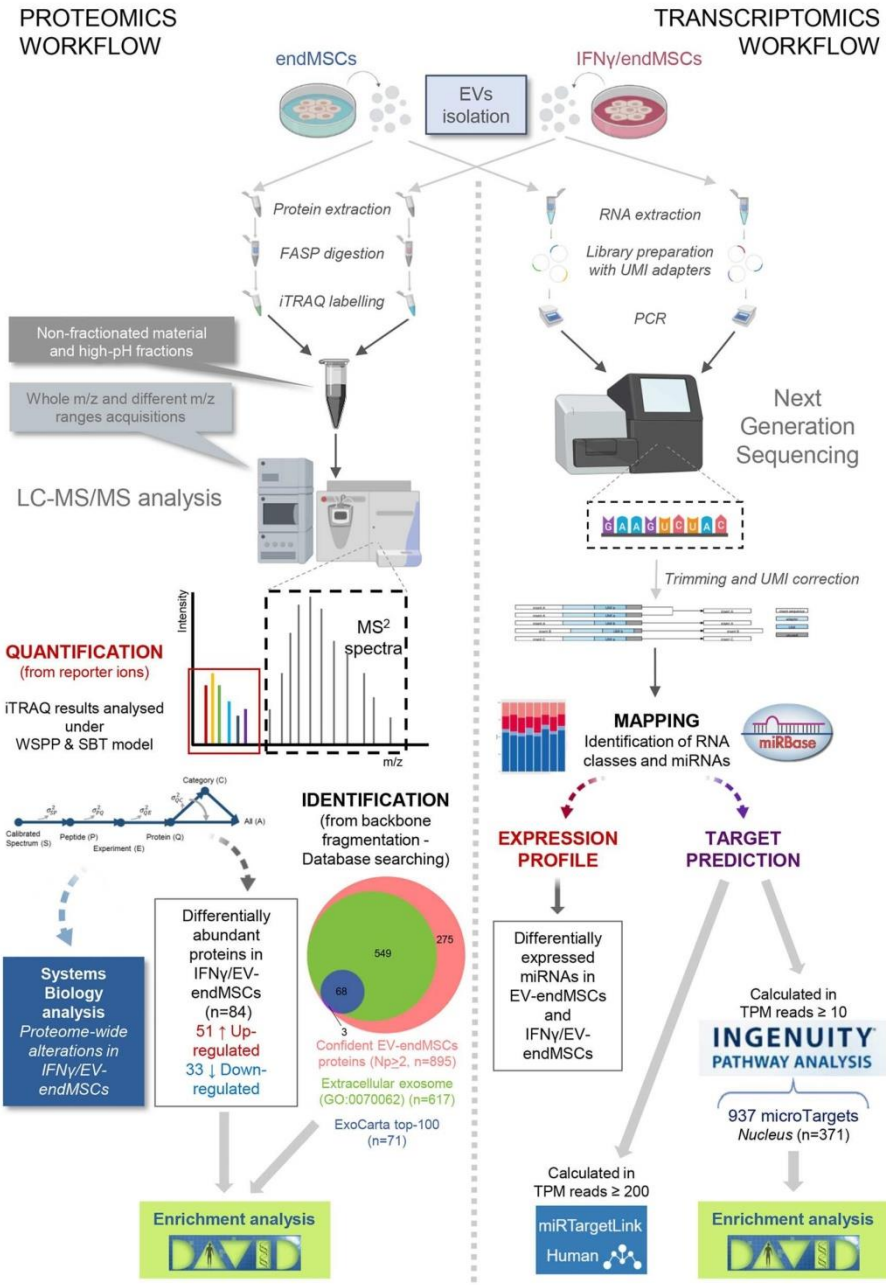


**FIGURE 1 |** Overview of the proteomic and transcriptomic approaches. For both studies, EV samples were obtained from endMSCs under two different conditions (IFNγ-treated and control cells). According to proteomic procedures (fully described in Materials and Methods section), iTRAQ technology allowed us to simultaneously obtain peptide identification and quantification from the MS2 spectra. We identified 895 confident proteins (at least two different peptide backbone

*(Continued)*

**FIGURE 1 |** fragmentation spectrum matched with reference sequences from database under 1% FDR). At the same time, quantification of peptide/protein levels were retrieved from the reporter ions (low m/z range in the MS2 spectra) being analyzed under the *WSPP* model (Navarro et al., 2014). In order to describe proteome-wide alterations, category analyses were performed based on the *SBT* model (García-Marqués et al., 2016). For the transcriptomics workflow, extracted total RNAs from EV samples were submitted to Next Generation sequencing. The UMI-corrected reads were aligned to miRBase (http://www.mirbase.org/) to discriminate the populations of RNAs in EVs cargo, and for the identification of the detected miRNAs in EV-endMSCs and IFNγ/EV-endMSCs. Human targeted genes were detected after an Ingenuity Pathway Analysis (IPA) on mapped microRNAs of control cells with TPM ≥ 10. Of the 937 identified microTargets, 371 were associated to the nucleus that may be the preferred site of EV-endMSCs targeting. miRTargetLink (https://ccb-web.cs.uni-saarland.de/mirtargetlink/) was used to identify multiple query nodes among identified miRNAs (TPM ≥ 200). Enrichment analyses of protein and microTarget lists were performed by DAVID software (https://david.ncifcrf.gov/) using Benjamini-Hochberg FDR for multiple test correction (FDR < 0.05). Images have been created with BioRender (https://app.biorender.com/), and BioVenn (http://www.biovenn.nl/). Two pictures in the trascriptomics workflow belong to the miRNA NGS Data Analysis Report from QIAGEN Genomic Services (Hilden, Germany). endMSCs, Endometrial-derived MSCs; EV, Extracellular Vesicles; EV-endMSCs, Extracellular Vesicles from Endometrial-derived stromal/Mesenchymal Stem Cells; FASP, Filter-Aided Sample Preparation; FDR, False Discovery Rate; HPLC-MS, High-Performance Liquid Chromatography coupled to Mass Spectrometry; IFNγ/EV-endMSCs, Extracellular Vesicles from IFNγ-primed Endometrial-derived stromal/Mesenchymal Stem Cells; IPA, Ingenuity Pathway Analysis; iTRAQ, Isobaric Tags for Relative and Absolute Quantitation; LC-MS/MS, Liquid chromatography tandem mass spectrometry; PCR, Polymerase Chain Reaction; SBT, Systems Biology Triangle; TPM, Tags Per Million; UMI, Unique Molecular Index; WSPP, Weighted Spectrum Peptide Protein.

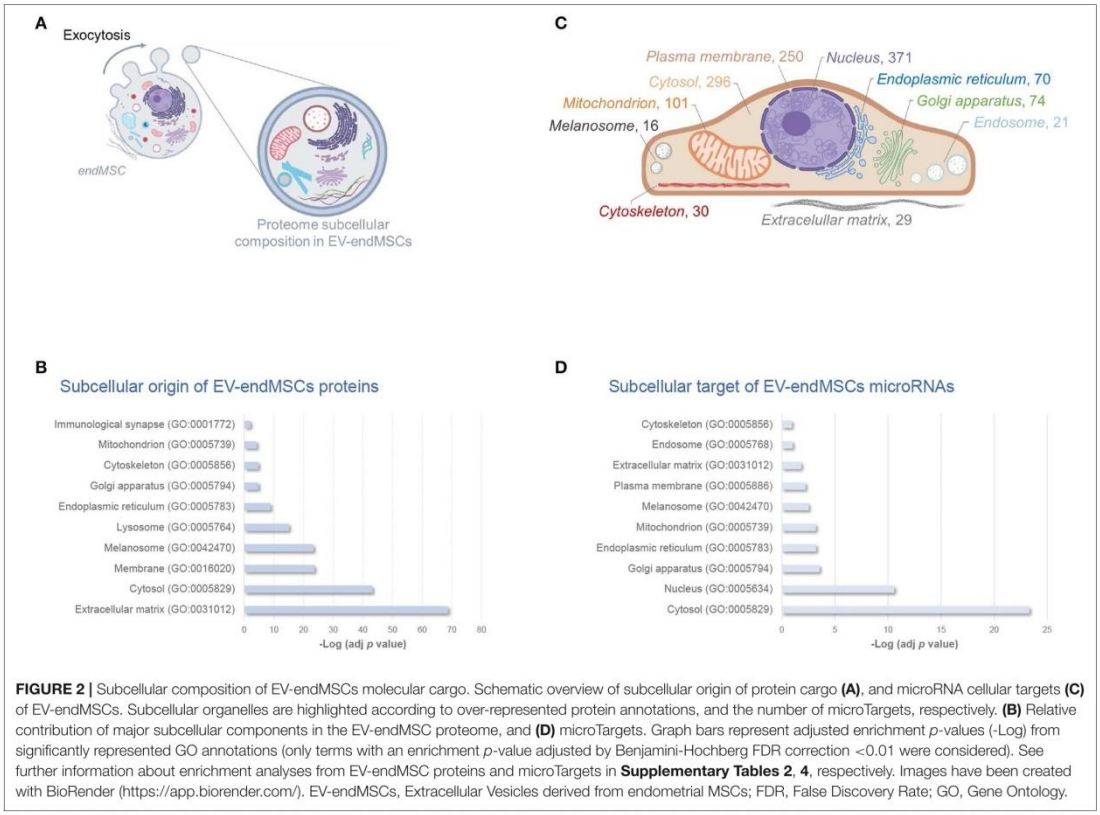


**FIGURE 2 |** Subcellular composition of EV-endMSCs molecular cargo. Schematic overview of subcellular origin of protein cargo **(A)**, and microRNA cellular targets **(C)** of EV-endMSCs. Subcellular organelles are highlighted according to over-represented protein annotations, and the number of microTargets, respectively. **(B)** Relative contribution of major subcellular components in the EV-endMSC proteome, and **(D)** microTargets. Graph bars represent adjusted enrichment *p*-values (-Log) from significantly represented GO annotations (only terms with an enrichment *p*-value adjusted by Benjamini-Hochberg FDR correction <0.01 were considered). See further information about enrichment analyses from EV-endMSC proteins and microTargets in **Supplementary Tables 2**, **4**, respectively. Images have been created with BioRender (https://app.biorender.com/). EV-endMSCs, Extracellular Vesicles derived from endometrial MSCs; FDR, False Discovery Rate; GO, Gene Ontology.

miRNA component was shown to affect *signaling transduction* (GO:0007165), *cell proliferation* (GO:0008283) and *apoptotic processes* (GO:0006915), among others ($p$-value < 0.001, 1% FDR, **Figure 3B**, **Supplementary Table 4**). Interestingly, *MAPK cascade* (GO:0000165), and *PI3K-Akt signaling* (hsa04151) pathways were also over-represented among microTargets ($p$-value < 0.001, 1% FDR) (**Figure 3B**), which in turn showed a significant enrichment within protein cargo (**Figure 3A**, **Supplementary Table 2**). Finally, results from tissue up-regulated gene annotations showed that microTargets were over-represented in brain ($n$ = 427), placenta ($n$ = 273 genes), epithelium ($n$ = 232), liver ($n$ = 147), and B-cells ($n$ = 32) among others ($p$-value < 0.01, 1% FDR, **Supplementary Table 4**).

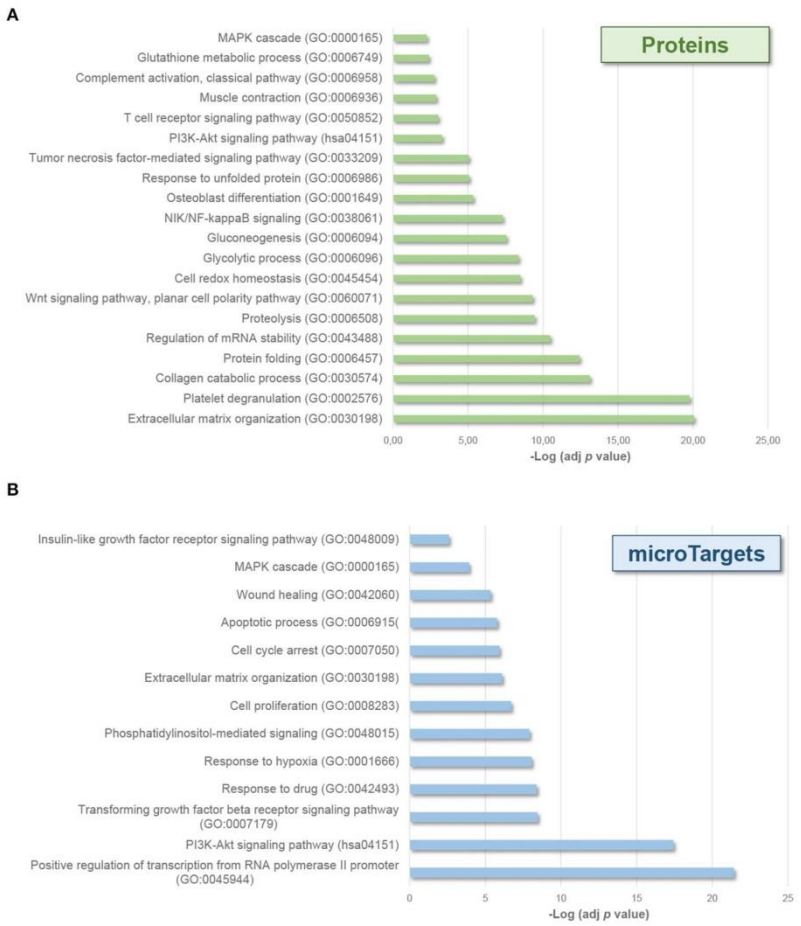


**FIGURE 3 |** Biological processes affected by EV-endMSCs molecular cargo. Graph bars represent adjusted enrichment *p*-values (–Log) of significantly enriched categories from proteins **(A)**, and microTargets **(B)**. Only terms with an enrichment *p*-value adjusted by Benjamini-Hochberg FDR correction <0.01 were considered. See further information about enrichment analyses from EV-endMSC proteins and microTargets in **Supplementary Tables 2**, **4**, respectively. EV-endMSCs, Extracellular Vesicles derived from endometrial MSCs; FDR, False Discovery Rate.

## Effect of IFNγ Priming in the EV-endMSCs Proteome Signature

With the aim of studying the modulation of protein composition in EV-endMSCs under IFNγ treatment, a comparative analysis of the proteome from EV-endMSCs ($n = 3$) and IFNγ/EV-endMSCs ($n = 3$) was carried out (**Figure 1**). The multiplexed quantitative proteomics approach provided an extensive dynamic range and great proteome coverage, allowing the simultaneous identification and quantification of hundreds of proteins in the same experiment, which offers an invaluable advantage for the analysis of limited sample amounts (Edwards and Haas, 2016; Jylhä et al., 2018), as the case for EVs samples. In this study, protein abundance changes in each sample were calculated in relation to the average values of each protein corresponding to control samples [$\log_2$-ratio expressed in units of standard deviation (Zq), **Supplementary Table 5**]. We have applied a robust and rigorous *ad-hoc* statistical analysis based on the WSPP model (Navarro et al., 2014), which has been repeatedly validated for the treatment of quantitative proteomics data in several models (Ruiz-Meana et al., 2014; Gómez-Serrano et al., 2016; Binek et al., 2017; Martínez-López et al., 2019).

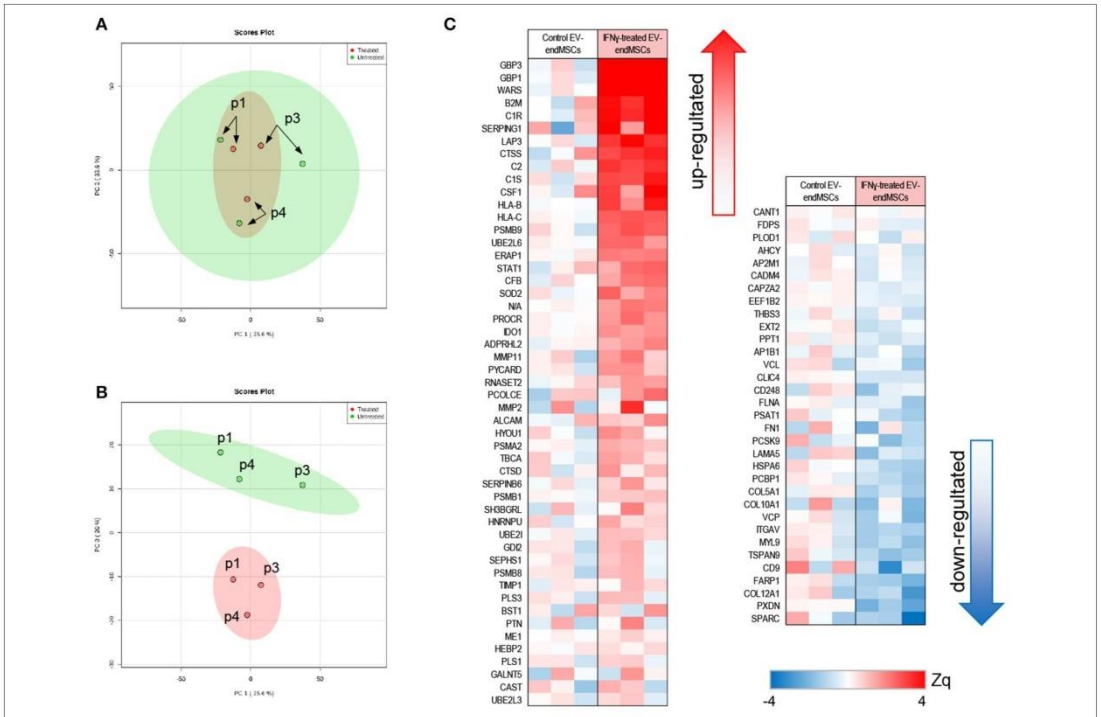


**FIGURE 4 |** Quantitative proteomic analysis of IFNγ/EV-endMSCs. A total of 895 proteins (number of peptides, Np, >2 at 1% FDR) quantified after iTRAQ proteomic approach were first subjected to Principal Component Analysis (PCA). **(A)** Score plot for PC1 (35.6% variance explained) vs. PC2 (33.6% variance explained). **(B)** Score plot for PC1 (35.6% variance explained) vs. PC3 (20% variance explained). Data display 95% confidence regions. Patient origin ($n = 3$) are indicated on the plots as p1, p3, and p4. IFNγ/EV-endMSCs (treated) and EV-endMSCs (untreated, control) samples are indicated in red and green, respectively. **(C)** Quantitative proteomics results. Protein profile changes were analyzed by WSPP model (Navarro et al., 2014) to identified significantly altered proteins comparing IFNγ/EV-endMSCs and EV-endMSCs samples. Protein values (Zq) are reported as the standardized variable, which is defined as the mean corrected $\log_2$-ratio expressed in units of standard deviation. Protein ratio of each sample was calculated against an internal standard (IS) based on the average of iTRAQ reporters from EV-endMSCs control samples. Statistical differences between Zq values of samples groups were evaluated by paired *t*-test. Significant protein abundance change was set at *p*-value <0.05. EV-endMSCs, Extracellular Vesicles derived from endometrial MSCs; IFNγ/EV-endMSCs, Extracellular Vesicles derived from IFNγ-primed endometrial MSCs; WSPP, Weighted Spectrum Peptide Protein.

The unsupervised study of proteomic results through PCA revealed substantial differences between EV-endMSCs and IFNγ/EV-endMSCs (**Figures 4A,B**, **Supplementary Figure 4**). Additionally, PCA analyses revealed that distribution of main protein components (PC1 *vs.* PC2) from the same individual behaved similarly, underlying a distinctive individual EV-endMSCs proteome background regardless of endMSCs treatment (**Figures 4A,B**). Despite inter-individual differences, IFNγ-priming of endMSCs caused an important effect on EVs proteome (**Figure 4B**). In order to evaluate the most representative candidates of this effect, differences in protein levels between samples groups were evaluated through paired *t*-test. A total of 84 proteins showed significant changes ($p$-value < 0.05) between EV-endMSCs and IFNγ/EV-endMSCs (51 and 33 proteins were up- and down-regulated, respectively) (**Figure 4C**, **Supplementary Table 5**). Notably, guanylate-binding proteins 1, and 3 (GBP1, GBP3) were highly up-regulated under IFNγ-treatment as well as proteins related to complement system, such as C1R (complement C1r subcomponent), C1S (complement C1s subcomponent), or SERPING1 (Plasma protease C1 inhibitor) (**Figure 4C**). Additionally, cytokines, such as CSF1 (also called M-CSF), cell adhesion molecules, like CD166 antigen—an important component of the immunological synapse (Kato et al., 2006; Gilsanz et al., 2013), and CD9 antigen—involved in platelet activation and aggregation (Worthington et al., 1990; Miao et al., 2001)—were also altered in IFNγ/EV-endMSCs. Enrichment analyses showed that IFNγ protein mediators were over-represented among differentially abundant proteins ($p$-value < 0.001, 5% FDR) (**Supplementary Table 6**). These analyses also pinpointed significant changes on proteins related to *angiogenesis* (GO:0001525), *collagen catabolism* (GO:0030574), *tumor necrosis factor signaling* (GO:0033209), *innate immune response*

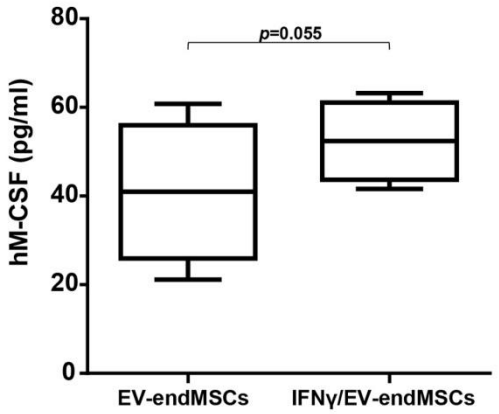


**FIGURE 5 |** Human M-CSF in extracellular vesicles derived from endometrial mesenchymal stem cells. The quantification of hM-CSF was performed by ELISA. EV-endMSCs from different donors were analyzed ($n = 4$). The lower boundary of the boxes indicates the 25th percentile and the upper boundary, the 75th percentile. Bars above and below the boxes indicate the 90th and 10th percentiles. The line within the boxes marks the median. A paired *t*-test was used to compare EV-endMSCs and IFNγ/EV-endMSCs.

(GO:0045087), and *proteasome core complex* (GO:0005839), among others.

Based on proteomic analyses and considering the biological relevance of human M-CSF on M1/M2 macrophage polarization, M-CSF was quantified by ELISA. EV-endMSCs and IFNγ/EV-endMSCs from different donors were analyzed ($n = 4$) and compared by a paired *t*-test. Human M-CSF levels appeared to be modified in IFNγ/EV-endMSCs, when compared to controls (**Figure 5**).

To study the impact of IFNγ-priming on protein functional dynamics, we additionally analyzed the normal distribution of protein quantifications predicted by the WSPP statistical model (Navarro et al., 2014) under the null hypothesis using the Systems Biology Triangle (SBT) algorithm (García-Marqués et al., 2016), which allows to detect alterations to protein function produced by the coordinated action of proteins in biological systems. Thus, a functional category was considered up- or down-regulated when the changes of its protein components fail to follow a normal distribution. In the comparison of protein profiles between EV-endMSCs and IFNγ/EV-endMSCs, a total of 117 functional categories were found significantly altered ($p$-value $< 0.05$), considering categories containing more than ten proteins (**Supplementary Table 7**). As expected, one of the largest category clusters, comprising 10 categories related to *antigen processing and presentation* (i.e., GO:0019882; GO:0002480; GO:0042605; GO:0002479; GO:0002486; GO:0002474; GO:0002486; GO:0003823; hsa04612), was increased. The majority of the corresponding protein components were up-regulated (e.g., HLA class I histocompatibility antigens, proteasome subunits, beta-2-microglobulin and heat shock proteins). In agreement with the enrichment analysis, *innate immune response* (GO:0045087) was up-regulated, with a significant increase of B2M, SERPING1, CSF1, PYCARD, and HLA-B and C proteins, among others. In addition, *adaptive immune response* (GO:0002250) encompassing differentially abundant proteins, such as ERAP1, ALCAM, and CTSS were also up-regulated (**Figure 6A**, **Supplementary Table 8A**). Notably, *complement activation* (GO:0006958) composed of C1R, C1S, SERPING1, or C2 immune mediators (**Figure 6B**, **Supplementary Table 8B**) was significantly up-regulated. Finally, functional proteome profiling revealed that several cell signaling pathways were also altered (**Supplementary Table 7**). This cluster contained several proteins with statistically significant increased abundance when comparing EV-endMSCs and IFNγ/EV-endMSCs. Some remarkable examples are the *IFNγ-mediated signaling pathway* (GO:0060333) and *NIK/NF-kappaB signaling* (GO:0038061), *T cell receptor signaling pathway* (GO:0050852) and *MAPK cascade* (GO:0000165), mostly related to the *proteasome complex* (GO:0000502). This complex includes significantly up-regulated subunits, such as PSMB10, PSMB9, PSME1, and PSME2 (**Figure 6C**, **Supplementary Table 8C**).

## microRNAome Alterations in EV-endMSCs Under IFNγ Priming

A comparative analysis of the miRNA expression profile was carried out in EV-endMSCs ($n = 4$) and IFNγ/EV-endMSCs ($n = 4$) (**Figure 1**). PCA analysis demonstrated that EV-endMSCs microRNAome does not discriminate as much as proteome does (**Supplementary Figure 5**).

The comparison of miRNA expression among EV-endMSCs and IFNγ/EV-endMSCs led to 18 significantly altered miRNAs ($p$-value $< 0.05$), four of them with an FDR $< 0.05$ (hsa-miR-196b-5p, hsa-miR-1246, hsa-miR-92a-3p, hsa-miR-150-5p) (**Table 1**, **Supplementary Table 9**). Next, we aimed to obtain a better understanding of the functional impact of these altered miRNAs at the cell, for which we performed IPA analysis to determine the potential microTargets.

According to IPA analysis, only two miRNAs (hsa-miR-150-5p and hsa-miR-196b-5p) showed *Experimentally observed* target annotation (**Figure 7**). The genes targeted by hsa-miR-150-5p are involved in acute-phase response and signaling in macrophages (*Akt, CEBPB*), IL signaling (*CSF1R*), adipogenesis (*EGR2*), inhibition of angiogeneisis (*VEGFA*), endocytosis, macropinocytosis (*PDGFB*), and glucocorticoid receptor signaling (*CEBPB*), among others. On the other hand, among the genes targeted by hsa-miR-196b-5p, there were *ANXA1* and *KRT5* (implicated in glucocorticoid receptor signaling), as well as *IKBKB* and *S100A9* (both associated to IL-mediated cell signaling). The full list of microTargets from the differentially expressed miRNAs and their functional pathways are described in **Supplementary Table 10**.

## Macrophage Polarization Assay

Human monocytes were *in vitro* cultured and differentiated toward M1-macrophages and M2-macrophages using GM-CSF and M-CSF, respectively. Similarly, human monocytes were co-cultured with EV-endMSCs ($n = 4$) and IFNγ/EV-endMSCs ($n$

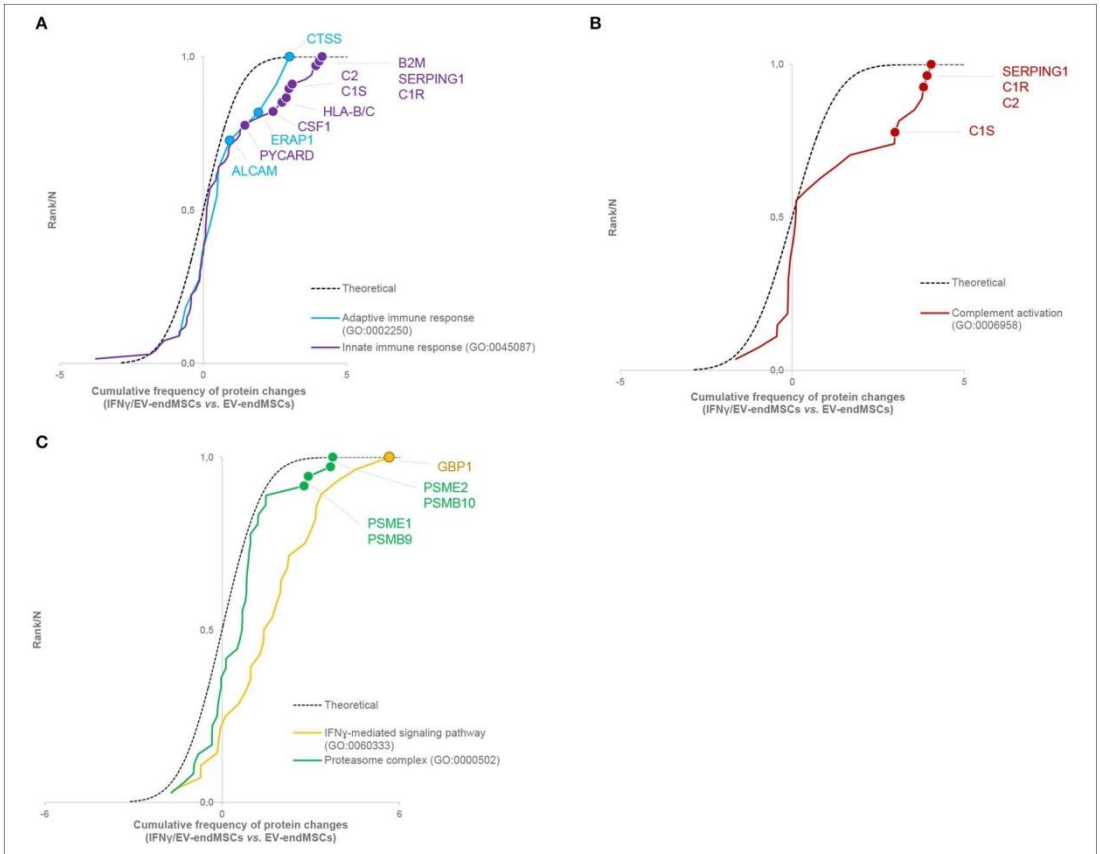


**FIGURE 6 |** Systems biology analysis of the IFNγ effect on EV-endMSC proteome. Quantitative proteomics results were analyzed using the Systems Biology Triangle (SBT) model (García-Marqués et al., 2016) to detect coordinated protein changes in the functional pathways. Functional categories were considered significantly changed at *p*-value <0.05. Results show the cumulative distribution of average difference of Zq values from proteins of interesting categories. A right-wards shift from the theoretical curve represents a global tendency of up-regulation in IFNγ/EV-endMSCs *vs*. EV-endMSCs. **(A)** *Innate immune response* (GO:0045087), and *adaptive immune response* (GO:0002250). **(B)** *Complement activation* (GO:0006958). **(C)** *IFNγ-mediated signaling pathway* (GO:0060333), and *proteasome complex* (GO:0000502). The complete sets of protein changes from each category are listed in **Supplementary Tables 8A–C**, respectively. EV-endMSCs, Extracellular Vesicles derived from endometrial MSCs; IFNγ/EV-endMSCs, Extracellular Vesicles derived from IFNγ-primed endometrial MSCs.

= 4). At day 6, the flow cytometry analysis of CD206 allowed us to quantify the monocyte-to-macrophage differentiation and polarization (**Figure 8**). Our results demonstrated that EV-endMSCs and IFNγ/EV-endMSCs triggered the macrophage differentiation toward M2 phenotype ($p < 0.05$). As expected, significant differences were found when we compared M1-differentiated cells and EVs-differentiated cells. However, our study did not reveal any significant difference between EV-endMSCs and IFNγ/EV-endMSCs.

Finally, for a more detailed characterization, *in vitro* differentiated monocytes co-cultured with EV-endMSCs and IFNγ/EV-endMSCs were also analyzed by qPCR. In this analysis, M1/M2 cytokines (*IL1b*, *TNF*, *TGFb,* and *NOS2)* did not reveal any conclusive result in terms of gene expression (**Supplementary Figure 6**).

## DISCUSSION

The extracellular vesicles (EVs) derived from MSCs are gaining interest among researchers (Keshtkar et al., 2018), and a proof of that is the increasing number of related publications (Roy et al., 2018). MSCs can be isolated from very different sources, however, endometrial tissue-resident MSCs are especially attractive from a therapeutic point of view because of their remarkable proliferating capacity, effective regenerative, and angiogenic potential (Tempest et al., 2018).

**TABLE 1 |** Significantly expressed miRNAs in IFNγ/EV-endMSCs.

| miRNA | logFC | *p*-value | FDR |
|---|---|---|---|
| **hsa-miR-196b-5p** | 1.07 | < 0.0001 | **0.00019** |
| **hsa-miR-1246** | −1.12 | < 0.0001 | **0.00616** |
| **hsa-miR-92a-3p** | −1.34 | 0.0001 | **0.01187** |
| **hsa-miR-150-5p** | −1.87 | 0.00023 | **0.02956** |
| hsa-miR-299-5p | −4.32 | 0.00055 | 0.05749 |
| hsa-miR-146a-5p | −1.88 | 0.00114 | 0.09818 |
| hsa-miR-378a-3p | −1.45 | 0.00763 | 0.49394 |
| hsa-miR-27a-5p | 0.99 | 0.01104 | 0.61100 |
| hsa-miR-484 | −2.12 | 0.01614 | 0.61698 |
| hsa-miR-409-3p | −0.80 | 0.01816 | 0.61698 |
| hsa-miR-490-3p | 1.15 | 0.01853 | 0.61698 |
| hsa-miR-30c-5p | −0.87 | 0.02242 | 0.61698 |
| hsa-miR-10b-5p | 0.34 | 0.02252 | 0.61698 |
| hsa-miR-574-5p | 1.25 | 0.02263 | 0.61698 |
| hsa-miR-486-5p | −1.25 | 0.02619 | 0.64869 |
| hsa-miR-17-5p | 1.20 | 0.02630 | 0.64869 |
| hsa-miR-376c-3p | 0.96 | 0.03618 | 0.67893 |
| hsa-miR-146b-5p | −0.59 | 0.03790 | 0.67893 |

*miRNA expression level is expressed as log fold change (logFC) between IFNγ/EV-endMSCs (n = 4), and EV-endMSCs groups (n = 4). The comparison of expression levels between groups led to 18 significantly altered microRNAs (p < 0.05), 4 of them presenting 5% FDR (bold highlighted) based on Benjamini-Hochberg FDR adjusted p-values. The full list of differentially expressed miRNAs is described in* ***Supplementary Table 9****. EV-endMSCs: Extracellular Vesicles derived from endometrial MSCs; FDR: False Discovery Rate; IFNγ/EV-endMSCs: Extracellular Vesicles derived from IFNγ-primed endometrial MSCs.*

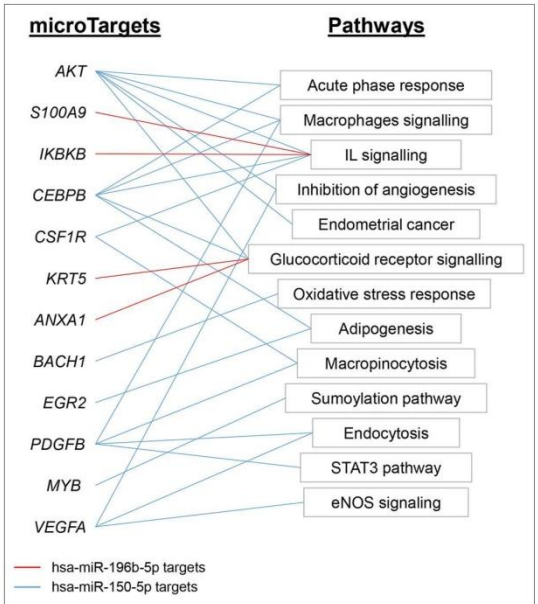


**FIGURE 7 |** Functional analysis of miRNAs expression profile EV-endMSCs. Ingenuity Pathway Analyses were performed to identify the microTargets of those miRNAs with *Experimentally observed* annotation. Figure shows interesting/representative pathways targeted by hsa-miR-196b-5p (red) and hsa-miR-150-5p (blue). Full lists of functional pathways involving *Experimentally observed* targeted genes (microTargets) are shown in **Supplementary Table 10**. EV-endMSCs, Extracellular Vesicles derived from endometrial MSCs.

The main objective of this study was focused on an exhaustive characterization of EVs released by menstrual blood-derived endMSCs (EV-endMSCs). Moreover, our interest was also focused on the biological consequences of IFNγ-priming on EV-endMSC, unraveling the proteome and microRNAome of these brand-new therapeutic tools (Murphy et al., 2019), and finding for them new and safe clinical applications.

As well as stem/stromal cells derived from placenta (Silini and Parolini, 2018), amniotic fluid (Ramasamy et al., 2018), and Wharton's jelly (Joerger-Messerli et al., 2016), MSCs from endometrial tissue can be easily expanded using standardized protocols, and without ethical concerns. This aspect is an important issue, since the simplicity of isolation protocols by non-invasive procedures and the robust expansion capacity of stem cells are crucial for a successful clinical translation of adult stem cells (Bunpetch et al., 2017).

From a methodological point of view, the *in vitro* isolation of EV-endMSCs was a simple and laborious procedure that required the collection of cell culture supernatants every 3 days and subsequent centrifugations, filtrations, and size-exclusion concentrations. Because of the complexity and variability of EVs released by *in vitro* cultured cells (exosomes, microvesicles, apoptotic bodies), and the variety of isolation protocols (ultracentrifugations, size-exclusion chromatography, field flow fractionation), the characterizations and isolations of released vesicles have been recently reviewed by the International Society for Extracellular Vesicles (Théry et al., 2018). In our study, the isolation/enrichment protocols for EV-endMSCs collection were developed according to previous studies from our group, after comparing different isolation protocols (Álvarez et al., 2015). The workflow for molecular characterization was performed using two strategies: high throughput proteomic analysis, and next generation sequencing (NGS) for miRNAs. In order to simplify and clarify the relevance of these results, the proteomic and miRNAs analyses will be separately discussed.

The study of EV-endMSCs proteome was performed with a high-throughput quantitative proteomic approach based on multiplex peptide stable isotope labeling, whose applicability on EV proteome profiling has been extensively studied and reviewed (Raimondo et al., 2011; Pocsfalvi et al., 2016; Greening et al., 2017). We considered more appropriate to characterize the untreated EV-endMSCs proteome (whose cells were not treated with IFNγ) before moving toward the absolute quantification of proteins due to IFNγ-priming. We found that the 69% of the entire EV-endMSCs proteome composition was associated to the GO term *Extracellular exosome* (GO:0070062), demonstrating the relatively high purity of the vesicles. Among these proteins, 71 were included in the 100 top-identified

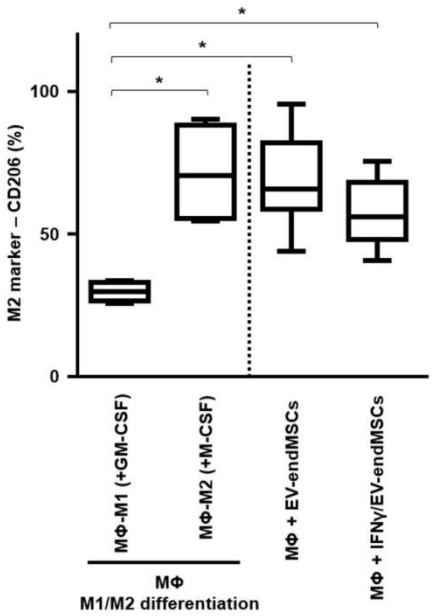


**FIGURE 8 |** *In vitro* M1/M2 Macrophage differentiation assay. Monocytes were firstly isolated from peripheral blood cells by plastic adherence. The M1 differentiation was performed in the presence of 50 ng/ml of human Granulocyte-Macrophages Colony-Stimulating Factor (GM-CSF). The M2 differentiation was performed in the presence of 50 ng/ml of human Macrophages Colony-Stimulating Factor (GM-CSF). M1-differentiated Macrophages (MΦ-M1) and M2-differentiated Macrophages (MΦ-M2) were analyzed at day 6 of differentiation. In parallel, EV-endMSCs and IFNγ/EV-endMSCs were added to monocytes at day 0 and *in vitro* cultured for 6 days. Similarly, monocytes were differentiated toward M1 Macrophages (MΦ-M1) in the presence of EV-endMSCs and IFNγ/EV-endMSCs. The macrophages were then trypsinized and the surface expression of CD206 (M2 marker) was determined by flow cytometry in $CD14^+$ cells. The lower boundary of the boxes indicates the 25th percentile and the upper boundary, the 75th percentile. Bars above and below the boxes indicate the 90th and 10th percentiles. The line within the boxes marks the median. No significant differences were observed between EV-endMSCs and IFNγ/EV-endMSCs. *$p \leq 0.05$.

proteins in ExoCarta database. Since ExoCarta is one of the most reliable database about EVs biomolecules (Rosa-Fernandes et al., 2017) and it has been commonly used by several authors to characterize the proteomic profiles of EVs (Jeannin et al., 2018; Arab et al., 2019; Göran Ronquist, 2019), our results further confirmed the vesicular origin of identified proteins. Surprisingly, the first identified protein was serotransferrin (see **Supplementary Table 1**). However, serotransferrin should not be considered a component of the released EVs since its presence may be the consequence of using an insulin-transferrin-selenium solution for *in vitro* cell culture and EV collection, as previously described by other authors (Tauro et al., 2012; Garcia et al., 2015; Chen et al., 2017).

It is important to note that EVs are considered critical mediators of cell to cell communication through the exchange of different molecules, such as proteins, DNA, RNA species, and metabolites (Caruso Bavisotto et al., 2019). Remarkably, EVs cargo can be modulated by different stimuli to the source cell, exerting pleiotropic effects on the recipient cell (Yoon et al., 2014). Being EVs natural carriers of proteins, which are essential for organism function and homeostasis, we aimed to investigate the subcellular origins of the EV-carried proteins. In accordance with other authors (Raimondo et al., 2011; Yuan et al., 2019), the Gene Ontology analysis of the EV-endMSCs proteome demonstrated an enrichment of proteins classified by the terms *Cytosol* (GO:0005829), *Extracellular space* (GO:0005615), *Membrane* (GO:0016020), and *Extracellular matrix* (GO:0031012). The inclusion of our EV-proteins in these four categories is understandable, considering that they are necessary for EV biogenesis, release, and uptake (Abels and Breakefield, 2016; Mathieu et al., 2019). In addition, the proteins classified within these categories are involved in different biological processes, such as cellular migration (Sung et al., 2015), invasion (Mu et al., 2013), embryo implantation (Desrochers et al., 2016), tumor metastasis (Hoshino et al., 2015; Sedgwick et al., 2015), and neutrophils recruitment during inflammation (Majumdar et al., 2016), among others.

Furthermore, the EV-endMSCs proteome was composed by proteins classified in the significantly enriched GO term *Mitochondrion* (GO:0005739). Even though this category was not reported by the above mentioned authors describing EV proteomes (Raimondo et al., 2011; Yuan et al., 2019), recent studies have outlined the existence of a mitochondrial-endolysosomal axis (Soto-Heredero et al., 2017; Picca et al., 2019a), where mitochondrial molecules are carried by EVs and exert their effect in processes like mitochondrial quality control (Picca et al., 2019b), senescence (Eitan et al., 2017), and "inflamm-aging" (Prattichizzo et al., 2017).

The presence of several EV-endMSCs proteins related to the *Immunological synapse* (GO:0001772) confirmed the findings of other researchers, who already associated EVs to mechanisms like T cell-antigen presenting cell interaction (Choudhuri et al., 2014), antigen-specific T-cell activation induced by dendritic cell (Théry et al., 2002), MHC class-II mediated antigen presentation (Roche and Furuta, 2015), and T-helper 1 cells differentiation (Qazi et al., 2009). In contrast to other authors who detected the presence of nuclear (Raimondo et al., 2011; Yuan et al., 2019) and ribosomal EV proteins (Ung et al., 2014), the EV-endMSCs proteome was not significantly enriched in these components.

As previously mentioned, the comparative analysis between EV-endMSCs and IFNγ/EV-endMSCs has revealed statistically significant differences in a wide range of proteins with different biological functions. In an attempt to determine the most relevant results from this exhaustive analysis, we focused our interest on immunomodulatory proteins that may have a key role in the therapeutic efficacy of these EVs. Of course, we are aware that this selection is questionable and, for sure, many other proteins may deserve a proper discussion and further investigation.

The identification of CSF-1 (also called M-CSF), in EV-endMSCs, and the differential expression observed on IFNγ/EV-endMSCs, could be considered one of the most relevant results from this study. The changes observed for this protein were further confirmed by ELISA. The immunoassay corroborated the significant differences observed in the proteomic analysis between EV-endMSCs and IFNγ/EV-endMSCs. It is widely accepted that CSF-1 is a primary regulator for macrophages (Jones and Ricardo, 2013) and it has been associated with M2 polarization and shifts toward homeostatic/reparative state (Hamilton, 2008; Hamilton et al., 2014). Additionally, CSF-1 has been found to modulate inflammatory responses, promoting the expansion and viability of macrophages in patients with inflammatory-mediated diseases (Lenzo et al., 2012; Hamilton and Achuthan, 2013). In the context of stem cell-based therapies, preclinical studies in myocardial infarction have demonstrated the immunomodulatory capacity of MSCs promoting the shift from M1 to M2 macrophages (Cho et al., 2014). More recently, a deep analysis of MSCs-macrophages interactions have shown that MSCs triggered the proliferation/differentiation of macrophages toward M2 by cell-to-cell contact, and by soluble factors where CSF-1 has a key role (Takizawa et al., 2017). All these findings, together with the identification of CSF-1 in these vesicles, and its significant increase in EVs from IFNγ-primed cells, may suggest that EV-endMSCs promote a M2 polarization. In accordance with this idea, an *in vitro* functional assay was performed using EV-endMSCs and IFNγ/EV-endMSCs. These vesicles were co-cultured with peripheral blood monocytes and macrophage differentiation/polarization demonstrated that both control EV-endMSCs and IFNγ/EV-endMSCs favored macrophages differentiation toward M2. In agreement with these *in vitro* results, our research group has recently demonstrated that extracellular vesicles from cardiosphere-derived cells stimulate M2 differentiation in the acute phase of porcine myocardial infarction (López et al., accepted).

Another relevant protein that was found in the proteome of EV-endMSCs and that increased in IFNγ/EV-endMSCs was ERAP1 (an aminopeptidase). Considering that ERAP1 is directly involved in the MHC class I presentation process (Cifaldi et al., 2012), the upregulation of this molecule under IFNγ treatment is not surprising. ERAP-1 is also involved in numerous biological processes and the presence of this protein in EV-endMSCs may have some other consequences. Firstly, the presence of ERAP1 has been found to increase the shedding of cytokine receptors (Cui et al., 2002), and to modulate the overall innate immune response (Aldhamen et al., 2013). Therefore, it is expected that the presence of ERAP1 in EV-endMSCs may have an impact in the inflammatory signaling on target cells. Secondly, ERAP-1 is also involved in cell proliferation, migration and angiogenesis upon stimulation with VEGF (Miyashita et al., 2002; Reeves and James, 2017), so the presence of this molecule in EV-endMSCs may be responsible, at least in part, for the pro-angiogenic effects observed on endMSCs (Hayati et al., 2011; Zhang et al., 2016).

The third protein showing an increase on IFNγ/EV-endMSCs (and classified as immunomodulatory), was PYCARD (also called ASC). This protein is an adaptor for inflammasomes that activate caspase-1 (Taxman et al., 2011) which also regulate the transcription of cytokines through NF-κB activation pathway (Stehlik et al., 2002). Interestingly, PYCARD has been found to inhibit the NF-κB activation mediated by proinflammatory cytokines. Based on that, the presence of this protein in EV-endMSCs may reduce the susceptibility to inflammatory stimuli in target cells. In other words, the interactions between EV-endMSCs and inflammatory cells could modulate the intracellular signaling pathways toward a less inflammatory phenotype.

Together with proteins, miRNA species are essential components of EV cargo (Abels and Breakefield, 2016). For this reason, the characterization of the proteomic profile was followed by an NGS analysis to define the RNA signature of EV-endMSCs. Firstly, our results demonstrated that miRNAs in EV-endMSCs are underrepresented over other small RNAs, which is in agreement with other studies developed in exosomes (Jenjaroenpun et al., 2013; Baglio et al., 2015; Tosar et al., 2015; Sork et al., 2018). Ingenuity Pathways Analyses allowed us to understand the pathways and biological mechanisms of miRNAs dataset. These analyses revealed that, among the 937 miRNAs with more than 10 TPMs, the genes *PTEN*, *CDK6*, *BCL2*, *CCND1*, and *MET* were targeted by 5 to 8 different miRNAs. These genes are directly involved in intracellular signaling, and cell proliferation, so the internalization of the above-mentioned miRNAs in target cells would have a significant impact on these intracellular pathways. Additionally, the quantification of miRNAs revealed that hsa-let-7a-5p, hsa-miR-143-3p, hsa-miR-21-5p, hsa-let-7b-5p, hsa-let-7f-5p, hsa-miR-16-5p, and hsa-miR-199a-3p were abundantly expressed, having an average of more than 200 TPMs. A networks analysis to identify multiple query nodes was performed with miRTargetLink (Wong and Wang, 2015; Liu and Wang, 2019). According to this analysis, 4 of the top-abundant miRNAs (hsa-miR-143-3p, hsa-miR-16-5p, hsa-miR-21-5p, and hsa-let-7b-5p) showed a validated interaction with *IGF1R*. This result may indicate that different miRNAs from EV-endMSCs could inhibit the IGF1R signaling in target cells and, subsequently the IGF1R-related pathways to modulate proliferation, survival, cell adhesion, etc. (Girnita et al., 2014). Finally, miRNA expression profile of EV-endMSCs and IFNγ/EV-endMSCs samples showed four differentially expressed miRNAs (FDR $\leq$ 0.005). Moreover, the IPA analysis revealed that two *Experimentally observed* miRNAs, hsa-miR-150-5p and hsa-miR-196b-5p, target some genes involved in *Glucocorticoid Receptor Signaling*, *IL-6/8/12 Signaling*, and in the *Role of Macrophages*. However, when we tried to validate the expression by qPCR of hsa-mir-1246, hsa-mir-150-5p, hsa-mir-196b-5p, and hsa-mir-92a-3p, we did not obtain conclusive results. PCR amplification of low abundant miRNAs in extracellular vesicles can be a challenge. Unfortunately, the four differentially expressed miRNAs (FDR $<$ 0.05) that we tried to amplify by qPCR were between the least abundant detected by NGS. Hence, we could not validate these miRNAs, even using commercially available optimized probes.

In summary, our qualitative, quantitative, bioinformatics, and *in vitro* analyses of proteins and miRNAs have provided

some clues and hints to unravel the molecules involved in the biological effect of these vesicles. This result, together with proteomics and the macrophage polarization assay suggests that EV-endMSCs may have an immunomodulatory effect in inflammatory conditions.

## DATA AVAILABILITY STATEMENT

The datasets generated and analyzed for this study can be found in the European Nucleotide Archive (https://www.ebi.ac.uk/ena) with accession number PRJEB34442 and via ProteomeXchange (http://www.proteomexchange.org/) with identifier PXD015465 (https://www.ebi.ac.uk/pride/archive/projects/PXD015465).

## AUTHOR CONTRIBUTIONS

FM, MG-S, FS-M, IJ, and JC conceived and designed the experiments. FM, MG-S, JV, EL, VÁ, JS-C, and RB performed the experiments and analyzed the data. FM, MG-S, IJ, and JC wrote the manuscript.

## FUNDING

This study was supported by competitive grants, such as: CIBER-CV (CB16/11/00494 grant to FS-M, CB16/11/00277 grant to JV); Miguel Servet I grant from Instituto de Salud Carlos III to JC (CP17/00021 and MS17/00021 co-financed by FEDER and FSE); Ayuda Grupos de Investigación de Extremadura. Consejería de Economía, Ciencia y Agenda Digital to FS-M (GR18199 cofinanced by FEDER); MAFRESA S.L. grant to FM; Instituto de Salud Carlos III grant to JC (PI18/0911 co-financed by FEDER); Junta de Extremadura to JC (IB16168 grant) co-financed by FEDER; Spanish Ministry of Science, Innovation and Universities to JV (BIO2015-67580-P grant and PGC2018-097019-B-I00 grant), through the Carlos III Institute of Health-Fondo de Investigación Sanitaria grant PRB3 to JV (IPT17/0019-ISCIII-SGEFI/ERDF, ProteoRed), Fundació MaratóTV3 to JV (grant 122/C/2015) and la Caixa Banking Foundation to JV (project code HR17-00247). CNIC was supported by Instituto de Salud Carlos III (ISCIII), Ministerio de Ciencia, Innovación y Universidades (MCNU) and the Pro CNIC Foundation, and it is a Severo Ochoa Center of Excellence (SEV-2015-0505). Sara Borrell grant (co-financed by FSE) to EL. Cell culture *in vitro* studies were performed at the ICTS Nanbiosis (Unit 14, Stem Cell Therapy). The funders had no role in study designs, data collection and analysis, decision to publish, or preparation of the manuscript.

## ACKNOWLEDGMENTS

The authors acknowledge the contribution of Carlos Carrasco and Sara Pérez (Bachelor students from University of Extremadura) in the cell culture collection and extracellular vesicle isolations. Special thanks to our colleague Joaquín González for the technical support in figures handling.

## SUPPLEMENTARY MATERIAL

The Supplementary Material for this article can be found online at: https://www.frontiersin.org/articles/10.3389/fbioe.2019.00431/full#supplementary-material

## REFERENCES

Abels, E. R., and Breakefield, X. O. (2016). Introduction to extracellular vesicles: biogenesis, RNA cargo selection, content, release, and uptake. *Cell. Mol. Neurobiol.* 36, 301–312. doi: 10.1007/s10571-016-0366-z

Aldhamen, Y. A., Seregin, S. S., Rastall, D. P. W., Aylsworth, C. F., Pepelyayeva, Y., Busuito, C. J., et al. (2013). Endoplasmic reticulum aminopeptidase-1 functions regulate key aspects of the innate immune response. *PLoS ONE* 8:e69539. doi: 10.1371/journal.pone.0069539

Álvarez, V., Blázquez, R., Sánchez-Margallo, F. M., DelaRosa, O., Jorge, I., Tapia, A., et al. (2015). Comparative study of isolated human mesenchymal stem cell derived exosomes for clinical use. *Acta Bioquim. Clin. Latinoam.* 49, 311–320. Available online at: http://www.scielo.org.ar/scielo.php?script=sci_isoref&pid=S0325-29572015000300004&lng=en&tlng=es

Álvarez, V., Sánchez-Margallo, F. M., Macías-García, B., Gómez-Serrano, M., Jorge, I., Vázquez, J., et al. (2018). The immunomodulatory activity of extracellular vesicles derived from endometrial mesenchymal stem cells on $CD4^+$ T cells is partially mediated by TGFbeta. *J. Tissue Eng. Regen. Med.* 12, 2088–2098. doi: 10.1002/term.2743

Arab, T., Raffo-Romero, A., Van, C. C., Lemaire, Q., Le, F. M.-C., Drago, F., et al. (2019). Proteomic characterisation of leech microglia extracellular vesicles (EVs): comparison between differential ultracentrifugation and Optiprep$^{TM}$ density gradient isolation. *J. Extracell. Vesicles* 8:1603048. doi: 10.1080/20013078.2019.1603048

Bagheri-Mohammadi, S., Karimian, M., Alani, B., Verdi, J., Tehrani, R. M., and Noureddini, M. (2019). Stem cell-based therapy for Parkinson's disease with a focus on human endometrium-derived mesenchymal stem cells. *J. Cell. Physiol.* 234, 1326–1335. doi: 10.1002/jcp.27182

Baglio, S. R., Rooijers, K., Koppers-Lalic, D., Verweij, F. J., Pérez Lanzón, M., Zini, N., et al. (2015). Human bone marrow- and adipose-mesenchymal stem cells secrete exosomes enriched in distinctive miRNA and tRNA species. *Stem Cell Res. Ther.* 6:127. doi: 10.1186/s13287-015-0116-z

Binek, A., Fernández-Jiménez, R., Jorge, I., Camafeita, E., López, J. A., Bagwan, N., et al. (2017). Proteomic footprint of myocardial ischemia/reperfusion injury: longitudinal study of the at-risk and remote regions in the pig model. *Sci. Rep.* 7:12343. doi: 10.1038/s41598-017-11985-5

Blázquez, R., Sánchez-Margallo, F. M., Álvarez, V., Matilla, E., Hernández, N., Marinaro, F., et al. (2018). Murine embryos exposed to human endometrial MSCs-derived extracellular vesicles exhibit higher VEGF/PDGF AA release, increased blastomere count and hatching rates. *PLoS ONE* 13:e0196080. doi: 10.1371/journal.pone.0196080

Bonzon-Kulichenko, E., Pérez-Hernández, D., Núñez, E., Martínez-Acedo, P., Navarro, P., Trevisan-Herraz, M., et al. (2011). A robust method for quantitative high-throughput analysis of proteomes by 18O labeling. *Mol. Cell Proteomics* 10:M110.003335. doi: 10.1074/mcp.M110.003335

Bunpetch, V., Wu, H., Zhang, S., and Ouyang, H. (2017). From "Bench to Bedside": current advancement on large-scale production of mesenchymal stem cells. *Stem Cells Dev.* 26, 1662–1673. doi: 10.1089/scd.2017.0104

Caruso Bavisotto, C., Scalia, F., Marino Gammazza, A., Carlisi, D., Bucchieri, F., Conway de Macario, E., et al. (2019). Extracellular vesicle-mediated cell–cell communication in the nervous system: focus on neurological diseases. *Int. J. Mol. Sci.* 20:434. doi: 10.3390/ijms20020434

Chan, R. W. S., Schwab, K. E., and Gargett, C. E. (2004). Clonogenicity of human endometrial epithelial and stromal cells. *Biol. Reprod.* 70, 1738–1750. doi: 10.1095/biolreprod.103.024109

Chen, L., Xiang, B., Wang, X., and Xiang, C. (2017). Exosomes derived from human menstrual blood-derived stem cells alleviate fulminant hepatic failure. *Stem Cell Res. Ther.* 8:9. doi: 10.1186/s13287-016-0453-6

Chinnadurai, R., Copland, I. B., Patel, S. R., and Galipeau, J. (2014). IDO-independent suppression of T cell effector function by IFN-γ-licensed human mesenchymal stromal cells. *J. Immunol.* 192, 1491–1501. doi: 10.4049/jimmunol.1301828

Cho, D.-I., Kim, M. R., Jeong, H., Jeong, H. C., Jeong, M. H., Yoon, S. H., et al. (2014). Mesenchymal stem cells reciprocally regulate the M1/M2 balance in mouse bone marrow-derived macrophages. *Exp. Mol. Med.* 46:e70. doi: 10.1038/emm.2013.135

Chong, J., Soufan, O., Li, C., Caraus, I., Li, S., Bourque, G., et al. (2018). MetaboAnalyst 4.0: towards more transparent and integrative metabolomics analysis. *Nucleic Acids Res.* 46, W486–W494. doi: 10.1093/nar/gky310

Choudhuri, K., Llodrá, J., Roth, E. W., Tsai, J., Gordo, S., Wucherpfennig, K. W., et al. (2014). Polarized release of TCR-enriched microvesicles at the T cell immunological synapse. *Nature* 507:118. doi: 10.1038/nature12951

Cifaldi, L., Romania, P., Lorenzi, S., Locatelli, F., and Fruci, D. (2012). Role of endoplasmic reticulum aminopeptidases in health and disease: from infection to cancer. *Int. J. Mol. Sci.* 13, 8338–8352. doi: 10.3390/ijms13078338

Cui, X., Hawari, F., Alsaaty, S., Lawrence, M., Combs, C. A., Geng, W., et al. (2002). Identification of ARTS-1 as a novel TNFR1-binding protein that promotes TNFR1 ectodomain shedding. *J. Clin. Invest.* 110, 515–526. doi: 10.1172/JCI13847

DelaRosa, O., Lombardo, E., Beraza, A., Mancheño-Corvo, P., Ramirez, C., Menta, R., et al. (2009). Requirement of IFN-gamma-mediated indoleamine 2,3-dioxygenase expression in the modulation of lymphocyte proliferation by human adipose-derived stem cells. *Tissue Eng. Part A* 15, 2795–2806. doi: 10.1089/ten.TEA.2008.0630

Desrochers, L. M., Bordeleau, F., Reinhart-King, C. A., Cerione, R. A., and Antonyak, M. A. (2016). Microvesicles provide a mechanism for intercellular communication by embryonic stem cells during embryo implantation. *Nat. Commun.* 7:11958. doi: 10.1038/ncomms11958

Doyle, L. M., and Wang, M. Z. (2019). Overview of extracellular vesicles, their origin, composition, purpose, and methods for exosome isolation and analysis. *Cells* 8:E727. doi: 10.3390/cells8070727

Du, X., Yuan, Q., Qu, Y., Zhou, Y., and Bei, J. (2016). Endometrial mesenchymal stem cells isolated from menstrual blood by adherence. *Stem Cells Int.* 2016:3573846. doi: 10.1155/2016/3573846

Edwards, A., and Haas, W. (2016). Multiplexed quantitative proteomics for high-throughput comprehensive proteome comparisons of human cell lines. *Methods Mol. Biol.* 1394, 1–13. doi: 10.1007/978-1-4939-3341-9_1

Eitan, E., Green, J., Bodogai, M., Mode, N. A., Bæk, R., Jørgensen, M. M., et al. (2017). Age-related changes in plasma extracellular vesicle characteristics and internalization by leukocytes. *Sci. Rep.* 7:1342. doi: 10.1038/s41598-017-01386-z

Gao, J., Scheenstra, M. R., van Dijk, A., Veldhuizen, E. J. A., and Haagsman, H. P. (2018). A new and efficient culture method for porcine bone marrow-derived M1- and M2-polarized macrophages. *Vet. Immunol. Immunopathol.* 200, 7–15. doi: 10.1016/j.vetimm.2018.04.002

Garcia, N. A., Ontoria-Oviedo, I., González-King, H., Diez-Juan, A., and Sepúlveda, P. (2015). Glucose starvation in cardiomyocytes enhances exosome secretion and promotes angiogenesis in endothelial cells. *PLoS ONE* 10:e0138849. doi: 10.1371/journal.pone.0138849

García-Marqués, F., Trevisan-Herraz, M., Martínez-Martínez, S., Camafeita, E., Jorge, I., Lopez, J. A., et al. (2016). A novel systems-biology algorithm for the analysis of coordinated protein responses using quantitative proteomics. *Mol. Cell Proteomics* 15, 1740–1760. doi: 10.1074/mcp.M115.055905

Gargett, C. E., Schwab, K. E., and Deane, J. A. (2016). Endometrial stem/progenitor cells: the first 10 years. *Hum. Reprod. Update* 22, 137–163. doi: 10.1093/humupd/dmv051

Gilsanz, A., Sánchez-Martín, L., Gutiérrez-López, M. D., Ovalle, S., Machado-Pineda, Y., Reyes, R., et al. (2013). ALCAM/CD166 adhesive function is regulated by the tetraspanin CD9. *Cell. Mol. Life Sci.* 70, 475–493. doi: 10.1007/s00018-012-1132-0

Girnita, L., Worrall, C., Takahashi, S.-I., Seregard, S., and Girnita, A. (2014). Something old, something new and something borrowed: emerging paradigm of insulin-like growth factor type 1 receptor (IGF-1R) signaling regulation. *Cell. Mol. Life Sci.* 71, 2403–2427. doi: 10.1007/s00018-013-1514-y

Gómez-Serrano, M., Camafeita, E., García-Santos, E., López, J. A., Rubio, M. A., Sánchez-Pernaute, A., et al. (2016). Proteome-wide alterations on adipose tissue from obese patients as age-, diabetes- and gender-specific hallmarks. *Sci. Rep.* 6:25756. doi: 10.1038/srep25756

Göran Ronquist, K. (2019). Extracellular vesicles and energy metabolism. *Clin. Chim. Acta* 488, 116–121. doi: 10.1016/j.cca.2018.10.044

Greening, D. W., Xu, R., Gopal, S. K., Rai, A., and Simpson, R. J. (2017). Proteomic insights into extracellular vesicle biology–defining exosomes and shed microvesicles. *Expert Rev. Proteomics* 14, 69–95. doi: 10.1080/14789450.2017.1260450

Hamilton, J. A. (2008). Colony-stimulating factors in inflammation and autoimmunity. *Nat. Rev. Immunol.* 8, 533–544. doi: 10.1038/nri2356

Hamilton, J. A., and Achuthan, A. (2013). Colony stimulating factors and myeloid cell biology in health and disease. *Trends Immunol.* 34, 81–89. doi: 10.1016/j.it.2012.08.006

Hamilton, T. A., Zhao, C., Pavicic, P. G., and Datta, S. (2014). Myeloid colony-stimulating factors as regulators of macrophage polarization. *Front. Immunol.* 5:554. doi: 10.3389/fimmu.2014.00554

Harting, M. T., Srivastava, A. K., Zhaorigetu, S., Bair, H., Prabhakara, K. S., Toledano Furman, N. E., et al. (2018). Inflammation-stimulated mesenchymal stromal cell-derived extracellular vesicles attenuate inflammation. *Stem Cells* 36, 79–90. doi: 10.1002/stem.2730

Hayati, A.-R., Nur Fariha, M.-M., Tan, G.-C., Tan, A.-E., and Chua, K. (2011). Potential of human decidua stem cells for angiogenesis and neurogenesis. *Arch. Med. Res.* 42, 291–300. doi: 10.1016/j.arcmed.2011.06.005

Hoshino, A., Costa-Silva, B., Shen, T.-L., Rodrigues, G., Hashimoto, A., Tesic Mark, M., et al. (2015). Tumour exosome integrins determine organotropic metastasis. *Nature* 527, 329–335. doi: 10.1038/nature15756

Huang, D. W., Sherman, B. T., and Lempicki, R. A. (2009a). Bioinformatics enrichment tools: paths toward the comprehensive functional analysis of large gene lists. *Nucleic Acids Res.* 37, 1–13. doi: 10.1093/nar/gkn923

Huang, D. W., Sherman, B. T., and Lempicki, R. A. (2009b). Systematic and integrative analysis of large gene lists using DAVID bioinformatics resources. *Nat. Protoc.* 4, 44–57. doi: 10.1038/nprot.2008.211

Jeannin, P., Chaze, T., Giai Gianetto, Q., Matondo, M., Gout, O., Gessain, A., et al. (2018). Proteomic analysis of plasma extracellular vesicles reveals mitochondrial stress upon HTLV-1 infection. *Sci. Rep.* 8:5170. doi: 10.1038/s41598-018-23505-0

Jenjaroenpun, P., Kremenska, Y., Nair, V. M., Kremenskoy, M., Joseph, B., and Kurochkin, I. V. (2013). Characterization of RNA in exosomes secreted by human breast cancer cell lines using next-generation sequencing. *PeerJ* 1:e201. doi: 10.7717/peerj.201

Joerger-Messerli, M. S., Marx, C., Oppliger, B., Mueller, M., Surbek, D. V., and Schoeberlein, A. (2016). Mesenchymal stem cells from Wharton's jelly and amniotic fluid. *Best Pract. Res. Clin. Obstet. Gynaecol.* 31, 30–44. doi: 10.1016/j.bpobgyn.2015.07.006

Jones, C. V., and Ricardo, S. D. (2013). Macrophages and CSF-1: implications for development and beyond. *Organogenesis* 9, 249–260. doi: 10.4161/org.25676

Jorge, I., Navarro, P., Martínez-Acedo, P., Núñez, E., Serrano, H., Alfranca, A., et al. (2009). Statistical model to analyze quantitative proteomics data obtained by 18O/16O labeling and linear ion trap mass spectrometry: application to the study of vascular endothelial growth factor-induced angiogenesis in endothelial cells. *Mol. Cell Proteomics* 8, 1130–1149. doi: 10.1074/mcp.M800260-MCP200

Jylhä, A., Nättinen, J., Aapola, U., Mikhailova, A., Nykter, M., Zhou, L., et al. (2018). Comparison of iTRAQ and SWATH in a clinical study with multiple time points. *Clin. Proteomics* 15:24. doi: 10.1186/s12014-018-9201-5

Kato, Y., Tanaka, Y., Hayashi, M., Okawa, K., and Minato, N. (2006). Involvement of CD166 in the activation of human γδT cells by tumor cells sensitized with nonpeptide antigens. *J. Immunol.* 177, 877–884. doi: 10.4049/jimmunol.177.2.877

Keerthikumar, S., Chisanga, D., Ariyaratne, D., Al Saffar, H., Anand, S., Zhao, K., et al. (2016). ExoCarta: a web-based compendium of exosomal cargo. *J. Mol. Biol.* 428, 688–692. doi: 10.1016/j.jmb.2015.09.019

Keshtkar, S., Azarpira, N., and Ghahremani, M. H. (2018). Mesenchymal stem cell-derived extracellular vesicles: novel frontiers in regenerative medicine. *Stem Cell Res. Ther.* 9:63. doi: 10.1186/s13287-018-0791-7

Kim, N., and Cho, S.-G. (2016). Overcoming immunoregulatory plasticity of mesenchymal stem cells for accelerated clinical applications. *Int. J. Hematol.* 103, 129–137. doi: 10.1007/s12185-015-1918-6

Kozomara, A., Birgaoanu, M., and Griffiths-Jones, S. (2019). miRBase: from microRNA sequences to function. *Nucleic Acids Res.* 47, D155–D162. doi: 10.1093/nar/gky1141

Kyurkchiev, S., Shterev, A., and Dimitrov, R. (2010). Assessment of presence and characteristics of multipotent stromal cells in human endometrium and decidua. *Reprod. Biomed. Online* 20, 305–313. doi: 10.1016/j.rbmo.2009.12.011

Lenzo, J. C., Turner, A. L., Cook, A. D., Vlahos, R., Anderson, G. P., Reynolds, E. C., et al. (2012). Control of macrophage lineage populations by CSF-1 receptor and GM-CSF in homeostasis and inflammation. *Immunol. Cell Biol.* 90, 429–440. doi: 10.1038/icb.2011.58

Liang, C., Jiang, E., Yao, J., Wang, M., Chen, S., Zhou, Z., et al. (2018). Interferon-γ mediates the immunosuppression of bone marrow mesenchymal stem cells on T-lymphocytes *in vitro*. *Hematology* 23, 44–49. doi: 10.1080/10245332.2017.1333245

Liu, W., and Wang, X. (2019). Prediction of functional microRNA targets by integrative modeling of microRNA binding and target expression data. *Genome Biol.* 20:18. doi: 10.1186/s13059-019-1629-z

Liu, Y., Niu, R., Li, W., Lin, J., Stamm, C., Steinhoff, G., et al. (2019). Therapeutic potential of menstrual blood-derived endometrial stem cells in cardiac diseases. *Cell. Mol. Life Sci.* 76, 1681–1695. doi: 10.1007/s00018-019-03019-2

López, E., Blázquez, R., Marinaro, F., Álvarez, V., Blanco, V., Báez, C., et al. (accepted). The intrapericardial delivery of extracellular vesicles from cardiosphere-derived cells stimulates M2 polarization during the acute phase of porcine myocardial infarction. *Stem Cell Rev. Rep.*

Lv, Y., Xu, X., Zhang, B., Zhou, G., Li, H., Du, C., et al. (2014). Endometrial regenerative cells as a novel cell therapy attenuate experimental colitis in mice. *J. Transl. Med.* 12:344. doi: 10.1186/s12967-014-0344-5

Majumdar, R., Tameh, A. T., and Parent, C. A. (2016). Exosomes mediate LTB4 release during neutrophil chemotaxis. *PLoS Biol.* 14:e1002336. doi: 10.1371/journal.pbio.1002336

Marinaro, F., Macías-García, B., Sánchez-Margallo, F. M., Blázquez, R., Álvarez, V., Matilla, E., et al. (2019). Extracellular vesicles derived from endometrial human mesenchymal stem cells enhance embryo yield and quality in an aged murine model. *Biol. Reprod.* 100, 1180–1192. doi: 10.1093/biolre/ioy263

Martínez-Bartolomé, S., Navarro, P., Martín-Maroto, F., López-Ferrer, D., Ramos-Fernández, A., Villar, M., et al. (2008). Properties of average score distributions of SEQUEST: the probability ratio method. *Mol. Cell Proteomics* 7, 1135–1145. doi: 10.1074/mcp.M700239-MCP200

Martínez-López, D., Camafeita, E., Cedó, L., Roldan-Montero, R., Jorge, I., García-Marqués, F., et al. (2019). APOA1 oxidation is associated to dysfunctional high-density lipoproteins in human abdominal aortic aneurysm. *EBioMedicine* 43, 43–53. doi: 10.1016/j.ebiom.2019.04.012

Mathieu, M., Martin-Jaular, L., Lavieu, G., and Théry, C. (2019). Specificities of secretion and uptake of exosomes and other extracellular vesicles for cell-to-cell communication. *Nat. Cell. Biol.* 21, 9–17. doi: 10.1038/s41556-018-0250-9

Miao, W.-M., Vasile, E., Lane, W. S., and Lawler, J. (2001). CD36 associates with CD9 and integrins on human blood platelets. *Blood* 97, 1689–1696. doi: 10.1182/blood.V97.6.1689

Miyashita, H., Yamazaki, T., Akada, T., Niizeki, O., Ogawa, M., Nishikawa, S., et al. (2002). A mouse orthologue of puromycin-insensitive leucyl-specific aminopeptidase is expressed in endothelial cells and plays an important role in angiogenesis. *Blood* 99, 3241–3249. doi: 10.1182/blood.v99.9.3241

Mu, W., Rana, S., and Zöller, M. (2013). Host matrix modulation by tumor exosomes promotes motility and invasiveness. *Neoplasia* 15:875. doi: 10.1593/neo.13786

Murphy, D. E., de Jong, O. G., Brouwer, M., Wood, M. J., Lavieu, G., Schiffelers, R. M., et al. (2019). Extracellular vesicle-based therapeutics: natural versus engineered targeting and trafficking. *Exp. Mol. Med.* 51:32. doi: 10.1038/s12276-019-0223-5

Najar, M., Krayem, M., Meuleman, N., Bron, D., and Lagneaux, L. (2017). Mesenchymal stromal cells and toll-like receptor priming: a critical review. *Immune Netw.* 17, 89–102. doi: 10.4110/in.2017.17.2.89

Navarro, P., Trevisan-Herraz, M., Bonzon-Kulichenko, E., Núñez, E., Martínez-Acedo, P., Pérez-Hernández, D., et al. (2014). General statistical framework for quantitative proteomics by stable isotope labeling. *J. Proteome Res.* 13, 1234–1247. doi: 10.1021/pr4006958

Navarro, P., and Vázquez, J. (2009). A refined method to calculate false discovery rates for peptide identification using decoy databases. *J. Proteome Res.* 8, 1792–1796. doi: 10.1021/pr800362h

Ngwa, J. S., Manning, A. K., Grimsby, J. L., Lu, C., Zhuang, W. V., and Destefano, A. L. (2011). Pathway analysis following association study. *BMC Proc.* 5:S18. doi: 10.1186/1753-6561-5-S9-S18

Nikoo, S., Ebtekar, M., Jeddi-Tehrani, M., Shervin, A., Bozorgmehr, M., Kazemnejad, S., et al. (2012). Effect of menstrual blood-derived stromal stem cells on proliferative capacity of peripheral blood mononuclear cells in allogeneic mixed lymphocyte reaction. *J. Obstet. Gynaecol. Res.* 38, 804–809. doi: 10.1111/j.1447-0756.2011.01800.x

Nikoo, S., Ebtekar, M., Jeddi-Tehrani, M., Shervin, A., Bozorgmehr, M., Vafaei, S., et al. (2014). Menstrual blood-derived stromal stem cells from women with and without endometriosis reveal different phenotypic and functional characteristics. *Mol. Hum. Reprod.* 20, 905–918. doi: 10.1093/molehr/gau044

Peron, J. P. S., Jazedje, T., Brandão, W. N., Perin, P. M., Maluf, M., Evangelista, L. P., et al. (2012). Human endometrial-derived mesenchymal stem cells suppress inflammation in the central nervous system of EAE mice. *Stem Cell Rev.* 8, 940–952. doi: 10.1007/s12015-011-9338-3

Picca, A., Guerra, F., Calvani, R., Bucci, C., Lo Monaco, M. R., Bentivoglio, A. R., et al. (2019a). Mitochondrial dysfunction and aging: insights from the analysis of extracellular vesicles. *Int. J. Mol. Sci.* 20:E805. doi: 10.3390/ijms20040805

Picca, A., Guerra, F., Calvani, R., Bucci, C., Lo Monaco, M. R., Bentivoglio, A. R., et al. (2019b). Mitochondrial-derived vesicles as candidate biomarkers in Parkinson's disease: rationale, design and methods of the EXosomes in PArkiNson Disease (EXPAND) study. *Int. J. Mol. Sci.* 20:E2373. doi: 10.3390/ijms20102373

Pocsfalvi, G., Stanly, C., Vilasi, A., Fiume, I., Capasso, G., Turiák, L., et al. (2016). Mass spectrometry of extracellular vesicles. *Mass Spectrom. Rev.* 35, 3–21. doi: 10.1002/mas.21457

Prattichizzo, F., Micolucci, L., Cricca, M., De Carolis, S., Mensà, E., Ceriello, A., et al. (2017). Exosome-based immunomodulation during aging: a nano-perspective on inflamm-aging. *Mech. Ageing Dev.* 168, 44–53. doi: 10.1016/j.mad.2017.02.008

Qazi, K. R., Gehrmann, U., Domange Jordö, E., Karlsson, M. C. I., and Gabrielsson, S. (2009). Antigen-loaded exosomes alone induce Th1-type memory through a B-cell-dependent mechanism. *Blood* 113, 2673–2683. doi: 10.1182/blood-2008-04-153536

Raimondo, F., Morosi, L., Chinello, C., Magni, F., and Pitto, M. (2011). Advances in membranous vesicle and exosome proteomics improving biological understanding and biomarker discovery. *Proteomics* 11, 709–720. doi: 10.1002/pmic.201000422

Ramasamy, T. S., Velaithan, V., Yeow, Y., and Sarkar, F. H. (2018). Stem cells derived from amniotic fluid: a potential pluripotent-like cell source for cellular therapy? *Curr. Stem Cell Res. Ther.* 13, 252–264. doi: 10.2174/1574888X13666180115093800

Reeves, E., and James, E. (2017). Tumour and placenta establishment: The importance of antigen processing and presentation. *Placenta* 56, 34–39. doi: 10.1016/j.placenta.2017.02.025

Robinson, M. D., and Oshlack, A. (2010). A scaling normalization method for differential expression analysis of RNA-seq data. *Genome Biol.* 11:R25. doi: 10.1186/gb-2010-11-3-r25

Roche, P. A., and Furuta, K. (2015). The ins and outs of MHC class II-mediated antigen processing and presentation. *Nat. Rev. Immunol.* 15, 203–216. doi: 10.1038/nri3818

Rosa-Fernandes, L., Rocha, V. B., Carregari, V. C., Urbani, A., and Palmisano, G. (2017). A perspective on extracellular vesicles proteomics. *Front. Chem.* 5:102. doi: 10.3389/fchem.2017.00102

Rossignoli, F., Caselli, A., Grisendi, G., Piccinno, S., Burns, J. S., Murgia, A., et al. (2013). Isolation, characterization, and transduction of endometrial decidual tissue multipotent mesenchymal stromal/stem cells from menstrual blood. *Biomed. Res. Int.* 2013:901821. doi: 10.1155/2013/901821

Roy, S., Hochberg, F. H., and Jones, P. S. (2018). Extracellular vesicles: the growth as diagnostics and therapeutics; a survey.

*J. Extracell. Vesicles* 7:1438720. doi: 10.1080/20013078.2018.1438720

Ruiz-Meana, M., Núñez, E., Miro-Casas, E., Martínez-Acedo, P., Barba, I., Rodriguez-Sinovas, A., et al. (2014). Ischemic preconditioning protects cardiomyocyte mitochondria through mechanisms independent of cytosol. *J. Mol. Cell. Cardiol.* 68, 79–88. doi: 10.1016/j.yjmcc.2014.01.001

Saleh, L., Otti, G. R., Fiala, C., Pollheimer, J., and Knöfler, M. (2011). Evaluation of human first trimester decidual and telomerase-transformed endometrial stromal cells as model systems of *in vitro* decidualization. *Reprod. Biol. Endocrinol.* 9:155. doi: 10.1186/1477-7827-9-155

Sangiorgi, B., and Panepucci, R. A. (2016). Modulation of immunoregulatory properties of mesenchymal stromal cells by toll-like receptors: potential applications on GVHD. *Stem Cells Int.* 2016:9434250. doi: 10.1155/2016/9434250

Schüring, A. N., Schulte, N., Kelsch, R., Röpke, A., Kiesel, L., and Götte, M. (2011). Characterization of endometrial mesenchymal stem-like cells obtained by endometrial biopsy during routine diagnostics. *Fertil. Steril.* 95, 423–426. doi: 10.1016/j.fertnstert.2010.08.035

Sedgwick, A. E., Clancy, J. W., Balmert, M. O., and D'Souza-Schorey, C. (2015). Extracellular microvesicles and invadopodia mediate non-overlapping modes of tumor cell invasion. *Sci. Rep.* 5:14748. doi: 10.1038/srep14748

Showalter, M. R., Wancewicz, B., Fiehn, O., Archard, J. A., Clayton, S., Wagner, J., et al. (2019). Primed mesenchymal stem cells package exosomes with metabolites associated with immunomodulation. *Biochem. Biophys. Res. Commun.* 512, 729–735. doi: 10.1016/j.bbrc.2019.03.119

Silini, A. R., and Parolini, O. (2018). Placental cells and derivatives: advancing clinical translation. *Cell Transplant.* 27, 1–2. doi: 10.1177/0963689717745332

Song, Y., Dou, H., Li, X., Zhao, X., Li, Y., Liu, D., et al. (2017). Exosomal miR-146a contributes to the enhanced therapeutic efficacy of interleukin-1β-primed mesenchymal stem cells against sepsis. *Stem Cells* 35, 1208–1221. doi: 10.1002/stem.2564

Sork, H., Corso, G., Krjutskov, K., Johansson, H. J., Nordin, J. Z., Wiklander, O. P. B., et al. (2018). Heterogeneity and interplay of the extracellular vesicle small RNA transcriptome and proteome. *Sci. Rep.* 8, 1–12. doi: 10.1038/s41598-018-28485-9

Soto-Heredero, G., Baixauli, F., and Mittelbrunn, M. (2017). Interorganelle communication between mitochondria and the endolysosomal system. *Front. Cell Dev. Biol.* 5:95. doi: 10.3389/fcell.2017.00095

Stehlik, C., Fiorentino, L., Dorfleutner, A., Bruey, J.-M., Ariza, E. M., Sagara, J., et al. (2002). The PAAD/PYRIN-family protein ASC is a dual regulator of a conserved step in nuclear factor kappaB activation pathways. *J. Exp. Med.* 196, 1605–1615. doi: 10.1084/jem.20021552

Sun, Y., Ren, Y., Yang, F., He, Y., Liang, S., Guan, L., et al. (2019). High-yield isolation of menstrual blood-derived endometrial stem cells by direct red blood cell lysis treatment. *Biol. Open* 8:bio.038885. doi: 10.1242/bio.038885

Sung, B. H., Ketova, T., Hoshino, D., Zijlstra, A., and Weaver, A. M. (2015). Directional cell movement through tissues is controlled by exosome secretion. *Nat. Commun.* 6:7164. doi: 10.1038/ncomms8164

Takizawa, N., Okubo, N., Kamo, M., Chosa, N., Mikami, T., Suzuki, K., et al. (2017). Bone marrow-derived mesenchymal stem cells propagate immunosuppressive/anti-inflammatory macrophages in cell-to-cell contact-independent and -dependent manners under hypoxic culture. *Exp. Cell Res.* 358, 411–420. doi: 10.1016/j.yexcr.2017.07.014

Tan, J., Li, P., Wang, Q., Li, Y., Li, X., Zhao, D., et al. (2016). Autologous menstrual blood-derived stromal cells transplantation for severe Asherman's syndrome. *Hum. Reprod.* 31, 2723–2729. doi: 10.1093/humrep/dew235

Tauro, B. J., Greening, D. W., Mathias, R. A., Ji, H., Mathivanan, S., Scott, A. M., et al. (2012). Comparison of ultracentrifugation, density gradient separation, and immunoaffinity capture methods for isolating human colon cancer cell line LIM1863-derived exosomes. *Methods* 56, 293–304. doi: 10.1016/j.ymeth.2012.01.002

Taxman, D. J., Holley-Guthrie, E. A., Huang, M. T.-H., Moore, C. B., Bergstralh, D. T., Allen, I. C., et al. (2011). The NLR adaptor ASC/PYCARD regulates DUSP10, mitogen-activated protein kinase (MAPK), and chemokine induction independent of the inflammasome. *J. Biol. Chem.* 286, 19605–19616. doi: 10.1074/jbc.M111.221077

Tempest, N., Maclean, A., and Hapangama, D. K. (2018). Endometrial stem cell markers: current concepts and unresolved questions. *Int. J. Mol. Sci.* 19:E3240. doi: 10.3390/ijms19103240

The Gene Ontology Consortium (2017). Expansion of the gene ontology knowledgebase and resources. *Nucleic Acids Res.* 45, D331–D338. doi: 10.1093/nar/gkw1108

Théry, C., Duban, L., Segura, E., Véron, P., Lantz, O., and Amigorena, S. (2002). Indirect activation of naïve $CD4^+$ T cells by dendritic cell-derived exosomes. *Nat. Immunol.* 3, 1156–1162. doi: 10.1038/ni854

Théry, C., Witwer, K. W., Aikawa, E., Alcaraz, M. J., Anderson, J. D., Andriantsitohaina, R., et al. (2018). Minimal information for studies of extracellular vesicles 2018 (MISEV2018): a position statement of the International Society for Extracellular Vesicles and update of the MISEV2014 guidelines. *J. Extracell. Vesicles* 7:1535750. doi: 10.1080/20013078.2018.1535750

Tosar, J. P., Gámbaro, F., Sanguinetti, J., Bonilla, B., Witwer, K. W., and Cayota, A. (2015). Assessment of small RNA sorting into different extracellular fractions revealed by high-throughput sequencing of breast cell lines. *Nucleic Acids Res.* 43, 5601–5616. doi: 10.1093/nar/gkv432

Trevisan-Herraz, M., Bagwan, N., García-Marqués, F., Rodriguez, J. M., Jorge, I., Ezkurdia, I., et al. (2019). SanXoT: a modular and versatile package for the quantitative analysis of high-throughput proteomics experiments. *Bioinformatics* 35, 1594–1596. doi: 10.1093/bioinformatics/bty815

Ung, T. H., Madsen, H. J., Hellwinkel, J. E., Lencioni, A. M., and Graner, M. W. (2014). Exosome proteomics reveals transcriptional regulator proteins with potential to mediate downstream pathways. *Cancer Sci.* 105, 1384–1392. doi: 10.1111/cas.12534

Wang, J., Chen, S., Zhang, C., Stegeman, S., Pfaff-Amesse, T., Zhang, Y., et al. (2012). Human endometrial stromal stem cells differentiate into megakaryocytes with the ability to produce functional platelets. *PLoS ONE* 7:e44300. doi: 10.1371/journal.pone.0044300

Wiśniewski, J. R., Ostasiewicz, P., and Mann, M. (2011). High recovery FASP applied to the proteomic analysis of microdissected formalin fixed paraffin embedded cancer tissues retrieves known colon cancer markers. *J. Proteome Res.* 10, 3040–3049. doi: 10.1021/pr200019m

Wong, N., and Wang, X. (2015). miRDB: an online resource for microRNA target prediction and functional annotations. *Nucleic Acids Res.* 43, D146–D152. doi: 10.1093/nar/gku1104

Worthington, R. E., Carroll, R. C., and Boucheix, C. (1990). Platelet activation by CD9 monoclonal antibodies is mediated by the Fc gamma II receptor. *Br. J. Haematol.* 74, 216–222. doi: 10.1111/j.1365-2141.1990.tb02568.x

Yin, J. Q., Zhu, J., and Ankrum, J. A. (2019). Manufacturing of primed mesenchymal stromal cells for therapy. *Nat. Biomed. Eng.* 3, 90–104. doi: 10.1038/s41551-018-0325-8

Yoon, Y. J., Kim, O. Y., and Gho, Y. S. (2014). Extracellular vesicles as emerging intercellular communicasomes. *BMB Rep.* 47, 531–539. doi: 10.5483/BMBRep.2014.47.10.164

Yuan, O., Lin, C., Wagner, J., Archard, J. A., Deng, P., Halmai, J., et al. (2019). Exosomes derived from human primed mesenchymal stem cells induce mitosis and potentiate growth factor secretion. *Stem Cells Dev.* 28, 398–409. doi: 10.1089/scd.2018.0200

Zhang, Y., Lin, X., Dai, Y., Hu, X., Zhu, H., Jiang, Y., et al. (2016). Endometrial stem cells repair injured endometrium and induce angiogenesis via AKT and ERK pathways. *Reproduction* 152, 389–402. doi: 10.1530/REP-16-0286

Zhao, Y., Lan, X., Wang, Y., Xu, X., Lu, S., Li, X., et al. (2018). Human endometrial regenerative cells attenuate bleomycin-induced pulmonary fibrosis in mice. *Stem Cells Int.* 2018:3475137. doi: 10.1155/2018/3475137

**Conflict of Interest:** The authors declare that the research was conducted in the absence of any commercial or financial relationships that could be construed as a potential conflict of interest.

*Copyright © 2019 Marinaro, Gómez-Serrano, Jorge, Silla-Castro, Vázquez, Sánchez-Margallo, Blázquez, López, Álvarez and Casado. This is an open-access article distributed under the terms of the Creative Commons Attribution License (CC BY). The use, distribution or reproduction in other forums is permitted, provided the original author(s) and the copyright owner(s) are credited and that the original publication in this journal is cited, in accordance with accepted academic practice. No use, distribution or reproduction is permitted which does not comply with these terms.*

PLOS ONE

RESEARCH ARTICLE

# Murine embryos exposed to human endometrial MSCs-derived extracellular vesicles exhibit higher VEGF/PDGF AA release, increased blastomere count and hatching rates

**Rebeca Blázquez[1,2‡], Francisco Miguel Sánchez-Margallo[1,2‡], Verónica Álvarez[1‡], Elvira Matilla[3], Nuria Hernández[3], Federica Marinaro[1], María Gómez-Serrano[4], Inmaculada Jorge[2,4], Javier G. Casado[1,2*], Beatriz Macías-García[3]**

**1** Stem Cell Therapy Unit, Jesús Usón Minimally Invasive Surgery Centre, Cáceres, Spain, **2** CIBER de Enfermedades Cardiovasculares, Madrid, Spain, **3** Assisted Reproduction Unit, Jesús Usón Minimally Invasive Surgery Centre, Cáceres, Spain, **4** Centro Nacional de Investigaciones Cardiovasculares (CNIC), Madrid, Spain

‡ These authors are co-first authors on this work.
* jgarcia@ccmijesususon.com

Check for updates

OPEN ACCESS

**Citation:** Blázquez R, Sánchez-Margallo FM, Álvarez V, Matilla E, Hernández N, Marinaro F, et al. (2018) Murine embryos exposed to human endometrial MSCs-derived extracellular vesicles exhibit higher VEGF/PDGF AA release, increased blastomere count and hatching rates. PLoS ONE 13(4): e0196080. https://doi.org/10.1371/journal.pone.0196080

**Editor:** Gijs B Afink, Academic Medical Centre, University of Amsterdam, NETHERLANDS

**Received:** December 21, 2017

**Accepted:** April 5, 2018

**Published:** April 23, 2018

**Copyright:** © 2018 Blázquez et al. This is an open access article distributed under the terms of the Creative Commons Attribution License, which permits unrestricted use, distribution, and reproduction in any medium, provided the original author and source are credited.

**Data Availability Statement:** All relevant data are within the paper and its Supporting Information files.

**Funding:** This work was supported in part by CIBER-CV (CB16/11/00494). One grant from Junta de Extremadura (Ayuda a grupos catalogados de la Junta de Extremadura, GR15175). Two grants from Junta de Extremadura to JGC (TA13042 and IB16168 co-financed by FEDER/FSE). One grant to

## Abstract

Endometrial Mesenchymal Stromal Cells (endMSCs) are multipotent cells with immunomodulatory and pro-regenerative activity which is mainly mediated by a paracrine effect. The exosomes released by MSCs have become a promising therapeutic tool for the treatment of immune-mediated diseases. More specifically, extracellular vesicles derived from endMSCs (EV-endMSCs) have demonstrated a cardioprotective effect through the release of anti-apoptotic and pro-angiogenic factors. Here we hypothesize that EV-endMSCs may be used as a co-adjuvant to improve *in vitro* fertilization outcomes and embryo quality. Firstly, endMSCs and EV-endMSCs were isolated and phenotypically characterized for *in vitro* assays. Then, *in vitro* studies were performed on murine embryos co-cultured with EV-endMSCs at different concentrations. Our results firstly demonstrated a significant increase on the total blastomere count of expanded murine blastocysts. Moreover, EV-endMSCs triggered the release of pro-angiogenic molecules from embryos demonstrating an EV-endMSCs concentration-dependent increase of VEGF and PDGF-AA. The release of VEGF and PDGF-AA by the embryos may indicate that the beneficial effect of EV-endMSCs could be mediating not only an increase in the blastocyst's total cell number, but also may promote endometrial angiogenesis, vascularization, differentiation and tissue remodeling. In summary, these results could be relevant for assisted reproduction being the first report describing the beneficial effect of human EV-endMSCs on embryo development.

B-MC (IB16159 co-financed by FEDER/FSE). One grant "Miguel Servet I" from Instituto de Salud Carlos III to JGC (CP17/00021 co-financed by FEDER/FSE). One grant "Juan de la Cierva" to B-MC from Spanish Ministry of Economy, Industry and Competitiveness (IJCI-2014-19428). The funders had no role in study designs, data collection and analysis, decision to publish or preparation of the manuscript.

**Competing interests:** The authors have declared that no competing interests exist.

## Introduction

Mesenchymal Stromal Cells (MSCs) are ubiquitous multipotent progenitor cells that can be found in bone marrow, umbilical cord, placenta or adipose tissue among others [1]. Their main features are plastic adherence, high proliferative potential, differentiation potential towards osteogenic, adipogenic and chondrogenic lineages and their self-renewal capacity [2]. Due to their immunomodulatory and anti-inflammatory activities, these cells have been considered for the treatment of a wide variety of clinical conditions including cirrhosis or articular damage [3,4]. However, invasive extraction of MSCs by means of tissue biopsies and the need for later expansion are limiting factors for their clinical application.

MSCs release paracrine factors that have also been shown to effectively mediate tissue repair and regeneration [5] offering a good cell-free alternative to direct MSCs application. Among all the paracrine factors, special attention is being put on exosomes, which are small vesicles (40–150 nm) of endosomal origin that mediate cell to cell communication. These vesicles are known to be composed of RNAs, DNA, lipids and proteins, although these components may vary depending upon cell type and physiological or pathological status [6,7].

Recently, MSCs have been isolated from human menstruation offering the advantage of being a non-invasive source of multipotent cells that can grow twice faster than bone marrow-derived MSCs [1]. This intense proliferative potential is aimed to maintain the dynamic remodeling of the endometrium [8] during the menstrual cycle. This cycle consists of a secretory and a proliferative phase which is followed by a profound desquamation of the endometrium during menstruation, being repeated over 400 times throughout the women's reproductive life [9]. Hence, endometrial MSCs offer the advantage of being a reliable and cost-effective source of multipotent cells. Recent studies have demonstrated that exosomes derived from menstrual MSCs alleviate apoptosis in a mouse model of fulminant hepatic failure [10] and decrease tumor-induced angiogenesis in prostate PC3 tumor cells [11].

Regarding the role of extracellular vesicles derived from endometrial MSCs (EV-endMSCs) in early pregnancy, it is known that the endometrium establishes a complex interplay with the embryo being this cell to cell communication mediated in part by exosome release [12]. This dynamic communication is partly mediated by cytokines and growth factors that are involved in pregnancy. For example, T cell-derived cytokines such as GM-CSF or IL-3 have been demonstrated to be important growth factors for the trophoblast, while TGF-ß, CSF-1 and LIF are involved in implantation determining embryo survival and viable offspring delivery [13,14].

Preimplantation development requires a transcriptional control for a precise coordination of multiple cell-fate decisions [15]. It requires the reprogramming of parental epigenomes to a totipotent state and the epigenetic programs are essential for lineage decisions and differentiation [16]. Several dynamic changes occurs during blastocyst formation and the polarization model seems to be the best model to incorporate most known information [17]. Once the oocyte is fertilized, the embryo undergoes symmetric and asymmetric divisions during morula to blastocyst transition. When it reaches the expanded blastocyst stage, it will escape from the zona pellucida (embryo hatching), being this a mandatory step for successful implantation [18,19]. Even when endometrial MSCs exosomes are presumed to vehicle many soluble factors including cytokines and growth factors, the effect that these vesicles may exert as coadjutants during embryo culture still remains unexplored. Therefore, the aim of the present study was to isolate and characterize human endometrial MSCs and their extracellular vesicles; then to evaluate their biological effect these EV- MSCs were co-cultured with murine 2 cell embryos produced *in utero*. Embryo development and hatching were *in vitro* evaluated.

Our results firstly demonstrate the beneficial effect of EV-endMSCs on embryo developmental competence, total cell number and embryo hatching. Moreover, the analysis of soluble

factors released by co-cultured embryos evidenced a significant increase of VEGF and PDGF-AA secretion which have been associated with enhanced angiogenesis, vascularization, differentiation and tissue remodeling possibly aiming to enhance endometrial receptivity.

## Materials and methods

### Isolation and *in vitro* expansion of endometrial mesenchymal stromal cells

Endometrial Mesenchymal Stromal Cells (endMSCs) were isolated from menstrual blood of four healthy women (Fig 1) according to previously described protocols [20,21]. Inclusion criteria for women were: females without infection, no hormone therapy and ages between 30–40 years. The exclusion criteria were: females with HBV, HCV or HIV infection, immune disorders and under hormone treatments. The samples were collected on day 2 or 3 of the menstrual cycle by the use of a menstrual cup. Written informed consent was obtained from all donors under the auspices of the Minimally Invasive Surgery Centre Research Ethics Committee, which approved this study. Briefly, menstrual blood was diluted 1:2 in PBS and centrifuged at 450 x g for 10 minutes. Supernatants were discarded in order to remove the residues of cervical mucus and cells were re-suspended in DMEM containing 10% fetal bovine serum (FBS), 1% penicillin/streptomycin and 1% glutamine. Cells were seeded onto tissue culture flasks and

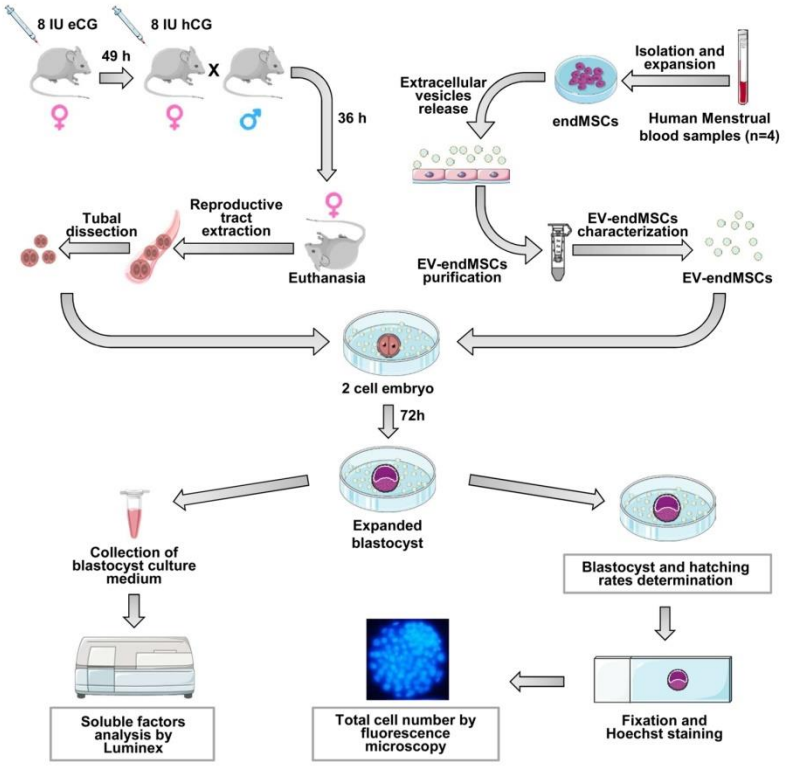


**Fig 1. Description of the study and methodological design.**

https://doi.org/10.1371/journal.pone.0196080.g001

expanded at 37˚C in 95% air and 5% $CO_2$ atmosphere. Non-adherent cells were removed after 24h. Adherent cells were cultured to 80% confluency and detached using PBS containing 0.25% trypsin (v/v). Cells were seeded again at a density of 5000 cells/$cm^2$. Culture medium was changed every three days.

## Phenotypical and functional characterization of endMSCs

The differentiation assay of endMSCs was performed when the cells reached 80% of confluence. Standard *in vitro* differentiation assays were used to promote osteogenic, adipogenic and chondrogenic differentiation. Cells were cultured for 21 days with differentiation specific media (Stem Pro Adipogenesis, Chondrogenesis and Osteogenesis Differentiation Kits, Gibco, Thermo Fisher Scientific, MA, USA) which was replaced every three days. Cells were stained to evidence adipogenic, chondrogenic and osteogenic differentiation with Oil Red O, Alcian Blue 8GX and Alizarin Red S stains, respectively. Differentiated cells were observed by optical microscopy. The degree of adipogenic, chondrogenic and osteogenic differentiations was determined by extracting the stain with 6M guanidine-HCl (Alcian Blue 8GX and Alizarin Red S stains) or pure isopropanol (Oil Red O stain). The absorbance of the extracts was quantified at 490 nm (Oil Red O and Alizarin Red S stains) and at 600 nm (Alcian Blue 8GX).

For the phenotypic analysis, $2 \times 10^5$ endMSCs were stained with human monoclonal antibodies (mAbs) against CD29, CD31, CD34, CD44, CD45, CD49d, CD49f, CD56, CD73, CD90, CD105 and HLA-DR using the appropriate concentrations of mAbs in the presence of PBS containing 2% FBS. The endMSCs and mAbs were incubated for 30 min at 4˚C. The cells were washed and re-suspended in PBS. Isotype-matched antibodies were used as negative controls. The flow cytometric analysis was performed on a FACScalibur cytometer (BD Biosciences, CA, USA) after acquisition of $10^5$ events.

Viable cells were selected using forward and side scatter characteristics and fluorescence was analyzed using CellQuest software (BD Biosciences, CA, USA). Isotype-matched negative control antibodies were used in the experiments. The percentage of positive cells above the negative control (isotype controls) was determined. Cells were analyzed at passages 3–4.

## Isolation, purification and characterization of extracellular vesicles from endMSCs

An enriched fraction of endMSCs-derived exosomes, contained in the isolated extracellular vesicles, was obtained from endMSCs cultured in 175 $cm^2$ flasks using a previously optimized protocol [22]. When cells reached a confluence of 80%, culture medium (DMEM containing 10% FBS) was replaced by exosome isolation medium (DMEM containing 1% insulin–transferrin–selenium). The endMSCs supernatants were collected every 3–4 days and centrifuged at 1000 x g for 10 min and 5000 x g for 20 min at 4˚C to eliminate dead cells and debris. Subsequently, the supernatants were filtered twice using a sterile cellulose acetate filter of 0.45 μm and then on of 0.20 μm (Corning, NY, USA). About 15 ml of these endMSCs supernatants were ultra-filtered through 3kDa MWCO Amicon® Ultra Devices (Merck-Millipore, MA, USA) at 4000 x g for 1 hour at 4˚C. The concentrated supernatants were collected and stored at -20˚C. Prior to *in vitro* experiments, the concentration of microvesicles was indirectly measured by quantifying the protein content by a Bradford assay (BioRad Laboratories, CA, USA).

The concentration and size of purified EV-endMSCs were quantified by nanoparticle tracking analysis (NanoSight Ltd, Amesbury, UK) equipped with fast video capture that relates the rate of Brownian motion to particle size. Results were analyzed using the particle-tracking analysis software package version 2.2. The equipment configuration for this analysis was: frames processed: 900. 899; frames per second: 30; calibration: 166 nm/pixel; automatic

defocus: Auto; detection threshold: 4 Multi; minimum size expected: Auto; tracking minimum size: 100 nm; temperature: 24–28˚C; viscosity: 0.80–0.95 cP.

For the flow cytometric analysis by fluorescent activated cells sorting, EV-endMSCs were bounded to latex beads and labeled with fluorophore-conjugated antibodies as described by Théry et al. [23]. Briefly, EV-endMSCs (5 μg of exosomal proteins) were conjugated overnight at 4˚C with 10 μl of Aldehyde/Sulfate latex beads, 4% w/v, 4 μm (Molecular Probes, OR, USA). 110 μl of 1M glycine were added to each tube and incubated for 30 minutes. Then the samples were centrifuged and re-suspended in a final volume of 0.5 ml PBS, containing 0.5% bovine serum albumin (BSA; w/v). These EV-endMSCs-coated beads were incubated for 30 minutes at 4˚C with anti-CD9 and anti-CD63 human monoclonal antibodies (BD Biosciences, CA, USA). The EV-endMSCs -coated beads were washed and re-suspended in PBS+BSA. The flow cytometry analysis was performed on a FACScalibur cytometer (BD Biosciences, CA, USA) after acquisition of $10^5$ events. Isotype-matched negative control antibodies were used in all the experiments. The percentage of positive cells above the negative control (isotype controls) was determined.

## Soluble factor analysis

At the third day of embryo culture, the embryos were fixed as described below and the cell culture media were individually collected and stored at -20˚C for later soluble factors analyses (Fig 1). As negative controls, KSOM medium with or without EV-endMSCs were used and their quantifications were subtracted to the corresponding study groups. The murine-specific soluble factors analyzed were chosen for their importance in the first phases of embryo development: GM-CSF, VEGF, IGF-I, IL-6, M-CSF, EGF and PDGF-AA. These soluble factors were analyzed using a bead-based Magnetic multiplexed Luminex Assay (LXSAMSM, R&D systems, MN, USA) according to the manufacturer's instructions. The concentrations of the different factors were expressed as pg/ml.

## Animals and superovulation protocol

All the experimental procedures were reviewed and approved by the Ethical Committee of the Jesús Usón Minimally Invasive Surgery Centre. B6D2F1 mice were housed under a 12 h light/12 h dark cycle, at a controlled temperature (19–23˚C) with free access to food and water. Females were intraperitoneally (IP) injected with 8 IU of equine chorionic gonadotropin (eCG, Veterin Corion, Divasa Farmavic) followed 49 h later by 8 IU of IP human chorionic gonadotropin (hCG, Foligon, MSD) to trigger ovulation (Fig 1).

## *In vivo* embryo recovery and culture

Female mice (8–12 weeks old) were hormonally stimulated to trigger ovulation as previously described; after hCG injection, females were paired with B6D2 males in a 1:1 ratio. After 36 hours from the hCG injection, females were sacrificed by cervical dislocation and the embryos were collected from the oviducts in M2 (Sigma-Aldrich, Barcelona, spain); these 2-cell embryos were washed in fresh KSOM (Merck-Millipore, Madrid, Spain) and placed in 100 μl droplets (9–12 embryos/droplet) devoid of EV-endMSCs (control) or in KSOM droplets added with 10, 20, 40 or 80 μg/ml of EV-endMSCs from the four different donors individually and media was not replaced throughout the entire culture; embryos were incubated in a 5% $CO_2$/95% air atmosphere at 37˚C and 100% humidity. For each experiment, 2 cell murine embryos were obtained from 3 different females (36 hours post-hCG) and pooled prior embryo culture (12 different females used in total). The number of initial 2 cell embryos and

the percentage of embryos reaching the expanded blastocyst stage as well as embryo hatching after 75 hours in culture were recorded (Fig 1).

### Total cell number

The number of cells in an embryo is a well-known indicator of embryo viability and quality [24]. Therefore, in view of the previous data, after embryo hatching assessment, the blastocysts obtained were fixed in 4% formaldehyde in PBS added with 0.01% of polyvinyl alcohol (PVA; w/v) at 4˚C for 12 hours and stained with 2.5 μg/ml of Hoechst 33342 (Eugene, OR, USA) in PBS added with PVA for 10 minutes at 37˚C. Then, the blastocysts were mounted on glass slides with glycerol, covered with coverslips and sealed. Embryos were then visualized (Fig 1) using a fluorescence microscope (Nikon Elipse TE2000-S) equipped with an ultraviolet lamp. Cell number was analyzed using the Fiji Image-J Software (1.45q, Wayne Rasband, NIH, USA).

### Statistical analysis

For total cell number analysis data were tested for normality using a Shapiro–Wilk test; results are reported as mean ± standard deviation (SD). Groups were compared using a one way ANOVA due their Gaussian distribution and homoscedasticity. When statistically significant differences were found, a Bonferroni post-hoc test was used to compare pairs of values. Blastocyst and hatching rates were compared among groups by Chi-square test with the Yates correction for continuity. The Fisher's Exact Test was used when a value of less than 5 was expected in any treatment. A Student t-test for paired comparisons was performed on VEGF and PDGF-AA measurements. The correlation between VEGF and PDGF-AA was calculated using the Pearson correlation coefficient. Statistical analyses were performed using Sigma Plot software version 12.3 for Windows (Systat Software, IL, USA) or with SPSS-21 software (SPSS, IL, USA); $p < 0.05$ was considered as statistically significant.

## Results

### Phenotypic profile of endMSCs

The phenotypic analysis of endMSCs cultures was carried out by flow cytometry. As reported by the representative histograms (Fig 2A), endMSCs were negative for CD31, CD34, CD45, HLA-DR and positive for the stemness markers CD29, CD44, CD49d, CD49f, CD56, CD73, CD90 and CD105. The differentiation towards the adipogenic, chondrogenic and osteogenic lineages was confirmed by microscopic analysis (Fig 2B) and stain quantification (Fig 2C).

### Size distribution, concentration and exosome specific markers in EV-endMSCs

In order to quantify the proteins in the enriched fraction of exosomes, a Bradford assay was performed ranging their protein concentrations between 350 and 750 μg/ml. The nanoparticle tracking analysis of EV-endMSCs revealed that the mean size and standard deviation of isolated vesicles from four different donors was 153.5±63.05 nm, while their concentration was $3.31x10^{11} \pm 3.8x10^{9}$ particles/ml. Fig 3A shows a representative analysis of nanoparticle tracking analysis. Finally, the EV-endMSCs were phenotypically characterized by flow cytometry with specific exosomal markers. The analysis of CD9 and CD63 demonstrated a positive expression of these exosome-related proteins (Fig 3B).

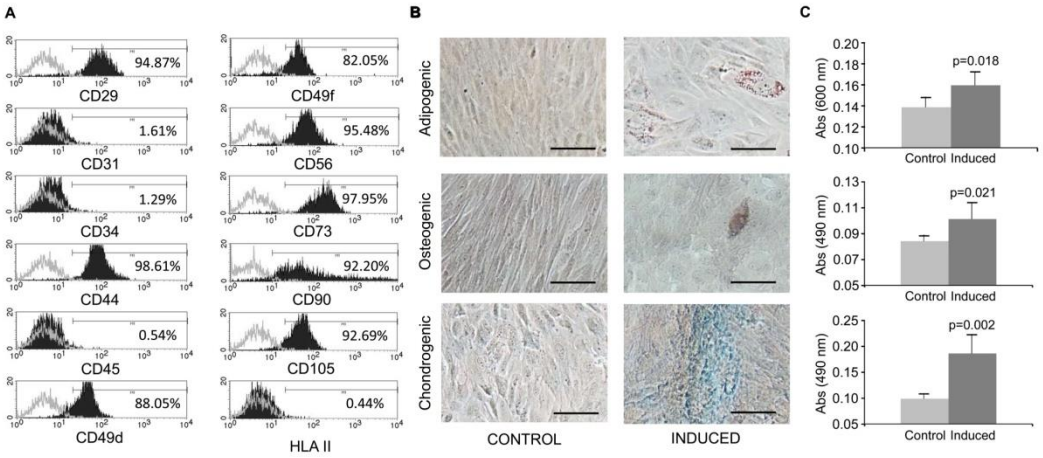


**Fig 2. Phenotypical characterization and differentiation potential of endMSCs.** (A) Flow cytometry analysis of endMSCs isolated from menstrual blood. A representative histogram together with the expression levels is shown. The expression of cell surface markers is represented as the percentage of positive cells (black lined histogram) above the negative control (grey lined histogram). (B) *In vitro* differentiation potential of endMSCs. The cells were *in vitro* cultured for 21 days with standard medium (Control) or with specific differentiation media for adipogenic, osteogenic and chondrogenic lineages (Induced). Differentiation towards adipocytes, osteocytes and chondrocytes was evidenced by Oil Red O, Alizarin Red and Alcian Blue 8GX respectively. Scale bar: 100 μm. (C) The adipogenic (above), osteogenic (middle) and chondrogenic (below) differentiation degree was quantified by determining the absorbance of the extracts at 490 nm (Oil Red O and Alizarin Red S staining) and at 600 nm (Alcian Blue 8GX). Four independent experiments using four different cell lines were performed and a Mann-Whitney U test was used. p-values are shown in the figure.

https://doi.org/10.1371/journal.pone.0196080.g002

## Development to the blastocyst stage, embryo hatching and total cell number count

Our results showed that the developmental competence of the embryos did not vary disregarding EV-endMSCs addition or the dosage used. The blastocyst rate of the control embryos devoid of EV-endMSCs was 86.8%, this percentage was 98.2% for the 10 μg/ml dose, 92.9% for 20 μg/ml, 79.6% when 40 μg/ml of EV-endMSCs were added and 84.9% for the 80 μg/ml dose and no statistically significant differences were observed between groups ($p>0.05$; Table 1). Conversely, total cell number was significantly enhanced ranging from 73.8–75.6 cells/embryo (37–41 blastocysts evaluated per treatment) when EV-endMSCs were added exceeding the non-EV-endMSCs added control (61.2 ± 19.6 cells/embryo, n = 44; $p<0.05$), demonstrating that EV-endMSCs significantly promoted blastomere division during embryonic development (Fig 4). Furthermore, as seen in Table 1, embryo hatching was consistently enhanced for all the EV-endMSCs dosages tested, although statistically significant differences were only observed between the control (20.5% hatching embryos) and the 20 μg/ml and 40 μg/ml EV-endMSCs dosages (54.1 and 47.6% of hatching embryos respectively; $p<0.05$).

## Quantification of soluble factors secreted during embryo development *in vitro*

The analysis of soluble factors was performed at the third day of embryo culture. Unfortunately, the analysis of murine molecules: GM-CSF, IGF-I, IL-6, M-CSF and EGF were below the detection limits of the technique and the quantification of these molecules was impossible at this time point (data not acquired). On the contrary, blastocyst-released PDGF-AA and VEGF were detectable in all supernatants at day 3 of embryo culture for all the different EV-

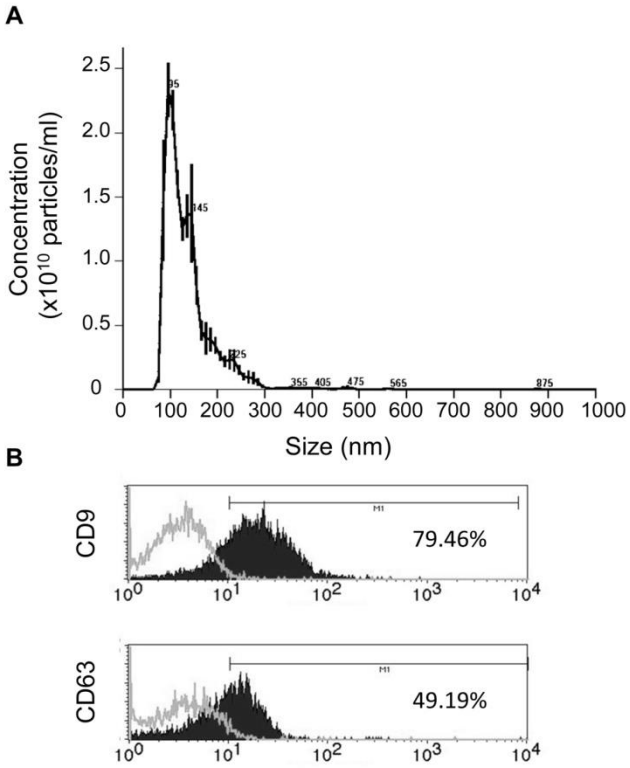


**Fig 3. Characterization of EV-endMSCs.** (A) Representative graph of nanoparticle tracking analysis to quantify size distribution and particle concentration of EV-endMSCs. (B) Flow cytometry analysis on EV-endMSCs for exosomal markers CD9 and CD63. A representative histogram together with the expression levels is shown. The expression of cell surface markers is represented as as the percentage of positive cells (black lined histogram) above the negative control (grey lined histogram).

https://doi.org/10.1371/journal.pone.0196080.g003

endMSCs dosages tested. Our results demonstrated an EV-endMSCs concentration-dependent increase of VEGF and PDGF-AA released by the embryos (Fig 5). It is important to note that the hypothetical presence of VEGF or PDGF-AA factors from EV-endMSCs was

**Table 1. Embryo development to the blastocyst stage and hatching rates.**

| Treatment | Initial 2 cell embryos | Blastocyst (%) | Hatching (%) |
|---|---|---|---|
| Control | 53 | 86.8[a] | 20.5[a] |
| 10 μg/ml EV-endMSCs | 56 | 98.2[a] | 39.0[a,b] |
| 20 μg/ml EV-endMSCs | 57 | 92.9[a] | 54.1[b] |
| 40 μg/ml EV-endMSCs | 49 | 79.6[a] | 47.6[b] |
| 80 μg/ml EV-endMSCs | 53 | 84.9[a] | 40[a,b] |

The initial number of 2 cell embryos retrieved in uterus (n) as well as blasocyst rate in % and hatching embryos in % is provided (hatching rates were calculated as the number of blastocysts that hatched/total blastocyst number per treatment); different superscripts represent statistically significant differences ($p<0.05$).

https://doi.org/10.1371/journal.pone.0196080.t001

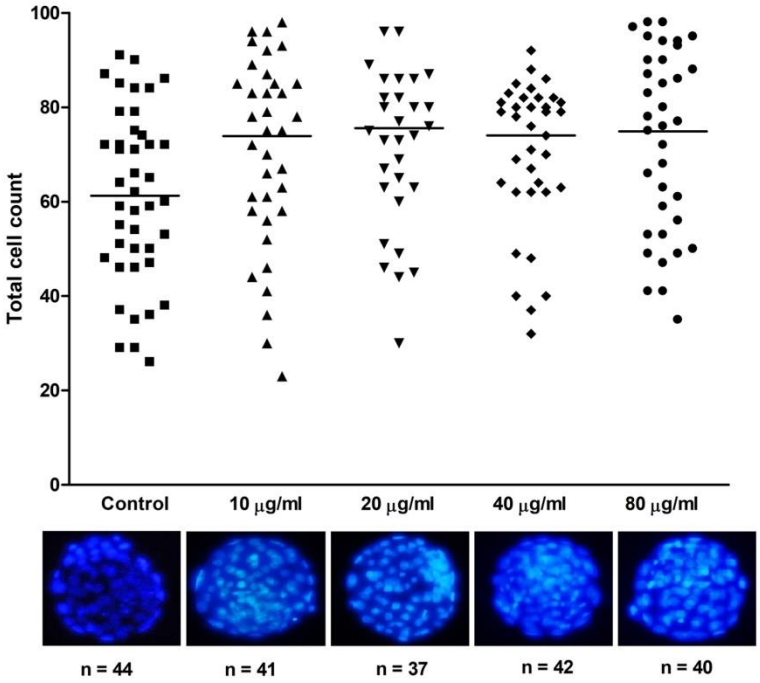


**Fig 4. Total cell number of murine blastocysts cultured in presence or absence of EV-endMSCs.** Total cell number of the obtained expanded blastocysts was obtained after Hoechst 33342 staining and subsequent evaluation by fluorescence microscopy. For each treatment, the individual blastomere count is represented. Horizontal bars show the mean values. All the treatments differ statistically from the control ($p<0.05$). Representative micrographs of expanded blastocysts cultured with varying dosages of EV-endMSCs are shown.

https://doi.org/10.1371/journal.pone.0196080.g004

considered and negative controls (culture medium with/without EV-endMSCs) were included for the different samples and this background was subtracted for each sample. However, as we could not discard cross-reactivity between human and mouse PDGF-AA in the Luminex assay, there is a possibility that residual human PDGF-AA with exosomal origin coming from embryos could have interfered in the measurements. The separated values of the experimental samples and negative control samples are shown in S1 Fig.

In the case of PDGF-AA, significant differences were found between negative controls (embryos cultured in the absence of EV-endMSCs) and embryos co-cultured with EV-endMSCs. The EV-endMSCs added at 10 μg/ml, 20 μg/ml, 40 μg/ml and 80 μg/ml showed the following p values: $p = 0.021$, $p = 0.014$, $p = 0.064$ and $p = 0.031$ respectively (Fig 5A).

In the case of VEGF, several significant differences were found between negative controls (blastocysts cultured without EV-endMSCs) and blastocysts co-cultured with EV-endMSCs. The EV-endMSCs supplemented at 10 μg/ml, 20 μg/ml, 40 μg/ml and 80 μg/ml showed the following p values: $p = 0.249$, $p = 0.018$, $p = 0.060$ and $P<0.001$ respectively (Fig 5B).

Finally, as shown in Fig 5C, our results demonstrated that the released VEGF and PDGF-AA produced by the blastocyst during their development *in vitro* were very significantly correlated ($r = 0.812$, $p<0.001$).

## Discussion

Exosomes derived from MSCs are a matter of study as they are known to exert a therapeutic role in different physiological and pathological conditions. In the case of endMSCs, these cells

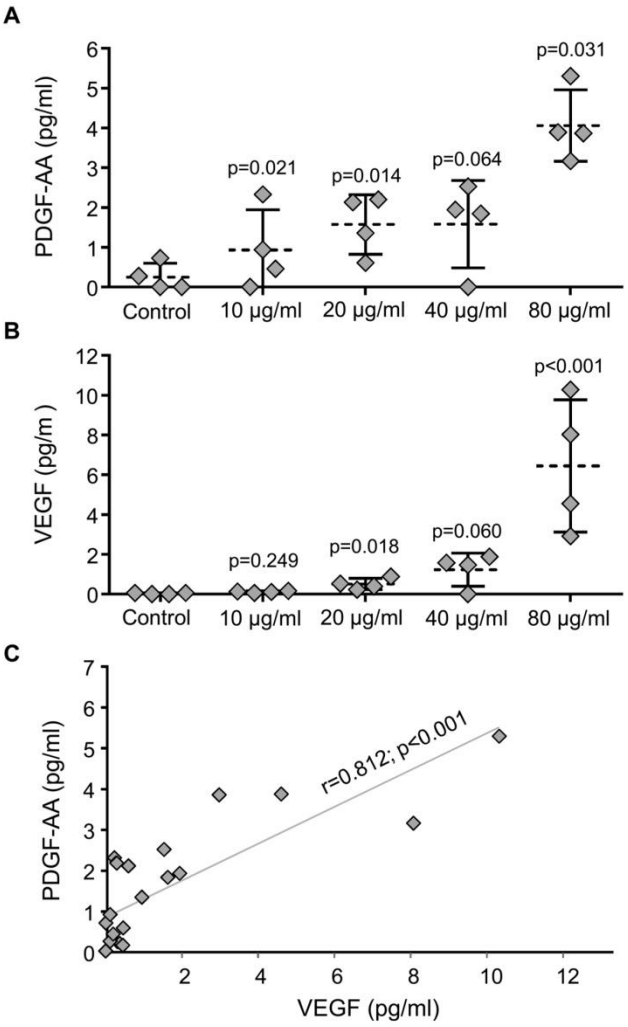


**Fig 5. Quantification of VEGF and PDGF-AA secreted during embryo culture.** Soluble factors released by the developing embryos co-cultured with EV-endMSCS were quantified by the Luminex xMAP technology at the third day of embryo culture. (A) PDGF-AA secreted by blastocyst embryos. All the data were compared by Student t-test for paired comparisons with respect to control group. The mean (dotted line) ±SD from four independent experiments, as well as individual measures (rhombuses), are shown. (B) VEGF secreted by blastocyst embryos. All the data were compared by Student t-test for paired comparisons with respect to control group. The mean (dotted line) ±SD from four independent experiments, as well as individual measures (rhombuses), are shown. (C) Correlation between PDGF-AA and VEGF. Correlation line as well as individual measures (rhombuses) are represented. The Pearson correlation coefficient (r) together with its significance level (p) is shown.

https://doi.org/10.1371/journal.pone.0196080.g005

participate in tissue remodeling which is essential for the endometrium [25] exhibiting immunomodulatory potential through the release of soluble factors [26]. These cells can be easily obtained during menstruation and their expansion, characterization and subsequent exosome retrieval can be achieved in the laboratory. Specifically, human exosomes released in the uterus have been demonstrated to profoundly influence implantation and embryo-maternal crosstalk [8].

Additionally, it has been demonstrated that *in vitro* produced bovine embryos release exosomes and that their composition varies depending on the embryo competence [27]; on the other hand it has been shown that, when the culture medium is not replaced during the entire embryo culture, the blastocyst rate, total cell number and calving significantly improve in bovine cloned embryos [28]. These effects have been related to exosome secretion by the embryos in the culture medium as removal of these exosomes by medium replacement impairs embryo development, while its supplementation to exosome-depleted embryos increases embryo quality [28]. Taken together, these reports reflect the complex interplay existing between the maternal environment and the embryo as exosome release and uptake determines embryo competence, quality and birth rate.

Even when exosomal content is still under study, what it is already known is that exosomes are locally released and are meant to interact and transfer their cargo to the target cells. Although the exact mechanisms are under study, in the case of the uterine environment these mechanisms are even more intricate, as the exosome content also depends on the hormonal environment and gestational status [29,30]. Several studies have been conducted to understand their *in vitro* features such as protein cargo [8] or micro RNA content [31] although the role that they may play *in vivo* or the optimal dosage to be used remains unexplored. Based on the previously mentioned literature, we aimed to elucidate if human EV-endMSCs influenced the soluble factors released by blastocyst, the development and hatching of blastocysts or the blastomere proliferation of murine embryos obtained *in vivo*. Our results did not evidence any effect of EV-endMSCs on embryo development as the blastocyst rates remained unchanged between treatments (over 79% blastocyst rate for all the treatments tested). These data are in agreement with previous reports in the bovine species in which exosomes derived from homologous oviductal explants did not increase the blastocyst yield [32,33]. However, core differences exist in both experimental settings as bovine *in vitro* produced embryos exhibit consistently lower developmental competence than B6D2F1 murine *in vivo* obtained two cell embryos [34]. Nevertheless, our results do not evidence any toxic effect of the EV-endMSCs dosages tested, and thus, the ones used in the present study can be considered non-toxic. As embryo development to the blastocyst stage does not predict embryo quality, the expanded blastocysts obtained were fixed and stained with Hoechst 33342 in order to determine their quality by total blastomere counts [35]. Interestingly, our results demonstrated an increase in blastomere count at all the EV-endMSCs dosages tested over the control demonstrating a positive effect of these microvesicles on embryonic total cell number. However, embryo transfer will be performed in next studies to rule out an increased incidence of embryonic aneuploidies in embryos supplemented with EV-endMSCs, although their incidence is very low in this species [36]. As previously mentioned, homologous oviductal exosomes increase the quality of bovine embryos in terms of survival rate after cryopreservation and gene expression [32,33]. In addition, exosomes derived from cloned bovine embryos also enhanced total cell number and the inner cell mass/trophoectoderm cell of the embryos [28] and these results parallel the ones obtained in the present work. To further confirm that EV-endMSCs increase embryo quality *in vitro*, hatching rates were also evaluated. Interestingly, statistically significant differences in hatching rates were only detected in the 20 and 40 μg/ml dosages compared against control, although for the 10 and 80 μg/ml dosages hatching rates were almost doubled

compared to the non-microvesicles added treatment. It is known that embryo hatching in the mouse is achieved by an embryonic-mediated lytic mechanism and by the pressure of the expanding blastocele/blastocyst against the zona [37]. However, the exact mechanism of hatching is still controversial as some authors claim that the lytic mechanism is predominant and the blastocyst pressure is less relevant [38]; thus our results parallel those of Gordon *et al.* who described that enzymatic digestion of the zona pellucida using Tyrode's solution better induces embryo hatching compared to mineral injection under the zona to mimic the mechanical embryo pressure as, even when total cell number significantly increases in each EV-endMSCs treatment, hatching rates improve significantly only for the 20 and 40 μg/ml dosages. These results reflect that the 10 μg/ml is a low dose while with the 80 μg/ml dosage we may be working at saturation conditions; therefore the 20–40 μg/ml dosages seem to be adequate reference ranges to work with. Our preliminary proteomic analyses of the EV-endMSCs have revealed a wide range of proteins closely related to embryo development and implantation (manuscript in preparation). As an example, transferrin [39], vinculin [40], and fibronectin [41,42] have been demonstrated to promote embryo development being essential in the early embryo development and survival. Thus, EV-endMSC could be promoting embryo blastomere division and hatching by the specific protein cargo released to the embryo culture medium. In addition, core proteins related to embryo implantation such as matrix metalloproteinase-2, -3 and -9 [43,44], or E-cadherin [45] were also identified. In summary, according to the proteomic profile of EV-endMSCs and the enhanced hatching observed in our EV-endMSCs embryos (positively related with embryo implantation [46]), our results may indicate a higher implantation potential of the obtained embryos, but this theory has to be further confirmed.

Apart from the analysis of embryo developmental competence, total blastomere count and blastocyst/hatching rate; we aimed to evaluate the release of soluble factors by murine embryos. It is known that embryos release cytokines that play a role in embryonic development, embryo-maternal recognition and maintenance of the proper hormonal environment [47]. However, the exact molecules that modulate the development of the pre-implantation embryo still remains a matter of study [48]. In this study, our analysis was firstly focused on the quantification of GM-CSF which has been demonstrated to promote blastocyst development [49], embryo implantation [50] as well as embryo survival [51]. Unfortunately, in our experimental conditions, the quantification analysis by Luminex xMAP detection was not sensitive enough to quantify murine GM-CSF. In fact, the detection limit of our Luminex assay was 11.65 pg/ml, while the detection limit by commercially available ELISAs is usually between 4 to 5 pg/ml. Based on that, future studies for quantifying murine GM-CSF will be performed by ELISA tests or by using blastocysts supernatants at different time points. Similarly to murine GM-CSF, the analyses of murine IL-6, M-CSF, EGF and IGF-I were also below the detection limit. Previous studies in human embryo culture-conditioned media have demonstrated that IL-6 was undetectable in embryo supernatants [52]. However, we should not rule out that ELISA (with better detection limit: 24.56 pg/ml for Luminex *vs.* 7–8 pg/ml for ELISA), may provide a more reliable quantitative analysis of this cytokine which has been found to be secreted by trophoblast cells [53]. In the case of IGF-I and EGF, these two growth factors were also undetectable in our experimental conditions. The IGF-I has been reported to promote blastocyst development [49] and is positively correlated with embryo quality when present in high concentrations in the follicular fluid [54]. In the case of EGF, this molecule stimulates trophoblast development having a key role in the implantation process [55,56].

Although several soluble molecules were undetectable in the culture medium of murine embryos, detectable levels were observed for VEGF and PDGF-AA. VEGF is intensely synthesized by blastocysts during embryo development in humans [57] and PDGF-AA has been associated to enhanced embryo quality and developmental potential [58]. In our experimental

conditions, the addition of EV-endMSCs to embryo cell culture triggered the release of these two growth factors and this release was EV-endMSCs concentration-dependent.

In the case of VEGF, the synthesis of this molecule has been initially described during embryonic angiogenesis [59] and seems to be the responsible of vascularization in placenta and decidua when secreted by trophoblastic giant cells [60]. In fact, the angiogenic potential of exosomes from different origins (human placenta-derived MSCs [61], umbilical cord blood [62] endothelial cells [63], human-induced pluripotent stem cell-derived MSCs [64] or bone marrow derived MSCs [65], among others) has been reported. Finally, and similarly to our experimental conditions, in mouse models, the role of VEGF has been associated with embryo implantation and embryonic vasculogenesis [66].

Regarding PDGF-AA and embryo development, the first expression analysis demonstrating the expression of PDGF-AA in embryonic murine cells [67]. This molecule has been linked with early embryo development and more recently, it has been associated with the regulation of programmed cell death mediating the fine-tuning formation of the primitive endoderm at the end of the preimplantation period [68]. In general, PDGF-AA has been defined as a mitogenic factor driving the proliferation of undifferentiated cells [69] and in later maturation stages it has been associated with cell differentiation, tissue remodeling, patterning and morphogenesis [70].

Interestingly, even when the effect of human EV-endMSCs was tested on murine embryos, the embryos increased the secretion of VEGF and PDGF-AA of murine origin. This fact highlights that EV-endMSCs exert their effect in a non-species-specific manner and suggest that the murine model can be a good candidate to further investigate the efficacy of EV-endMSCs of human origin on these embryos.

To summarize, to the authors' best knowledge, this is the first report describing the lack of toxicity and beneficial effect of human EV-endMSCs on embryos of any species. The increased release of VEGF and PDGF-AA may indicate that the beneficial effect could be mediating not only an enhanced embryo quality reflected by a significant increase in total cell number per blastocyst and embryo hatching, but also supporting angiogenesis, vascularization, differentiation and tissue remodeling of the endometrium after embryo hatching in view of the soluble factors released. These results confirm a beneficial effect of EV-endMSCs in the field of assisted reproduction and aim to impulse future research in this still underexplored area.

## Supporting information

**S1 Fig. Quantification of VEGF and PDGF-AA secreted during embryo culture.** VEGF (A) and PDF-AA (B) concentrations measured by Luminex in experimental samples (box and whiskers diagrams, corresponding to embryos exposed to different concentrations of EV-endMSCs) and negative control samples used as background (plot diagrams, corresponding to culture medium with different concentrations of EV-endMSCs). The means±SD from four independent experiments are shown.
(TIF)

## Acknowledgments

Soluble factors were analyzed by the ICTS Nanbiosis (Unit 14. Cell therapy at CCMIJU). Maintenance of animals was performed by the ICTS Nanbiosis (Unit 22. Animal housing at CCMIJU). In vivo embryo recovery and culture was performed by the ICTS Nanbiosis (Unit 23. Assisted Reproduction at CCMIJU). Special thanks to our student Eva Alegre Cortés for data management.

## Author Contributions

**Conceptualization:** Francisco Miguel Sánchez-Margallo, Verónica Álvarez, Javier G. Casado, Beatriz Macías-García.

**Data curation:** Rebeca Blázquez, Francisco Miguel Sánchez-Margallo, Federica Marinaro, Inmaculada Jorge, Javier G. Casado, Beatriz Macías-García.

**Formal analysis:** Rebeca Blázquez, Francisco Miguel Sánchez-Margallo, Verónica Álvarez, Elvira Matilla, Federica Marinaro, Inmaculada Jorge, Javier G. Casado, Beatriz Macías-García.

**Funding acquisition:** Francisco Miguel Sánchez-Margallo, Javier G. Casado, Beatriz Macías-García.

**Investigation:** Rebeca Blázquez, Francisco Miguel Sánchez-Margallo, Verónica Álvarez, Nuria Hernández, Federica Marinaro, María Gómez-Serrano, Javier G. Casado, Beatriz Macías-García.

**Methodology:** Rebeca Blázquez, Francisco Miguel Sánchez-Margallo, Verónica Álvarez, Elvira Matilla, Nuria Hernández, Federica Marinaro, María Gómez-Serrano, Javier G. Casado, Beatriz Macías-García.

**Project administration:** Francisco Miguel Sánchez-Margallo, Verónica Álvarez, Javier G. Casado, Beatriz Macías-García.

**Resources:** Verónica Álvarez, Elvira Matilla, Javier G. Casado, Beatriz Macías-García.

**Supervision:** Rebeca Blázquez, Francisco Miguel Sánchez-Margallo, Javier G. Casado, Beatriz Macías-García.

**Validation:** Rebeca Blázquez, María Gómez-Serrano, Javier G. Casado, Beatriz Macías-García.

**Visualization:** Elvira Matilla, Beatriz Macías-García.

**Writing – original draft:** Rebeca Blázquez, Francisco Miguel Sánchez-Margallo, Verónica Álvarez, Federica Marinaro, Javier G. Casado, Beatriz Macías-García.

**Writing – review & editing:** Rebeca Blázquez, Francisco Miguel Sánchez-Margallo, Elvira Matilla, Nuria Hernández, Federica Marinaro, María Gómez-Serrano, Inmaculada Jorge, Javier G. Casado, Beatriz Macías-García.

## References

1. Khoury M, Alcayaga-Miranda F, Illanes SE, Figueroa FE. The promising potential of menstrual stem cells for antenatal diagnosis and cell therapy. Front Immunol. 2014; 5: 205. https://doi.org/10.3389/fimmu.2014.00205 PMID: 24904569
2. Uder C, Brückner S, Winkler S, Tautenhahn H-M, Christ B. Mammalian MSC from selected species: Features and applications. Cytometry A. 2018; 93: 32–49. https://doi.org/10.1002/cyto.a.23239 PMID: 28906582
3. Burke J, Hunter M, Kolhe R, Isales C, Hamrick M, Fulzele S. Therapeutic potential of mesenchymal stem cell based therapy for osteoarthritis. Clin Transl Med. 2016; 5: 27. https://doi.org/10.1186/s40169-016-0112-7 PMID: 27510262
4. Volarevic V, Nurkovic J, Arsenijevic N, Stojkovic M. Concise review: Therapeutic potential of mesenchymal stem cells for the treatment of acute liver failure and cirrhosis. Stem Cells. 2014; 32: 2818–2823. https://doi.org/10.1002/stem.1818 PMID: 25154380
5. Rani S, Ryan AE, Griffin MD, Ritter T. Mesenchymal Stem Cell-derived Extracellular Vesicles: Toward Cell-free Therapeutic Applications. Mol Ther. 2015; 23: 812–823. https://doi.org/10.1038/mt.2015.44 PMID: 25868399

6. Théry C, Zitvogel L, Amigorena S. Exosomes: composition, biogenesis and function. Nat Rev Immunol. 2002; 2: 569–579. https://doi.org/10.1038/nri855 PMID: 12154376
7. Wang L, Yu Z, Wan S, Wu F, Chen W, Zhang B, et al. Exosomes Derived from Dendritic Cells Treated with Schistosoma japonicum Soluble Egg Antigen Attenuate DSS-Induced Colitis. Front Pharmacol. 2017; 8: 651. https://doi.org/10.3389/fphar.2017.00651 PMID: 28959207
8. Greening DW, Nguyen HPT, Elgass K, Simpson RJ, Salamonsen LA. Human Endometrial Exosomes Contain Hormone-Specific Cargo Modulating Trophoblast Adhesive Capacity: Insights into Endometrial-Embryo Interactions. Biol Reprod. 2016; 94: 38. https://doi.org/10.1095/biolreprod.115.134890 PMID: 26764347
9. Mutlu L, Hufnagel D, Taylor HS. The endometrium as a source of mesenchymal stem cells for regenerative medicine. Biol Reprod. 2015; 92: 138. https://doi.org/10.1095/biolreprod.114.126771 PMID: 25904012
10. Chen L, Xiang B, Wang X, Xiang C. Exosomes derived from human menstrual blood-derived stem cells alleviate fulminant hepatic failure. Stem Cell Res Ther. 2017; 8: 9. https://doi.org/10.1186/s13287-016-0453-6 PMID: 28115012
11. Alcayaga-Miranda F, González PL, Lopez-Verrilli A, Varas-Godoy M, Aguila-Díaz C, Contreras L, et al. Prostate tumor-induced angiogenesis is blocked by exosomes derived from menstrual stem cells through the inhibition of reactive oxygen species. Oncotarget. 2016; 7: 44462–44477. https://doi.org/10.18632/oncotarget.9852 PMID: 27286448
12. Homer H, Rice GE, Salomon C. Review: Embryo- and endometrium-derived exosomes and their potential role in assisted reproductive treatments-liquid biopsies for endometrial receptivity. Placenta. 2017; 54: 89–94. https://doi.org/10.1016/j.placenta.2016.12.011 PMID: 28043656
13. Chaouat G, Dubanchet S, Ledée N. Cytokines: Important for implantation? J Assist Reprod Genet. 2007; 24: 491–505. https://doi.org/10.1007/s10815-007-9142-9 PMID: 18044017
14. Salamonsen LA, Evans J, Nguyen HPT, Edgell TA. The Microenvironment of Human Implantation: Determinant of Reproductive Success. Am J Reprod Immunol. 2016; 75: 218–225. https://doi.org/10.1111/aji.12450 PMID: 26661899
15. Cui W, Mager J. Transcriptional Regulation and Genes Involved in First Lineage Specification During Preimplantation Development. Adv Anat Embryol Cell Biol. 2018; 229: 31–46. https://doi.org/10.1007/978-3-319-63187-5_4 PMID: 29177763
16. Marcho C, Cui W, Mager J. Epigenetic dynamics during preimplantation development. Reproduction. 2015; 150: R109–120. https://doi.org/10.1530/REP-15-0180 PMID: 26031750
17. Johnson MH. From mouse egg to mouse embryo: polarities, axes, and tissues. Annu Rev Cell Dev Biol. 2009; 25: 483–512. https://doi.org/10.1146/annurev.cellbio.042308.113348 PMID: 19575654
18. Kim HJ, Park SB, Yang JB, Choi YB, Lee KH. Effects of laser-assisted hatching and exposure time to vitrification solution on mouse embryo development. Clin Exp Reprod Med. 2017; 44: 193–200. https://doi.org/10.5653/cerm.2017.44.4.193 PMID: 29376016
19. Park SB, Kim HJ, Choi YB, Ahn KH, Lee KH, Yang JB, et al. The effect of various assisted hatching techniques on the mouse early embryo development. Clin Exp Reprod Med. 2014; 41: 68–74. https://doi.org/10.5653/cerm.2014.41.2.68 PMID: 25045630
20. Moreno R, Rojas LA, Villellas FV, Soriano VC, García-Castro J, Fajardo CA, et al. Human Menstrual Blood-Derived Mesenchymal Stem Cells as Potential Cell Carriers for Oncolytic Adenovirus. Stem Cells Int. 2017;2017. https://doi.org/10.1155/2017/3615729 PMID: 28781596
21. Zemel'ko VI, Kozhukharova IB, Alekseenko LL, Domnina AP, Reshetnikova GF, Puzanov MV, et al. Neurogenic potential of human mesenchymal stem cells isolated from bone marrow, adipose tissue and endometrium: a comparative study. Tsitologiia. 2013; 55: 101–110. PMID: 23718072
22. Álvarez V, Blázquez R, Sánchez-Margallo FM, DelaRosa O, Jorge I, Tapia A, et al. Comparative study of isolated human mesenchymal stem cell derived exosomes for clinical use. Acta bioquim clin latinoam. 2015; 49: 311–320.
23. Théry C, Amigorena S, Raposo G, Clayton A. Isolation and characterization of exosomes from cell culture supernatants and biological fluids. Curr Protoc Cell Biol. 2006;3.22: 1–29. https://doi.org/10.1002/0471143030.cb0322s30 PMID: 18228490
24. Alpha Scientist in Reproductive Medicine and ESHRE Special Interest Group of Embryology. The Istanbul consensus workshop on embryo assessment: proceedings of an expert meeting. Hum Reprod. 2011; 26: 1270–1283. https://doi.org/10.1093/humrep/der037 PMID: 21502182
25. Elsheikh E, Sylvén C, Ericzon B- G, Palmblad J, Mints M. Cyclic variability of stromal cell-derived factor-1 and endothelial progenitor cells during the menstrual cycle. Int J Mol Med. 2011; 27: 221–226. https://doi.org/10.3892/ijmm.2010.570 PMID: 21132258

26. Wang H, Jin P, Sabatino M, Ren J, Civini S, Bogin V, et al. Comparison of endometrial regenerative cells and bone marrow stromal cells. J Transl Med. 2012; 10: 207. https://doi.org/10.1186/1479-5876-10-207 PMID: 23038994

27. Mellisho EA, Velásquez AE, Nuñez MJ, Cabezas JG, Cueto JA, Fader C, et al. Identification and characteristics of extracellular vesicles from bovine blastocysts produced in vitro. PLoS ONE. 2017; 12: e0178306. https://doi.org/10.1371/journal.pone.0178306 PMID: 28542562

28. Qu P, Qing S, Liu R, Qin H, Wang W, Qiao F, et al. Effects of embryo-derived exosomes on the development of bovine cloned embryos. PLoS ONE. 2017; 12: e0174535. https://doi.org/10.1371/journal.pone.0174535 PMID: 28350875

29. Burns G, Brooks K, Wildung M, Navakanitworakul R, Christenson LK, Spencer TE. Extracellular Vesicles in Luminal Fluid of the Ovine Uterus. Ye X, editor. PLoS ONE. 2014; 9: e90913. https://doi.org/10.1371/journal.pone.0090913 PMID: 24614226

30. Nguyen HPT, Simpson RJ, Salamonsen LA, Greening DW. Extracellular Vesicles in the Intrauterine Environment: Challenges and Potential Functions. Biology of Reproduction. 2016; 95: 109–109. https://doi.org/10.1095/biolreprod.116.143503 PMID: 27655784

31. Altmäe S, Koel M, Võsa U, Adler P, Suhorutšenko M, Laisk-Podar T, et al. Meta-signature of human endometrial receptivity: a meta-analysis and validation study of transcriptomic biomarkers. Sci Rep. 2017; 7: 10077. https://doi.org/10.1038/s41598-017-10098-3 PMID: 28855728

32. Lopera-Vasquez R, Hamdi M, Maillo V, Gutierrez-Adan A, Bermejo-Alvarez P, Ramírez MÁ, et al. Effect of bovine oviductal extracellular vesicles on embryo development and quality *in vitro*. Reproduction. 2017; 153: 461–470. https://doi.org/10.1530/REP-16-0384 PMID: 28104825

33. Lopera-Vásquez R, Hamdi M, Fernandez-Fuertes B, Maillo V, Beltrán-Breña P, Calle A, et al. Extracellular Vesicles from BOEC in In Vitro Embryo Development and Quality. Sturmey R, editor. PLOS ONE. 2016; 11: e0148083. https://doi.org/10.1371/journal.pone.0148083 PMID: 26845570

34. Gu Y, Li Y, Huang X, Zheng J, Yang J, Diao H, et al. Reproductive Effects of Two Neonicotinoid Insecticides on Mouse Sperm Function and Early Embryonic Development In Vitro. Wang H, editor. PLoS ONE. 2013; 8: e70112. https://doi.org/10.1371/journal.pone.0070112 PMID: 23922925

35. Xu J, Cheung T., Chan ST, Ho P., Yeung WS. Human oviductal cells reduce the incidence of apoptosis in cocultured mouse embryos. Fertility and Sterility. 2000; 74: 1215–1219. https://doi.org/10.1016/S0015-0282(00)01618-6 PMID: 11119753

36. Daughtry BL, Chavez SL. Chromosomal instability in mammalian pre-implantation embryos: potential causes, detection methods, and clinical consequences. Cell Tissue Res. 2016; 363: 201–225. https://doi.org/10.1007/s00441-015-2305-6 PMID: 26590822

37. Montag M, Koll B, Holmes P, van der Ven null. Significance of the number of embryonic cells and the state of the zona pellucida for hatching of mouse blastocysts in vitro versus in vivo. Biol Reprod. 2000; 62: 1738–1744. PMID: 10819778

38. Gordon JW, Dapunt U. A new mouse model for embryos with a hatching deficiency and its use to elucidate the mechanism of blastocyst hatching. Fertil Steril. 1993; 59: 1296–1301. PMID: 8495780

39. Nasr-Esfahani MH, Johnson MH. How does transferrin overcome the in vitro block to development of the mouse preimplantation embryo? J Reprod Fertil. 1992; 96: 41–48. PMID: 1432973

40. Duband JL, Thiery JP. Spatio-temporal distribution of the adherens junction-associated molecules vinculin and talin in the early avian embryo. Cell Differ Dev. 1990; 30: 55–76. PMID: 2112421

41. Tsuiki A, Preyer J, Hung TT. Effects of fibronectin and its peptide fragment on preimplantation mouse embryo. Am J Obstet Gynecol. 1989; 160: 724–728. PMID: 2522738

42. Fresco VM, Kern CB, Mohammadi M, Twal WO. Fibulin-1 Binds to Fibroblast Growth Factor 8 with High Affinity: EFFECTS ON EMBRYO SURVIVAL. J Biol Chem. 2016; 291: 18730–18739. https://doi.org/10.1074/jbc.M115.702761 PMID: 27402846

43. Lahav-Baratz S, Shiloh H, Koifman M, Kraiem Z, Wiener-Megnazi Z, Ishai D, et al. Early embryo-endometrial signaling modulates the regulation of matrix metalloproteinase-3. Fertil Steril. 2004; 82 Suppl 3: 1029–1035. https://doi.org/10.1016/j.fertnstert.2004.06.026 PMID: 15474069

44. Reponen P, Leivo I, Sahlberg C, Apte SS, Olsen BR, Thesleff I, et al. 92-kDa type IV collagenase and TIMP-3, but not 72-kDa type IV collagenase or TIMP-1 or TIMP-2, are highly expressed during mouse embryo implantation. Dev Dyn. 1995; 202: 388–396. https://doi.org/10.1002/aja.1002020408 PMID: 7626795

45. Li R, Yu C, Gao R, Liu X, Lu J, Zhao L, et al. Effects of DEHP on endometrial receptivity and embryo implantation in pregnant mice. J Hazard Mater. 2012; 241–242: 231–240. https://doi.org/10.1016/j.jhazmat.2012.09.038 PMID: 23046697

46. Gabrielsen A, Fedder J, Agerholm I. Parameters predicting the implantation rate of thawed IVF/ICSI embryos: a retrospective study. Reprod Biomed Online. 2006; 12: 70–76. PMID: 16454938

47. Zolti M, Ben-Rafael Z, Meirom R, Shemesh M, Bider D, Mashiach S, et al. Cytokine involvement in oocytes and early embryos. Fertility and Sterility. 1991; 56: 265–272. https://doi.org/10.1016/S0015-0282(16)54483-5 PMID: 2070856

48. Tríbulo P, Siqueira LGB, Oliveira LJ, Scheffler T, Hansen PJ. Identification of potential embryokines in the bovine reproductive tract. J Dairy Sci. 2018; 101: 690–704. https://doi.org/10.3168/jds.2017-13221 PMID: 29128220

49. Robertson SA, Chin PY, Glynn DJ, Thompson JG. Peri-conceptual cytokines—setting the trajectory for embryo implantation, pregnancy and beyond. Am J Reprod Immunol. 2011; 66 Suppl 1: 2–10. https://doi.org/10.1111/j.1600-0897.2011.01039.x PMID: 21726333

50. Zhou W, Chu D, Sha W, Fu L, Li Y. Effects of granulocyte-macrophage colony-stimulating factor supplementation in culture medium on embryo quality and pregnancy outcome of women aged over 35 years. J Assist Reprod Genet. 2016; 33: 39–47. https://doi.org/10.1007/s10815-015-0627-7 PMID: 26660059

51. Ziebe S, Loft A, Povlsen BB, Erb K, Agerholm I, Aasted M, et al. A randomized clinical trial to evaluate the effect of granulocyte-macrophage colony-stimulating factor (GM-CSF) in embryo culture medium for in vitro fertilization. Fertil Steril. 2013; 99: 1600–1609. https://doi.org/10.1016/j.fertnstert.2012.12.043 PMID: 23380186

52. Barañao RI, Piazza A, Rumi LS, Polak de Fried E. Determination of IL-1 and IL-6 levels in human embryo culture-conditioned media. Am J Reprod Immunol. 1997; 37: 191–194. PMID: 9083616

53. Goyal P, Brünnert D, Ehrhardt J, Bredow M, Piccenini S, Zygmunt M. Cytokine IL-6 secretion by trophoblasts regulated via sphingosine-1-phosphate receptor 2 involving Rho/Rho-kinase and Rac1 signaling pathways. Mol Hum Reprod. 2013; 19: 528–538. https://doi.org/10.1093/molehr/gat023 PMID: 23538947

54. Mehta BN, Chimote NM, Chimote MN, Chimote NN, Nath NM. Follicular fluid insulin like growth factor-1 (FF IGF-1) is a biochemical marker of embryo quality and implantation rates in in vitro fertilization cycles. J Hum Reprod Sci. 2013; 6: 140–146. https://doi.org/10.4103/0974-1208.117171 PMID: 24082656

55. Han J, Li L, Hu J, Yu L, Zheng Y, Guo J, et al. Epidermal growth factor stimulates human trophoblast cell migration through Rho A and Rho C activation. Endocrinology. 2010; 151: 1732–1742. https://doi.org/10.1210/en.2009-0845 PMID: 20150581

56. Lim HJ, Dey SK. HB-EGF: a unique mediator of embryo-uterine interactions during implantation. Exp Cell Res. 2009; 315: 619–626. https://doi.org/10.1016/j.yexcr.2008.07.025 PMID: 18708050

57. Artini PG, Valentino V, Monteleone P, Simi G, Parisen-Toldin MR, Cristello F, et al. Vascular endothelial growth factor level changes during human embryo development in culture medium. Gynecol Endocrinol. 2008; 24: 184–187. https://doi.org/10.1080/09513590801893117 PMID: 18382903

58. Cerkiene Z, Eidukaite A, Usoniene A. Immune factors in human embryo culture and their significance. Medicina (Kaunas). 2010; 46: 233–239.

59. Flamme I, von Reutern M, Drexler HC, Syed-Ali S, Risau W. Overexpression of vascular endothelial growth factor in the avian embryo induces hypervascularization and increased vascular permeability without alterations of embryonic pattern formation. Dev Biol. 1995; 171: 399–414. https://doi.org/10.1006/dbio.1995.1291 PMID: 7556923

60. Achen MG, Gad JM, Stacker SA, Wilks AF. Placenta growth factor and vascular endothelial growth factor are co-expressed during early embryonic development. Growth Factors. 1997; 15: 69–80. PMID: 9401819

61. Komaki M, Numata Y, Morioka C, Honda I, Tooi M, Yokoyama N, et al. Exosomes of human placenta-derived mesenchymal stem cells stimulate angiogenesis. Stem Cell Res Ther. 2017; 8: 219. https://doi.org/10.1186/s13287-017-0660-9 PMID: 28974256

62. Hu Y, Rao S-S, Wang Z-X, Cao J, Tan Y-J, Luo J, et al. Exosomes from human umbilical cord blood accelerate cutaneous wound healing through miR-21-3p-mediated promotion of angiogenesis and fibroblast function. Theranostics. 2018; 8: 169–184. https://doi.org/10.7150/thno.21234 PMID: 29290800

63. Lombardo G, Dentelli P, Togliatto G, Rosso A, Gili M, Gallo S, et al. Activated Stat5 trafficking Via Endothelial Cell-derived Extracellular Vesicles Controls IL-3 Pro-angiogenic Paracrine Action. Sci Rep. 2016; 6: 25689. https://doi.org/10.1038/srep25689 PMID: 27157262

64. Liu X, Li Q, Niu X, Hu B, Chen S, Song W, et al. Exosomes Secreted from Human-Induced Pluripotent Stem Cell-Derived Mesenchymal Stem Cells Prevent Osteonecrosis of the Femoral Head by Promoting Angiogenesis. Int J Biol Sci. 2017; 13: 232–244. https://doi.org/10.7150/ijbs.16951 PMID: 28255275

65. Shabbir A, Cox A, Rodriguez-Menocal L, Salgado M, Van Badiavas E. Mesenchymal Stem Cell Exosomes Induce Proliferation and Migration of Normal and Chronic Wound Fibroblasts, and Enhance Angiogenesis In Vitro. Stem Cells Dev. 2015; 24: 1635–1647. https://doi.org/10.1089/scd.2014.0316 PMID: 25867197

66. Zhang J, Wang L, Cai L, Cao Y, Duan E. The expression and function of VEGF at embryo implantation "window" in the mouse. ChinSciBull. 2001; 46: 409–411. https://doi.org/10.1007/BF03183277

67. Rappolee DA, Brenner CA, Schultz R, Mark D, Werb Z. Developmental expression of PDGF, TGF-alpha, and TGF-beta genes in preimplantation mouse embryos. Science. 1988; 241: 1823–1825. PMID: 3175624

68. Artus J, Kang M, Cohen-Tannoudji M, Hadjantonakis A-K. PDGF signaling is required for primitive endoderm cell survival in the inner cell mass of the mouse blastocyst. Stem Cells. 2013; 31: 1932–1941. https://doi.org/10.1002/stem.1442 PMID: 23733391

69. Betsholtz C, Karlsson L, Lindahl P. Developmental roles of platelet-derived growth factors. Bioessays. 2001; 23: 494–507. https://doi.org/10.1002/bies.1069 PMID: 11385629

70. Hoch RV, Soriano P. Roles of PDGF in animal development. Development. 2003; 130: 4769–4784. https://doi.org/10.1242/dev.00721 PMID: 12952899

Received: 15 May 2018 | Revised: 9 August 2018 | Accepted: 10 August 2018
DOI: 10.1111/rda.13314

Check for updates

SHORT COMMUNICATION

WILEY Reproduction in Domestic Animals

# Extracellular vesicles derived from endometrial human mesenchymal stem cells improve IVF outcome in an aged murine model

Federica Marinaro[1] | Eva Pericuesta[2] | Francisco Miguel Sánchez-Margallo[1,3] | Javier G. Casado[1,3] | Verónica Álvarez[1] | Elvira Matilla[1] | Nuria Hernández[1] | Rebeca Blázquez[1,3] | Lauro González-Fernández[4] | Alfonso Gutiérrez-Adán[2] | Beatriz Macías-García[1]

[1]Jesús Usón Minimally Invasive Surgery Centre (CCMIJU), Cáceres, Spain

[2]Department of Animal Reproduction, INIA, Madrid, Spain

[3]CIBER de Enfermedades Cardiovasculares, Madrid, Spain

[4]SINTREP Group, University of Extremadura, Cáceres, Spain

**Correspondence**
Javier G. Casado, Jesús Usón Minimally Invasive Surgery Centre (CCMIJU), Cáceres, SPAIN.
Email: jgarcia@ccmijesususon.com

**Funding information**
Instituto de Salud Carlos III, CIBER-CV, Grant/Award Number: CB16/11/00494; Consejería de Economía e Infraestructuras, Junta de Extremadura, Grant/Award Number: IB16168 and IB16159; Instituto de Salud Carlos III, Miguel Servet Grants, Grant/Award Number: CP17/00021; Spanish Ministry of Economy, Industry and Competitiveness, Grant/Award Number: AGL2015-73249-JIN, AGL2015-66145 and AGL2017-84681-R

**Contents**

Advanced age reduces the success of in vitro fertilization (IVF) being this effect partly mediated by an overproduction of reactive oxygen species (ROS) that trigger apoptosis. It has been demonstrated that extracellular vesicles derived from endometrial mesenchymal stem cells (EV-endMSCs) exert an antioxidant effect and can be used as IVF coadjutants. In this work, endMSCs were isolated from human menstrual blood ($n$ = 4) and characterized according to multipotentiality and surface marker expression prior EV-endMSCs isolation. Oocytes were obtained from 21 B6D2 mice (24 weeks) and coincubated with sperm from young males (8–12 weeks). Presumptive zygotes were incubated in the presence of 0, 10, 20, 40 or 80 μg/ml of EV-endMSCs in KSOM medium. Blastocyst yield was evaluated, and 25 blastocysts per group were used for qPCR. Blastocyst rate was 29.4% in control; 45.2% for 10 μg/ml, 62.9% for 20 μg/ml, 55.5% for 40 μg/ml and 53.8% in the 80 μg/ml ($n$ = 124–130 oocytes) being all the increases significantly different when compared against control ($p < 0.05$). The 20–80 μg/ml treatments decreased the expression of glutathione peroxidase (*Gpx1*), and the 10–40 μg/ml treatments reduced the expression of superoxide dismutase (*Sod1*; $p < 0.05$) compared to control; *Bax* mRNA expression did not vary. Our results suggest that the increased developmental competence of the embryos could be partly mediated by the EV-endMSCs' ROS scavenger activity.

KEYWORDS
animal disease model, extracellular vesicles, IVF, mesenchymal stem cells, qPCR, ROS

## 1 | INTRODUCTION

Advanced woman age is a poor prognostic factor for fertility in humans as it decreases egg's competence and increases the risk of miscarriage (Rasool & Shah, 2018). This declined fertility has been linked to impaired reactive oxygen species (ROS) metabolism, mitochondrial dysfunction and apoptosis induction in the aged oocyte (Igarashi et al., 2016; Miao, Kikuchi, Sun, & Schatten, 2009; Mihalas, Redgrove, McLaughlin, & Nixon, 2017). Continuous embryo culture in vitro is known to decrease the embryo developmental competence due to ROS build-up, being this more evident in aged oocytes. Hence, the optimization of embryo culture using appropriate animal models could

help to enhance the efficiency of in vitro fertilization (IVF) cycles (Highet et al., 2017). Recently, endometrial mesenchymal stem/stromal cells (endMSCs) and their extracellular vesicles (EV-endMSCs) have been isolated from human menstruation (Khoury, Alcayaga-Miranda, Illanes, & Figueroa, 2014) and have been shown to exhibit ROS scavenger activity (Alcayaga-Miranda et al., 2016). Thus, the aim of the present work was to evaluate whether EV-endMSCs could be used as an adjuvant to improve IVF outcomes in aged mice. Furthermore, the expression levels of *Sod1* and *Gpx1* in murine embryos were evaluated as both of them are known to be natural first-line defences against ROS; in addition, potential changes in *Bax* expression were also evaluated to assess whether EV-endMSCs could potentially ameliorate apoptosis during embryo culture.

## 2 | MATERIALS AND METHODS

### 2.1 | Isolation, in vitro expansion, phenotypical characterization and multipotentiality of endometrial mesenchymal stromal/stem cells

Endometrial mesenchymal stromal/stem cells (endMSCs) were isolated from menstrual blood after a written informed consent; all procedures were approved by the JUMISC Ethics Committee (Ref. 009/17). The endMSCs and EV-endMSCs were isolated and characterized as previously described (see Blázquez et al., 2018 for a complete protocol). In brief, menstrual blood was centrifuged at 450 × *g* for 10 min. Pellets were resuspended in DMEM containing 10% foetal bovine serum (FBS), 1% penicillin/streptomycin and 1% glutamine. Cells were seeded onto tissue culture flasks, expanded at 37°C in 95% air and 5% $CO_2$ atmosphere to 80% confluency and detached using PBS containing 0.25% trypsin (v/v); cells were seeded again, and culture medium was changed every 3 days. To isolate the EV-endMSCs, cell culture medium was replaced by DMEM containing 1% insulin–transferrin–selenium. The endMSCs supernatants were collected every 3–4 days. These supernatants were firstly centrifuged and then filtered using a sterile cellulose acetate filters (0.45 μm followed by a 0.2 μm pore size, Corning, NY, USA). Filtered supernatants were then concentrated using 3 kDa MWCO Amicon® Ultra Devices (Merck Millipore, MA, USA) centrifuged at 4,000 × *g* for 1 hr at 4°C.

### 2.2 | Superovulation protocol

B6D2F1 mice superovulation was performed by intraperitoneal injection of 10 IU of equine chorionic gonadotropin and 10 IU of human chorionic gonadotropin (hCG) 49 hr apart (Blázquez et al., 2018).

### 2.3 | In vitro fertilization

Twenty-four-week-old female mice ($n = 21$) were euthanized 12 hr after hCG administration. Cumulus–oocyte complexes were recovered and placed in 500 μl of pre-equilibrated human tubal fluid (HTF; Merck Millipore, Madrid, Spain) layered with mineral oil. Two B6D2F1/J males aged 8–12 weeks were euthanized ($n = 16$) for each IVF session; epididymal sperm was extracted and capacitated as previously described (Blázquez et al., 2018). The oocytes were inseminated with $2 \times 10^6$ sperm/ml (pooled from both males). After 6 hr, presumptive zygotes were rinsed in KSOM medium (Merck Millipore, Madrid, Spain) and transferred to 100 μL droplets of KSOM added with 0, 10, 20, 40 or 80 μg/ml of EV-endMSCs using previously validated EV-endMSCs dosages in murine embryos (Blázquez et al., 2018). Follow-up of the embryos was performed for 4 days. Eight different IVF sessions in eight different days were run and 2–3 females per day used.

### 2.4 | RNA isolation and reverse transcription

Six independent samples of blastocysts from six different IVF sessions ($n = 25$ blastocysts per treatment, 125 embryos in total) cultured with and without EV-endMSCs (0, 10, 20, 40 and 80 μg/ml) were used. Three independent groups of blastocysts per experimental condition were pooled and processed for poly(A) RNA extraction using the Dynabeads mRNA Direct Extraction Kit (Dynal Biotech, Oslo, Norway), following the manufacturer's instructions (Bermejo-Álvarez, Rizos, Rath, Lonergan, & Gutierrez-Adan, 2008). The reverse transcription reaction was performed as recommended by the manufacturer (Epicentre Technologies Corp, Madison, WI, USA).

### 2.5 | Gene expression analysis

The mRNA expression levels of the selected genes were determined by real-time quantitative polymerase chain reaction (qPCR) using specific primers (Table 1). All qPCRs were performed, according to the manufacturer's instructions, using the GoTaq qPCR Master Mix (Promega, Madrid, Spain) coupled to SYBR Green in a Rotor-Gene 6000 Real-Time Cycler (Corbett Research, Sydney, Australia). For each experimental group, duplicates of three different cDNA samples were used for all genes of interest. Melt curve analyses were performed.

Relative expression levels were quantified by the comparative cycle threshold ($\Delta\Delta C_T$) method (Livak & Schmittgen, 2001; Schmittgen & Livak, 2008) normalizing the values with the reference gene *H2AFZ*.

### 2.6 | Statistical analysis

For qPCR analysis, data were tested for normality using a Shapiro–Wilk test and compared by a one-way ANOVA followed by multiple pairwise comparisons using the Tukey test; values are expressed as mean ± standard deviation (*SD*). Blastocyst rates were compared by chi-square test with the Yates correction for continuity. The Fisher's exact test was used when a value of <5 was expected in any treatment. Statistical analyses were performed using Sigma Plot software version 12.3 for Windows (Systat Software, IL, USA) or with SPSS 21 software (SPSS, IL, USA); $p < 0.05$ was considered as statistically significant.

**TABLE 1** List of primers used in this study

| Entrez gene symbol | Gene name | Accession no. | Forward primer (5′–3′) | Reverse primer (5′–3′) | Product length |
|---|---|---|---|---|---|
| *H2afz* | H2A histone family, member Z | NM_001316995.1 | AGGACGACTAGCCATGGACGTGTG | CCACCACCAGCAATTGTAGCCTTG | 209 |
| *Gpx1* | Glutathione peroxidase 1 | NM_001329527.1 | GCAACCAGTTTGGGCATCA | CTCGCACTTTTCGAAGAGCATA | 116 |
| *Bax* | BCL2-associated X protein | NM_007527.3 | AAGCTGAGCGAGTGTCTCCGGCG | GCCACAAAGATGGTCACTGTCTGCC | 361 |
| *Sod1* | Superoxide Dismutase 1 | NM_174615 | GTGCAAGGCACCATCCACTTCG | CACCATCGTGCGGCCAATGATG | 309 |

## 3 | RESULTS

### 3.1 | Phenotypic profile of endMSCs and EV-endMSCs characterization

Coinciding with our previous report, endMSCs were negative for CD31, CD34, CD45 and HLA-DR and positive for the stemness markers CD29, CD44, CD49d, CD49f, CD56, CD73, CD90 and CD105. Adipogenic, chondrogenic and osteogenic differentiation was confirmed by microscopic analysis and stain quantification (Blázquez et al., 2018). The protein concentration of the enriched EV-endMSCs was determined by the Bradford assay and ranged between 350 and 750 μg/ml. The mean size and standard deviation were 153.5 ± 63.05 nm. Finally, the EV-endMSCs phenotypical characterization by flow cytometry demonstrated a positive expression of the CD9 and CD63 exosome-related proteins.

### 3.2 | Development to the blastocyst stage

The expanded blastocyst rate increased when EV-endMSCs were added to the embryo culture medium at any of the dosages tested (Table 2; $p < 0.05$).

### 3.3 | Differential expression of candidate genes

*Gpx1* expression was downregulated in the 20–80 μg/ml EV-endMSCs dosages while *Sod1* expression decreased in the 10–40 μg/ml dosages when compared against control ($p < 0.05$); the expression of *Bax* did not vary ($p > 0.05$; Figure 1).

## 4 | DISCUSSION AND CONCLUSION

Our results show that EV-endMSCs increase the developmental competence of IVF-derived embryos from aged females being the maximum effect observed for the 20 μg/ml dose. Hence, EV-endMSCs seem to partially alleviate oocyte ageing as also observed when embryo culture medium is supplemented with caffeine or nitric oxide (Miao et al., 2009).

**TABLE 2** Blastocyst rates obtained after embryo culture using varying doses of EV-endMSCs

| | Oocytes | Blastocyst rate (Day 4) |
|---|---|---|
| Control | 126 | 37 (29.4)[a] |
| 10 μg/ml | 124 | 56 (45.2)[b] |
| 20 μg/ml | 124 | 78 (62.9)[b] |
| 40 μg/ml | 128 | 71 (55.5)[b] |
| 80 μg/ml | 130 | 70 (53.8)[b] |

Embryo development to the blastocyst stage was recorded in the different treatments used. The values are presented as total number and (percentage); values bearing different letters in the same column differ statistically from the control ($p < 0.05$).

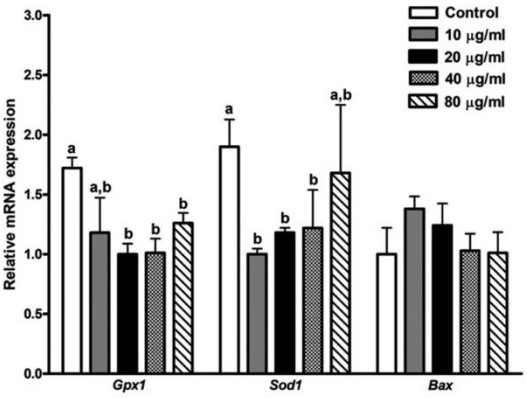


**FIGURE 1** Relative RNA abundance of candidate genes. Murine blastocysts were used for RNA quantification ($n = 25$ embryos/treatment) of candidate genes related to apoptosis and oxidative stress. Bars represent mean and *SD*; values bearing different letters differ statistically from control ($P < 0.05$)

Then, we aimed to assess whether the effect of EV-endMSCs on the embryonic developmental competence was mediated by increased ROS scavenger defences or inhibition of the intrinsic apoptotic pathway (Guérin, El Mouatassim, & Ménézo, 2001). Our results suggest that

EV-endMSCs exert an exogenous ROS scavenger activity during embryo culture that diminishes the need of the embryo to produce endogenous glutathione peroxidase 1 and superoxide dismutase 1 in a dose-dependent manner. This hypothesis is also supported by the work performed by Maitre, Jornot, and Junod (1993) who proposed that intracellular $O_2$ metabolites themselves are the signals that modify the antioxidant enzymes gene expression. Coinciding with our findings, EV-endMSCs have also been shown to diminish angiogenesis in prostate tumour by means of their ROS scavenger activity (Alcayaga-Miranda et al., 2016), demonstrating again the therapeutic potential of EV-endMSCs. This is the first report where EV-endMSCs have been used to improve IVF outcome in an aged model. EV-endMSCs enhance the developmental competence of murine IVF-derived zygotes, and this effect seems to be mediated by their ROS scavenger activity. Other sources of EV like the ones released from bovine oviductal explants have been demonstrated to enhance embryo quality (Lopera-Vasquez et al., 2017), and thus, EV-endMSCs should be also considered as candidates to enrich embryo culture media in veterinary IVF settings. More research is needed to fully elucidate the optimal dosages and the mechanisms underlying the observed effect.

## ACKNOWLEDGEMENTS

This work was supported in part by CIBER-CV (CB16/11/00494). Two projects were from Junta de Extremadura (IB16168 and IB16159 cofinanced by FEDER/FSE). One grant "Miguel Servet I" was from Instituto de Salud Carlos III to JGC (CP17/00021 cofinanced by FSE. In vitro studies were performed at the ICTS Nanbiosis (Units 14, 22 and 23). This work was partially funded by AGL2015-73249-JIN, AGL2015-66145 and AGL2017-84681-R (AEI/FEDER/UE) from the Spanish Ministry of Economy, Industry and Competitiveness. Special Thanks to MAFRESA for their support to Jesús Usón Minimally Invasive Surgery Centre. The funders had no role in study design, data collection and analysis, decision to publish or preparation of the manuscript.

## CONFLICT OF INTEREST

The authors declare no conflict of interests.

## AUTHOR CONTRIBUTIONS

Javier García Casado, Beatriz Macías-García and Francisco Miguel Sánchez-Margallo conceived and designed the experiments and obtained the funding. Verónica Álvarez, Rebeca Blázquez, Elvira Matilla, Nuria Hernández, Federica Marinaro, Lauro González-Fernández, Eva Pericuesta, Alfonso Gutiérrez-Adán and Beatriz Macías-García performed the experiments and analysed the data. All the authors wrote the manuscript and approved the final version.

## REFERENCES

Alcayaga-Miranda, F., González, P. L., Lopez-Verrilli, A., Varas-Godoy, M., Aguila-Díaz, C., Contreras, L., & Khoury, M. (2016). Prostate tumor-induced angiogenesis is blocked by exosomes derived from menstrual stem cells through the inhibition of reactive oxygen species. *Oncotarget*, *7*, 44462–44477.

Bermejo-Álvarez, P., Rizos, D., Rath, D., Lonergan, P., & Gutierrez-Adan, A. (2008). Epigenetic differences between male and female bovine blastocysts produced in vitro. *Physiological Genomics*, *32*, 264–272. https://doi.org/10.1152/physiolgenomics.00234.2007

Blázquez, R., Sánchez-Margallo, F. M., Álvarez, V., Matilla, E., Hernández, N., Marinaro, F., … Macías-García, B. (2018). Murine embryos exposed to human endometrial MSCs-derived extracellular vesicles exhibit higher VEGF/PDGF AA release, increased blastomere count and hatching rates. *PLoS One*, *13*, e0196080. https://doi.org/10.1371/journal.pone.0196080

Guérin, P., El Mouatassim, S., & Ménézo, Y. (2001). Oxidative stress and protection against reactive oxygen species in the pre-implantation embryo and its surroundings. *Human Reproduction Update*, *7*, 175–189. https://doi.org/10.1093/humupd/7.2.175

Highet, A. R., Bianco-Miotto, T., Pringle, K. G., Peura, A., Bent, S., Zhang, J., … Roberts, C. T. (2017). A novel embryo culture media supplement that improves pregnancy rates in mice. *Reproduction*, *153*, 327–340. https://doi.org/10.1530/REP-16-0517

Igarashi, H., Takahashi, T., Abe, H., Nakano, H., Nakajima, O., & Nagase, S. (2016). Poor embryo development in post-ovulatory in vivo -aged mouse oocytes is associated with mitochondrial dysfunction, but mitochondrial transfer from somatic cells is not sufficient for rejuvenation. *Human Reproduction*, *31*, 2331–2338. https://doi.org/10.1093/humrep/dew203

Khoury, M., Alcayaga-Miranda, F., Illanes, S. E., & Figueroa, F. E. (2014). The promising potential of menstrual stem cells for antenatal diagnosis and cell therapy. *Frontiers in Immunology*, *5*, 205.

Livak, K. J., & Schmittgen, T. D. (2001). Analysis of relative gene expression data using real-time quantitative PCR and the 2(-Delta Delta C(T)) Method. *Methods*, *25*, 402–408. https://doi.org/10.1006/meth.2001.1262

Lopera-Vasquez, R., Hamdi, M., Maillo, V., Gutierrez-Adan, A., Bermejo-Alvarez, P., Ramírez, M. Á., … Rizos, D. (2017). Effect of bovine oviductal extracellular vesicles on embryo development and quality in vitro. *Reproduction*, *153*, 461–470. https://doi.org/10.1530/REP-16-0384

Maitre, B., Jornot, L., & Junod, A. F. (1993). Effects of inhibition of catalase and superoxide dismutase activity on antioxidant enzyme mRNA levels. *American Journal of Physiology. Lung Cellular and Molecular Physiology*, *265*, L636–L643. https://doi.org/10.1152/ajplung.1993.265.6.L636

Miao, Y.-L., Kikuchi, K., Sun, Q.-Y., & Schatten, H. (2009). Oocyte aging: cellular and molecular changes, developmental potential and reversal possibility. *Human Reproduction Update*, *15*, 573–585. https://doi.org/10.1093/humupd/dmp014

Mihalas, B. P., Redgrove, K. A., McLaughlin, E. A., & Nixon, B. (2017). Molecular mechanisms responsible for increased vulnerability of the ageing oocyte to oxidative damage. *Oxidative Medicine and Cellular Longevity*, *2017*, 1–22. https://doi.org/10.1155/2017/4015874

Rasool, S., & Shah, D. (2018). The futile case of the aging ovary: is it mission impossible? A focused review. *Climacteric*, *21*, 22–28. https://doi.org/10.1080/13697137.2017.1410784

Schmittgen, T. D., & Livak, K. J. (2008). Analyzing real-time PCR data by the comparative C(T) method. *Nature Protocols*, *3*, 1101–1108. https://doi.org/10.1038/nprot.2008.73

**How to cite this article:** Marinaro F, Pericuesta E, Sánchez-Margallo FM, et al. Extracellular vesicles derived from endometrial human mesenchymal stem cells improve IVF outcome in an aged murine model. *Reprod Dom Anim*. 2018;53(Suppl. 2);46–49. https://doi.org/10.1111/rda.13314

*Biology of Reproduction*, 2019, 100(5), 1180–1192
doi:10.1093/biolre/ioy263
Research Article
Advance Access Publication Date: 28 December 2018

Research Article

# Extracellular vesicles derived from endometrial human mesenchymal stem cells enhance embryo yield and quality in an aged murine model†

**Federica Marinaro[1,‡], Beatriz Macías-García[2,*,‡], Francisco Miguel Sánchez-Margallo[1,3], Rebeca Blázquez[1,3], Verónica Álvarez[1], Elvira Matilla[2], Nuria Hernández[2], María Gómez-Serrano[3,4], Inmaculada Jorge[3,4], Jesús Vázquez[3,4], Lauro González-Fernández[5], Eva Pericuesta[6], Alfonso Gutiérrez-Adán[6] and Javier G. Casado[1,3]**

[1]Stem Cell Therapy Unit, Jesús Usón Minimally Invasive Surgery Centre (JUMISC), Cáceres, Spain; [2]Assisted Reproduction Unit, Jesús Usón Minimally Invasive Surgery Centre, Cáceres, Spain; [3]CIBER de Enfermedades Cardiovasculares (CIBERCV), Madrid, Spain; [4]Centro Nacional de Investigaciones Cardiovasculares (CNIC), Madrid, Spain; [5]Research Group of Intracellular Signaling and Technology of Reproduction (SINTREP), Institute of Biotechnology in Agriculture and Livestock (INBIO G+C), University of Extremadura, Cáceres, Spain and [6]INIA, Department of Animal Reproduction, Madrid, Spain

*__Correspondence__: Assisted Reproduction Unit, JUMISC, N-521, Km 41.8, 10071, Cáceres. Tel: +34 927181032; E-mail: bea_macias@hotmail.com

†__Grant Support:__ This work was supported by one grant "Miguel Servet I" from Instituto de Salud Carlos III to JGC (CD17/00021 co-financed by FSE); one grant MAFRESA S.L. to FM.
__Conference presentations:__ Federica Marinaro, Eva Pericuesta, Francisco Miguel Sánchez-Margallo, Javier García Casado, Verónica Álvarez, Elvira Matilla, Nuria Hernández, Rebeca Blázquez, Lauro González-Fernández, Alfonso Gutiérrez-Adán, and Beatriz Macías-García. Extracellular vesicles derived from endometrial human mesenchymal stem cells improve IVF outcome in an aged murine model. Reproduction in Domestic Animals 53:46-49. DOI: 10.1111/rda.13314. 22nd Annual ESDAR Conference 2018 Córdoba (Spain) September 27th-29th, 2018. Student oral competition.
‡Federica Marinaro and Beatriz Macías-García equally contributed to the present work and should be considered as co-first authors.
Edited by Dr. Peter J. Hansen

Received 31 July 2018; Revised 22 October 2018; Accepted 26 December 2018

## Abstract

Advanced age is a risk factor undermining women's fertility. Hence, the optimization of assisted reproduction techniques is an interdisciplinary challenge that requires the improvement of in vitro culture systems. Here, we hypothesize that supplementation of embryo culture medium with extracellular vesicles from endometrial-derived mesenchymal stem cells (EV-endMSCs) may have a positive impact on the embryo competence of aged oocytes. In this work, 24 weeks old B6D2 female mice were used as egg donors and in vitro fertilization assays were performed using males from the same strain (8–12 weeks); the presumptive zygotes were incubated in the presence of 0, 10, 20, 40, or 80 $\mu$g/ml of EV-endMSCs. The results from the proteomic analysis of EV-endMSCs



© The Author(s) 2018. Published by Oxford University Press on behalf of Society for the Study of Reproduction. All rights reserved.
For permissions, please e-mail: journals.permissions@oup.com

Downloaded from https://academic.oup.com/biolreprod/article/100/5/1180/5266294 by guest on 20 April 2021

and the classification by Reactome pathways allowed us to identify proteins closely related with the fertilization process. Moreover, in our aged murine model, the supplementation of the embryo culture medium with EV-endMSCs improved the developmental competence of the embryos as well as the total blastomere count. Finally, gene expression analysis of murine blastocysts showed significant changes on core genes related to cellular response to oxidative stress, metabolism, placentation, and trophectoderm/inner cell mass formation. In summary, we demonstrate that EV-endMSCs increase the quality of the embryos, and according to proteomic and genomic analysis, presumably by modulating the expression of antioxidant enzymes and promoting pluripotent activity. Therefore, EV-endMSCs could be a valuable tool in human assisted reproduction improving the developmental competence of aged oocytes and increasing the odds of implantation and subsequent delivery.

### Summary Sentence

The supplementation of embryo culture medium with extracellular vesicles from endometrial-derived mesenchymal stem cells increases the quality of aged embryos.

**Key words:** embryo culture, stem cells, proteomics, gene expression, oxidative stress, aging.

## Introduction

Advanced woman age is one of the most detrimental prognostic factors for fertility in humans as it decreases egg's competence. Nowadays, social, educational, and financial pressures have delayed motherhood until the final thirties or forties, declining overall fertility and increasing the risk of miscarriage [1]. When motherhood needs to be delayed, egg freezing is the assisted reproductive technique of choice to preserve the oocyte´s quality, but this has to be planned in advance which is not the most common scenario [2]. In aged women (>40 years), the use of assisted reproductive techniques is recommended if conception does not occur after 6 months. However, even when these techniques improve fertilization rates, blastocyst development is compromised and live births considerably decreased compared to oocytes´ from younger donors [3]. This decline in fertility has been partly linked to an oxidative stress imbalance in the aged oocyte resulting in impaired reactive oxygen species (ROS) metabolism and decreased capacity for protein/DNA repair [4]. Nevertheless, optimization of embryo culture when aged oocytes are used is a challenge that could enhance embryo development and quality [5].

Nowadays, adult stem cells are under investigation to improve the fertilization rates in assisted reproduction. Placental derived mesenchymal stem cells (MSCs) are currently under evaluation in a clinical trial for improving implantation rates (Clinicaltrials.gov Identifier NCT01649752). Moreover, the therapeutic potential of autologous MSCs is evaluated in women suffering premature ovarian failure (Clinicaltrials.gov Identifier NCT02062931).

Special attention has been focused on the extracellular vesicles released by MSCs. They are known to mediate cell-to-cell communication by means of their specific cargo (RNAs, DNA, lipids, proteins, cytokines, and growth factors) [6, 7] and are secreted by different cell types including endometrial and oviductal cells [7–9]. Furthermore, these extracellular vesicles have been used as coadjuvants in assisted reproduction [10]. Their addition to bovine embryo culture medium has been found to enhance blastocyst quality [8, 11] and to improve the quality of homologous embryos through embryo-to-embryo communication when derived from porcine parthenotes and bovine embryos [12, 13].

Few years ago endometrial-derived Mesenchymal Stem Cells (endMSCs) and their extracellular vesicles (EV-endMSC) were isolated from menstrual blood [14] and they were found to alleviate human hepatic failure by diminishing active caspase 3 and apoptosis [15], to decrease prostate tumor-induced angiogenesis by modulating ROS production, diminishing vascular endothelial growth factor (VEGF) secretion and nuclear factor kappa B activity [16] and to exert cardioprotective effects through the microRNA miR-21 [17]. EV-endMSCs' importance in human reproduction has been demonstrated by the fact that they seem to be involved in the embryo-maternal interactions [6] and in endometrial receptivity [18].

In view of these reports, and according to previous results from our group which demonstrated that human EV-endMSCs in embryo culture medium increased cell proliferation and hatching rates in a murine model [10], we hypothesize that human EV-endMSCs may have a beneficial effect on the developmental competence of embryos derived from aged females mice.

In order to validate this hypothesis, embryo division kinematics follow-up, blastocyst quality as well as the expression of specific genes were evaluated in zygotes derived from old mice (24 weeks old) after addition of EV-endMSCs. Additionally, the proteomic profile of the EV-endMSCs used for supplementation of embryo culture medium was characterized and classified using Gene Ontology and Reactome Pathway Database.

## Materials and methods

### Isolation and in vitro expansion of endometrial mesenchymal stromal/stem cells

Endometrial Mesenchymal Stromal/Stem Cells were isolated from menstrual blood of four healthy women according to previously described protocols [10]. Samples were collected on day 2 or 3 of the menstrual cycle in a menstrual cup. Written informed consent was obtained from all donors under the auspices of the Minimally Invasive Surgery Centre Research Ethics Committee, which approved this study. Menstrual blood was diluted 1:2 in PBS and centrifuged at 450 x g for 10 min. Supernatants were discarded in order to remove cervical mucus debris and cells were re-suspended in Dulbecco's Modified Eagle's medium (DMEM) containing 10% fetal bovine serum (FBS), 1% penicillin/streptomycin, and 1% glutamine. Cells were seeded onto tissue culture flasks and expanded at 37°C in 95% air and 5% $CO_2$ atmosphere. Non-adherent cells were removed after 24 h. Adherent cells were cultured to 80% confluency and detached using PBS containing 0.25% trypsin (v/v). Cells were seeded again at a density of 5000 cells/cm$^2$. Culture medium was changed every 3 days.

Downloaded from https://academic.oup.com/biolreprod/article/100/5/1180/5266294 by guest on 20 April 2021

### Phenotypical characterization and multipotentiality of endMSCs

For the phenotypic analysis, $2 \times 10^5$ endMSCs were stained with human monoclonal antibodies (mAbs) against CD29, CD44, CD73, CD90, CD105, CD117, CD14, CD20, CD31, CD34, CD45, CD80, and HLA-DR using the appropriate concentrations of mAbs in the presence of PBS containing 2% FBS. The endMSCs and mAbs were incubated for 30 min at 4°C. Cells were then washed and re-suspended in PBS. Isotype-matched antibodies were used as negative controls. The flow cytometric analysis was performed on a FACScalibur cytometer (BD Biosciences, CA, USA) after acquisition of $10^5$ events. Viable cells were selected using forward and side scatter characteristics and fluorescence was analyzed using CellQuest software (BD Biosciences, CA, USA). The mean relative fluorescence intensity was calculated by dividing the mean fluorescent intensity (MFI) by the MFI of its negative control. The differentiation assays of endMSCs were performed for 21 days with differentiation specific media, which was replaced every 3 days. Oil Red O, Alcian Blue, and Alizarin Red S staining were performed to evidence adipogenic, chondrogenic and osteogenic differentiation, respectively. Cells were analyzed at passages 3–4.

### Isolation, purification and characterization of extracellular vesicles derived from endMSCs

Extracellular vesicles derived from endMSCs (EV-endMSCs) were obtained from endMSCs using a previously optimized protocol [10]. DMEM cell culture medium (product code: L0102, Biowest, Nuaillé, France) supplemented by 10% FBS was used for endMSCs expansion. When cells reached 80% of confluence, it was replaced by DMEM containing 1% insulin–transferrin–selenium (product code: 41400045, ThermoFisher Scientific, Waltham, MA, USA). End-MSCs at passages 4–5 were used for extracellular vesicles isolation. The endMSCs supernatants were collected every 3–4 days and centrifuged at 1000 x g for 10 min and 5000 x g for 20 min at 4°C. These supernatants were filtered using sterile cellulose acetate filters. Firstly, with a 0.45 $\mu$m pore size and secondly with a 0.2 $\mu$m pore size (Corning, NY, USA). Filtered supernatants were then concentrated using 3kDa MWCO Amicon® Ultra Devices (Merck-Millipore, MA, USA) centrifuged at 4000 x g for 1 h at 4°C. The concentrated supernatants were stored at −20°C for the subsequent proteomic analysis and co-incubation with the zygotes.

Prior to in vitro experiments, the protein content of microvesicles was quantified by a Bradford assay (BioRad Laboratories, CA, USA). The concentration and size of purified extracellular vesicles were quantified by nanoparticle tracking analysis (NanoSight Ltd, Amesbury, UK) and analyzed using the particle-tracking analysis software package version 2.2.

### Protein identification by high-resolution liquid chromatography coupled to mass spectrometry-based proteomic analyses

The characterization of EV-endMSCs from three different donors was performed by high-throughput proteomic analysis according to previously described protocols [19-23]. For proteomic analysis, protein extracts were incubated with trypsin using the Filter Aides Sample Preparation digestion kit (Expedeon), as previously described [24]. The resulting peptides were labeled using 8plex-iTRAQ reagents (Sciex) according to manufacturer's instructions and desalted on OASIS HLB extraction cartridges (Waters Corp.). Half of the tagged peptides were directly analyzed by LC-MS/MS in different acquisition runs, and the remaining peptides were separated into three fractions using the high pH reversed-phase peptide fractionation kit (Thermo Fisher Scientific). High-resolution LC-MS analysis of iTRAQ-labelled peptides was carried out on an Easy nLC 1000 nano-HPLC apparatus (Thermo Scientific) coupled to QExactive mass spectrometer (Thermo Fisher Scientific). Peptides were injected onto a C18 reversed phase nano-column (75 $\mu$m I.D. and 50 cm, Acclaim PepMap100, Thermo Scientific) in buffer A (0.1% formic acid (v/v)) and eluted with a 180 min lineal gradient of buffer B (90% acetonitrile, 0.1% formic acid (v/v)). MS runs consisted of enhanced FT-resolution spectra (140 000 resolution) in the 390–1 500 m/z range and separated 390–700, 650–900, and 850–1500 m/z ranges followed by data-dependent MS/MS spectra of the 15 most intense parent ions acquired along the chromatographic run. HCD fragmentation was performed at 30% of normalized collision energy. A total of 14 MS data sets, 8 from unfractionated material and 6 from the corresponding fractions, were registered with 42 h total acquisition time. For peptide identification the MS/MS spectra were searched with the SEQUEST HT algorithm implemented in Proteome Discoverer 2.1 (Thermo Scientific). The results were analyzed using the probability ratio method [25] and the false discovery rate (FDR) of peptide identification was calculated based on the search results against a decoy database using the refined method [23]. Peptide and scan counting was performed assuming as positive events those with a FDR equal or lower than 1%. Enrichment analysis was performed by using the DAVID functional annotation database [26, 27].

### Reagents

All the reagents were purchased from Sigma-Aldrich (Barcelona, Spain) unless otherwise stated.

### Animals and superovulation protocol

All the experimental procedures were reviewed and approved by the Ethical Committee of the Junta de Extremadura (CGA/mbr). B6D2F1 mice were housed under a 12 h light/12 h dark cycle, at a controlled temperature (19–23°C) with free access to food and water. Females were intraperitoneally (IP) injected with 8 IU of equine chorionic gonadotropin (eCG, Veterin Corion, Divasa Farmavic) followed 49 h later by 8 IU of IP human chorionic gonadotropin (hCG, Foligon, MSD) to trigger ovulation.

### In vitro fertilization

Twenty four weeks old female mice (n = 24) were euthanized 12 h after hCG administration by cervical dislocation, and cumulus-oocyte complexes were recovered from oviducts and placed in 500 $\mu$l of pre-equilibtrated Human Tubal fluid (HTF; Merck-Millipore, Madrid, Spain) covered with mineral oil. Two male B6D2F1/J mice aged 8–12 weeks were euthanized (n = 16) for each IVF day by cervical dislocation and were ventrally dissected to remove the cauda epididymis. Once located, the epididymis and attached vas deferens were sectioned and transferred to two different a Petri dishes containing 500 $\mu$l of pre-equilibrated HTF covered with mineral oil. Spermatozoa were obtained by gently pressing the cauda epididymis through the vas deferens and were allowed to capacitate for 45 min at 37°C in a 5% $CO_2$/95% air atmosphere at 100% humidity. At the end of the incubation, sperm concentration was measured using a Makler chamber (Irvine Scientific, CA, USA). The pool of cumulus-oocytes complexes obtained from all the females were released from the ampullas into a petri dish containing 500 $\mu$l of equilibrated HTF covered with mineral oil. Then,

Downloaded from https://academic.oup.com/biolreprod/article/100/5/1180/5266294 by guest on 20 April 2021

the oocytes were inseminated with $2 \times 10^6$ sperm/ml pooled from both males ($0.5 \times 10^6$ total sperm from each male); gametes were co-incubated for 6 h, and the presumptive zygotes were washed in 500 $\mu$l of clean KSOM medium after co-incubation (Merck-Millipore, Madrid, Spain). Then, zygotes were randomly allocated to 100 $\mu$l droplets of KSOM supplemented with 0, 10, 20, 40, or 80 $\mu$g/ml of EV-endMSCs and cultured until they reached the expanded blastocyst stage (4 days). Eight different IVF sessions in eight different days were run and 3 females (n = 24) and 2 males (n = 16) per day were used. Moreover, in order to show the differences between aged and non-aged oocytes in parallel with supplementation of EVs, we performed IVF on young B6D2 female mice (8–12 weeks, n = 3). These IVF sessions were performed in accordance with the protocol used for the aged mice using plain KSOM as embryo culture.

### Total cell number

The number of cells in an embryo is a well-known indicator of embryo quality [28]. Therefore, to further evaluate embryo quality, some of the expanded blastocysts obtained were fixed in 4% formaldehyde in PBS added with 0.01% of polyvinyl alcohol (PVA; w/v) at 4°C for 12 h and stained with 2.5 $\mu$g/ml of Hoechst 33342 (Eugene, OR, USA) in PBS added with PVA for 10 min at 37°C. Then, the blastocysts were mounted on glass slides with glycerol, covered with coverslips and sealed using nails polish. The embryos were then visualized using a fluorescence microscope (Nikon Eclipse TE2000-S) equipped with an ultraviolet lamp. Cell number was analyzed using the Fiji Image-J Software (1.45q, Wayne Rasband, NIH, USA).

### RNA isolation and reverse transcription

Six independent samples of embryos cultured with and without EV-endMSCs (n = 25 expanded blastocysts per treatment) under each experimental condition (10 $\mu$g/ml, 20 $\mu$g/ml, 40 $\mu$g/ml, and 80 $\mu$g/ml of EV-endMSCs; n = 25 embryos/treatment) were used. Three independent groups of 8–9 embryos at blastocyst stage per experimental group were pooled and processed for poly(A) RNA extraction. Poly(A) RNA was extracted using the Dynabeads mRNA Direct Extraction Kit (Dynal Biotech, Oslo, Norway) following the manufacturer's instructions with minor modifications as described by Bermejo-Alvarez and coworkers [29]. After 5 min of incubation in lysis buffer and another 5 min with lysis buffer and Dynabeads, poly(A) RNA attached to the Dynabeads was extracted with a magnet and washed twice in washing buffer A and washing buffer B. RNA was then eluted with 10 mM Tris–HCl, pH 7.5. Immediately after extraction, the reverse transcription (RT) reaction was performed as recommended by the manufacturer (Epicentre Technologies Corp, Madison, WI, USA). Briefly, oligo-dT (0.2 $\mu$M) and random primers (0.5 $\mu$M) were added to each RNA sample and were heated for 5 min at 70°C to denature the secondary RNA structure. Next, the tubes were incubated at 25°C for 10 min to promote the annealing of the primers. Then, the RNA was reverse-transcribed for 60 min at 37°C in a final volume of 40 $\mu$L containing 0.375 mM dNTPs (Biotools, Madrid, Spain), 6.25 U RNasin RNAse inhibitor (Promega), 10 × MMLV-RT buffer with 8 mM dithiothreitol and 5 U MMLV high performance reverse transcriptase (Epicentre Technologies Corp, Madison, WI, USA), followed by incubation at 85°C for 5 min to inactivate the RT enzyme.

### Gene expression analysis

The mRNA expression levels of the selected genes were determined by real-time quantitative RT polymerase chain reaction (qRT-PCR) using specific primers designed with Primer-BLAST (http://www.ncbi.nlm.nih.gov/tools/primer-blast/) to span exon-exon boundaries when possible. Primers (Table 2) were previously validated for adequate primer efficiency; the specificity of their PCR products was confirmed by electrophoresis on a 2% agarose gel. All target genes showed efficiencies between 97 and 100% and correlation coefficients close to 1.0.

All PCR reactions were performed in a final volume of 20 $\mu$L, containing 0.25 mM of forward and reverse primers, 10 $\mu$L of GoTaq qPCR Master Mix (Promega) with SYBR Green as double-stranded DNA-specific fluorescent dye, and 2 $\mu$L of each cDNA sample using a Rotorgene 6000 Real Time Cycler (Corbett Research, Sydney, Australia). For each experimental group, three different cDNA samples were used in two repetitions for all genes of interest. The PCR program consisted of an initial denaturalization step at 94°C for 2 min, followed by 35 cycles of denaturalization at 94°C for 10 s, annealing at 56°C for 30 s, extension at 72°C for 15 s and 10 s of fluorescence acquisition defined for each primer. At the end of each PCR run, melt curve analyses were performed for all genes to ensure single product amplification and exclude the possible interference of dimers.

Values were normalized using as housekeeping gene H2A histone family, member Z (*H2afz*) that was tested in previous studies [30]. Relative expression levels were quantified by the comparative cycle threshold (ΔΔCT) method [31]. Fluorescence was acquired in each cycle to determine the threshold cycle during the log-linear phase of the reaction at which fluorescence increased above background for each sample. According to the comparative CT method, the ΔCT value was determined by subtracting the mean CT value of the housekeeping gene for each sample from each gene CT value of the sample. Calculation of ΔΔCT involved using the highest sample ΔCT value (i.e. the sample with the lowest target expression) as an arbitrary constant to subtract from all other ΔCT sample values. Fold changes in the relative gene expression of the target were determined using the formula $2^{-\Delta\Delta CT}$ [32].

### Internalization assay

To analyze the uptake of the EV-endMSCs by the embryos, the extracellular vesicles were stained with 2% of SYTO RNA Select green fluorescent cell stain (Thermo Fisher Scientific) at 37°C for 30 min. PBS without exosomes added with 2% of SYTO RNA Select green fluorescent cell stain was used as control. To remove the remaining dye, all the samples (including the control PBS) were centrifuged on exosome spin columns (MW 3000, Thermo Fisher Scientific) according to manufacturer's instructions. Exosomes concentration was indirectly measured in a Bradford assay. Finally, after IVF, 25 murine zygotes were co-cultured with labeled EV-endMSCs at different concentrations or stained with PBS as negative control. Internalization (green fluorescence) was confirmed by fluorescent microscopy. Additionally, embryos were stained with 2.5 mg/ml of Hoechst 33342 (Eugene, OR, USA) for 10 min at 37°C to visualize DNA.

### Statistical analysis

For total cell number and gene expression analysis, data were tested for normality using a Shapiro–Wilk test; results are reported as mean ± standard deviation (SD). Groups were compared using a one way ANOVA due their Gaussian distribution and

Downloaded from https://academic.oup.com/biolreprod/article/100/5/1180/5266294 by guest on 20 April 2021

**Table 1.** Reactome functional annotation of EV-endMSCs proteins. Proteins were classified and subsequently analyzed according to their involvement in crucial pathways related to in vitro fertilization and embryo implantation. Selected pathways were *Metabolism* (R-HSA-1430728) (n = 114 identified proteins), *Developmental biology* (R-HSA-1266738) (n = 74), and *Cellular response to oxidative stress* (R-HSA-2262752) (n = 23). Color scale represents the protein abundance according to total peptide counting from LC/MS analyses. Additional information regarding LC/MS protein identification is displayed in Supplementary Table S1.

| Metabolism (R-HSA-1430728) | | Developmental Biology (R-HSA-1266738) | | Cellular response to oxidative stress (R-HSA-2262752) |
|---|---|---|---|---|
| A2M | CD44 | MYH9 | TUBA1B | P4HB |
| AGRN | CBR1 | COL6A3 | DPYSL2 | MMP3 |
| LRP1 | GLO1 | COL3A1 | PSMA5 | TPM1 |
| ENO1 | FH | VCL | MYH11 | HSPA1B |
| P4HB | PSME1 | FN1 | CFL1 | TXNRD1 |
| IQGAP1 | UBA52 | COL5A2 | SEMA7A | ANXA1 |
| HSPG2 | RBP1 | MMP2 | PDGFRB | GSTP1 |
| TKT | PSMA2 | LAMB1 | PSMA4 | PRDX1 |
| ALDH1A1 | TCN2 | COL6A1 | PSMA6 | CST3 |
| PSAP | PSME2 | AGRN | ACTR3 | PARK7 |
| LUM | PGLS | MSN | CAP1 | TXN |
| GPI | PSMA3 | LAMC1 | PSME1 | SOD3 |
| LDHA | PSMA1 | COL5A1 | UBA52 | APEX1 |
| TXNRD1 | RPLP2 | TLN1 | PSMA2 | SOD2 |
| VCAN | CTGF | IQGAP1 | PSME2 | PDGFD |
| LDHB | CMPK1 | SPTAN1 | SPTBN1 | AXL |
| NT5E | PSMB1 | HSPA8 | PSMA3 | PRDX5 |
| GPC1 | GSTO1 | MYH10 | PEA15 | SOD1 |
| ATP5B | PSMB4 | EZR | PSMA1 | PRDX2 |
| ALB | ALDOC | ALCAM | PEBP1 | PDGFRA |
| MDH2 | ADH5 | CDH2 | PSMB1 | PTPRK |
| EXT2 | ME1 | COL6A2 | PSMB4 | PRDX6 |
| PGK1 | HK1 | GPC1 | COL2A1 | CYCS |
| PSAT1 | PGD | ACTB | PSMB3 | |
| NAGLU | DDAH2 | AP2B1 | PSMB7 | |
| HEXA | GAPDH | NRP1 | PDGFRA | |
| AP2B1 | GOT2 | NEO1 | ARPC4 | |
| ALDOA | PSMB3 | ITGB1 | FABP4 | |
| BGN | MARCKS | HSP90AA1 | MYL9 | |
| IDH1 | GLRX | YWHAB | PDLIM7 | |
| TPI1 | NME1 | PFN1 | PSMB9 | |
| HSP90AA1 | MAN2B2 | PSMA7 | MYH14 | |
| CNDP2 | GALNS | MYL6 | SEMA3A | |
| LTA4H | RPLP1 | ACTR2 | ACTN2 | |
| HEXB | PSMB7 | ARPC2 | PRNP | |
| PSMA7 | GM2A | MYL12A | SDC2 | |
| GSTP1 | FABP4 | HSP90AB1 | PLXNC1 | |

Downloaded from https://academic.oup.com/biolreprod/article/100/5/1180/5266294 by guest on 20 April 2021

**Table 1.** Continued

| Metabolism (R-HSA-1430728) | | Developmental Biology (R-HSA-1266738) | Cellular response to oxidative stress (R-HSA-2262752) |
|---|---|---|---|
| PCSK9 | GC | | |
| GSS | PSMB9 | | |
| PTGDS | ENO3 | | |
| PSMA5 | RPL12 | | |
| PGAM1 | SDC4 | | |
| EXT1 | FDPS | | |
| MDH1 | CYCS | | |
| BTD | DBI | | |
| DCN | ACP5 | | |
| KPNB1 | FABP5 | | |
| MANBA | PGK2 | | |
| TXN | RPS28 | | |
| GBE1 | PGAM2 | | |
| GNS | SDC2 | | |
| APOE | HBB | | |
| B4GAT1 | APOA1 | | |
| PSMA4 | SDC1 | | |
| SEC23A | NME2 | | |
| PSMA6 | PRSS1 | | |
| TALDO1 | CKM | | |

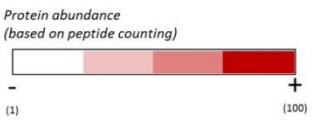


homoscedasticity. When statistically significant differences were found, a Bonferroni post-hoc test was used to compare pairs of values in the blastomere count experiment, while for the expression of candidate genes, the ANOVA was followed by multiple pairwise comparisons using the Tukey method. Blastocyst rates were compared among groups by Chi-square test with the Yates correction for continuity. The Fisher's Exact Test was used when a value of less than 5 was expected in any treatment. Statistical analyses were performed using Sigma Plot software version 12.3 for Windows (Systat Software, IL, USA) or with SPSS-21 software (SPSS, IL, USA); $P < 0.05$ was considered as statistically significant.

## Results

### Characterization of endMSCs and EV-endMSCs

The characterization of endMSCs and EV-endMSCs has been previously published by our group [10, 33]. The phenotypical analysis evidenced that endMSCs were positive for CD29, CD44, CD73, CD90, CD105, and CD117, and negative for CD14, CD20, CD31, CD34, CD45, CD80, and HLA-DR. The differentiation potential of these cells toward adipogenic, chondrogenic, and osteogenic lineages was confirmed by selective staining and microscopic analysis after co-culture with differentiation specific media. Regarding EV-endMSCs, the nanoparticle tracking analysis showed that the mean size of the vesicles was 153.5 ± 63.05 nm, while their concentration was $3.31 \times 10^{11} \pm 3.8 \times 10^{9}$ particles/ml. Additionally, the analysis of CD9 and CD63 by flow cytometry demonstrated a positive expression of these exosomal markers.

### High-throughput proteomics analysis of EV-endMSCs

This proteomic analysis allowed us to identify a wide range of proteins in EV-endMSCs (n = 1802). The relative abundance of each protein, represented in Table 1, was estimated in accordance to the peptide counting from LC/MS analyses and was quantified by means

Downloaded from https://academic.oup.com/biolreprod/article/100/5/1180/5266294 by guest on 20 April 2021

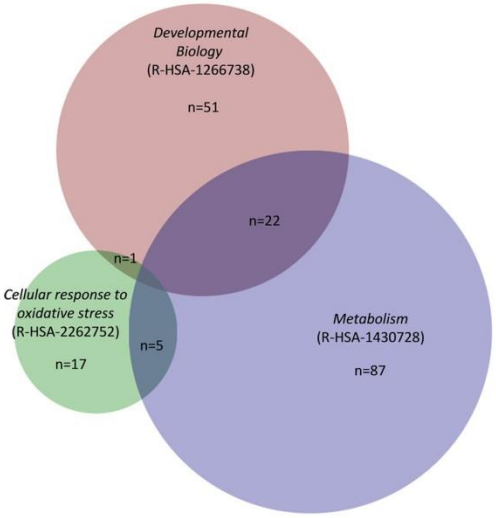


**Figure 1.** High-throughput proteomic analysis on EV-endMSCs. Protein extracts from EV-endMSCs were processed by high-resolution liquid chromatography coupled to mass spectrometry-based proteomic analyses. The functional enrichment analysis was performed by Reactome Pathway Database in the most representative proteins identified (n = 580). The Venn diagram shows unique and overlapped proteins in these three Reactome pathways.

of the intensities of iTRAQ reporters which were used to tag the peptides of each sample. Reporter ion intensities of each protein were normalized to the total ion intensity of the sample dataset. Functional analysis according to the Gene Ontology annotation database [34, 35] was performed with the most representative proteins identified, accordingly to their abundance (n = 580), considering negligible proteins with abundance lower than 0.005%.

First, the protein data set was classified according to the "cellular component" annotation. In this analysis, a total of 395 proteins were classified as *"Extracellular Vesicles"* (GO:1903561 $P < 0.01$, 5% FDR; data not shown). In a subsequent analysis using the Reactome Pathway Database [36], we sorted out the proteins according to their involvement in crucial pathways related to fertilization and embryo implantation. Some interesting Reactome pathways were: *Metabolism* (R-HSA-1430728; n = 114 proteins), *Developmental biology* (R-HSA-1266738; n = 74 proteins), and *Cellular response to oxidative stress* (R-HSA-2262752; n = 23 proteins). Figure 1 shows the Venn diagram with unique and overlapped proteins among these three Reactome pathways. Additionally, Table 1 lists the proteins identified and classified in the aforementioned Reactome categories. Of note, 45 out of 114 proteins identified in the *Metabolism pathway* were also classified by Gene-Ontology in the *Immune System Process* (GO:0002376). Similarly, 26 out of 114 were involved in the *Regulation of Cell Differentiation* (GO:0045595). Furthermore, the number of identified peptides (peptide counting) for each protein together with the Gene name, UniProt Accession Code and the Reactome Pathway it belongs are listed in the Supplementary Table S1.

### Development to the blastocyst stage and total cell number count

EV-endMSC addition to the embryo culture medium did not influence embryo division at days 1 and 2 of culture compared to control (Table 3; $P > 0.05$). However, when the embryos reached the morula stage (day 3), the 20 $\mu$g/ml and 80 $\mu$g/ml dosages of EV-endMSCs significantly enhanced the percentage of embryos that developed in culture compared to control (Table 3, $P < 0.05$). Our results showed that the blastocyst rate after 4 days of culture significantly increased when EV-endMSCs were added to the embryo culture medium at any of the dosages tested (Table 3; $P < 0.01$). Interestingly, the maximum blastocyst yield was observed for the 20 $\mu$g/ml dose (62.9% blastocyst rate) compared to the control (29.4%) at day 4 of culture.

In parallel, expanded blastocyst total cell number significantly increased for all the EV-endMSCs dosages tested varying from 32.4 ± 12.9 blastomeres per embryo (mean ± SD) in the control group to 48.5 ± 14.4 for the 40 $\mu$g/ml, being this the maximum value obtained (Figure 2; $P < 0.05$).

In order to emphasize the differences in developmental competence and kinematics of embryos obtained from young and aged female mice, new IVF assays were performed in 8–12 week-old females in absence of EV-endMSCs. In our experimental conditions, the blastocyst rate in young females reached 89.6%, which was consistently higher than the percentages obtained in aged females (supplementary Table S2). To highlight the marked age-dependent differences found in IVF outcomes, a chi-square test was performed to compare the developmental competence and embryo kinematics of young (8–12 weeks) *vs.* aged (24–26 weeks) B6D2 females. As it can be observed in the Supplementary Table S2, blastocyst development was severely compromised with increasing age in our B6D2 females at all the stages studied.

### Differential expression of embryo-related genes

The gene expression analysis was performed by quantitative PCR in blastocysts at day 4 of culture. Based on the proteomic analysis, several candidate genes were selected according to their involvement in the following Reactome categories: *Metabolism* (acetyl-coenzyme A carboxylase alpha –*Acaca*-, glyceraldehyde-3-phosphate dehydrogenase –*Gapdh*-), *Cellular response to oxidative stress* (glutathione peroxidase 1 -*Gpx1*- and superoxide dismutase 1 -*Sod1*-), and *Developmental biology* (placental growth factor –*Pgf*-, VEGF A –*Vegfa*-, POU domain, class 5, transcription factor 1 -*Pou5f1*- and sex determining region Y-box 2 -*Sox2*-). These four genes were also subclassified according to their involvement in placentation (*Pgf*, *Vegfa*) and trophectoderm/inner cell mass formation (*Pou5f1* and *Sox2*).

When compared against control, the relative RNA abundance for *Gpx1* was downregulated in the 20–80 $\mu$g/ml EV-endMSCs while *Sod1* expression was consistently lower in the 10–40 $\mu$g/ml doses ($P < 0.05$). Relative *Vegfa* and *Gapdh* expression increased at all the EV-endMSCs doses used compared to control ($P < 0.05$) except for the 80 $\mu$g/ml dose which did not differ from the non-EV-endMSCs added treatment ($P > 0.05$). *Sox2* expression was upregulated for the 10, 20, and 40 $\mu$g/ml dosages compared to control ($P < 0.05$), while its expression did not change when EV-endMSC at 80 $\mu$g/ml were added ($P > 0.05$; Figure 3).

In addition, the relative RNA abundance of *Acaca, Pgf and Pouf51* did not vary despite EV-endMSC supplementation ($P > 0.05$; Figure 3).

Downloaded from https://academic.oup.com/biolreprod/article/100/5/1180/5266294 by guest on 20 April 2021

**Table 2.** List of primers.

| Ehtrez gene symbol | Gene name | Accesion no. | Forward primer (5'-3') | Reverse primer (5'-3') | Product length |
|---|---|---|---|---|---|
| *H2ajz* | H2A his tone family, member Z | NM_001316995.1 | AGGACGACTAGCCATGGACGTGTG | CCACCACCAGCAATTGTAGCCTTG | 209 |
| *Gpxl* | Glutathiones peroxidase 1 | NM.001329527.1 | GCAACCAGTTTGGCATCA | CTCGCACTTTTCGAAGAGCATA | 116 |
| *Pgf* | Placental growth factor | NM.001271705.1 | CTCTCTGGAACACAGGCAGA | CCGTAGCTGTACCACGAAGA | 100 |
| *Vegfa* | Vascular endothelial growth factor A | NM.009505 | CACAGCAGATGTGAATGCAG | TTTACACGTCTGCGGATCTTG | 94 |
| *Acaca* | acetyl-Coenzyme A carboxylase alpha | XM.011248666.1 | AAACCAGCACTCCCGATTCAT | GGCCAAACCATCCTGTAAGC | 175 |
| *Pou5f1* | POU domain, class 5, transcription factor 1 | NM.013633 | TAGGTGAGCCGTCTTTCCAC | GCTTAGCCAGGTTCGAGGAT | 159 |
| *Sox2* | SRY (sex determining region Y)-box2 | NM.011443.4 | GCACATGAACGGCTGGAGCAACG | TGCTGCGAGTAGGACATGCTGTAGG | 206 |
| *Bax* | BCL2-associated X protein | NM.007527.3 | AACGCTGAGCGAGTGTCTCCGGCG | GCCACAAAGATGGTCACTGTCTGCC | 361 |
| *Gapdh* | Qyceraldehyde-3-phosphate dehydrogenase | NM.001289726.1 | AGGTCGGTGTGAACGGATTTG | TGTAGACCATGTAGTTGAGGTCA | 122 |
| *Sod1* | Superoxide dismutase 1 | NM.174615 | GTGCAAGGCCACCATCCACTTCG | CACCATCGTGCCGCCAATGATG | 309 |
| *Gadd45a* | Growth arrest and DNA damage inducible alpha | BC023815.1 | CTTCTGGTCGCACGGGAAGG | GCTCCACCGCGGCAGTCACC | 277 |

### EV-endMSCs uptake

Fluorescent labelling of EV-endMSCs allowed us to confirm that these vesicles are effectively internalized by the embryos after 24 h of co-culture. The absence of fluorescence in the negative control demonstrated that non-specific fluorescence was not interfering with the fluorescence observed from the labeled EV-endMSCs. Based on the fluorescence analysis, we demonstrated that EV-endMSCs co-cultured with murine embryos at different concentrations were rapidly internalized (Figure 4).

## Discussion

In the present study, we demonstrate that extracellular vesicles released from human endometrial MSCs can be used as an embryo culture supplement to partially recover the developmental competence of aged oocytes. In our setting, not only the developmental competence of the embryos was improved (Table 3), but also the total blastomere count (Figure 2). This is in accordance with the report of Qu et al., who demonstrated that bovine embryos subjected to somatic cell nuclear transfer produce exosomes that enhance the development to the blastocyst stage as well as their quality [13].

Even when embryo culture conditions have lesser influence on the developmental potential of the early embryo than the initial oocyte quality [37], our results in an aged murine model demonstrate that EV-endMSCs enhance the developmental competence as well as the quality of the embryos produced. These results may have discrepancies with former reports in mice and bovine where addition of extracellular vesicles did not enhance the embryo's developmental competence [8, 10, 11]. However, it is important to note that, in our previous report [10], these EV-endMSCs were co-cultured with two-cell embryos retrieved from young females (aged 8–12 weeks), which have a notably superior developmental competence than the aged murine model used in the present work. This consideration can also be confirmed by our results regarding the developmental competences of zygotes retrieved from young and aged females (Supplementary Table S2). As expected, in absence of the EVs supplementation, embryos from young female mice exhibited significantly higher developmental competence when compared to the embryos from aged females. Hence, naturally aging mice can be considered important models for the investigation of occurring declines in reproductive capacity and impaired viability of the oocyte [38].

In the case of the bovine species [8, 11], embryo culture medium was enriched with homologous oviductal extracellular vesicles and the reduced developmental competence of in vitro matured oocytes could not be overcome when these vesicles were used. This divergence can be explained not only by the molecular differences that may exist between human EV-endMSCs and bovine oviductal extracellular vesicles, but also by the inherent reduced developmental competence of bovine oocytes harvested in prophase I [39].

On the other hand, MSCs have been previously used for embryo culture in porcine, bovine, and murine models; even when contradictory results have been reported, it has been proposed that MSCs secrete growth factors that may have a positive impact during embryo culture enhancing embryo quality [40-42].

Next, in order to further understand the mechanisms involved in the beneficial effects of EV-MCs on the embryo development, a high throughput proteomic analysis was performed in these EV-endMSCs. First, the most abundant identified proteins were classified according to specific Reactome pathways which are closely related with the fertilization process: *Metabolism* (a total of 114 proteins),

Downloaded from https://academic.oup.com/biolreprod/article/100/5/1180/5266294 by guest on 20 April 2021

**Table 3.** *Embryo division kinematics and blastocyst rate.* Murine oocytes from aged females (24 weeks old) were subjected to IVF and the number of oocytes used as well as their embryo division dynamics was recorded at days 1 to 4 of embryo culture. All values are presented as total number and (percentage); values bearing different letters in the same column differ statistically from the control ($P < 0.05$).

| | Oocytes | 2 cells (day 1) | 8 cells (day 2) | Morula (day 3) | Blastocyst (day 4) |
|---|---|---|---|---|---|
| Control | 126 | 93 (7.38) | 82 (65.1) | 71(56.3)[a] | 37 (29.4)[a] |
| 10 $\mu$g/ml | 124 | 98 (79) | 95 (76.6) | 83 (66.9)[a] | 56 (45.2)[b] |
| 20 $\mu$g/ml | 124 | 102 (82.3) | 96(77.4) | 95 (76.6)[b] | 78 (62.9)[b] |
| 40 $\mu$g/ml | 128 | 97 (75.8) | 88 (68.8) | 86 (67.2)[a] | 71 (55.5)[b] |
| 80 $\mu$g/ml | 130 | 104 (80) | 100 (76.9) | 93 (71.5)[b] | 70 (53.8)[b] |

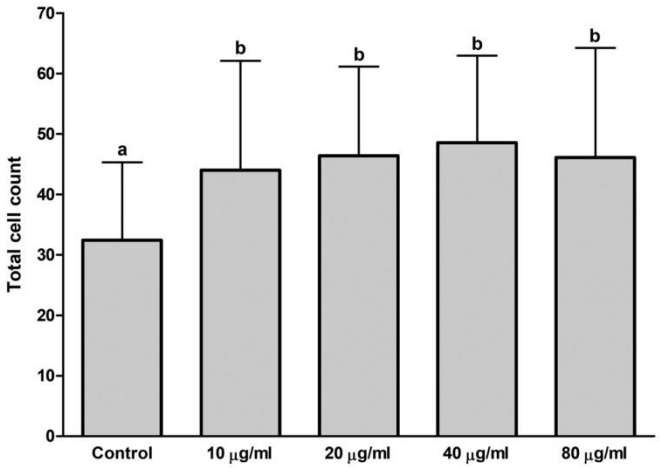


**Figure 2.** Total cell number of murine blastocysts cultured in presence or absence of EV-endMSCs. Total cell number of the expanded blastocysts was obtained after Hoechst 33342 staining and subsequent evaluation by fluorescence microscopy. For each treatment, the individual blastomere count is represented; the number of embryos evaluated were 15 for control, 24 for the 10 $\mu$g/ml treatment, 31 for the 20 $\mu$g/ml treatment, 38 for the 40 $\mu$g/ml treatment, and 31 for the 80 $\mu$g/ml treatment. Bars show the mean ± SD. All the treatments differ statistically from the control ($P < 0.05$).

*Developmental biology* (a total of 74 proteins), and *Cellular response to oxidative stress* (a total of 23 proteins; Table 1).

Some of the most abundant proteins found in our proteomic analysis deserve better investigation. For example, fibronectin (FN1) was reported to be essential for embryogenesis, from the two-cell stage to tissue morphogenesis [43-46]. Vinculin (VCL) and alpha2 macroglobulin (A2M), other abundant proteins found in our analysis, were established to be important during early development [47, 48]. Moreover, A2M as well as matrix metalloproteinase-3 (MMP-3) and agrin (AGRN) were related to implantation [49-51]. In addition, matrix metalloproteinase -2 (MMP-2) and laminin beta 1 (LAMB1) were associated to the developing human embryo and the early phases of human pregnancy [52, 53].

Interestingly, the proteomic analysis revealed the presence of four different insulin-like growth factor-binding protein (IGFBP) isoforms (-4, -5, -6, -7) in all EV-endMSCs samples. The presence of these proteins is relevant considering that previous reports have demonstrated that the addition of IGFBP to embryo culture medium protects the inner cell mass from apoptosis and increases mitochondrial membrane potential in oocytes [54]. Our proteomic analysis has also demonstrated a very high abundance of serum albumin (the fourth in terms of absolute quantification), which is largely used for the supplementation of commercial media in IVF [55] and has been reported to alleviate ROS production in vitro in neurons and sperm [56, 57].

To further confirm if the proteomic results can, at least in part, explain the improvement in the developmental competence and embryo quality, gene expression analysis in the resulting blastocysts was performed on core genes related to *Cellular response to oxidative stress, Metabolism, Placentation, and Trophectoderm/inner cell mass formation.*

Regarding the *cellular response to oxidative stress* category, previous studies have evidenced that one of the main constraints blunting the developmental competence of aged oocytes relies on their reduced ability to counteract ROS [58]. Furthermore, a recently published report from Mihalas *et al.*, has demonstrated that immature aged oocytes undergo a decrease in proteasome activity when subjected to an oxidative environment leading to the accumulation of damaged and/or dysfunctional proteins contributing to the age-dependent drop in oocyte quality [59].

Interestingly, the expression of *Sod1* (as well as *Gpx1)* consistently decreased at the 20 and 40 $\mu$g/ml EV-endMSCs dosages

Downloaded from https://academic.oup.com/biolreprod/article/100/5/1180/5266294 by guest on 20 April 2021

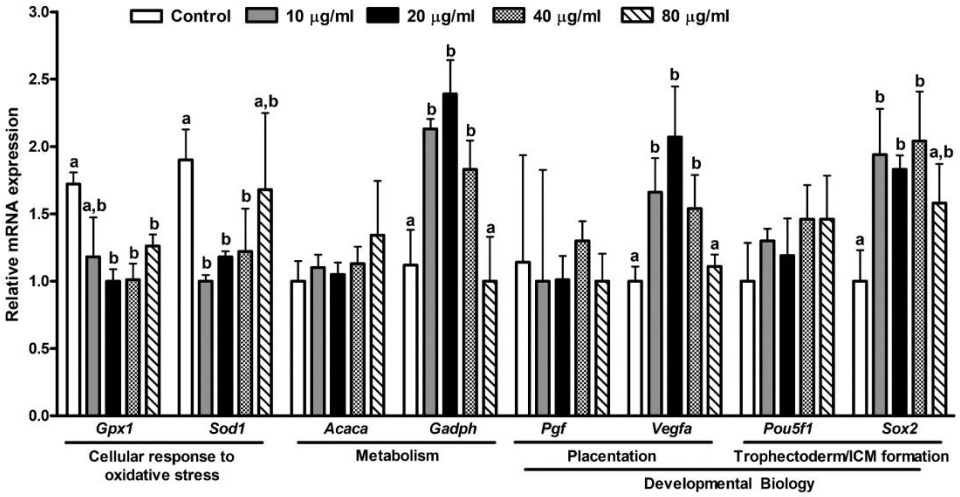


**Figure 3.** Relative mRNA expression of candidate genes. Relative mRNA levels of candidate genes related to the proteome categories cellular response to oxidative stress, metabolism, and developmental biology (n = 25 embryos/treatment). Bars represent mean ± SD; values bearing different letters differ statistically from the control ($P < 0.05$).

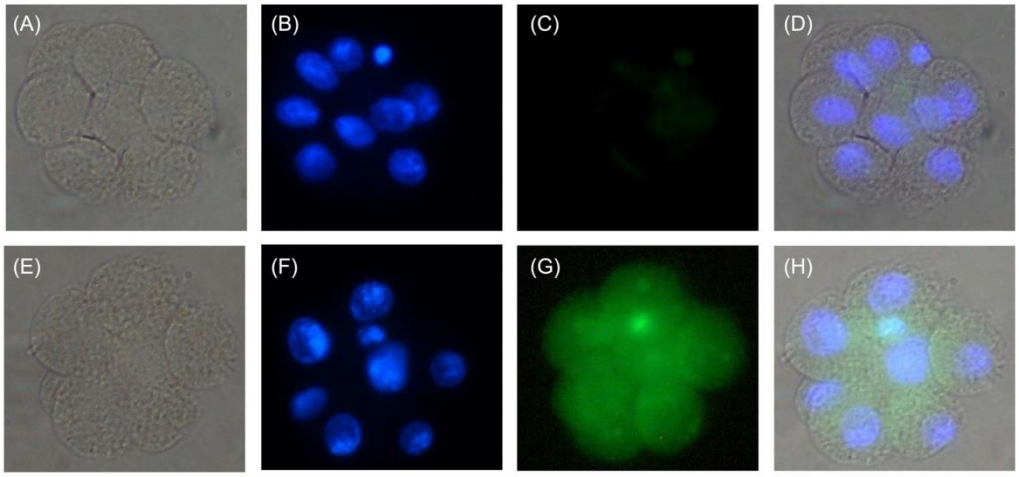


**Figure 4.** Internalization of EV-endMSCs by the embryos. EV-endMSCs were labeled with SYTO RNA select green fluorescent cell stain and co-cultured at different concentrations with embryos for 24 h. Additionally, embryos were stained with Hoechst to visualize DNA. The figure shows representative images of an embryo co-cultured with EV-endMSCs at 80 μg/ml (E, F, G, H). Representative images of the control (embryos co-cultured with stained PBS) are also shown (A, B, C, D). A and E: bright field microscopy showing a representative embryo. B and F: visualization of Hoechst fluorescence under fluorescence microscopy. C and G: visualization of SYTO RNA Select fluorescence under fluorescence microscopy. D: merged image of A, B and C. H: merged image of E, F and G.

coinciding with the highest embryo yields obtained in the present work (Figure 3 and Table 3). The diminished expression of *Gpx1* and *Sod1* suggests that EV-endMSCs exert an exogenous ROS scavenger activity during embryo culture (Figure 3). As a matter of fact, a good correlation between mRNA, proteins, and antioxidant enzyme activities in rat embryos subjected to diabetic environment has already been demonstrated [60]. In the pre-implantation embryo, antioxidant enzymes (including SOD1 and GPX1) are primarily regulated at the pre-transcriptional level, and the transcripts are translated to produce active enzymes [61]. Moreover, it was postulated that embryo's defense against ROS depends the intracellular ROS levels that trigger the expression of antioxidant genes as demonstrated in human umbilical vein endothelial cells [62] and mouse zygotes [63]. It has to be noted that, in our work, EV-endMSCs were added to zygotes. In view of all the previous literature and considering that major gene activation occurs in the 2-cell embryo, if less *Sod1* and

Downloaded from https://academic.oup.com/biolreprod/article/100/5/1180/5266294 by guest on 20 April 2021

*Gpx1*mRNA is found in the embryos, it is likely that lower ROS levels are triggering their expression. Agreeing with our findings, but in the setting of prostate tumors, EV-endMSCs have also been shown to diminish angiogenesis in tumoral cells by means of their ROS scavenger activity [16], demonstrating again the ROS scavenger potential of EV-endMSCs is an unexplored scenario.

Additionally, the expression levels of *Pou5f1* and *Sox2* were also analyzed. The gene *Pou5f1* is a homeodomain transcription factor of the POU (Pit-Oct-Unc), family that encodes the OCT4 protein. This protein has been shown to be a critical regulator of cellular pluripotency in murine embryos [64]. Additionally, the transcription factor SOX2 forms a complex with OCT4 and participates in the maintenance of self-renewal of the pluripotent inner cell mass, being essential for the formation of the trophoectoderm in the preimplantation embryo [65]. Our results demonstrate that the expression of *Pou5f1* did not vary between treatments but the expression of *Sox2* raised for the 10–40 $\mu$g/ml EV-endMSCs dosages coinciding with the maximum blastocyst rates and total cell number (Table 3 and Figure 3). It is known that morulae developed from *Sox2-/-* zygotes get arrested at this stage and fail to cavitate [65] and form a proper inner cell mass [66]; in addition, rescue experiments using cell-permeant SOX2 protein result in increased blastocyst rate and restoration of SOX2 protein levels in murine blastocysts knock-down of *Sox2* using short interfering RNA [65]. Hence, the increased expression of *Sox2* together with the enhanced developmental competence and cell number of our embryos further corroborate the boosting effect on embryo quality mediated by EV-MSCs supplementation.

Regarding to metabolism-related genes, it has been demonstrated that fully pluripotent stem lines exhibit higher ATP levels compared with initial pluripotent stem cells [67]. These observations are coincident with the increased *Gapdh* expression and increased total cell number observed in our embryos for the 10–40 $\mu$g/ml EV-endMSCs dosages. It is widely known that GAPDH activity is involved in the glycolytic pathway triggering the conversion of glyceraldehyde-3-phosphate to 1,3-diphosphoglycerate to provide energy in the form of ATP. Hence, the increased expression of *Sox2* in our aged murine model suggests that firstly, EV-endMSCs increases the quality of the embryos through the self-renewal of the pluripotent inner cell mass and the establishment of the trophectoderm lineage [65]. Secondly, the increased expression of *Gapdh* suggests an increase of embryo quality through the enhancement of metabolism during embryonic development.

Conversely, our results did not show significant differences in the expression levels of the *Acaca* gene, suggesting that fatty acid metabolism is not affected by EV-endMSCs supplementation to the embryo culture medium.

Aside from quality-related genes and metabolism-related genes, we aimed to determine if the produced embryos could potentially exhibit higher implantation ability. Our experiments revealed that *Vegfa* consistently increased when EV-endMSCs were added at the 10–40 $\mu$g/ml dosages. Previous reports have demonstrated that mouse-derived embryos treated with either recombinant human VEGF, or VEGF isoforms 121 and 165, exhibit higher embryo development with quicker cavitation, increased blastomere number, improved implantation rates, and fetal limb development compared to controls [68]. Furthermore, recent findings from our research group have demonstrated that murine embryos exposed to EV-endMSCs exhibit higher VEGF and PDGF-AA release, confirming the results of the present study [8]. Therefore, the addition of EV-endMSCs to IVF-derived murine zygotes obtained from aged females increased the quality of the embryos, presumably due to their ROS scavenger and pluripotent-promoting activity. Furthermore, in light of the previously mentioned reports it is tempting to speculate that the resulting embryos may also exhibit higher implantation potential.

To the authors' best knowledge, this is the first report describing the proteomic profiling of EV-endMSCs based on Reactome pathways. Moreover, our in vitro assays have demonstrated their therapeutic potential to rescue the developmental competence of aged oocytes in a murine model. Hence, their beneficial effect should be taken in account as it may be a valuable tool in human ARTs improving the efficiency of the current techniques and increasing the odds of implantation and subsequent delivery.

## Supplemental data

Supplementary data are available at *BIOLRE* online.

**Supplementary Table S1. Proteins identified in EV-endMSCs LC/MS analyses at 1% FDR (n = 1802).** Protein descriptions, UniProt accession codes and the corresponding genes names (N/A means "Not assigned") are displayed. **Np** refers to the number of peptides identified for each protein. The FDR for peptide identification was set at 1%. Green symbols indicate those proteins annotated within the Reactome pathways discussed on the text (Table 1).

**Supplementary Table S2. Developmental competence of embryos derived from young and aged B6D2 females.** The initial number of two cell embryos used, as well as blastocyst rates in % is provided. Values bearing different letters in a column differ statistically ($P < 0.001$).

## Acknowledgements

The authors wish to acknowledge the generous donation of the menstrual blood. In addition, the work from the animal housing staff Luis Dávila, Marisa Higuero and Víctor Pérez who exquisitely took care of the animals used in this study is greatly appreciated. The collaboration between CCMIJU and INIA was enabled by the Red de Excelencia PIVEV (Ref. AGL2016-81890-REDT; Ministerio de Ciencia, Innovación y Universidades).

## Funding

This work was supported in part by CIBER-CV (CB16/11/00494, CB16/11/00277). One project and grant "Miguel Servet I" from Instituto de Salud Carlos III to JGC (CP17/00021 and CD17/00021 co-financed by FEDER and FSE). One grant from MAFRESA S.L. to FM. One project from Instituto de Salud Carlos III to JGC (PI18/0911 cofinanced by FEDER).

The competitive projects from the Ministry of Science, Innovation, and Universities (AGL2015-73249-JIN, AGL2015-66145, AGL2017-84681-R (AEI/FEDER/UE)), and the Carlos III Institute of Health-Fondo de Investigación Sanitaria (PRB2, PT13/0001/0017-ISCIII-SGEFI/FEDER; PBR3, PT17/0019/0003 ISCIII-SGEFI/FEDER; ProteoRed), and the Fundación La Marato TV3 (20153731(122/C/2015)). The CNIC is supported by the Ministry of Science, Innovation and Universities and the Pro CNIC Foundation, and is a Severo Ochoa Center of Excellence (SEV-2015-0505). All in vitro studies were performed at the ICTS Nanbiosis (Units 14, 22, and 23). The funders had no role in study designs, data collection and analysis, decision to publish, or preparation of the manuscript.

**Competing Interests:** The authors have declared that no competing interests exist.

Downloaded from https://academic.oup.com/biolreprod/article/100/5/1180/5266294 by guest on 20 April 2021

## References


1. Rasool S, Shah D. The futile case of the aging ovary: is it mission impossible? A focused review. *Climacteric* 2018;**21**(1):22–28.
2. Allahbadia GN. Social egg freezing: developing countries are not exempt. *J Obstet Gynecol India*. 2016;**66**(4):213–217.
3. O'Brien YM, Ryan M, Martyn F, Wingfield MB. A retrospective study of the effect of increasing age on success rates of assisted reproductive technology. *Int J Gynecol Obstet* 2017;**138**(1):42–46.
4. Mihalas BP, Redgrove KA, McLaughlin EA, Nixon B. Molecular mechanisms responsible for increased vulnerability of the ageing oocyte to oxidative damage. *Oxid Med Cell Longev* 2017;**2017**:1–22.
5. Highet AR, Bianco-Miotto T, Pringle KG, Peura A, Bent S, Zhang J, Nottle MB, Thompson JG, Roberts CT. A novel embryo culture media supplement that improves pregnancy rates in mice. *Reproduction* 2017;**153**(3):327–340.
6. Greening DW, Nguyen HPT, Elgass K, Simpson RJ, Salamonsen LA. Human Endometrial Exosomes Contain Hormone-Specific Cargo Modulating Trophoblast Adhesive Capacity: Insights into Endometrial-Embryo Interactions1. *Biol Reprod*. 2016 ;**94**(2). Available at: https://academic.oup.com/biolreprod/article-lookup/doi/10.1095/biolreprod.115.134890. Accessed 28 November 2017.
7. Théry C, Zitvogel L, Amigorena S. Exosomes: composition, biogenesis and function. *Nat Rev Immunol* 2002;**2**(8):569–579.
8. Lopera-Vasquez R, Hamdi M, Maillo V, Gutierrez-Adan A, Bermejo-Alvarez P, Ramírez MÁ, Yáñez-Mó M, Rizos D. Effect of bovine oviductal extracellular vesicles on embryo development and quality *in vitro*. *Reproduction*. 2017;**153**(4):461–470.
9. Wang L, Yu Z, Wan S, Wu F, Chen W, Zhang B, Lin D, Liu J, Xie H, Sun X, Wu Z. Exosomes derived from dendritic cells treated with schistosoma japonicum soluble egg antigen attenuate DSS-induced colitis. *Front Pharmacol* 2017;**8**:651.
10. Blázquez R, Sánchez-Margallo FM, Álvarez V, Matilla E, Hernández N, Marinaro F, Gómez-Serrano M, Jorge I, Casado JG, Macías-García B. Murine embryos exposed to human endometrial MSCs-derived extracellular vesicles exhibit higher VEGF/PDGF AA release, increased blastomere count and hatching rates. Afink GB, ed. *PLoS One* 2018;**13**(4):e0196080.
11. Lopera-Vásquez R, Hamdi M, Fernandez-Fuertes B, Maillo V, Beltrán-Breña P, Calle A, Redruello A, López-Martín S, Gutierrez-Adán A, Yañez-Mó M, Ramirez MÁ, Rizos D et al. Extracellular vesicles from BOEC in in vitro embryo development and quality. *PLoS One* 2016;**11**(2):e0148083.
12. Saadeldin IM, Kim SJ, Choi YB, Lee BC. Improvement of cloned embryos development by co-culturing with parthenotes: a possible role of exosomes/microvesicles for embryos paracrine communication. *Cell Reprogram* 2014;**16**(3):223–234.
13. Qu P, Qing S, Liu R, Qin H, Wang W, Qiao F, Ge H, Liu J, Zhang Y, Cui W, Wang Y. Effects of embryo-derived exosomes on the development of bovine cloned embryos. *PLoS One* 2017;**12**(3):e0174535.
14. Khoury M, Alcayaga-Miranda F, Illanes SE, Figueroa FE. The promising potential of menstrual stem cells for antenatal diagnosis and cell therapy. *Front Immunol* 2014;**5**:205.
15. Chen L, Xiang B, Wang X, Xiang C. Exosomes derived from human menstrual blood-derived stem cells alleviate fulminant hepatic failure. *Stem Cell Res Ther* 2017; ;**8**(1). Available at: http://stemcellres.biomedcentral.com/articles/10.1186/s13287-016-0453-6. Accessed 02 March 2018.
16. Alcayaga-Miranda F, González PL, Lopez-Verrilli A, Varas-Godoy M, Aguila-Díaz C, Contreras L, Khoury M. Prostate tumor-induced angiogenesis is blocked by exosomes derived from menstrual stem cells through the inhibition of reactive oxygen species. *Oncotarget* 2016; ;**7**(28). Available at: http://www.oncotarget.com/fulltext/9852. Accessed 02 March 2018.
17. Wang K, Jiang Z, Webster KA, Chen J, Hu H, Zhou Y, Zhao J, Wang L, Wang Y, Zhong Z, Ni C, Li Q et al. Enhanced cardioprotection by human endometrium mesenchymal stem cells driven by exosomal microRNA-21. *STEM CELLS Transl Med* 2017;**6**(1):209–222.
18. Homer H, Rice GE, Salomon C. Review: embryo- and endometrium-derived exosomes and their potential role in assisted reproductive treatments–liquid biopsies for endometrial receptivity. *Placenta* 2017;**54**:89–94.
19. Bonzon-Kulichenko E, Pérez-Hernández D, Núñez E, Martínez-Acedo P, Navarro P, Trevisan-Herraz M, Ramos Mdel C, Sierra S, Martínez-Martínez S, Ruiz-Meana M, Miró-Casas E, García-Dorado D et al. A robust method for quantitative high-throughput analysis of proteomes by 18O labeling. *Mol Cell Proteomics MCP* 2011;**10**(1):M110.003335.
20. García-Marqués F, Trevisan-Herraz M, Martínez-Martínez S, Camafeita E, Jorge I, Lopez JA, Méndez-Barbero N, Méndez-Ferrer S, Del Pozo MA, Ibáñez B, Andrés V, Sánchez-Madrid F et al. A novel systems-biology algorithm for the analysis of coordinated protein responses using quantitative proteomics. *Mol Cell Proteomics* 2016;**15**(5):1740–1760.
21. Jorge I, Navarro P, Martínez-Acedo P, Núñez E, Serrano H, Alfranca A, Redondo JM, Vázquez J. Statistical model to analyze quantitative proteomics data obtained by 18O/16O labeling and linear ion trap mass spectrometry: application to the study of vascular endothelial growth factor-induced angiogenesis in endothelial cells. *Mol Cell Proteomics MCP* 2009;**8**(5):1130–1149.
22. Navarro P, Trevisan-Herraz M, Bonzon-Kulichenko E, Núñez E, Martínez-Acedo P, Pérez-Hernández D, Jorge I, Mesa R, Calvo E, Carrascal M, Hernáez ML, García F et al. General statistical framework for quantitative proteomics by stable isotope labeling. *J Proteome Res* 2014;**13**(3):1234–1247.
23. Navarro P, Vázquez J. A refined method to calculate false discovery rates for peptide identification using decoy databases. *J Proteome Res* 2009;**8**(4):1792–1796.
24. Wiśniewski JR, Ostasiewicz P, Mann M. High recovery FASP applied to the proteomic analysis of microdissected formalin fixed paraffin embedded cancer tissues retrieves known colon cancer markers. *J Proteome Res* 2011;**10**(7):3040–3049.
25. Martínez-Bartolomé S, Navarro P, Martín-Maroto F, López-Ferrer D, Ramos-Fernández A, Villar M, García-Ruiz JP, Vázquez J. Properties of average score distributions of SEQUEST. *Mol Cell Proteomics* 2008;**7**(6):1135–1145.
26. Huang DW, Sherman BT, Lempicki RA. Systematic and integrative analysis of large gene lists using DAVID bioinformatics resources. *Nat Protoc* 2009;**4**(1):44–57.
27. Huang DW, Sherman BT, Lempicki RA. Bioinformatics enrichment tools: paths toward the comprehensive functional analysis of large gene lists. *Nucleic Acids Res* 2009;**37**(1):1–13.
28. Alpha Scientist in Reproductive Medicine and ESHRE Special Interest Group of Embryology. The Istanbul consensus workshop on embryo assessment: proceedings of an expert meeting. *Hum Reprod* 2011;**26**(6):1270–1283.
29. Bermejo-Álvarez P, Rizos D, Rath D, Lonergan P, Gutierrez-Adan A. Epigenetic differences between male and female bovine blastocysts produced in vitro. *Physiol Genomics* 2008;**32**(2):264–272.
30. Bermejo-Alvarez P, Rizos D, Rath D, Lonergan P, Gutierrez-Adan A. Sex determines the expression level of one third of the actively expressed genes in bovine blastocysts. *Proc Natl Acad Sci USA* 2010;**107**(8):3394–3399.
31. Schmittgen TD, Livak KJ. Analyzing real-time PCR data by the comparative CT method. *I* 2008;**3**(6):1101–1108.
32. Livak KJ, Schmittgen TD. Analysis of Relative Gene Expression Data Using Real-Time Quantitative PCR and the 2???CT Method. *Methods* 2001;**25**(4):402–408.
33. Álvarez V, Sánchez-Margallo FM, Macías-García B, Gómez-Serrano M, Jorge I, Vázquez J, Blázquez R, Casado JG. The immunomodulatory activity of extracellular vesicles derived from endometrial mesenchymal stem cells on CD4+ T cells is partially mediated by TGFbeta. *J Tissue Eng Regen Med* 2018;**12**(10):2088–98.
34. Ashburner M, Ball CA, Blake JA, Botstein D, Butler H, Cherry JM, Davis AP, Dolinski K, Dwight SS, Eppig JT, Harris MA, Hill DP et al. Gene ontology: tool for the unification of biology. *Nat Genet* 2000;**25**(1):25–29.
35. The Gene Ontology Consortium. Expansion of the gene ontology knowledgebase and resources. *Nucleic Acids Res* 2017;**45**(D1):D331–D338.


Downloaded from https://academic.oup.com/biolreprod/article/100/5/1180/5266294 by guest on 20 April 2021

36. Fabregat A, Jupe S, Matthews L, Sidiropoulos K, Gillespie M, Garapati P, Haw R, Jassal B, Korninger F, May B, Milacic M, Roca CD et al. The reactome pathway knowledgebase. *Nucleic Acids Res*. 2018;**46**(D1):D649–D655.
37. Lonergan P, Fair T. Maturation of oocytes in vitro. *Annu Rev Anim Biosci* 2016;**4**(1):255–268.
38. Thouas GA, Trounson AO, Jones GM. Effect of female age on mouse oocyte developmental competence following mitochondrial injury1. *Biol Reprod* 2005;**73**(2):366–373.
39. Lonergan P, Fair T. In vitro-produced bovine embryos—dealing with the warts.*Theriogenology*. 2008;**69**(1):17–22.
40. Bhardwaj R, Ansari MM, Parmar MS, Chandra V, Sharma GT. Stem cell conditioned media contains important growth factors and improves in vitro buffalo embryo production. *Anim Biotechnol* 2016;**27**(2):118–125.
41. Opiela J, Bülbül B, Romanek J. Varied approach of using MSCs for bovine embryo in vitro culture. *Anim Biotechnol* 2018;1–8.
42. Park H-Y, Kim E-Y, Lee S-E, Choi H-Y, Moon JJ, Park M-J, Son YJ, Lee JB, Jeong CJ, Lee DS, Riu KJ, Park SP. Effect of human adipose tissue-derived mesenchymal-stem-cell bioactive materials on porcine embryo development. *Mol Reprod Dev* 2013;**80**(12):1035–1047.
43. de Almeida PG, Pinheiro GG, Nunes AM, Gonçalves AB, Thorsteinsdôttir S. Fibronectin assembly during early embryo development: A versatile communication system between cells and tissues. *Dev Dyn Off Publ Am Assoc Anat* 2016;**245**(4):520–35.
44. Larson RC, Ignotz GG, Currie WB. Effect of fibronectin on early embryo development in cows. *Reproduction* 1992;**96**(1):289–297.
45. Raddatz E, Monnet-Tschudi F, Verdan C, Kucera P. Fibronectin distribution in the chick embryo during formation of the blastula. *Anat Embryol* 1991;**183**(1):57–65.
46. Tsuiki A, Preyer J, Hung TT. Effects of fibronectin and its peptide fragment on preimplantation mouse embryo. *Am J Obstet Gynecol* 1989;**160**(3):724–728.
47. Duband JL, Thiery JP. Spatio-temporal distribution of the adherens junction-associated molecules vinculin and talin in the early avian embryo. *Cell Differ Dev* 1990;**30**(1):55–76.
48. Hong S-K, Dawid IB. Alpha2 macroglobulin-like is essential for liver development in zebrafish. *PLoS One* 2008;**3**(11):e3736.
49. Coppock HA, White A, Aplin JD, Westwood M. Matrix metalloprotease-3 and -9 proteolyze insulin-like growth factor-binding protein-11. *Biol Reprod*. 2004;**71**(2):438–443.
50. Bauersachs S, Mitko K, Ulbrich SE, Blum H, Wolf E. Transcriptome studies of bovine endometrium reveal molecular profiles characteristic for specific stages of estrous cycle and early pregnancy. *Exp Clin Endocrinol Diabetes* 2008;**116**(07):371–384.
51. Esadeg S, He H, Pijnenborg R, Van Leuven F, Croy BA. Alpha-2 macroglobulin controls trophoblast positioning in mouse implantation sites. *Placenta* 2003;**24**(10):912–921.
52. Pereza N, Ostojić S, Volk M, Kapović M, Peterlin B. Matrix metalloproteinases 1, 2, 3 and 9 functional single-nucleotide polymorphisms in idiopathic recurrent spontaneous abortion. *Reprod Biomed Online*. 2012;**24**(5):567–575.
53. Roediger M, Miosge N, Gersdorff N. Tissue distribution of the laminin $\beta$1 and $\beta$2 chain during embryonic and fetal human development. *J Mol Hist* 2010;**41**(2-3):177–184.
54. Ascari IJ, Alves NG, Jasmin J, Lima RR, Quintão CCR, Oberlender G, Moraes EA, Camargo LSA. Addition of insulin-like growth factor I to the maturation medium of bovine oocytes subjected to heat shock: effects on the production of reactive oxygen species, mitochondrial activity and oocyte competence. *Domest Anim Endocrinol* 2017;**60**:50–60.
55. Blake D, Svalander P, Jin M, Silversand C, Hamberger L. Protein supplementation of human IVF culture media. *J Assist Reprod Genet* 2002;**19**(3):137–143.
56. Macias-Garcia B, Gonzalez-Fernandez L, Loux SC, Rocha AM, Guimaraes T, Pena FJ, Varner DD, Hinrichs K. Effect of calcium, bicarbonate, and albumin on capacitation-related events in equine sperm. *Reproduction* 2014;**149**(1):87–99.
57. Vega L, Arroyo ÁA, Tabernero A, Medina JM. Albumin-blunted deleterious effect of amyloid-? by preventing the internalization of the peptide into neurons. *JAD* 2009;**17**(4):795–805.
58. Tatone C, Amicarelli F, Carbone MC, Monteleone P, Caserta D, Marci R, Artini PG, Piomboni P, Focarelli R. Cellular and molecular aspects of ovarian follicle ageing. *Hum Reprod Update* 2008;**14**(2):131–142.
59. Mihalas BP, Bromfield EG, Sutherland JM, De Iuliis GN, McLaughlin EA, Aitken RJ, Nixon B. Oxidative damage in naturally aged mouse oocytes is exacerbated by dysregulation of proteasomal activity. *J Biol Chem* 2018;**293**(49):18944–18964.
60. Forsberg H, Borg LA, Cagliero E, Eriksson UJ. Altered levels of scavenging enzymes in embryos subjected to a diabetic environment. *Free Radic Res* 1996;**24**(6):451–459.
61. Guérin P, El Mouatassim S, Ménézo Y. Oxidative stress and protection against reactive oxygen species in the pre-implantation embryo and its surroundings. *Hum Reprod Update* 2001;**7**(2):175–189.
62. Maître B, Jornot L, Junod AF. Effects of inhibition of catalase and superoxide dismutase activity on antioxidant enzyme mRNA levels. *Am J Physiol* 1993;**265**(6 Pt 1):L636–643.
63. Schultz RM. Regulation of zygotic gene activation in the mouse. *Bioessays*. 1993;**15**(8):531–538.
64. Wu G, Schöler HR. Role of Oct4 in the early embryo development. *Cell Regeneration* 2014;**3**(1):3: 7.
65. Keramari M, Razavi J, Ingman KA, Patsch C, Edenhofer F, Ward CM, Kimber SJ. Sox2 is essential for formation of trophectoderm in the preimplantation embryo. *PLoS One* 2010;**5**(11):e13952.
66. Rizzino A, Wuebben EL. Sox2/Oct4: A delicately balanced partnership in pluripotent stem cells and embryogenesis. *Biochim Biophys Acta* 2016;**1859**(6):780–791.
67. Zhang Y, Cui P, Li Y, Feng G, Tong M, Guo L, Li T, Liu L, Li W, Zhou Q. Mitochondrially produced ATP affects stem cell pluripotency *via* Actl6a-mediated histone acetylation. *FASEB J*. 2018;**32**(4):1891–1902.
68. Binder NK, Evans J, Gardner DK, Salamonsen LA, Hannan NJ. Endometrial signals improve embryo outcome: functional role of vascular endothelial growth factor isoforms on embryo development and implantation in mice. *Hum Reprod* 2014;**29**(10):2278–2286.


Downloaded from https://academic.oup.com/biolreprod/article/100/5/1180/5266294 by guest on 20 April 2021

## INFORME DE LOS DIRECTORES – GRADO DE CONTRIBUCIÓN

D. Javier García Casado, y Dña. Esther López Nieto como directores de la tesis titulada "TERAPIAS AVANZADAS BASADAS EN CÉLULAS MADRE Y VESÍCULAS EXTRACELULARES: CARACTERIZACIÓN Y APLICACIONES EN MODELOS ANIMALES", certificamos el factor de impacto y la categorización de las siguientes publicaciones incluidas en la tesis doctoral. Del mismo modo, se especifica cuál ha sido la participación del doctorando.

Marinaro F, Casado JG, Blázquez R, Brun MV, Marcos R, Santos M, Duque FJ, López E, Álvarez V, Usón A, Sánchez-Margallo FM. Laparoscopy for the Treatment of Congenital Hernia: Use of Surgical Meshes and Mesenchymal Stem Cells in a Clinically Relevant Animal Model. Front Pharmacol. PMID: 33101010. Article. 2020 Sep.

IF: 4.225.

Categoría: PHARMACOLOGY & PHARMACY

Revista dentro del 25%: Si

Contribución del doctorando: Desarrollo experimental, análisis y discusión de los resultados, elaboración y escritura del manuscrito

López E, Marinaro F, de Pedro MLÁ, Sánchez-Margallo FM, Gómez-Serrano M, Ponath V, Pogge von Strandmann E, Jorge I, Vázquez J, Fernández-Pereira LM, Crisóstomo V, Álvarez V, Casado JG. The Immunomodulatory Signature of Extracellular Vesicles From Cardiosphere-Derived Cells: A Proteomic and miRNA Profiling. Front Cell Dev Biol. PMID: 32582685. Article. 2020 Jun. IF: 5.186.

Categoría: DEVELOPMENTAL BIOLOGY

Revista dentro del 25%: Si

Contribución del doctorando: Desarrollo experimental, análisis y discusión de los resultados, revisión y correcciones del manuscrito

Marinaro F, Gómez-Serrano M, Jorge I, Silla-Castro JC, Vázquez J, Sánchez-Margallo FM, Blázquez R, López E, Álvarez V, Casado JG. Unraveling the Molecular Signature of Extracellular Vesicles From Endometrial-Derived Mesenchymal Stem Cells: Potential Modulatory Effects and Therapeutic Applications. Front Bioeng Biotechnol. PMID: 31921832.Article. 2019 Dec 20. IF: 3.644.

Categoría: MULTIDISCIPLINARY SCIENCES

Revista dentro del 25%: No (Q2)

Contribución del doctorando: Desarrollo experimental, análisis y discusión de los resultados, elaboración y escritura del manuscrito

López E, Blázquez R, Marinaro F, Álvarez V, Blanco V, Báez C, González I, Abad A, Moreno B, Sánchez-Margallo FM, Crisóstomo V, Casado JG. The Intrapericardial Delivery of Extracellular Vesicles from Cardiosphere-Derived Cells Stimulates M2 Polarization during the Acute Phase of Porcine Myocardial Infarction. Stem Cell Rev Rep. PMID: 31865532. Article. 2020 Jun.

IF: 5.316.

Categoría: MEDICINE, RESEARCH & EXPERIMENTAL

Revista dentro del 25%: Si

Contribución del doctorando: Desarrollo experimental, análisis y discusión de los resultados, revisión y correcciones del manuscrito

Marinaro F, Pericuesta E, Sanchez-Margallo FM, Casado JG, Alvarez V, Matilla E, Hernandez N, Blazquez R, Gonzalez-Fernandez L, Gutierrez-Adan Alfonso, Macias-Garcia B. Extracellular vesicles derived from endometrial human mesenchymal stem cells improve IVF outcome in an aged murine model. Reprod Domest Anim. PMID: 30238659. Article. 2018

IF: 1.21

Categoría: VETERINARY

Revista dentro del 25%: No (Q2)

Contribución del doctorando: Desarrollo experimental, análisis y discusión de los resultados, elaboración y escritura del manuscrito

López E, Sánchez-Margallo FM, Álvarez V, Blázquez R, Marinaro F, Abad A, Martín H, Báez C, Blanco V, Crisóstomo V, Casado JG. Identification of very early inflammatory markers in a porcine myocardial infarction model. BMC Vet Res. PMID: 30898123. 2019.

IF: 1.835.

Categoría: VETERINARY

Revista dentro del 25%: Si

Contribución del doctorando: Desarrollo experimental, análisis y discusión de los resultados, revisión y correcciones del manuscrito

Marinaro F, Macías-García B, Sánchez-Margallo FM, Blázquez R, Álvarez V, Matilla E, Hernández N, Gómez-Serrano M, Jorge I, Vázquez J, González-Fernández L, Pericuesta E, Gutiérrez-Adán A, Casado JG. Extracellular vesicles derived from endometrial human mesenchymal stem cells enhance embryo yield and quality in an aged murine model. Biol Reprod. PMID: 30596891. Article. 2019 May.

IF: 3.322.

Categoría: REPRODUCTIVE BIOLOGY

Revista dentro del 25%: Si

Contribución del doctorando: Desarrollo experimental, análisis y discusión de los resultados, elaboración y escritura del manuscrito

Marinaro F, Sánchez-Margallo FM, Álvarez V, López E, Tarazona R, Brun MV, Blázquez R, Casado JG. Meshes in a mess: Mesenchymal stem cell-based therapies for soft tissue reinforcement. Acta Biomater. PMID: 30500445. Review. 2019 Feb.

IF: 7.242.

Categoría: BIOMATERIALS

Revista dentro del 25%: Si

Contribución del doctorando: Desarrollo experimental, análisis y discusión de los resultados, elaboración y escritura del manuscrito

Blázquez R, Álvarez V, Antequera-Barroso JA, Báez-Díaz C, Blanco V, Maestre J, Moreno-Lobato B, López E, Marinaro F, Casado JG, Crisóstomo V, Sánchez-Margallo FM. Altered hematological, biochemical and immunological parameters as predictive biomarkers of severity in experimental myocardial infarction. Vet Immunol Immunopathol. PMID: 30459001. Article. 2018 Nov.

IF: 1.632.

Categoría: VETERINARY

Revista dentro del 25%: Si

Contribución del doctorando: Desarrollo experimental, análisis y discusión de los resultados, revisión y correcciones del manuscrito

Blázquez R, Sánchez-Margallo FM, Álvarez V, Usón A, Marinaro F, Casado JG. Fibrin glue mesh fixation combined with mesenchymal stem cells or exosomes modulates the inflammatory reaction in a murine model of incisional hernia. Acta Biomater. PMID: 29462710. Article. 2018 Apr.

IF: 6.383.

Categoría: BIOMATERIALS

Revista dentro del 25%: Si

Contribución del doctorando: Desarrollo experimental, análisis y discusión de los resultados, revisión y correcciones del manuscrito

Blázquez R, Sánchez-Margallo FM, Álvarez V, Matilla E, Hernández N, Marinaro F, Gómez-Serrano M, Jorge I, Casado JG, Macías-García B. Murine embryos exposed to human endometrial MSCs-derived

extracellular vesicles exhibit higher VEGF/PDGF AA release, increased blastomere count and hatching rates. PLoS One. PMID: 29684038. Article. 2018 Apr 23.

IF: 2.766.

Categoría: MULTIDISCIPLINARY SCIENCES

Revista dentro del 25%: Si

Contribución del doctorando: Desarrollo experimental, análisis y discusión de los resultados, revisión y correcciones del manuscrito

# COPYRIGHT

## OPEN ACCESS JOURNALS

Publishers: Public Library of Science, Biomed central, Frontiers Media

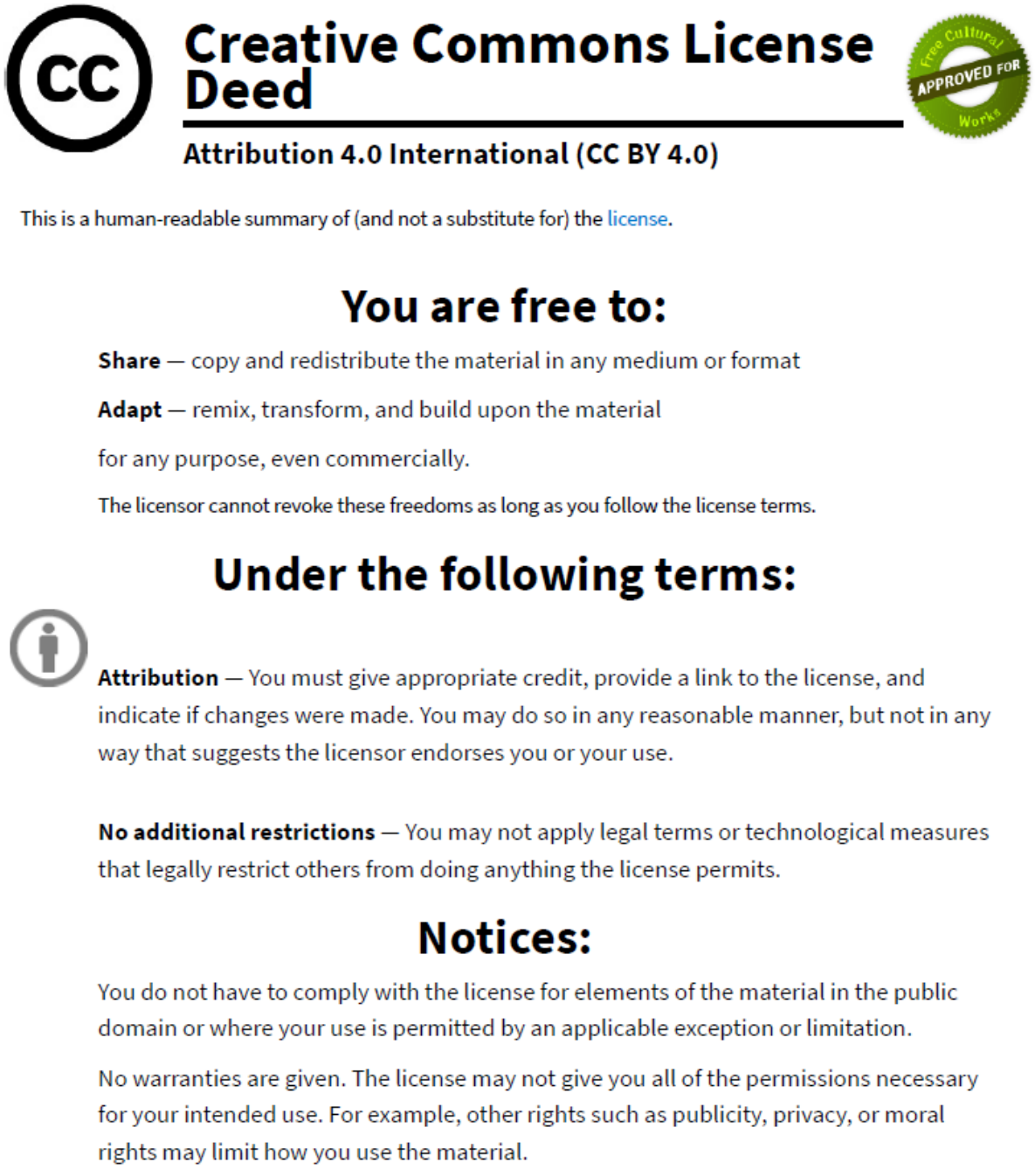

**Creative Commons License Deed**

**Attribution 4.0 International (CC BY 4.0)**

This is a human-readable summary of (and not a substitute for) the license.

**You are free to:**

**Share** — copy and redistribute the material in any medium or format

**Adapt** — remix, transform, and build upon the material

for any purpose, even commercially.

The licensor cannot revoke these freedoms as long as you follow the license terms.

**Under the following terms:**

**Attribution** — You must give appropriate credit, provide a link to the license, and indicate if changes were made. You may do so in any reasonable manner, but not in any way that suggests the licensor endorses you or your use.

**No additional restrictions** — You may not apply legal terms or technological measures that legally restrict others from doing anything the license permits.

**Notices:**

You do not have to comply with the license for elements of the material in the public domain or where your use is permitted by an applicable exception or limitation.

No warranties are given. The license may not give you all of the permissions necessary for your intended use. For example, other rights such as publicity, privacy, or moral rights may limit how you use the material.

## NON-OPEN ACCESS JOURNALS

Publishers: Elsevier, Springer, Wiley-Blackwell

Copyright Clearance Center RightsLink®

Home | Help | Email Support | Federica Marinaro

Fibrin glue mesh fixation combined with mesenchymal stem cells or exosomes modulates the inflammatory reaction in a murine model of incisional hernia

**Author:** Rebeca Blázquez,Francisco Miguel Sánchez-Margallo,Verónica Álvarez,Alejandra Usón,Federica Marinaro,Javier G. Casado

**Publication:** Acta Biomaterialia

**Publisher:** Elsevier

**Date:** 15 April 2018

*© 2018 Acta Materialia Inc. Published by Elsevier Ltd. All rights reserved.*

Journal Author Rights

Please note that, as the author of this Elsevier article, you retain the right to include it in a thesis or dissertation, provided it is not published commercially. Permission is not required, but please ensure that you reference the journal as the original source. For more information on this and on your other retained rights, please visit: https://www.elsevier.com/about/our-business/policies/copyright#Author-rights

BACK | CLOSE WINDOW

© 2021 Copyright - All Rights Reserved | Copyright Clearance Center, Inc. | Privacy statement | Terms and Conditions
Comments? We would like to hear from you. E-mail us at customercare@copyright.com

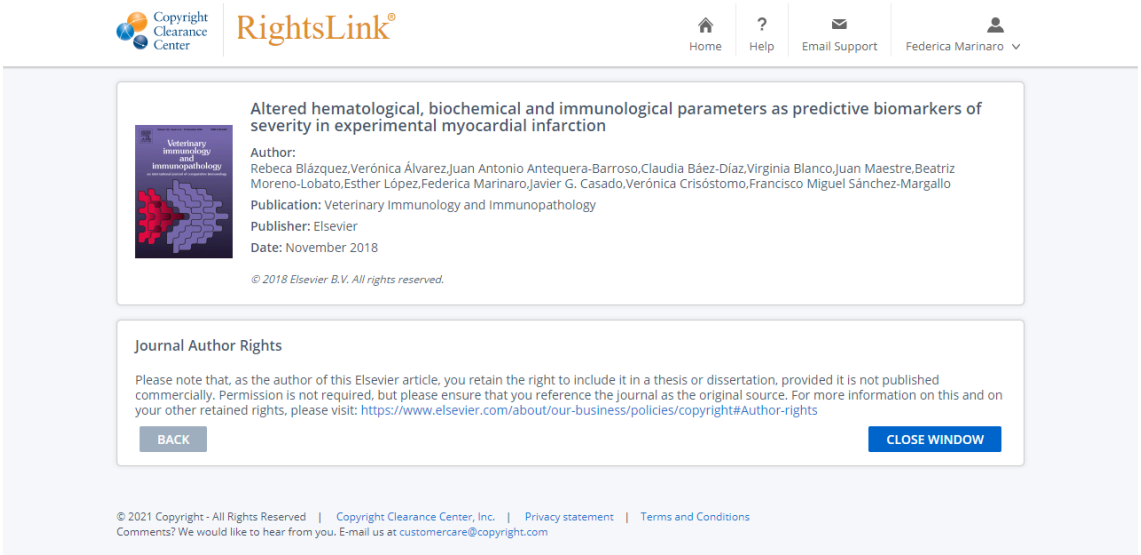

Copyright Clearance Center RightsLink®

Home | Help | Email Support | Federica Marinaro

Altered hematological, biochemical and immunological parameters as predictive biomarkers of severity in experimental myocardial infarction

**Author:**
Rebeca Blázquez,Verónica Álvarez,Juan Antonio Antequera-Barroso,Claudia Báez-Díaz,Virginia Blanco,Juan Maestre,Beatriz Moreno-Lobato,Esther López,Federica Marinaro,Javier G. Casado,Verónica Crisóstomo,Francisco Miguel Sánchez-Margallo

**Publication:** Veterinary Immunology and Immunopathology

**Publisher:** Elsevier

**Date:** November 2018

*© 2018 Elsevier B.V. All rights reserved.*

Journal Author Rights

Please note that, as the author of this Elsevier article, you retain the right to include it in a thesis or dissertation, provided it is not published commercially. Permission is not required, but please ensure that you reference the journal as the original source. For more information on this and on your other retained rights, please visit: https://www.elsevier.com/about/our-business/policies/copyright#Author-rights

BACK | CLOSE WINDOW

© 2021 Copyright - All Rights Reserved | Copyright Clearance Center, Inc. | Privacy statement | Terms and Conditions
Comments? We would like to hear from you. E-mail us at customercare@copyright.com

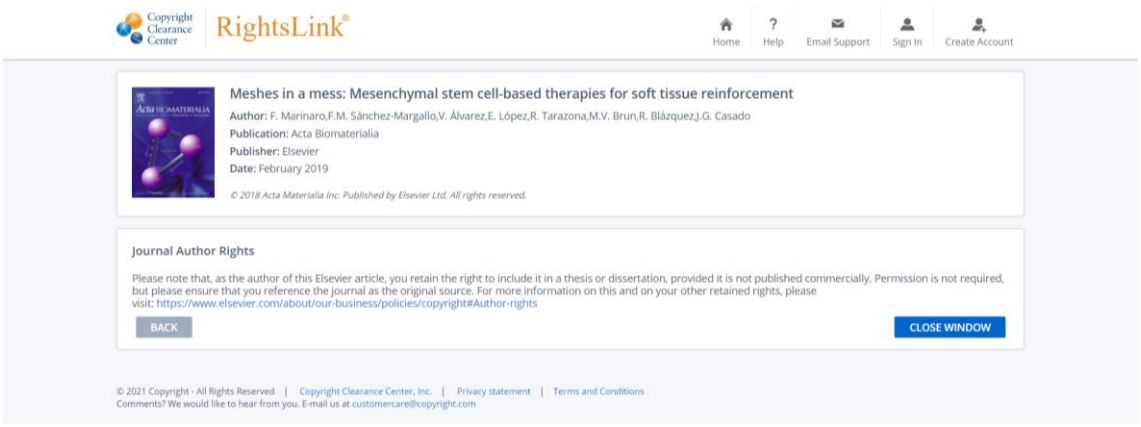

Copyright Clearance Center RightsLink®

Home | Help | Email Support | Sign in | Create Account

Meshes in a mess: Mesenchymal stem cell-based therapies for soft tissue reinforcement

**Author:** F. Marinaro,F.M. Sánchez-Margallo,V. Álvarez,E. López,R. Tarazona,M.V. Brun,R. Blázquez,J.G. Casado

**Publication:** Acta Biomaterialia

**Publisher:** Elsevier

**Date:** February 2019

*© 2018 Acta Materialia Inc. Published by Elsevier Ltd. All rights reserved.*

Journal Author Rights

Please note that, as the author of this Elsevier article, you retain the right to include it in a thesis or dissertation, provided it is not published commercially. Permission is not required, but please ensure that you reference the journal as the original source. For more information on this and on your other retained rights, please visit: https://www.elsevier.com/about/our-business/policies/copyright#Author-rights

BACK | CLOSE WINDOW

© 2021 Copyright - All Rights Reserved | Copyright Clearance Center, Inc. | Privacy statement | Terms and Conditions
Comments? We would like to hear from you. E-mail us at customercare@copyright.com

Copyright Clearance Center RightsLink®

Home | Help | Email Support | Federica Marinaro

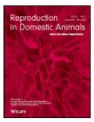

## Extracellular vesicles derived from endometrial human mesenchymal stem cells improve IVF outcome in an aged murine model

**Author:** Beatriz Macías-García, Alfonso Gutiérrez-Adán, Lauro González-Fernández, et al
**Publication:** Reproduction in Domestic Animals
**Publisher:** John Wiley and Sons
**Date:** Sep 21, 2018

*© 2018 Blackwell Verlag GmbH*

## Order Completed

Thank you for your order.

This Agreement between Miss. Federica Marinaro ("You") and John Wiley and Sons ("John Wiley and Sons") consists of your license details and the terms and conditions provided by John Wiley and Sons and Copyright Clearance Center.

Your confirmation email will contain your order number for future reference.

Printable Details

| | |
|---|---|
| License Number | 5025970911806 |
| License date | Mar 11, 2021 |

### Licensed Content

| | |
|---|---|
| Licensed Content Publisher | John Wiley and Sons |
| Licensed Content Publication | Reproduction in Domestic Animals |
| Licensed Content Title | Extracellular vesicles derived from endometrial human mesenchymal stem cells improve IVF outcome in an aged murine model |
| Licensed Content Author | Beatriz Macías-García, Alfonso Gutiérrez-Adán, Lauro González-Fernández, et al |
| Licensed Content Date | Sep 21, 2018 |
| Licensed Content Volume | 53 |
| Licensed Content Issue | S2 |
| Licensed Content Pages | 4 |

### Order Details

| | |
|---|---|
| Type of use | Dissertation/Thesis |
| Requestor type | Author of this Wiley article |
| Format | Print and electronic |
| Portion | Full article |
| Will you be translating? | No |

### About Your Work

| | |
|---|---|
| Title | Miss |
| Institution name | Jesús Usón Minimally Invasive Surgery Centre |
| Expected presentation date | Sep 2021 |

### Additional Data

### Requestor Location

| | |
|---|---|
| Requestor Location | Miss. Federica Marinaro<br>Carretera N-521 km 41.8<br><br>Cáceres, Cáceres 10071<br>Spain<br>Attn: Miss. Federica Marinaro |

### Tax Details

| | |
|---|---|
| Publisher Tax ID | EU826007151 |
| Customer VAT ID | ESG10347417 |

### Price

| | |
|---|---|
| Total | 0.00 EUR |

Would you like to purchase the full text of this article? If so, please continue on to the content ordering system located here: Purchase PDF
If you click on the buttons below or close this window, you will not be able to return to the content ordering system.

**Total: 0.00 EUR**

CLOSE WINDOW ORDER MORE

© 2021 Copyright - All Rights Reserved | Copyright Clearance Center, Inc. | Privacy statement | Terms and Conditions
Comments? We would like to hear from you. E-mail us at customercare@copyright.com

SPRINGER NATURE LICENSE
TERMS AND CONDITIONS

Mar 11, 2021

This Agreement between Miss. Federica Marinaro ("You") and Springer Nature ("Springer Nature") consists of your license details and the terms and conditions provided by Springer Nature and Copyright Clearance Center.

| | |
|---|---|
| License Number | 5025900554706 |
| License date | Mar 11, 2021 |
| Licensed Content Publisher | Springer Nature |
| Licensed Content Publication | Stem Cell Reviews and Reports |
| Licensed Content Title | Author Correction: The Intrapericardial Delivery of Extracellular Vesicles from Cardiosphere-Derived Cells Stimulates M2 Polarization during the Acute Phase of Porcine Myocardial Infarction |
| Licensed Content Author | Esther López et al |
| Licensed Content Date | Feb 27, 2020 |
| Type of Use | Thesis/Dissertation |
| Requestor type | academic/university or research institute |
| Format | print and electronic |
| Portion | full article/chapter |
| Will you be translating? | no |
| Circulation/distribution | 1 - 29 |
| Author of this Springer Nature content | yes |
| Title | Miss |
| Institution name | Jesús Usón Minimally Invasive Surgery Centre |
| Expected presentation date | Sep 2021 |
| Requestor Location | Miss. Federica Marinaro<br>Carretera N-521 km 41.8<br><br>Cáceres, Cáceres 10071<br>Spain<br>Attn: Miss. Federica Marinaro |
| Customer VAT ID | ESG10347417 |
| Total | 0.00 EUR |

# APPENDIX 2: CO-AUTHORED PUBLICATIONS NOT FORMING PART OF THIS THESIS

## INDEXED PUBLICATIONS NOT INCLUDED IN THIS THESIS

- R Blázquez, FM Sánchez-Margallo, J Reinecke, V Álvarez, E López, F Marinaro and JG Casado. *Conditioned Serum Enhances the Chondrogenic and Immunomodulatory Behavior of Mesenchymal Stem Cells*. Front Pharmacol. 2019 Jun 28;10:699. doi: 10.3389/fphar.2019.00699. eCollection 2019
- A Ballestin, JG Casado, E Abellan, FJ Vela, V Alvarez, A Uson, E Lopez, F Marinaro, R Blazquez, FM Sanchez-Margallo. *Ischemia-reperfusion injury in a rat microvascular skin free flap model: A histological, genetic, and blood flow study*. PLoS One. 2018 Dec 27;13(12):e0209624. doi: 10.1371/journal.pone. 0209624. eCollection 2018.

## NON-INDEXED PUBLICATIONS

- V Álvarez, FM Sánchez-Margallo, B Macías García, R Blázquez Durán, E López Nieto, F Marinaro, JM Gallardo Bolaños, J Giner Torres, M Rodríguez Martín, JA Gutiérrez Jiménez, A Gallardo Soler, J García Casado. *Evaluación de diferentes métodos de aislamiento de ADN circulante para la detección de fragmentos de cromosoma Y en yeguas gestante.* AETEL n.115 (2019)
- R Blázquez, FM Sánchez-Margallo, V Álvarez, A Usón, F Marinaro, J G. Casado. *Células madre y sus exosomas como terapia avanzada para tratar la hernia incisional: prueba de concepto en modelo murino*. An Real Acad Farm Vol. 84, Nº 1 (2018), pp. 39-51. ISSN (Online) 1697-4298

## PRESENTATIONS AND PROCEEDINGS

- F Marinaro, E López, M Pulido, V Álvarez, MÁ de Pedro, I Jardín, JJ López, FM Sánchez-Margallo, and JG Casado. *A multi-layered fibrin coating allows menstrual blood-derived mesenchymal stromal cells adhesion on polypropylene surgical meshes*. Poster at the Annual Meeting of International Society Gene & Cell Therapy (2021)
- E López, MÁ de Pedro, F Marinaro, M Pulido, V Álvarez, C Baez-Díaz, V Blanco, FM Sánchez Margallo, V Crisóstomo, JG Casado. *Infiltrated platelets in infarcted myocardium as a target for extracellular vesicles from endometrial-derived mesenchymal stromal cells after intrapericardial administration*. Oral presentation at the Annual Meeting of International Society Gene & Cell Therapy (2021)
- MÁ de Pedro, M Pulido, V Álvarez, F Marinaro, FM Sánchez-Margallo, E López, JG Casado. *Immunomodulatory effect of Extracellular Vesicles derived from endometrial MSCs on phenotype and functions of NK cells*. Poster at 42 Congreso de la Sociedad Española de Inmunología (2021)
- M Pulido, LM Fernández-Pereira, MÁ de Pedro, V Álvarez, F Marinaro, FM Sánchez-Margallo, E López, JG Casado. *Development of an in vitro protocol to analyse and quantify SARS-CoV-2–specific CD4+ and CD8+ T cells in COVID-19 patients by spike-derived peptides*. Poster at 42 Congreso de la Sociedad Española de Inmunología (2021)
- F Marinaro, MÁ de Pedro, M Gómez Serrano, I Jorge, E Delgado, E López, V Álvarez, JC Silla-Castro, J Vázquez, FM Sánchez Margallo, JG Casado. *Extracellular vesicles from endometrial-derived MSCs as coadjuvants for embryo culture mediums: omics and systems biology studies*. Poster at 36th ESHRE (European Society of Human Reproduction and Embryology) Annual Meeting (2020). Published in Human Reproduction, Volume 35, Issue Supplement 1, July 2020, Pages i1-i522
- F Marinaro, FM Sánchez Margallo, R Blázquez, MV Brun, E López, V Álvarez, A Usón, R Marcos, M Santos, FJ Duque, JG Casado. *Bone marrow mesenchymal stem cells accelerate wound healing after hernia repair with polypropylene surgical meshes.* Poster at 27th ESGTC (European Society of Gene and Cell Therapy) Congress (2019). Published in Human Gene Therapy Vol. 30, No. 11 (P675)
- E López, FM Sánchez-Margallo, F Marinaro, R Blázquez, V Álvarez, C Báez-Diaz, V Blanco-Blázquez, I González, A Abad, V Crisóstomo, JG Casado. *The inflammation mechanisms in myocardial infarction are altered after intrapericardial administration of cardiosphere-derived stem cells and their extracellular vesicles.* Poster at 27th ESGTC (European Society of Gene and Cell Therapy) Congress (2019). Published in Human Gene Therapy Vol. 30, No. 11 (P687)

- F Marinaro, JM Silva, A Barros, I Aroso, E Mancha, JG Casado, RL Reis, FM Sánchez Margallo. *A multilayered coating method for the application of stem cell therapy on polypropylene surgical meshes*. Oral presentation at 25th SEIQ Congress (Spanish Society of Surgical Investigation) (2019). Published in British Journal of Surgery, 106:S2, 5-18
- E Mancha, JC Gómez, E López, F Marinaro, A Macías, JP Carrasco, FM Sánchez, José Blas Pagador. *Assessment of cellular viability in bioprinted scaffold with alginate-gelatin hydrogel*. Oral presentation at 25th SEIQ Congress (Spanish Society of Surgical Investigation) (2019)
- E Mancha, JC Gómez, E López, F Marinaro, A Macías, JP Carrasco, FM Sánchez, José Blas Pagador. *Comparison between homemade and commercial bioprinter*. Oral presentation at 25th SEIQ Congress (Spanish Society of Surgical Investigation) (2019). Published in British Journal of Surgery, 106:S2, 5-18
- B Macías-García, F Marinaro, V Álvarez, L González-Fernández. *Effects of extracellular vesicles derived from human endometrial mesenchymal stem cells on porcine embryo development in vitro*. Poster at 35th Annual Meeting of the European Embryo Transfer Association (AETE), Murcia, Spain (2019). Published in Anim. Reprod., v.16, n.3, p.736, Jul./Sept. 2019
- FM Sanchez Margallo, F Marinaro, R Blazquez Duran, M Veloso Brun, JG Casado. *Laparoscopic implantation of mesenchymal stem cell-coated meshes in a swine model of abdominal hernia*. Oral presentation at 27th EAES (European Association of Endoscopic Surgery) Congress (2019)
- F Marinaro, E Pericuesta, V Álvarez, E Matilla, N Hernández, FM Sánchez-Margallo, R Blázquez, JG Casado, A Gutiérrez-Adán, B Macías-García. *The antioxidant activity of exosomes derived from endometrial human mesenchymal stem cells improves IVF outcome in an aged murine model.* Oral presentation at Annual ESDAR (European Society for Domestic Animal Reproduction) Conference 2018. Publication as Short Communication in Reprod Dom Anim. 53 (Suppl. 2):100–215
- E Alegre Cortés, F Marinaro, L González-Fernández, FM Sánchez-Margallo, B Macías-García. *Assessing the most effective way for overnight cooling of epididymal dog sperm prior freezing: in situ vs. extended.* Poster at Annual ESDAR (European Society for Domestic Animal Reproduction) Conference 2018. Publication in Reprod Dom Anim. 53 (Suppl. 2):100–215, P4.
- B Macías-García, L González-Fernández, F Marinaro, L Dávila, I Higuero, V Pérez, E Alegre-Cortés, FM Sánchez-Margallo. *N-acetylcysteine addition to canine sperm freezing extender*

*does not affect its post-thaw quality.* Poster at Annual ESDAR (European Society for Domestic Animal Reproduction) Conference 2018. Publication in Reprod Dom Anim. 53 (Suppl. 2):100–215, P177

- F Marinaro, FM Sánchez-Margallo, V Álvarez, R Blázquez, E López, B Macías-García, M Gómez-Serrano, I Jorge, J Vázquez, JG Casado. *IFNγ-preconditioning treatment increases immune system-related proteins in extracellular vesicles derived from human endometrial mesenchymal stromal cells.* Poster at *5th* European Congress of Immunology (2018). Publication in the Abstract book of the 5th European Congress of Immunology, P.A3.01.11.
- E López, V Alvarez, R Blázquez, F Marinaro, V Crisóstomo, C Báez, V Blanco, A Abad, JG Casado, FM Sánchez-Margallo. *Identification of very early inflammatory markers in a porcine myocardial infarction model*. Poster at 5th European Congress of Immunology (2018). Publication in the Abstract book of the 5th European Congress of Immunology, P.A3.07.08.
- F Marinaro, V Álvarez, R Blázquez, E López, B Macías-García, M Gómez-Serrano, I Jorge, J Vázquez, FM Sánchez-Margallo, JG Casado. *Proteomic profiling of the exosomes released by endometrial mesenchymal stem cells: possible relations with embryo development and implantation.* Poster oral presentation at 34rd Annual Meeting of the European Society of Human Reproduction and Embryology (2018). Publication in Human Reproduction, Abstracts of the 34rd Annual Meeting of the ESHRE. Volume 33, Suppl July 2018 pp. i1-i508, P-797, 2018.
- JG Casado, R Blázquez R, V Álvarez, J Antequera-Barroso, C Báez-Díaz, V Blanco, J Maestre, B Moreno, E López, F Marinaro, V Crisóstomo, FM Sánchez-Margallo. *Identification of early peripheral blood biomarkers to predict the severity of myocardial infarction in a porcine model*. Poster at 52nd Annual Scientific Meeting of the European Society for Clinical Investigation (2018). Publication in the European Journal of Clinical Investigation, Abstracts of the 52nd Annual Scientific Meeting of the ESCI. P105-T, Volume 48 Supplement 1 May 2018.
- J García-Casado, E López, V Álvarez, R Blázquez, F Marinaro, M Gómez-Serrano, I Jorge, J Vázquez, FM Sánchez-Margallo. *Isolation and proteomics analysis of microvesicles from cardiosphere-derived cells for cardiac repair therapy*. Poster at 52nd Annual Scientific Meeting of the European Society for Clinical Investigation (2018). Publication in the European Journal of Clinical Investigation, Abstracts of the 52nd Annual Scientific Meeting of the European Society for Clinical Investigation. P106-T, Volume 48, Supplement 1, May 2018.

## BOOK CHAPTERS

- F Marinaro, M Gómez Serrano et al. *Unraveling the Molecular Signature of Extracellular Vesicles From Endometrial-Derived Mesenchymal Stem Cells: Potential Modulatory Effects and Therapeutic Applications*. Martin J. Stoddart, Sandra Hofmann and Wolfgang Holnthoner, eds. *MSC Signaling in Regenerative Medicine*. Lausanne: Frontiers Media SA. DOI 10.3389/978-2-88966-320-0 ISSN 1664-8714.
- E López, F Marinaro, et al. *The Immunomodulatory Signature of Extracellular Vesicles From Cardiosphere-Derived Cells: A Proteomic and miRNA Profiling*. Khan, M., Sayed, N., Krishnamurthy, P., Tang, Y., eds. *Wireless Intercellular Communications in Cardiac Pathology: The Role of Exosomes*. Lausanne: Frontiers Media SA. doi: 10.3389/978-2-88966-179-4 ISSN 1664-8714

## AWARDS

- R. Blázquez, F.M. Sánchez-Margallo, V. Álvarez, A. Usón, F. Marinaro, J.G. Casado. *Stem cells and their exosomes as advanced therapy to treat incisional hernia: proof of concept in a murine model*. Concurso científico del curso 2017. Premio de la Real Academia Nacional de Farmacia.
- Tu tesis en un post-it. Asociación de Doctorandos de la Universidad de Extremadura.

# APPENDIX 3: INTERNATIONAL PHD MENTION

With this thesis, the requirements requested by University of Extremadura to obtain the International PhD mention were accomplished. The expected requirements are reported as follows:

a. During the training period necessary to obtain the doctoral degree, the doctoral student spent a three-month research stay outside of Spain in a prestigious higher education institution or research center, studying or carrying out research work related to the thesis.
b. The research stay took place at the 3B's Research group (University of Minho, Caldas das Taipas, Portugal), from the 1st March 2019 to the 31st May 2019. It was supervised by Dr. Alexandre Barros, Dr. Joana Marques Silva and Prof. Dr. Rui Reis.
c. This PhD thesis has been totally written in English, the most used language in scientific communication, which is not an official language in Spain.
d. Two acknowledged researchers with the PhD title, working in foreign institutions and from different countries respect to the one where the PhD Student carried out her research stay, were informed about this thesis:
    1) Dr. Sandro Sacchi, PhD. Researcher at Department of Life Sciences, University of Modena and Reggio Emilia (Italy)
    2) Dr. Diego Celdrán Bonafonte, DVM, PhD, MBA. Research Assistant Professor, Surgery, University Animal Care, Division of CT Surgery, College of Medicine, University of Arizona (USA)
e. Two acknowledged researchers, with the PhD title, different to the above-mentioned researchers and from a foreign research institution were invited to be part of the evaluating commission of this PhD thesis:
    1) Dr. Alexandra Marques, PhD. Principal investigator, Research Institute on Biomaterials, Biodegradables and Biomimetics (I3Bs), University of Minho (Portugal)
    2) Dr. Barbara Barboni, DVM, PhD. Full professor, Faculty of Biosciences and agro-food and environmental technology, University of Teramo (Italy)

3B's Research Group
I3Bs - Research Institute on Biomaterials, Biodegradables and Biomimetics of University of Minho
AvePark, Parque de Ciência e Tecnologia,
Zona Industrial da Gandra
4805-017 Barco GMR, Portugal

3B's Research Group

Biomaterials
Biodegradables
Biomimetics

# Research Stay Certification

The PhD Student Federica Marinaro has developed a research stay in the I3B's – Research Institute on Biomaterials, Biodegradables and Biomimetics of University of Minho in Guimãraes (Portugal) from March 1st to May 31st.

In witness thereof, we sign the present declaration in Guimãraes on May 31st, 2019.

Prof. Dr. Rui L. Reis
Director of 3B's
Research Group

Dr. Alexandre Barros
Assistant Researcher at
3B's Research Group

Dr. Joana Marques-Silva
Post Doc at 3B's
Research Group

UNIMORE
UNIVERSITÀ DEGLI STUDI DI MODENA E REGGIO EMILIA

Dipartimento di Scienze della Vita

Sede di Modena
Via Giuseppe Campi, 183
41125 - Modena, Italia
T +39 059 2055170 · 2055529 · 2055014
F +39 059 2055700

Sede di Reggio Emilia
Via Amendola 2
42122 - Reggio Emilia, Italia
T +39 0522 522036/ 67 · F +39 0522 522053

Sandro Sacchi, PhD
Dipartimento di Scienze della Vita
Via Campi 213/D
Tel. +393471819903
E-mail: sandro.sacchi@unimore.it
12th March 2021

To whom it may concern:

**Re: Doctoral thesis of Federica Marinaro**

Dear Sir/Madam,

I have been asked to act as referee of Federica Marinaro's doctoral thesis, "A*dult stem cell- and extracellular vesicle-based therapies: characterization and application in animal models*" (*Terapias avanzadas basadas en celulares madre y vesículas extracelulares: caracterización y aplicaciones en modelos animales*).

The data generated during her PhD are presented in ten original research articles, published in peer-reviewed, respected journals. All these papers show that Federica Marinaro has gained extensive laboratory (and research) experience during her PhD work and has developed and used a wide variety of techniques in her research. These techniques have been used to answer a set of novel and interesting hypotheses regarding adult stem cell and extracellular vesicle-based therapies, which have been carefully linked to important clinical needs. The breadth of approaches used in these studies, and more widely throughout the thesis, means that the candidate is well-placed for a successful future research career.

With these points in mind, I have no hesitation in recommending Federica Marinaro as a candidate to reach the International Doctorate Grade.

Yours faithfully,

Sandro Sacchi

Partita IVA e codice fiscale: 00427620364

THE UNIVERSITY OF ARIZONA
College of Medicine
Tucson

NEPHROLOGY DIVISION
DEPARTMENT OF MEDICINE

1501 N Campbell Ave
P.O. Box 245022
Tucson, AZ 85724
Ofc: 520-626-6371
Fax: 520-626-2024
www.deptmedicine.arizona.edu/nephrology

***D. Diego Celdrán Bonafonte, DVM, MSC, PhD.***
***Associate Scientific Investigator.***
***Division of Nephrology. College of Medicine.***
***The University of Arizona.***

*Sirva la presente carta Para acreditar que la tesis titulada "**Desarrollo y estudio del potencial inmunomodulador de tres novedosas estrategias para la aplicación de la terapia celular**", que será defendida por la doctoranda Rebeca Blázquez Durán, cumple ampliamente con todos los requisitos académicos, científicos y metodológicos para la obtención del grado de doctor.*

*Cabe destacar la elevada calidad científica del trabajo, su meticulosidad y el gran potencial de aplicación de los resultados obtenidos. Del mismo modo, solicito por medio de este **informe favorable**, que dicha tesis doctoral sea considerada como Tesis Doctoral Internacional.*

*Y para que así conste, firmo la presente*
*en Tucson, Arizona (USA) a 13 de Septiembre de 2016*

*Dr. Diego Celdrán Bonafonte*